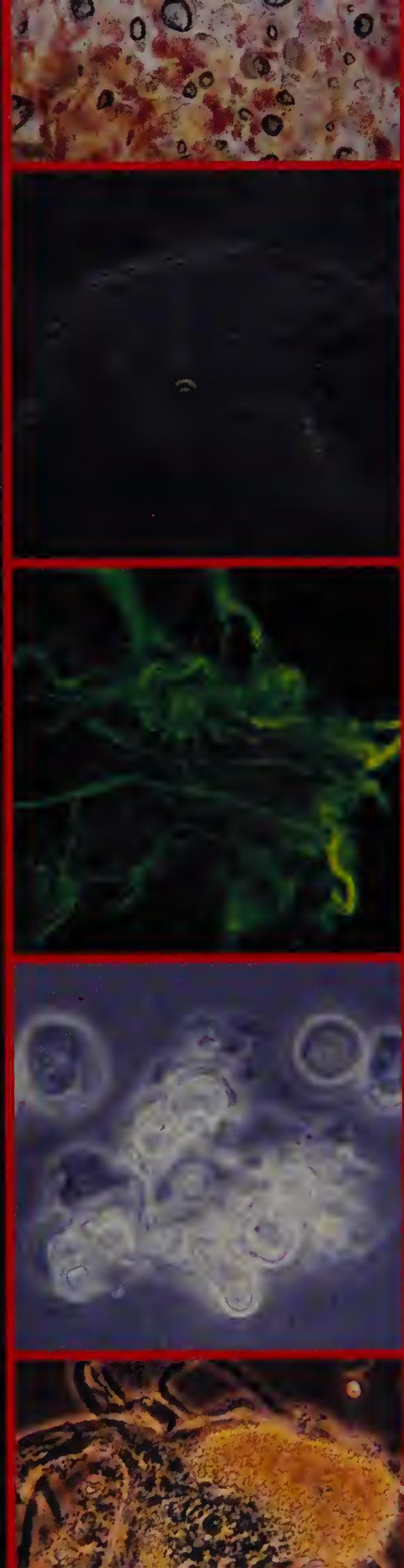


ATLAS OF THE CELLULAR STRUCTURE OF THE HUMAN NERVOUS SYSTEM

Harold Hillman
David Jarman



LIBRARY

JUN 25 1991

National Institutes of Health

**ATLAS OF THE
CELLULAR STRUCTURE
OF THE HUMAN
NERVOUS SYSTEM**

Strange, is it not? that of the myriads who
Before us pass'd the door of Darkness through
Not one returns to tell us of the Road,
Which to discover we must travel too.

Omar Khayyam (11th century)

The contemplation of things as they are,
without error or confusion, without
substitution or imposture, is in itself a
nobler thing than a whole harvest of
invention.

Francis Bacon (1605)

ATLAS OF THE CELLULAR STRUCTURE OF THE HUMAN NERVOUS SYSTEM

**Harold Hillman
David Jarman**

*Unity Laboratory of Applied Neurobiology,
University of Surrey, Guildford, Surrey, England*



ACADEMIC PRESS

Harcourt Brace Jovanovich, Publishers
London San Diego New York
Boston Sydney Tokyo Toronto

QM
525
H655
1991

ACADEMIC PRESS LTD.
24/28 Oval Road,
London NW1 7DX

United States Edition published by
ACADEMIC PRESS INC.
San Diego, California 92101-4311

Copyright © 1991 by
ACADEMIC PRESS LTD.

All Rights Reserved.

No part of this book may be reproduced in any form by photostat, microfilm, or any other means without written permission from the publishers

British Library Cataloguing in Publication Data

Hillman, H. (Harold) 1930-

Atlas of cellular structure of the human nervous system.

1. Man. Nervous system. Anatomy

I. Title II. Jarman, D.

611.8

ISBN 0-12-348770-6

Filmset by Oxprint Ltd , Oxford
Printed in Hong Kong

CONTENTS

v

Preface	vii	Section 5 CEREBELLUM	129
Acknowledgements	ix	Section 6 SPINAL CORD AND GANGLIA	141
List of figures	x		
Methods used	1	Section 7 CRANIAL NERVES AND RETINA	167
Section 1 COLOUR MACROGRAPHS OF THE BRAIN	3	Section 8 PERIPHERAL NERVES	183
Views of the intact brain		Section 9 PITUITARY, PINEAL AND ADRENAL GLANDS	195
Sections of the cerebrum and the cerebellum		Summary	203
Section 2 MICROSCOPIC CONSTITUENT ELEMENTS	21	Appendix	205
Section 3 CEREBRAL CORTEX	41	Selected references	209
Section 4 SUBCORTICAL STRUCTURES	71		

*This book is dedicated to our wives,
Elizabeth and Jean.*

PREFACE

The great microscopist and cytologist, J. R. Baker, wrote: 'Every cytological investigation should start, if possible, with the study of the living cell' (Baker, 1958). With pleasing exceptions, such as blood vessels in the web of toes, peripheral nerves *in situ* and sympathetic ganglia, this is rarely possible in the living animal, because the optical conditions for light microscopy are not optimal. Observations on tissue culture would be attractive, but, unfortunately, cells change in culture and their appearances are highly sensitive to the conditions of incubation. Therefore, the nearest one can approach the appearance of living cells is to dissect them out using minimal unnatural reagents, and try to observe them before their structure changes, or they become infected.

Study of unfixed human nervous tissue requires access to material from biopsy or from post mortems. Material from the former sources is hard to obtain, and samples from most parts of the central nervous system are not available. Therefore, in this atlas, most of the material is post mortem from human beings. Of course, some of the patients had been dead for 1–3 days before the post mortems, and undoubtedly autolysis will have occurred during this time. However, it is worth noting that: (i) this is a drawback of any human neuropathological study; (ii) as far as we are aware, no one has shown that morphological changes do occur shortly after death in the elements of the central nervous system; (iii) our practice was to discard tissues in which bacteria or fungi could be seen; (iv) we always compared the appearances of the human post-mortem specimens with those of the same structures from freshly killed rabbits, rats, guinea-pigs, lambs and mice. There were no differences between the same structures in the human brains and those in these mammals, except that we did not see lipofuscin in the central nervous systems of animals. Sometimes, when tissues such as retinas or median nerves were not obtainable from human beings, only animal tissues

could be used; (v) most of our samples were from middle-aged or old human beings, because children and young adults rarely came to post mortem.

In this atlas, we have attempted to make accurate observations on the building materials of the nervous system, rather than on its connections or physiology. Our philosophy has been that the structures speak for themselves, so that our comments are confined to drawing readers' attention to particular structural features and their incidence.

The early pioneers of microscopy, such as van Leeuwenhoek, Fontana, Swammerdam, Malpighi, Purkinje, Remak, Ehrenberg, and Valentin, examined tissues without the addition of fixatives. Fixatives had been used earlier to stop post-mortem changes, but were not widely employed until histological techniques were developed in the second half of the 19th century. The kinds of observations in the earlier literature on unstained cells of the central nervous system were no longer reported after the introduction of histological procedures, and are now rare in modern publications.

Tellyesniczky in 1898 made the first systematic investigations on the effects of staining procedures on the appearances and dimensions of tissue by light microscopy. He was followed by Ross, Baker, Frontera, Gersh, Kushida, Lodin, Cammermeyer and many others. They found that during staining procedures, whether or not they included freezing, the whole tissue shrank, each organelle not necessarily shrinking equally. Shrinkage occurred mainly during fixation, dehydration, and between dehydration and embedding or mounting. The apparent spaces seen around stained neurons were a graphic example of this phenomenon. The widely held belief that the embedding or mounting media reinflated the tissue components to their previous volumes turned out not to be the case (see Appendix, p. 205).

The following chemical effects could also change the appearance of the tissue: (i) precipitates can be formed

in the extracellular fluid, the cytoplasm and the axoplasm, firstly, as a consequence of fixation, secondly, from the dehydration of tissues previously containing 60–80 per cent water, and thirdly, when salts of heavy metals, such as silver, osmium, tungsten, lead, etc., react with the proteins and lipids of the tissue; (ii) the large volume of the reagents compared with that of the tissues results in extraction of water and solvent-soluble components, some of them structural. For example, fixatives extract proteins; ethanol and acetone extract lipids.

Since Stilling and Wallach in 1842 introduced serial sections, it has been appreciated that the size, shape or presence of any cell or organelle cannot be assessed from a single section.

The techniques of teasing and microdissection go back to van Leeuwenhoek in the 17th century and were

used in this century by Gray, Heilbrunn, the Chambers (father and son) and Hyden. Further, the observation of the fine structure of unfixed cells, previously pursued by bright field, dark ground and polarizing microscopy, was much enhanced by the invention of phase contrast microscopy by Zernike in 1934.

Hyden in Sweden in the 1960s studied the neurons of the Deiters' nucleus of rabbit using this approach, but — as far as we can find — no attempts have been made before to examine all main elements in the mammalian (including human) nervous system, under these conditions. We would be pleased to enter into discussion or correspondence with anyone who has made similar observations.

Many of the historical references are taken from Clarke and O'Malley (1968).

ACKNOWLEDGEMENTS

We are most grateful to the Handicapped Children's Aid Committee of London and to Dr D. Horrobin of Scotia Pharmaceuticals for supporting this work. Mr K. Shaughnessy and Mr J. Darbey of the Audio Visual Aids Unit of the University of Surrey took the colour macrographs. Dr R. Ainsworth and Mr R. Smythe kindly obtained the tissue for us. Mr E. Rosen, FRCS, from Manchester was good enough to supply us with the micrographs of the fundus. Mr A. V. Dodge, former President of the Quekett Microscopical Club, helped us much with the photography and the microscopy.

Miss P. Gunter, of Zeiss Oberkochen Ltd. at Welwyn Garden City, permitted us to use the laser scanning microscope. Mr M. J. Walker, of Stafford, took some flash photographs of our neurons, and Mr L. V. Martin, OBE, former President of the Quekett Microscopical Club, used his Hoffman modulation contrast to look at the structure of the nucleolus. Dr Susan Hall, of the Department of Anatomy, Guy's Hospital, London, and Cambridge University Press gave us permission to reproduce the micrograph of the mouse sciatic nerve. We extend our thanks to all these individuals.

LIST OF FIGURES

Section 1 Colour macrographs of the brain

Figure 1 Superior view of the brain.

Figure 2 Lateral view of the brain.

Figure 3 Inferior view of the brain to show some of the cranial nerves.

Figure 4 Inferior view of the brain to show the circle of Willis.

Figure 5 Pial vessels on the surface of the cortex.

Figure 6 Ventral view of the pons, showing two vertebral arteries joining to become the basilar artery, which leads to the circle of Willis.

Figure 7 The cerebellum to show the folia and the pial blood vessels.

Figure 8 The frontal lobe, showing the white and grey matter.

Figure 9 The white matter of the insula to show the distribution of small arteries.

Figure 10 Diagram to show the planes of the subsequent brain sections.

Figure 11 Section through the anterior part of the frontal lobe.

Figure 12 Section through the frontal lobe to show the genu of the corpus callosum and the anterior horns of the lateral ventricle.

Figure 13 Section through the frontal lobe and the head of the caudate nucleus.

Figure 14 Section through the caudate nucleus, the internal capsule and the putamen.

Figure 15 Section through the frontal and temporal lobes, the globus pallidus and the third ventricle.

Figure 16 Putamen, globus pallidus and internal capsule.

Figure 17 Section through the parietal and temporal lobes, showing the thalamus, the third ventricle and the infundibulum.

Figure 18 Close-up of the previous section.

Figure 19 Section through the parietal and temporal lobes to

show the hippocampus, the third ventricle and the mammillary bodies.

Figure 20 Section through the parietal and temporal lobes to show the substantia nigra, the hippocampus and the red nucleus.

Figure 21 Close-up of the previous figure.

Figure 22 The hippocampus and the choroid plexus.

Figure 23 Section through the parietal and temporal lobes, to show the pineal gland, the midbrain and the pons.

Figure 24 The midbrain and the cerebral peduncles.

Figure 25 View of the cerebellum and the midbrain from the anterior aspect.

Figure 26 Section through the cerebellum and the medulla.

Figure 27 Section through the pons.

Figure 28 View of the cerebellum and the midbrain from the posterior aspect.

Figure 29 The arbor vitae appearance of a folium of the cerebellum.

Section 2 Microscopic constituent elements

Figure 30 Isolated human hypoglossal neuron to show the dendritic tree.

Figure 31 Isolated human Purkinje cell showing long primary and branched secondary dendrites.

Figure 32 Isolated rabbit neuron from the lateral vestibular nucleus to show nuclear and nucleolar membranes, by phase contrast and by differential interference contrast microscopy.

Figure 33 Isolated rabbit lateral vestibular neuron photographed twice with an interval of 20 minutes, to show nucleolar and cytoplasmic movements.

Figure 34 Isolated human neurons from the arcuate nucleus to show the nucleolar membranes.

Figure 35 Teased human substantia nigral neurons and neuroglia, by phase contrast and stained with anti-neurofilament antibody.

- Figure 36** Isolated human ventral horn cell from the cervical spinal cord, to show intracellular lipofuscin.
- Figure 37** Isolated rat ventral horn cell from the cervical spinal cord, to show a neuroglial cell or a small neuron.
- Figure 38** Isolated rabbit ventral horn cell from the cervical spinal cord focused on the somal surface to show adherent beaded fibres.
- Figure 39** The same neuron as in the previous figure, but focused inside the cell to show the nucleus and paired nucleoli.
- Figure 40** Isolated human pituicytes.
- Figure 41** Isolated guinea-pig ganglion cell from the cervical spinal ganglion.
- Figure 42** Isolated guinea-pig ganglion cell from the myenteric plexus of the colon.
- Figure 43** Isolated human neurons or neuroglial cells from the red nucleus.
- Figure 44** Isolated rat cerebellar granule cells.
- Figure 45** Surface of the soma of an isolated rabbit ventral horn cell from the cervical spinal cord to show adherent beaded fibre endings.
- Figure 46** Nucleus and nucleolus of isolated rabbit lateral vestibular neuron.
- Figure 47** Nucleolar membrane and nucleolonema in isolated rabbit lateral vestibular neuron.
- Figures 48 and 49** Nucleus and nucleolus of isolated rabbit ventral horn cell to show the mitochondria and nucleolonema.
- Figure 50** Nucleus and nucleolus of isolated rabbit lateral vestibular neuron to show the nuclear membrane.
- Figure 51** Soma-dendritic junction of isolated rabbit lateral vestibular neuron to show granular appearance.
- Figure 52** Surface of the dendrite of an isolated rabbit ventral horn neuron to show the granular appearance compared with the previous figure.
- Figure 53** Isolated human dendrite from a Betz cell, to show the dendritic structure and adherent fine granules.
- Figure 54** Isolated human dendrite from a vagal nucleus neuron.
- Figure 55** Isolated human dendritic tree of an inferior vestibular neuron.
- Figure 56** Isolated human fine fibre from the cerebellar grey matter, to show adherent fine granules.
- Figure 57** Isolated human fine fibre from the previous tissue, showing that it has a smooth outline.
- Figure 58** Isolated rabbit dendrite from a ventral horn cell from the cervical spinal cord, to show a fine beaded fibre running along its upper edge.
- Figure 59** Isolated human ependymal cells from the wall of the lateral ventricle adjacent to the corpus callosum.
- Figure 60** Teased human putamen, to show fine granular material.
- Figure 61** Isolated rat beaded fibres from dorsal white matter of cervical spinal cord to show small axoplasmic granules within the beads.
- Figure 62** Teased human beaded fibres from the vestibulospinal tract.
- Figure 63** Isolated human beaded fibres from the pons, to show a side branch ending in a bead.
- Figure 64** Clump of neuroglial droplets from the human cerebellar white matter.
- Figure 65** Teased human optic nerve, to show droplets and neuroglial cells.
- Figure 66** Isolated droplets from rabbit dorsal column of the spinal cord.
- Figure 67** Isolated rat myelinated fibre from sciatic nerve, to show Schwann cell containing multiple nucleoli.
- Figure 68** Isolated rabbit myelinated fibre from sciatic nerve to show node of Ranvier and axon.
- Figure 69** Isolated rabbit myelinated nerve fibre from the sciatic nerve, to show intra-axonal inclusions.
- Figure 70** Partially teased rabbit sciatic nerve showing a dark Remak fibre between myelinated fibres.
- Figure 71** Isolated rabbit Remak fibres from the sciatic nerve.
- Figure 72** Isolated human capillary from the putamen.
- Figure 73** Isolated human capillary from the cerebellar cortex, showing endothelial cells and/or pericytes.
- Figure 74** Isolated rabbit capillary from the internal capsule to show endothelial cells and/or pericytes.

Section 3 Cerebral cortex

- Figure 75** Thin slab of adult rabbit frontal cortical grey matter, lightly coloured with methylene blue to show the incidence of neuron somas.
- Figure 76** Thin slab of human frontal cortical grey matter, lightly coloured with methylene blue to show the incidence of neuron somas.
- Figure 77** Thin slab of adult rat frontal cortical grey matter, unstained.
- Figure 78** Thin slab of human frontal cortical grey matter, to show neurons *in situ*.
- Figure 79** Thin slab of new-born lamb frontal cortical grey matter to show pyramidal neuronal somas *in situ*.
- Figure 80** Teased fine granular material from human frontal grey matter, to show individual or aggregates of granules.

- Figure 81** Teased human frontal grey matter, to show fine fibres.
- Figure 82** Teased human frontal grey matter, to show a neuron and associated neuroglia.
- Figure 83** Thin slab of human frontal region, to show grey-white matter boundary.
- Figure 84** Thin slab of human frontal white matter, to show beaded fibres and large droplets.
- Figure 85** Thin slab of rat frontal white matter, to show large beaded fibres *in situ*.
- Figure 86** Partially teased human frontal white matter, to show beaded fibres and droplets.
- Figure 87** Partially teased human frontal white matter, to show beaded fibres and droplets.
- Figure 88** Teased human frontal white matter, to show fine beaded fibres and small droplets.
- Figure 89** Thin slab of human parietal cortical grey matter, lightly coloured with methylene blue to show the incidence of neuron somas.
- Figure 90** Thin slab of human parietal grey matter, to show a Betz cell *in situ*.
- Figure 91** Thin slab of human parietal grey matter to show neuroglial nuclei and fine granular material *in situ*.
- Figure 92** Teased adult rabbit parietal grey matter, to show neurons and fine granules.
- Figure 93** Teased human parietal grey matter to show neuroglial nuclei or small neurons.
- Figure 94** Isolated human Betz cell from the parietal grey matter, to show nucleolar membrane, nucleolonema and dendrites.
- Figure 95** Isolated human Betz cell from parietal grey matter, to show intracellular lipofuscin, a nucleolar membrane and adherent neuroglia.
- Figure 96** Isolated human Betz cell, stained with anti-neurofilament 200 kD protein.
- Figure 97** Isolated human Betz cell, stained with anti-glial fibrillary acidic protein.
- Figure 98** Isolated clump of fine granular material from human parietal cortex, and a neuroglial nucleus or small cell below it.
- Figure 99** Partially teased thin slab of human parietal white matter, to show beaded fibres and large droplets.
- Figure 100** Thin slab of adult rabbit paraventricular parietal white matter, to show beaded fibres and droplets.
- Figure 101** Thin slab of guinea-pig parietal white matter to show fibres.
- Figure 102** Partially teased thin slab of human parietal white matter, to show beaded fibres travelling in several directions.

- Figure 103** As previous figure, showing teased beaded fibres and droplets.
- Figure 104** Thin slab of human temporal grey matter, lightly coloured with methylene blue to show the incidence of neuron somas.
- Figure 105** Thin slab of human temporal cortex, lightly coloured with methylene blue, covered by the pia mater on the left.
- Figure 106** Thin slab of human temporal grey matter, to show neuronal somas and beaded fibres.
- Figure 107** Thin slab of human temporal grey matter, to show a beaded fibre tract passing through.
- Figure 108** Teased human temporal grey matter, to show cells with large nuclei and fine granular material.
- Figure 109** Teased human temporal grey matter, to show small neurons or neuroglial nuclei and fine granular material.
- Figure 110** Teased human temporal white matter, to show beaded fibres and droplets.
- Figure 111** Thin slab of human temporal white matter, to show small beaded fibres.
- Figure 112** Thin slab of human occipital grey matter, lightly coloured with methylene blue to show the incidence of neuron somas.
- Figure 113** Thin slab of human occipital grey-white matter boundary, lightly coloured with methylene blue.
- Figure 114** Thin slab of human occipital grey matter, to show large beaded fibres.
- Figure 115** Thin slab of human occipital grey matter, to show neurons *in situ*.
- Figure 116** Thin slab of human occipital grey matter, to show birefringence of fibres.
- Figure 117** Thin slab of human occipital grey matter, to show a Meynert cell *in situ*.
- Figure 118** Teased human occipital grey matter, to show neuroglial nuclei and fine granular material.
- Figure 119** Isolated Meynert cell from human occipital grey matter.
- Figure 120** Teased rat occipital grey matter to show neuroglial nuclei or cells.
- Figure 121** Thin slab of new-born mouse occipital grey matter, to show neurons — some with double nucleoli.
- Figure 122** Teased new-born mouse occipital grey matter, to show neurons with little cytoplasm and fine fibres.
- Figure 123** Thin slab of new-born mouse occipital white matter, to show probable migration of cells.
- Figure 124** Thin slab of human occipital white matter, to show beaded fibres.
- Figure 125** Thin slab of human occipital white matter, to show teased beaded fibres and large droplets.

Section 4 Subcortical structures

Figure 126 Thin slab of human corpus callosum, to show beaded fibres.

Figure 127 Teased human corpus callosum, to show beaded fibres, which can occasionally be seen branching.

Figure 128 Teased human corpus callosum, showing large beaded fibre.

Figure 129 Teased human corpus callosum, to show birefringence of the sheath.

Figure 130 Thin slab of human internal capsule, to show beaded fibres.

Figure 131 Thin slab of human internal capsule, teased to show large beaded fibres and droplets.

Figure 132 Partially teased rabbit internal capsule, to show large and small droplets.

Figure 133 Thin slab of human caudate nucleus, to show blood vessels.

Figure 134 Thin slab of human caudate nucleus, to show the incidence of neuron somas.

Figure 135 Thin slab of human caudate nucleus, to show fine beaded fibres.

Figure 136 Partially teased human caudate nucleus, to show neuroglial nuclei and fine granules.

Figure 137 Partially teased human caudate nucleus, teased to show fine fibres.

Figure 138 Teased rat caudate nucleus, to show beaded fibres.

Figure 139 Thin slab of human putamen, lightly coloured with methylene blue to show the incidence of neuron somas.

Figure 140 Thin slab of human putamen, to show fine beaded fibres.

Figure 141 Partially teased white matter of a rat putamen, to show beaded fibres.

Figure 142 Teased human putamen, to show fine fibres.

Figure 143 Isolated human neuroglia or small neurons and fine granules from the putamen.

Figure 144 Thin slab of human globus pallidus, to show beaded fibres and a neuron with lipofuscin *in situ*.

Figure 145 Thin slab of human globus pallidus, to show fibres, some beaded.

Figure 146 Partially teased human globus pallidus, to show large droplets and fibres.

Figure 147 Thin slab of human thalamus, lightly coloured with methylene blue to show the incidence and appearance of neuron somas.

Figure 148 Thin slab of human dorsolateral nucleus of the thalamus, to show fibres and droplets.

Figure 149 Thin slab of human medial nucleus of the thalamus, to show neurons with intracellular lipofuscin.

Figure 150 Isolated human beaded fibres from the dorsolateral nucleus of the thalamus.

Figure 151 Isolated neurons from thalamus from a human and from rat.

Figure 152 Thin slab of human hypothalamus, to show neuron somas and beaded fibres.

Figure 153 Thin slab of human hypothalamus, to show capillaries and nuclei.

Figure 154 Teased human hypothalamus, to show neurons, fine fibres and neuroglial nuclei.

Figure 155 Isolated human hypothalamic neuron.

Figure 156 Thin slab of human fornix of the hypothalamus, to show beaded fibres.

Figure 157 Teased small droplets from a thin slab of human fornix of the hypothalamus.

Figure 158 Thin slab of human red nucleus, lightly coloured with methylene blue to show the incidence of neuron somas.

Figure 159 Thin slab of human red nucleus, to show the distribution of capillaries.

Figure 160 Partially teased human red nucleus, to show neurons with associated lipofuscin.

Figure 161 Thin slab of human red nucleus, to show fibre tracts and droplets.

Figure 162 Teased human red nucleus, to show beaded fibres and droplets.

Figure 163 Teased human red nucleus, to show unidentified spherical cells, possible neuron somas and neuroglial nuclei.

Figure 164 Thin slab of human substantia nigra, lightly coloured with methylene blue to show the high incidence of neuron somas.

Figure 165 Thin slab of human substantia nigra, to show the incidence of neuron somas.

Figure 166 Partially teased human substantia nigra, to show two neurons and beaded fibres.

Figure 167 Teased human substantia nigra, to show a neuron with adjacent fine granular material.

Figure 168 Teased human substantia nigral neuroglia from the previous specimen, to show fine granular material.

Figure 169 Isolated capillaries and beaded fibres from human substantia nigra.

Figure 170 Thin slab of the human mammillary body, to show neurons and beaded fibres.

Figure 171 Isolated neuron somas from a thin slab of the human mammillary body.

Figure 172 Teased fibres and small droplets from the same specimen as in the penultimate figure.

- Figure 173** Lipofuscin from the same specimen as in the previous figure, with polars uncrossed and with polars crossed to show birefringence.
- Figure 174** Thin slab of human superior colliculus, lightly coloured with methylene blue to show the incidence of neurons.
- Figure 175** Teased human superior colliculus, to show large refractile droplets and fine granules.
- Figure 176** Thin slab of human inferior colliculus.
- Figure 177** Teased human inferior colliculus, to show a neuron covered with lipofuscin and associated neuroglia.
- Figure 178** Thin slab of the human hippocampus, lightly coloured with methylene blue to show the incidence of neurons.
- Figure 179** Thin slab of the human hippocampus, lightly coloured with methylene blue to show the incidence and appearance of pyramidal neuron somas.
- Figure 180** Higher power view of the same specimen as in the previous figure, to show pyramidal neurons *in situ* and fine beaded fibres.
- Figure 181** Thin slab of rabbit hippocampus, lightly coloured with methylene blue, to show pyramidal layer and granule cell layer.
- Figure 182** Higher power view of the same specimen as in the previous figure, but enlarged granule cell layer with fine processes proceeding from the cells.
- Figure 183** Higher power view of the same specimen as in the previous figure, with the pyramidal cell layer enlarged.
- Figure 184** Thin slab of the human hippocampus, to show granule cell somas.
- Figure 185** Teased human hippocampus from the previous specimen to show granule cells and neuroglial nuclei.
- Figure 186** Teased human hippocampus, to show pyramidal neurons and their processes.
- Figure 187** Teased human hippocampal pyramidal neuron from the previous specimen.
- Figure 188** Thin slab of the human amygdala, to show neuron somas and beaded fibres.
- Figure 189** Teased human amygdala from the previous specimen, to show fine granular material.
- Figure 190** Teased human amygdala from the previous specimen, to show round and oval cells and fine granular material.
- Figure 191** Human choroid plexus from the posterior horn of the lateral ventricle, right side.
- Figure 192** Human choroid plexus from the previous specimen, to show blood vessels and villi.
- Figure 193** Human choroid plexus from the previous specimen, to show capillaries and what are believed to be calcareous deposits.
- Figure 194** Human choroid plexus from the previous

- specimen, to show blood vessels and calcareous deposits.
- Figure 195** Human choroid plexus from the previous specimen, to show a 'whorl' and connective tissue fibres.
- Figure 196** Rabbit paraventricular white matter to show droplets.
- Figure 197** Teased artery from rabbit choroid plexus from the lateral ventricle.
- Figure 198** Isolated human epithelial cells from the choroid plexus.
- Figure 199** Human ependymal cells and adjacent white matter stained with Holzer's stain.
- Figure 200** Rabbit capillary from the white matter adjacent to the third ventricle.
- Figure 201** Thin slab of human pyramid, to show fibres and large and small droplets.
- Figure 202** Thin slab of human pyramid from the previous specimen, to show the pyramid/arcuate nucleus boundary.
- Figure 203** Thin slab of human pons, to show beaded fibres and droplets.
- Figure 204** Partially teased human pons from the previous specimen, to show beaded fibres.
- Figure 205** Teased human pons from the previous specimen, to show beaded fibres and droplets.
- Figure 206** Isolated neurons from the teased human pontine nucleus.
- Figure 207** Teased guinea-pig pons to show refractile droplets.
- Figure 208** Thin slab of human olfactory nucleus, lightly coloured with methylene blue to show the incidence of neuron somas.
- Figure 209** Thin slab of human olfactory nucleus, to show a fibre tract *in situ*.
- Figure 210** The same thin slab of human olfactory nucleus as in the previous specimen, to show birefringence of some fibres.
- Figure 211** Isolated neuron from teased human olfactory nucleus, with adherent neuroglia.
- Figure 212** Isolated capillaries from teased human olfactory nucleus.
- Figure 213** Thin slab of human medial lemniscus, to show beaded fibres and droplets.
- Figure 214** Partially teased human medial lemniscus from the previous specimen, to show beaded fibres and droplets.
- Figure 215** Teased human medial lemniscus from the previous specimen, to show isolated droplets.
- Figure 216** Thin slab of human inferior vestibular nucleus, to show a neuron with lipofuscin *in situ* and beaded fibres.
- Figure 217** Partially teased human inferior vestibular nucleus from the previous specimen to show neuron and beaded fibres.

Figure 218 Isolated neuron from teased human inferior vestibular nucleus, with adherent neuroglia.

Figure 219 Isolated rabbit neuron from teased lateral vestibular nucleus to show nuclear and nucleolar membranes.

Figure 220 Isolated rabbit neuron soma from teased lateral vestibular nucleus, to show details of nucleolus.

Figure 221 Isolated human neuron from the lateral vestibular nucleus, stained with anti-neurofilament 200 kD protein, by phase contrast and after excitation with blue light of 450–490 nm.

Figure 222 Isolated human neuron from the lateral vestibular nucleus, stained with anti-glial fibrillary acidic protein, by phase contrast and after excitation with blue light of 450–490 nm.

Figure 223 Isolated human neuroglia from the lateral vestibular nucleus, stained with anti-neurofilament 200 kD protein, by phase contrast and after excitation with blue light of 450–490 nm.

Figure 224 Thin slab of human medullary white matter, to show beaded fibres *in situ*.

Figure 225 Thin slab of human dorsal nucleus of the vagus, to show a neuron *in situ* with large lipofuscin deposit.

Figure 226 Thin slab of human dorsal nucleus of the vagus, to show beaded fibres *in situ*.

Figure 227 Partially teased human dorsal nucleus of the vagus from the previous specimen, to show beaded fibres.

Figure 228 Isolated neuron from the dorsal nucleus of the vagus.

Figure 229 Thin slab of human hypoglossal nucleus, lightly coloured with methylene blue to show the incidence and appearance of neuron somas.

Figure 230 Thin slab of human hypoglossal nucleus, from the previous specimen, lightly coloured with methylene blue to show the appearance of the neuron soma *in situ*.

Figure 231 Thin slab of human hypoglossal nucleus, to show lipofuscin, beaded fibres and droplets.

Figure 232 Teased human hypoglossal nucleus, to show neurons and neuroglia.

Figure 233 Isolated human neuron from the hypoglossal nucleus of the previous specimen.

Figure 234 Isolated human neuron from the hypoglossal nucleus of the previous specimen.

Figure 235 Teased human white matter adjacent to the hypoglossal nucleus, to show beaded fibres.

Section 5 Cerebellum

Figure 236 Thin slab of human cerebellar cortex, to show Purkinje cells with dendrites *in situ*.

Figure 237 Thin slab of human cerebellar cortex, lightly coloured with methylene blue to show Purkinje cell somas *in situ*.

Figure 238 Thin slab of lamb cerebellar cortex to show Purkinje and granule cells *in situ*.

Figure 239 Partially teased lamb cerebellar cortex to show two Purkinje cells, one with two nucleoli and associated neuroglia.

Figure 240 Isolated human Purkinje cell.

Figure 241 Teased dendrites from the human Purkinje cell of the previous specimen.

Figure 242 Isolated human cerebellar granule cells and fine granular material.

Figure 243 Isolated fine granular material of human cerebellar grey matter.

Figure 244 Thin slab of human cerebellar white matter from the centre of a folium, to show fine beaded fibres.

Figure 245 Thin slab of human cerebellar white matter adjacent to the dentate nucleus, from the previous specimen, to show large beaded fibres and droplets.

Figure 246 Section of human cerebellar white matter, stained with Palmgren's stain, to show a tract of fine fibres.

Figure 247 Partially teased human cerebellar white matter adjacent to the dentate nucleus, to show beaded fibres and neuroglial cells.

Figure 248 Teased human cerebellar white matter, to show beaded fibres and droplets.

Figure 249 Thin slab of human dentate nucleus, to show a neuron with lipofuscin *in situ* and beaded fibres.

Figure 250 Thin slab of human dentate nucleus from the previous specimen, to show beaded fibres and droplets.

Figure 251 Isolated guinea-pig neuron with associated neuroglia from the dentate nucleus.

Figure 252 Teased neuroglia from the rabbit dentate nucleus, to show fine granular material.

Figure 253 Thin slab of human fastigial nucleus, to show neurons *in situ* with associated lipofuscin.

Figure 254 Thin slab of human white matter adjacent to the fastigial nucleus, from the previous specimen, to show beaded fibres and droplets.

Section 6 Spinal cord and ganglia

Figure 255 Dissection of rat spinal cord to show the position of dorsal root ganglia.

Figure 256 Section of injected cat spinal cord to show that there are more blood vessels in the grey than the white matter.

Figure 257 Section of cat spinal cord stained with a silver stain to show the distribution of black-staining ventral horn cells in the grey matter.

Figure 258 Partially teased rabbit substantia gelatinosa from the cervical spinal cord, to show fibres, believed to be myelinated.

Figure 259 Teased rabbit substantia gelatinosa from the cervical spinal cord, to show bipolar neurons and associated neuroglia.

Figure 260 Teased guinea-pig substantia gelatinosa from the cervical spinal cord, to show a small neuron, beaded fibres and fine granular material.

Figure 261 Thin slab of human anterior horn from the cervical spinal cord, to show anterior horn cell *in situ*.

Figure 262 Isolated rabbit ventral horn cells from the cervical spinal cord.

Figure 263 Isolated human anterior horn cell from the cervical spinal cord, to show the large intracellular lipofuscin deposits, the nucleus and the nucleolus.

Figure 264 Isolated rabbit anterior horn cell from the cervical spinal cord, to show the nucleolar membrane, small and medium size beaded fibres, and a capillary.

Figure 265 Isolated human anterior horn cell.

Figure 266 Isolated human anterior horn cell, stained with anti-neurofilament 200 kD protein, by phase contrast and after excitation with blue light of 450–490 nm.

Figure 267 Isolated human anterior horn cell, stained with anti-glial fibrillary acidic protein, by phase contrast and after excitation with blue light of 450–490 nm.

Figure 268 Isolated human neuroglia from the anterior horn, stained with anti-glial fibrillary acidic protein, by phase contrast and after excitation with blue light of 450–490 nm.

Figure 269 Thin slab of human gracile tract from the cervical spinal cord, to show beaded fibres *in situ*.

Figure 270 Thin slab of human cuneate tract from the cervical spinal cord, to show beaded fibres *in situ* and droplets.

Figure 271 Teased human cuneate tract from the previous specimen, to show beaded fibres.

Figure 272 Thin slab of fresh rat dorsal region of cervical spinal cord, to show beaded fibres and droplets.

Figure 273 Teased fresh rat beaded fibres from the dorsal cervical spinal cord.

Figure 274 Teased fresh guinea-pig dorsal white matter from the sacral spinal cord, to show droplets and neuroglial cells.

Figure 275 Teased freshly killed rabbit dorsal white matter from the cervical spinal cord, to show isolated droplets.

Figure 276 Thin slab of fresh guinea-pig lateral white matter from the cervical spinal cord to show fibres and droplets *in situ*.

Figure 277 Partially teased human vestibulospinal tract from the cervical spinal cord, to show beaded fibres and droplets.

Figure 278 Thin slab of guinea-pig filum terminale to show beaded fibres, droplets and neuroglial nuclei.

Figure 279 Teased fresh guinea-pig filum terminale to show beaded fibres.

Figure 280 Transverse section of a human ventral root

stained with Palmgren's stain to show nerve fibres.

Figure 281 Section of a human dorsal root ganglion stained with haematoxylin and eosin.

Figure 282 Isolated rat cervical spinal ganglion.

Figure 283 Partially teased rabbit cervical spinal ganglion, to show ganglion cells.

Figure 284 Isolated rat ganglion cell from cervical spinal ganglion.

Figure 285 Isolated rabbit ganglion cell from cervical spinal ganglion to show associated 'satellite' cells or synapses.

Figure 286 Dissected rabbit superior cervical ganglion.

Figure 287 Rat superior cervical ganglion to show nerve fibres *in situ*.

Figure 288 Partially teased superior cervical ganglion from 4-week-old rat, to show ganglion cells and nerve fibres.

Figure 289 Dissected rabbit vagal ganglion.

Figure 290 Partially teased rabbit vagal ganglion, to show ganglion cells, 'satellite' cells or synapses, and nerve fibres.

Figure 291 Teased rabbit ganglion cells from the previous specimen.

Figure 292 Partially teased mouse sympathetic nerve to the ileum, to show Remak fibres *in situ*.

Figure 293 Teased rabbit cervical sympathetic nerve, to show a beaded fibre and Remak fibres.

Figure 294 Teased guinea-pig cervical sympathetic nerve, to show Remak fibres.

Figure 295 Isolated mouse sublingual ganglion, to show ganglion cells *in situ*.

Figure 296 Partially teased mouse sublingual ganglion, to show ganglion cells and associated nerve fibres.

Figure 297 Myenteric plexus in guinea-pig colon *in situ*.

Figure 298 Dissected guinea-pig myenteric plexus of colon, to show ganglion cells *in situ*.

Figure 299 Guinea-pig myenteric plexus of colon *in situ*, to show ganglion cells.

Figure 300 Isolated guinea-pig ganglion cells from the myenteric plexus of colon to show multiple nucleoli.

Section 7 Cranial nerves and retina

Figure 301 Partially teased rabbit olfactory bulb to show different cell types.

Figure 302 Teased human olfactory bulb, to show spherical cells.

Figure 303 Thin slab of human olfactory tract, to show beaded fibres *in situ*.

- Figure 304** Partially teased human olfactory tract, to show fibres.
- Figure 305** Isolated beaded fibre from the previous specimen.
- Figure 306** Thin slab of human optic nerve, to show beaded fibres *in situ*.
- Figure 307** Teased human optic nerve, to show beaded fibres.
- Figure 308** Teased human neuroglial clump from the optic nerve.
- Figure 309** Isolated droplet and neuroglial cell from the previous specimen.
- Figure 310** Neuroglial nuclei and fine granular material teased from the optic nerve of rat.
- Figure 311** Teased rat oculomotor nerve, to show beaded and myelinated nerve fibres.
- Figure 312** Partially teased rat trigeminal nerve to show a ganglion cell and myelinated fibres.
- Figure 313** Isolated rabbit myelinated nerve fibre of the abducens nerve, showing the axon from which the sheath has been partly pulled off by teasing.
- Figure 314** Isolated rat myelinated and unmyelinated (Remak) fibres from the facial nerve.
- Figure 315** Isolated rat myelinated fibre from the glossopharyngeal nerve, to show a node of Ranvier.
- Figure 316** Teased rabbit vagus nerve to show myelinated fibres with intra-axonal inclusions.
- Figure 317** Isolated beaded fibre in rabbit vagus nerve.
- Figure 318** Normal fundus of a left eye, 30 degrees view. The optic nerve head shows a physiological cup with a cup to disc ratio of 0.2.
- Figure 319** As above, fundus of the right eye of another subject, to show variation of normal appearances.
- Figure 320** Unteased rabbit retina to show blood vessels and bundles of nerve fibres.
- Figure 321** Partially teased rabbit retina to show beaded fibres.
- Figure 322** Partially teased rabbit retina to show ganglion cells.
- Figure 323** Partially teased rabbit retina to show ganglion cells.
- Figure 324** Partially teased rabbit retina to show small ganglion cells and fine fibres.
- Figure 325** Partially teased rabbit retina, to show cell bodies of rods and cones. Inset: rod nuclei.
- Figure 326** Teased rabbit retina to show amacrine cells and rod nuclei.
- Figure 327** Isolated nuclei, probably of cones, from the

central area of rat retina.

Figure 328 Isolated nuclei, probably of rods, from the central area of rat retina.

Figure 329 Teased outer segments of rods and ganglion cells from rat retina.

Figure 330 Partially teased rabbit retina to show pigment cell layer.

Section 8 Peripheral nerves

Figure 331 Transverse section of a branch of rabbit sciatic nerve, stained by the Weigert-Pal method, to show the incidence of myelinated fibres.

Figure 332 Partially teased mouse phrenic nerve, to show beaded fibres.

Figure 333 Isolated guinea-pig myelinated nerve fibres from phrenic nerve.

Figure 334 Isolated guinea-pig Remak fibre from phrenic nerve.

Figure 335 Thin slab of guinea-pig diaphragm including terminations of phrenic nerve, to show neuromuscular junctions.

Figure 336 Unteased guinea-pig median nerve, to show beaded and myelinated fibres *in situ*.

Figure 337 Partially teased mouse median nerve, to show developing myelinated nerve fibres and Schwann cells *in situ*.

Figure 338 Isolated guinea-pig myelinated nerve fibres from median nerve.

Figure 339 Sciatic nerve of a living mouse *in situ*.

Figure 340 Unteased guinea-pig sciatic nerve, to show myelinated fibres.

Figure 341 Teased 4-week-old rat sciatic nerve, to show myelinated nerve fibres and a Schwann cell.

Figure 342 Teased rabbit sciatic nerve, to show beaded and myelinated nerve fibres and a Schwann cell.

Figure 343 Isolated rabbit myelinated fibres from sciatic nerve, to show node of Ranvier.

Figure 344 Isolated rat myelinated fibre from the sciatic nerve, to show Schmidt-Lantermann incisure on one side and intra-axonal particles.

Figure 345 Isolated rabbit sciatic fibre, to show apparatus of Golgi-Rezzonico.

Figure 346 Isolated rabbit myelinated fibre from the sciatic nerve, to show intra-axonal inclusions.

Figure 347 Isolated rabbit myelinated fibres from the sciatic nerve to show intra-axonal particles.

Figure 348 Isolated Remak fibre from rabbit sciatic nerve.

Figure 349 Teased rabbit sural nerve to show myelinated and Remak fibres.

Section 9 Pituitary, pineal and adrenal glands

Figure 350 Unteased human posterior pituitary gland, to show blood vessels *in situ*.

Figure 351 Isolated human pituicytes from the posterior lobe; fine granules can also be seen.

Figure 352 Thin slab of human pineal gland, showing pinealocytes *in situ*.

Figure 353 Partially teased human pineal gland, to show pinealocytes, fine nerve fibres and fine granular material.

Figure 354 Partially teased guinea-pig pineal gland, to show pinealocytes.

Figure 355 Partially teased guinea-pig pineal stalk, lower end, to show beaded fibres and endings.

Figure 356 Isolated human pinealocytes.

Figure 357 Brain sand from the previous specimen.

Figure 358 Another piece of human brain sand.

Figure 359 The same piece of brain sand as in the previous figure, but viewed through cross polars to show its birefringence.

Figure 360 Partially teased rabbit adrenal medulla to show chromaffin cells in columns.

Figure 361 Teased rabbit adrenal medulla to show chromaffin cells.

Figure 362 Isolated nuclei and fine granular material from rabbit adrenal medulla.

Appendix The effects of staining procedures on the appearances of rabbit medullary neuron somas.

METHODS USED

Most of the observations were made on human brains obtained at post mortem. The patients had been dead for 1–3 days, and had died from non-neurological causes. Their ages ranged from 46 to 95 years. The specimens were not fixed. They were put into plastic bags and taken to the Unity Laboratory of Applied Neurobiology of the University of Surrey within 20 minutes of their excision.

The human brains were initially cut into coronal sections and kept unfixed at 4°C. The slabs were photographed as soon as possible in natural colour.

When human tissues were not available, nervous tissue was taken from lambs which had died during birth and from adult rabbits, rats, guinea-pigs and mice killed by exposure to an overdose of ether. The brains, spinal cords, retinas, cranial nerves, ganglia and peripheral nerves were excised, and the specimens were teased and photographed, usually on the same day but sometimes up to 3 days later. In the latter cases they were placed in specimen bottles in an atmosphere saturated with water vapour, and stored in the refrigerator at 4°C.

Pieces of brain or spinal cord were cut into transverse sections and placed on the stage of a Zeiss zoom dissecting microscope, with magnification from 20 to 200 times. They were bathed in 150 mm NaCl solution (saline) to which about 1 mg methylene blue per 50 ml saline was added to show up the neuron somas and the general topography of the tissue. After this had been established, a small piece about 2 mm, by 2 mm, by 0.05–0.1 mm thick was cut with iris scissors, a scalpel blade, or a fine syringe needle. It was placed in saline in a parallel-walled chamber (Sartory *et al.*, 1971). This was made by cutting a circular hole in double-sided non-water-soluble tape, about 2 cm by 2 cm square, which was stuck on to a microscope slide. The masking tape was left on the upper surface, and a drop of saline was

placed in the circle to receive the tissue. The masking tape was removed, and a standard cover slip 0.17 mm thick was placed over the specimen with minimum pressure (Hillman, 1986a).

The small unteased pieces of tissue were observed with minimal teasing under less than optimal conditions to establish the appearances of the cells and nerve fibres *in situ* and to find out whether any appearances in the subsequently teased or microdissected tissues were artefacts produced by the teasing or microdissection itself. This became crucial, for example, when viewing varicosities on fibres and droplets in white matter, which other authors have thought to have resulted from manipulations.

Individual neurons and pieces of neuroglia were isolated by hand by the technique originally described by Hyden (1959), and detailed more recently (Hillman, 1986a). Neuron somas were dissected out by hand, using mounted stainless steel wires 30 µm or 70 µm in diameter, or tungsten wires 150 µm in diameter, brought to a point by the method of Dossel (1966). The somas were transferred on the wire to a drop of saline solution containing no methylene blue, in a parallel-walled chamber. Using the dissecting microscope, a small group of somas, clumps of neuroglia, myelinated fibres, or droplet or varicose fibres, could be placed under direct vision on any part of the slide. They were so isolated that they could be viewed optimally and photographed by phase contrast microscopy.

The specimens were then examined using a Zeiss research microscope and Neofluar objectives, with 6.3, 16, 40, 63 or 100 times magnification and numerical apertures of 0.20, 0.40 and 0.75, 0.9 and 1.3, respectively. Sometimes, two polars were used, when the objects observed were thought to be birefringent. A Zeiss Ikon Icarex 35 camera and Kodak Technical Pan Film 2415 were used, and calibration was performed

using a stage micrometer, with 10 μm divisions. All photographs were printed on Ilford Multigrade III paper. Ektachrome 160 was used for colour.

In all cases, the appearances of all elements seen in the human specimens were the same, although often larger than those in the animal specimens studied, except that lipofuscin granules were seen in human but not in animal brains. However, it must be said that most tissues originated from mature human beings and young adult animals. All the appearances of the neurons, neuroglial fibres, granules and droplets observed are reported.

Nearly all tissues were examined fresh by phase contrast microscopy but, nowadays, neurons and glial cells are often identified by their fluorescence on addition of monoclonal antibodies to neurofilament polypeptide or to glial fibrillary acidic protein (GFAP), respectively. Therefore, these antibodies have been used on some identified cells by the method of Debus *et al.* (1983).

Briefly the tissues were fixed in acetone, 5 per cent acetic acid in ethanol, or in buffered paraformaldehyde for 5 minutes at room temperature. They were washed three times with phosphate buffered saline (PBS), the

surplus PBS was drawn off, and 50 μl fetal calf serum was left on the cells for 20 minutes. The excess fetal calf serum was removed at room temperature, and 50 μl of the monoclonal antibody, anti-GFAP or anti-neurofilament 200 kD protein, was pipetted on to the preparation; it was left in a moist atmosphere for 12 hours at 4°C. It was washed three times with PBS at room temperature, the surplus PBS was removed, and 50 μl anti-mouse-IgG-FITC (fluorescein isothiocyanate) antibody was pipetted on to it, and left for 1 hour at room temperature, in a moist atmosphere in the dark. The antibodies were supplied by Boehringer Mannheim. The preparation was then washed three times with PBS, and mounted in a PBS/glycerol mixture (Citifluor AF1). The slides were sealed with nail varnish. At no time were the tissues allowed to dry out.

The slides were viewed with a Leitz Dialux 20 fluorescent microscope, using the epifluorescent mode and phase contrast objectives, with 16 or 40 times magnification and numerical apertures of 0.45 and 0.7, respectively. The photographs were taken with an Olympus OM2N camera and Ektachrome 400 colour film.

SECTION

1

COLOUR MACROGRAPHS OF THE BRAIN

Views of the intact brain

Sections of the cerebrum and the cerebellum



Figure 1 Superior view of the brain of a 74-year-old man ($\times 0.67$).

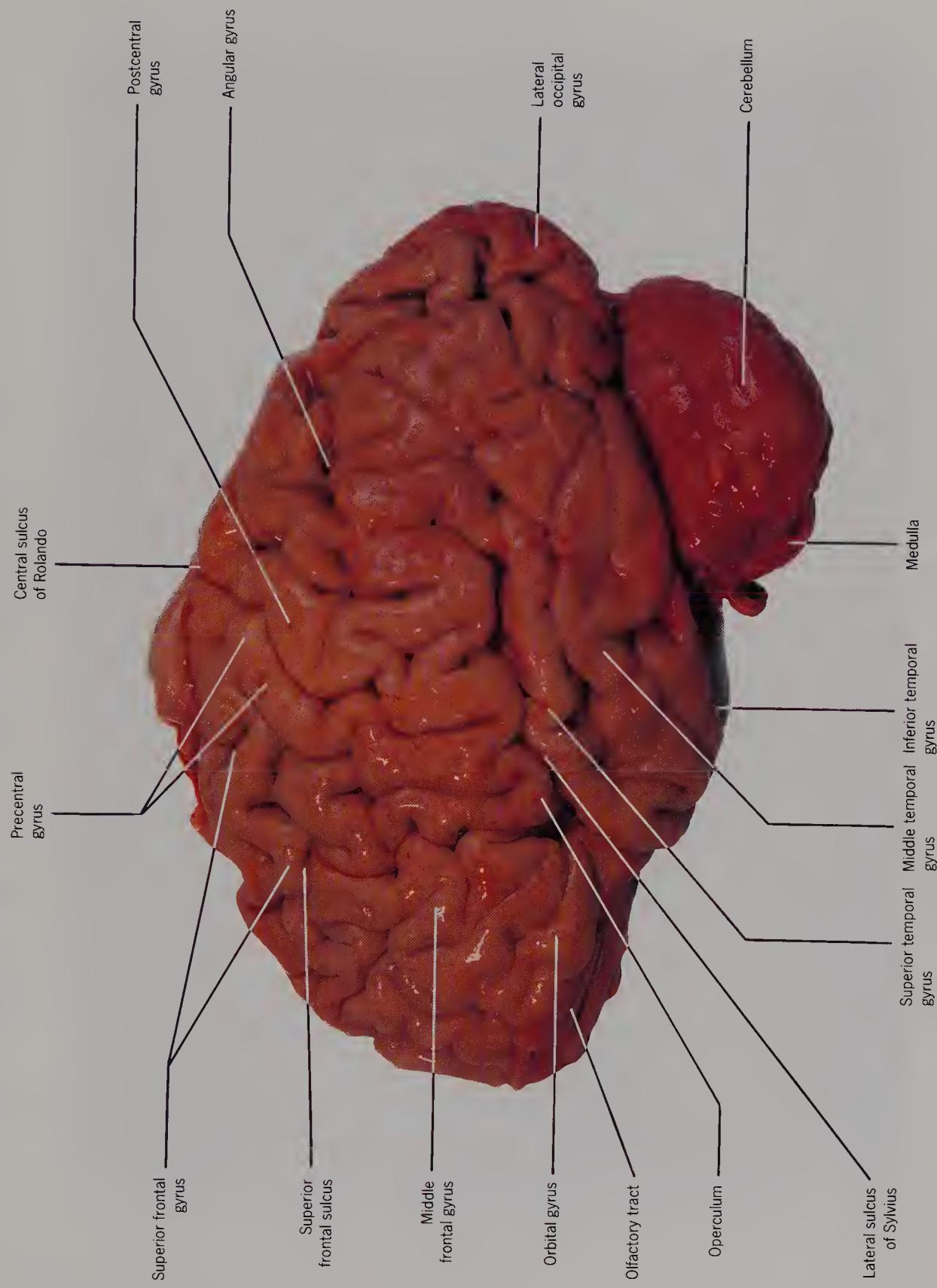


Figure 2 Lateral view of the brain of a 74-year-old man ($\times 0.67$).

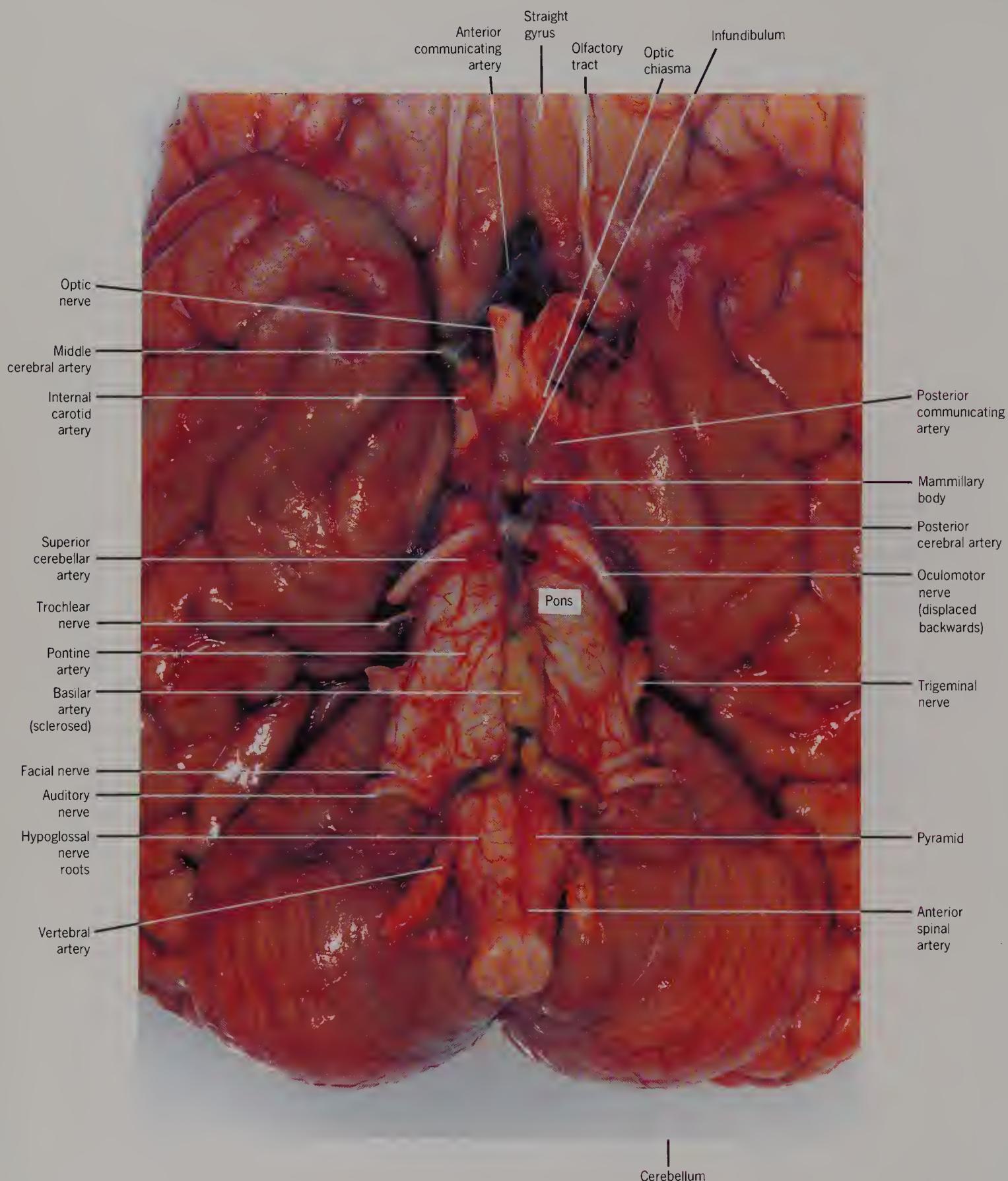


Figure 3 Inferior view of the brain of a 74-year-old man to show some of the cranial nerves. The oculomotor nerve should be pointing forwards ($\times 1$).

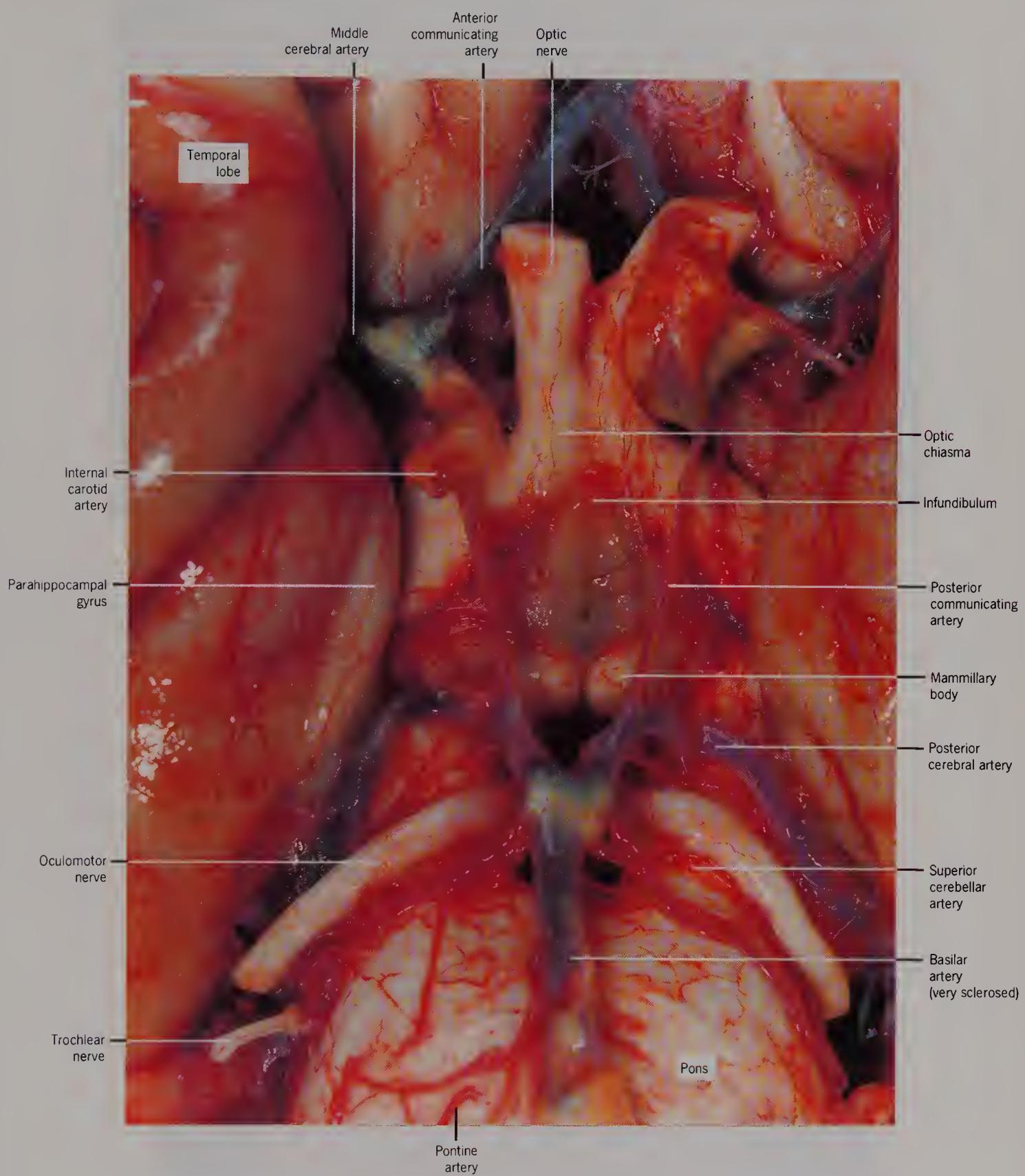


Figure 4 Inferior view of the brain of a 74-year-old man to show the circle of Willis. The sclerosis of the basilar artery ($\times 2.5$).

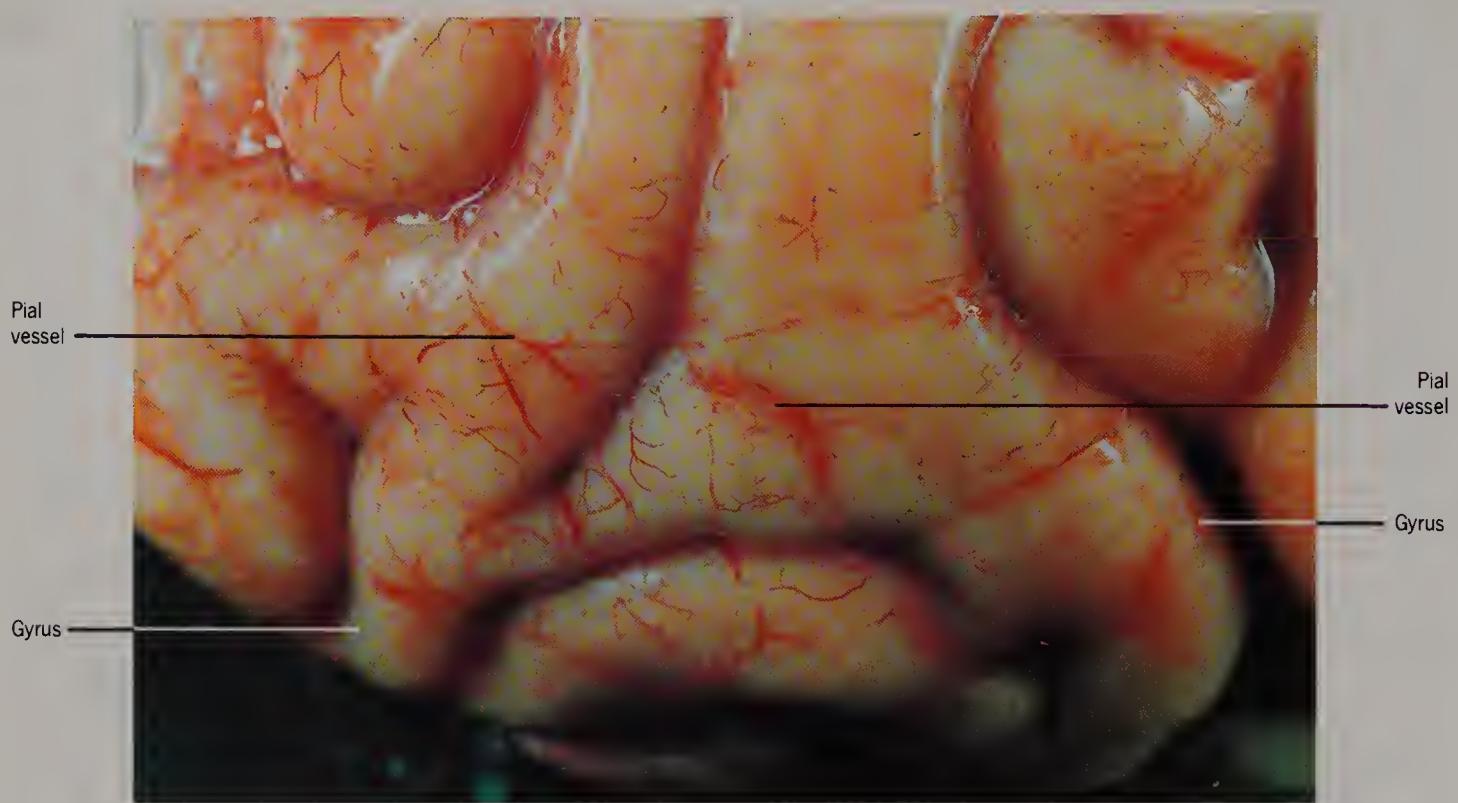


Figure 5 Pial vessels on the surface of the cortex ($\times 3.5$).

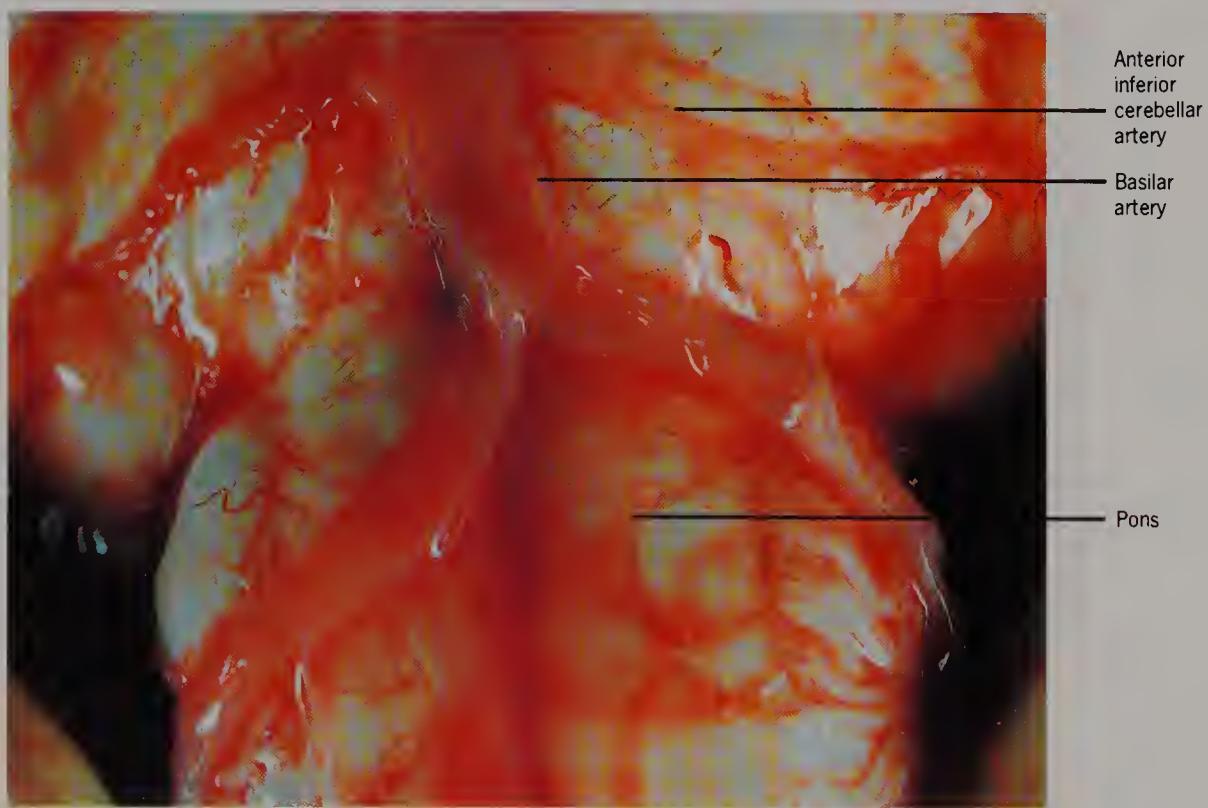


Figure 6 Ventral view of the pons, showing two vertebral arteries joining to become the basilar artery, which leads to the circle of Willis ($\times 3.5$).

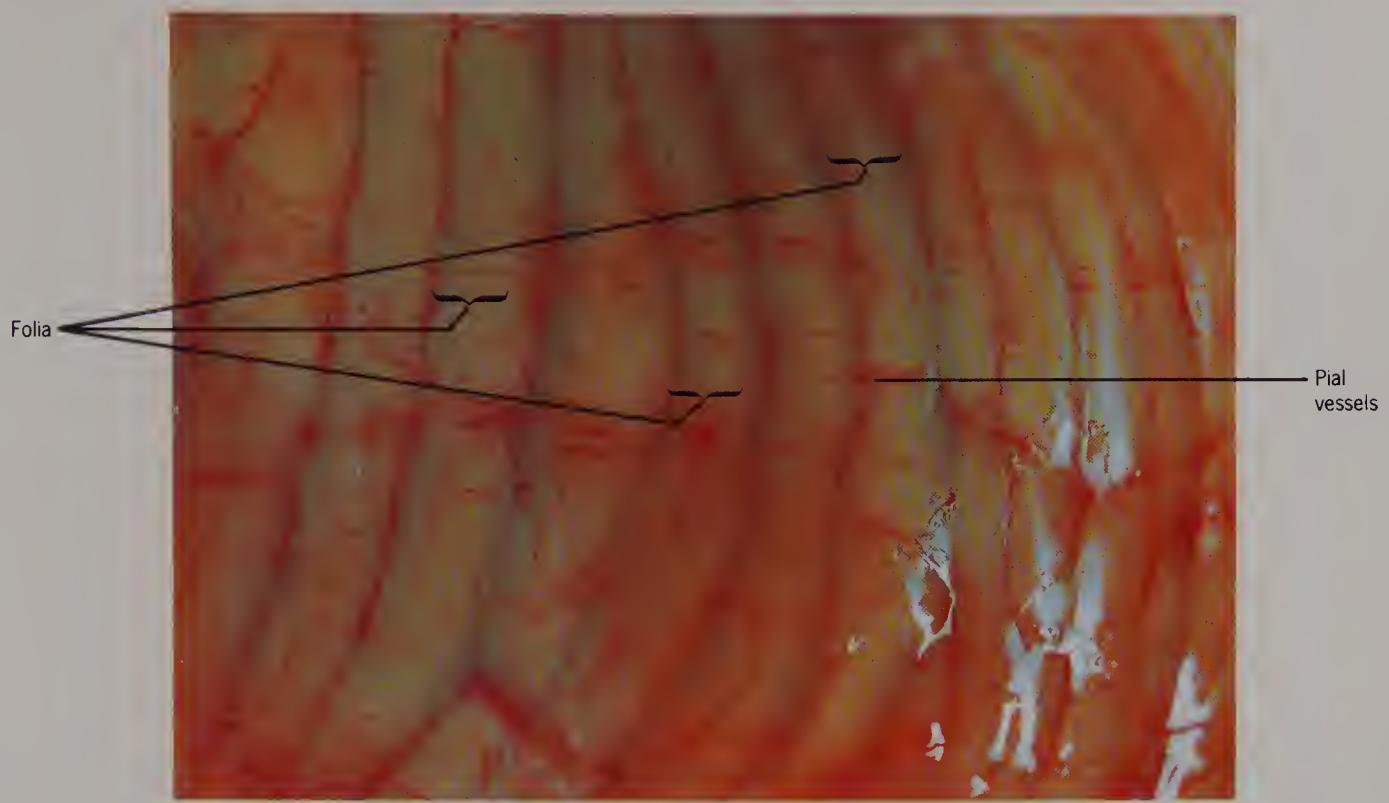


Figure 7 The cerebellum to show the folia and the pial blood vessels ($\times 3.5$).

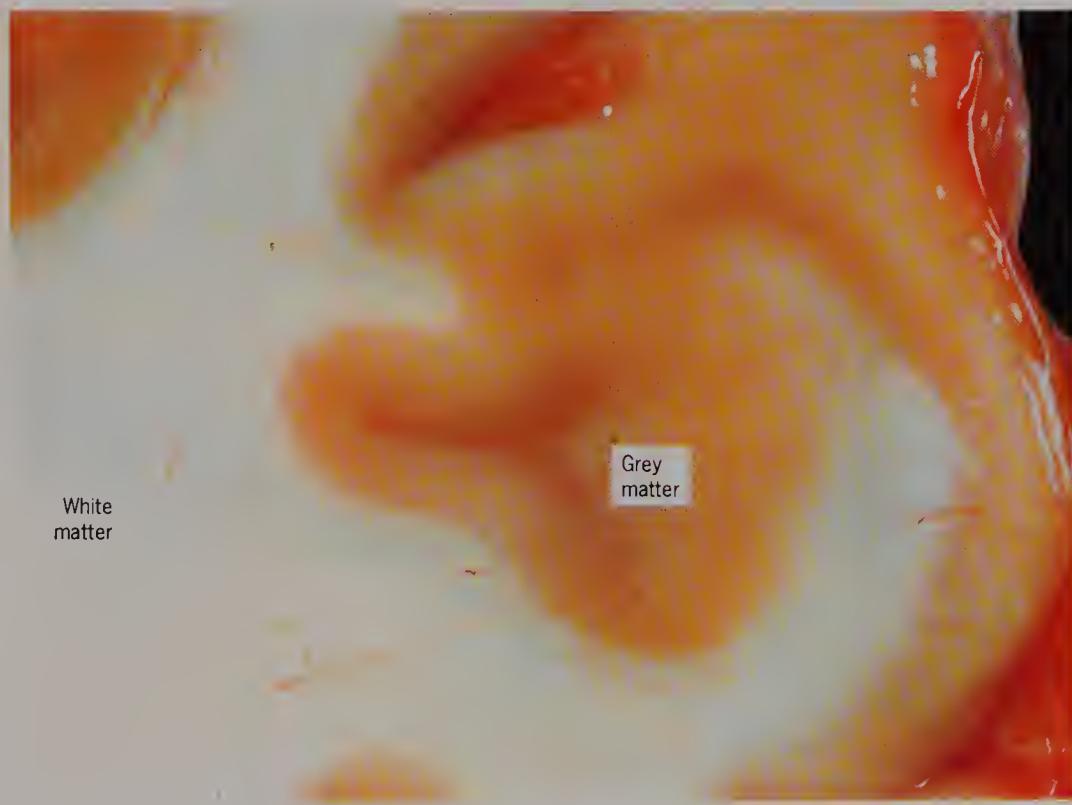


Figure 8 The frontal lobe, showing the white and grey matter, whose colour is light brown in the unfixed state ($\times 3.5$).

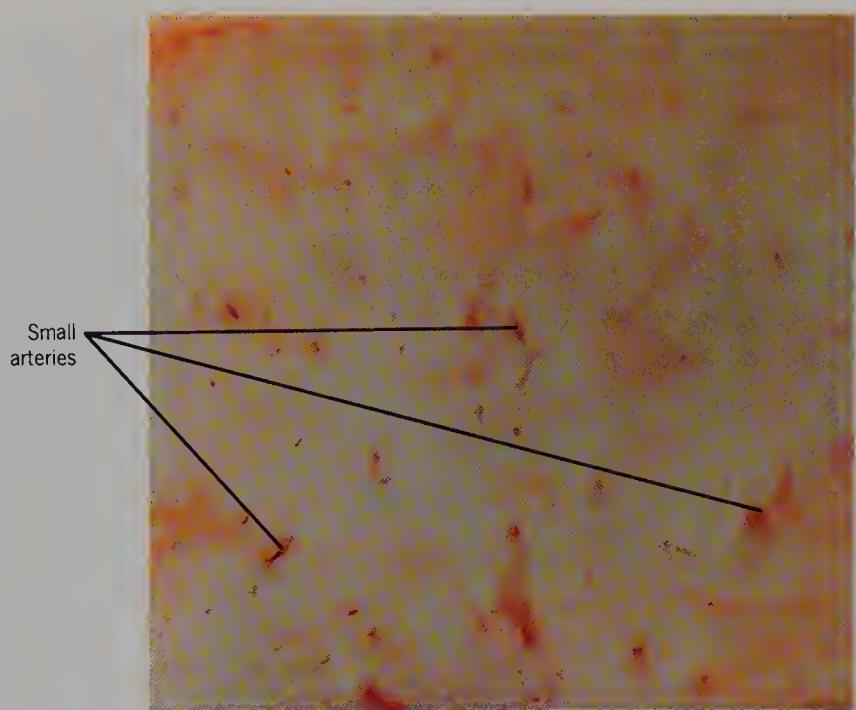


Figure 9 The white matter of the insula to show the distribution of small arteries ($\times 3.5$).

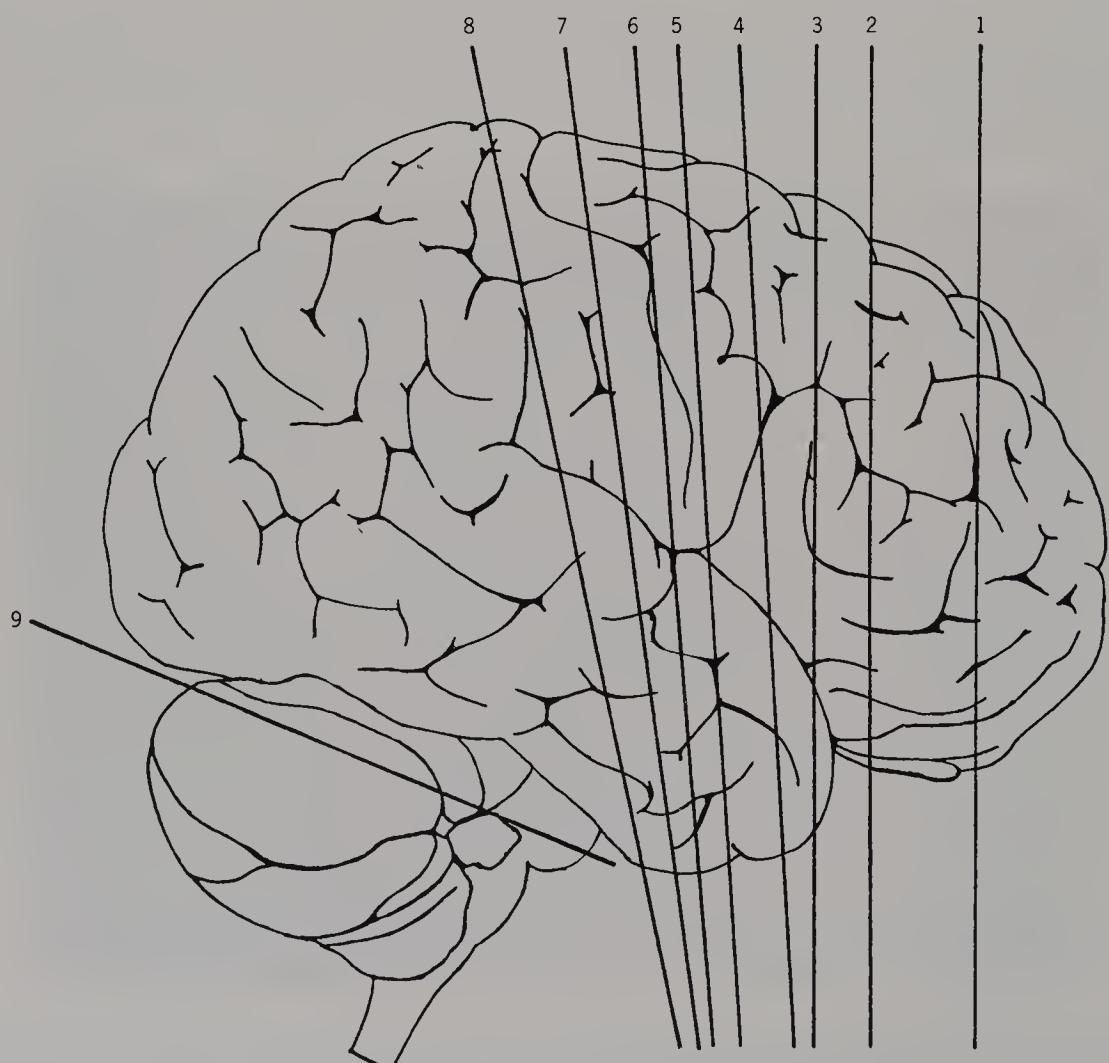


Figure 10 Diagram to show the planes of the subsequent brain sections (sections 1–9).

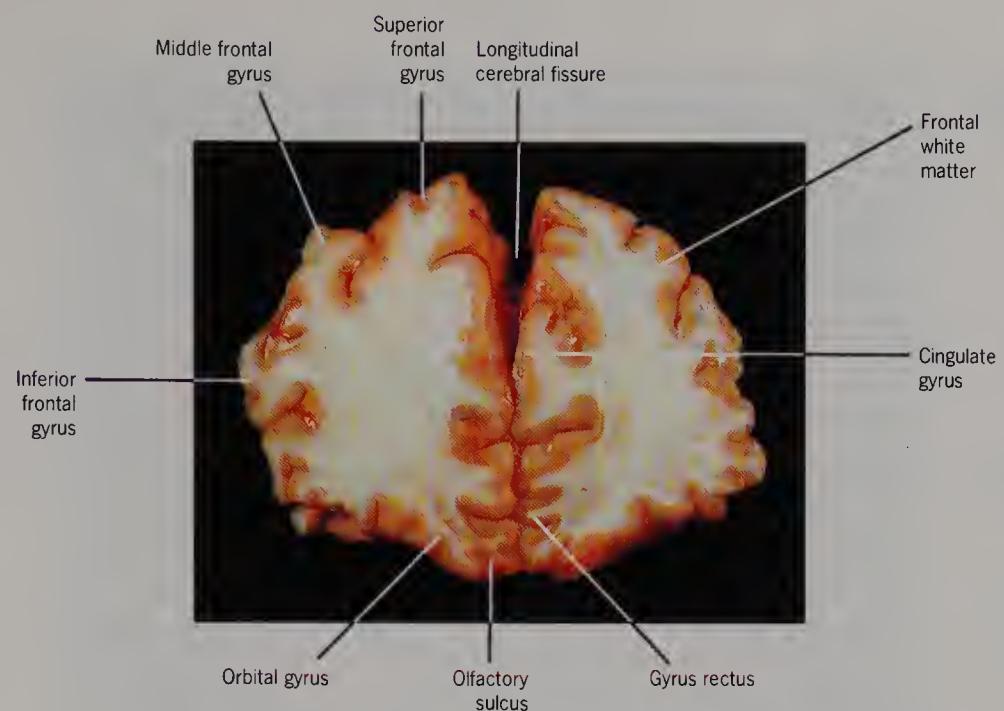


Figure 11 Section 1, through the anterior part of the frontal lobe ($\times 0.5$).

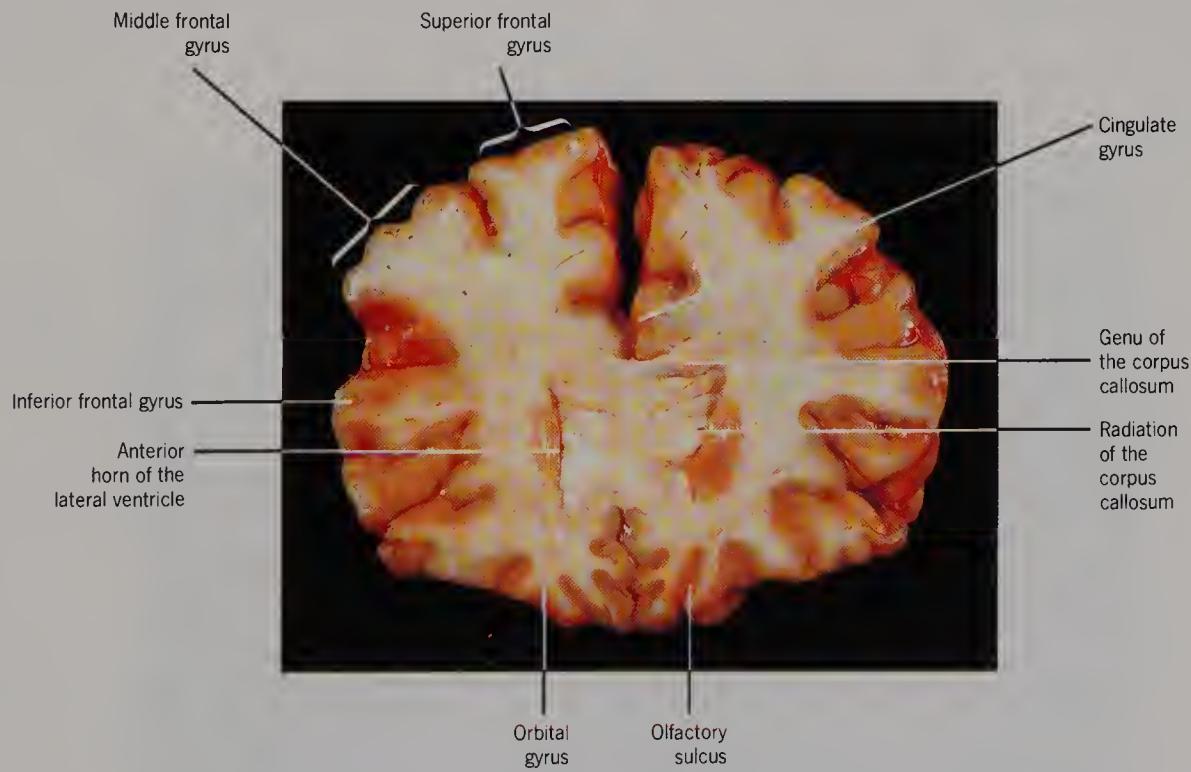


Figure 12 Section 2, through the frontal lobe to show the genu of the corpus callosum and the anterior horns of the lateral ventricle ($\times 0.5$).

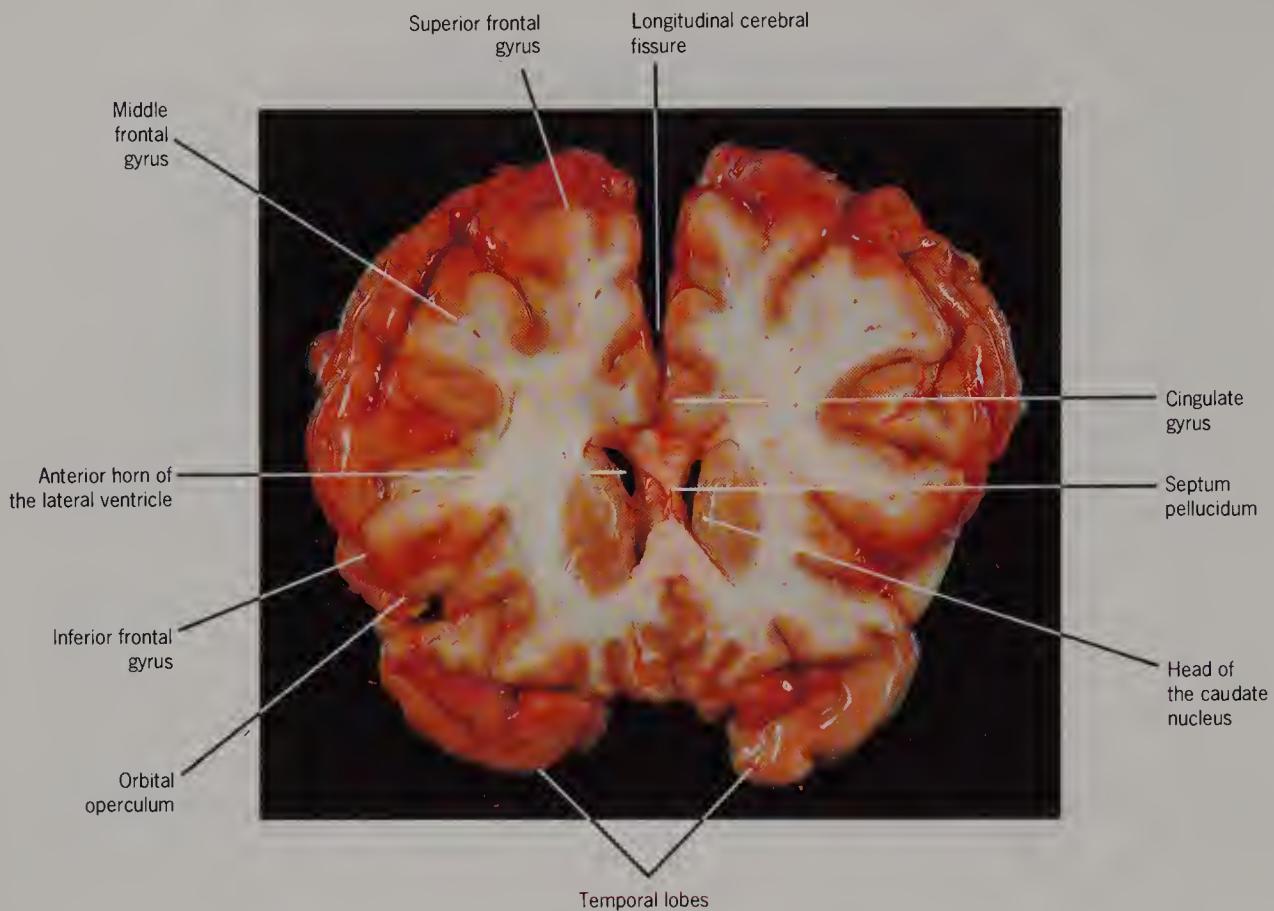


Figure 13 Section 3, through the frontal lobe and the head of the caudate nucleus. The temporal lobes can be seen below ($\times 0.5$).

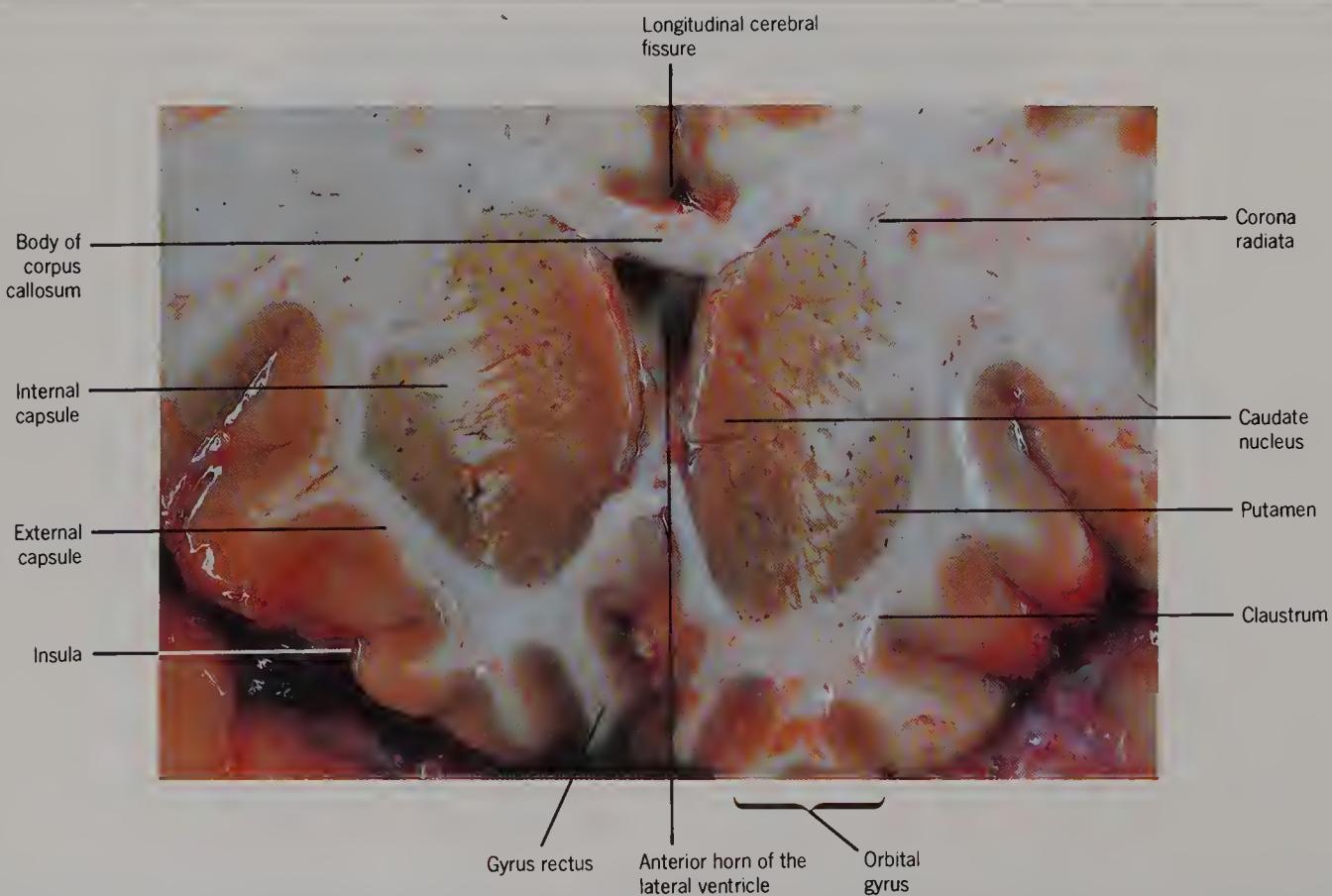


Figure 14 Section through the caudate nucleus, the internal capsule and the putamen ($\times 1.5$).

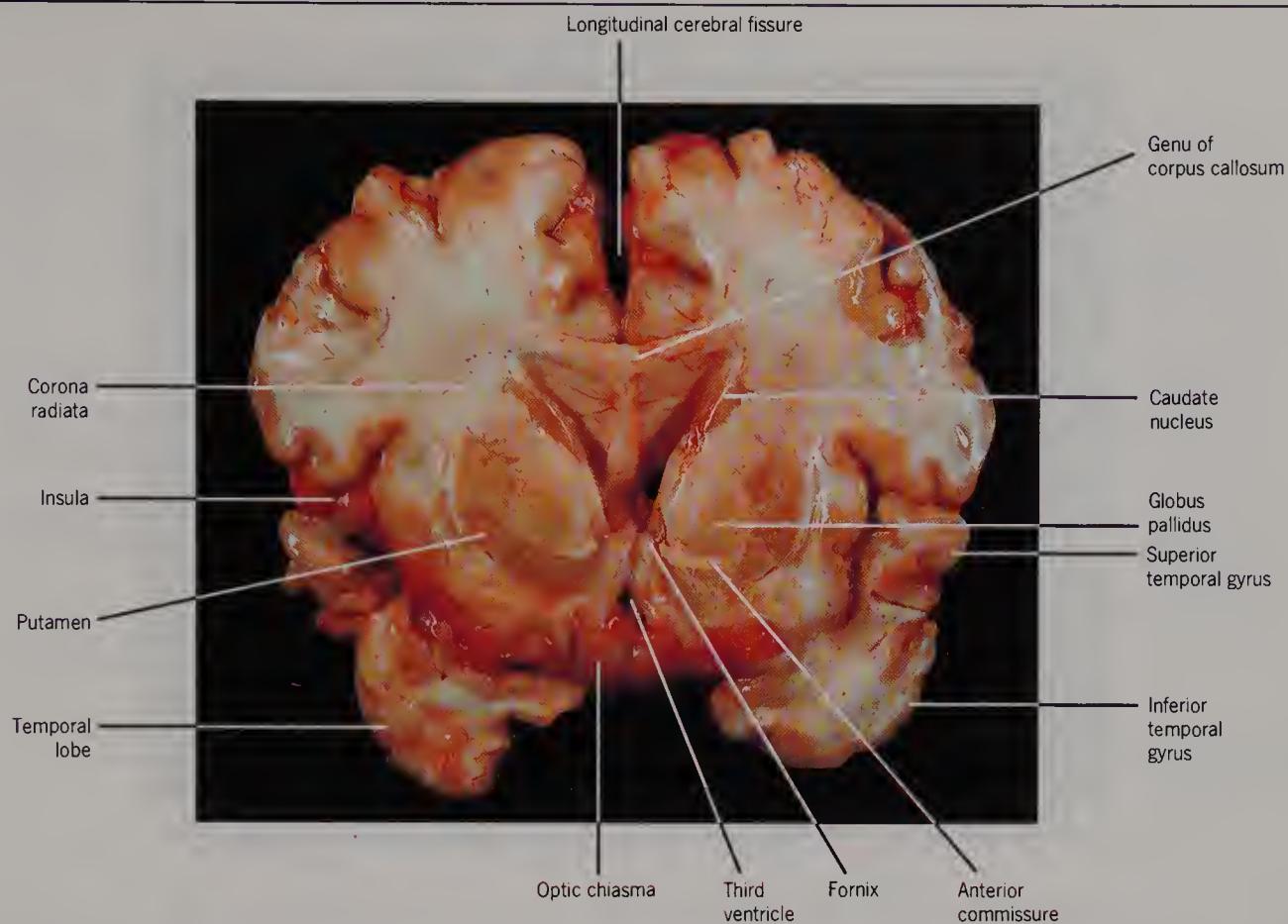


Figure 15 Section 4, through the frontal and temporal lobes, the globus pallidus and the third ventricle ($\times 0.5$).

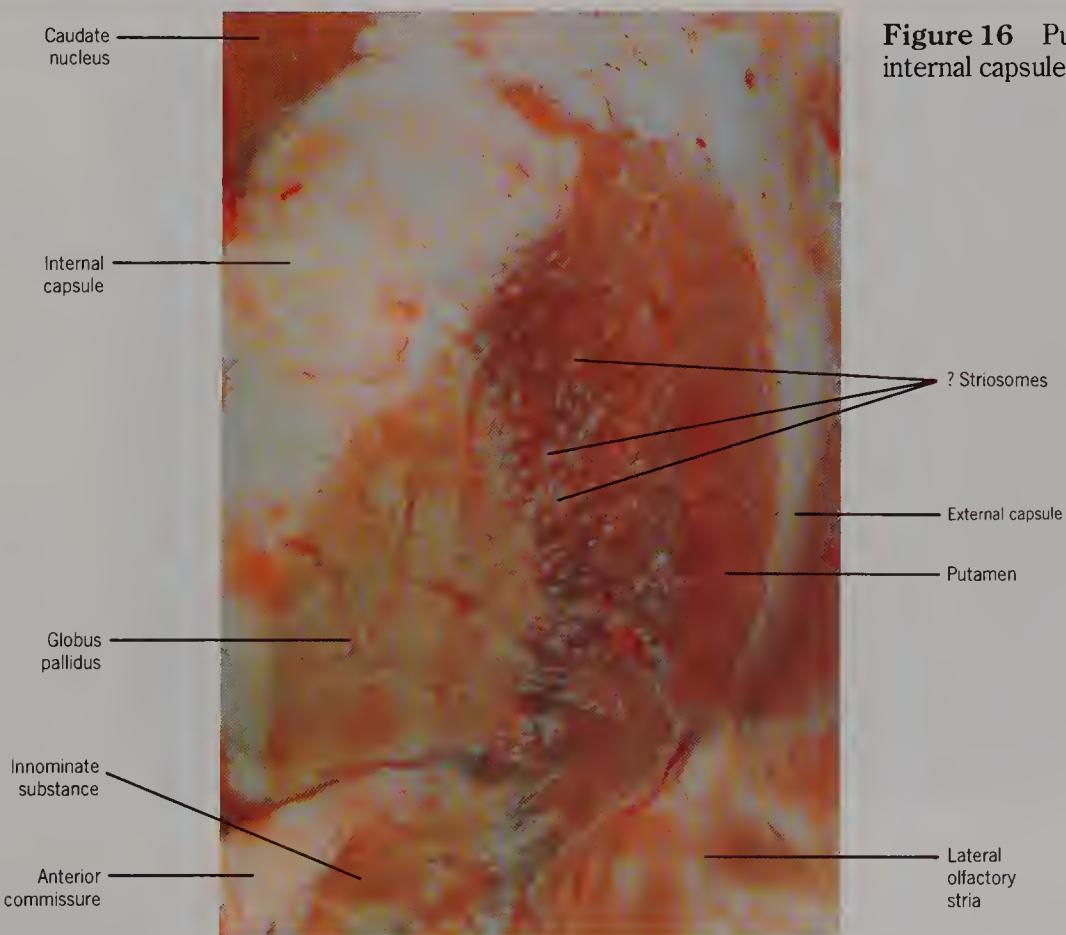


Figure 16 Putamen, globus pallidus and internal capsule ($\times 2.75$).

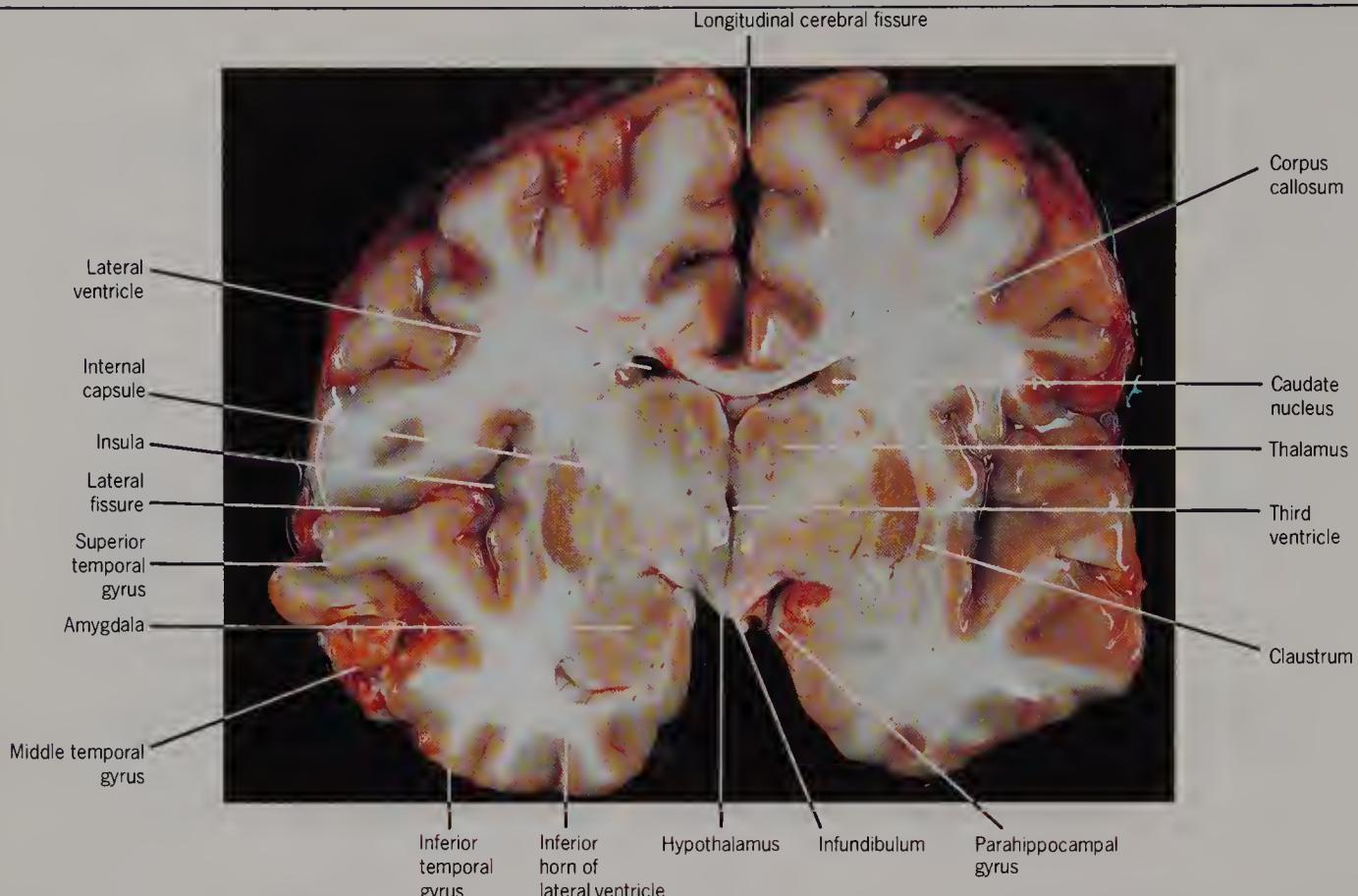


Figure 17 Section 5, through the parietal and temporal lobes, showing the thalamus, the third ventricle and the infundibulum ($\times 0.5$).

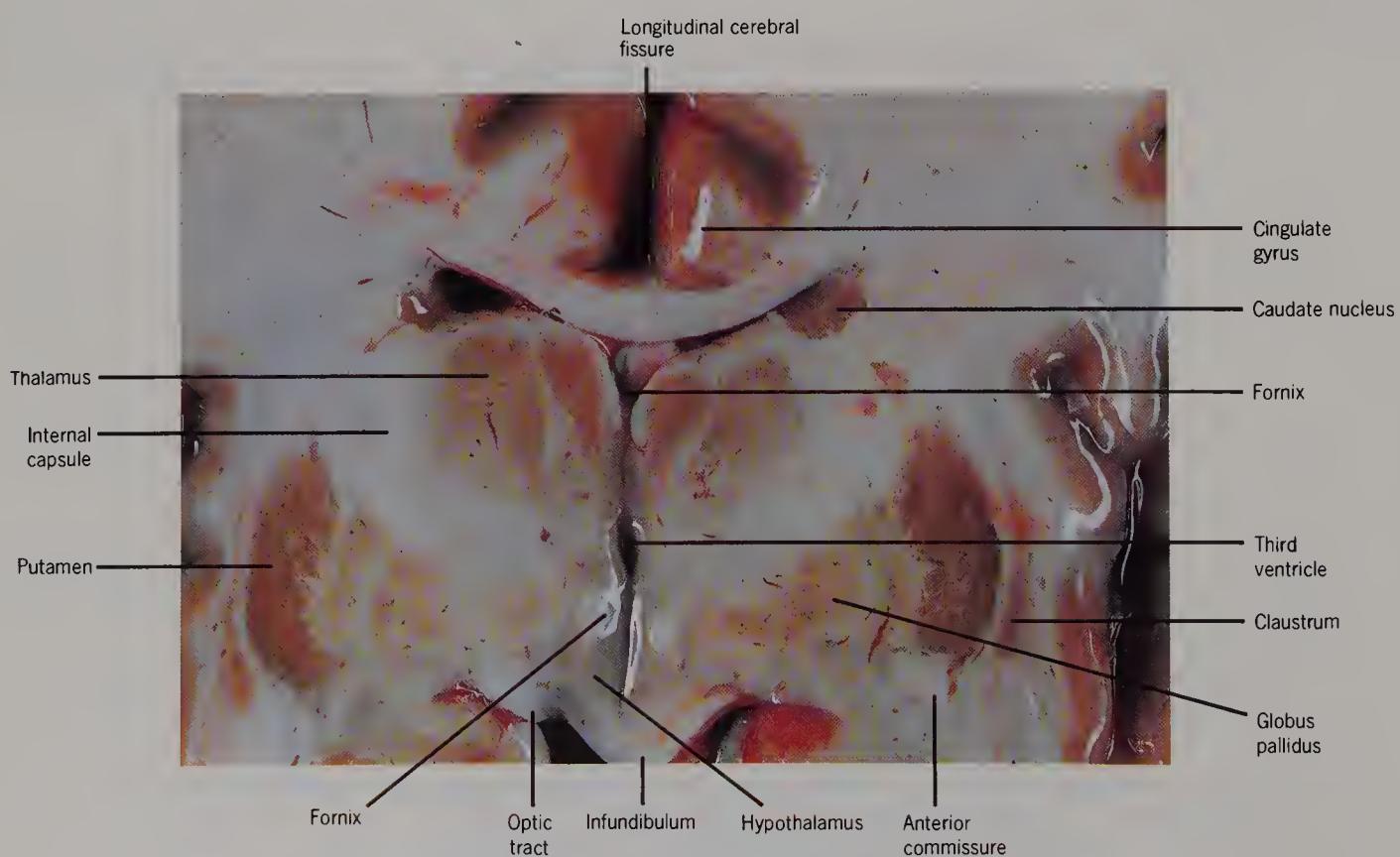


Figure 18 Close-up of the previous section ($\times 1.5$).

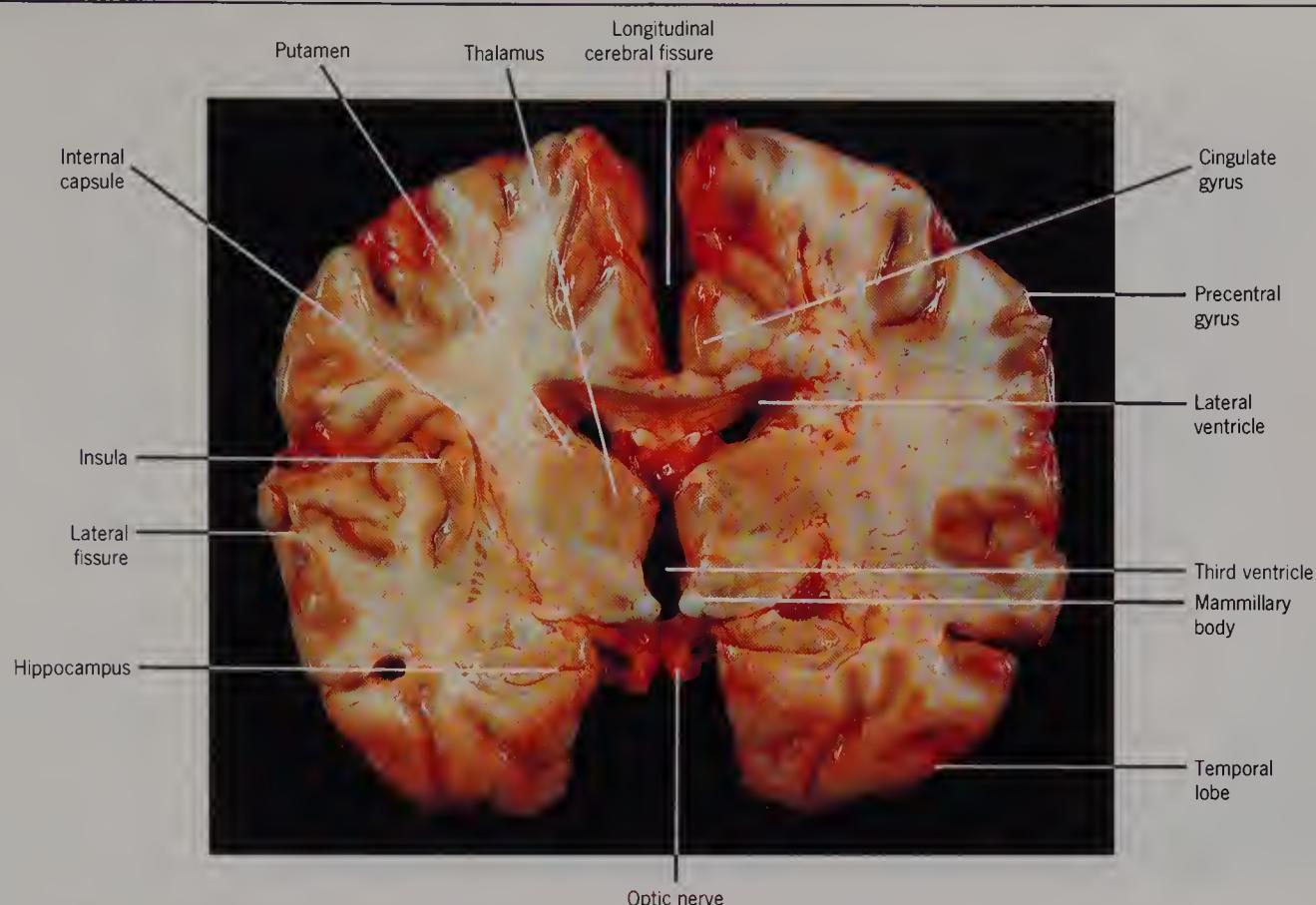


Figure 19 Section 6 through the parietal and temporal lobes to show the hippocampus, the third ventricle and the mammillary bodies ($\times 0.5$).

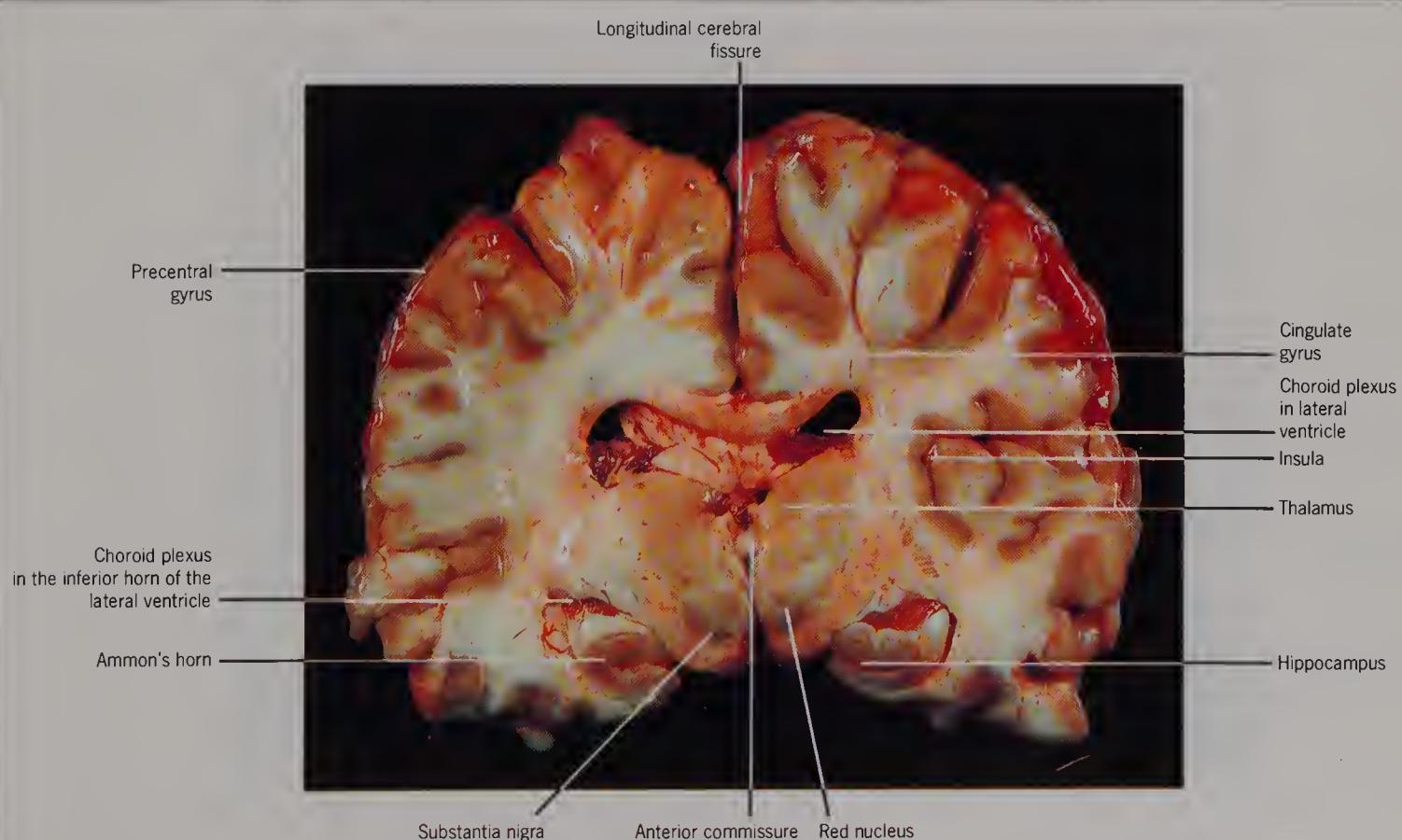


Figure 20 Section 7, through the parietal and temporal lobes to show the substantia nigra, the hippocampus and the red nucleus ($\times 0.5$).

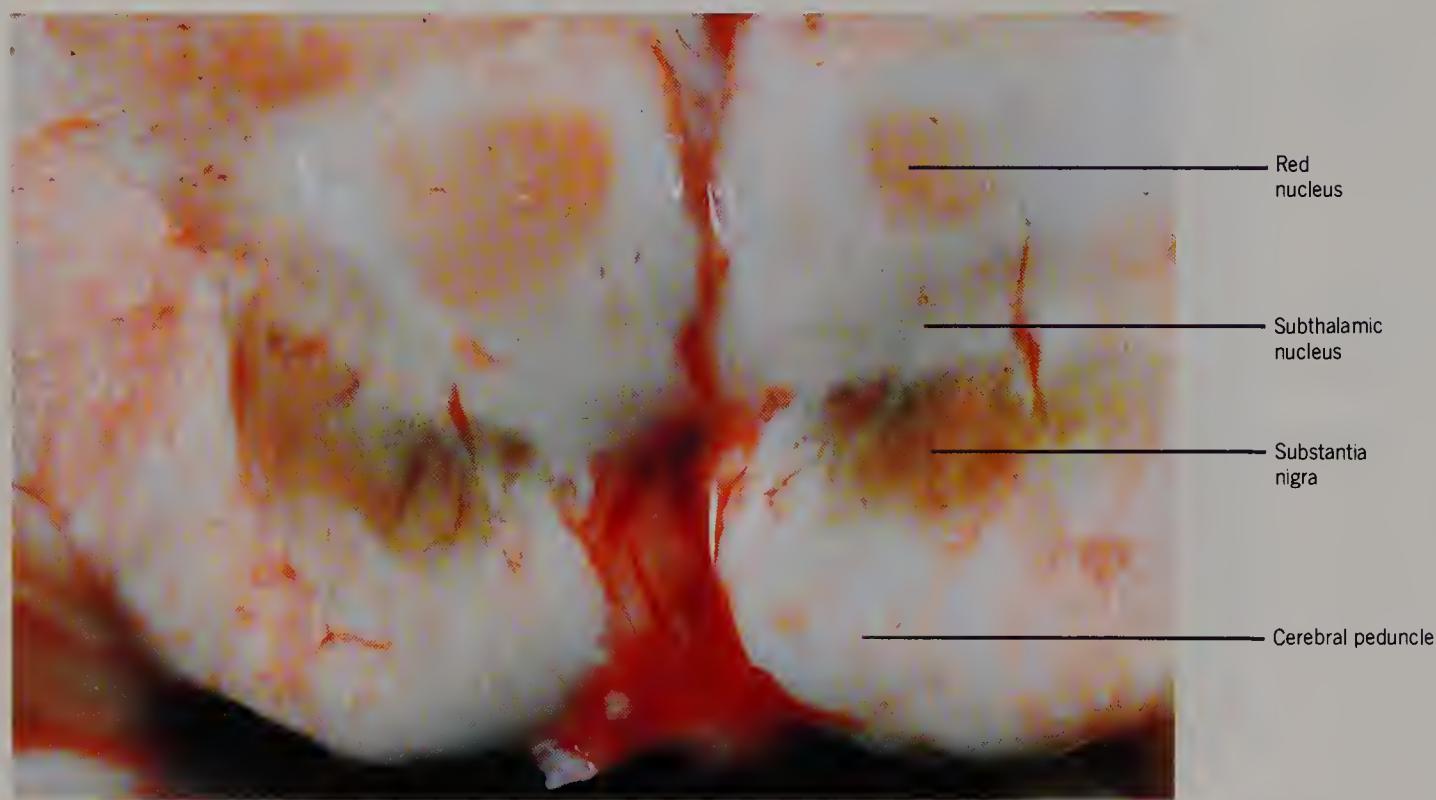


Figure 21 Close-up of the previous figure ($\times 3.5$).

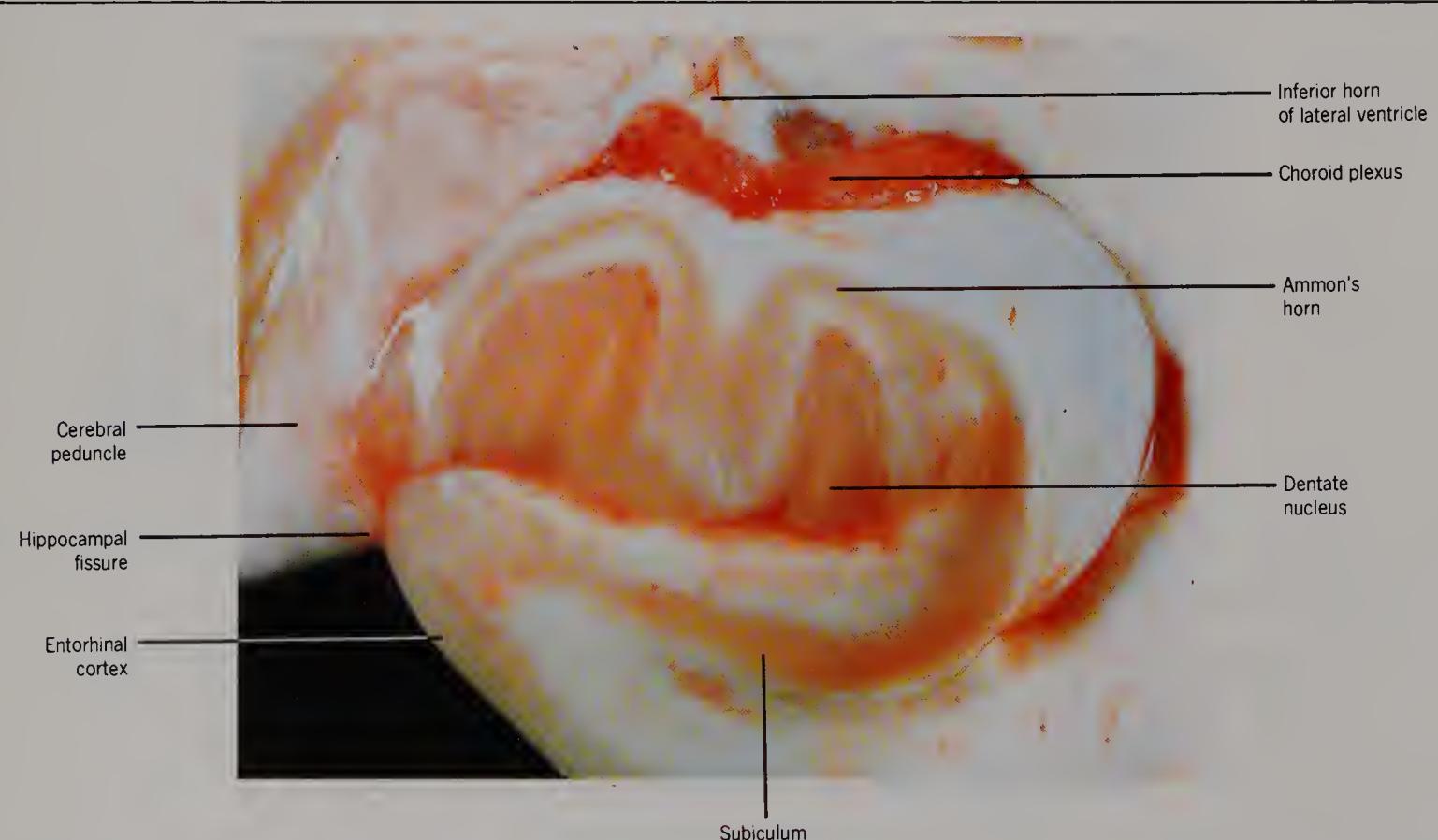


Figure 22 The hippocampus and the choroid plexus ($\times 3.5$).

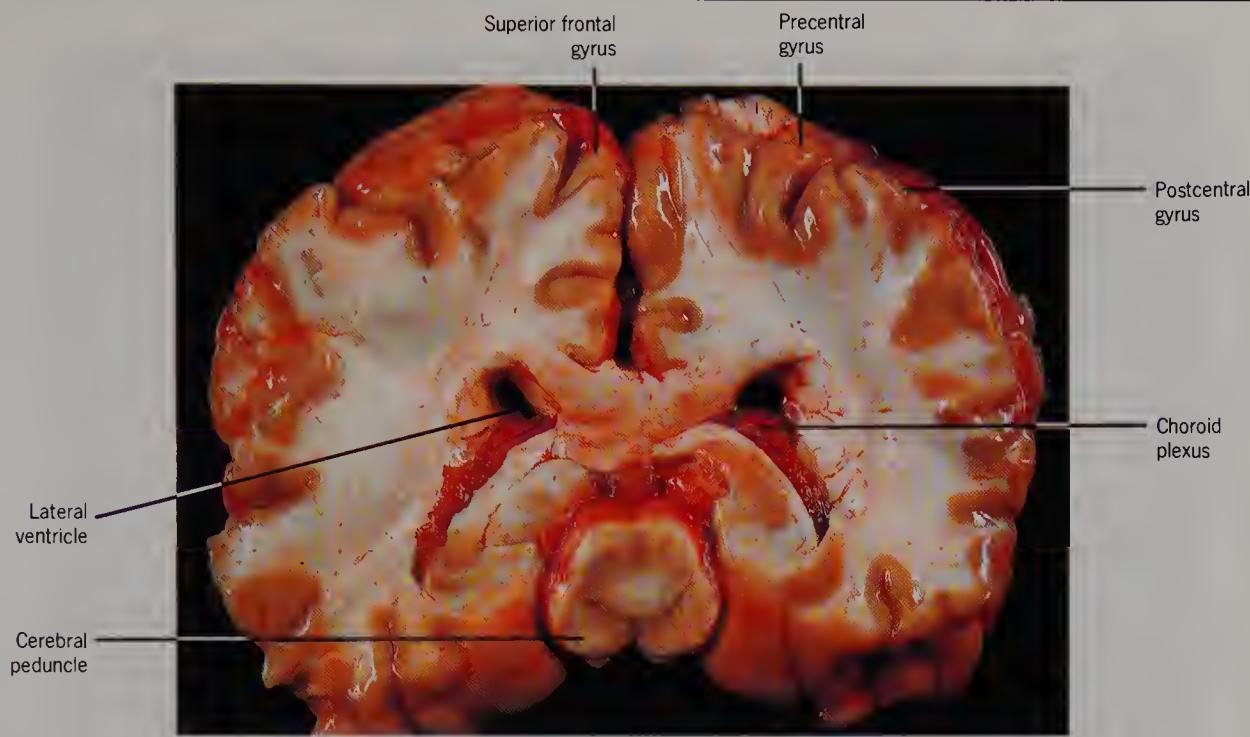


Figure 23 Section 8, through the parietal and temporal lobes, to show the pineal gland, the midbrain and the pons ($\times 0.5$).



Figure 24 The midbrain and the cerebral peduncles ($\times 2.75$).

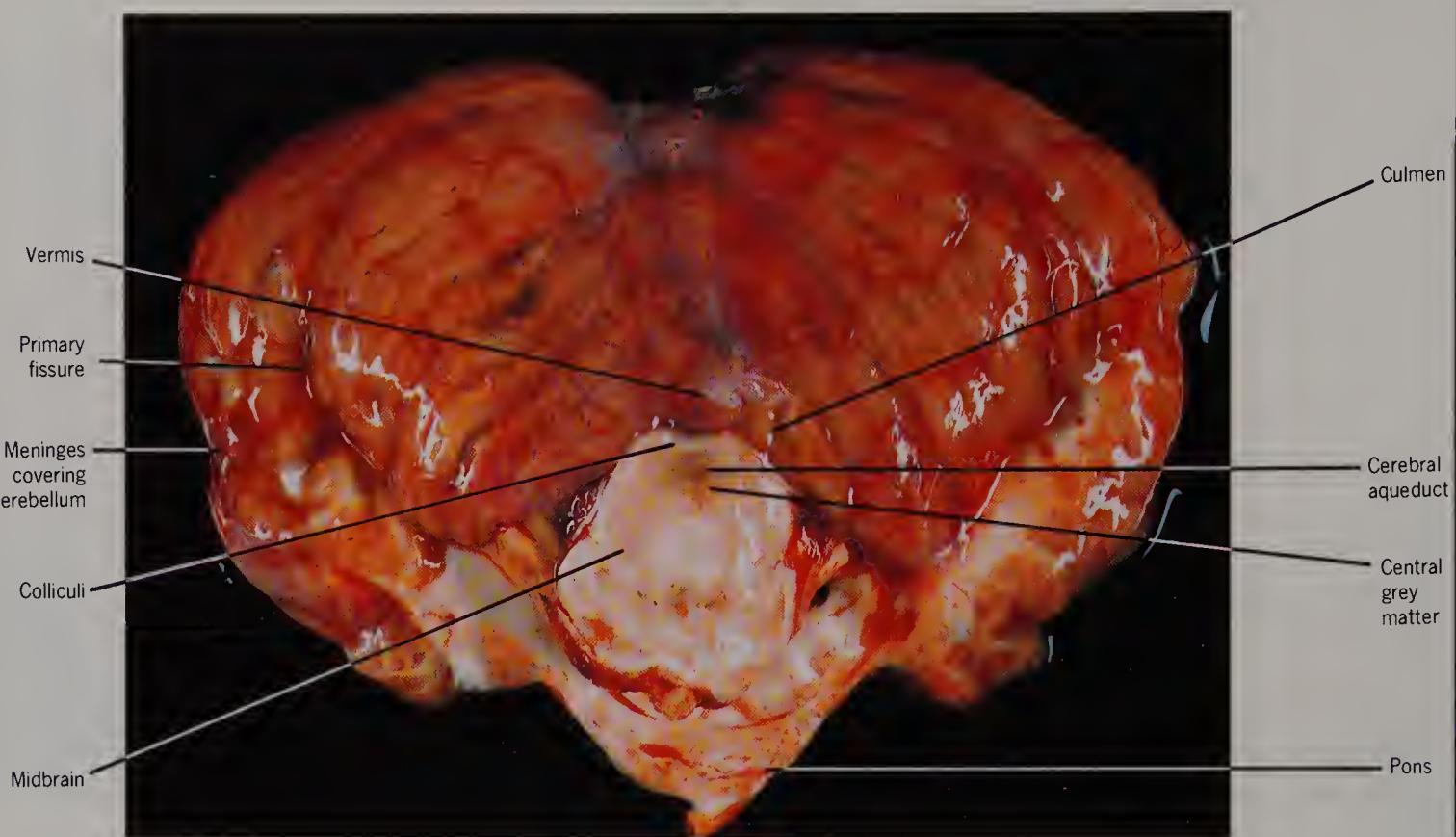


Figure 25 View of the cerebellum and the midbrain from the anterior aspect ($\times 0.75$).

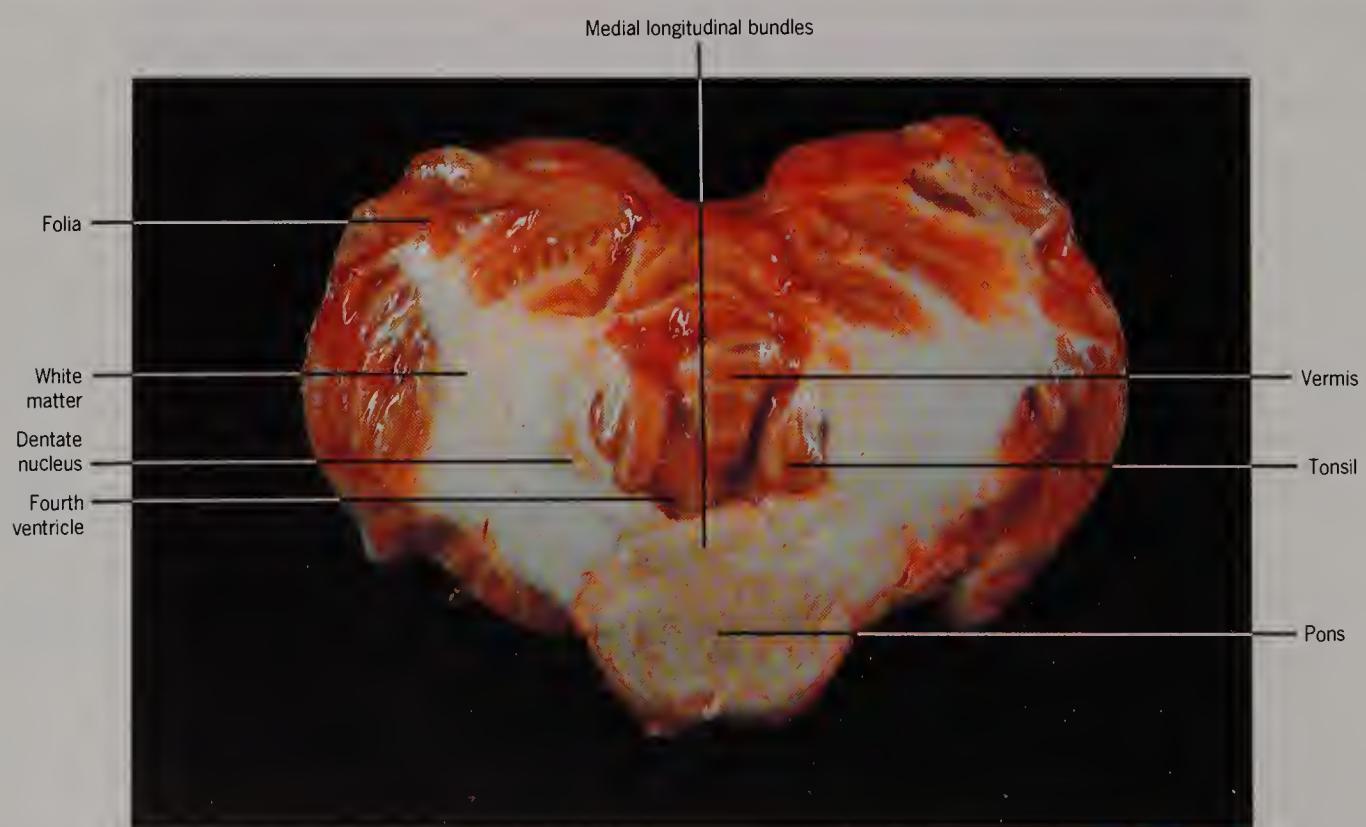


Figure 26 Section 9, through the cerebellum and medulla ($\times 0.5$).

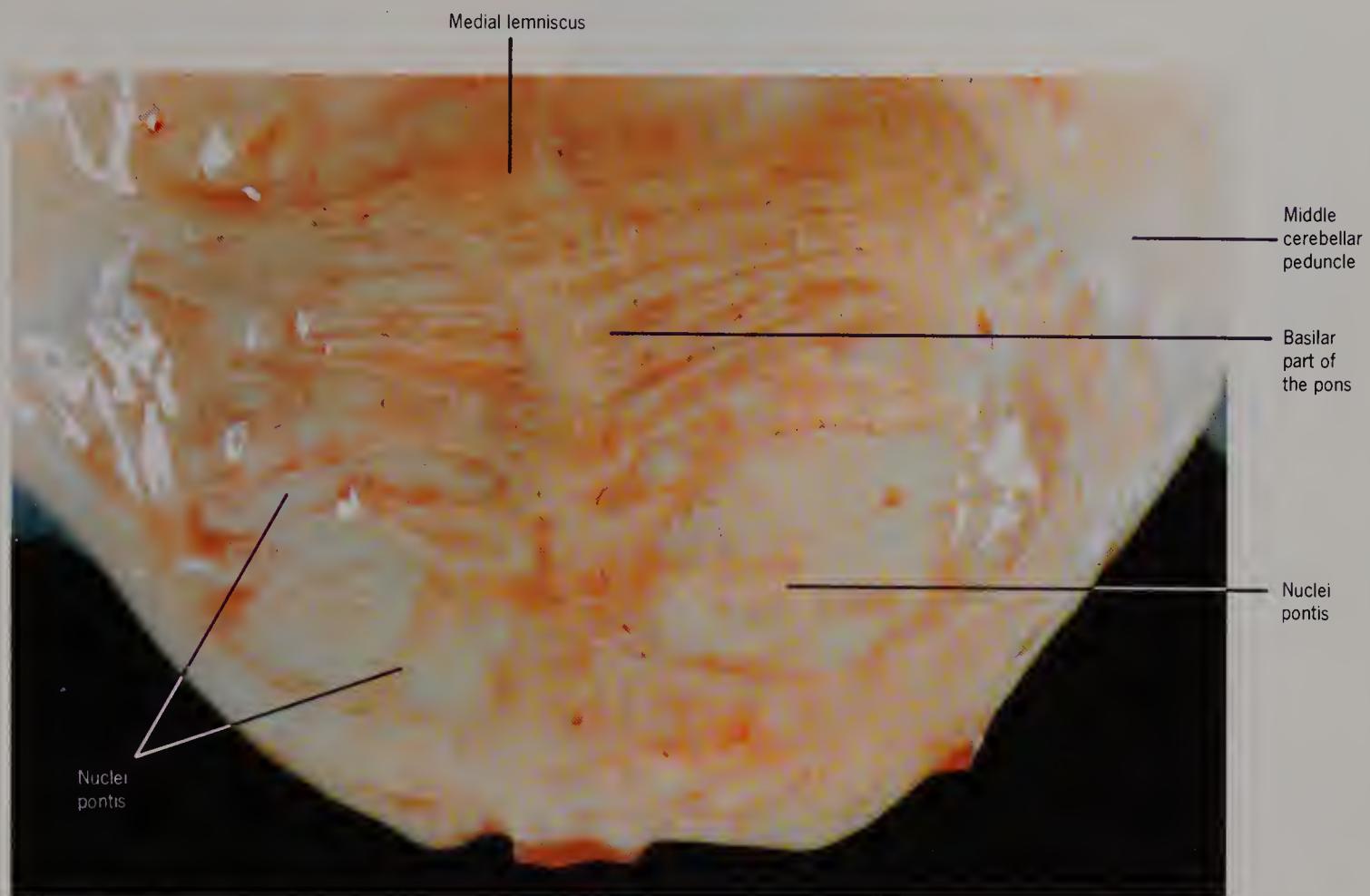


Figure 27 Section through the pons ($\times 3$).

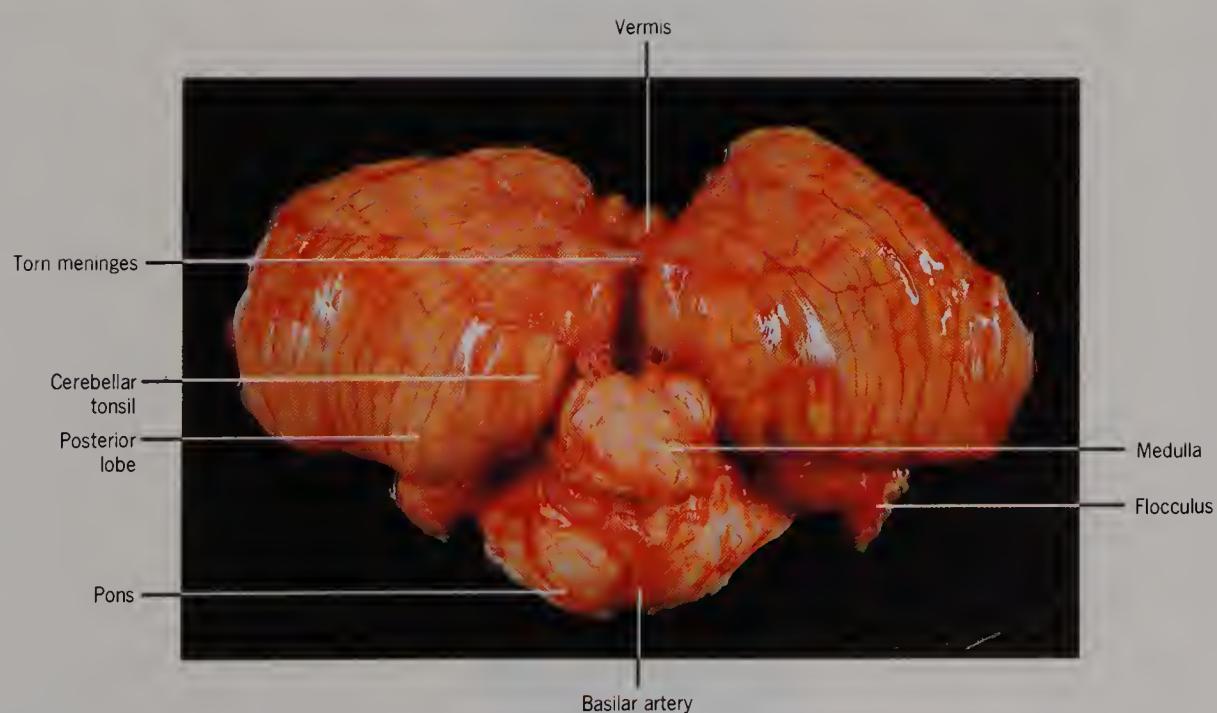


Figure 28 View of the cerebellum and the midbrain from the posterior aspect ($\times 0.5$).

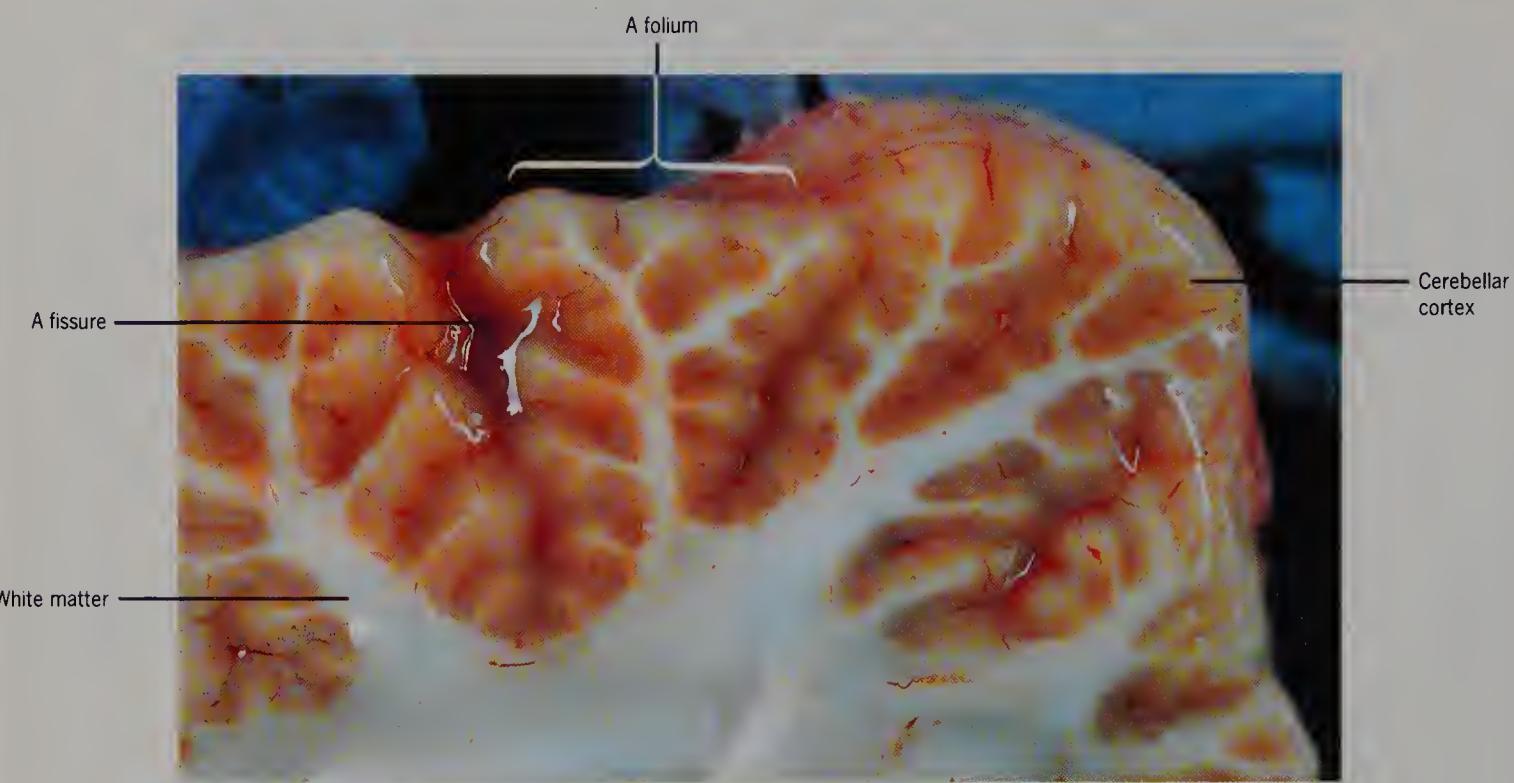


Figure 29 The arbor vitae appearance of a folium of the cerebellum ($\times 10$).

SECTION
2

MICROSCOPIC CONSTITUENT ELEMENTS



Figure 30 Isolated human hypoglossal neuron from a 62-year-old female, to show the dendritic tree (phase contrast, $\times 375$).

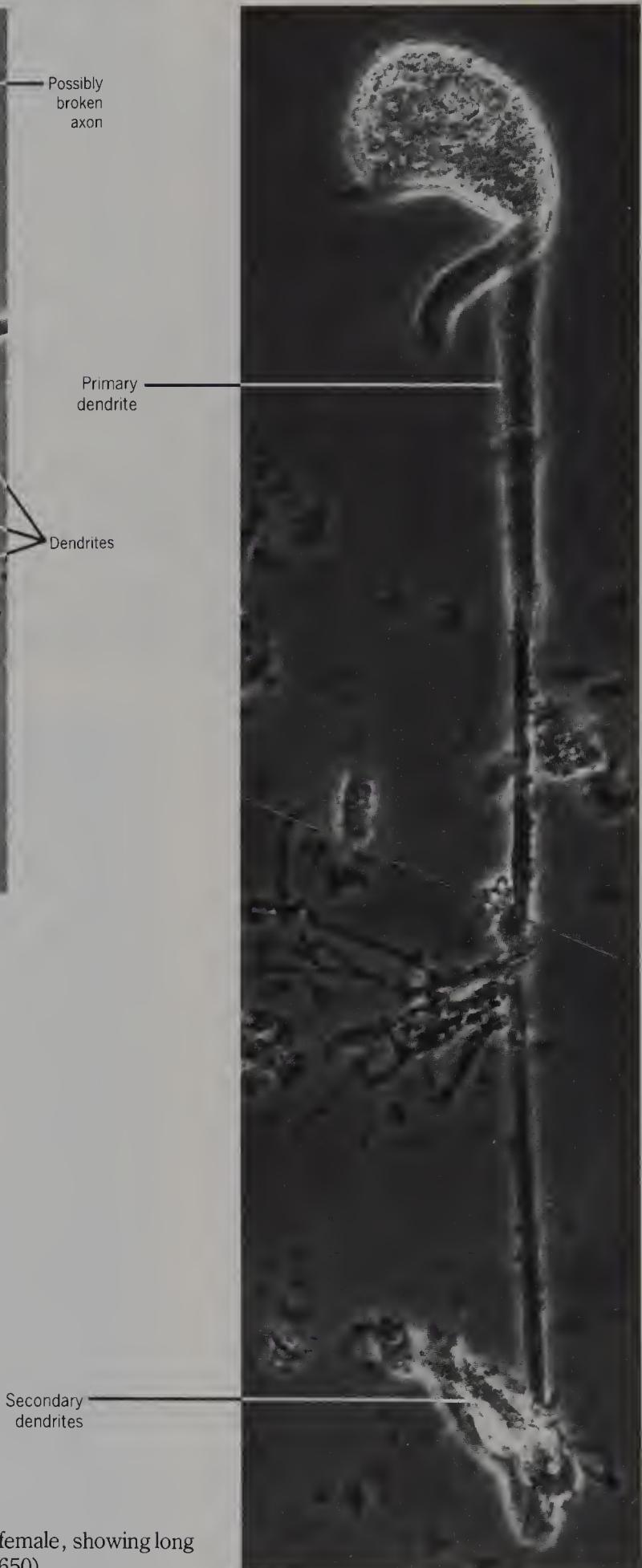


Figure 31 Isolated human Purkinje cell from a 46-year-old female, showing long primary and branched secondary dendrites (phase contrast, $\times 650$).

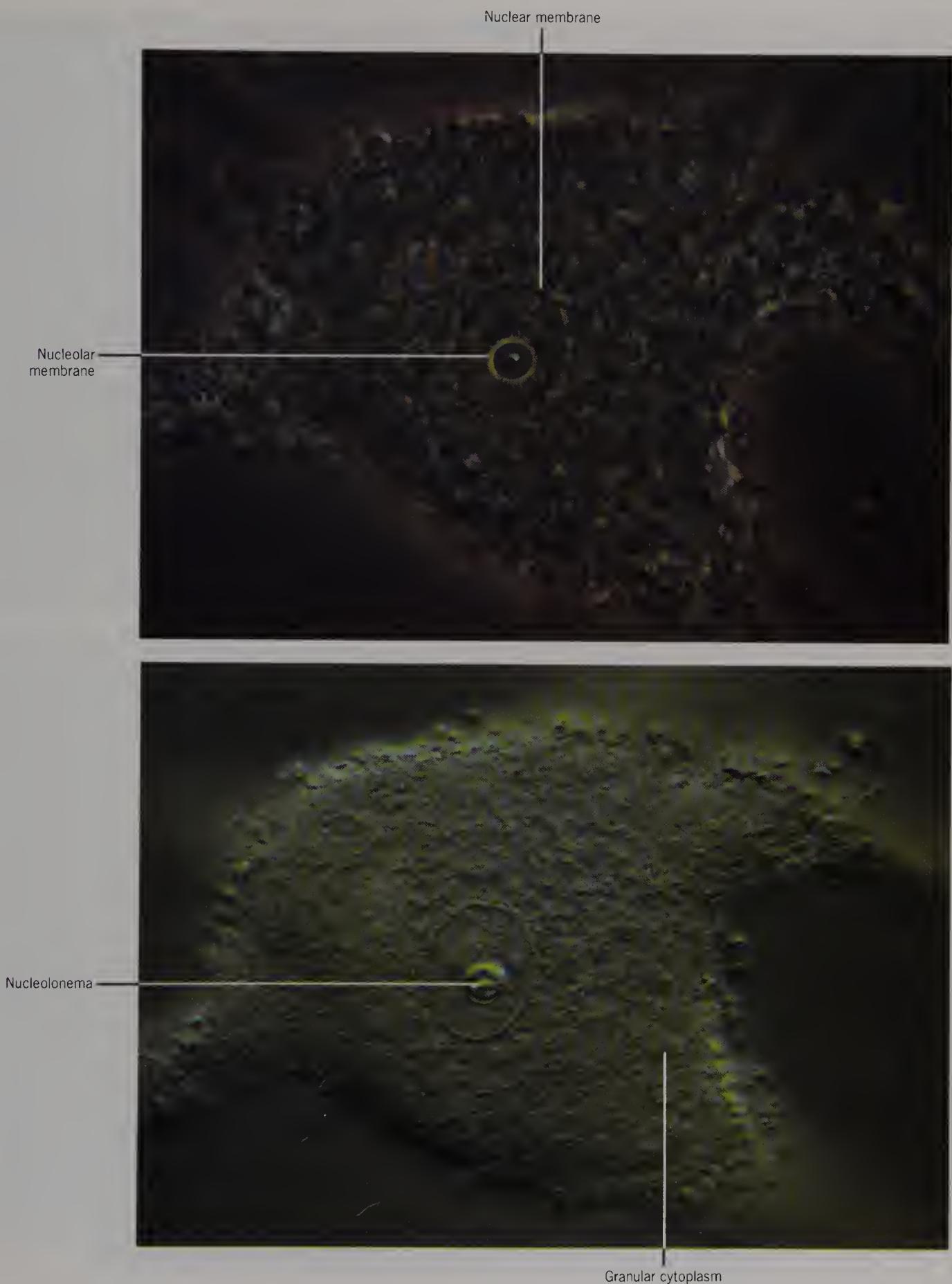


Figure 32 Isolated rabbit neuron from the lateral vestibular nucleus to show nuclear and nucleolar membranes, by phase contrast (above) and by differential interference contrast microscopy (below) ($\times 750$). (These photographs were kindly taken by Mr M. I. Walker, of Stafford, using flash illumination.)

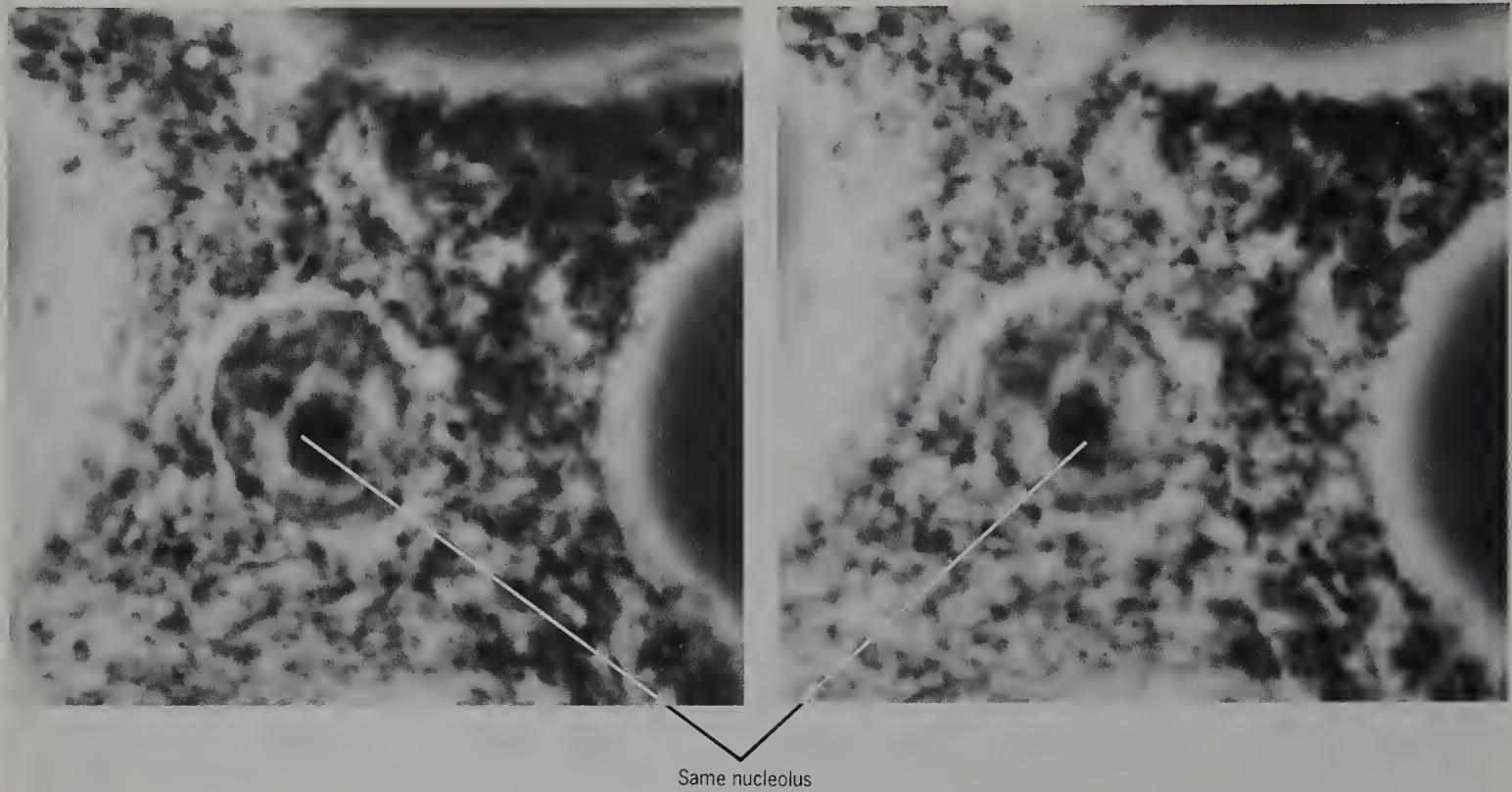


Figure 33 Isolated rabbit lateral vestibular neuron photographed twice with an interval of 20 minutes, to show nucleolar and cytoplasmic movements (phase contrast, $\times 2000$).

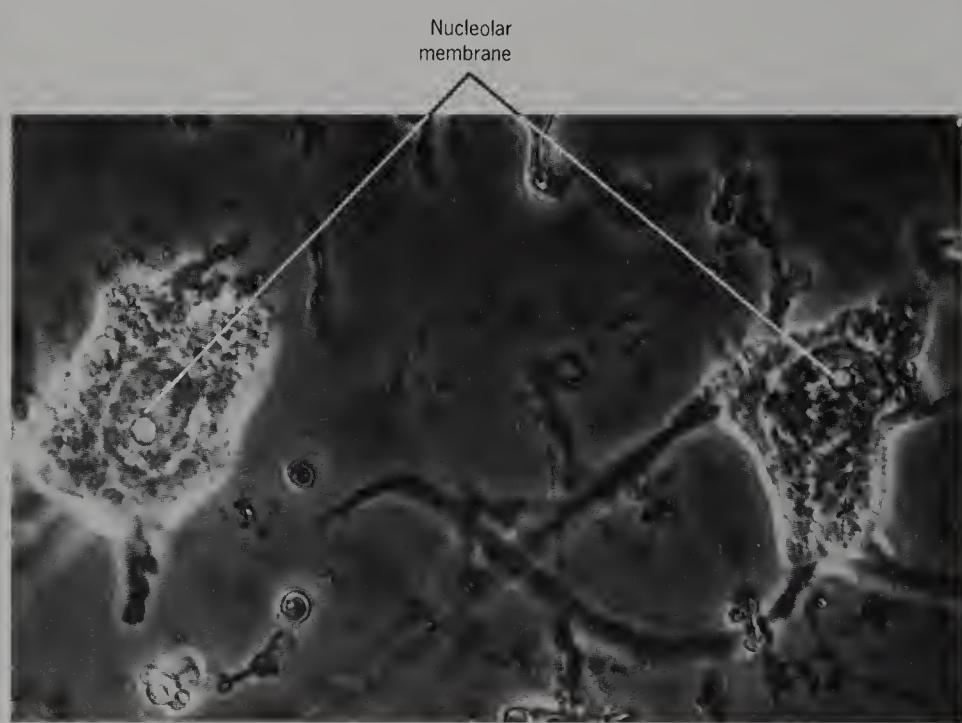


Figure 34 Isolated human neurons from the arcuate nucleus of a 71-year-old male, to show the nucleolar membranes (phase contrast, $\times 800$).



Figure 35 Teased human substantia nigral neurons and neuroglia from an 82-year-old male, by phase contrast (above) and stained with anti-neurofilament antibody (below) ($\times 500$).

Note the fluorescence throughout the neuron, but not of the fine granular material.



Figure 36 Isolated human ventral horn cell from the cervical spinal cord of a 75-year-old male, to show intracellular lipofuscin (phase contrast, $\times 800$).

Lipofuscin accumulates with age.

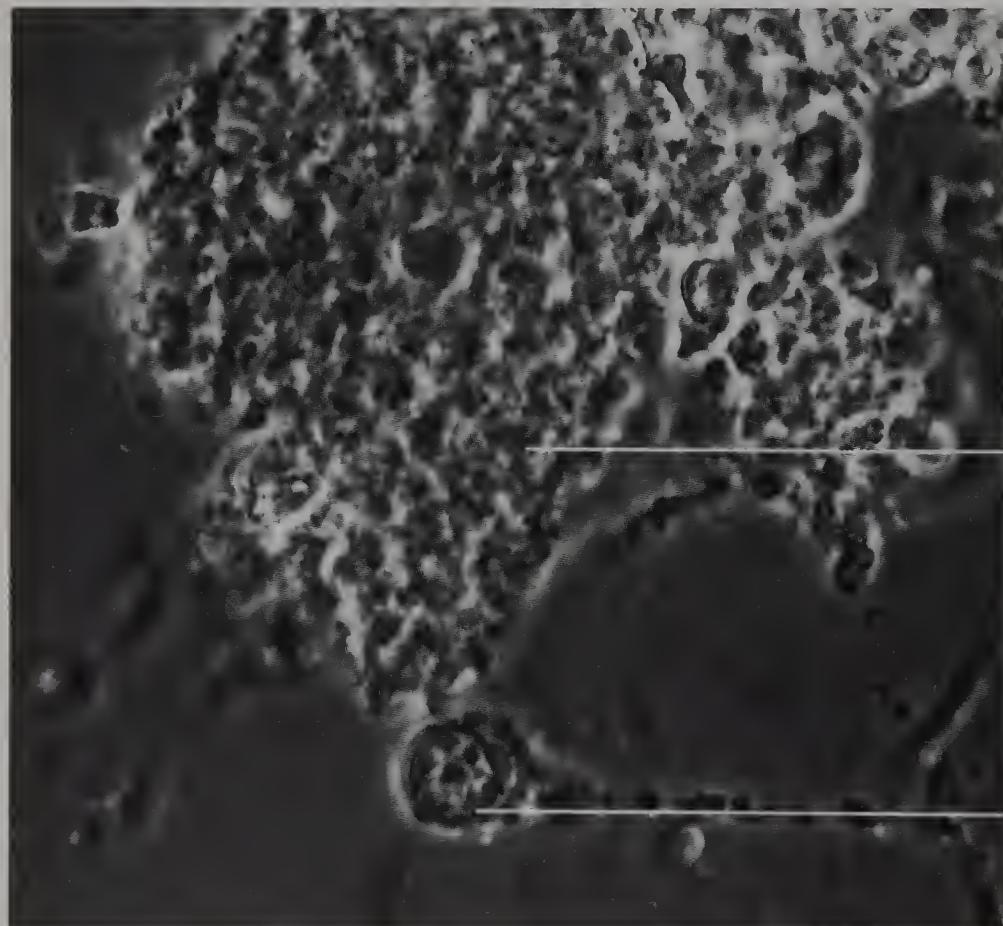


Figure 37 Isolated rat ventral horn cell from the cervical spinal cord, to show a neuroglial cell or a small neuron (phase contrast, $\times 800$).

Neuron

Small cell

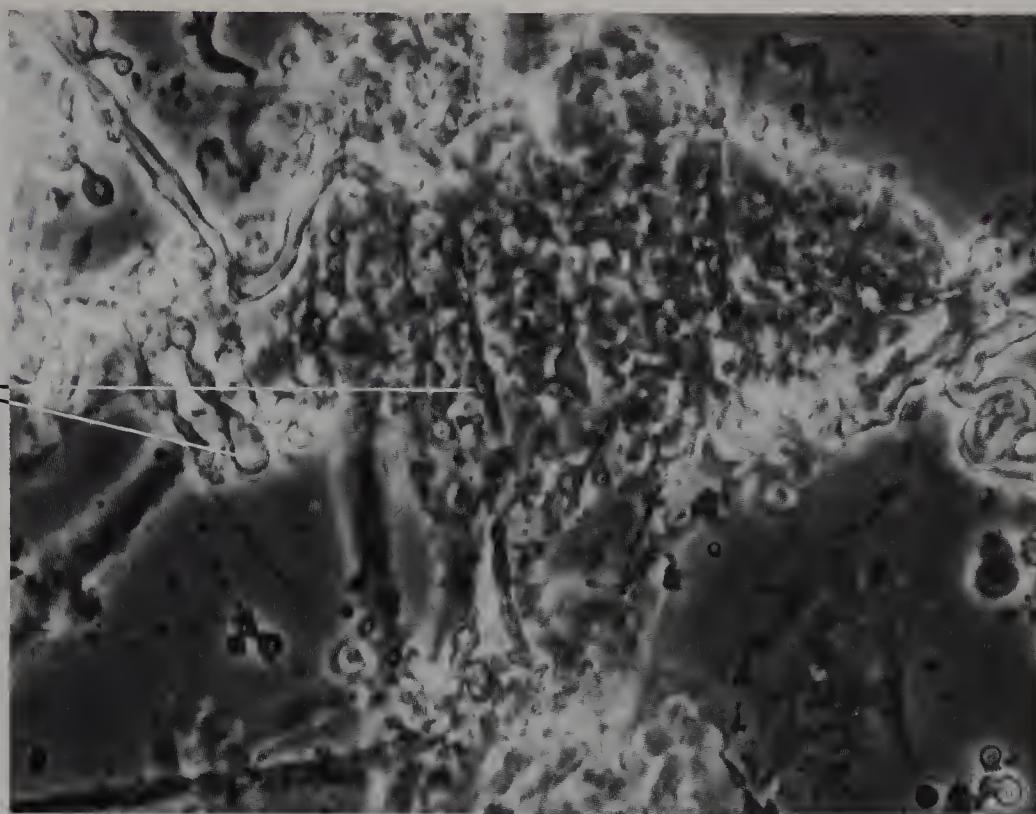


Figure 38 Isolated rabbit ventral horn cell from the cervical spinal cord focused on the somal surface to show adherent beaded fibres (phase contrast, $\times 650$).

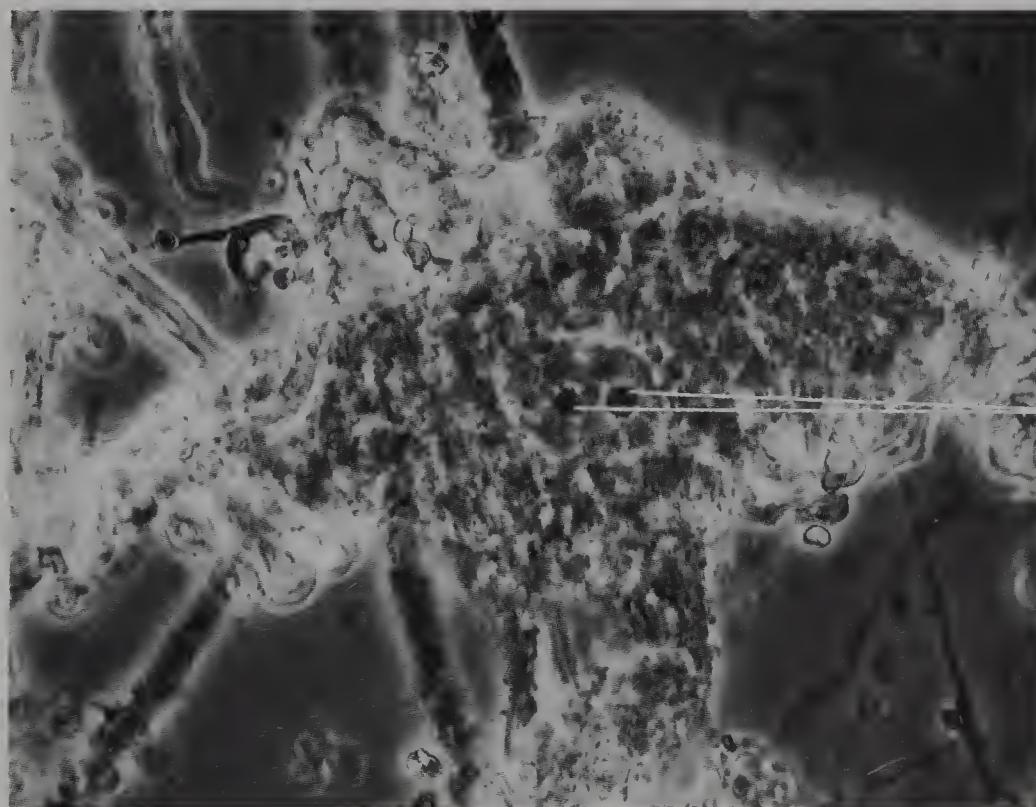


Figure 39 The same neuron as in the previous figure, but focused inside the cell to show the nucleus and paired nucleoli (phase contrast, $\times 650$).

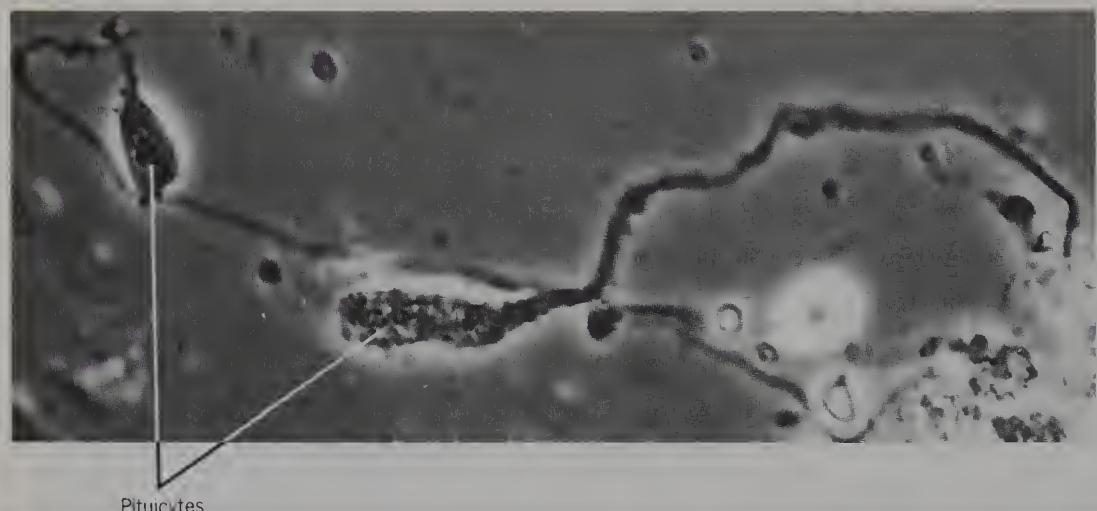


Figure 40 Isolated human pituicytes from a 54-year-old male (phase contrast, $\times 800$).

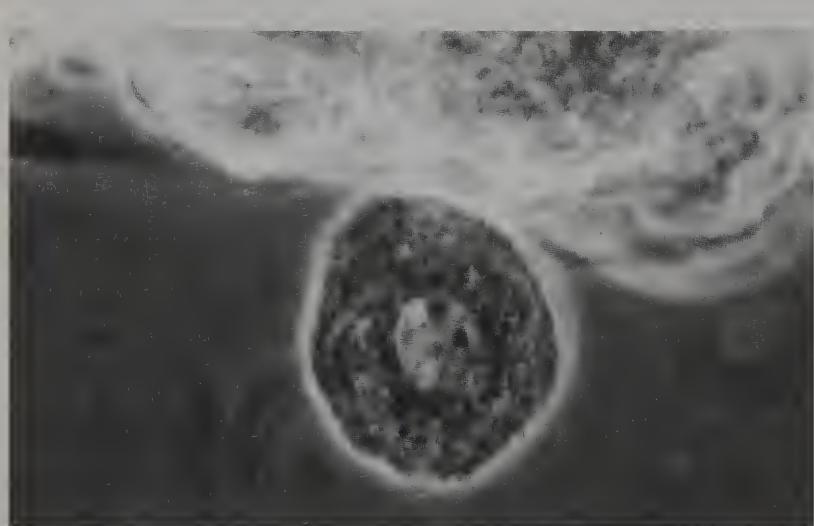


Figure 41 Isolated guinea-pig ganglion cell from the cervical spinal ganglion (phase contrast, $\times 800$).

There are multiple nucleoli in this and the next figure.

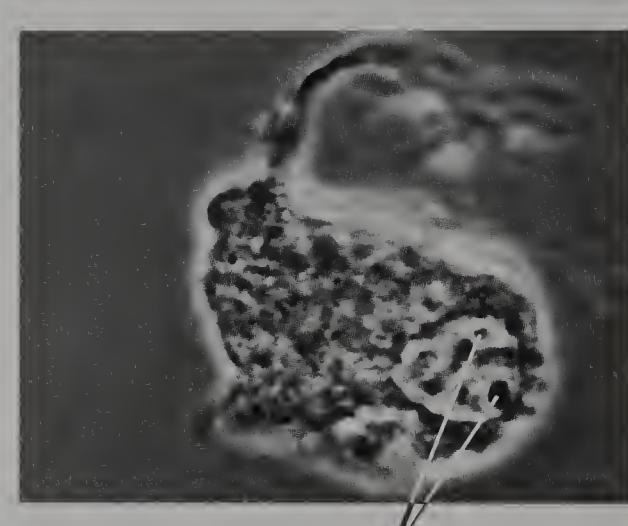


Figure 42 Isolated guinea-pig ganglion cell from the myenteric plexus of the colon (phase contrast, $\times 1300$).

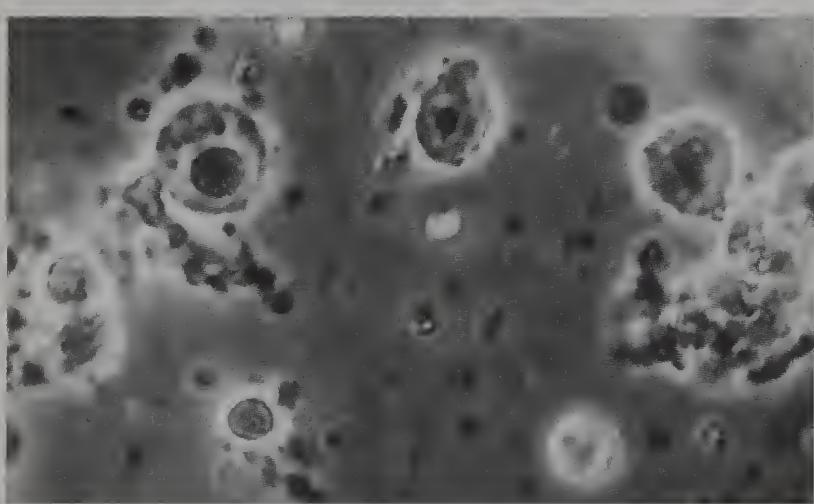


Figure 43 Isolated human neurons or neuroglial cells from the red nucleus of a 77-year-old male (phase contrast, $\times 800$).

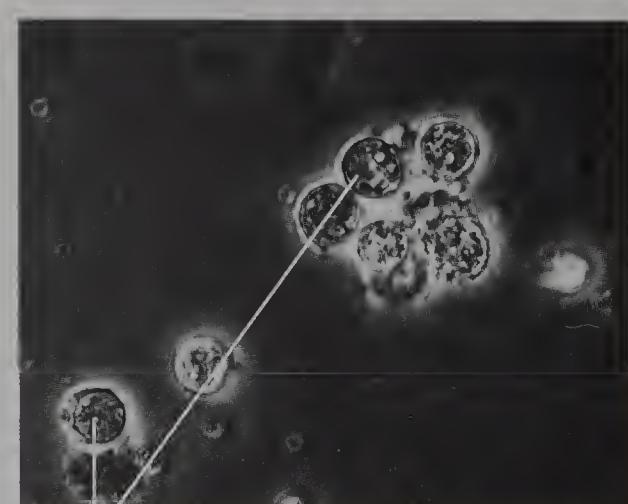


Figure 44 Isolated 1-week-old rat cerebellar granule cells (phase contrast, $\times 800$).

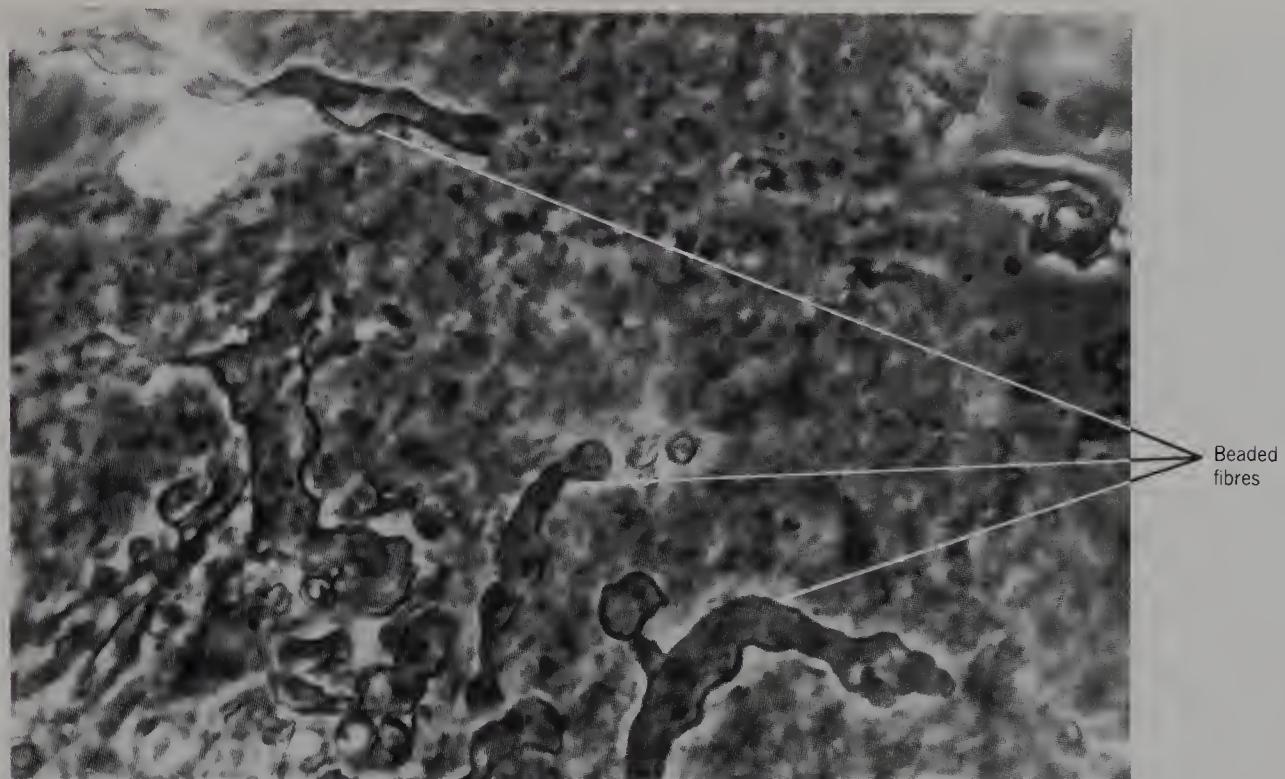


Figure 45 Surface of the soma of an isolated rabbit ventral horn cell from the cervical spinal cord to show adherent beaded fibre endings (phase contrast, $\times 1500$).

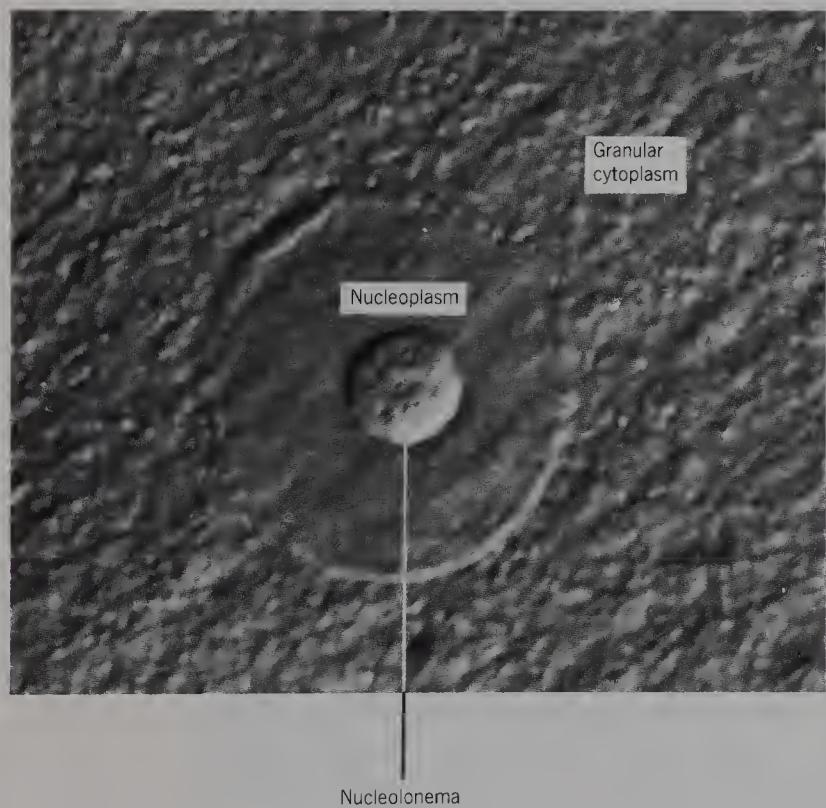


Figure 46 Nucleus and nucleolus of isolated rabbit lateral vestibular neuron (oblique negative phase contrast, $\times 1500$). (By kind permission of Mr L. V. Martin, OBE.)

Note the granularity of the cytoplasm and the transparency of the nucleoplasm.

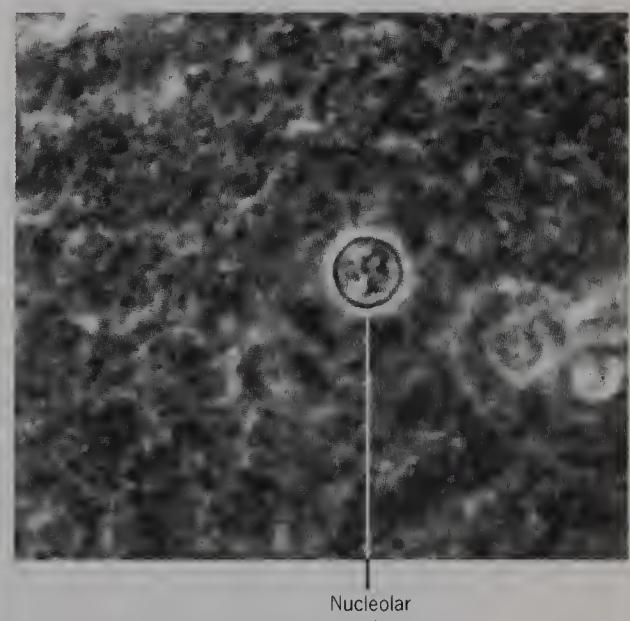


Figure 47 Nucleolar membrane and nucleolonema in isolated rabbit lateral vestibular neuron (phase contrast, $\times 1200$).



Figures 48 and 49 Nucleus and nucleolus of isolated rabbit ventral horn cell to show the mitochondria and nucleolonema. These two optical sections were 1 μm apart (Zeiss scanning differential interference contrast, $\times 4300$). (All differential interference micrographs were taken by kind permission of Miss P. Gunter of Zeiss Oberkochen.)



Figure 50 Nucleus and nucleolus of isolated rabbit lateral vestibular neuron to show the nuclear membrane (microscopy as in previous figure, $\times 4300$).

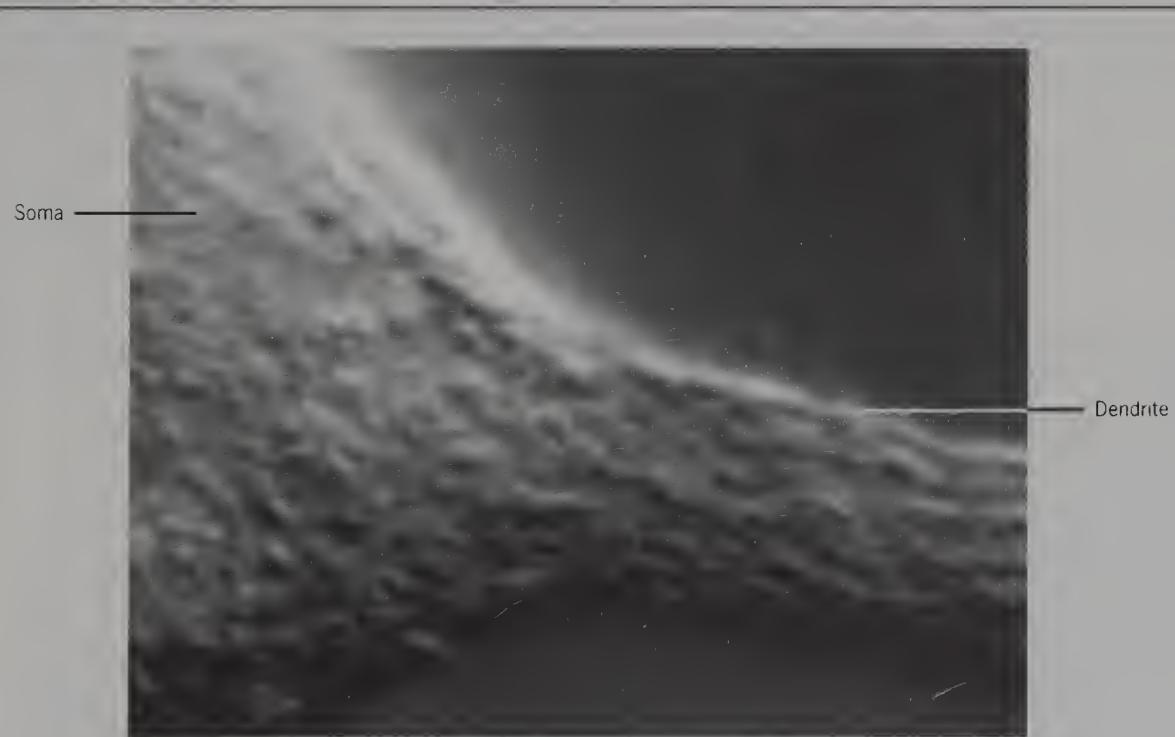


Figure 51 Soma-dendritic junction of isolated rabbit lateral vestibular neuron to show granular appearance (Zeiss scanning differential interference contrast, $\times 4300$).

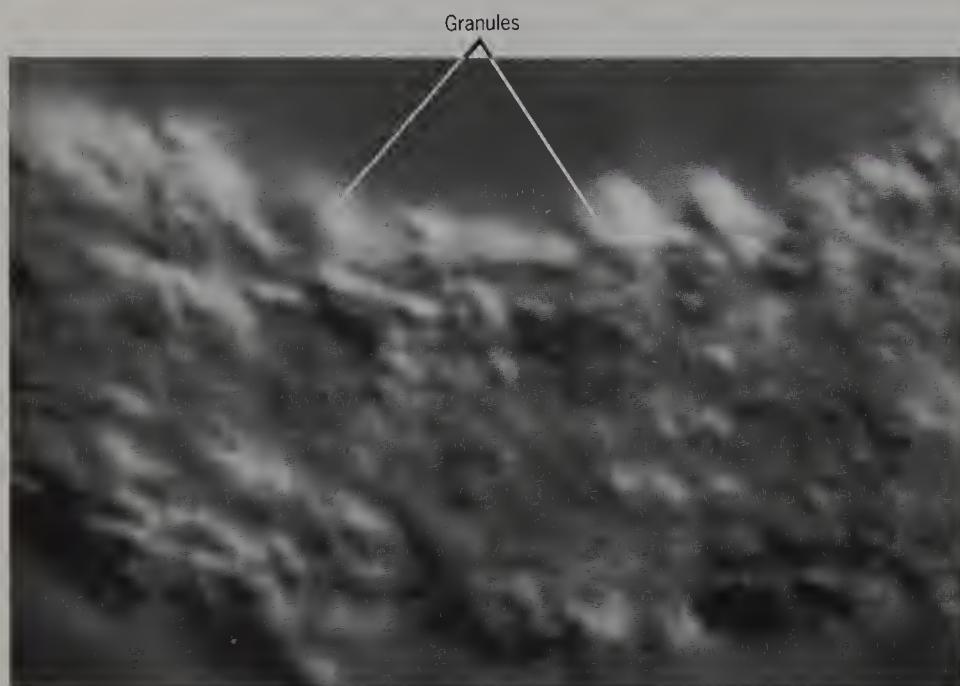


Figure 52 Surface of the dendrite of an isolated rabbit ventral horn neuron to show the granular appearance compared with the previous figure (microscopy as in previous figure, $\times 6800$).

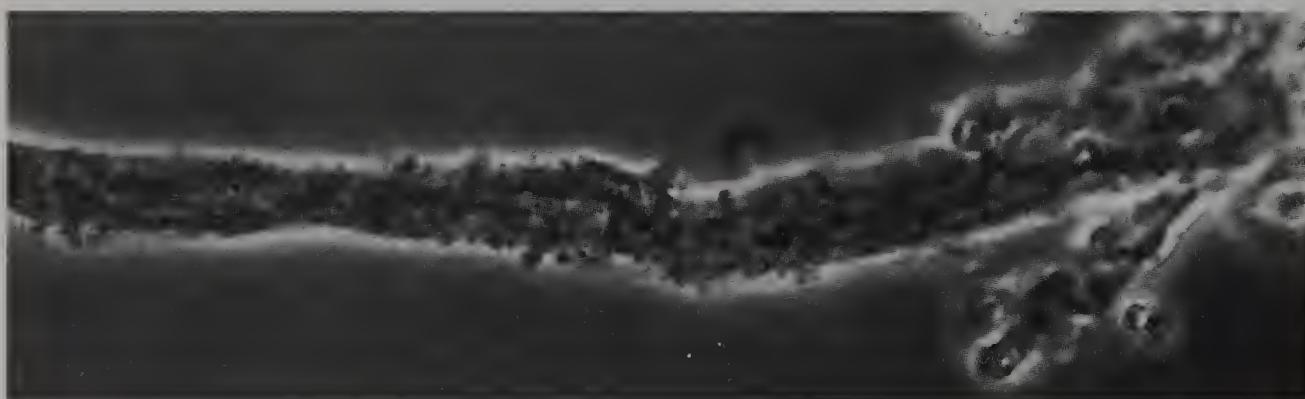


Figure 53 Isolated human dendrite from a Betz cell from a 55-year-old male, to show the dendritic structure and adherent fine granules (phase contrast, $\times 800$).

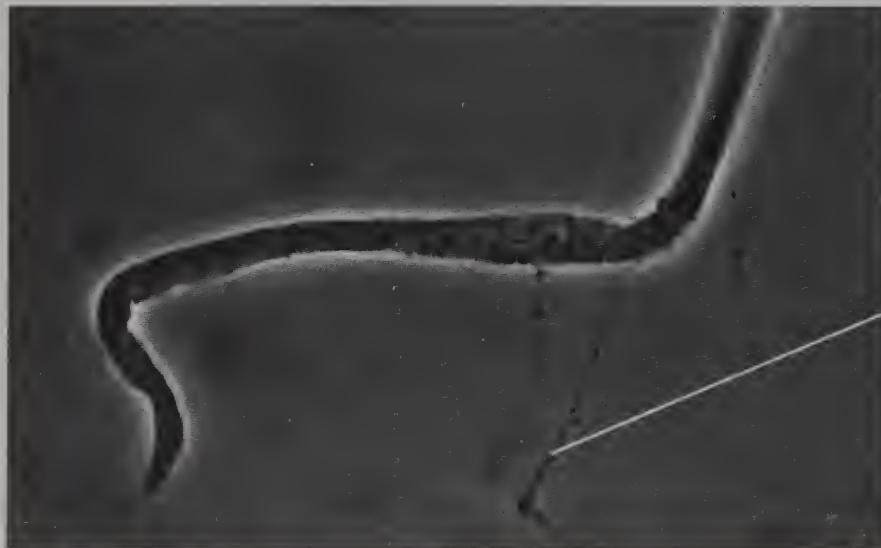


Figure 54 Isolated human dendrite from a vagal nucleus neuron of a 53-year-old male (phase contrast, $\times 800$).

Note the fine adherent dendrites.

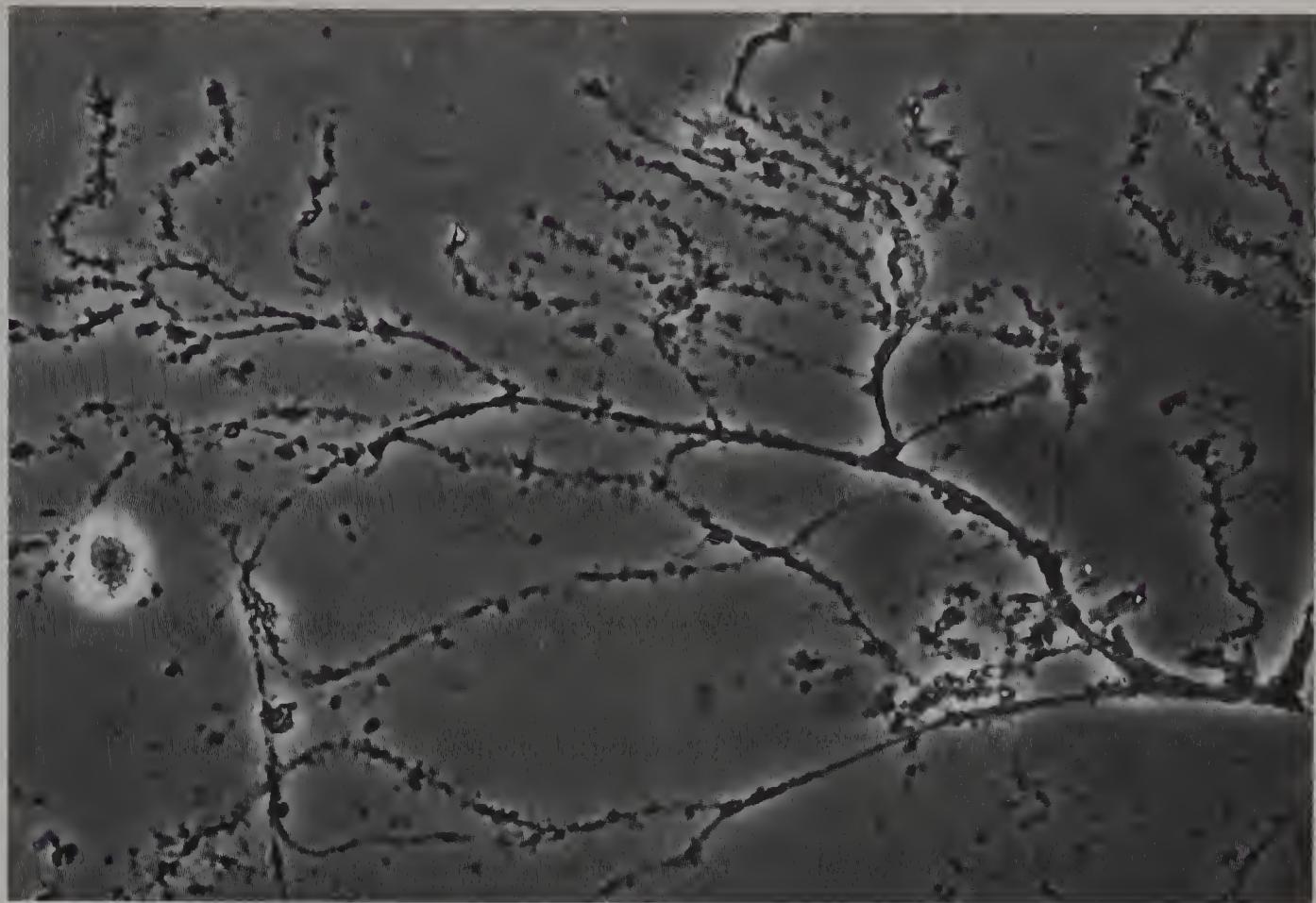


Figure 55 Isolated human dendritic tree of an inferior vestibular neuron from a 68-year-old male (phase contrast, $\times 750$).

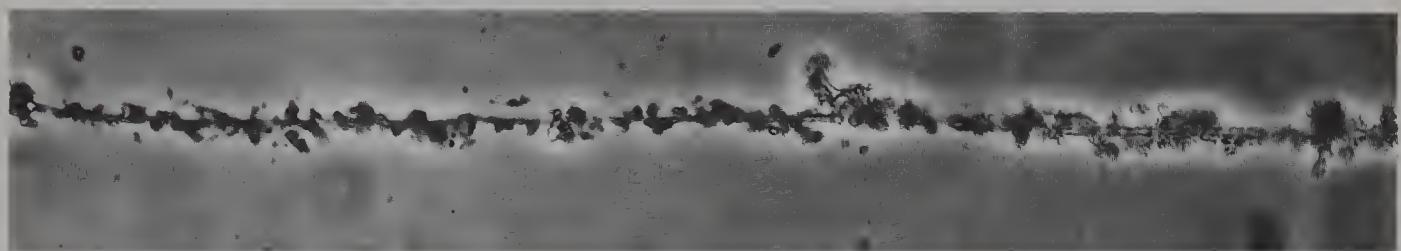


Figure 56 Isolated human fine fibre from the cerebellar grey matter from a 55-year-old male, to show adherent fine granules (phase contrast, $\times 750$).

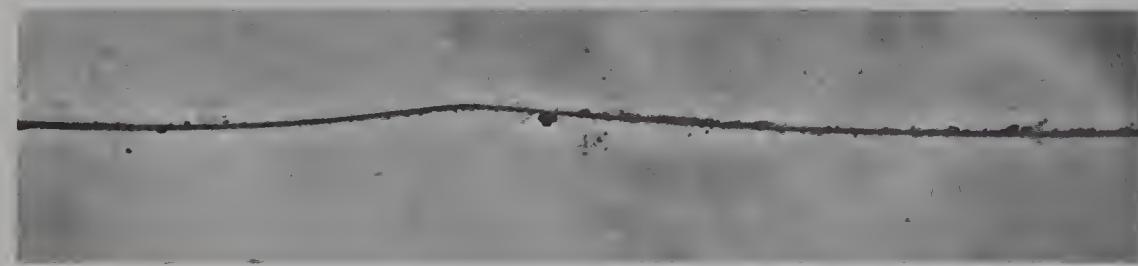


Figure 57 Isolated human fine fibre from the previous tissue, showing that it has a smooth outline (phase contrast, $\times 750$).

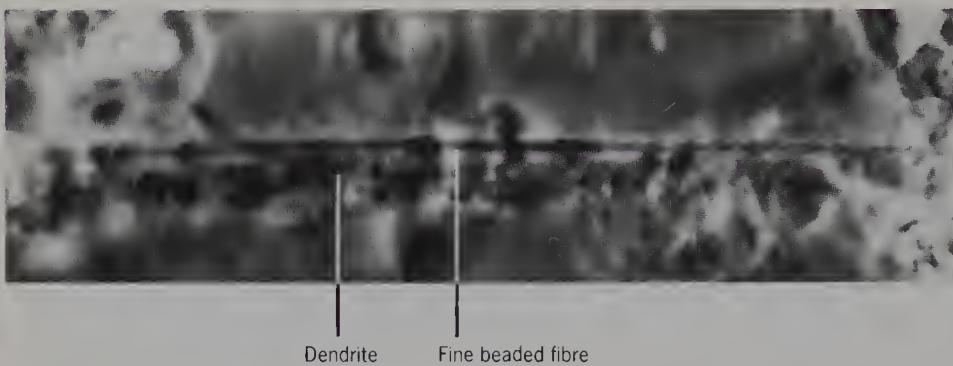


Figure 58 Isolated rabbit dendrite from a ventral horn cell from the cervical spinal cord, to show a fine beaded fibre running along its upper edge (phase contrast, $\times 2000$).

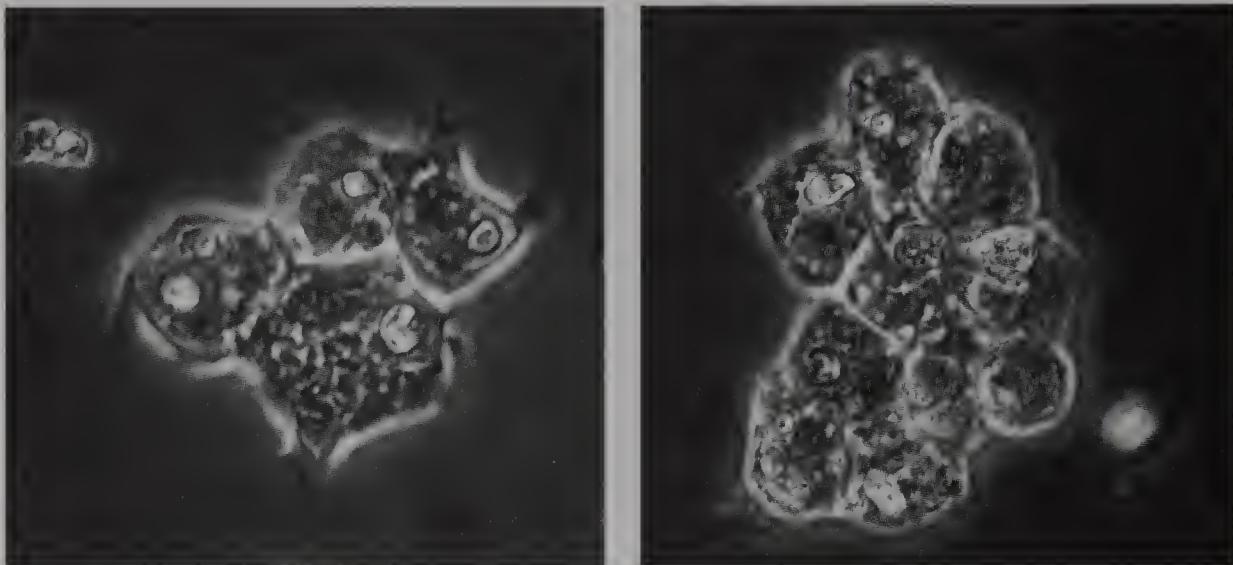


Figure 59 Isolated human ependymal cells from the wall of the lateral ventricle adjacent to the corpus callosum from a 68-year-old male (phase contrast, $\times 750$).

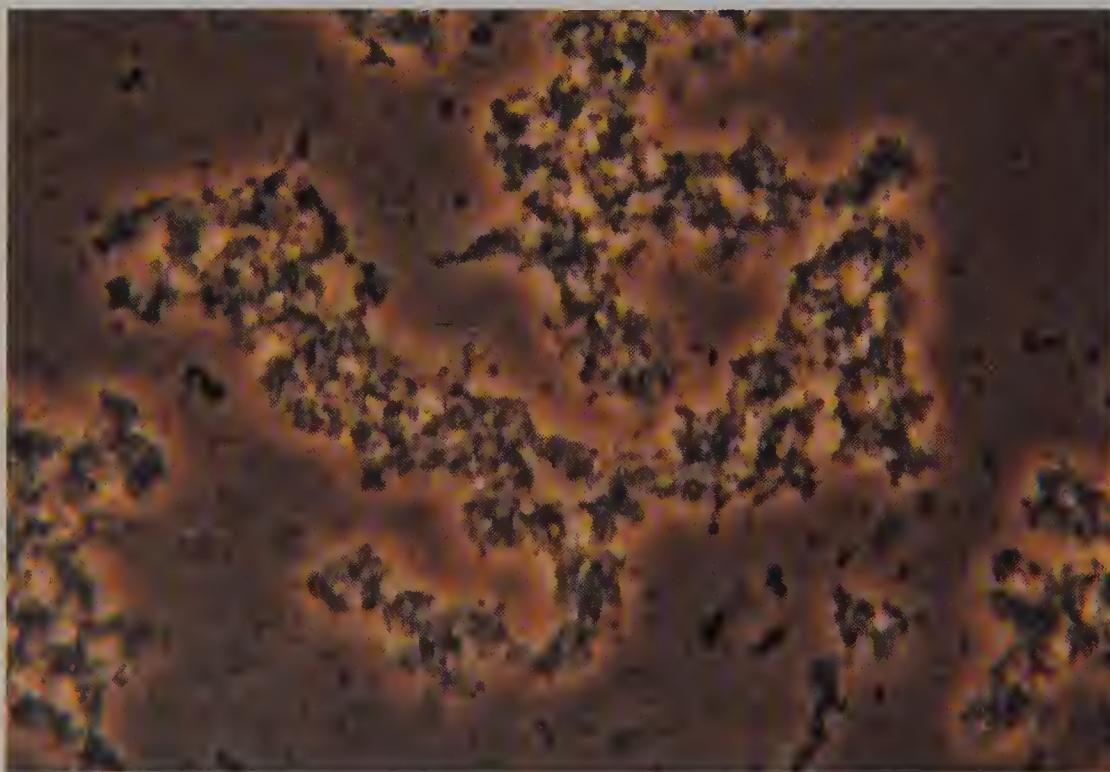


Figure 60 Teased human putamen from a 65-year-old female, to show fine granular material (phase contrast, $\times 750$).

This material is the major component of neuroglia in grey matter.

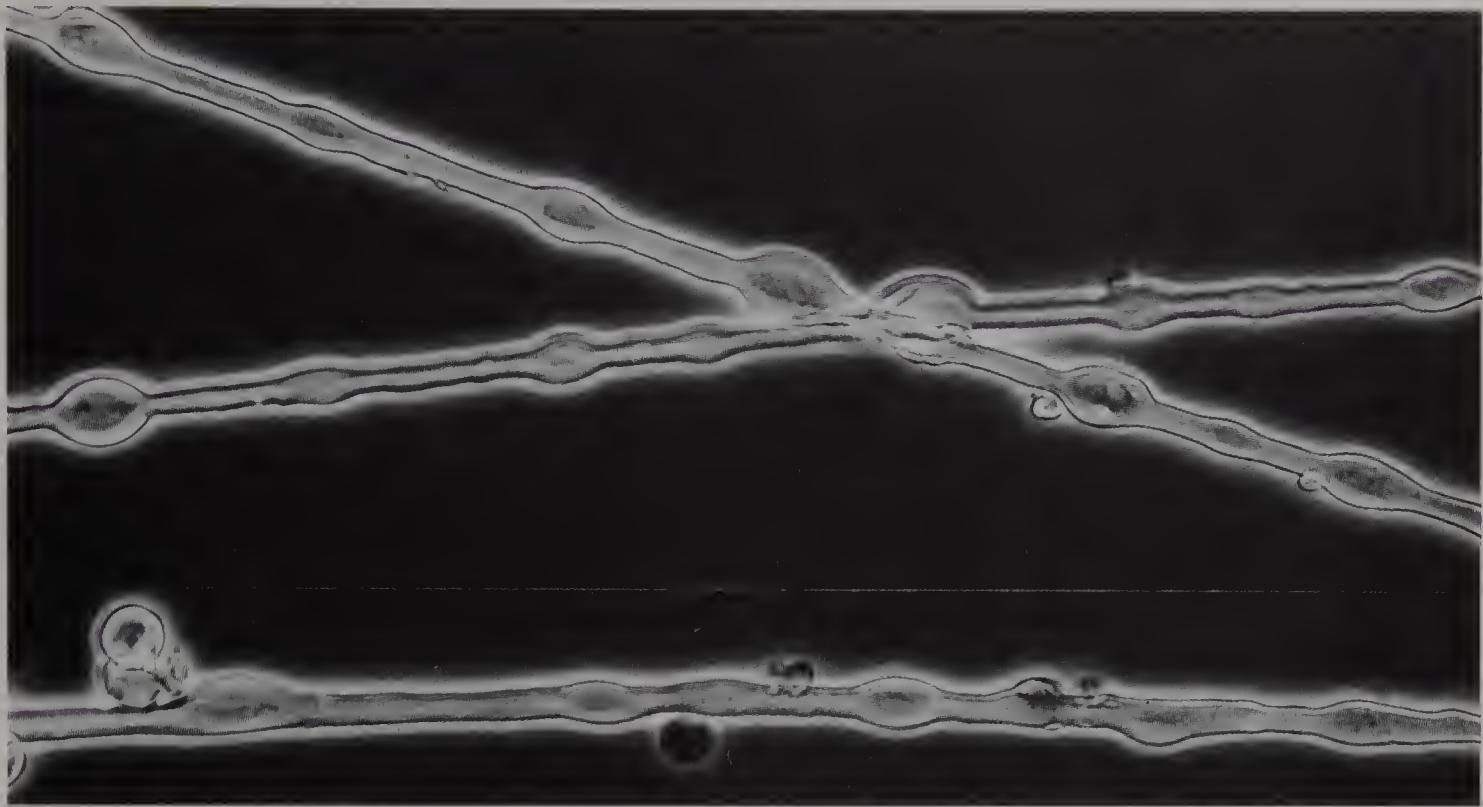


Figure 61 Isolated rat beaded fibres from dorsal white matter of cervical spinal cord to show small axoplasmic granules within the beads (phase contrast, $\times 800$).

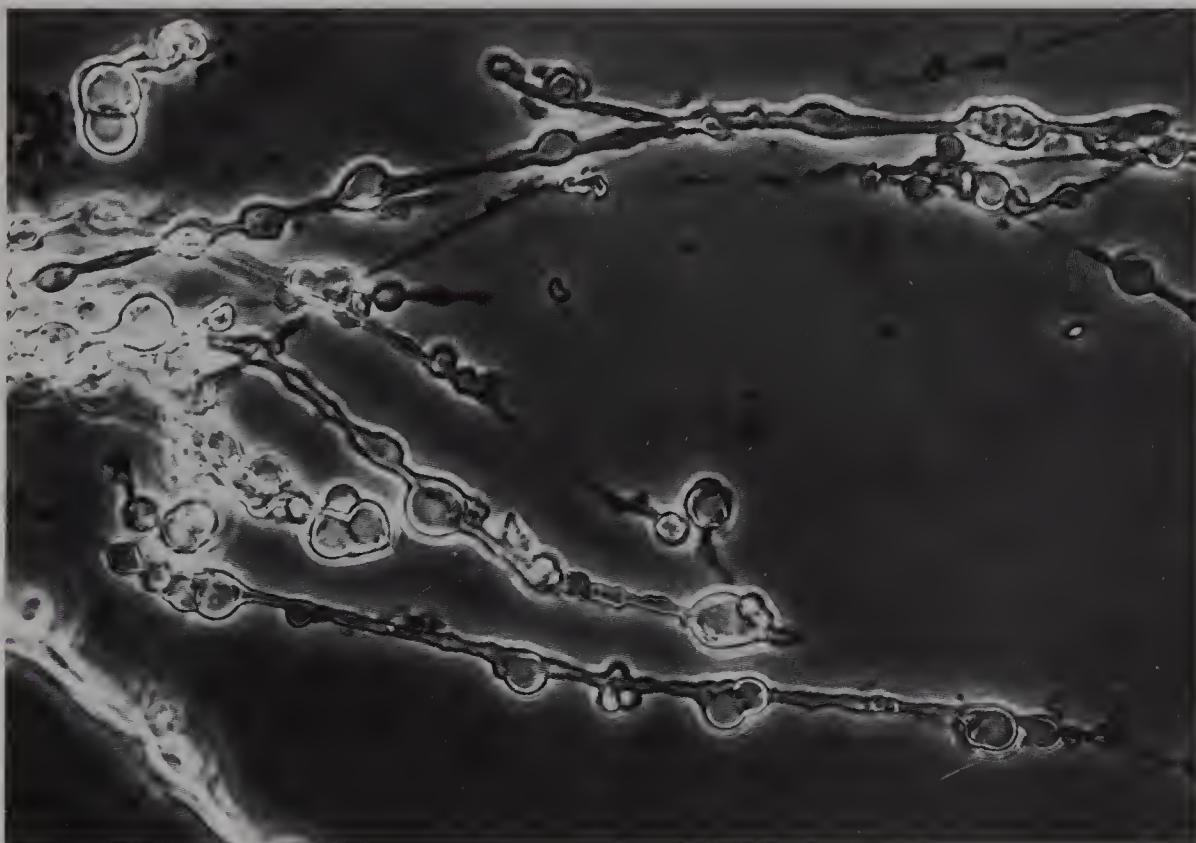


Figure 62 Teased human beaded fibres from the vestibulospinal tract of an 89-year-old female (phase contrast, $\times 800$).
The beads are refractile.

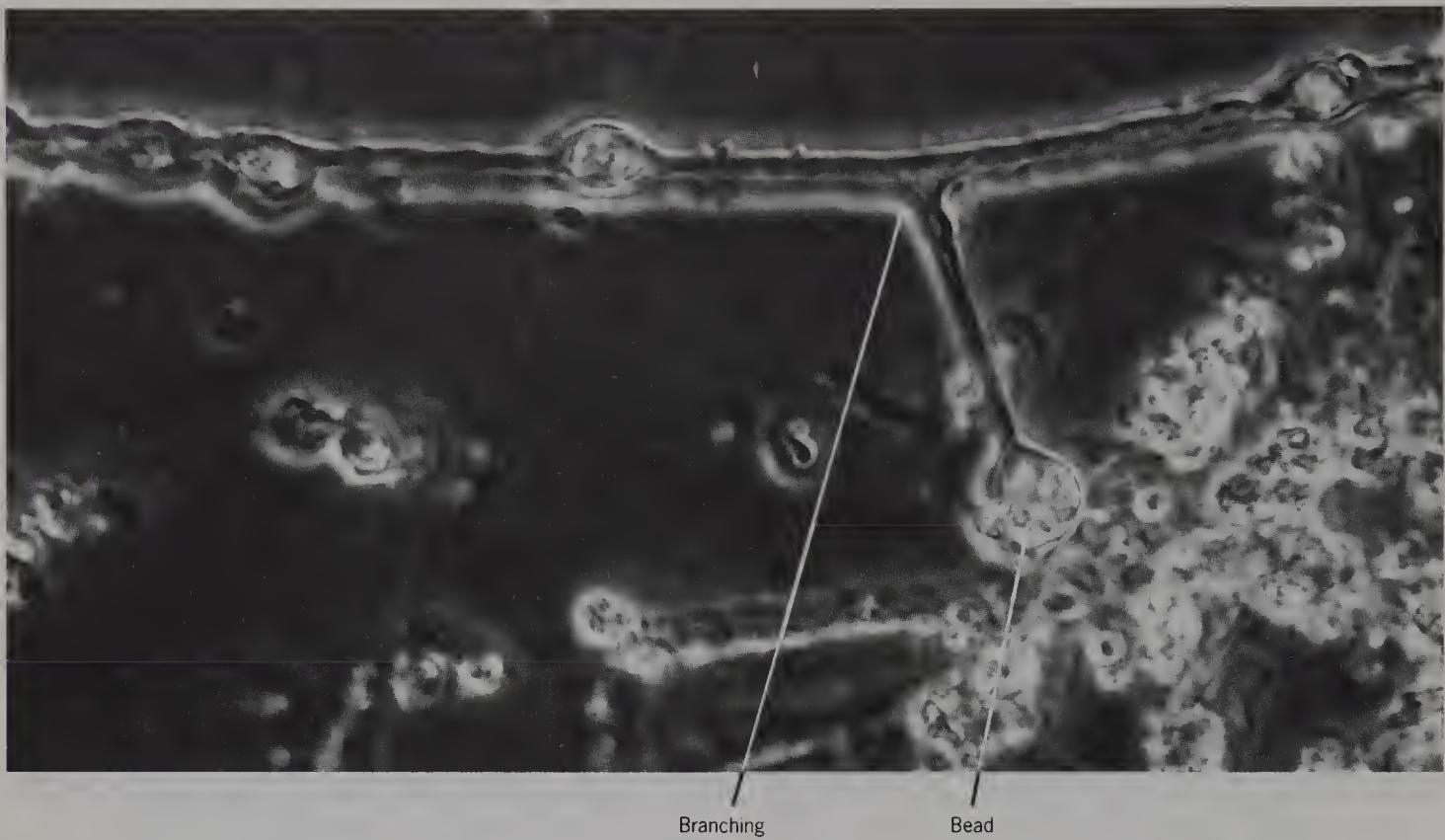


Figure 63 Isolated human beaded fibres from the pons of a 95-year-old female, to show a side branch ending in a bead (phase contrast, $\times 1300$).

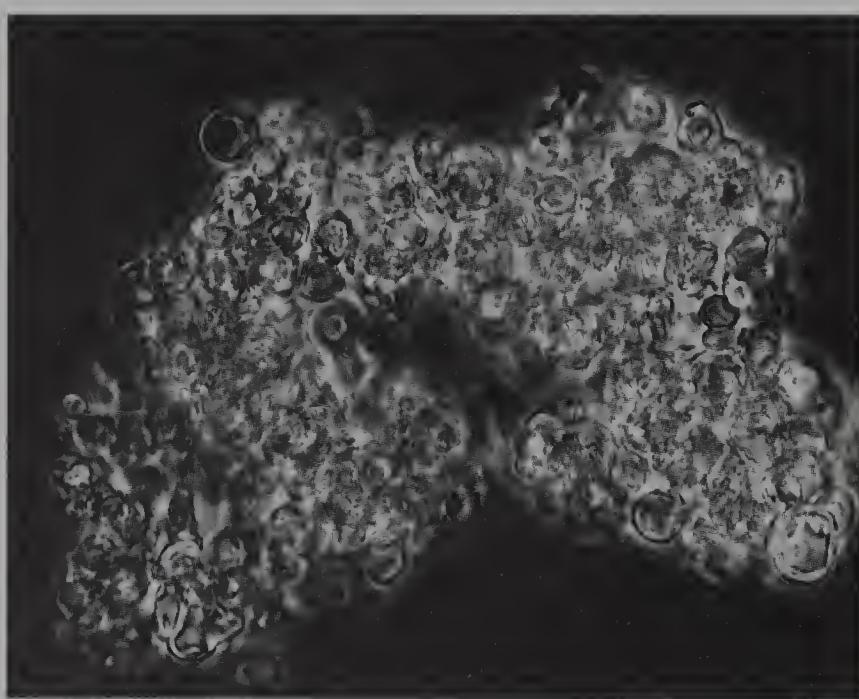


Figure 64 Clump of neuroglial droplets from the human cerebellar white matter of an 80-year-old female (phase contrast, $\times 800$).
Droplets are a major component of white matter.

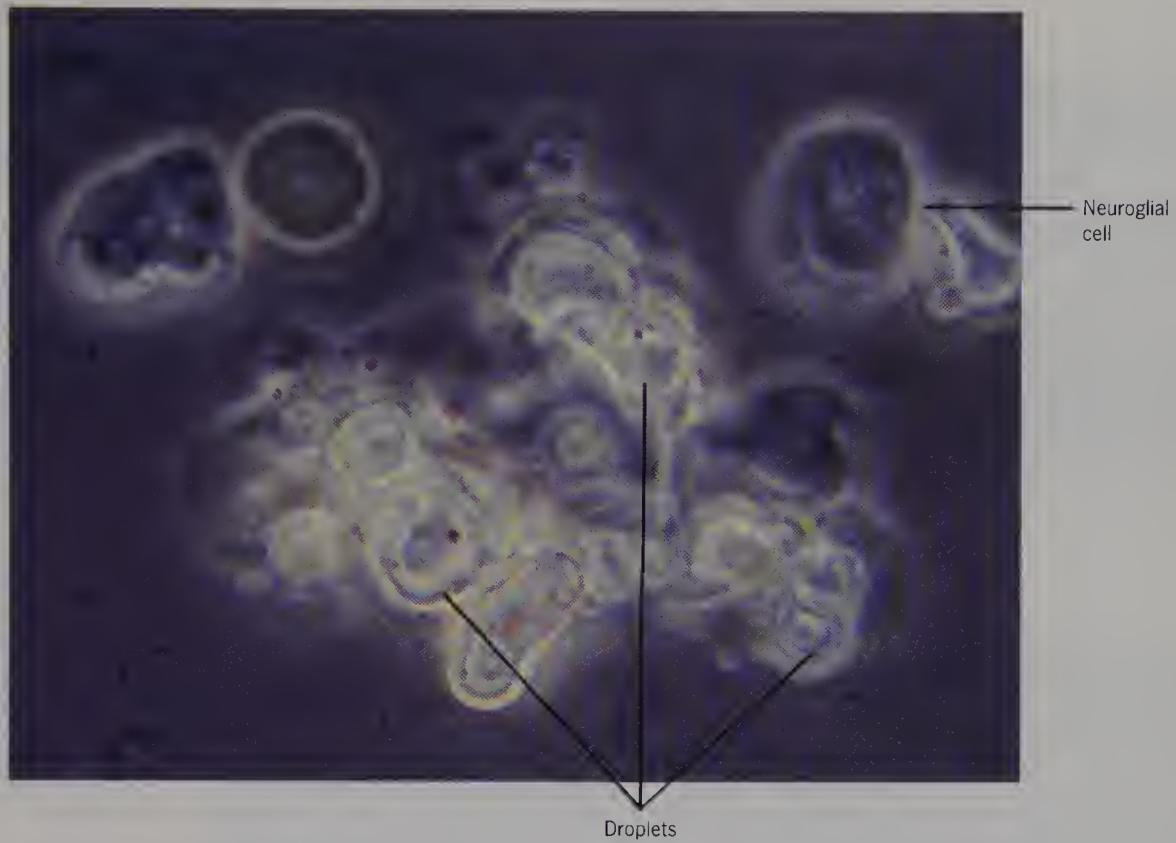


Figure 65 Teased human optic nerve from a 43-year-old male, to show droplets and neuroglial cells (phase contrast, $\times 1500$).

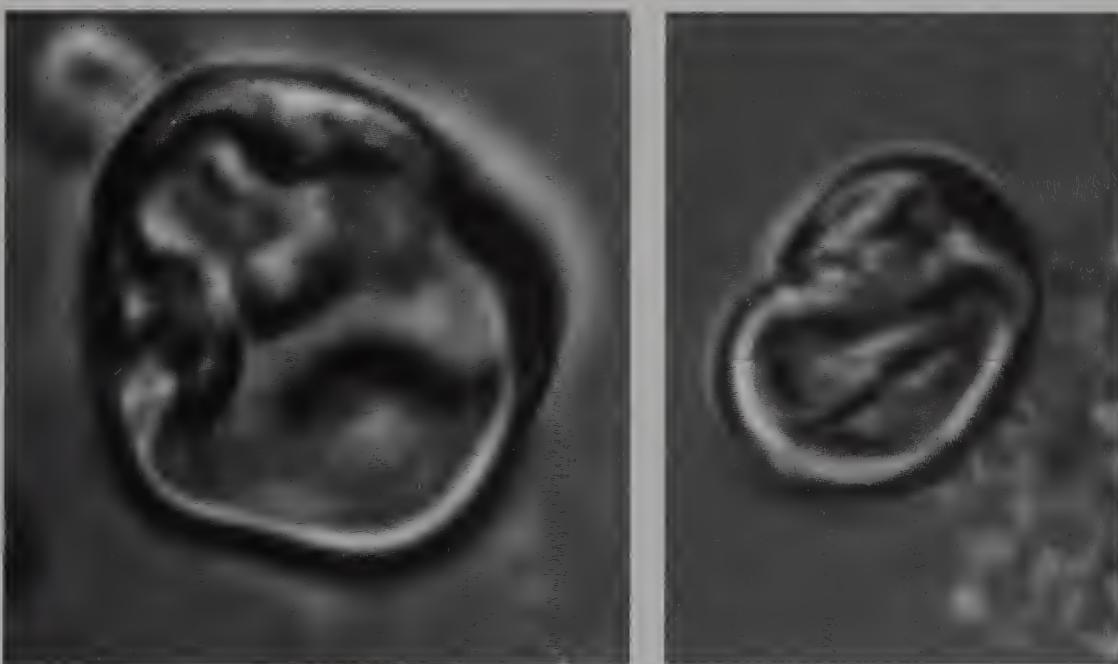


Figure 66 Isolated droplets from rabbit dorsal column of the spinal cord (Zeiss scanning differential interference contrast, $\times 4300$).

These have not been seen before at high power.

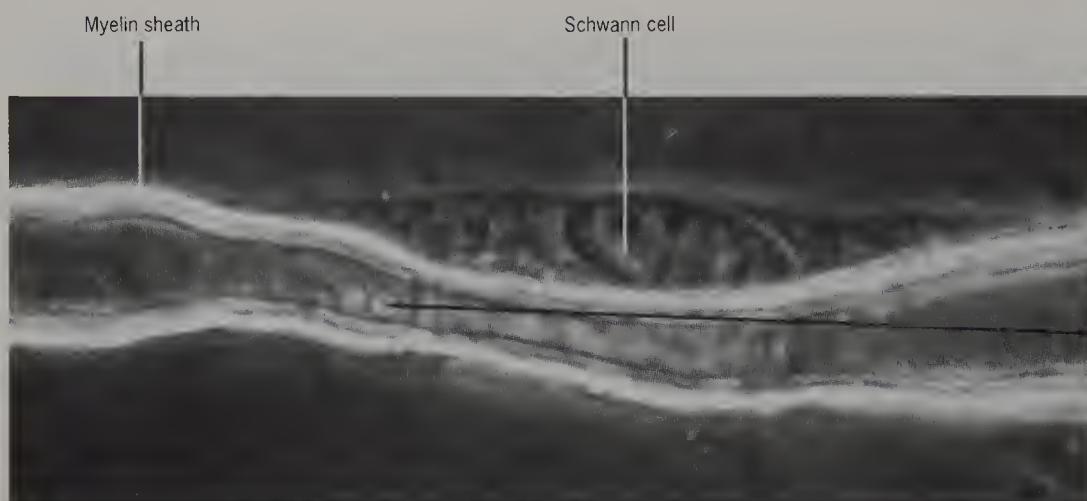


Figure 67 Isolated rat myelinated fibre from sciatic nerve, to show Schwann cell containing multiple nucleoli (phase contrast, $\times 1500$).

The Schwann cell was described in 1839.

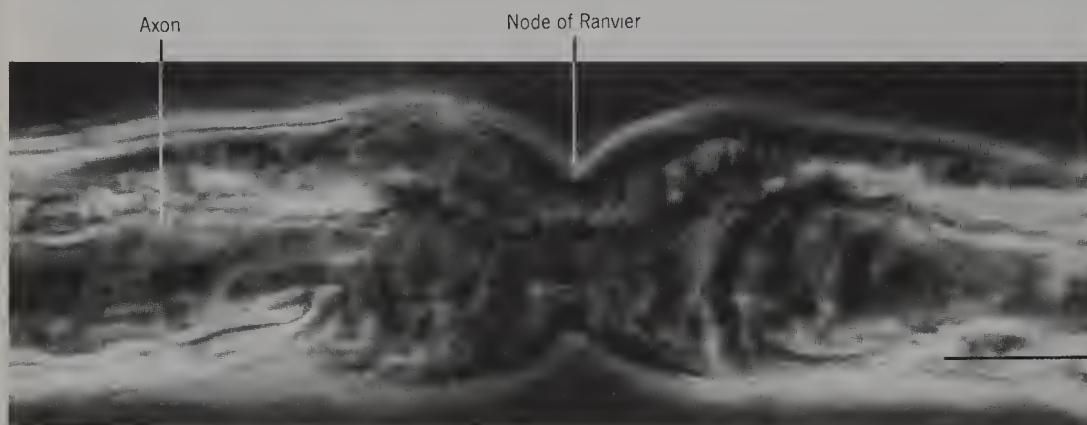


Figure 68 Isolated rabbit myelinated fibre from sciatic nerve to show node of Ranvier and axon (phase contrast, $\times 1500$).

The node of Ranvier was described in 1871.

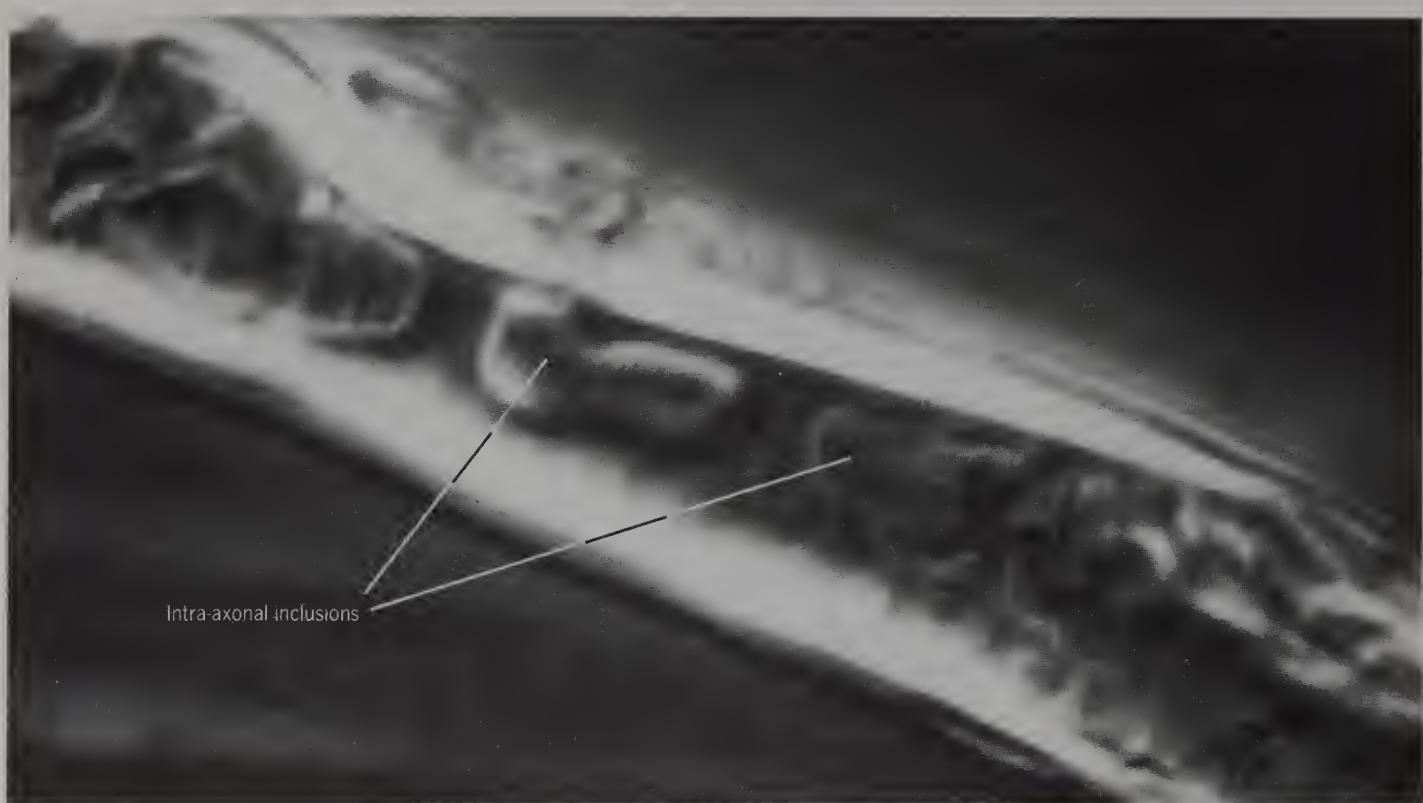


Figure 69 Isolated rabbit myelinated nerve fibre from the sciatic nerve, to show intra-axonal inclusions (Zeiss scanning differential interference contrast, $\times 4300$).



Figure 70 Partially teased rabbit sciatic nerve showing a dark Remak fibre between myelinated fibres (phase contrast, $\times 750$).

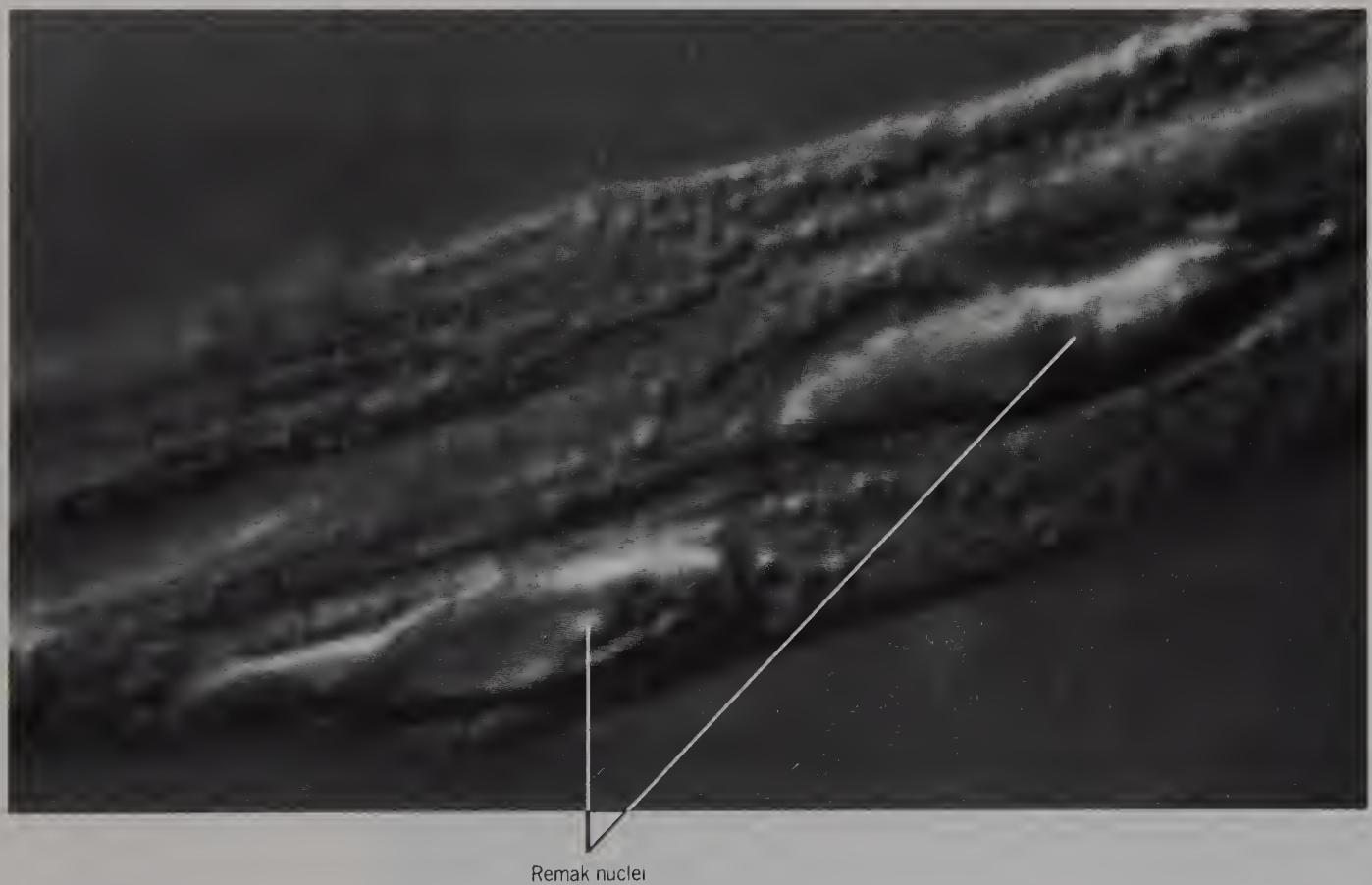


Figure 71 Isolated rabbit Remak fibres from the sciatic nerve (Zeiss scanning differential interference contrast, $\times 4000$).

The elongated nuclei seen on the outside are characteristic of Remak (unmyelinated) fibres.

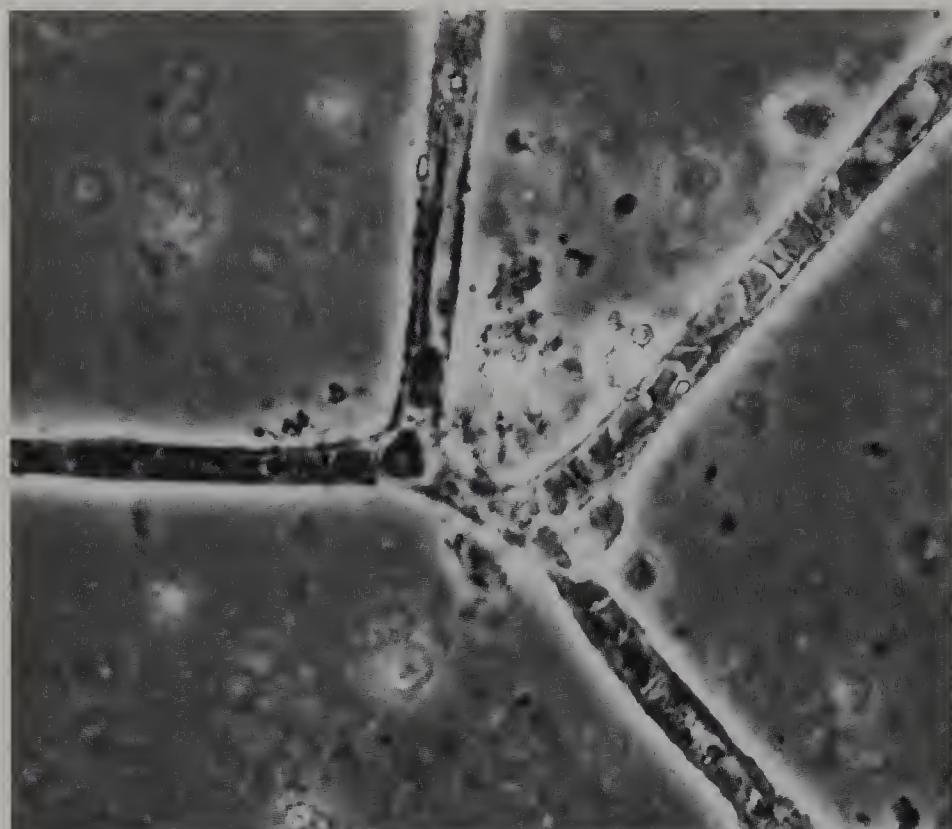


Figure 72 Isolated human capillary from the putamen of an 84-year-old male (phase contrast, $\times 750$).

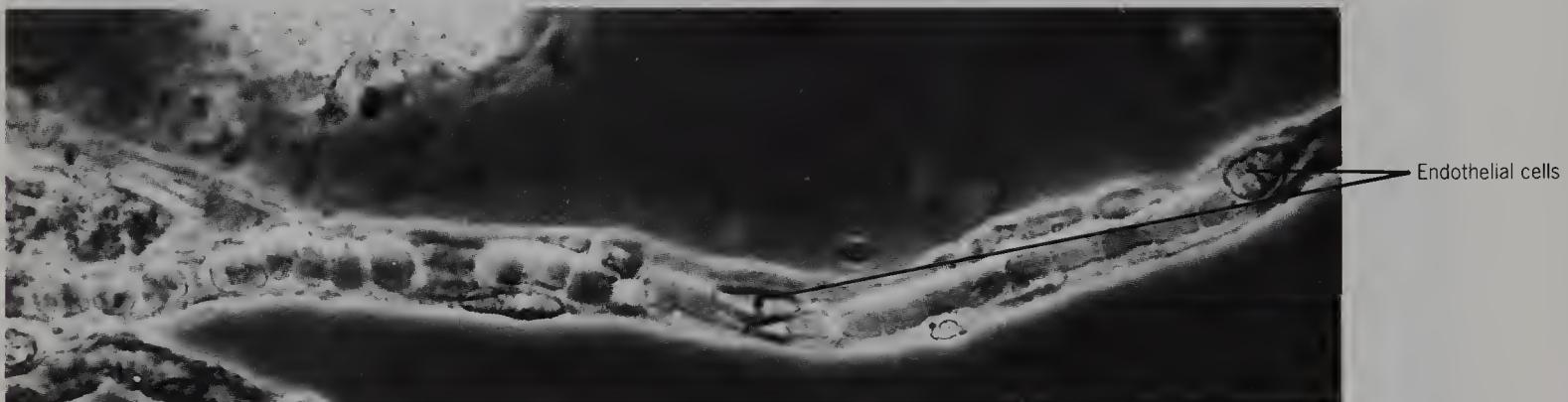


Figure 73 Isolated human capillary from the cerebellar cortex of a 55-year-old male, showing endothelial cells and/or pericytes (phase contrast, $\times 750$).

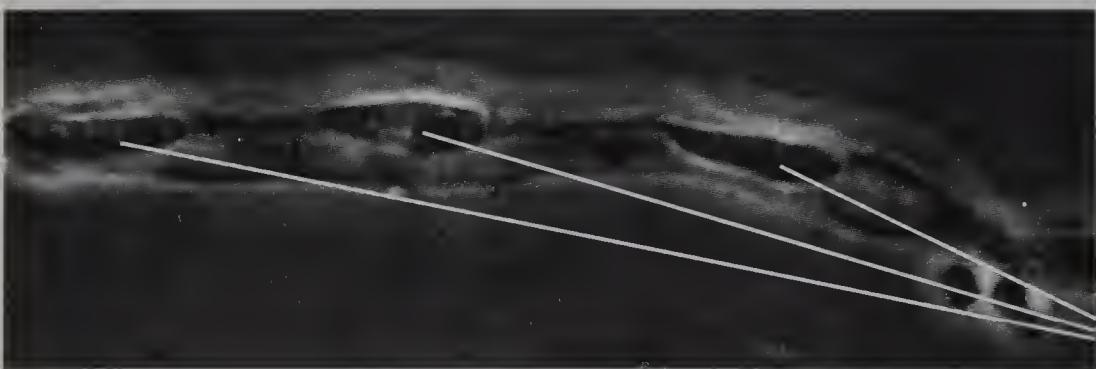


Figure 74 Isolated rabbit capillary from the internal capsule to show endothelial cells and/or pericytes (phase contrast, $\times 1500$).

Endothelial cells or pericytes

SECTION
3

CEREBRAL CORTEX

Figure 75 Thin slab of adult rabbit frontal cortical grey matter, lightly coloured with methylene blue to show the incidence of neuron somas; **a-f** are successive, but not continuous from the surface of the cortex to the white matter. The laminae are indicated with Roman numerals: I, plexiform; II, external granular; III, pyramidal; IV, internal granular; V, ganglionic; VI, multiform (bright field, $\times 85$).

The total thickness of the cortex in this specimen was 6 mm.



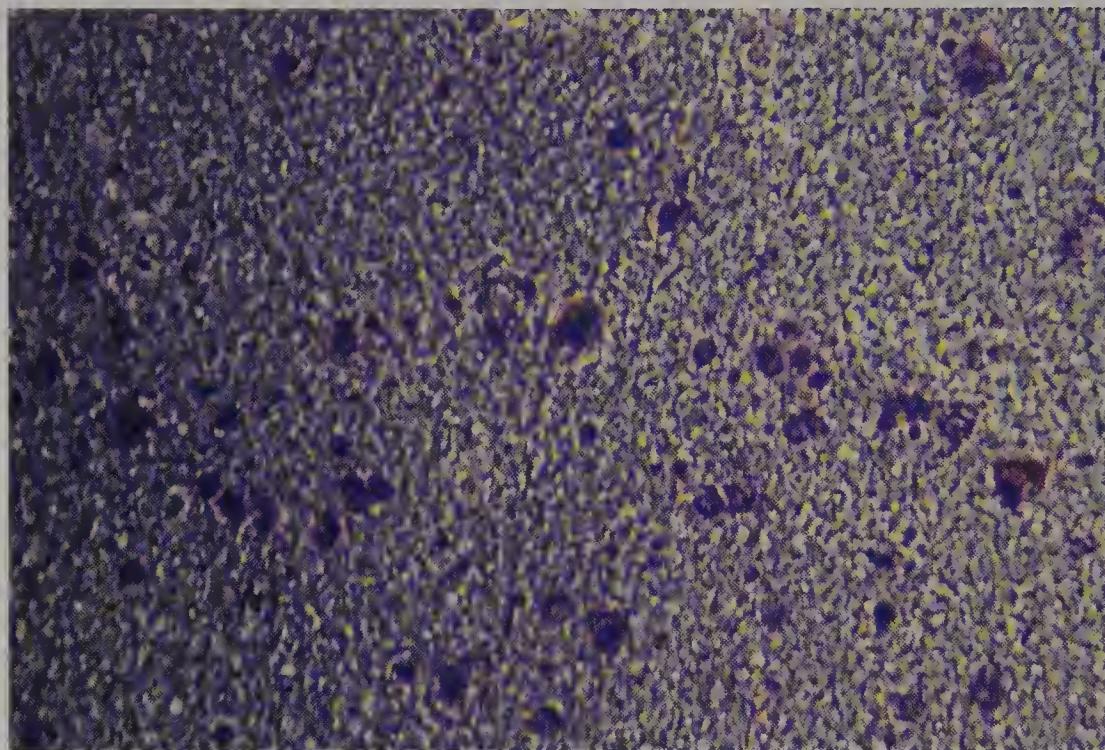


Figure 76 Thin slab of human frontal cortical grey matter from a 79-year-old male, lightly coloured with methylene blue to show the incidence of neuron somas (bright field, $\times 250$).

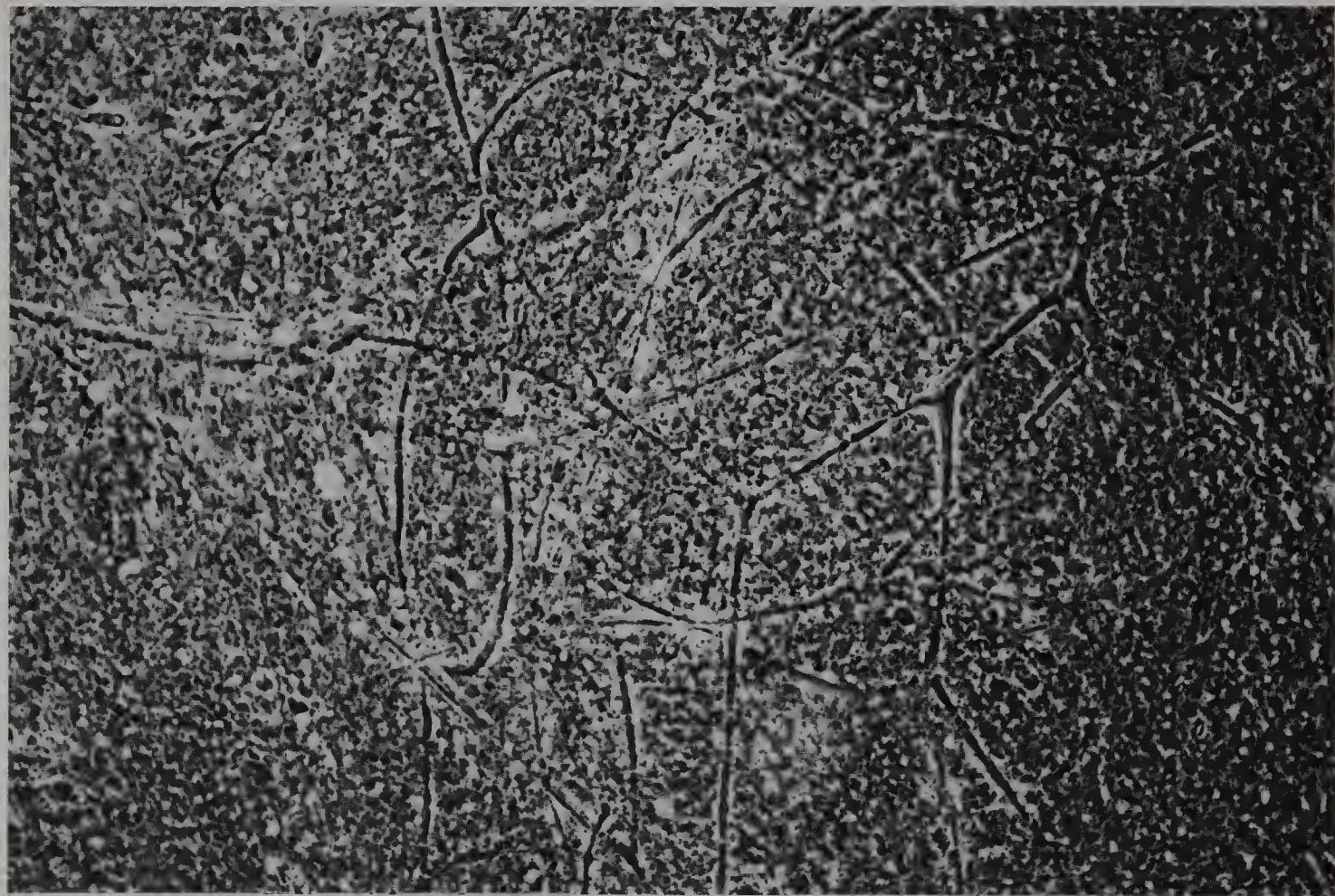


Figure 77 Thin slab of adult rat frontal cortical grey matter, unstained (phase contrast, $\times 335$).

There is a rich blood supply, which gives part of the colour to grey matter.

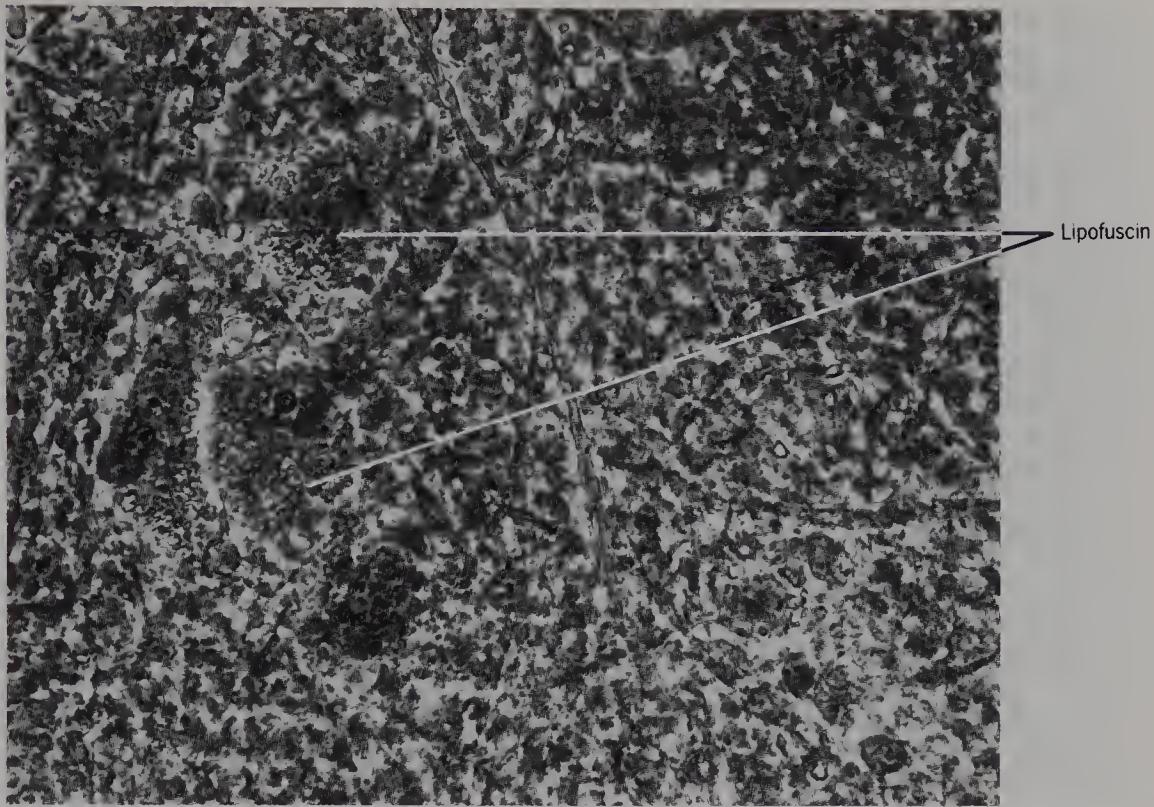


Figure 78 Thin slab of human frontal cortical grey matter from a 68-year-old male, to show neurons *in situ* (phase contrast, $\times 700$).

Lipofuscin is present in the cytoplasm of most adult human neurons.

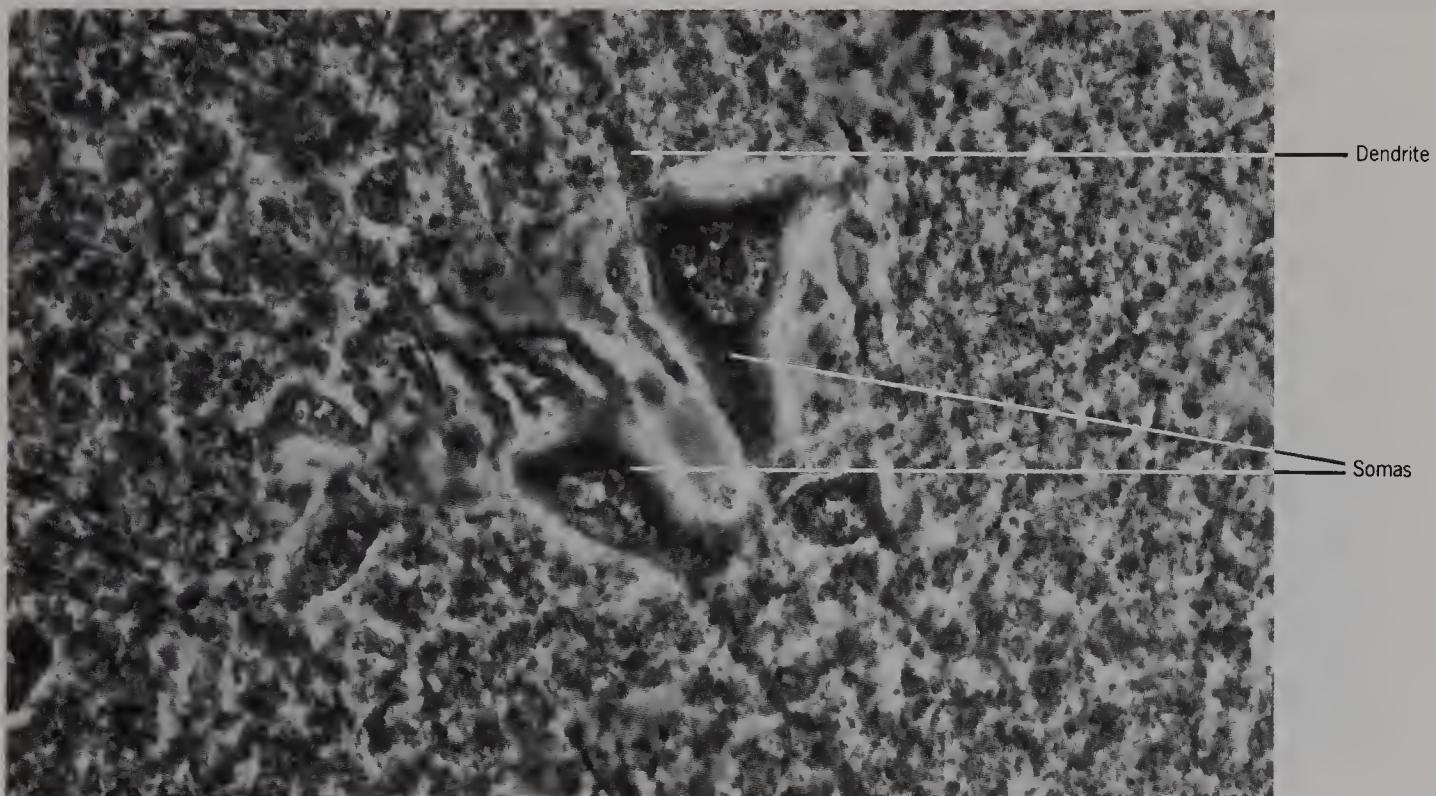


Figure 79 Thin slab of new-born lamb frontal cortical grey matter to show pyramidal neuronal somas *in situ* (phase contrast, $\times 700$).

The dendrites are visible and the nucleus has a low refractive index.

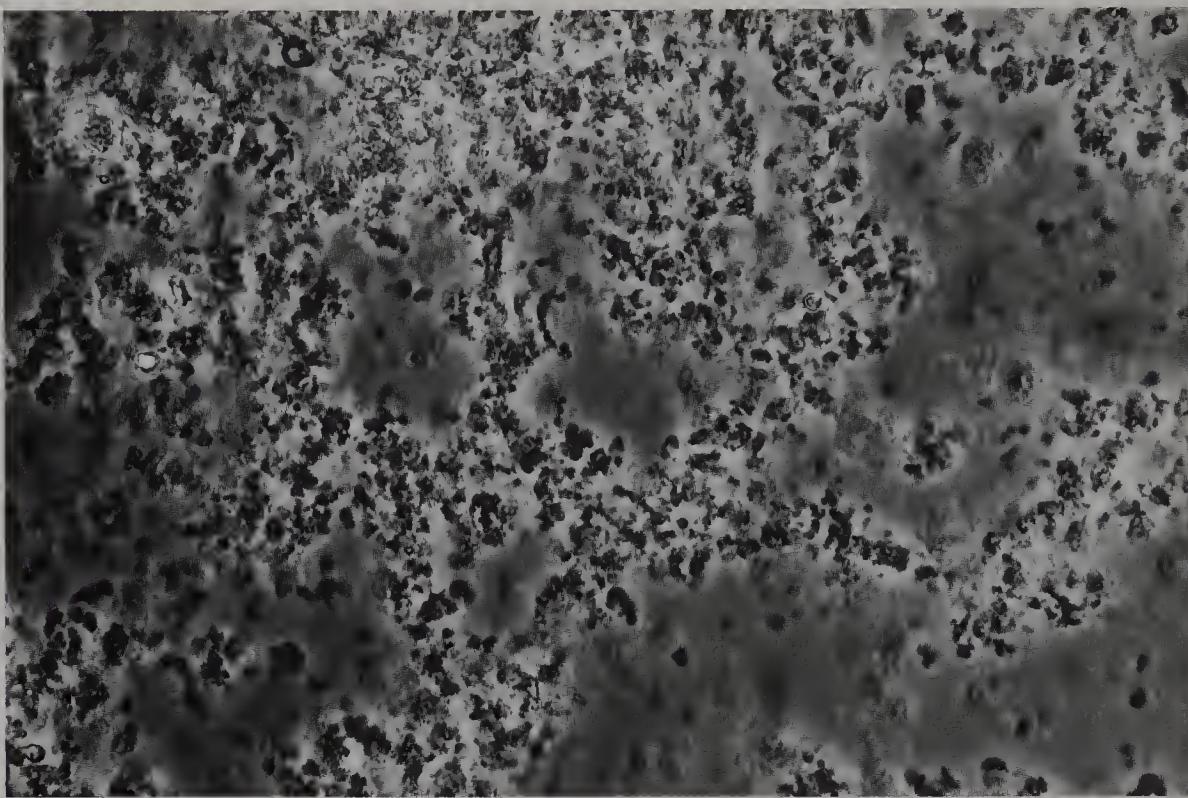


Figure 80 Teased fine granular material from human frontal grey matter from a 68-year-old male, to show individual or aggregates of granules (phase contrast, $\times 700$).

These fine dark granules occupy most of the volume between the neurons in grey matter.

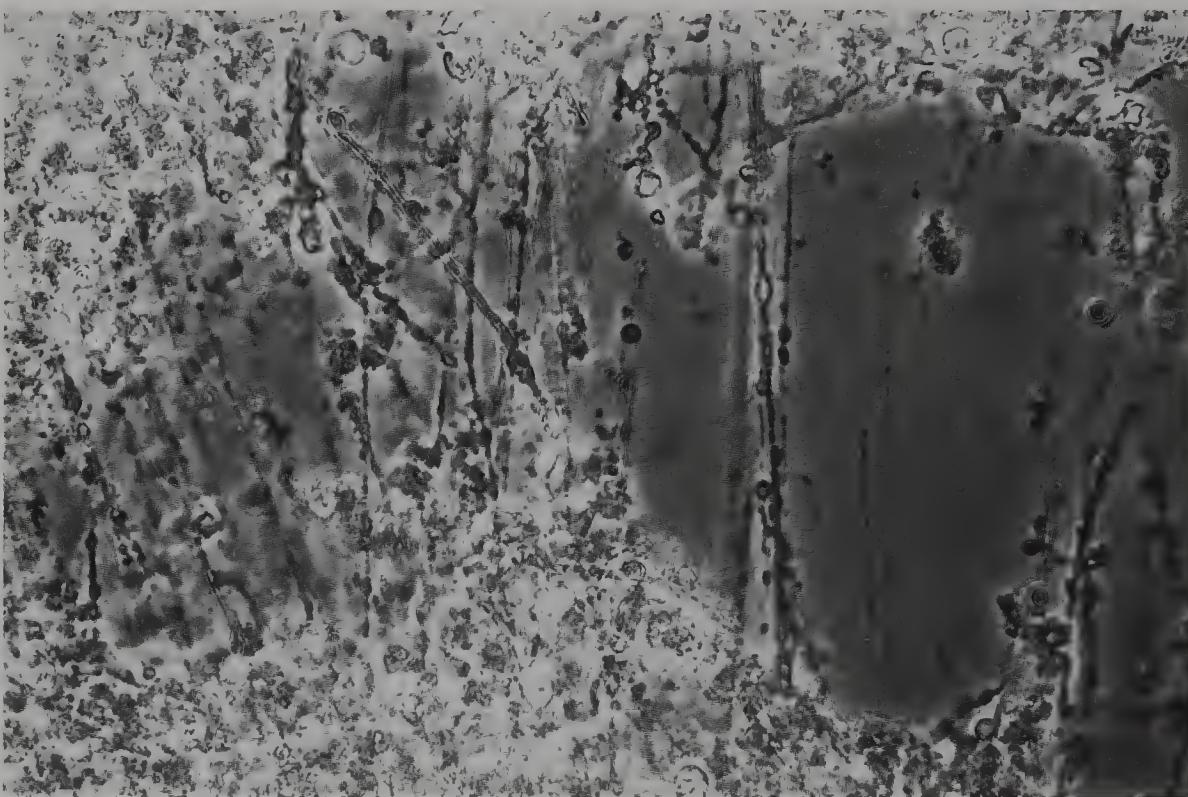


Figure 81 Teased human frontal grey matter from a 68-year-old male, to show fine fibres (phase contrast, $\times 700$).

The fibres are seen clearly only when the tissue is teased, and fine granules often adhere to them.

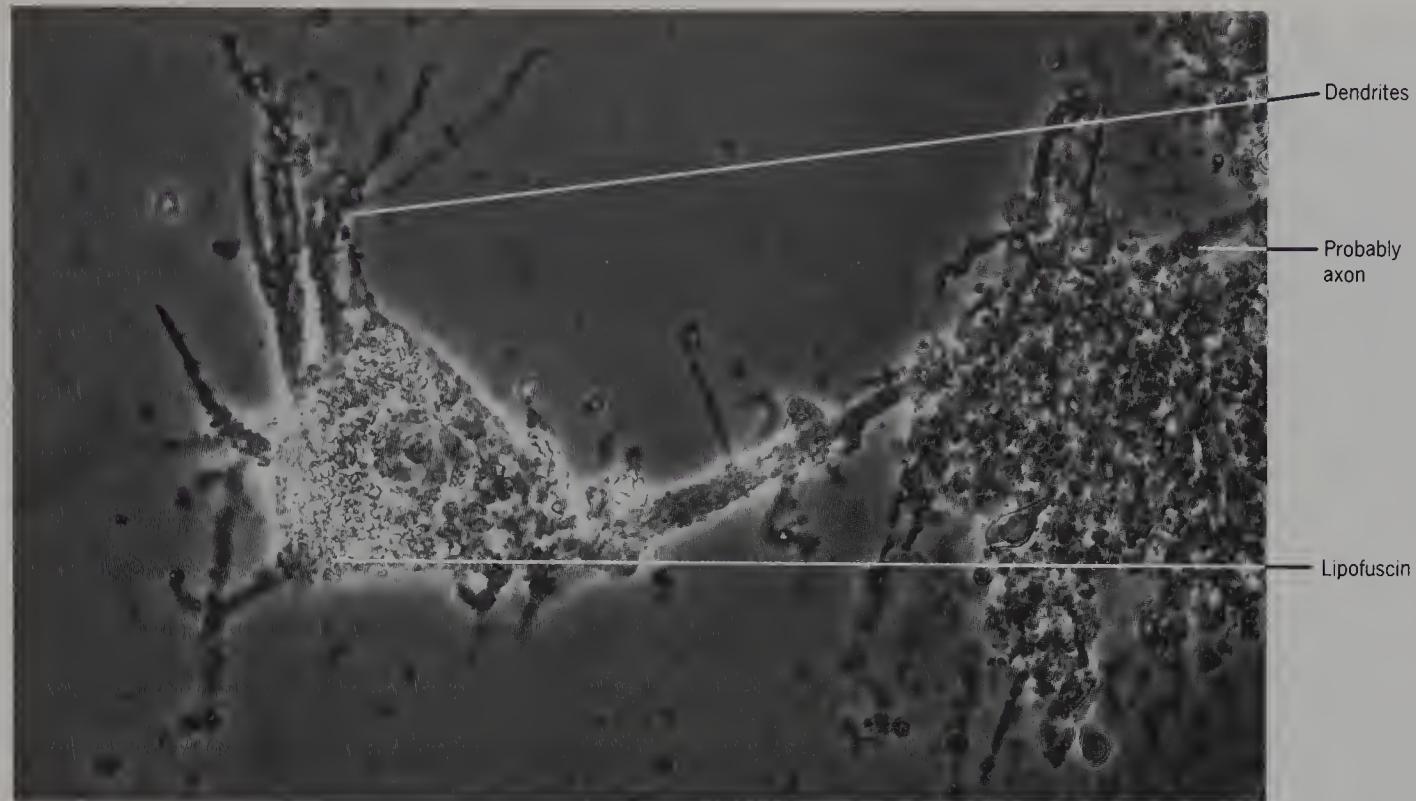


Figure 82 Teased human frontal grey matter from a 77-year-old male, to show a neuron and associated neuroglia (phase contrast, $\times 700$).

Note the number of primary dendrites.

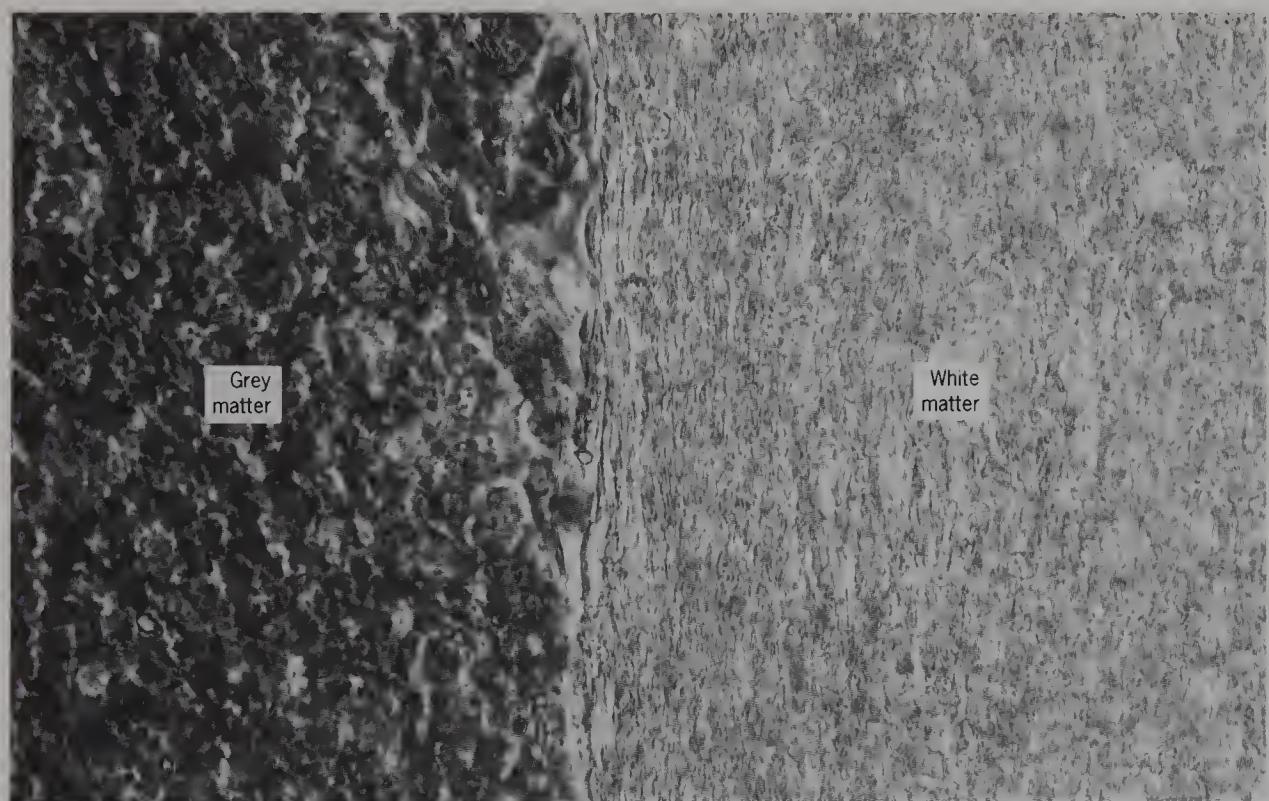


Figure 83 Thin slab of human frontal region from an 84-year-old male, to show grey–white matter boundary (phase contrast, $\times 700$).

The grey matter has a high refractive index. There are fibres in the white matter.

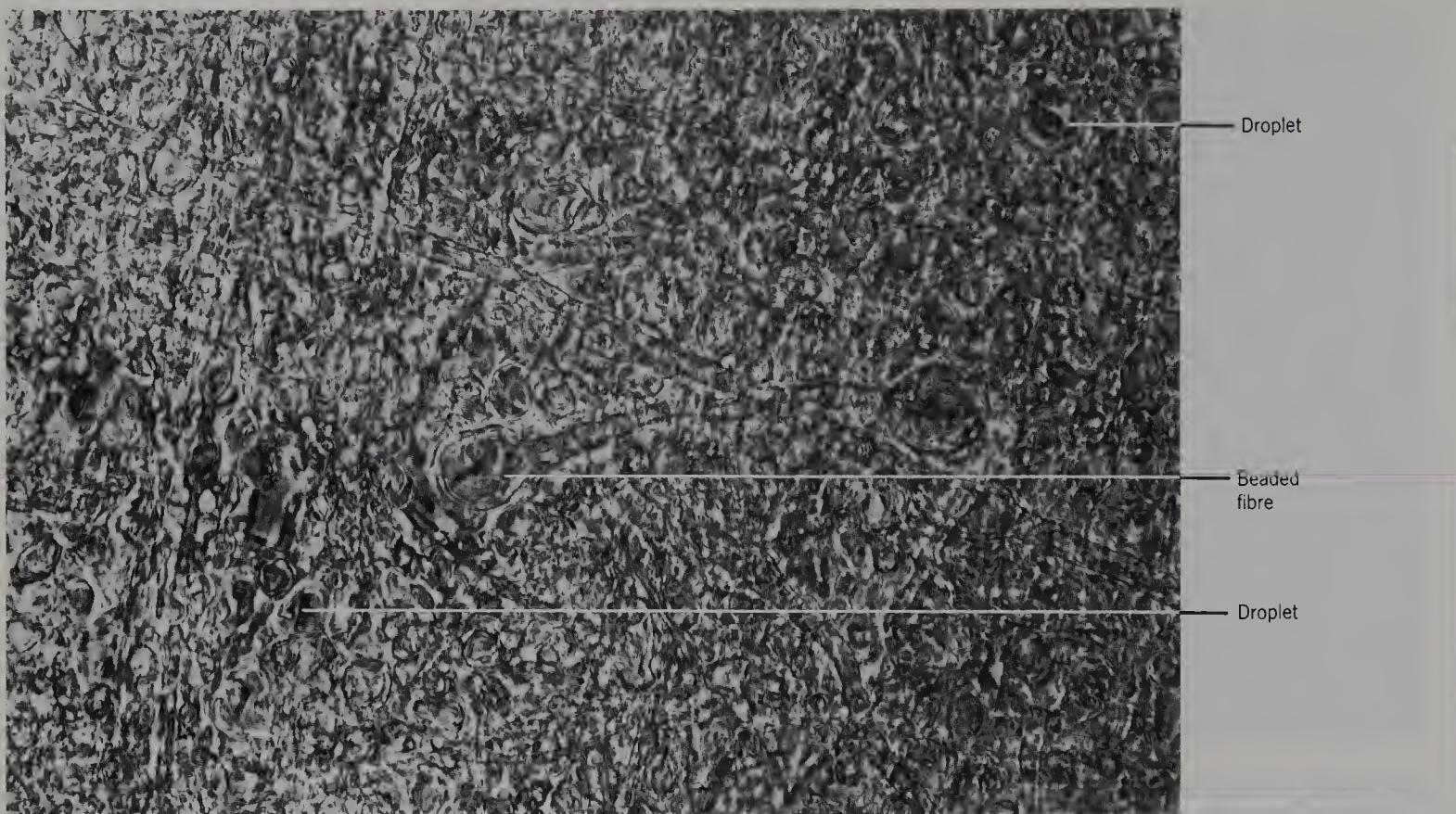


Figure 84 Thin slab of human frontal white matter from a 68-year-old male, to show beaded fibres and large droplets (phase contrast, $\times 700$).

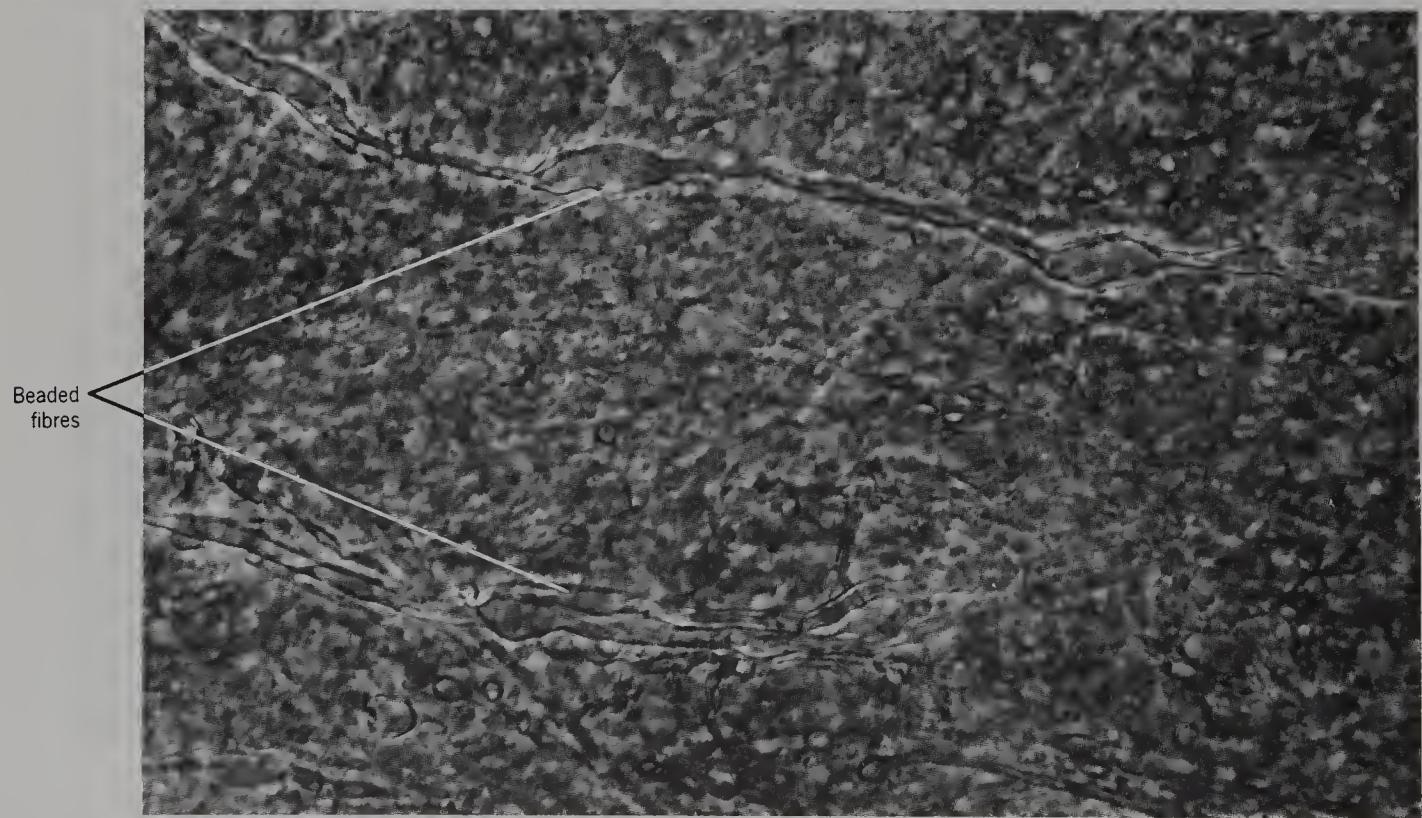


Figure 85 Thin slab of rat frontal white matter, to show large beaded fibres *in situ* (phase contrast, $\times 700$).

These droplets and beaded fibres were reported by Ehrenberg in 1833 and Remak in 1836, and more recently by Fernandez-Moran in 1952.

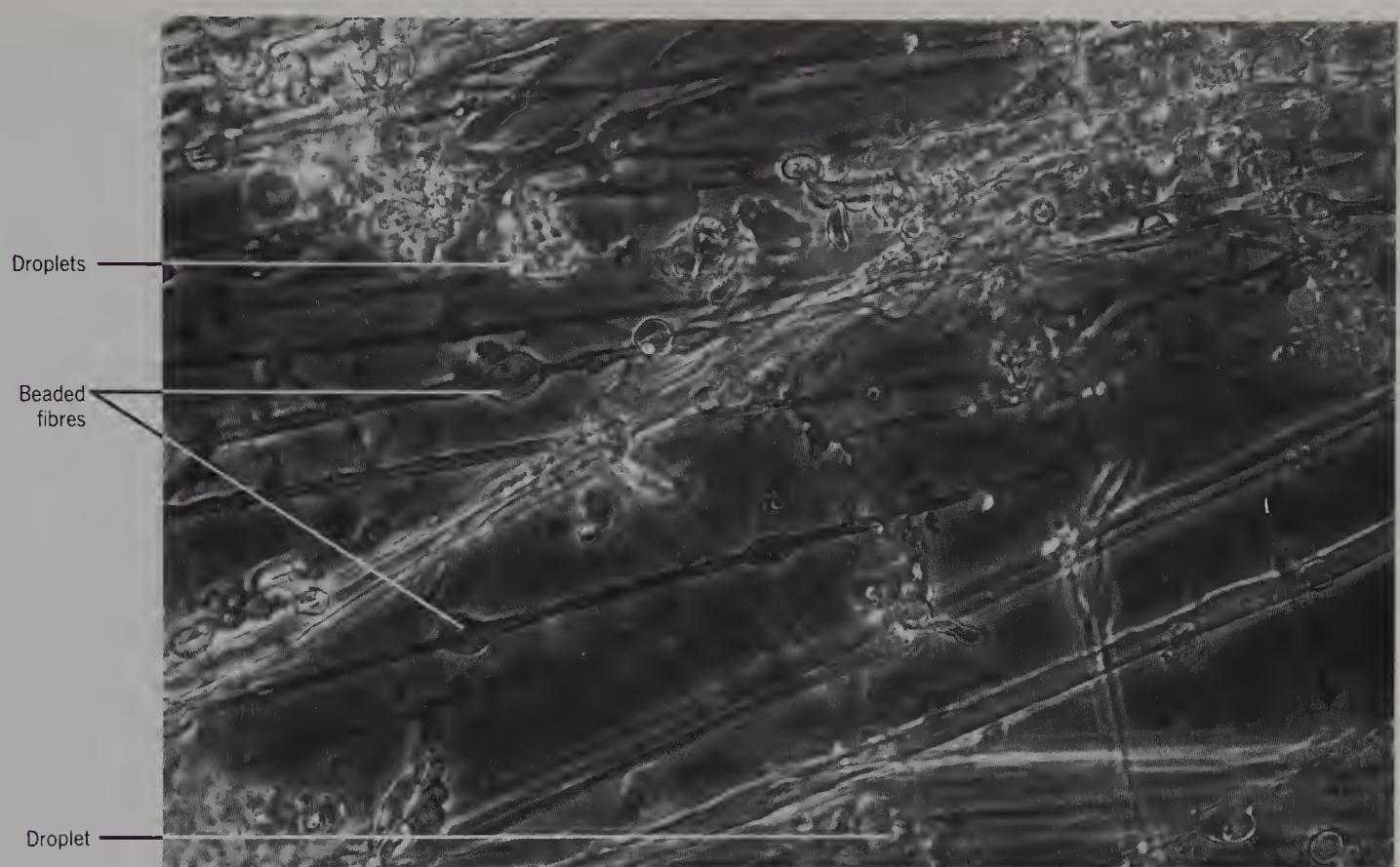


Figure 86 Partially teased human frontal white matter of an 84-year-old male, to show beaded fibres and droplets (phase contrast, $\times 700$).

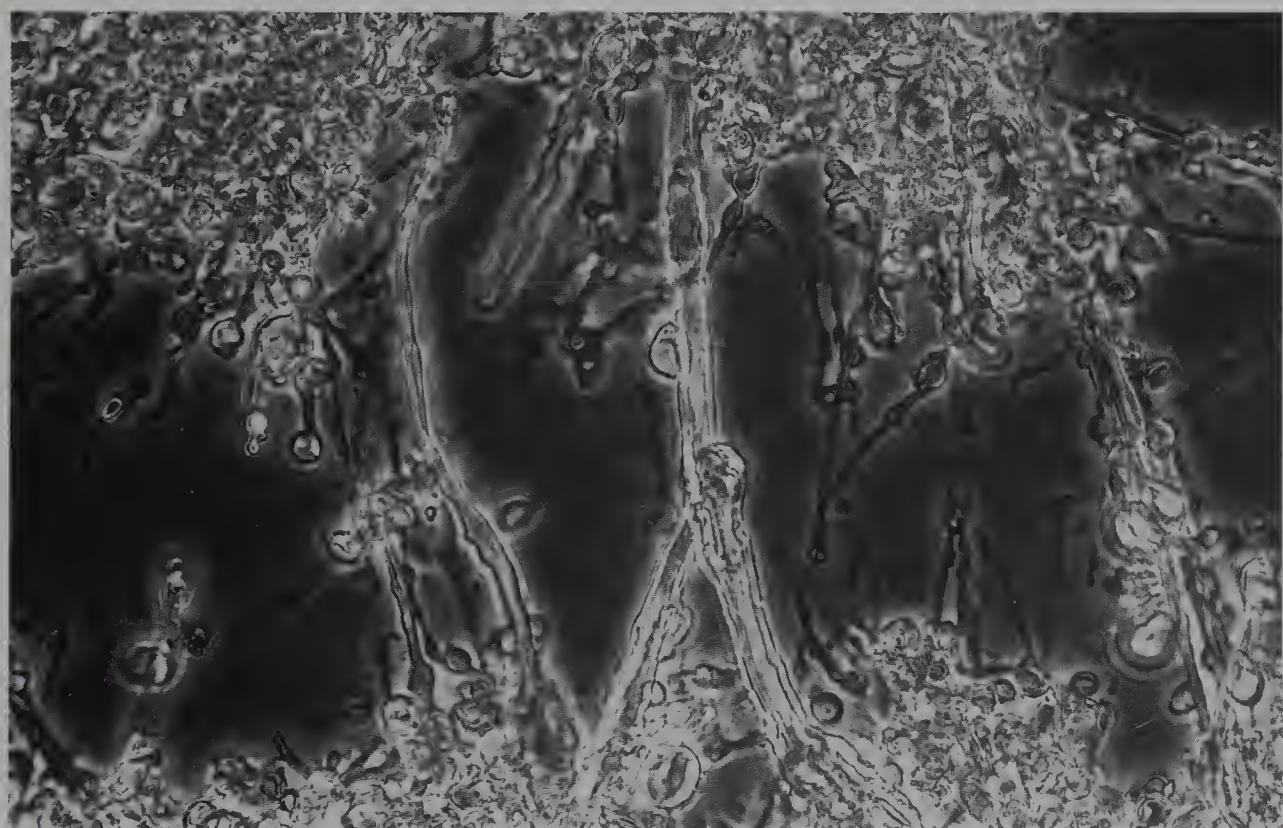


Figure 87 As previous figure, but from a 68-year-old male.

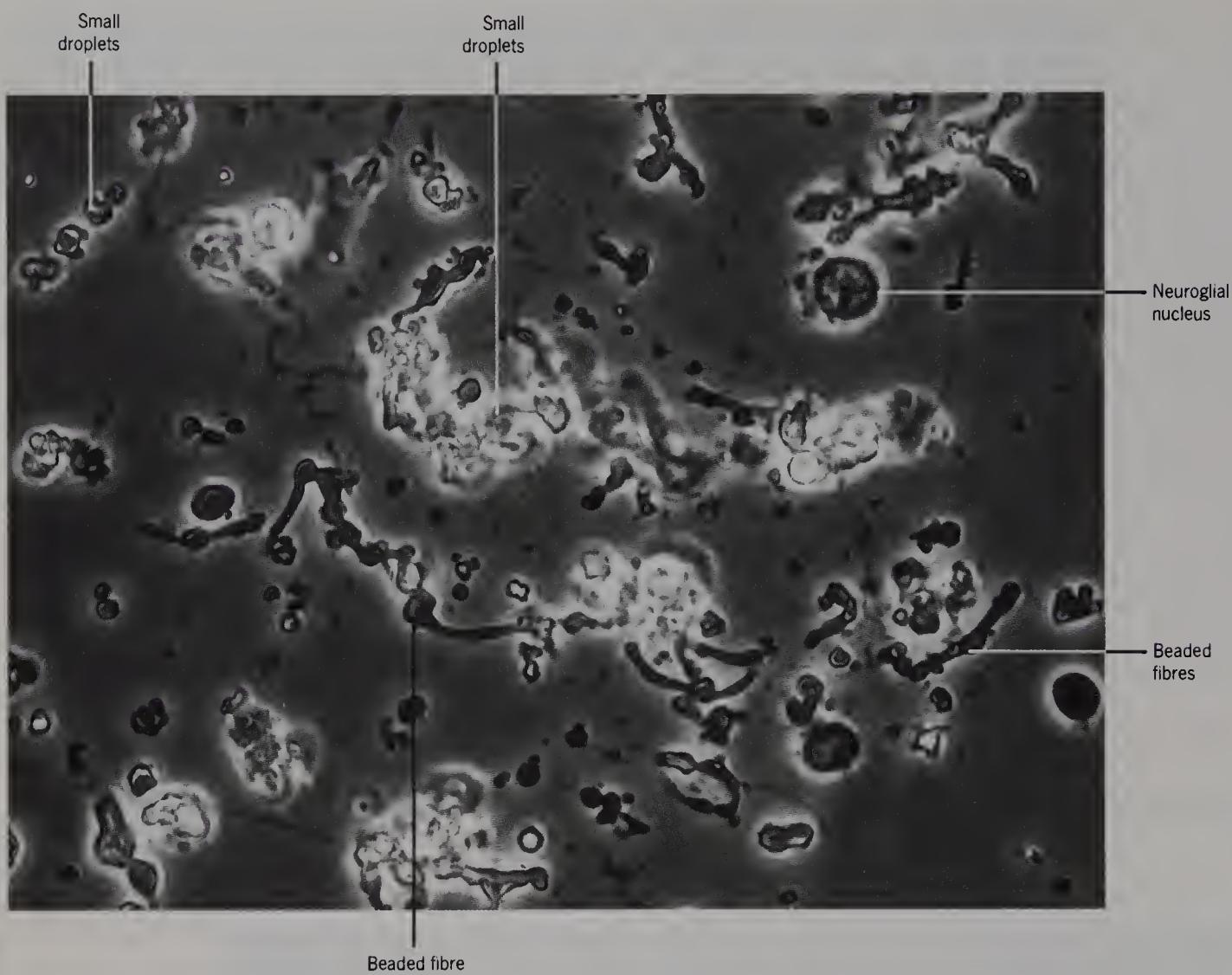


Figure 88 Teased human frontal white matter from a 77-year-old male, to show fine beaded fibres and small droplets (phase contrast, $\times 800$).

Neuroglial nuclei can be seen.

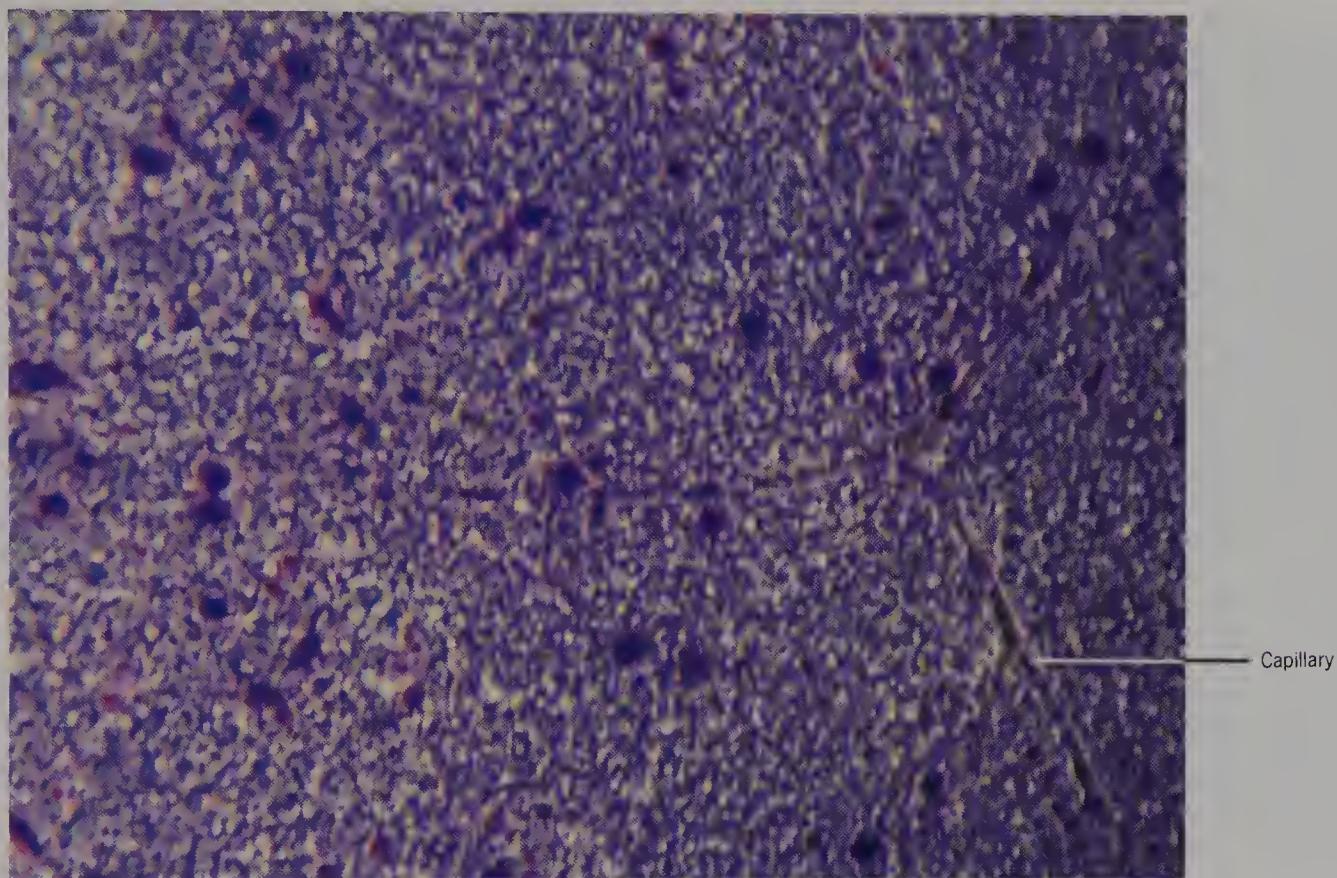


Figure 89 Thin slab of human parietal cortical grey matter from a 79-year-old male, lightly coloured with methylene blue to show the incidence of neuron somas (bright field, $\times 300$).

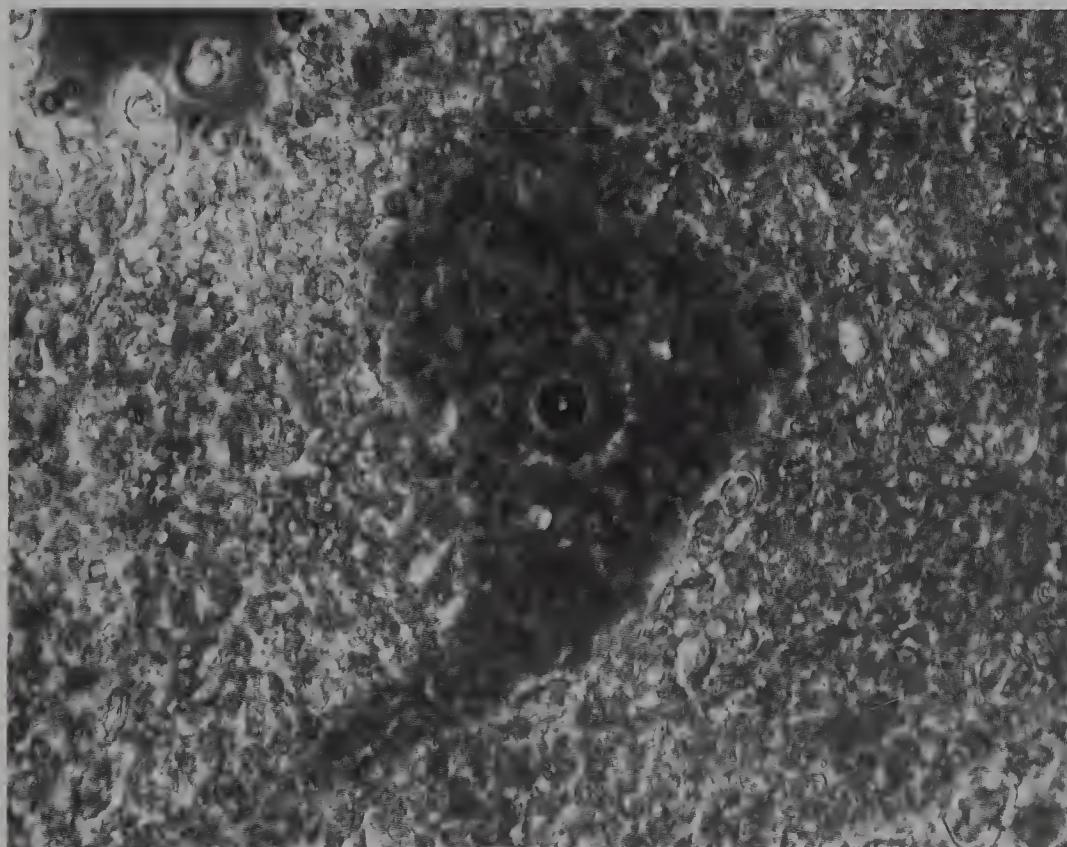


Figure 90 Thin slab of human parietal grey matter from a 53-year-old male, to show a Betz cell *in situ* (phase contrast, $\times 700$).

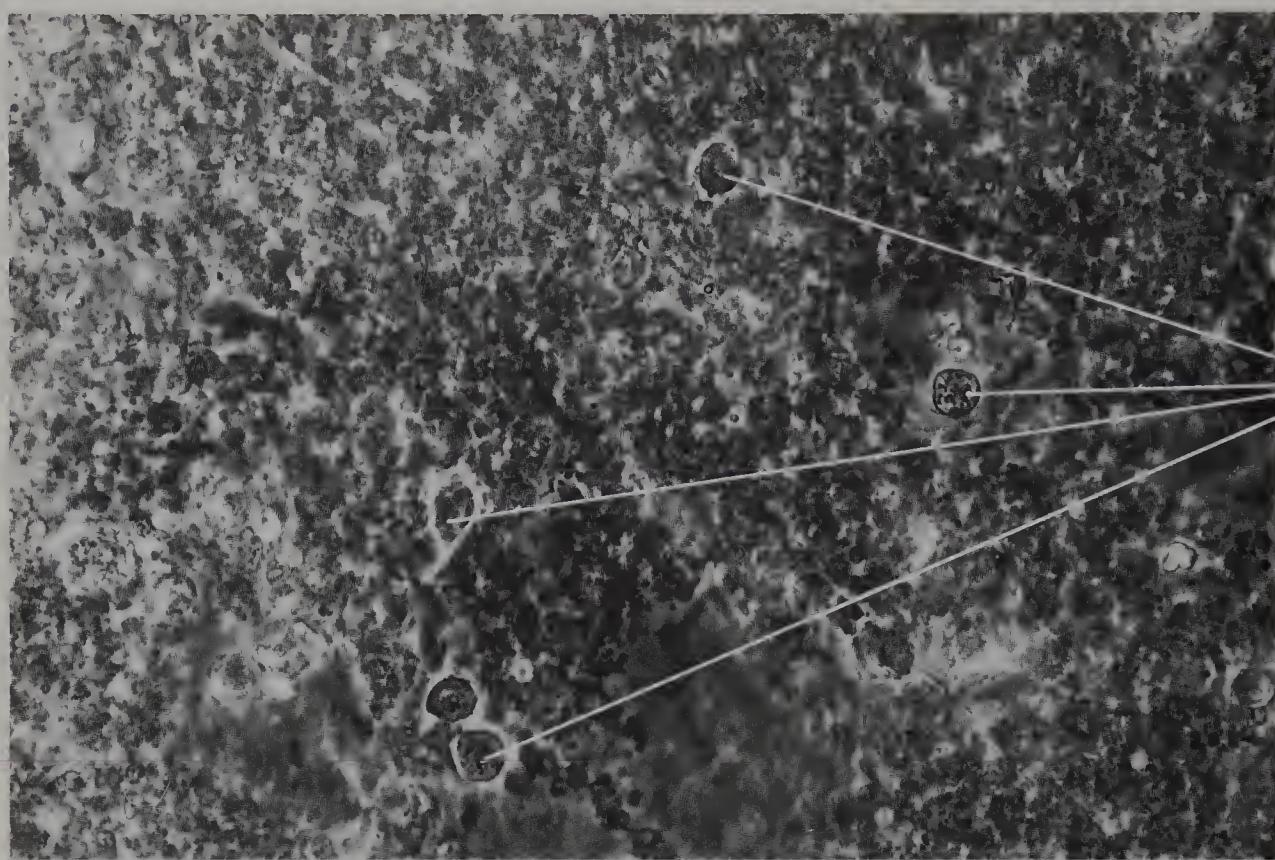


Figure 91 Thin slab of human parietal grey matter from a 68-year-old male to show neuroglial nuclei and fine granular material *in situ* (phase contrast, $\times 700$).

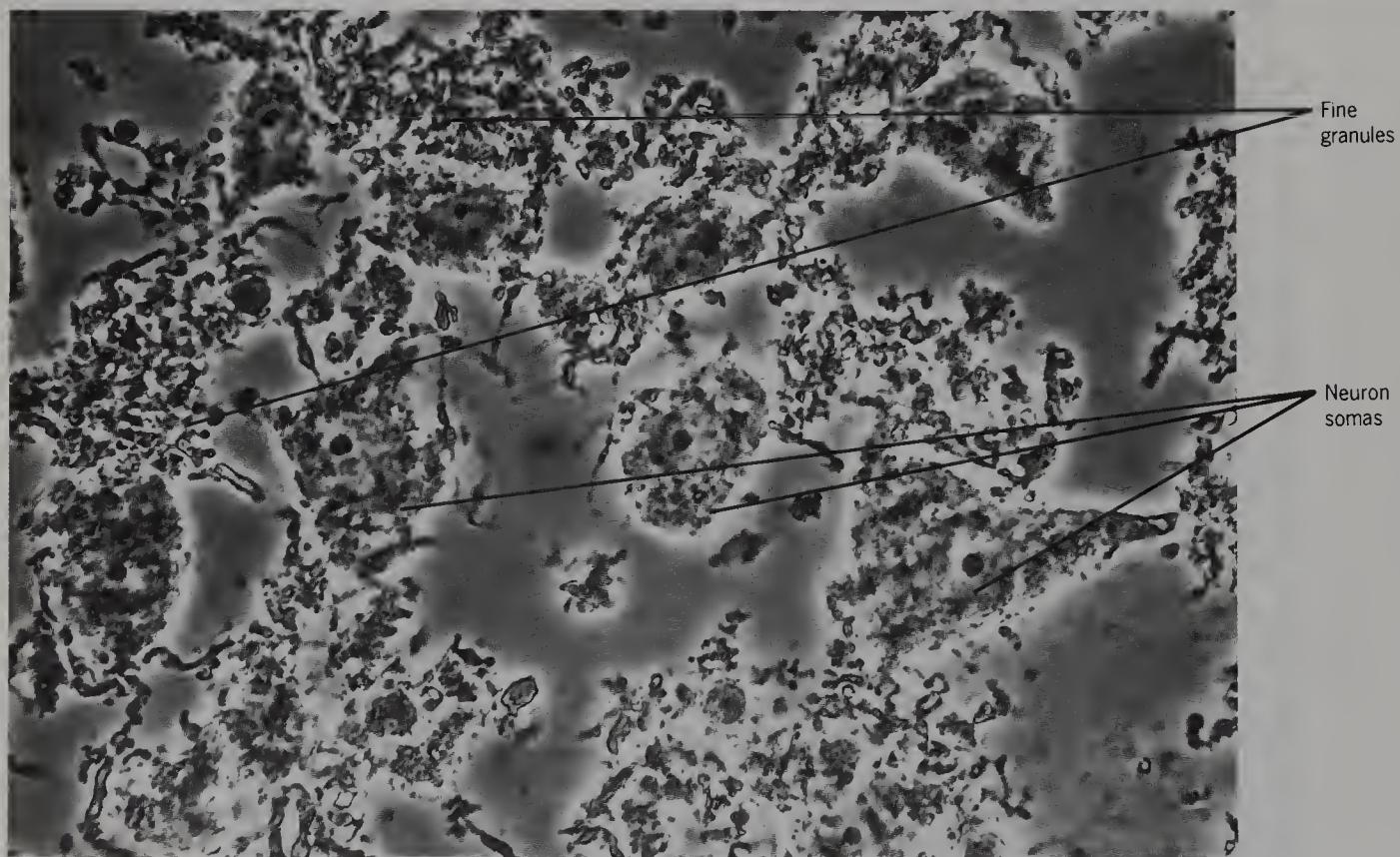


Figure 92 Teased adult rabbit parietal grey matter, to show neurons and fine granules (phase contrast, $\times 700$).

The appearance of isolated neurons was first reported by Remak in 1838.

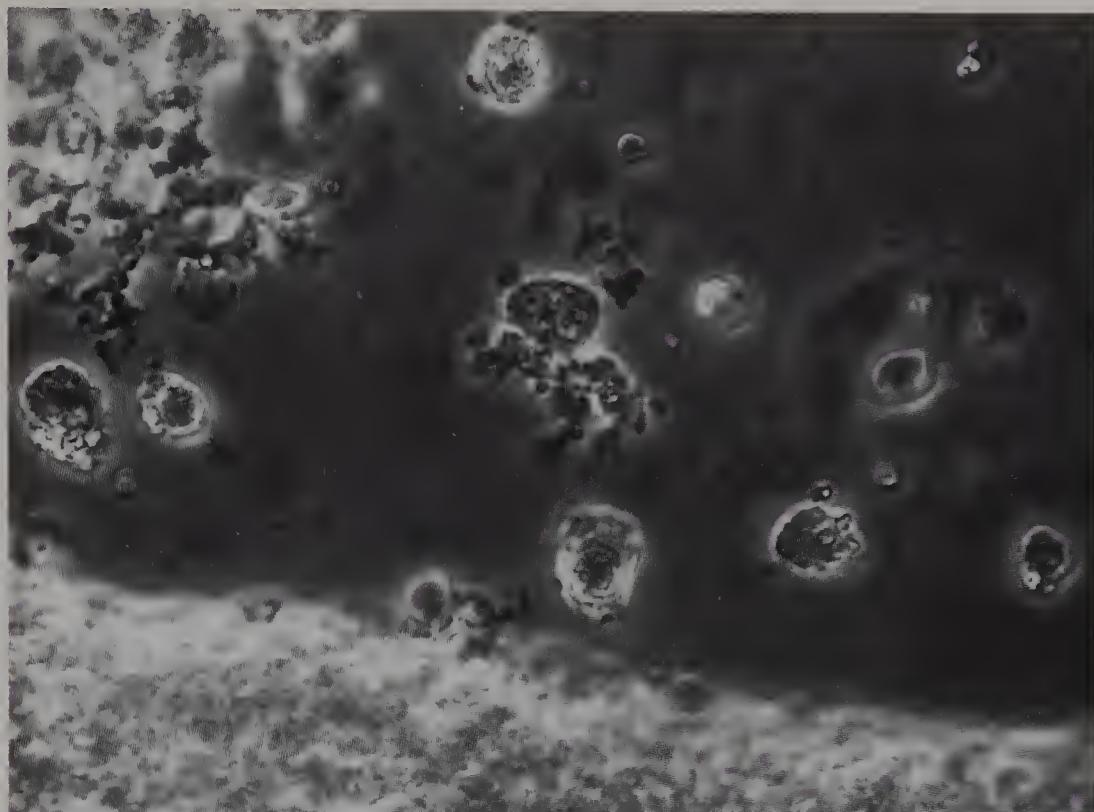


Figure 93 Teased human parietal grey matter from a 68-year-old male to show neuroglial nuclei or small neurons (phase contrast, $\times 700$).

Note the absence of fibres attached to these cells. Neuroglial nuclei were first described by Virchow in 1856.

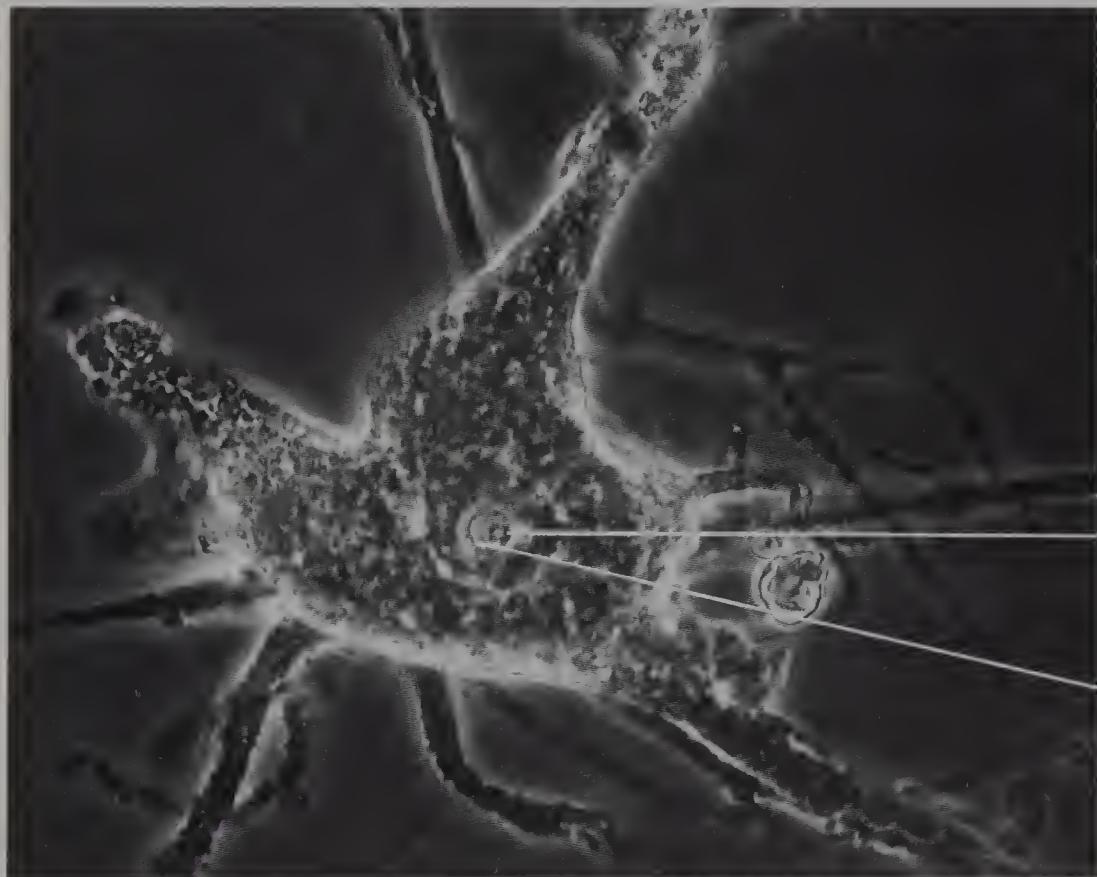


Figure 94 Isolated human Betz cell from the parietal grey matter of a 53-year-old male, to show nucleolar membrane, nucleolonema and dendrites (phase contrast, $\times 700$).

These Betz cells are rare. Betz also described the motor and sensory cortices in 1874.

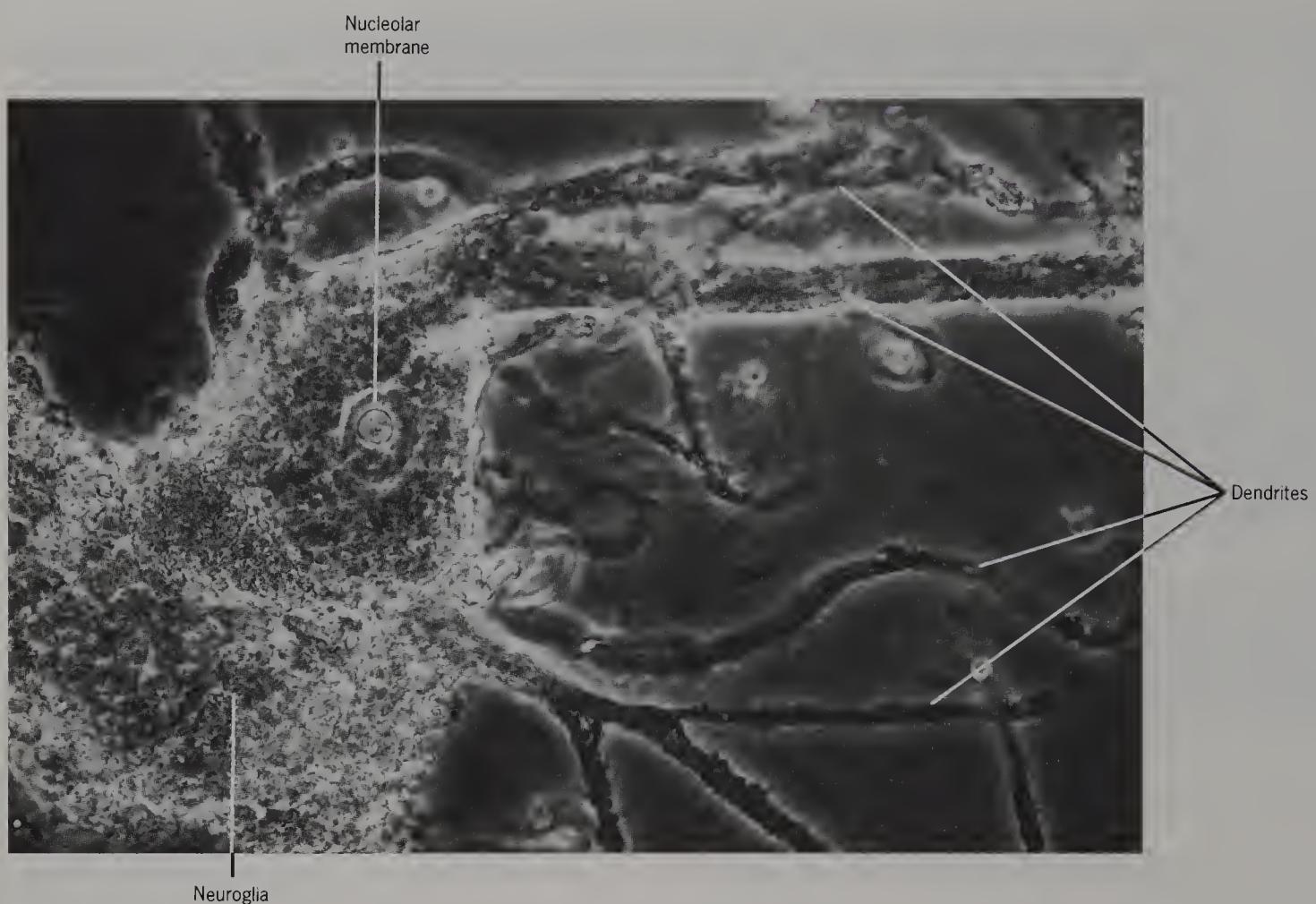


Figure 95 Isolated human Betz cell from parietal grey matter of a 55-year-old male, to show intracellular lipofuscin, a nucleolar membrane and adherent neuroglia (phase contrast, $\times 700$).

Lipofuscin was first seen in human brains by Obersteiner in 1903.

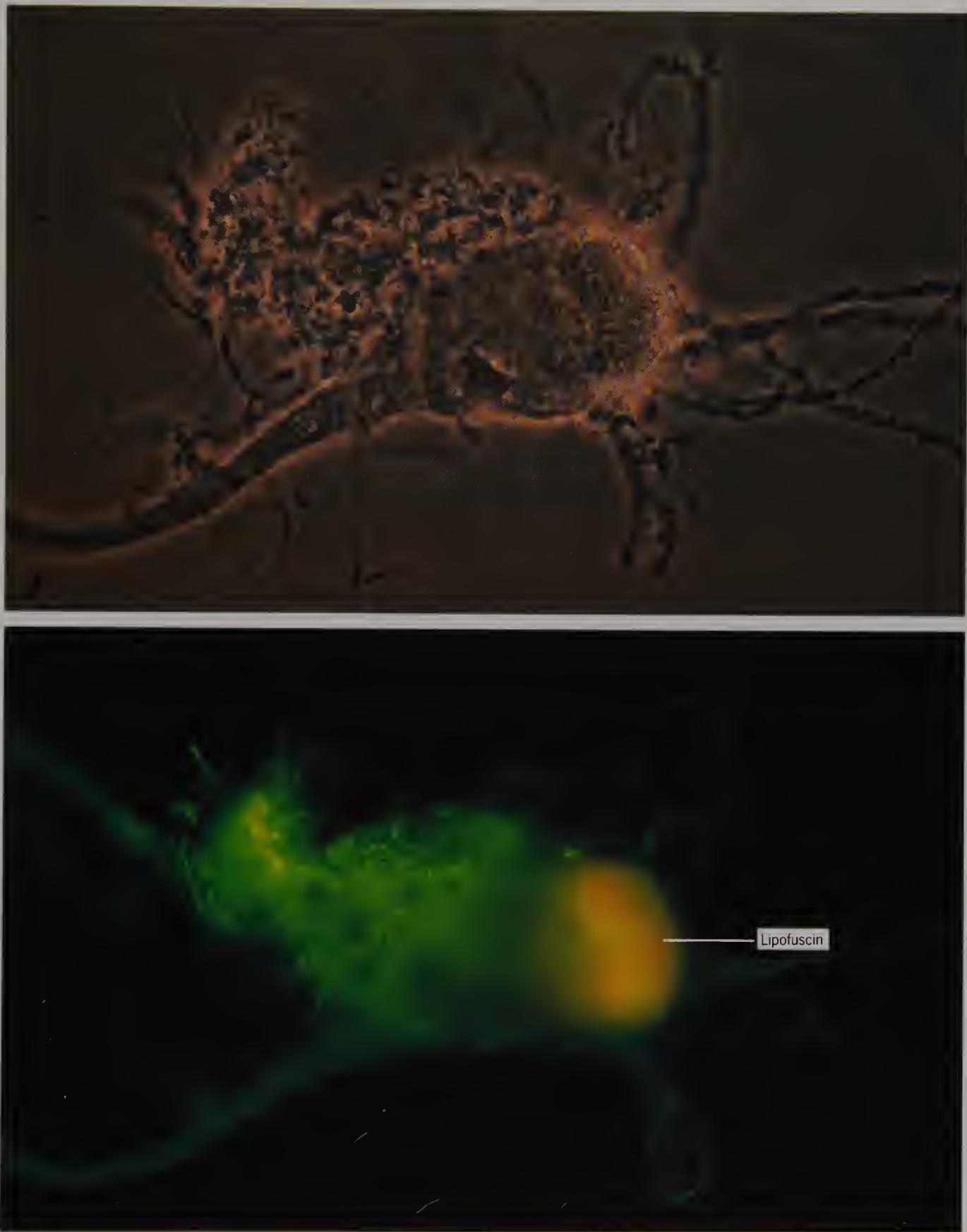


Figure 96 Isolated human Betz cell from an 82-year-old male, stained with anti-neurofilament 200 kD protein, by phase contrast (above) and after excitation with the blue light of 450–490 nm (below) ($\times 500$).

The autofluorescence of lipofuscin is increased after antibody staining. There is little fluorescence in dendrites or fine granular material, but some fine fibres in the neuroglia fluoresce intensely.

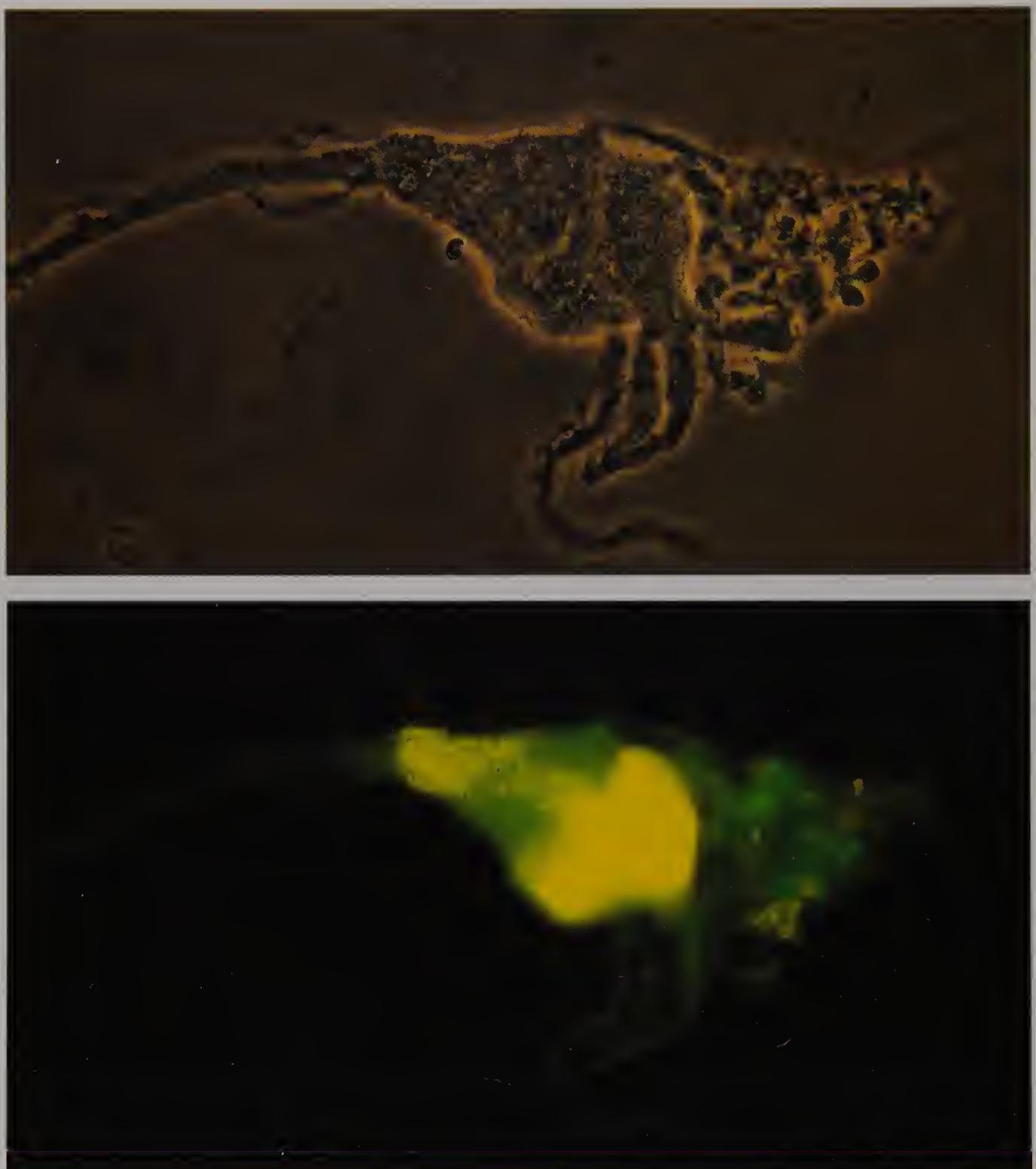


Figure 97 Isolated human Betz cell from an 82-year-old male, stained with anti-glial fibrillary acidic protein, by phase contrast (above) and after excitation with blue light of 450–490 nm (below) ($\times 500$).

Neither the dendrites nor the neuroglial fibres fluoresce. Compare with Figure 96.

Figure 98 Isolated clump of fine granular material from human parietal cortex of a 68-year-old male, and a neuroglial nucleus or small cell below it (phase contrast, $\times 800$).

This material is a major component of the neuroglia between neurons. Neuroglia was first described by Virchow in 1846.

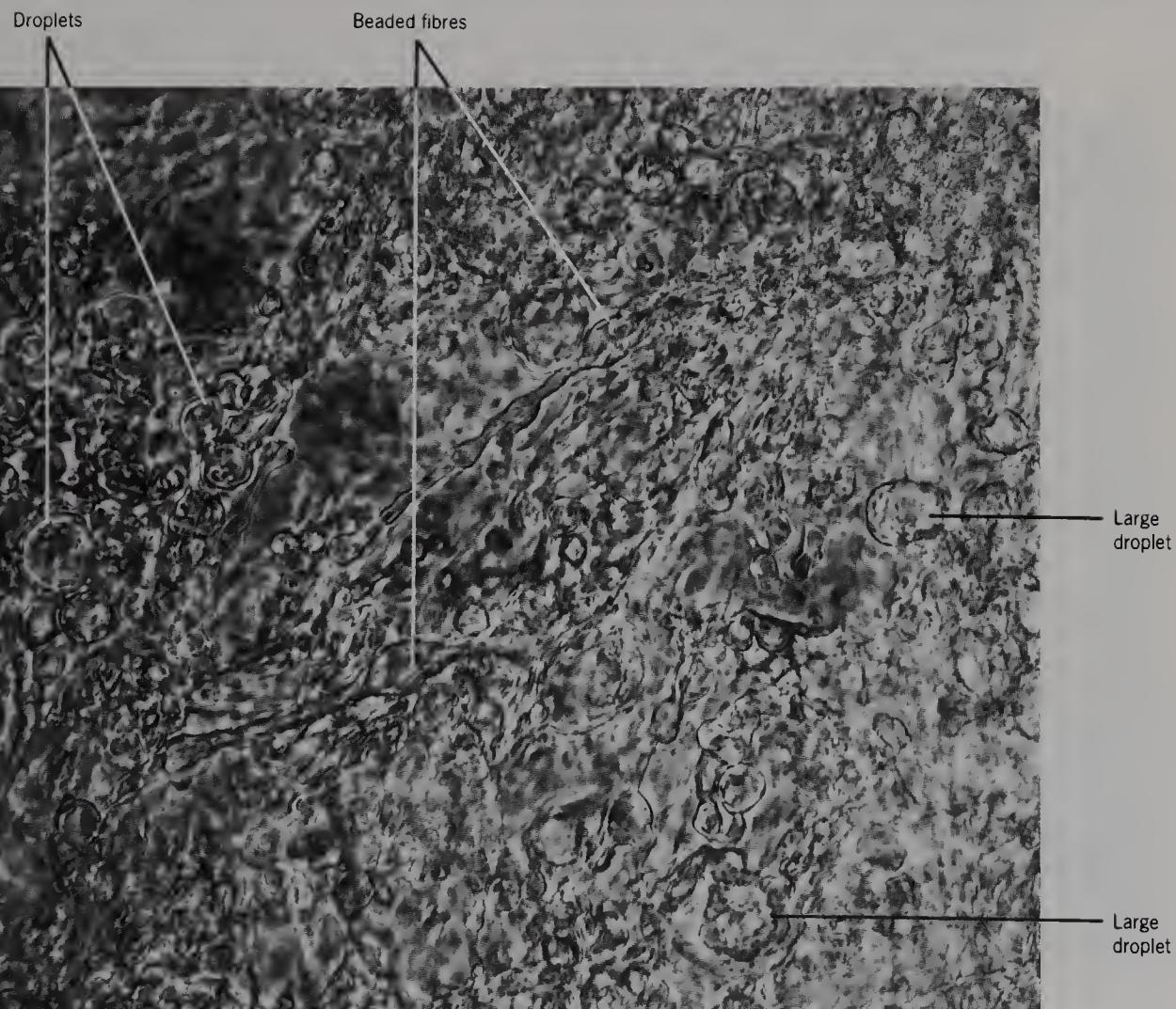


Figure 99 Partially teased thin slab of human parietal white matter from a 68-year-old male, to show beaded fibres and large droplets (phase contrast, $\times 800$).



Figure 100 Thin slab of adult rabbit paraventricular parietal white matter, to show beaded fibres and droplets (phase contrast, $\times 700$).

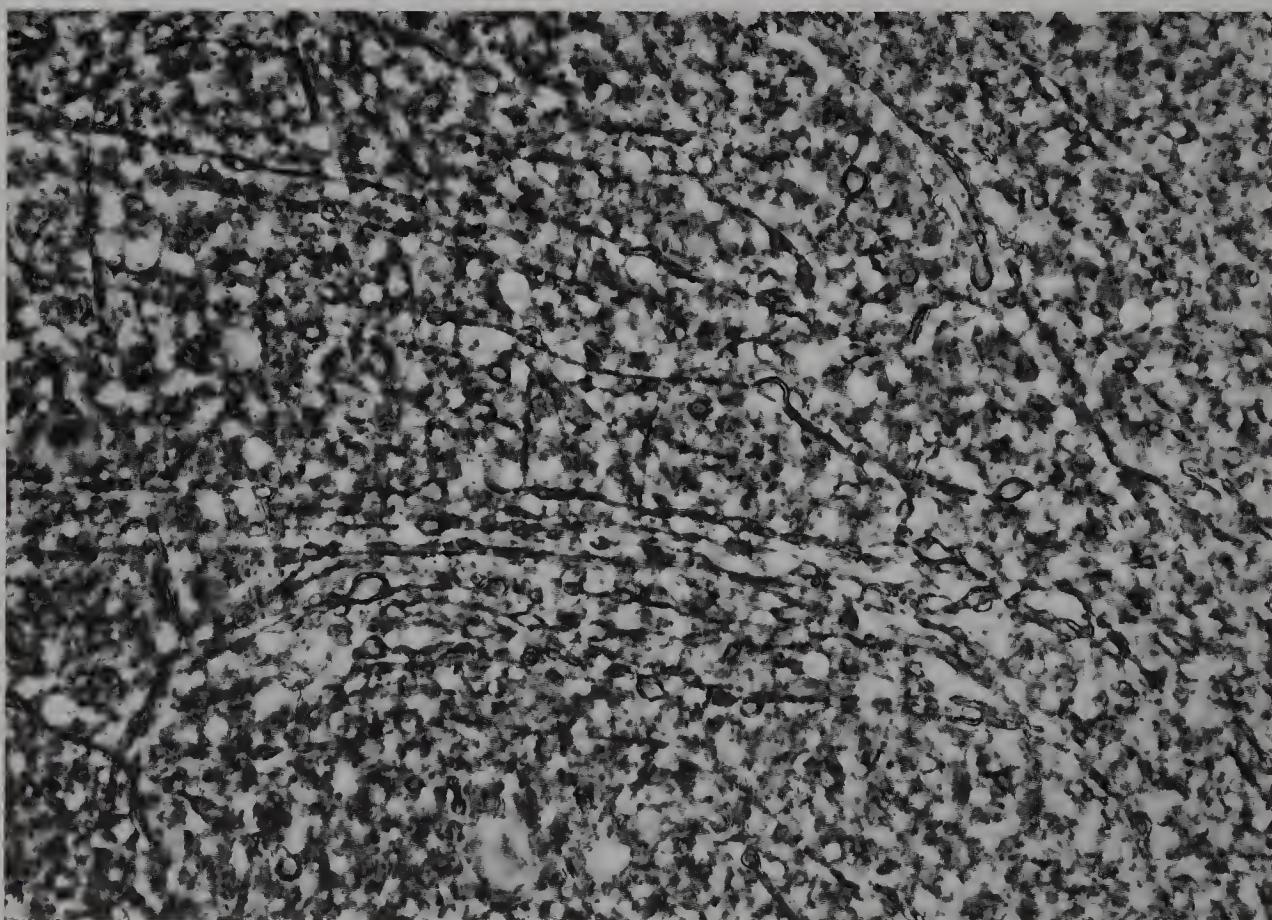


Figure 101 Thin slab of guinea-pig parietal white matter to show fibres (phase contrast, $\times 700$).

White matter was first described by de Vieussens in 1684.



Figure 102 Partially teased thin slab of human parietal white matter from a 68-year-old male, to show beaded fibres travelling in several directions (phase contrast, $\times 700$).

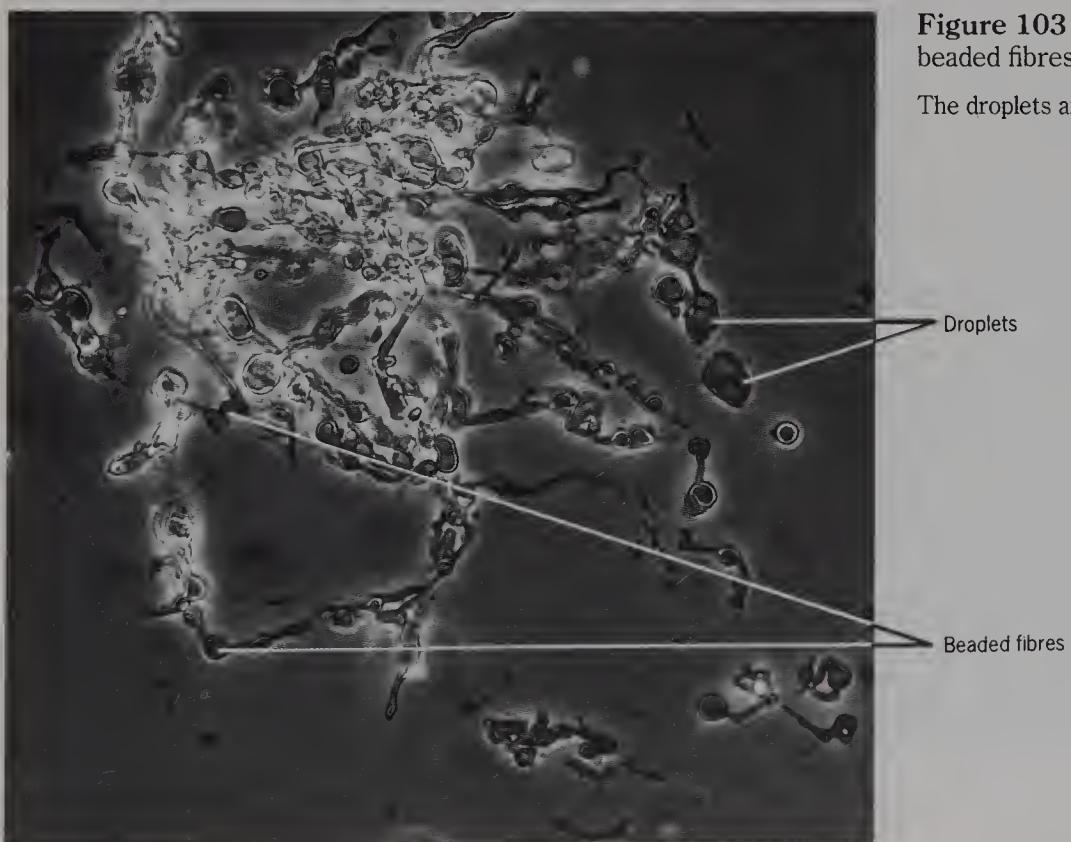


Figure 103 As previous figure, showing teased beaded fibres and droplets (phase contrast, $\times 700$).
The droplets are very refractile.



Figure 104 Thin slab of human temporal grey matter from a 79-year-old male, lightly coloured with methylene blue to show the incidence of neuron somas (bright field, $\times 110$).

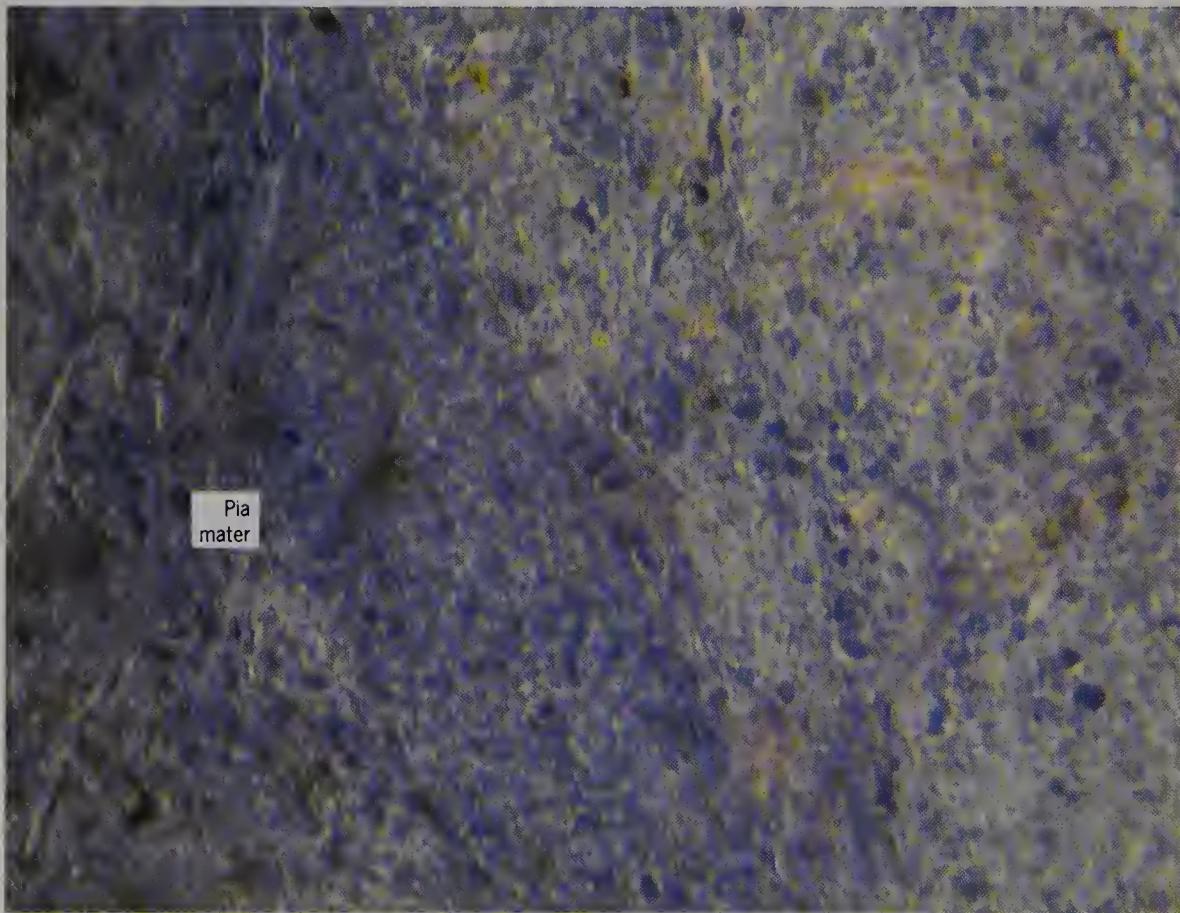


Figure 105 Thin slab of human temporal cortex from a 79-year-old male, lightly coloured with methylene blue, covered by the pia mater on the left (bright field, $\times 255$).

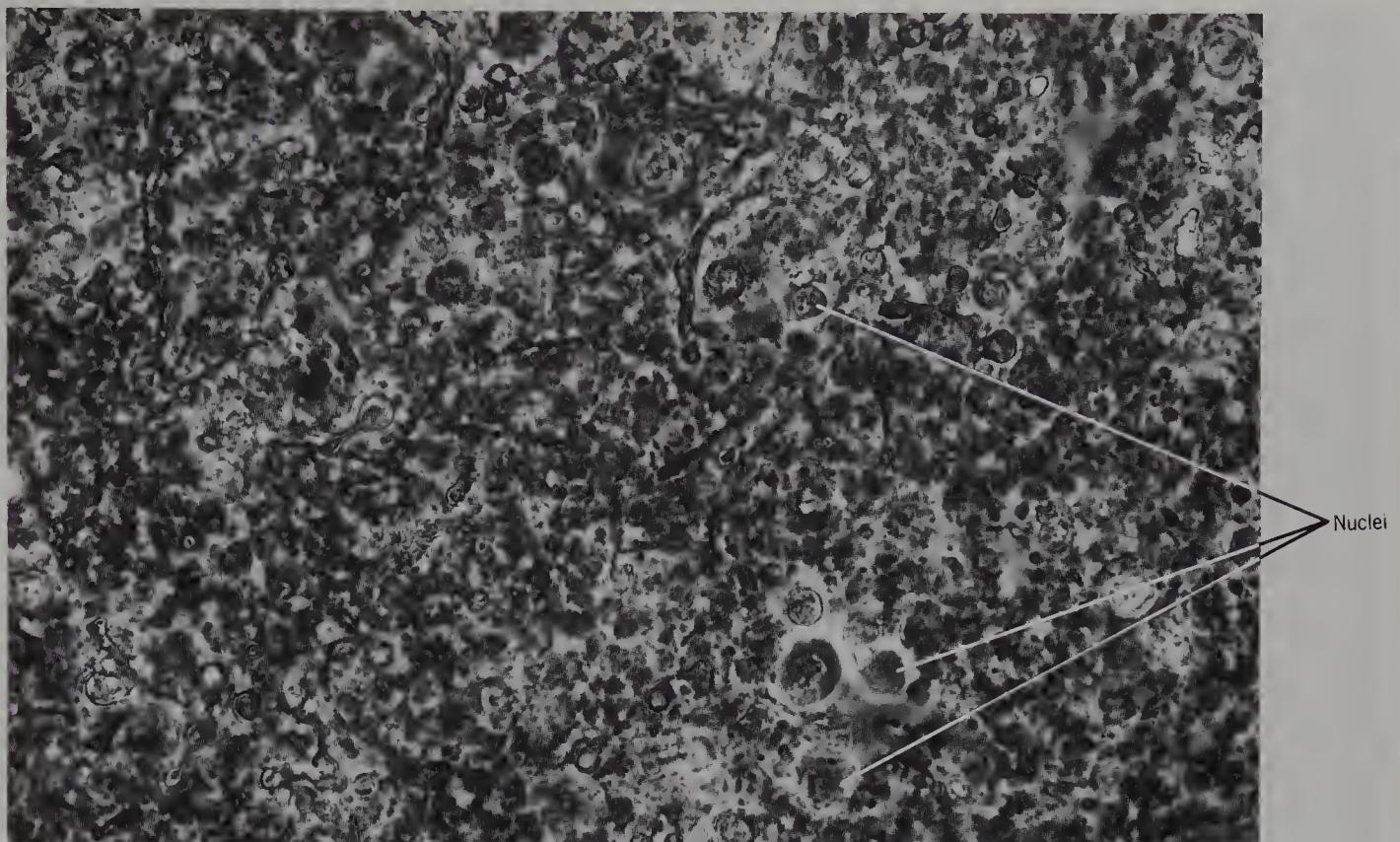


Figure 106 Thin slab of human temporal grey matter from a 73-year-old male, to show neuronal somas and beaded fibres (phase contrast, $\times 700$).

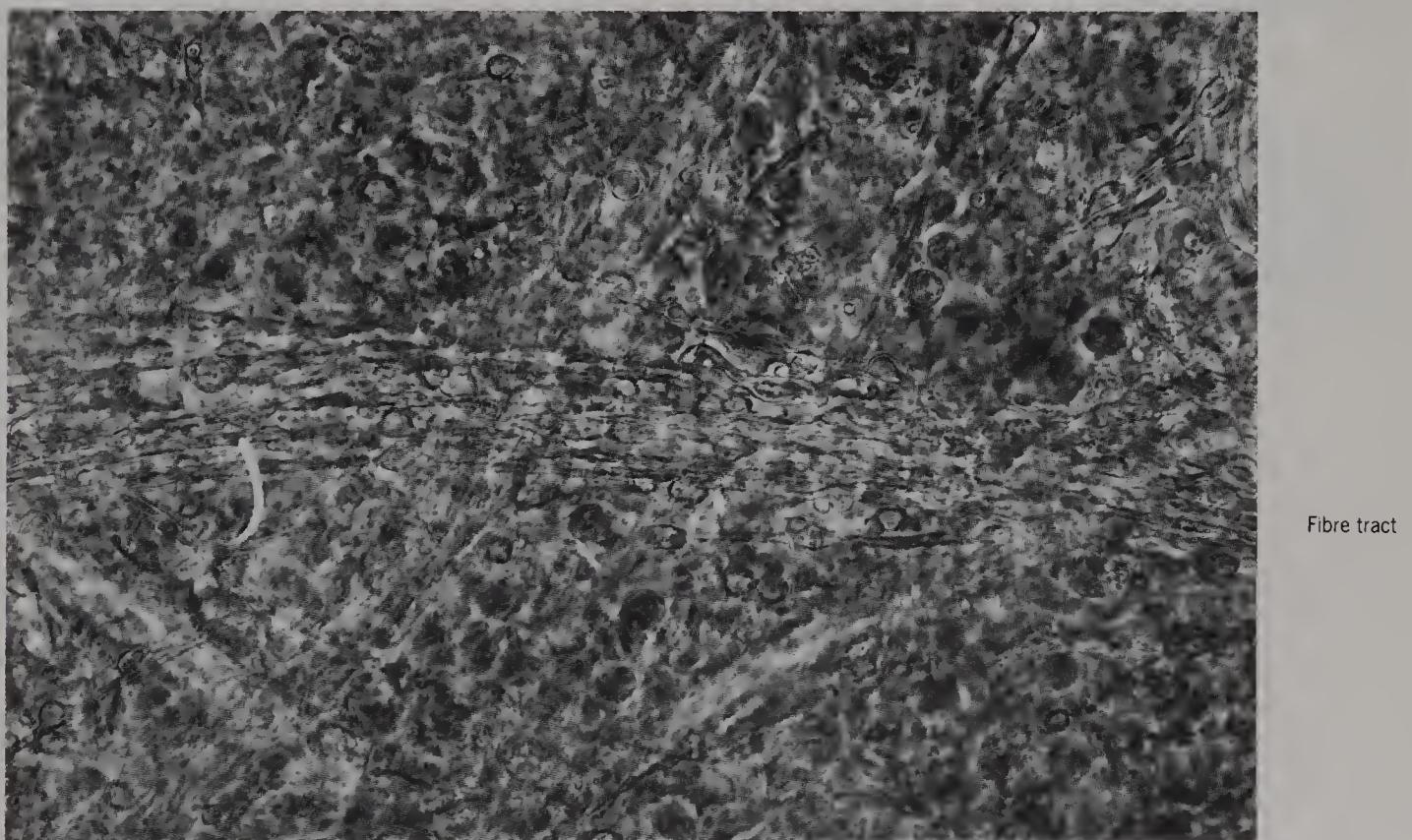


Figure 107 Thin slab of human temporal grey matter from an 84-year-old male, to show a beaded fibre tract passing through (phase contrast, $\times 700$).

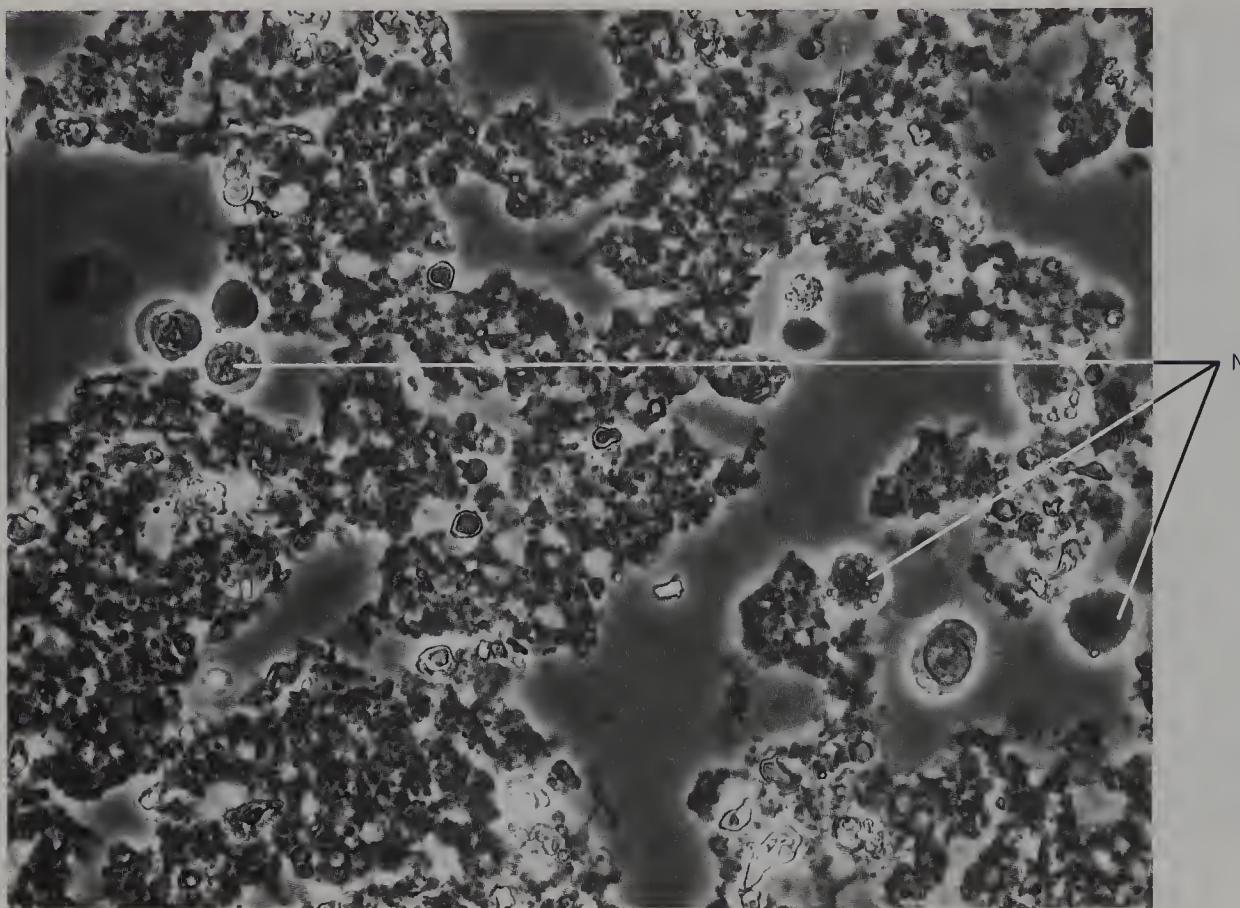
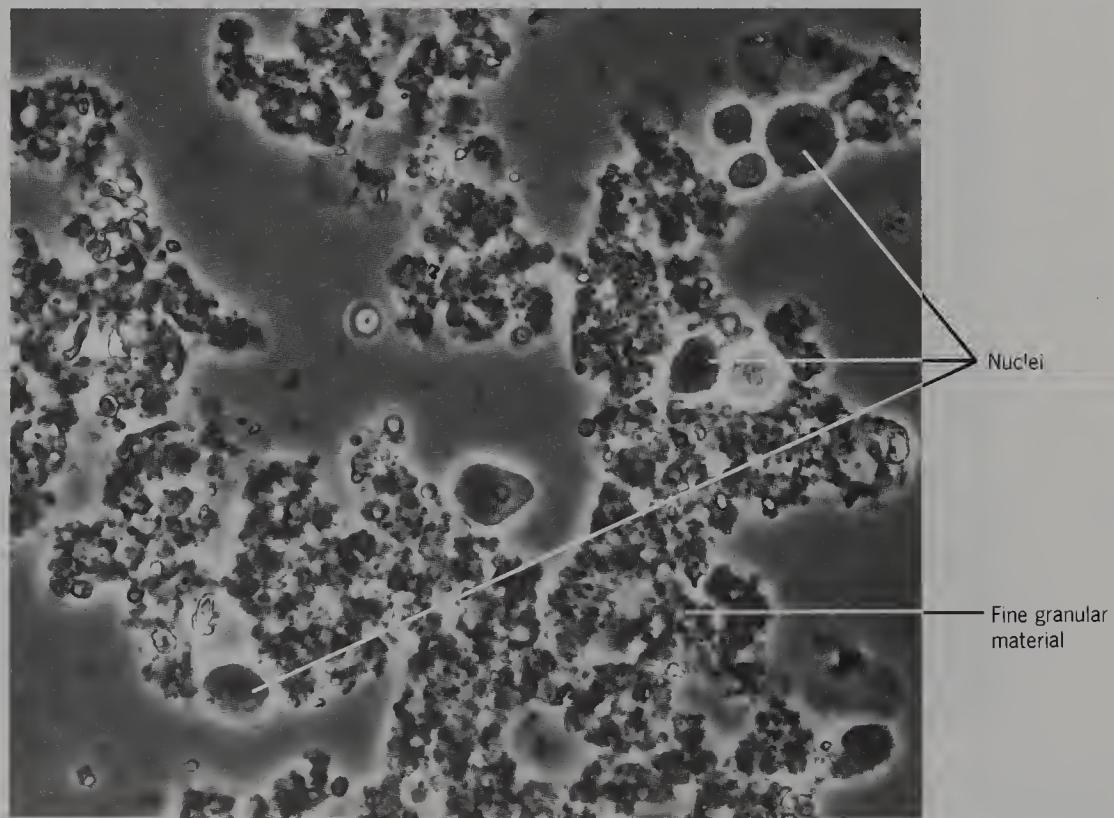


Figure 108 Teased human temporal grey matter of an 84-year-old male, to show cells with large nuclei and fine granular material (phase contrast, $\times 700$).

Figure 109 Teased human temporal grey matter from a 73-year-old male, to show small neurons or neuroglial nuclei and fine granular material (phase contrast, $\times 700$).



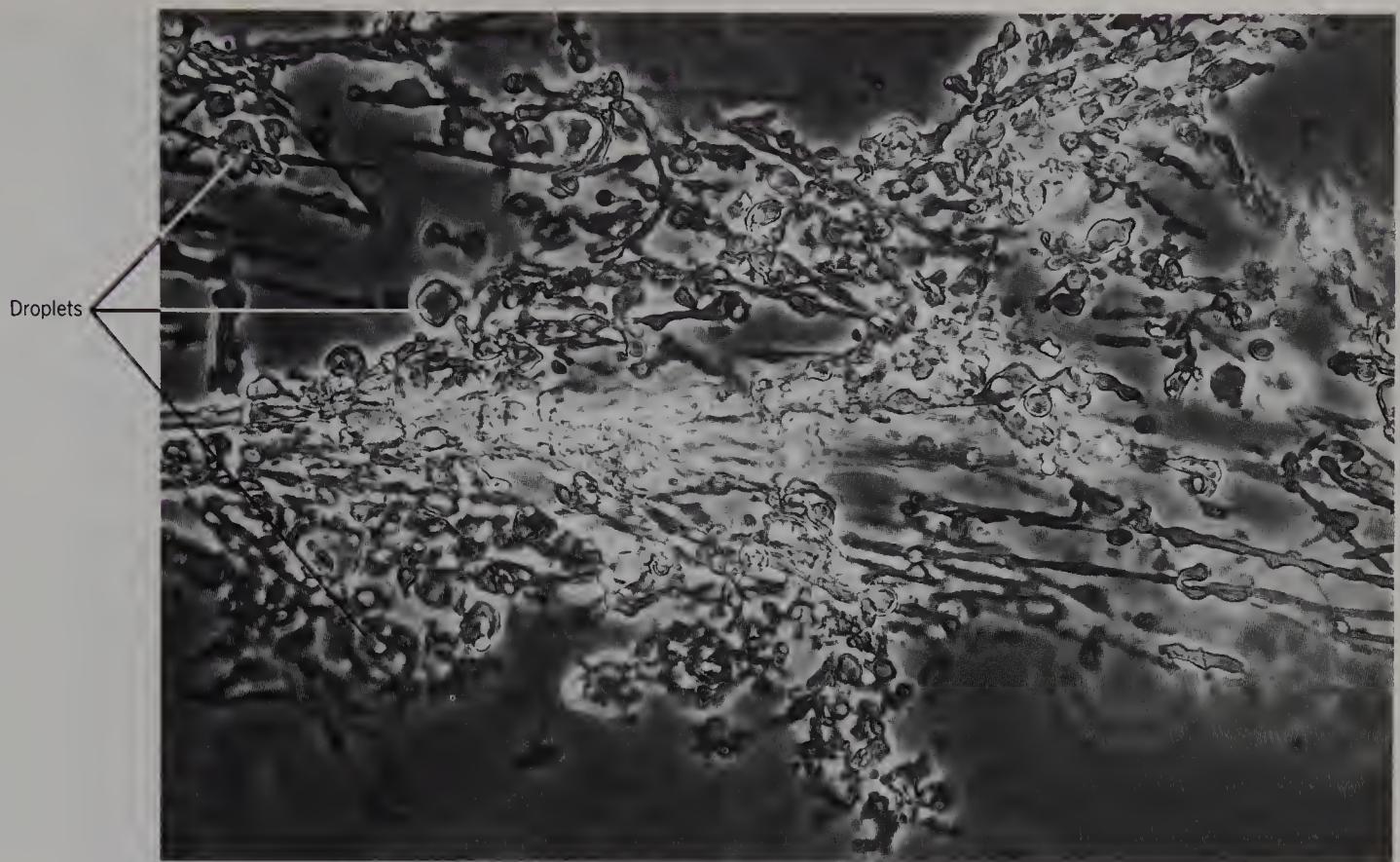


Figure 110 Teased human temporal white matter from an 84-year-old male, to show beaded fibres and droplets (phase contrast, $\times 700$).

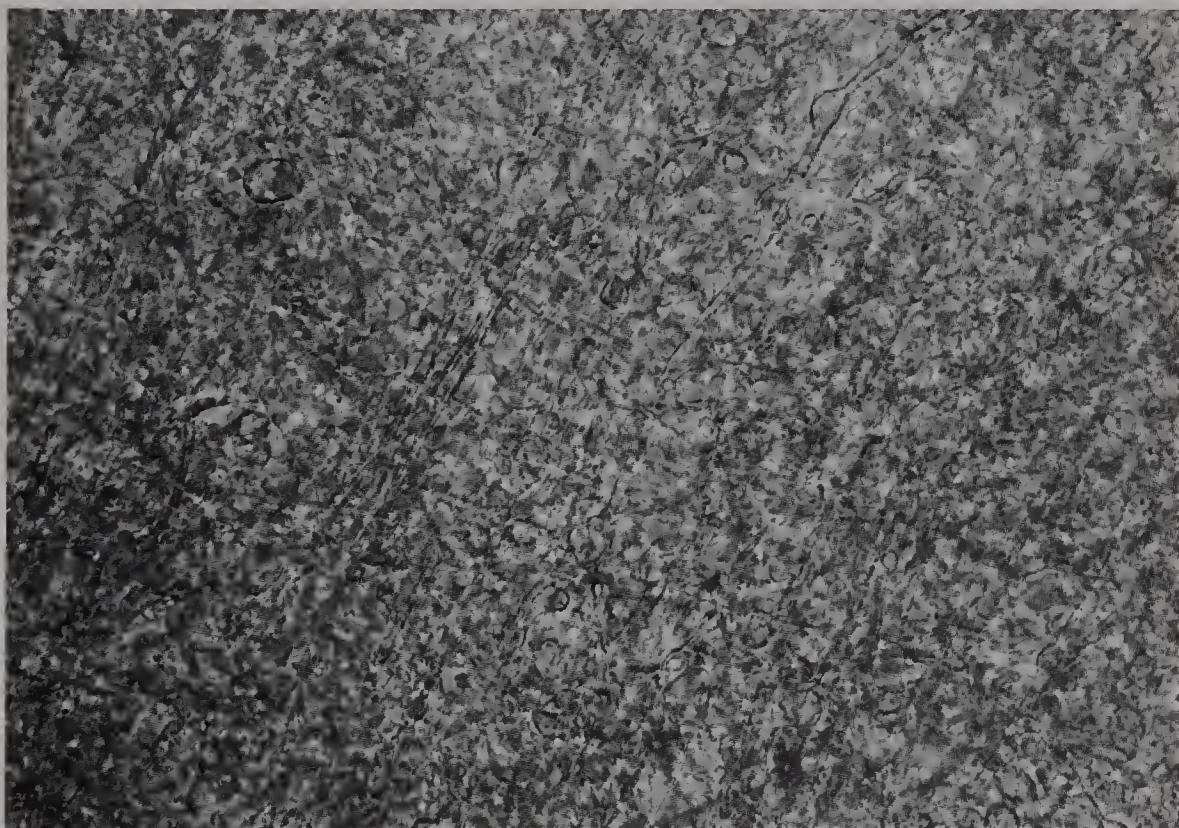


Figure 111 Thin slab of human temporal white matter from an 84-year-old male, to show small beaded fibres (phase contrast, $\times 640$).

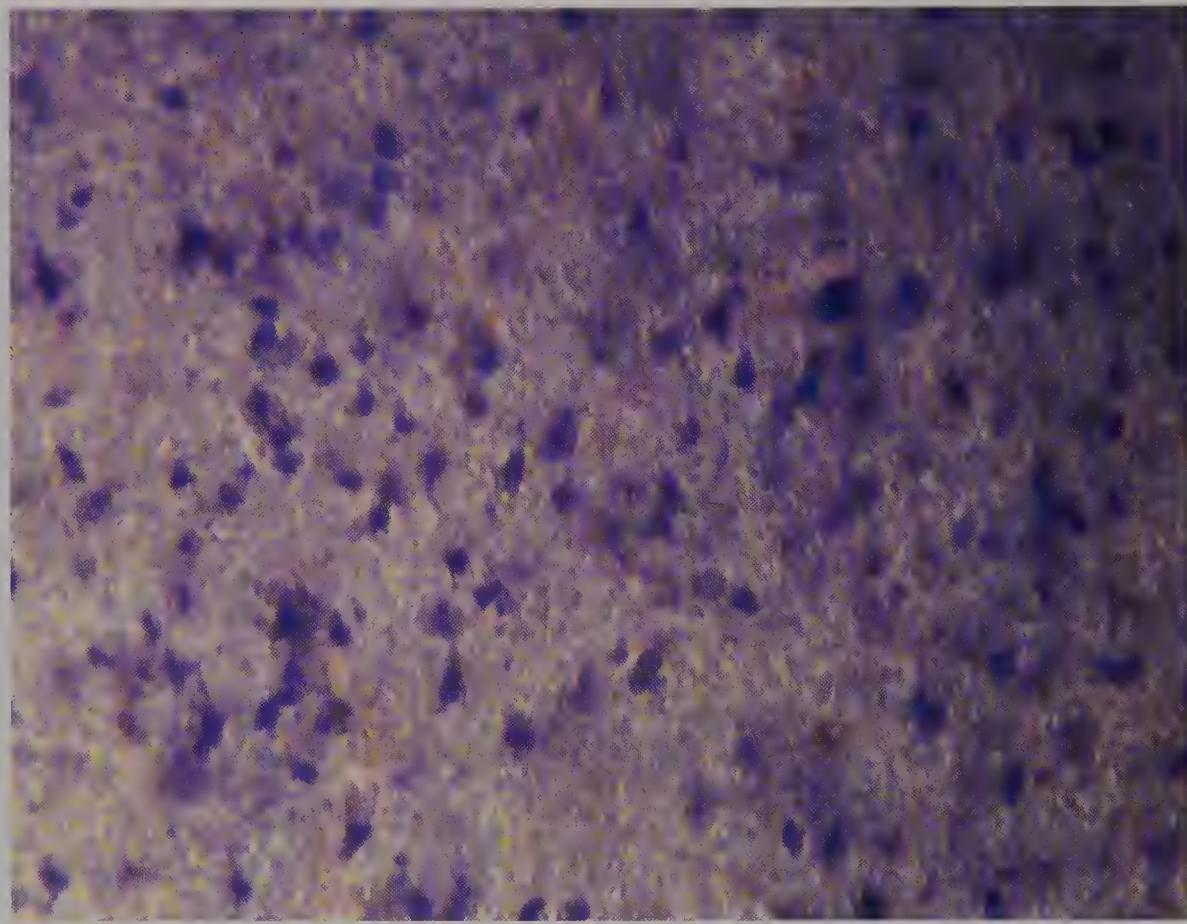
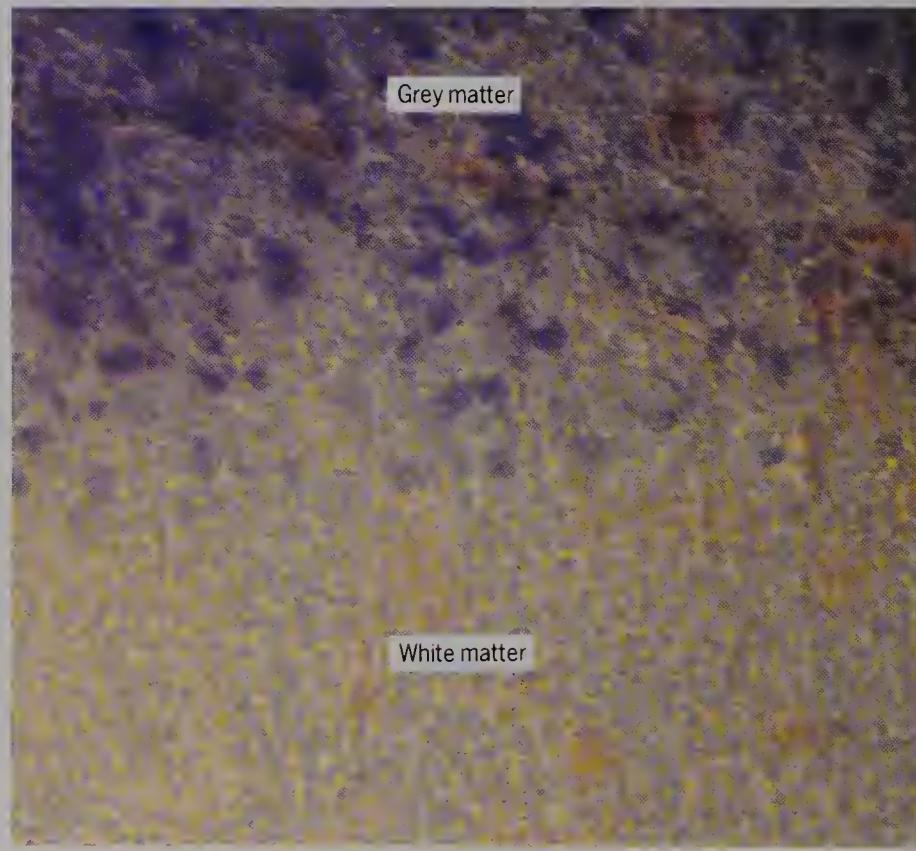


Figure 112 Thin slab of human occipital grey matter from a 79-year-old male, lightly coloured with methylene blue to show the incidence of neuron somas (bright field, $\times 300$).

Figure 113 Thin slab of human occipital grey-white matter boundary from a 79-year-old male, lightly coloured with methylene blue (bright field, $\times 300$).



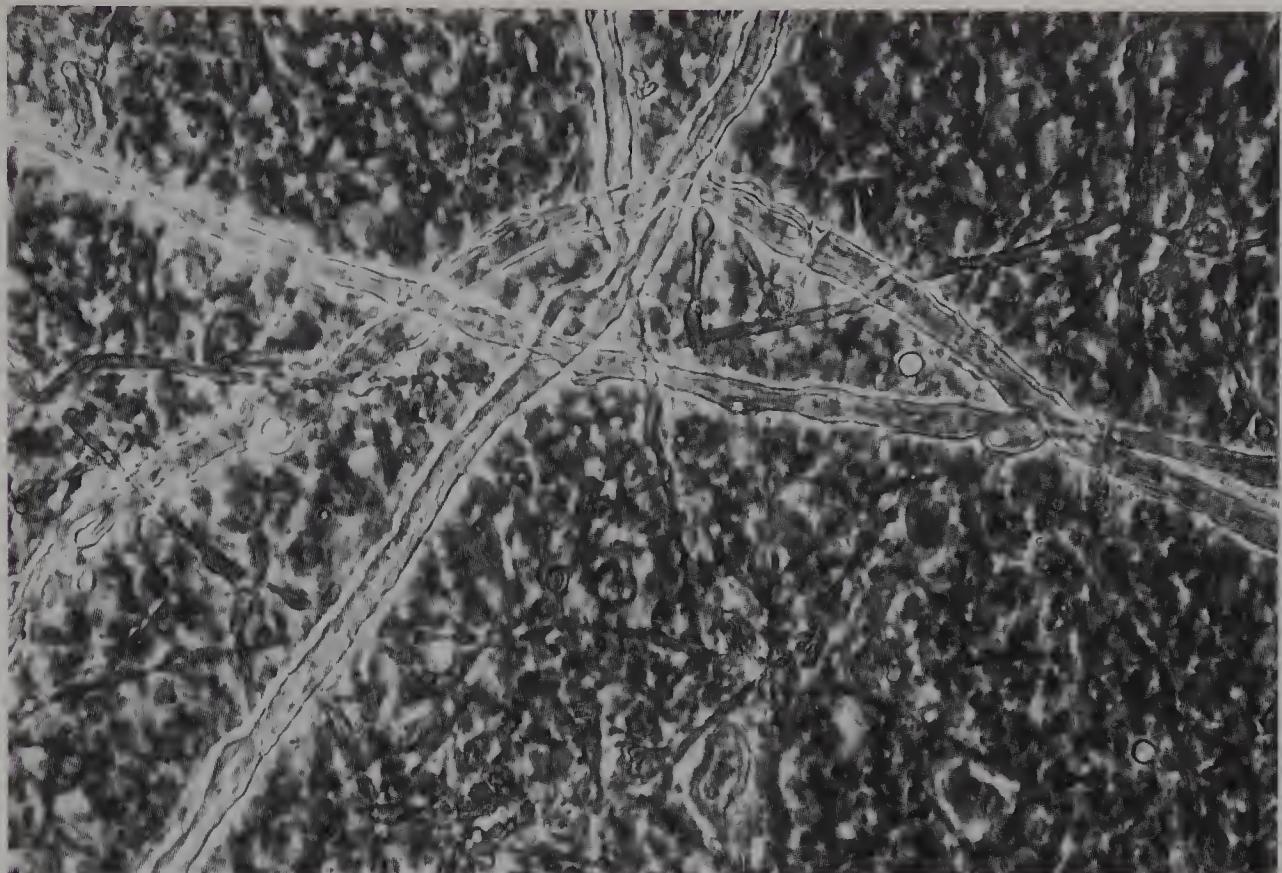


Figure 114 Thin slab of human occipital grey matter from a 68-year-old male, to show large beaded fibres (phase contrast, $\times 700$).



Figure 115 Thin slab of human occipital grey matter from a 68-year old male, to show neurons *in situ* (phase contrast, $\times 700$).



Figure 116 Thin slab of human occipital grey matter from a 55-year-old male, to show birefringence of fibres (polarized light, $\times 130$).

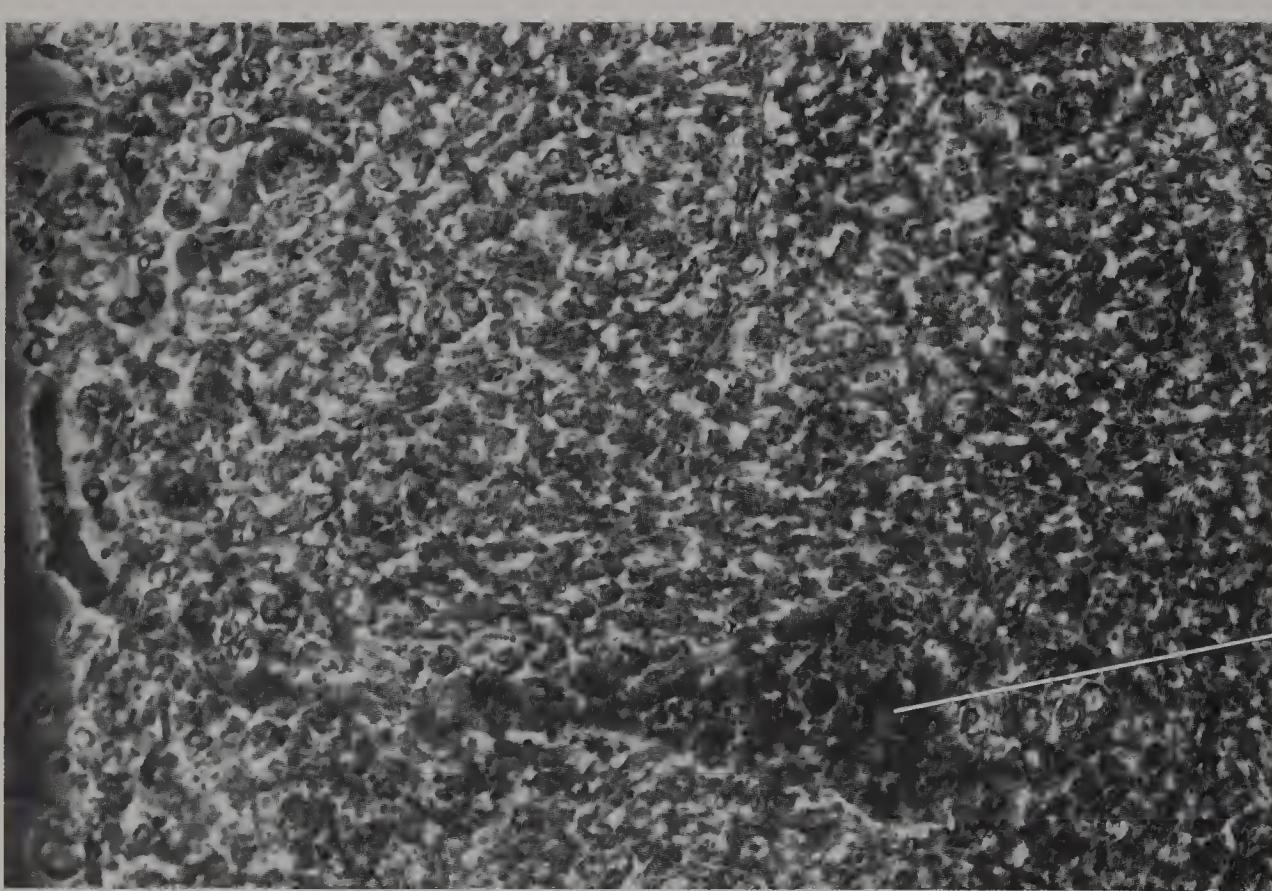


Figure 117 Thin slab of human occipital grey matter from a 73-year-old male, to show a Meynert cell *in situ* (phase contrast, $\times 700$).

There are few of these cells. They were first seen by Meynert in 1872.

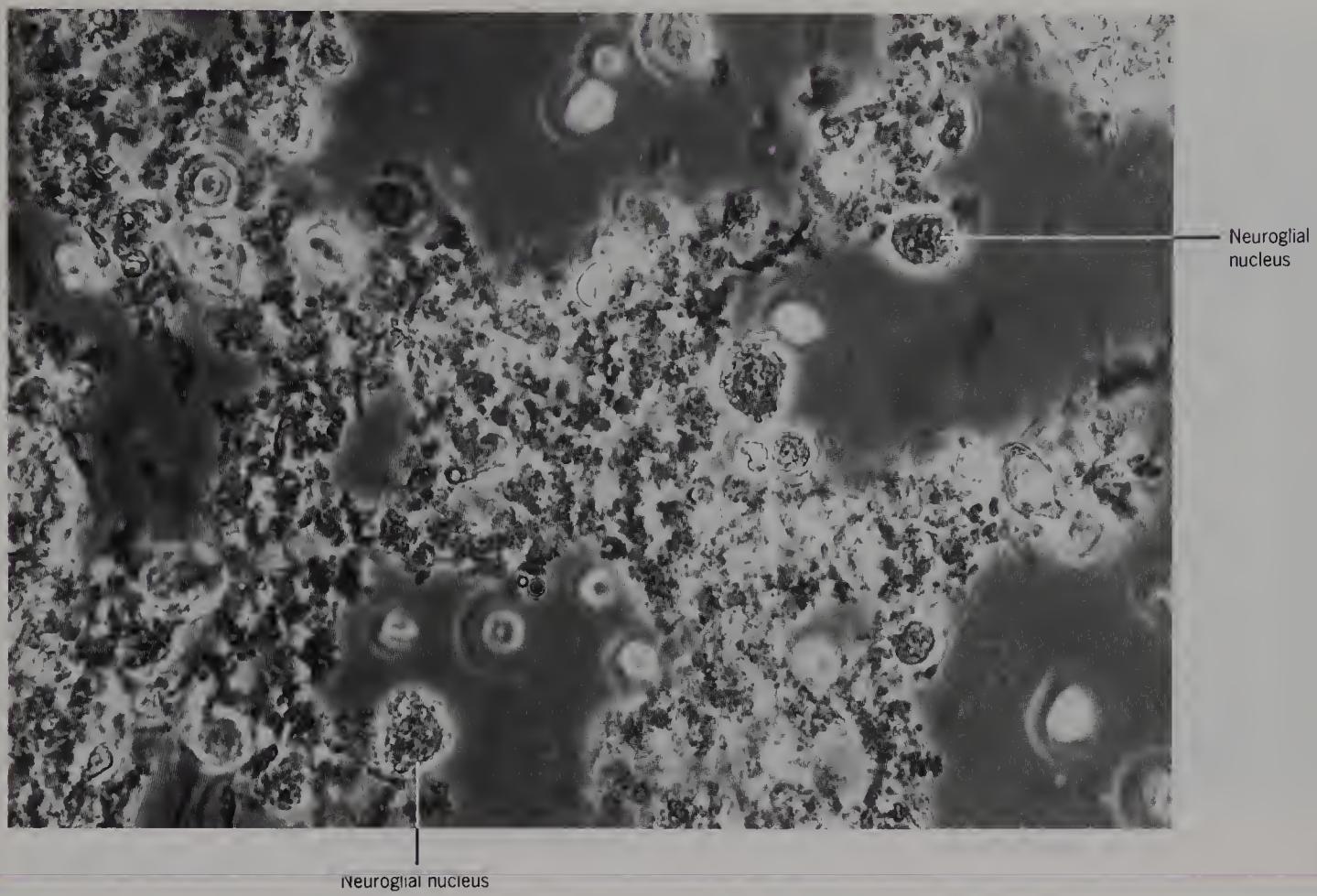


Figure 118 Teased human occipital grey matter from a 68-year-old male, to show neuroglial nuclei and fine granular material (phase contrast, $\times 700$).

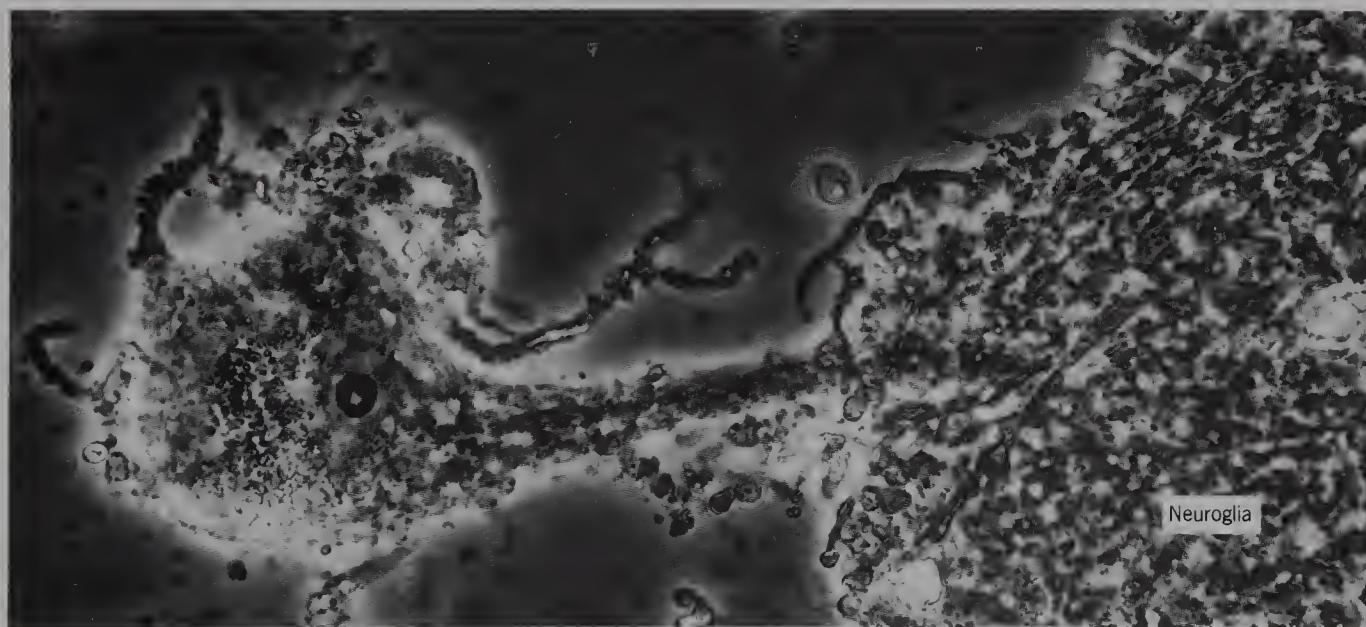


Figure 119 Isolated Meynert cell from human occipital grey matter from a 77-year-old male (phase contrast, $\times 800$).

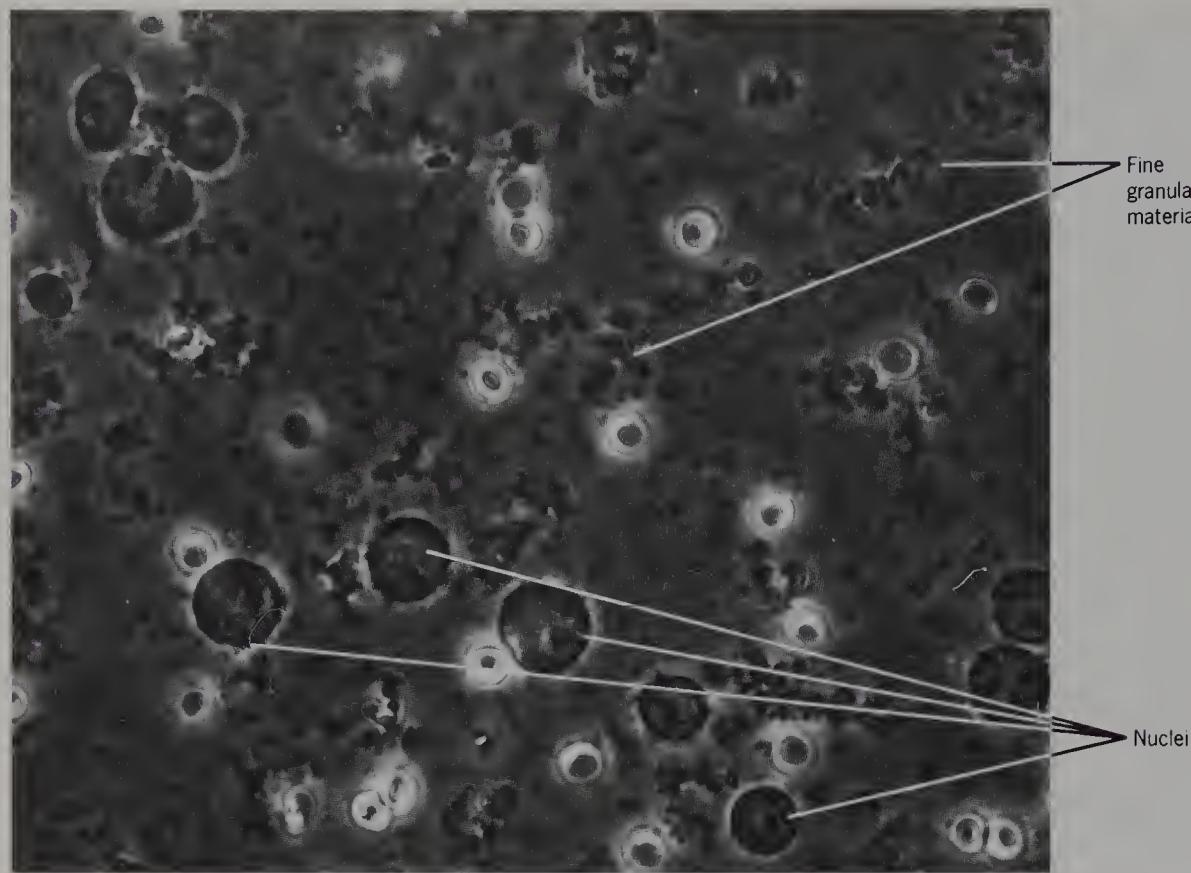


Figure 120 Teased rat occipital grey matter to show neuroglial nuclei or cells (phase contrast, $\times 700$).

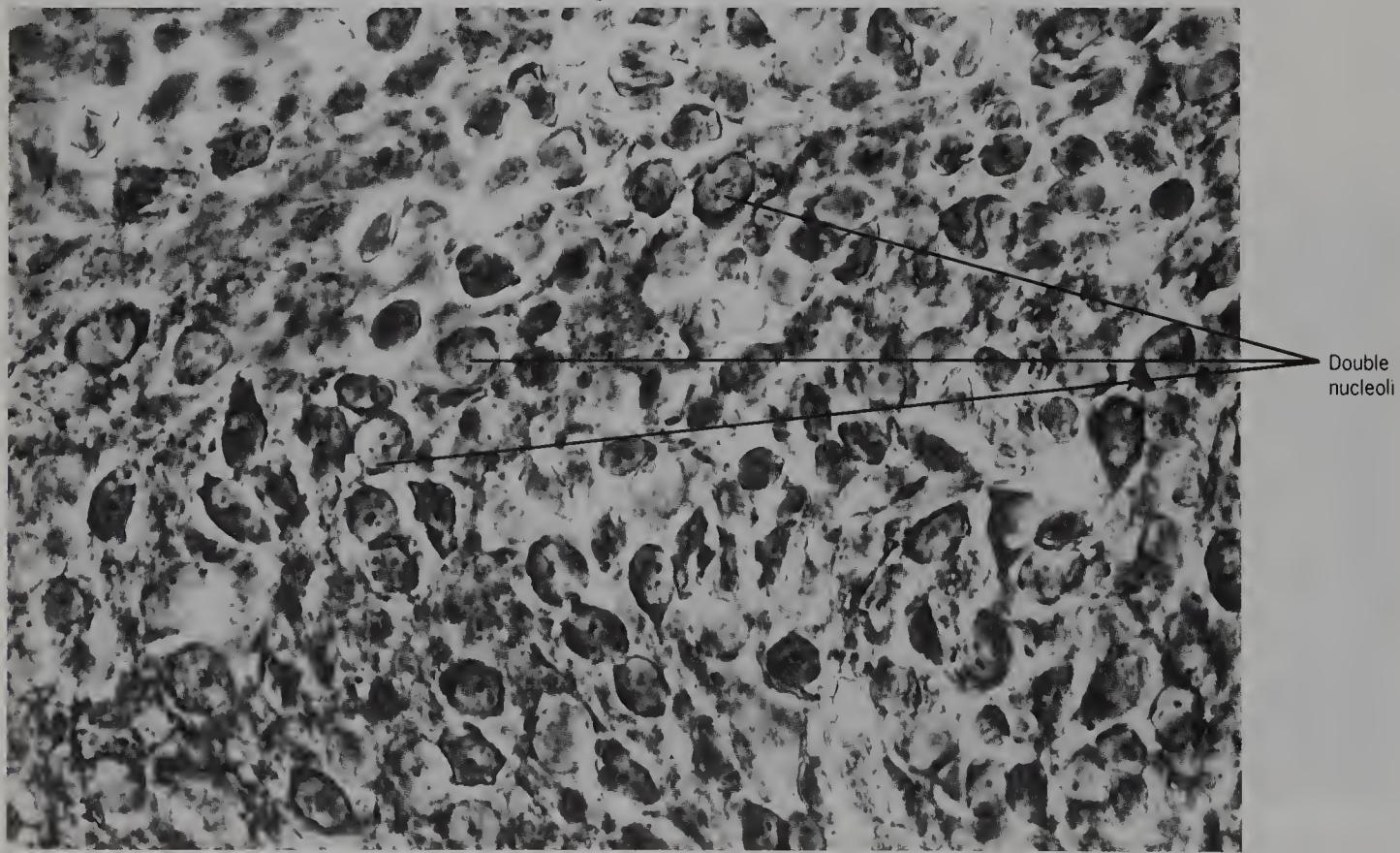


Figure 121 Thin slab of new-born mouse occipital grey matter, to show neurons — some with double nucleoli (phase contrast, $\times 700$).

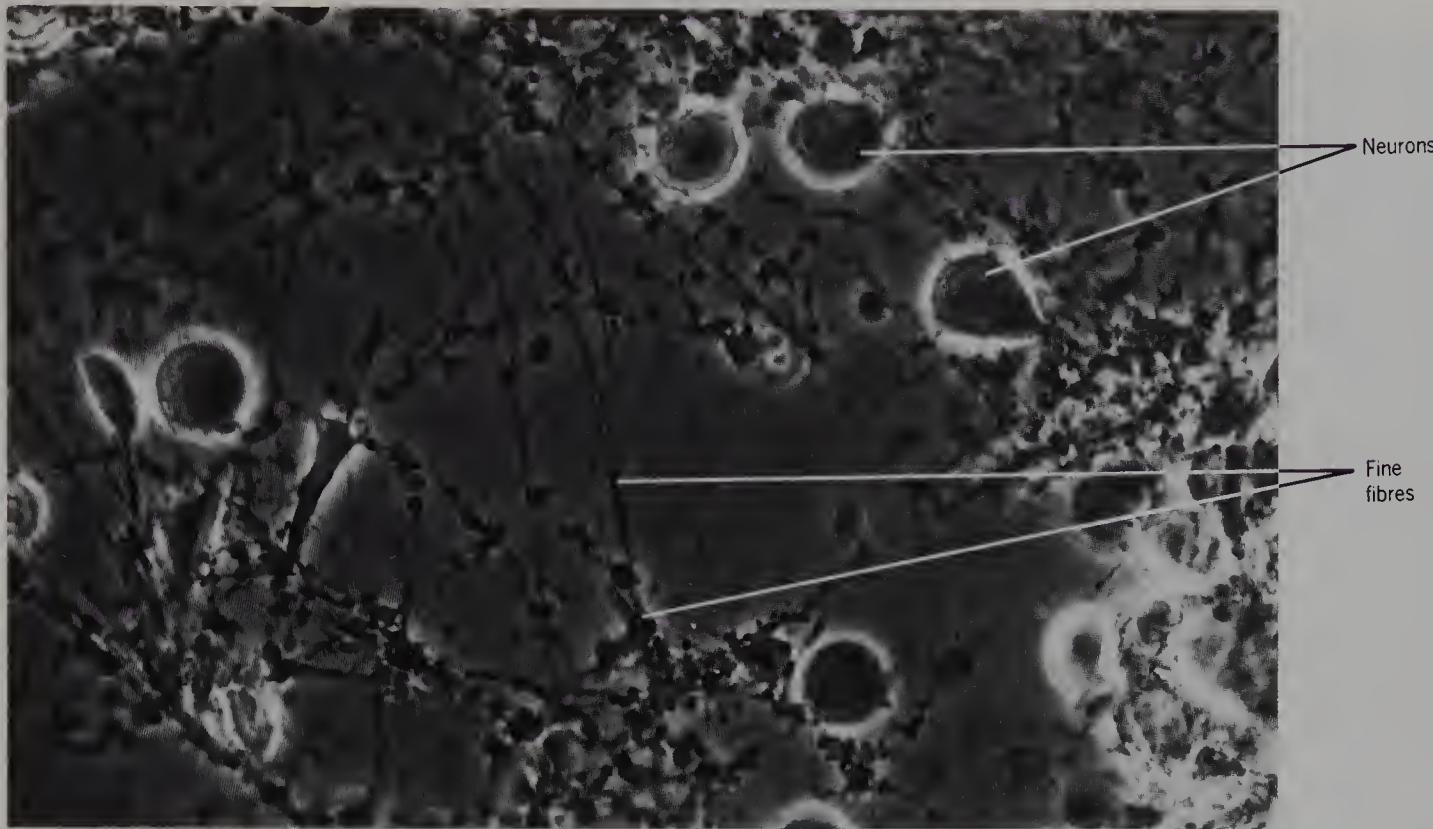


Figure 122 Teased new-born mouse occipital grey matter, to show neurons with little cytoplasm and fine fibres (phase contrast, $\times 700$).

Fine fibres can be seen only in the teased tissue.

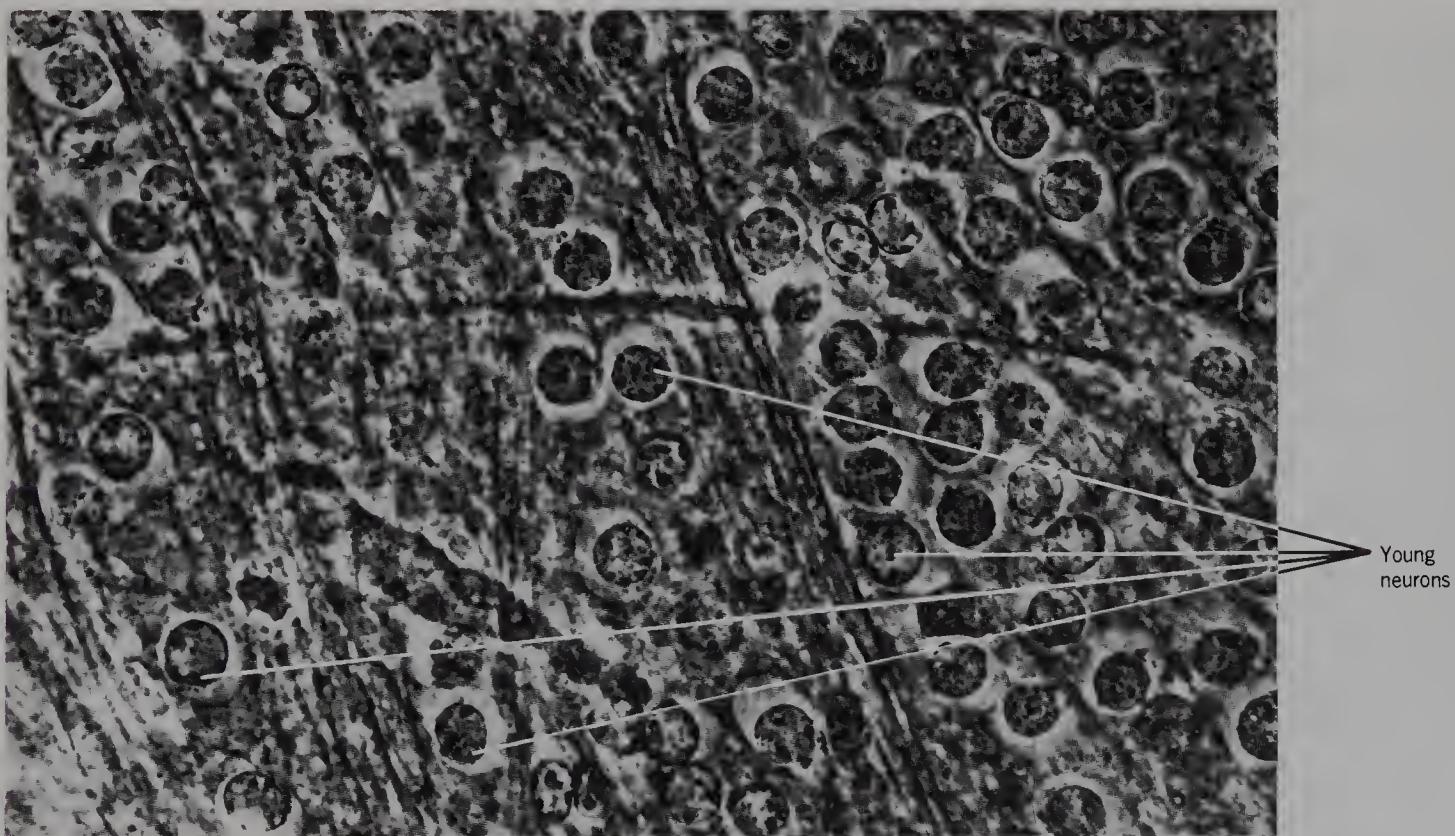


Figure 123 Thin slab of new-born mouse occipital white matter, to show probable migration of cells (phase contrast, $\times 700$).

The cytoplasm of the neurons is transparent at this age.



Figure 124 Thin slab of human occipital white matter from a 68-year-old male, to show beaded fibres (phase contrast, $\times 700$).

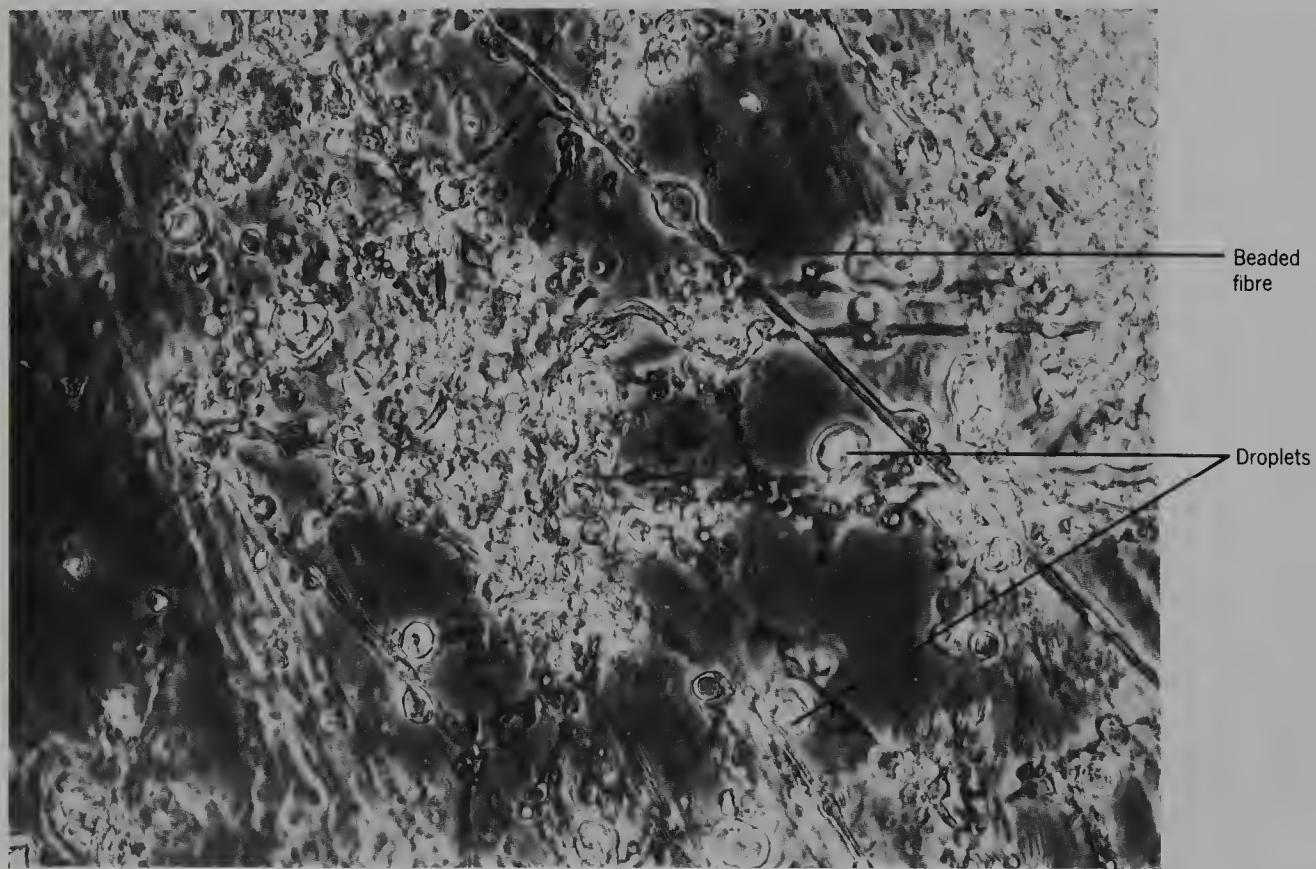


Figure 125 As previous figure, to show teased beaded fibres and large droplets (phase contrast, $\times 700$).

SECTION
4

SUBCORTICAL STRUCTURES



Figure 126 Thin slab of human corpus callosum from an 82-year-old female, to show beaded fibres (phase contrast, $\times 700$).

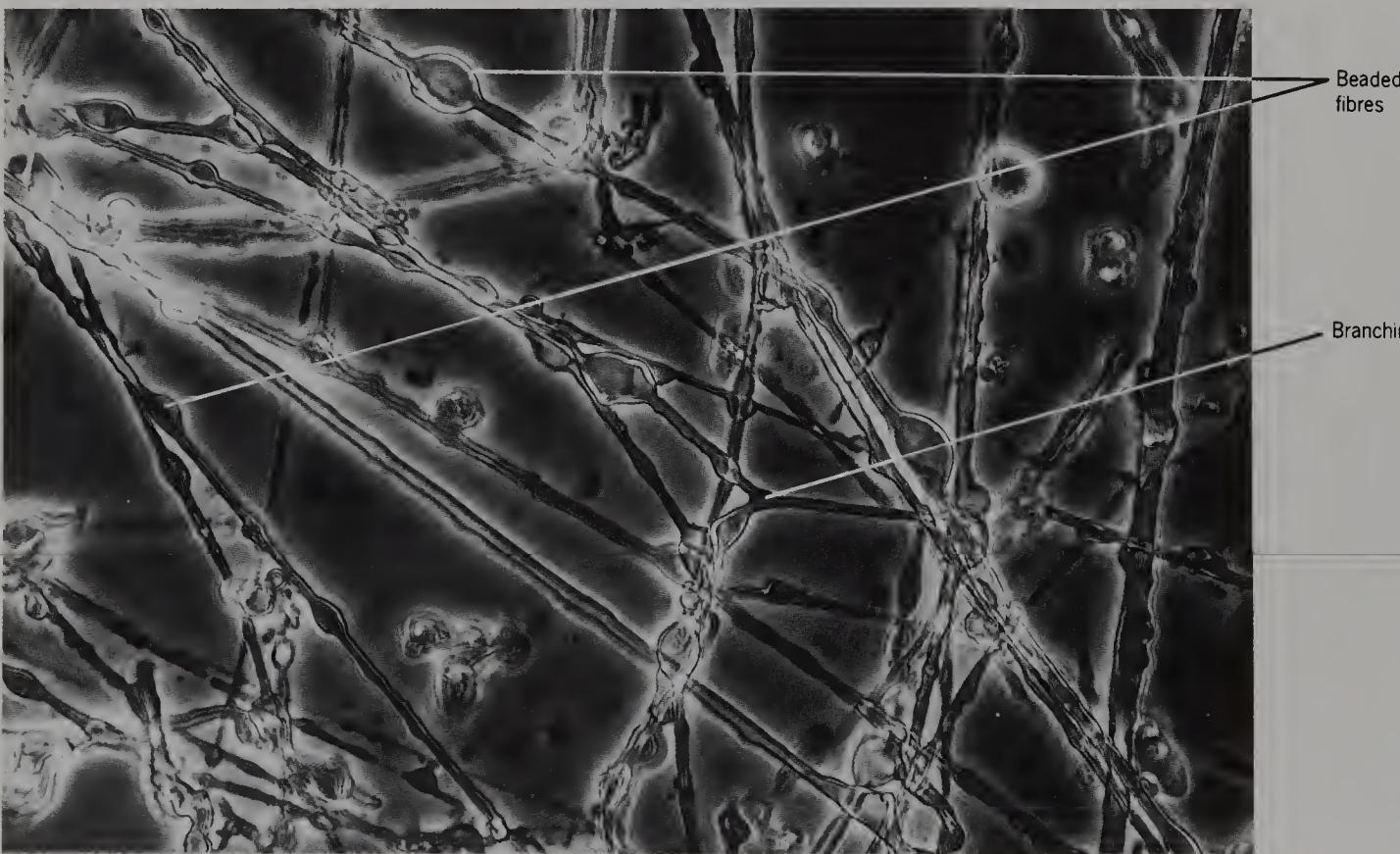


Figure 127 Teased human corpus callosum from a 77-year-old male, to show beaded fibres, which can occasionally be seen branching (phase contrast, $\times 700$).



Figure 128 As previous figure, but showing large beaded fibre (phase contrast, $\times 700$).

The large beads and droplets are transparent.



Figure 129 The same fibre as in the previous figure, to show birefringence of the sheath (polarized light, $\times 700$).



Figure 130 Thin slab of human internal capsule from an 84-year-old male, to show beaded fibres (phase contrast, $\times 700$).

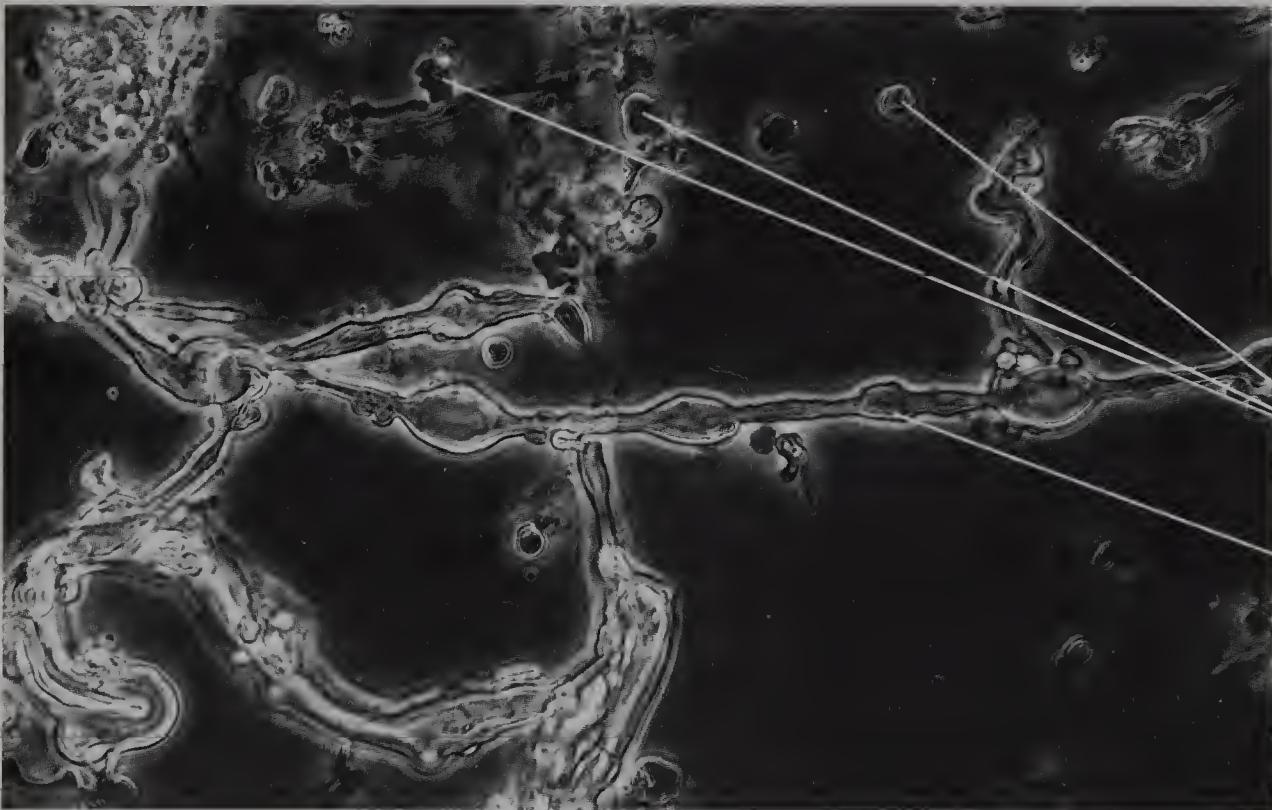


Figure 131 As previous figure, but teased to show large beaded fibres and droplets (phase contrast, $\times 700$).

There are granules within the beads.

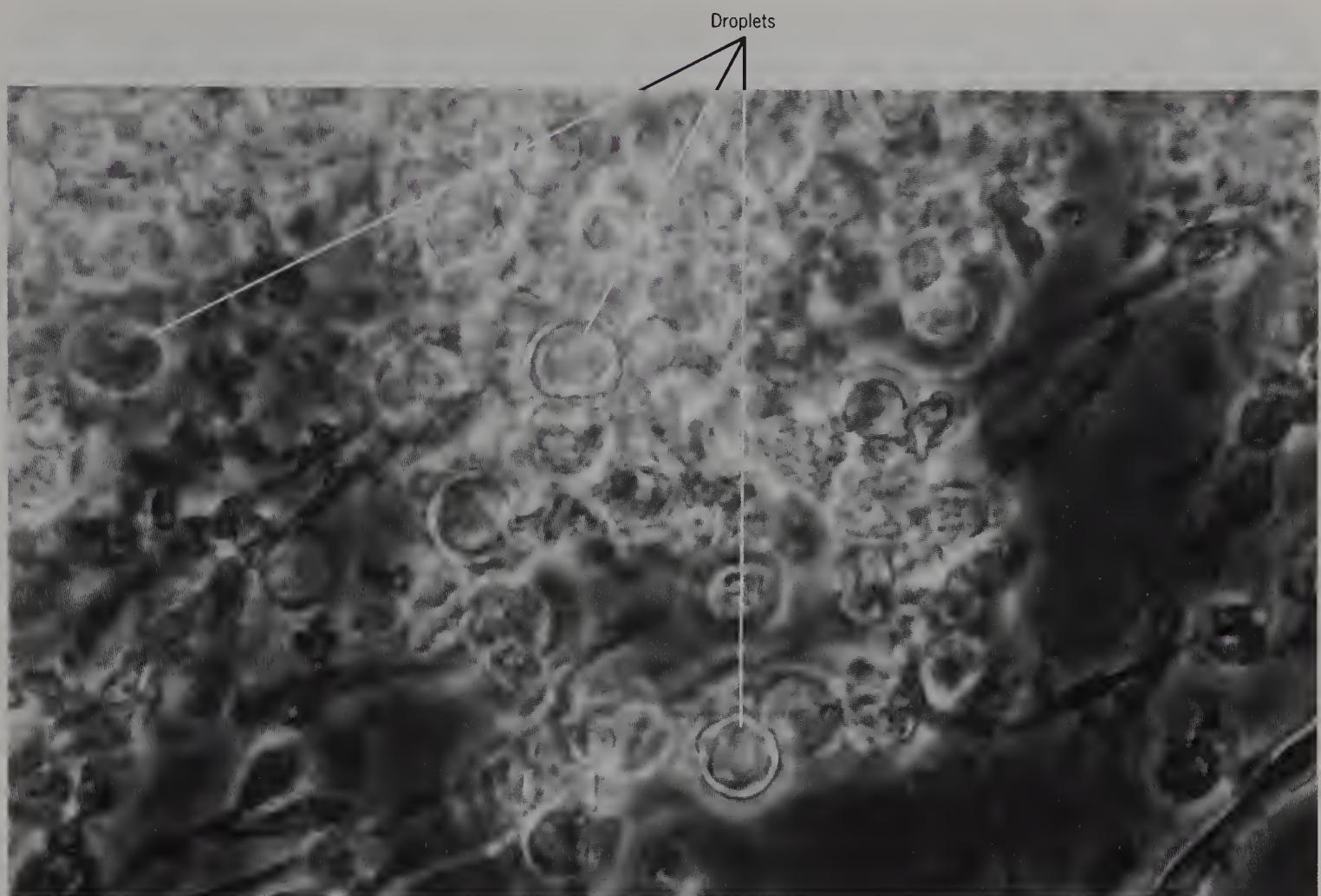


Figure 132 Partially teased rabbit internal capsule, to show large and small droplets (phase contrast, $\times 2000$).

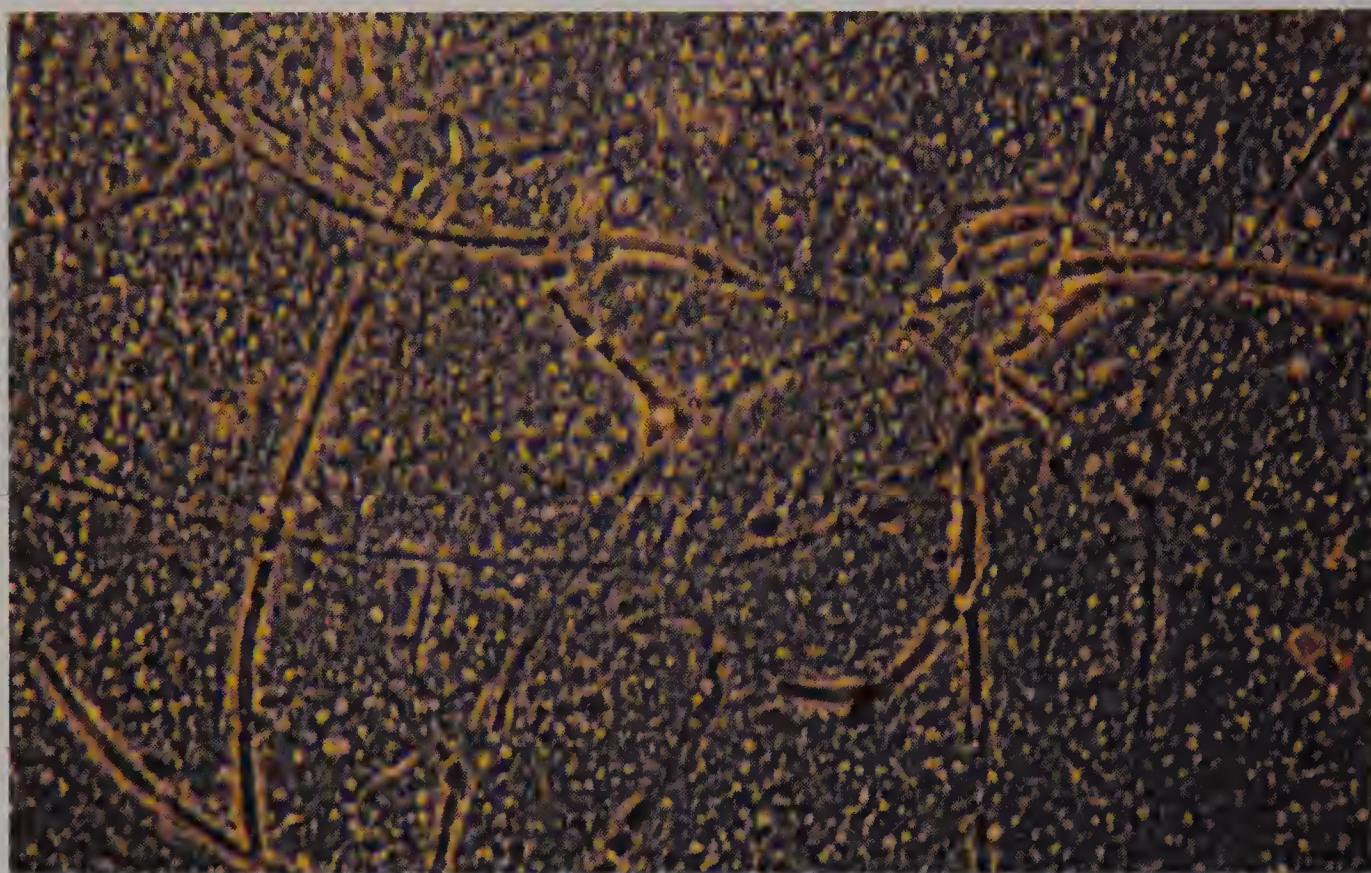


Figure 133 Thin slab of human caudate nucleus from a 65-year-old female, to show blood vessels (phase contrast, $\times 300$).

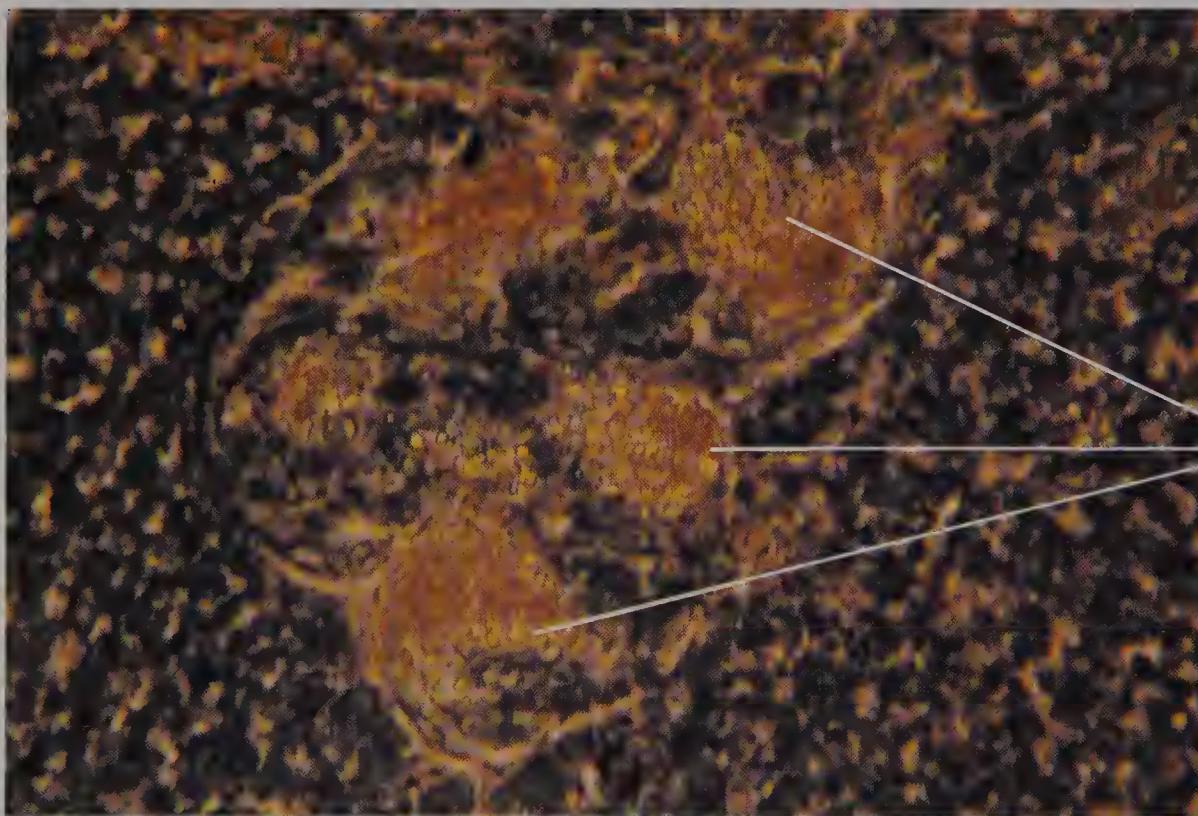


Figure 134 Thin slab of human caudate nucleus from a 65-year-old female, to show the incidence of neuron somas (bright field, $\times 700$).

The contrast is given by the lipofuscin.

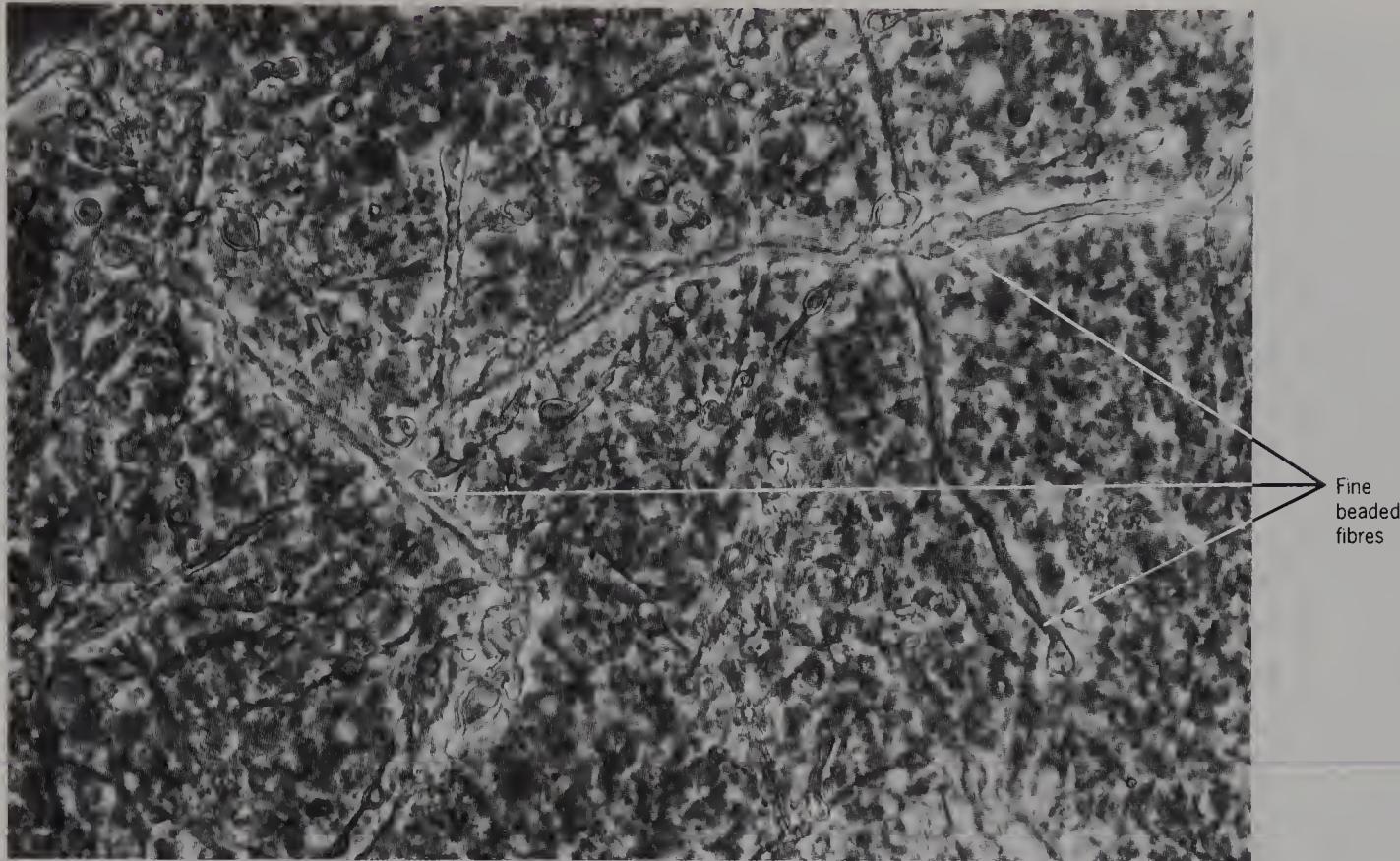


Figure 135 Thin slab of human caudate nucleus from an 80-year-old female, to show fine beaded fibres (phase contrast, $\times 700$).

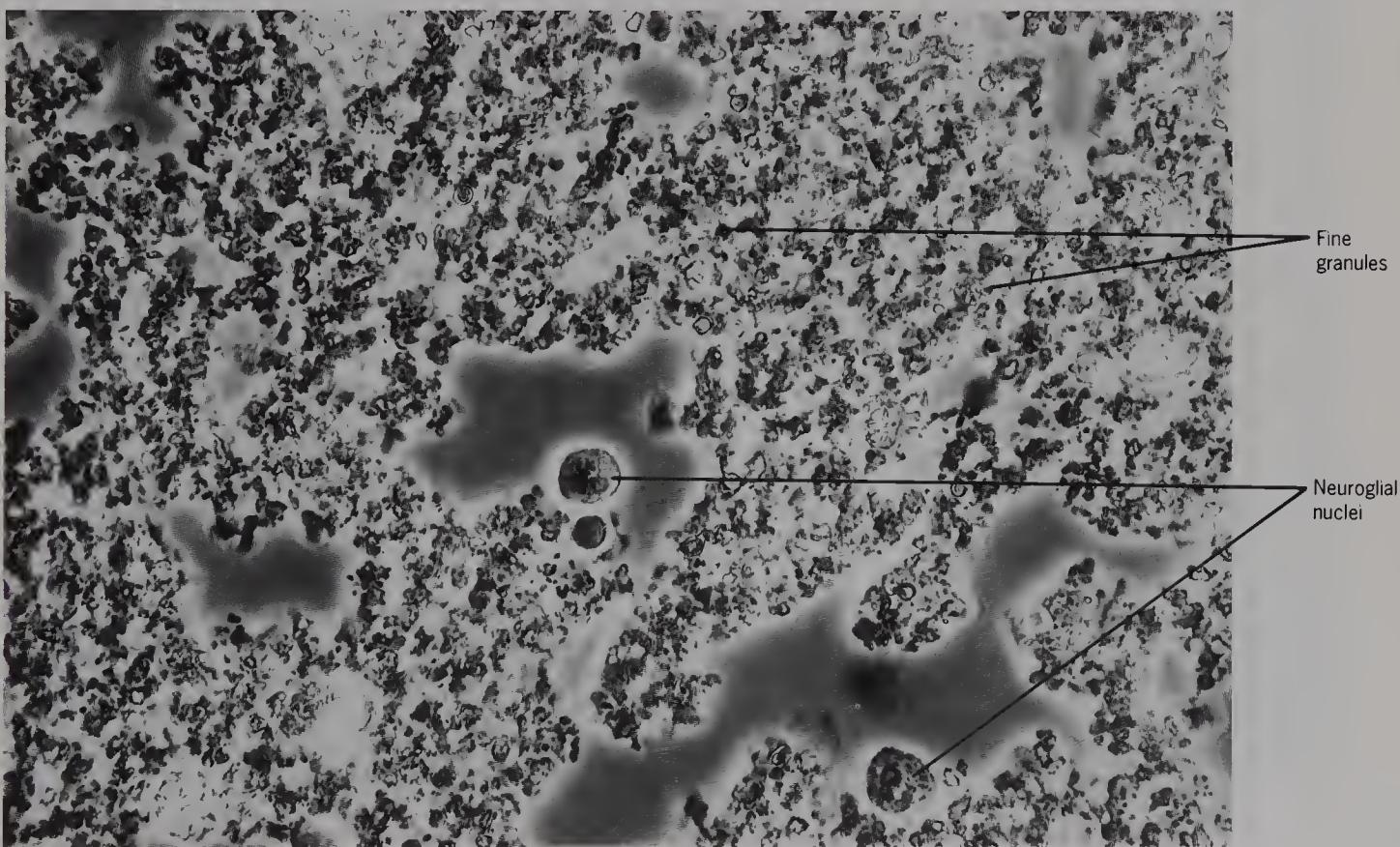


Figure 136 Partially teased human caudate nucleus from a 70-year-old male, to show neuroglial nuclei and fine granules (phase contrast, $\times 700$).

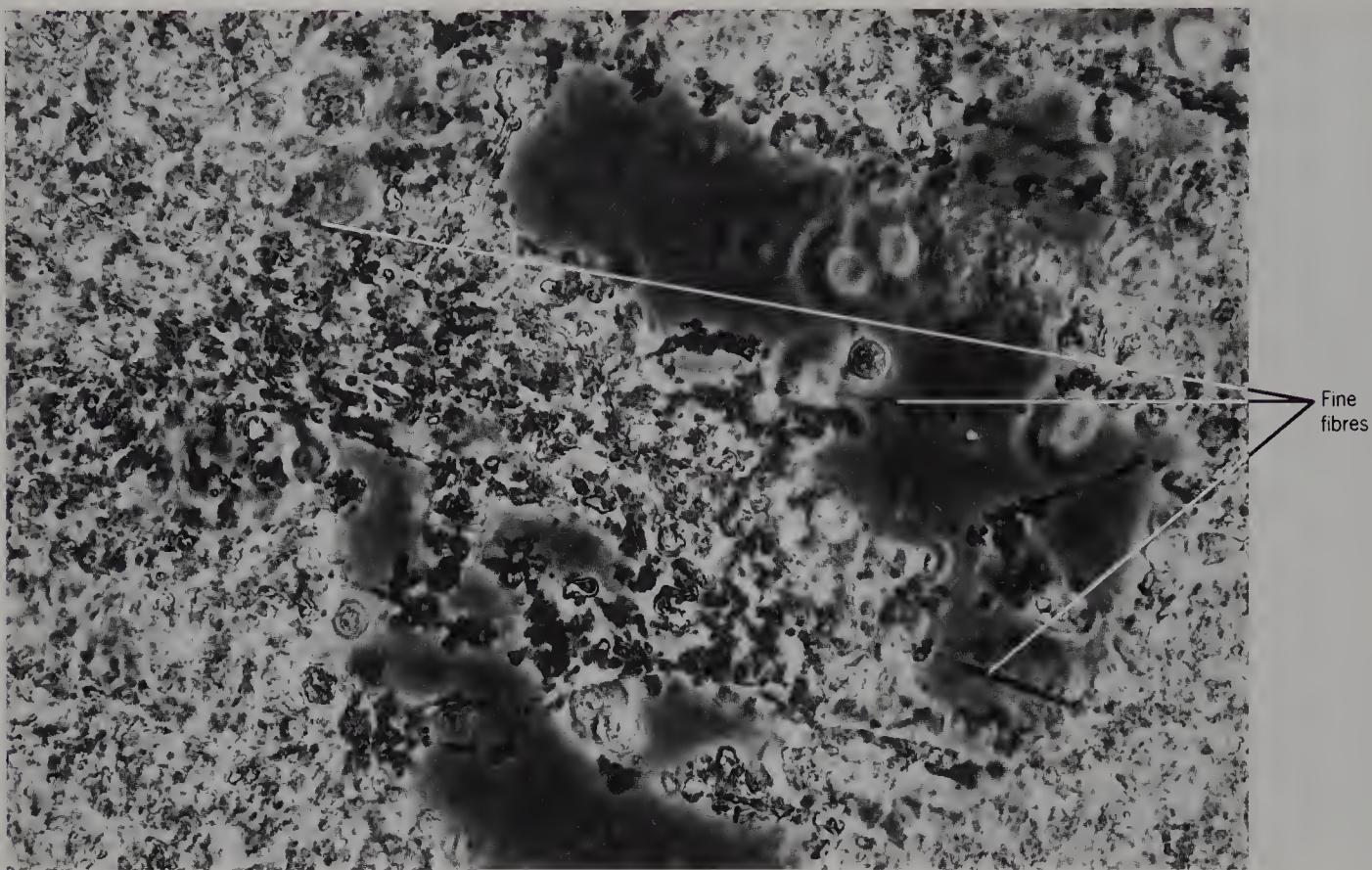


Figure 137 As previous specimen, but teased to show fine fibres (phase contrast, $\times 700$).

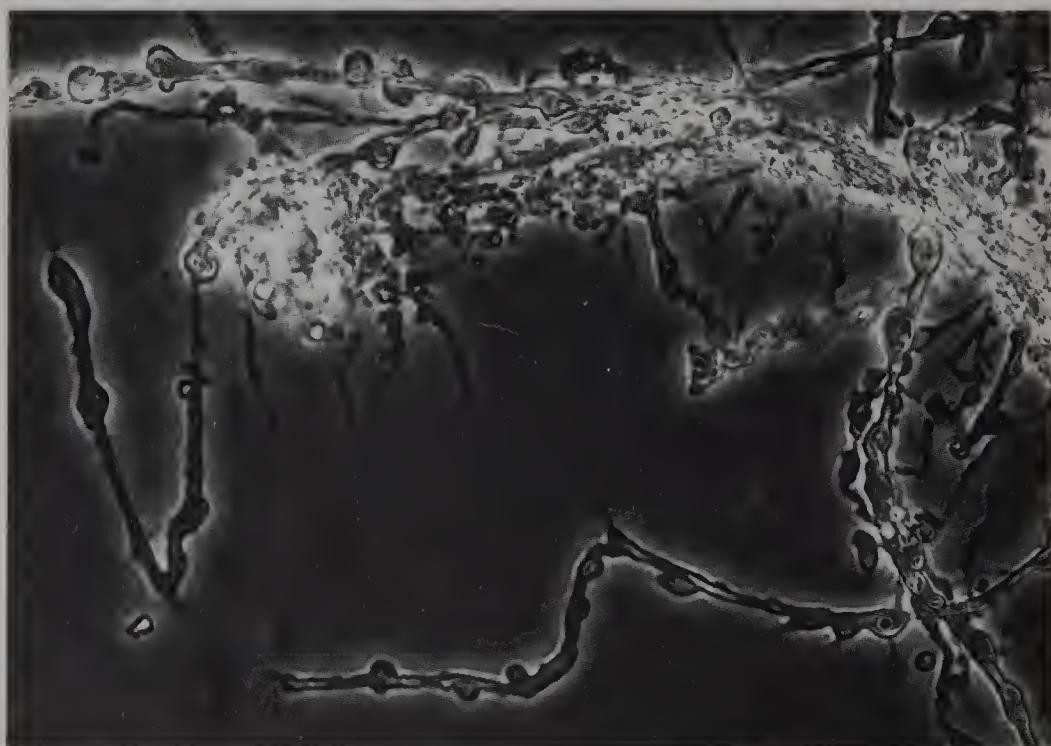


Figure 138 Teased rat caudate nucleus, to show beaded fibres (phase contrast, $\times 700$).

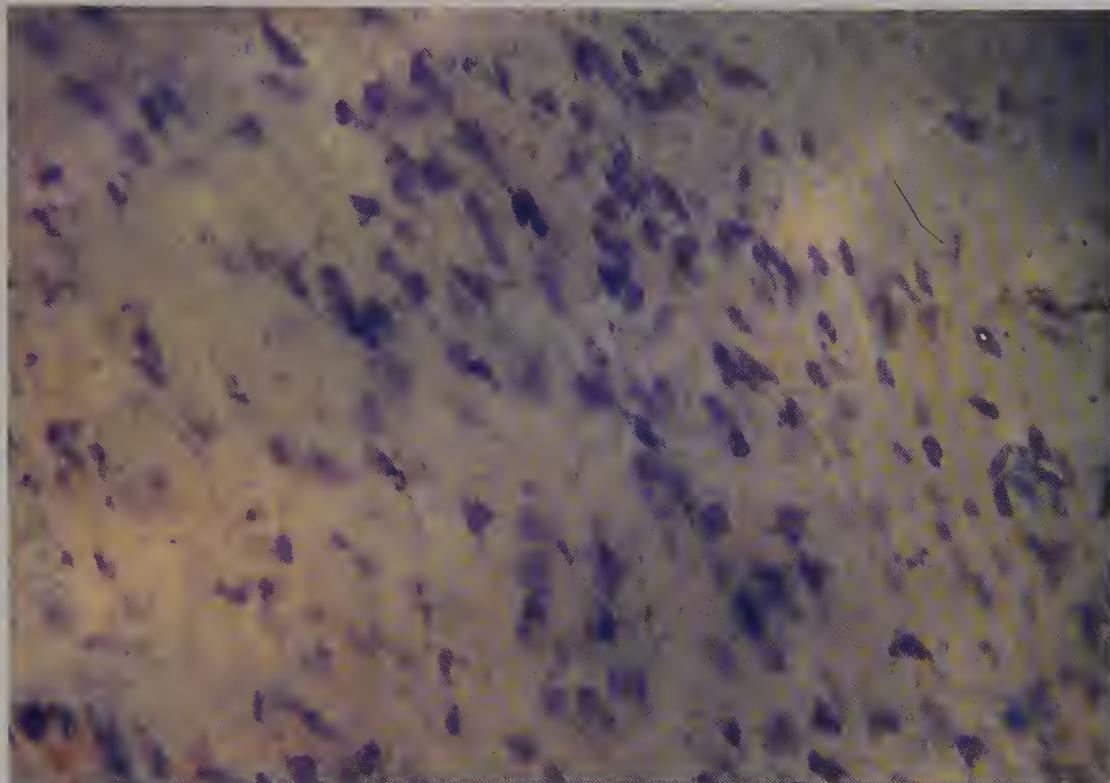


Figure 139 Thin slab of human putamen from a 60-year-old male, lightly coloured with methylene blue to show the incidence of neuron somas (bright field, $\times 100$).



Figure 140 Thin slab of human putamen from a 65-year-old female, to show fine beaded fibres (phase contrast, $\times 720$).



Figure 141 Partially teased white matter of a rat putamen, to show beaded fibres (phase contrast, $\times 700$).



Figure 142 Teased human putamen from a 65-year-old female, to show fine fibres (phase contrast, $\times 700$).

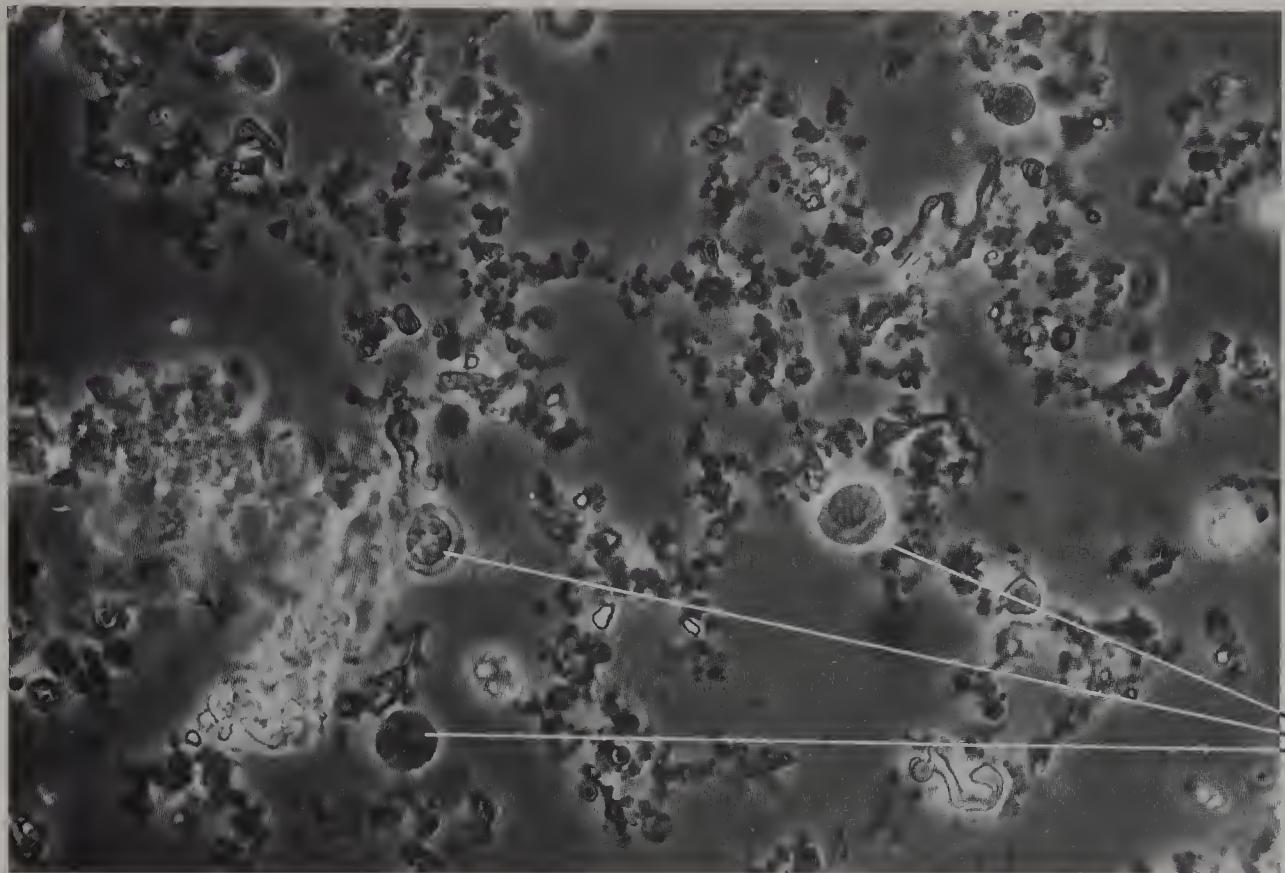


Figure 143 Isolated human neuroglia or small neurons and fine granules from the putamen of a 73-year-old male (phase contrast, $\times 700$).

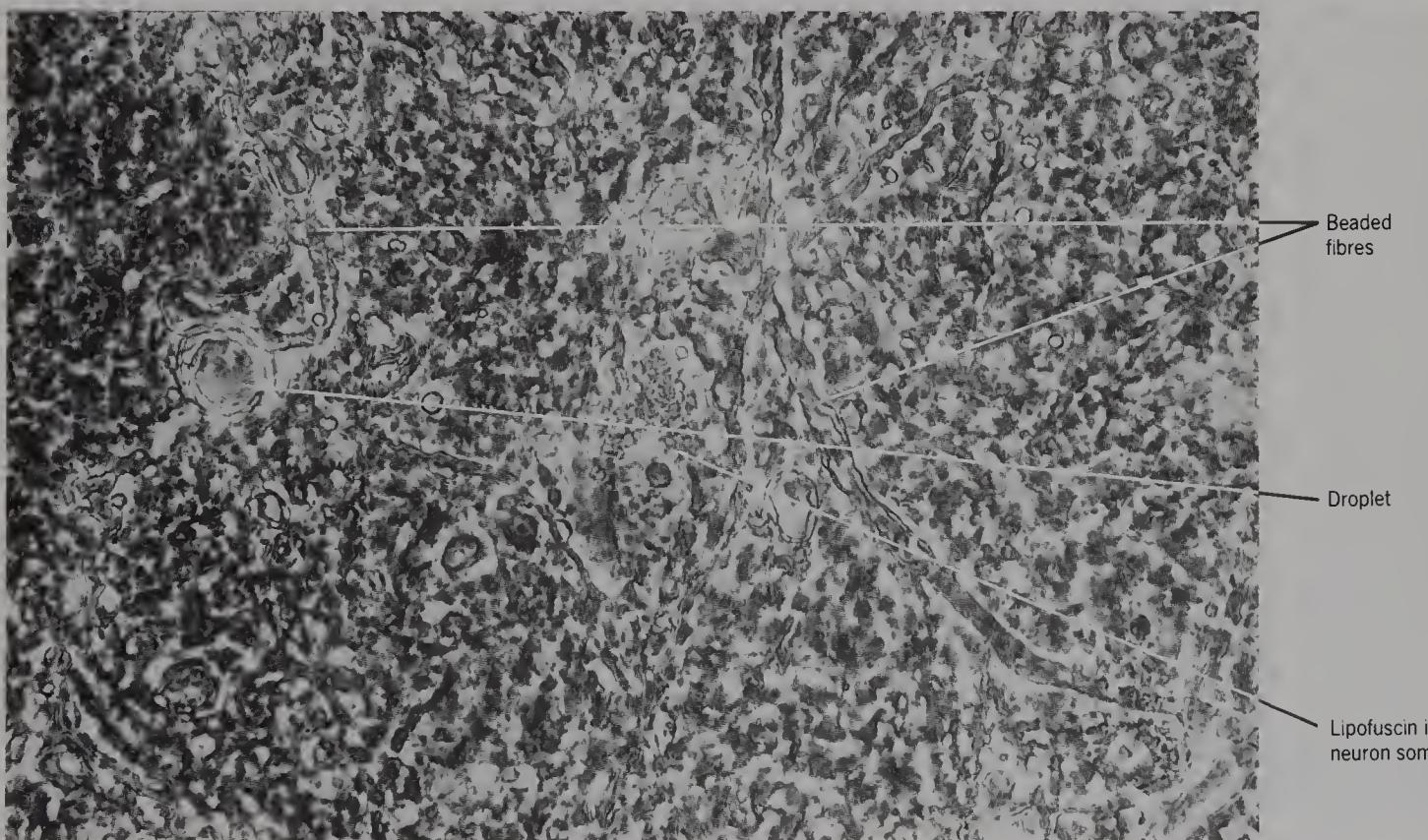


Figure 144 Thin slab of human globus pallidus from a 71-year-old male, to show beaded fibres and a neuron with lipofuscin *in situ* (phase contrast, $\times 700$).

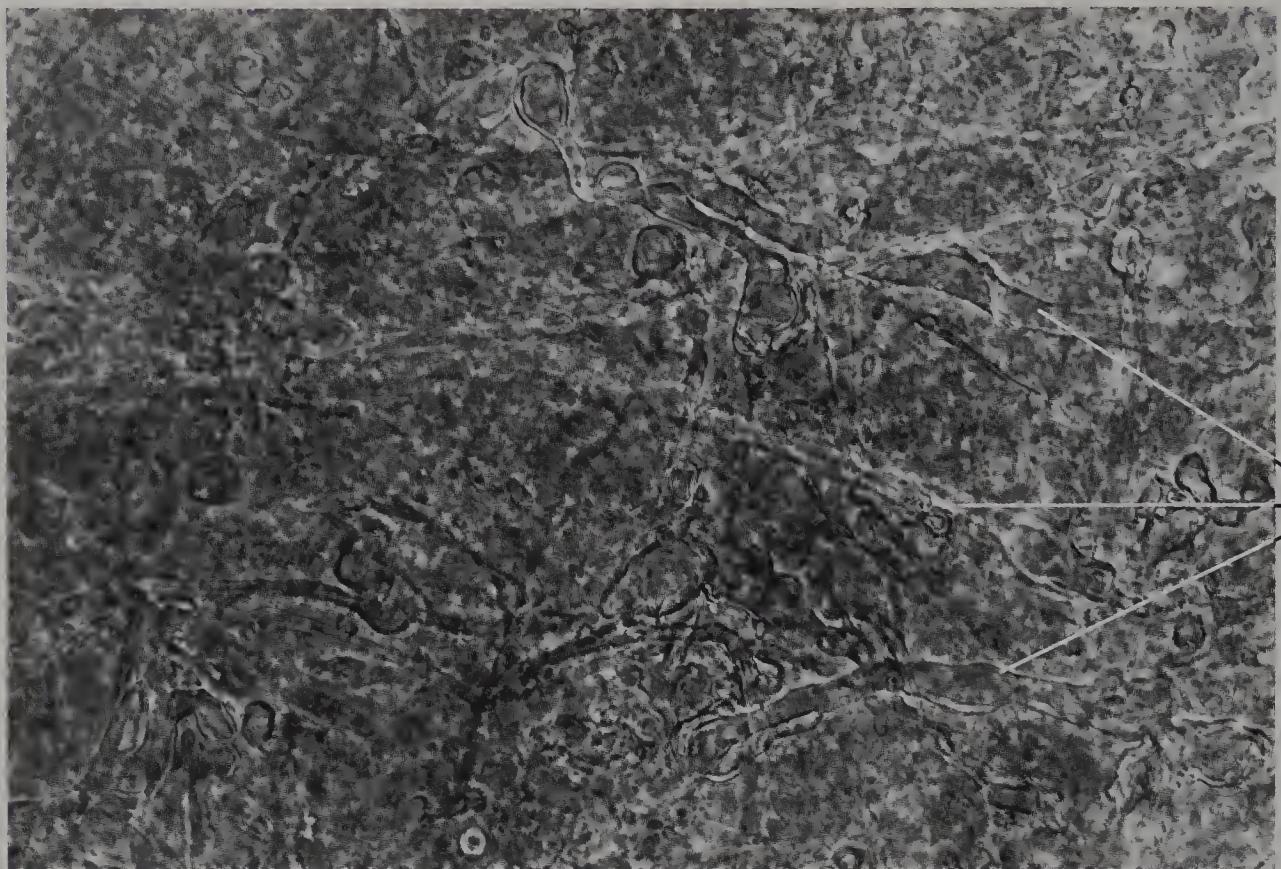


Figure 145 As previous specimen, to show fibres, some beaded (phase contrast, $\times 700$).



Figure 146 Partially teased human globus pallidus from a 95-year-old female, to show large droplets and fibres (phase contrast, $\times 700$).

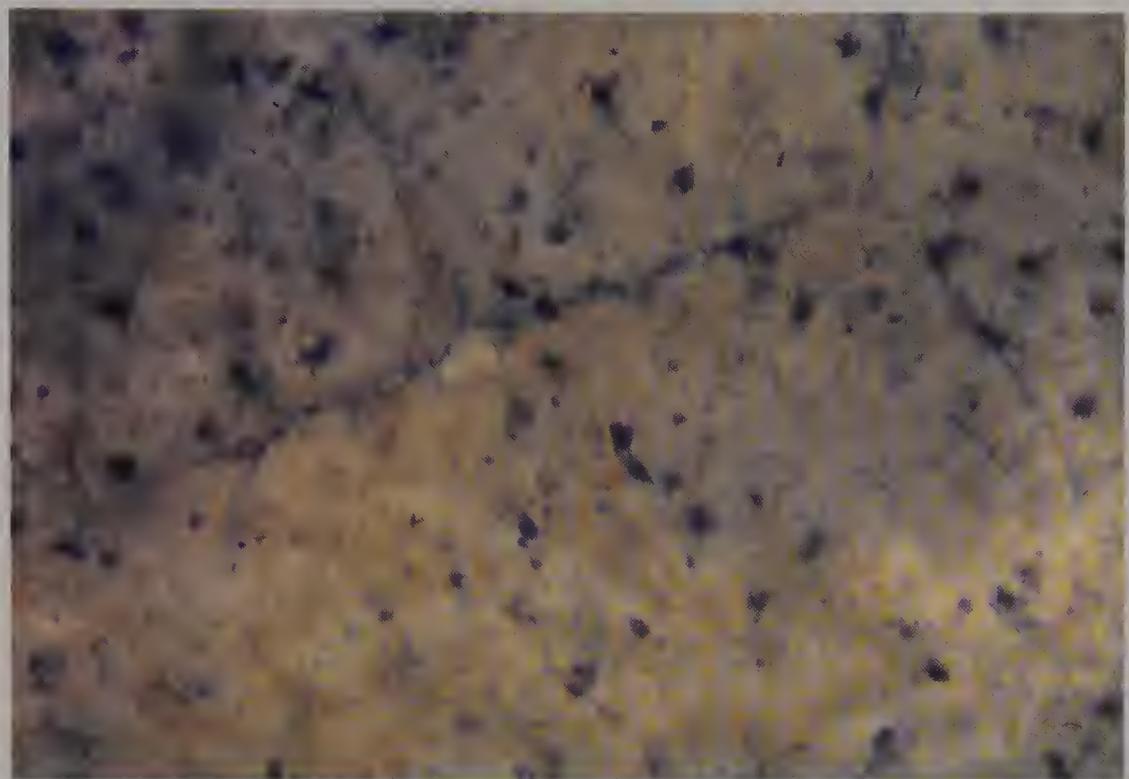


Figure 147 Thin slab of human thalamus from a 60-year-old male, lightly coloured with methylene blue to show the incidence and appearance of neuron somas (bright field, $\times 100$).

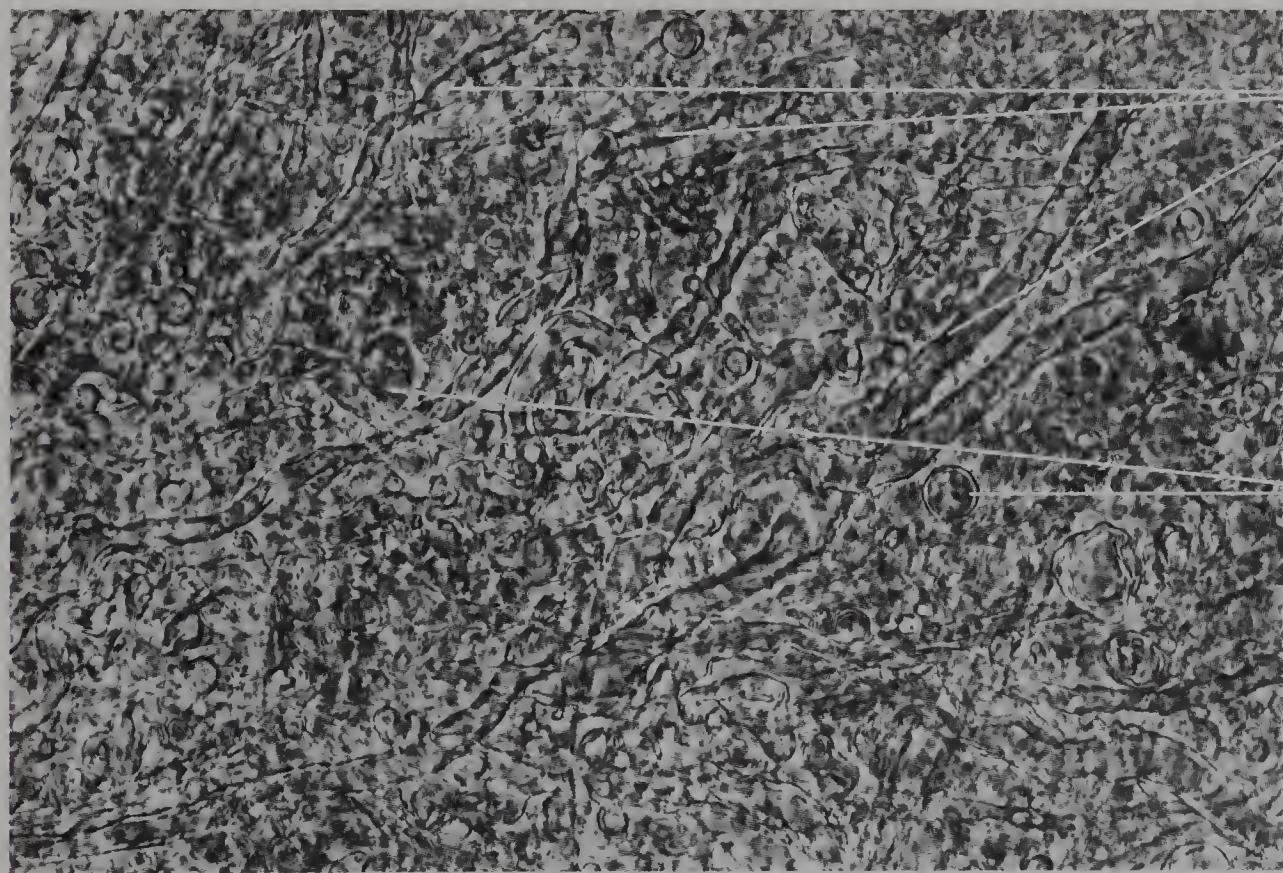


Figure 148 Thin slab of human dorsolateral nucleus of the thalamus from a 73-year-old male, to show fibres and droplets (phase contrast, $\times 700$).

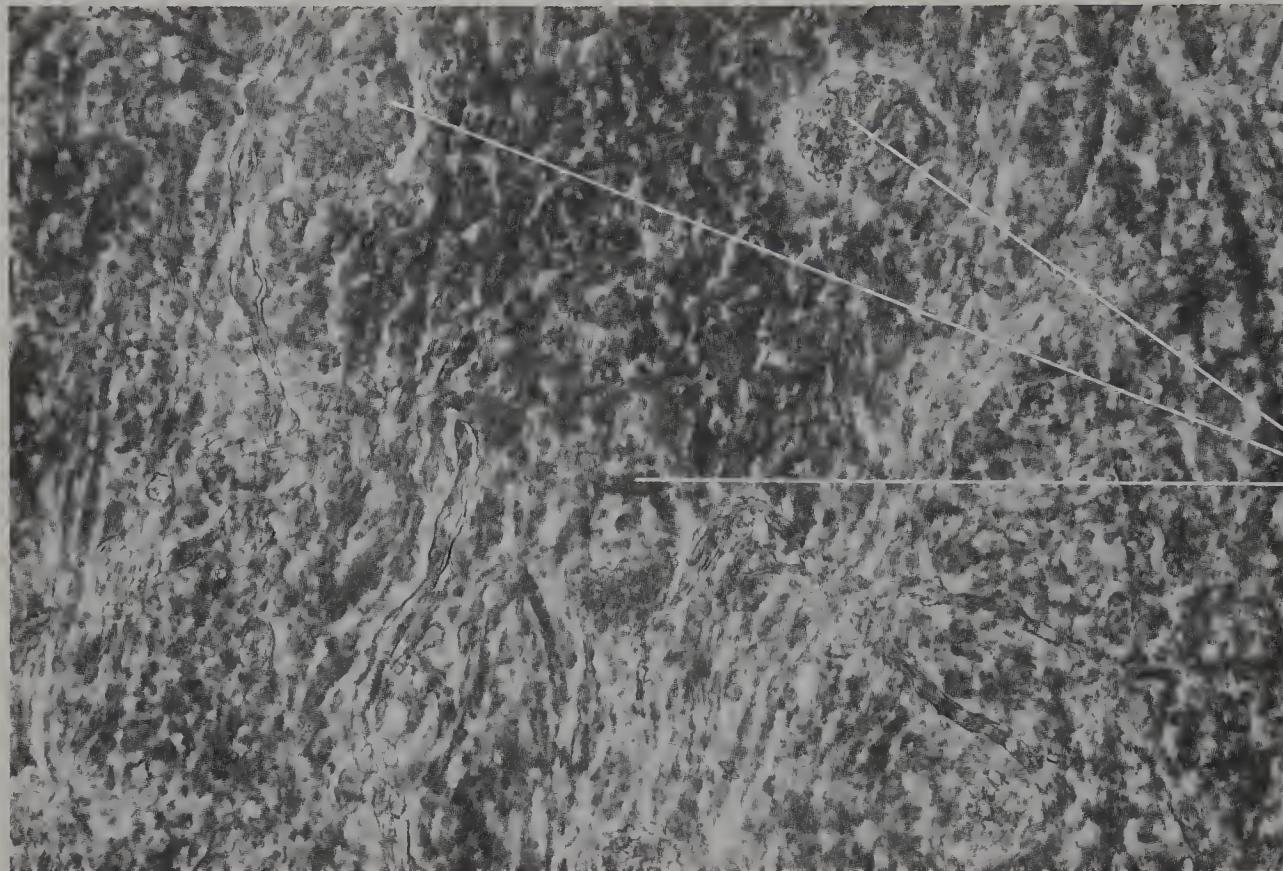


Figure 149 Thin slab of human medial nucleus of the thalamus, from a 73-year-old male, to show neurons with intracellular lipofuscin (phase contrast, $\times 700$).

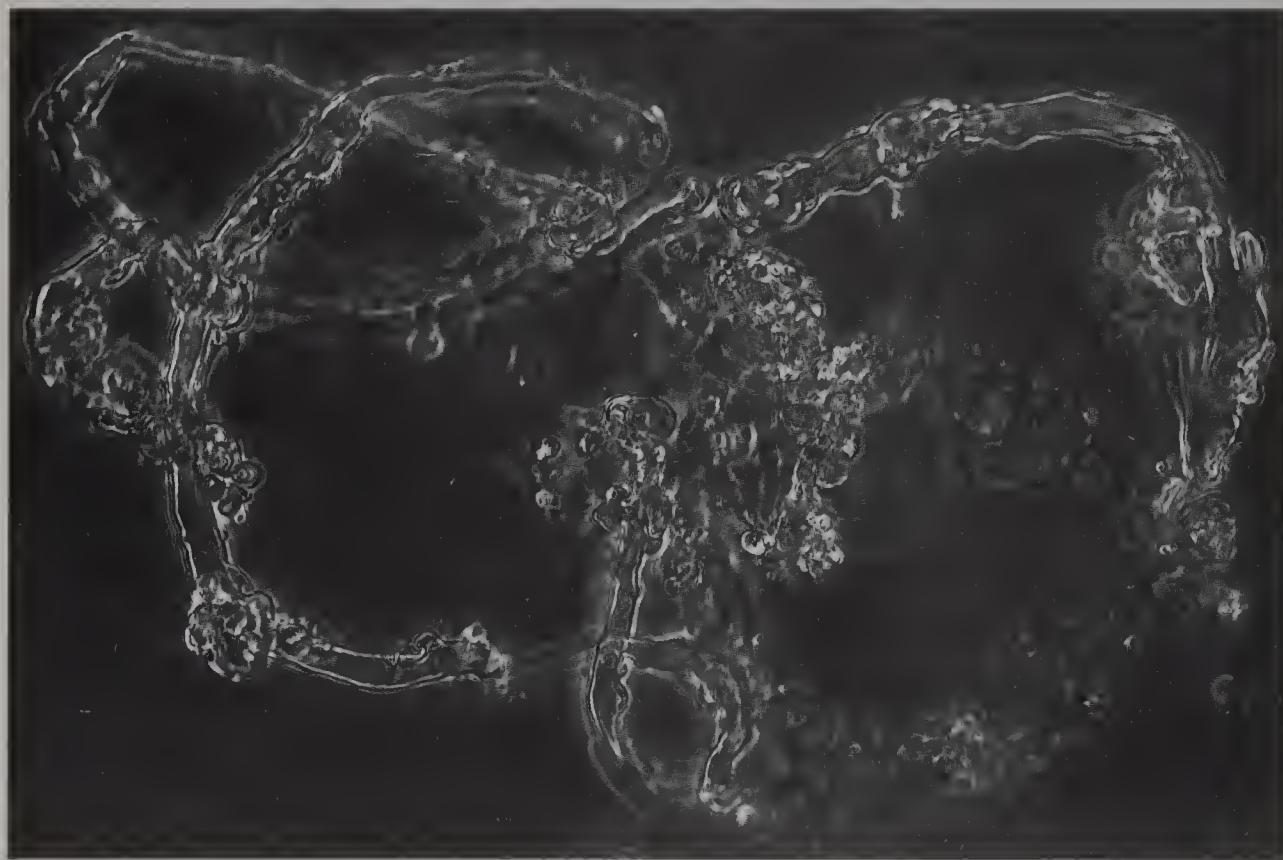


Figure 150 Isolated human beaded fibres from the dorsolateral nucleus of the thalamus from a 73-year-old male (dark ground, $\times 700$).

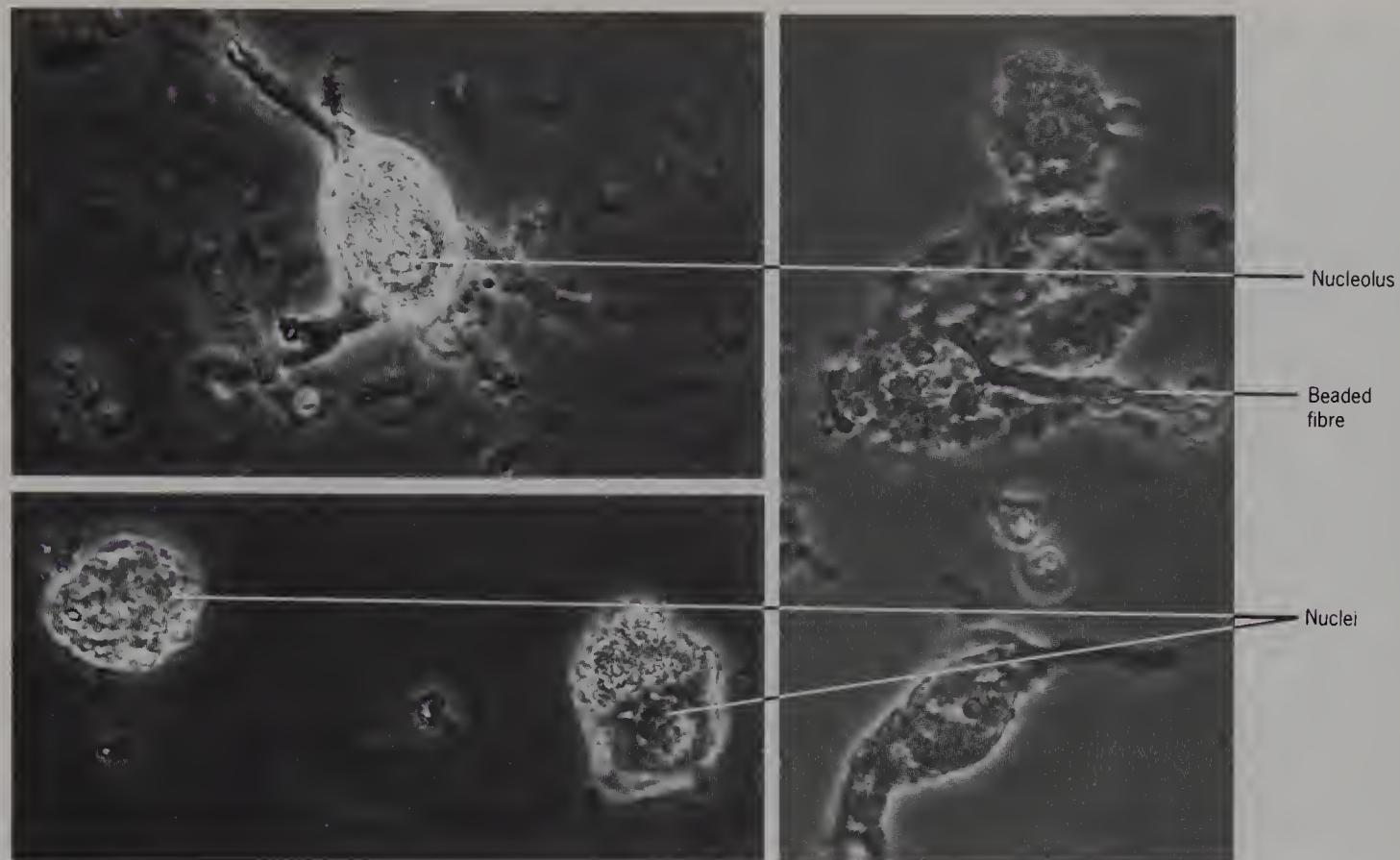


Figure 151 Isolated neurons from thalamus from a 73-year-old human male (left) and from rat (right) (phase contrast, $\times 700$).
The dendrites have presumably been detached during teasing of the neurons (bottom left).

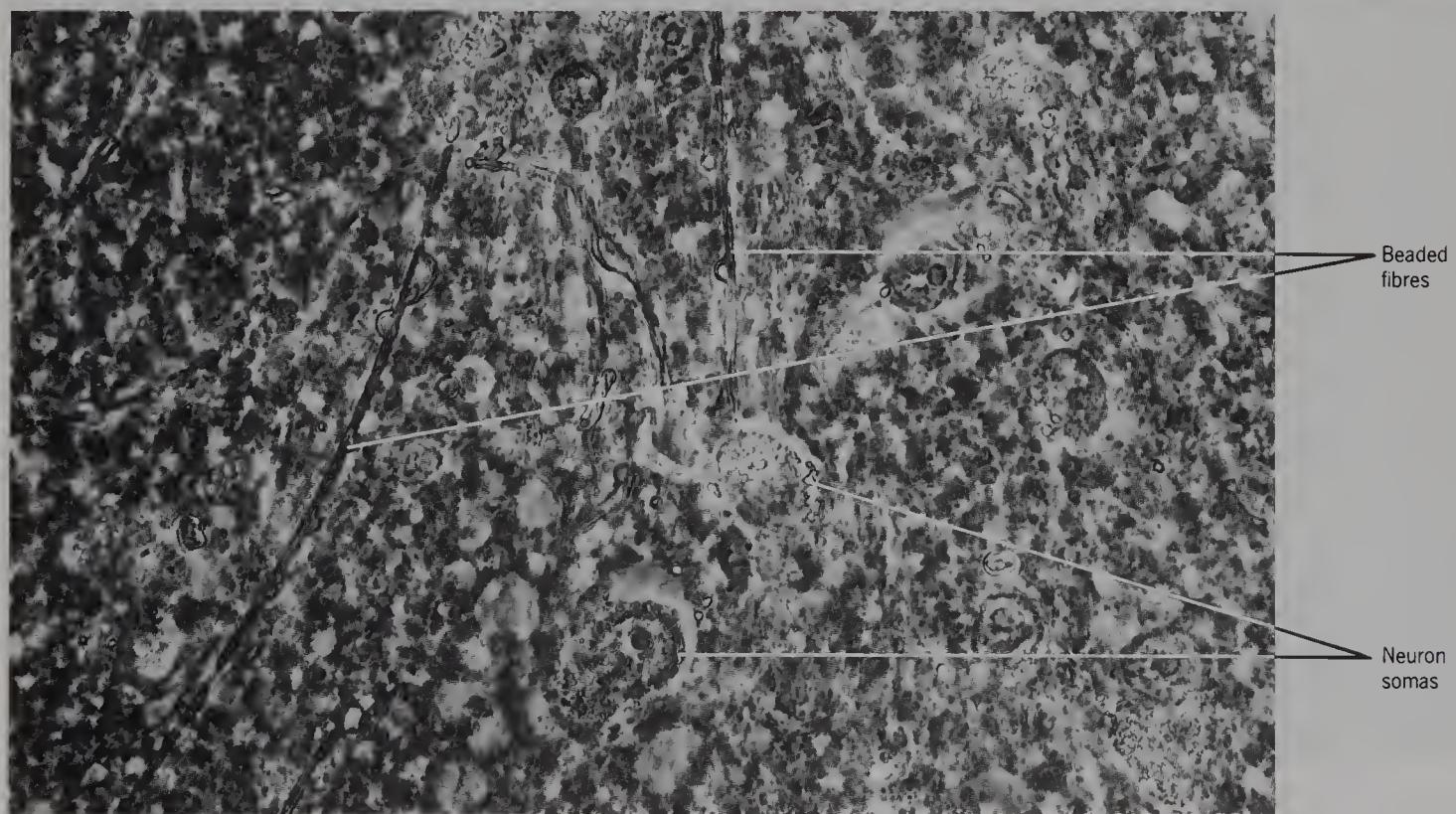


Figure 152 Thin slab of human hypothalamus from a 77-year-old male, to show neuron somas and beaded fibres (phase contrast, $\times 700$).

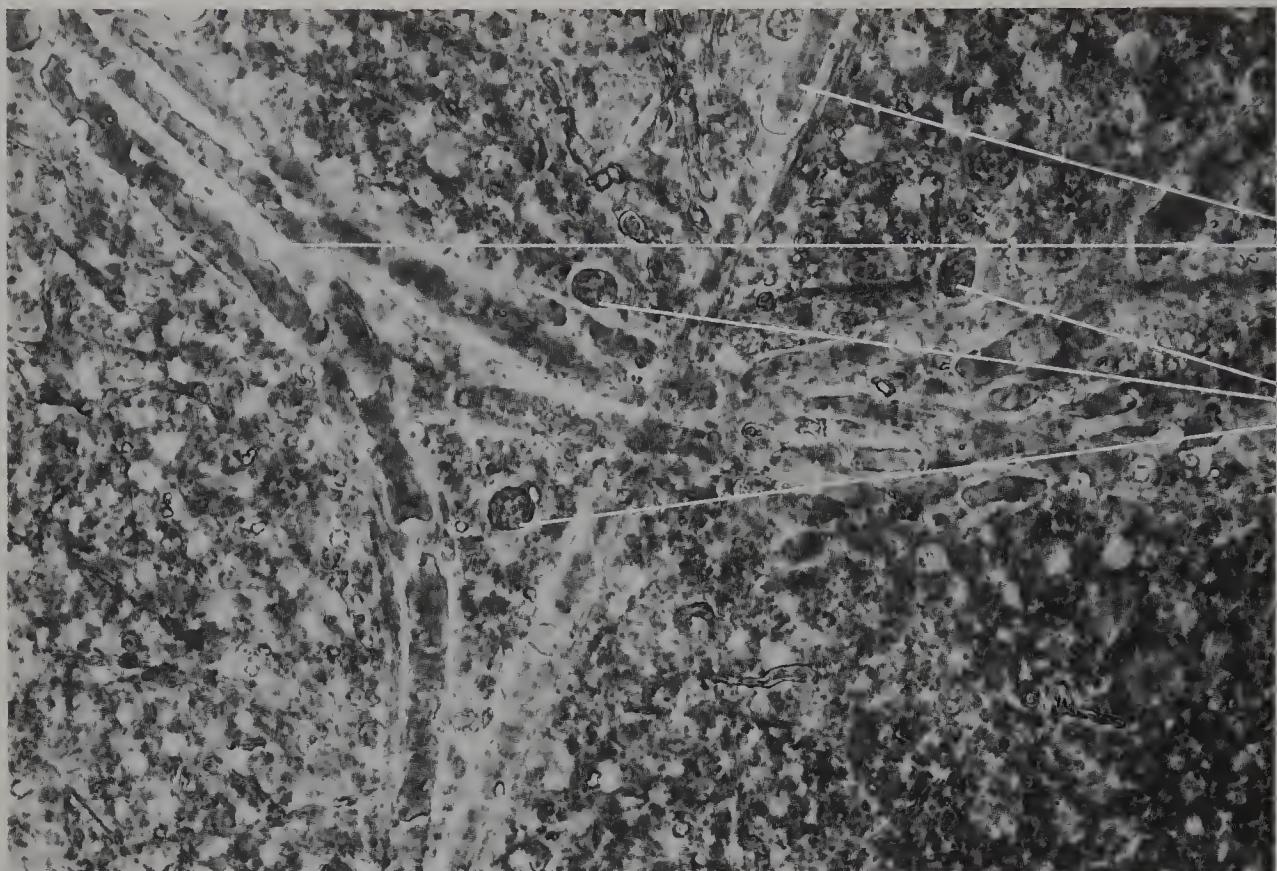


Figure 153 Thin slab of human hypothalamus from a 77-year-old male, to show capillaries and nuclei (phase contrast, $\times 700$).

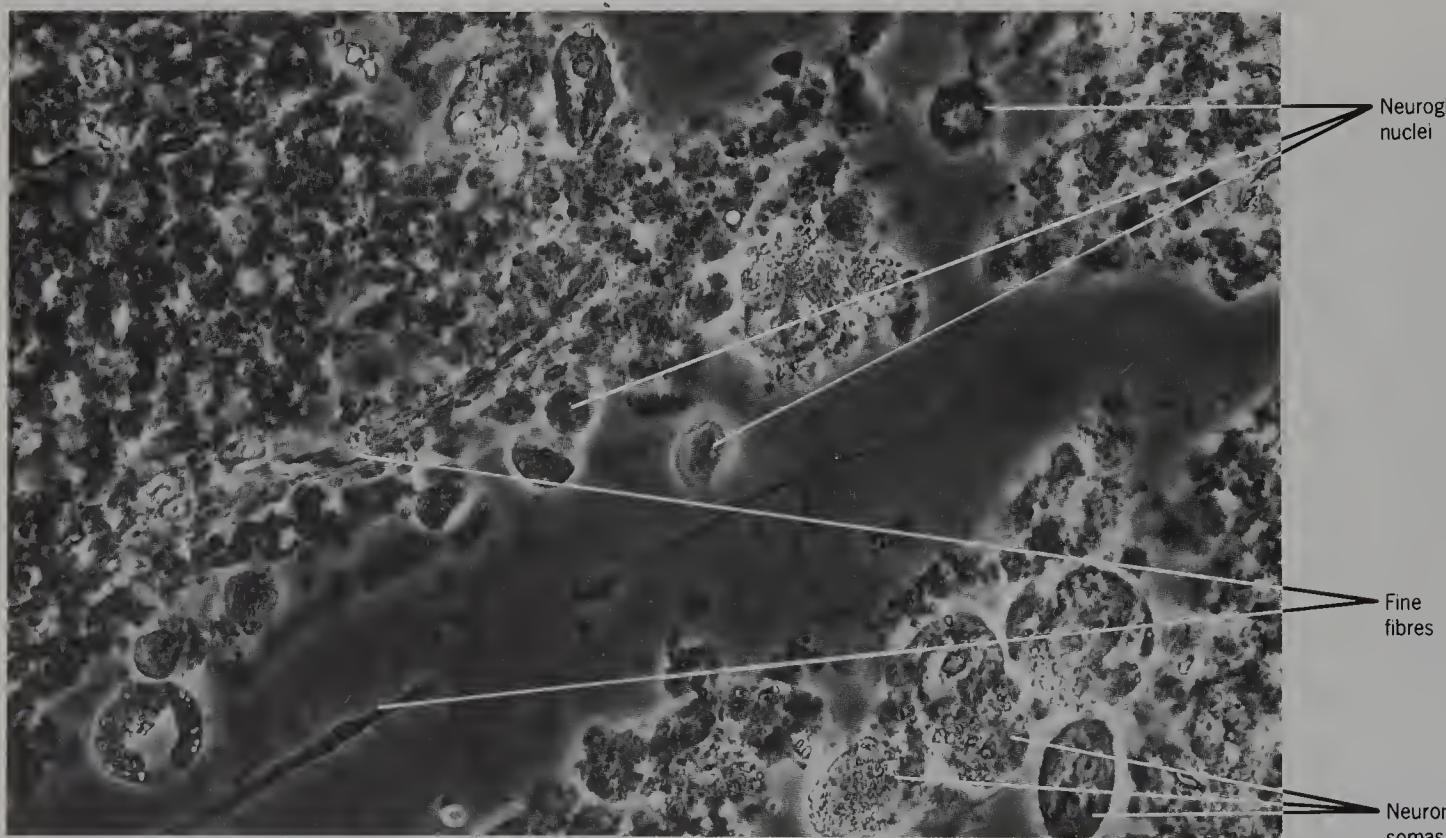


Figure 154 Teased human hypothalamus from a 77-year-old male, to show neurons, fine fibres and neuroglial nuclei (phase contrast, $\times 700$).

The neurons have few or no dendrites.

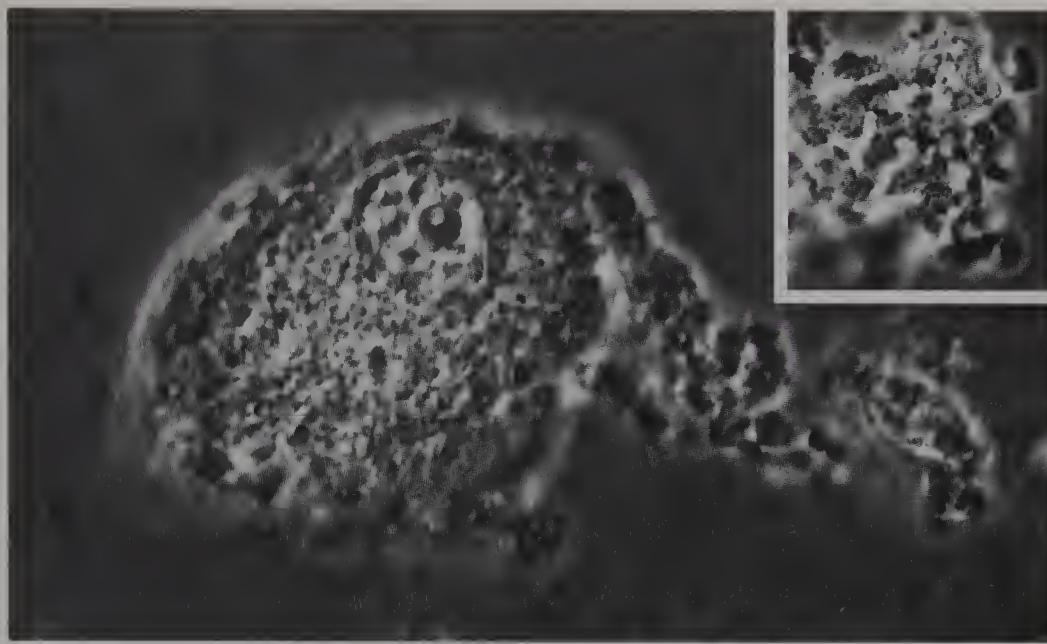


Figure 155 Isolated human hypothalamic neuron from a 53-year-old male (phase contrast, $\times 1140$). Inset: fine granular material adjacent to the latter (phase contrast, $\times 700$).

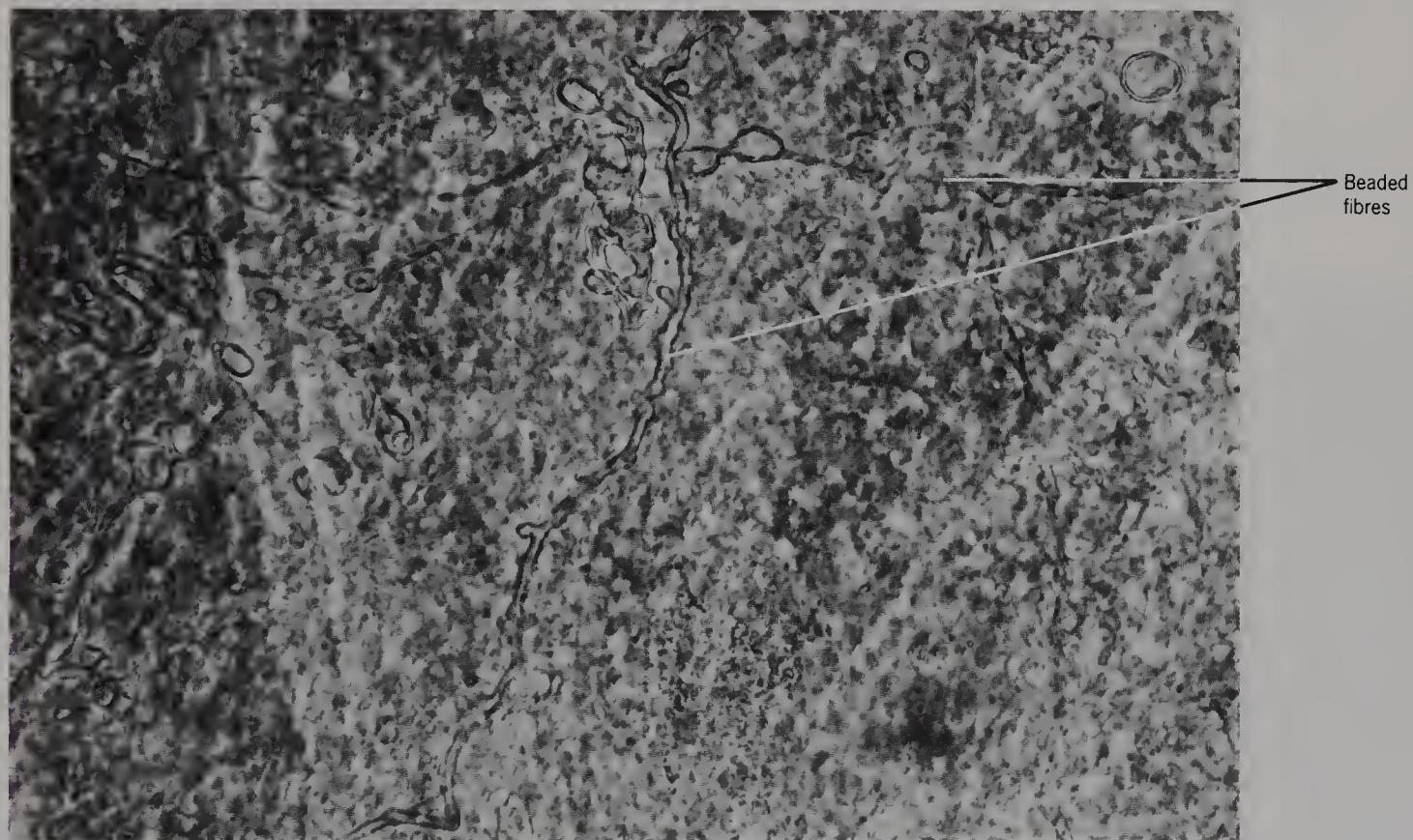


Figure 156 Thin slab of human fornix of the hypothalamus from a 77-year-old male, to show beaded fibres (phase contrast, $\times 700$).

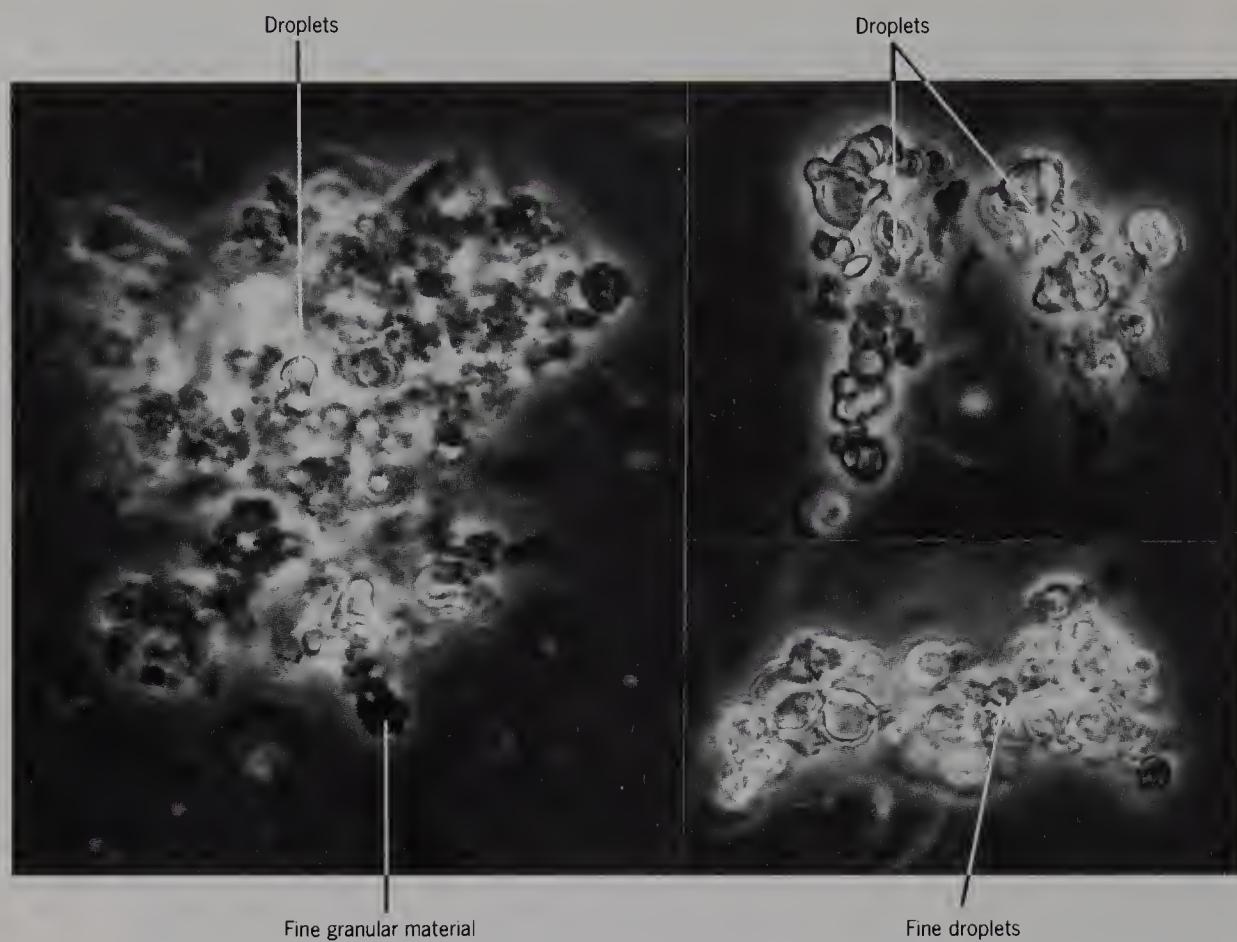


Figure 157 Teased small droplets from previous specimen (phase contrast, $\times 700$).

The droplets are refractile compared with the fine granular material, which is black.



Figure 158 Thin slab of human red nucleus from a 60-year-old male, lightly coloured with methylene blue to show the incidence of neuron somas (bright field, $\times 100$).

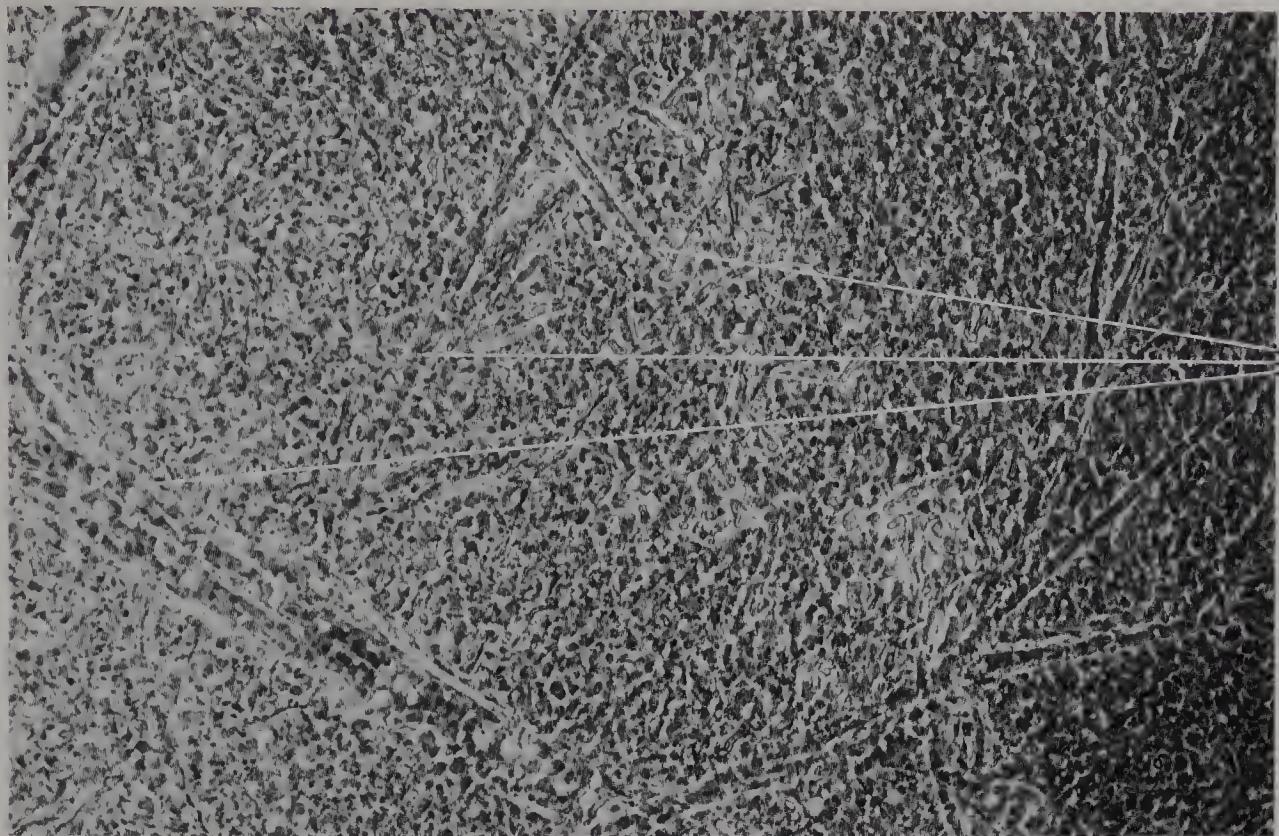


Figure 159 Thin slab of human red nucleus from a 77-year-old male, to show the distribution of capillaries (bright field, $\times 300$).

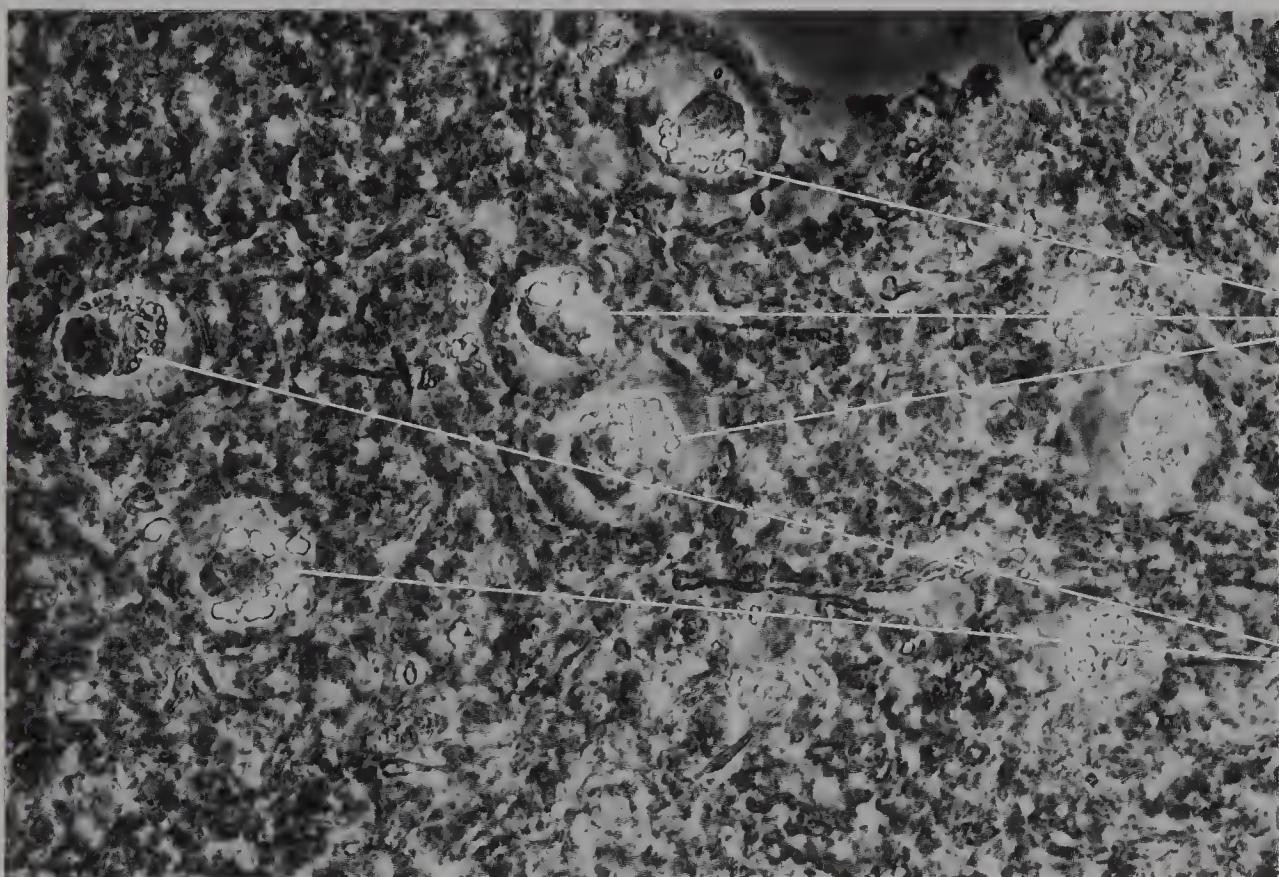


Figure 160 Partially teased human red nucleus from a 77-year-old male, to show neurons with associated lipofuscin (phase contrast, $\times 700$).



Figure 161 Thin slab of human red nucleus from a 73-year-old male, to show fibre tracts and droplets (phase contrast, $\times 700$).

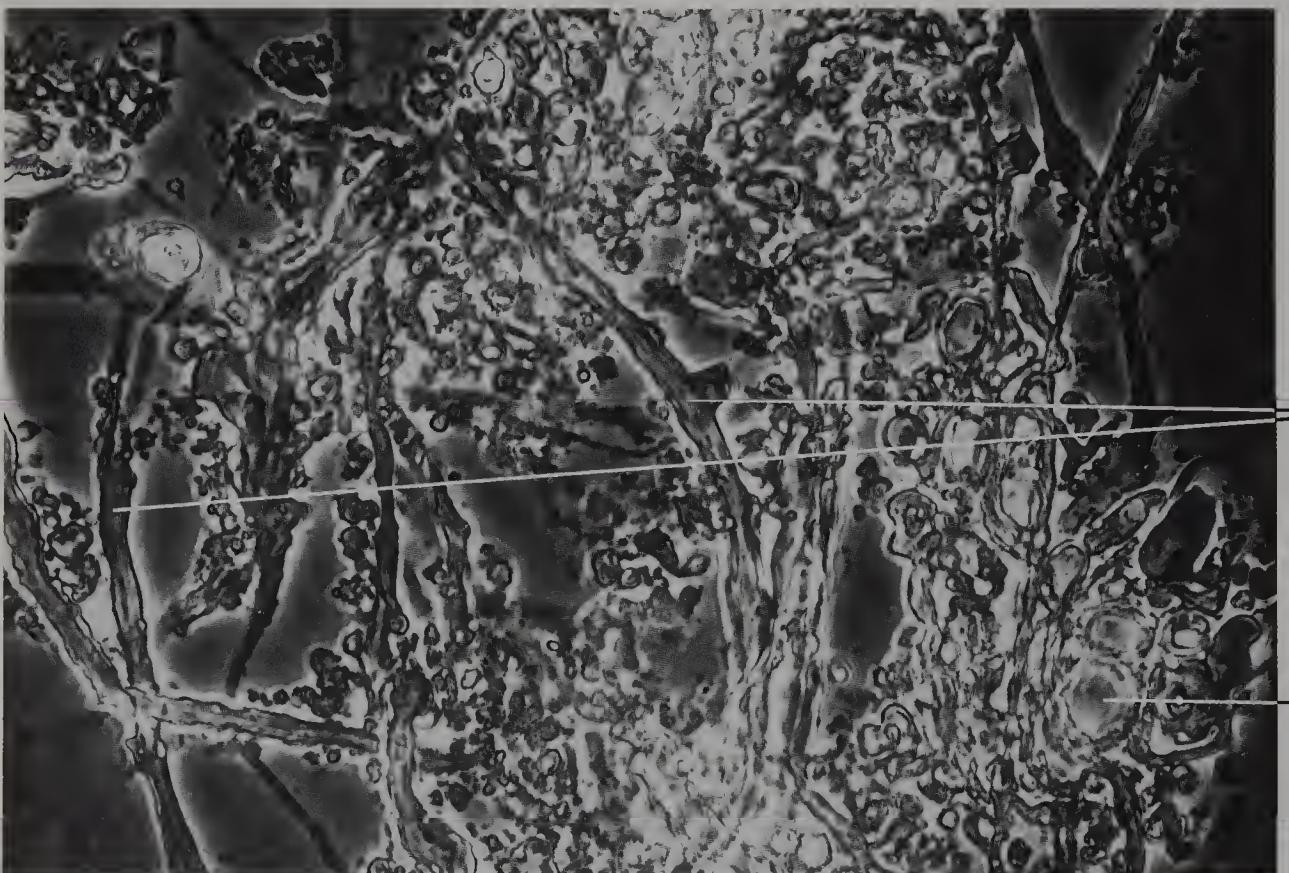


Figure 162 Teased human red nucleus from a 73-year-old male, to show beaded fibres and droplets (phase contrast, $\times 700$).

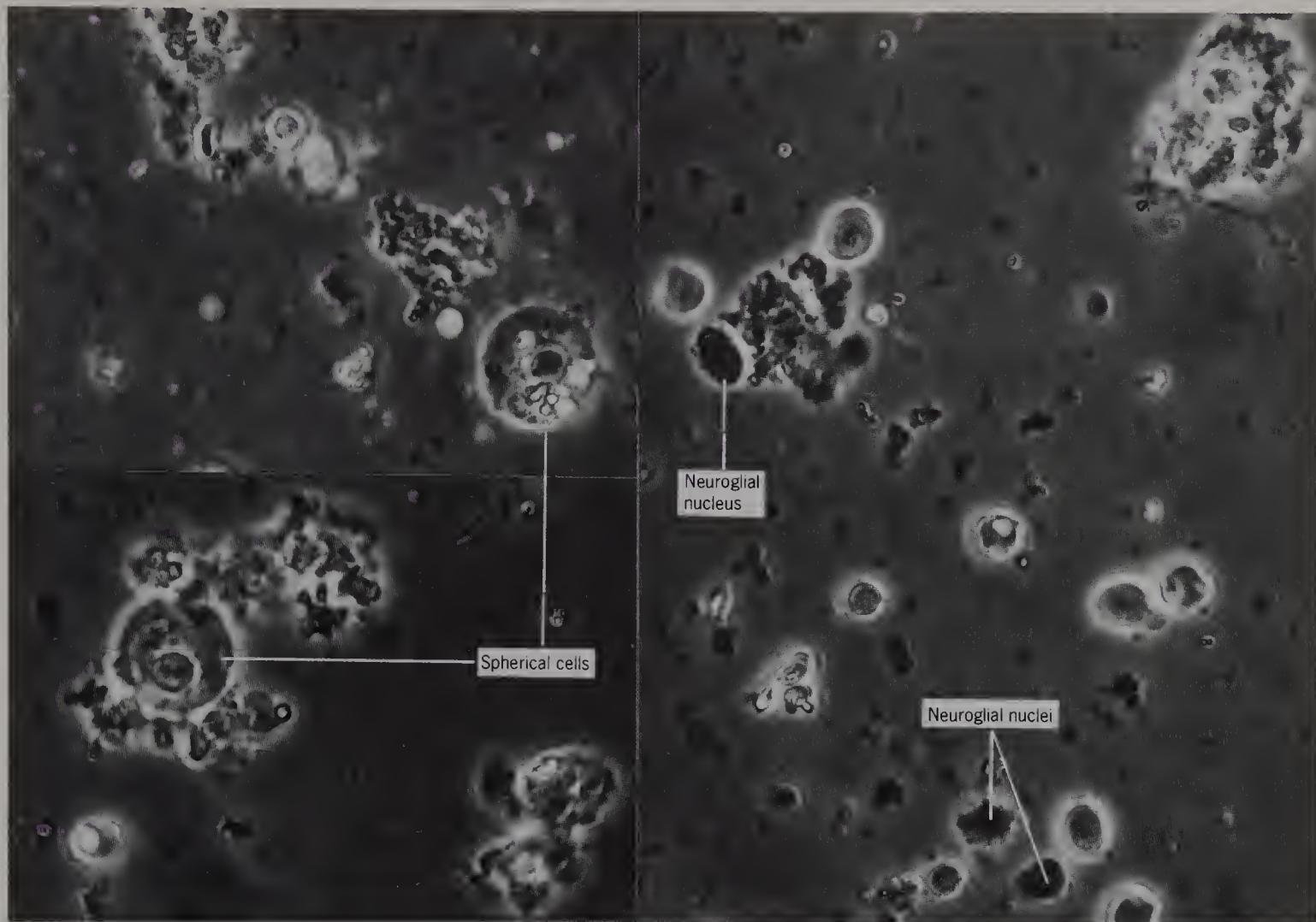


Figure 163 Teased human red nucleus from a 77-year-old male, to show unidentified spherical cells, possible neuron somas and neuroglial nuclei (phase contrast, $\times 700$).

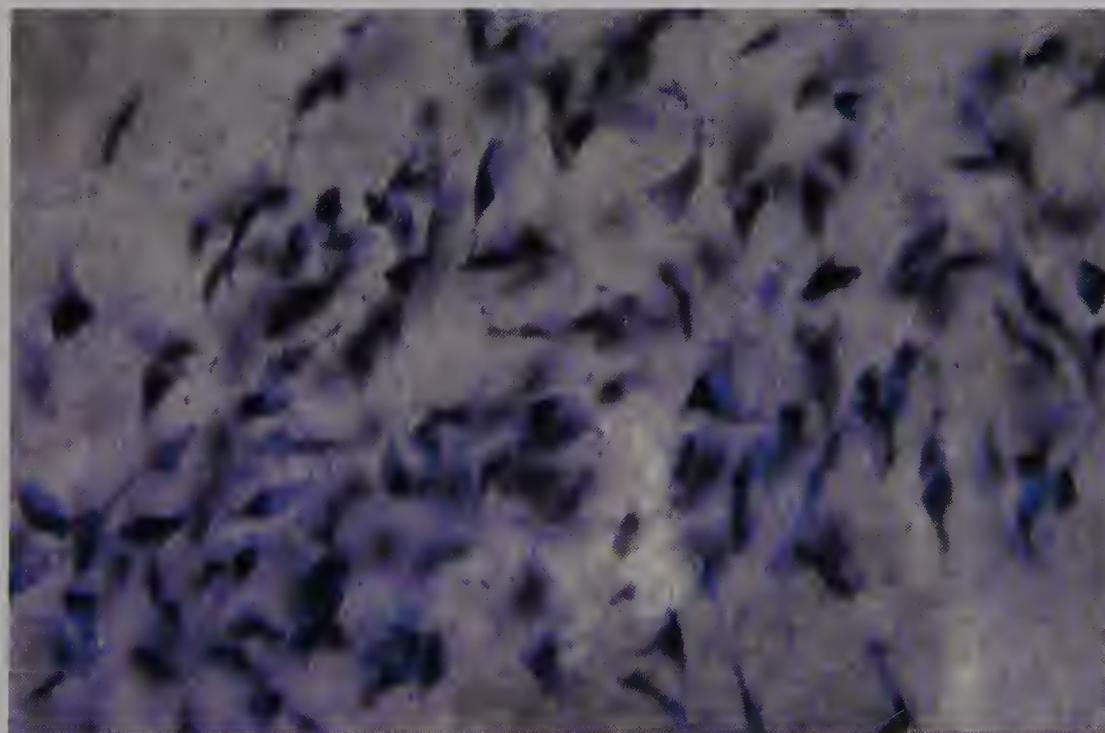


Figure 164 Thin slab of human substantia nigra from a 60-year-old male, lightly coloured with methylene blue to show the high incidence of neuron somas (bright field, $\times 100$).

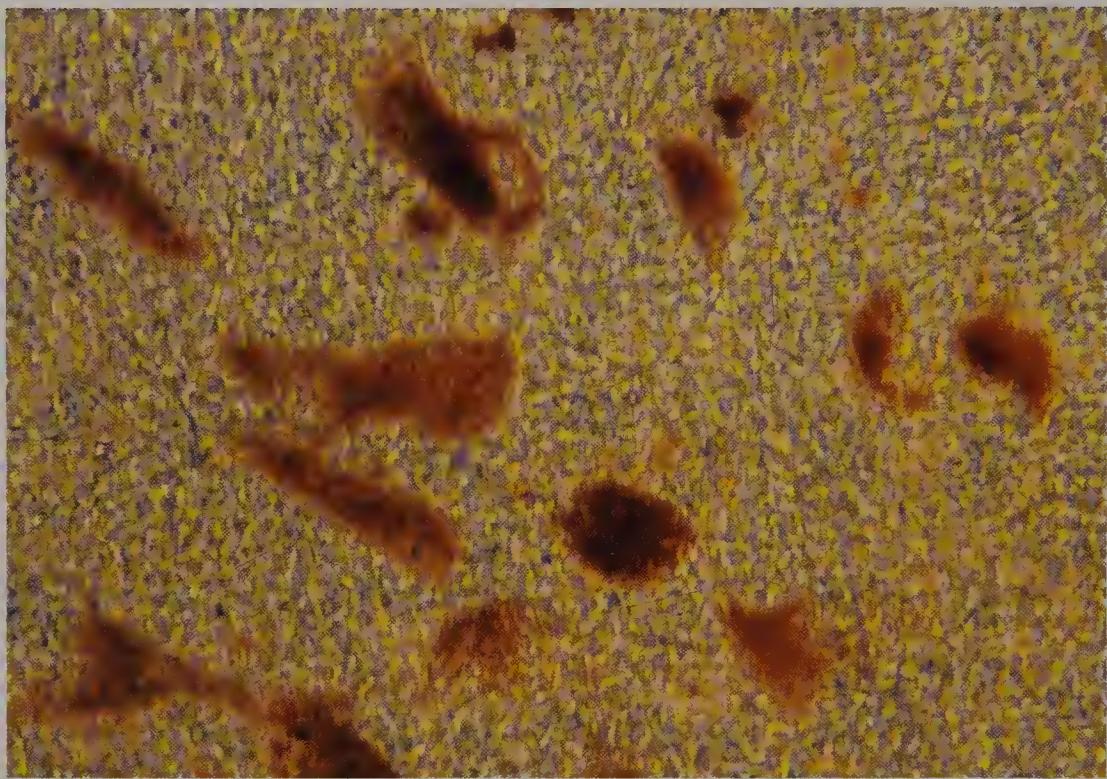


Figure 165 Thin slab of human substantia nigra from an 84-year-old male, to show the incidence of neuron somas (bright field, $\times 255$).

The melanin is naturally brown and in the brain is found only in neurons of the substantia nigra.

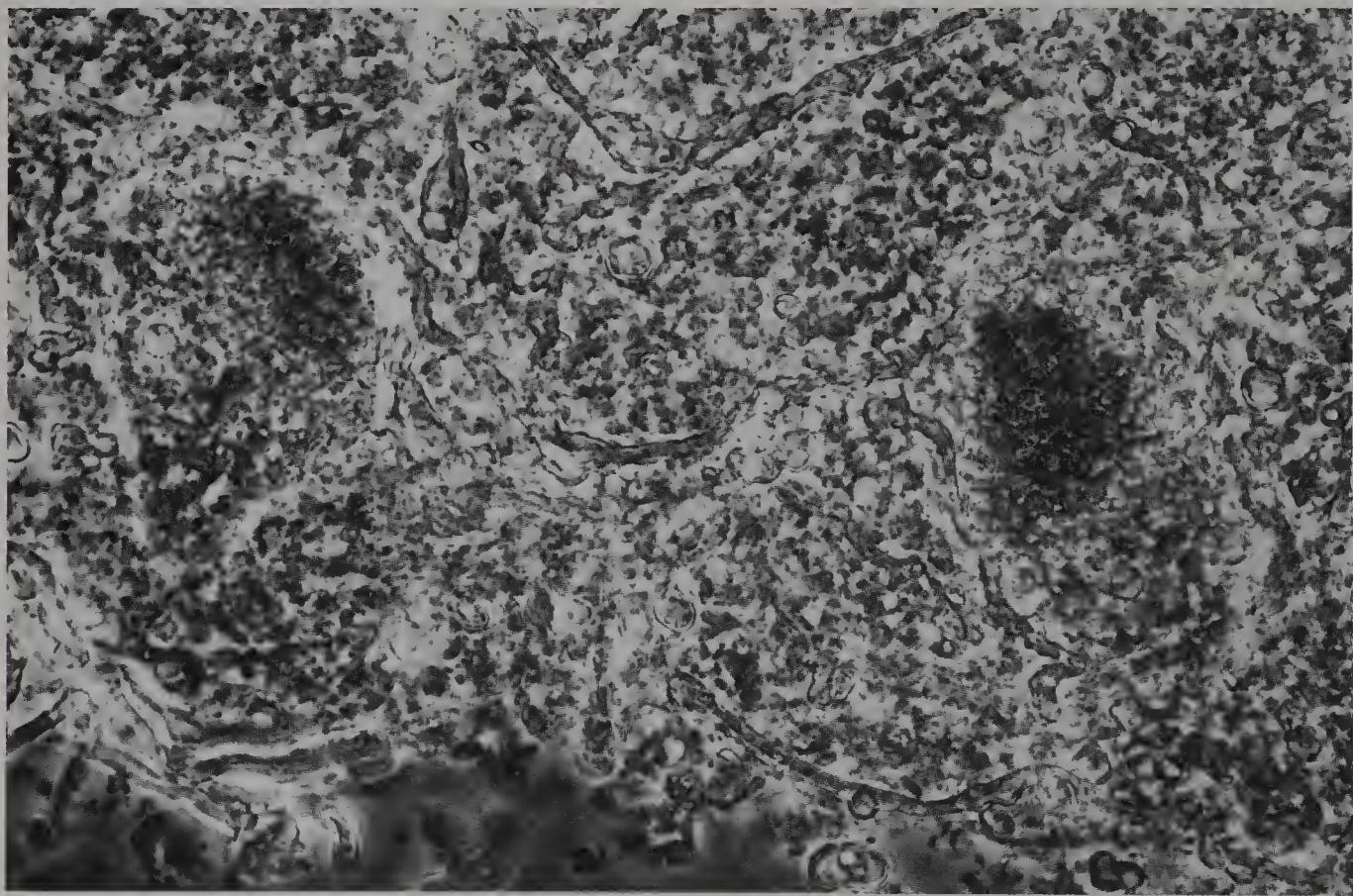


Figure 166 Partially teased human substantia nigra, from a 73-year-old male, to show two neurons and beaded fibres (phase contrast, $\times 800$).

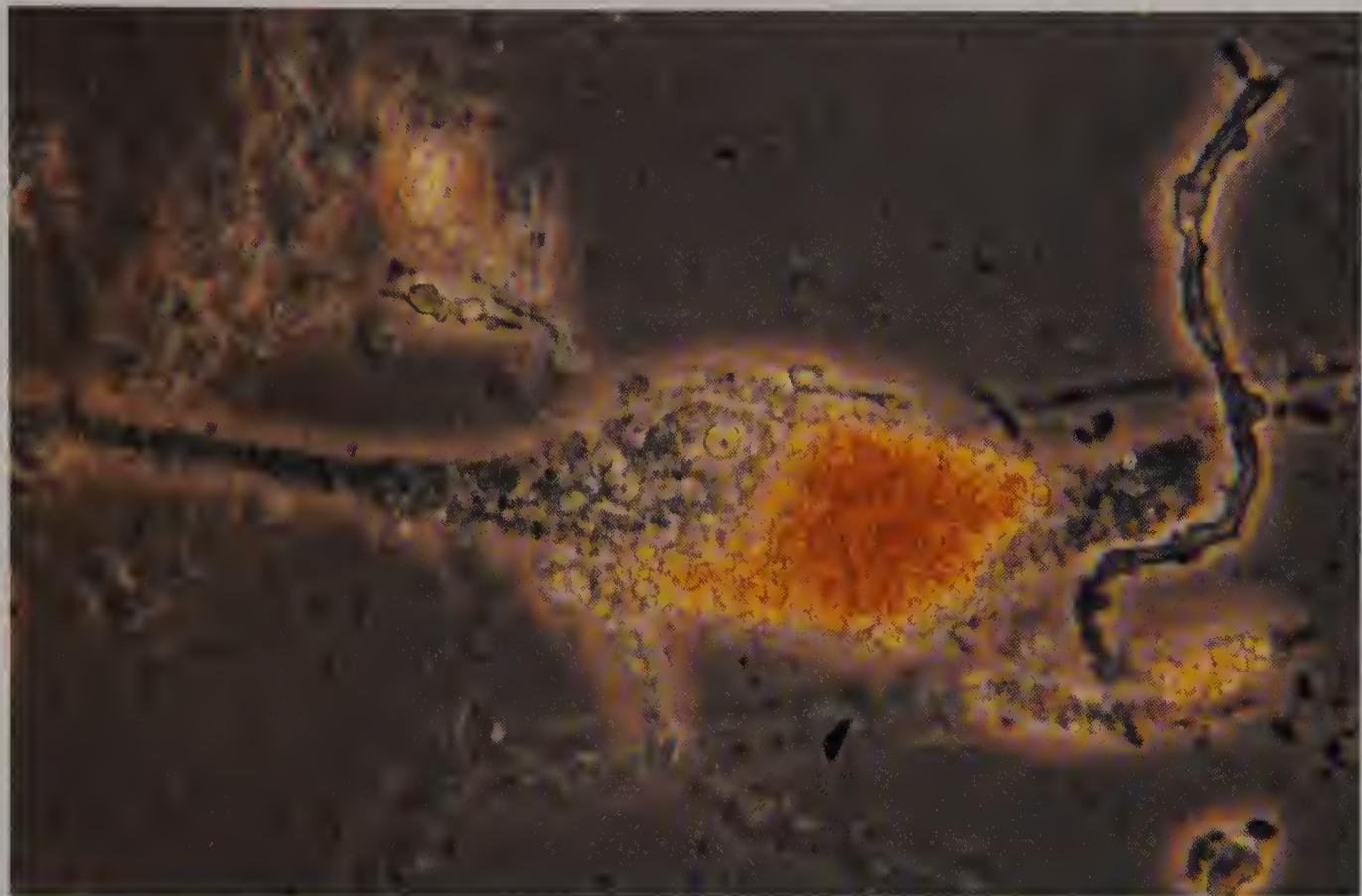


Figure 167 Teased human substantia nigra from a 74-year-old male, to show a neuron with adjacent fine granular material (phase contrast, $\times 610$).



Figure 168 Teased human substantia nigral neuroglia from the previous specimen, to show fine granular material (phase contrast, $\times 800$).

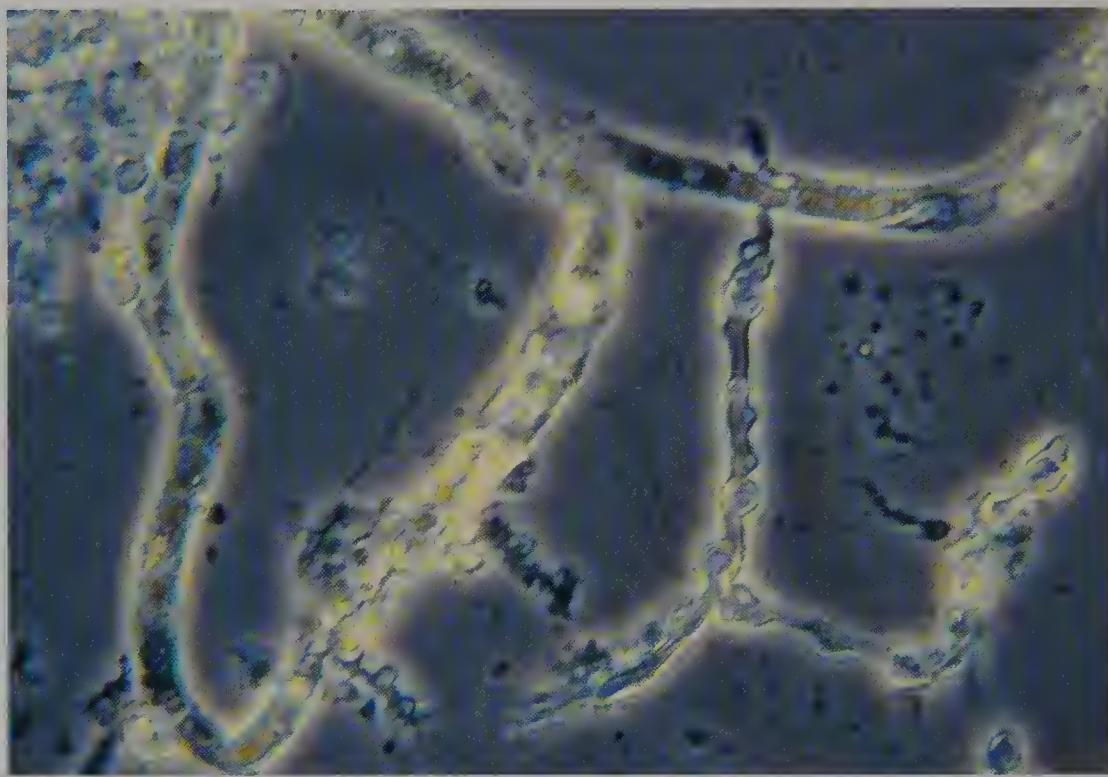


Figure 169 Isolated capillaries and beaded fibres from human substantia nigra of an 84-year-old male (phase contrast, $\times 610$).

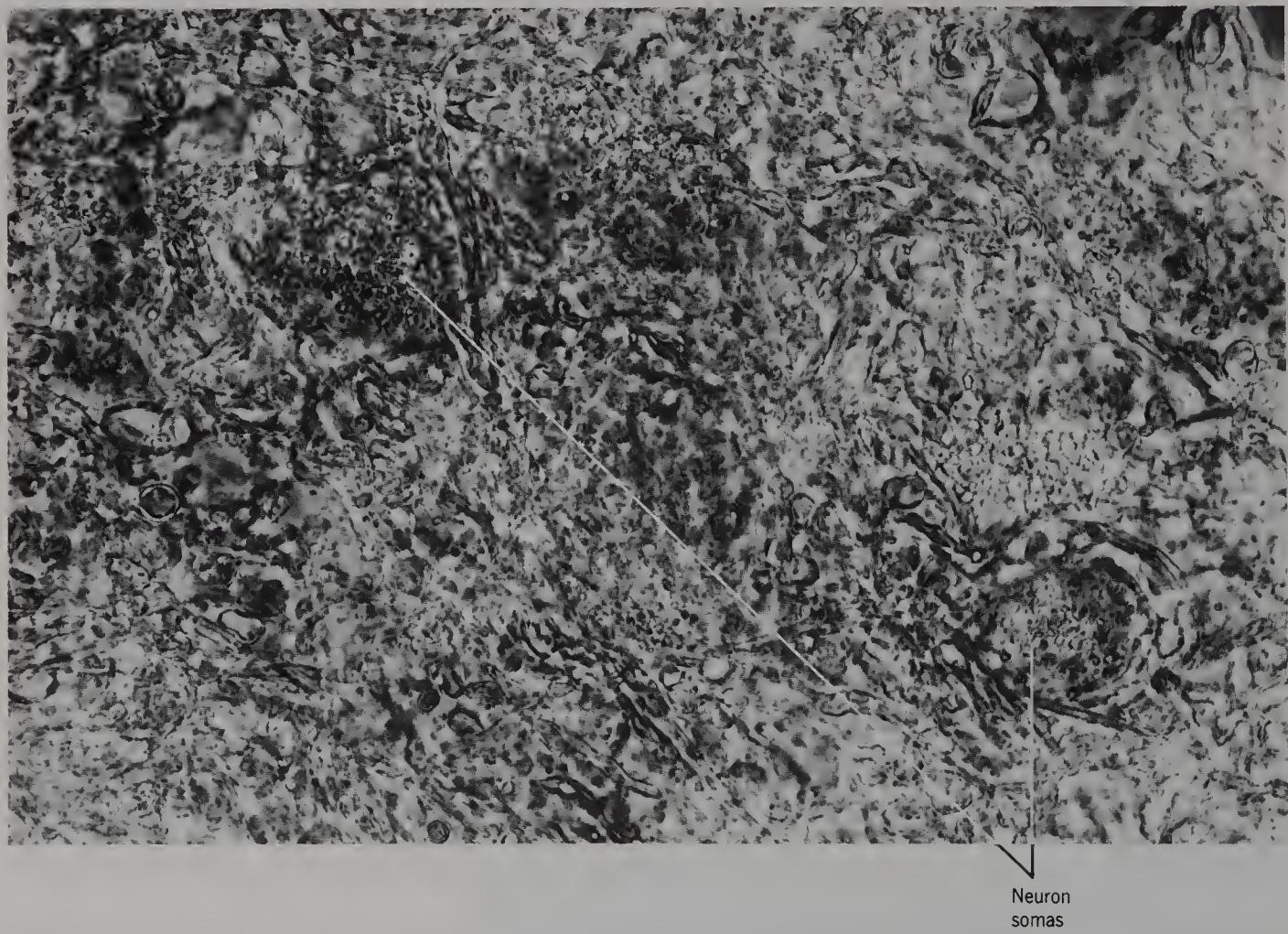


Figure 170 Thin slab of the human mammillary body from a 77-year-old male, to show neurons and beaded fibres (phase contrast, $\times 800$).

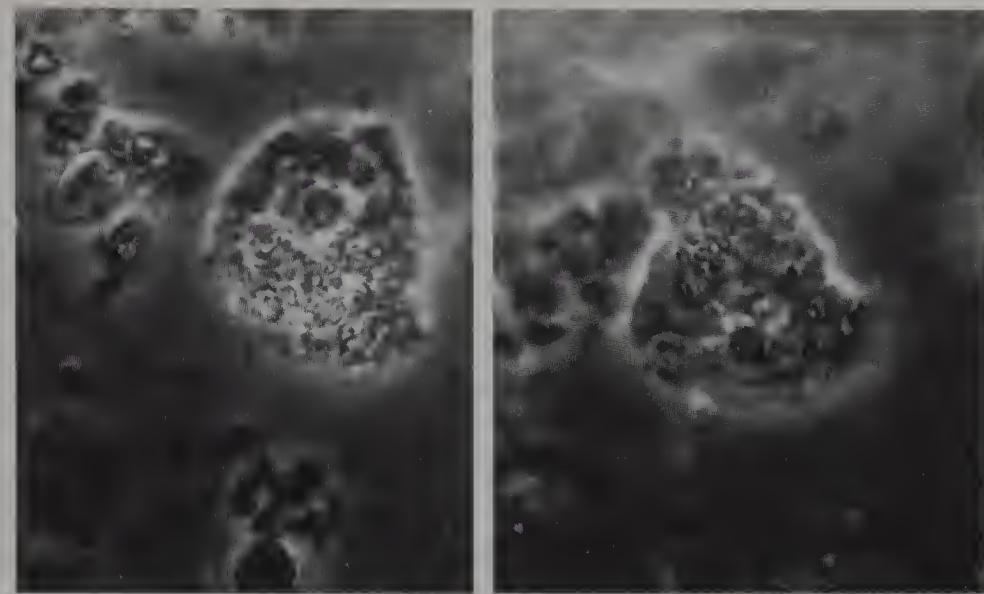


Figure 171 Isolated neuron somas from the previous specimen (phase contrast, $\times 800$).

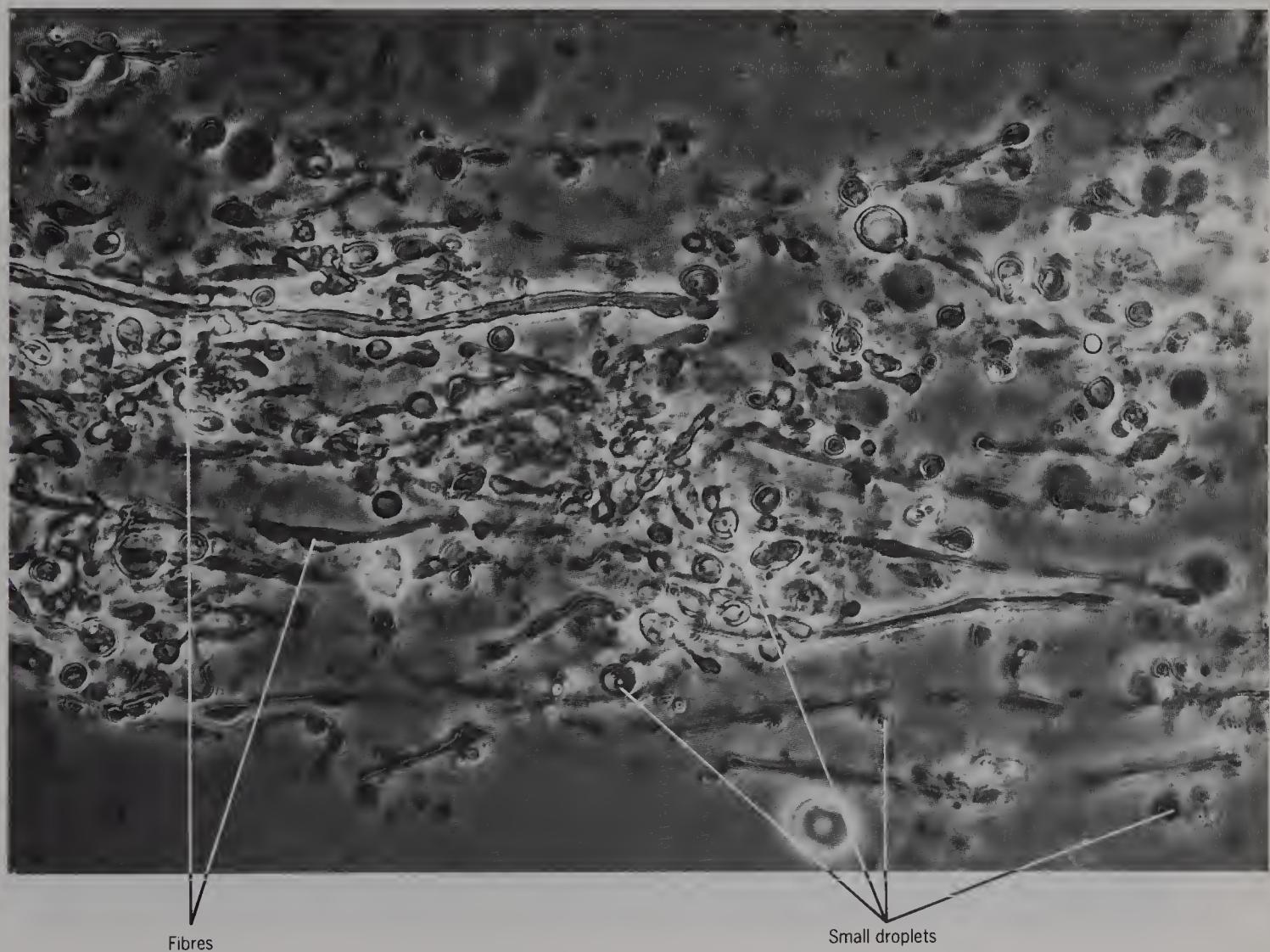


Figure 172 Teased fibres and small droplets from the same specimen as in the penultimate figure (phase contrast, $\times 800$).

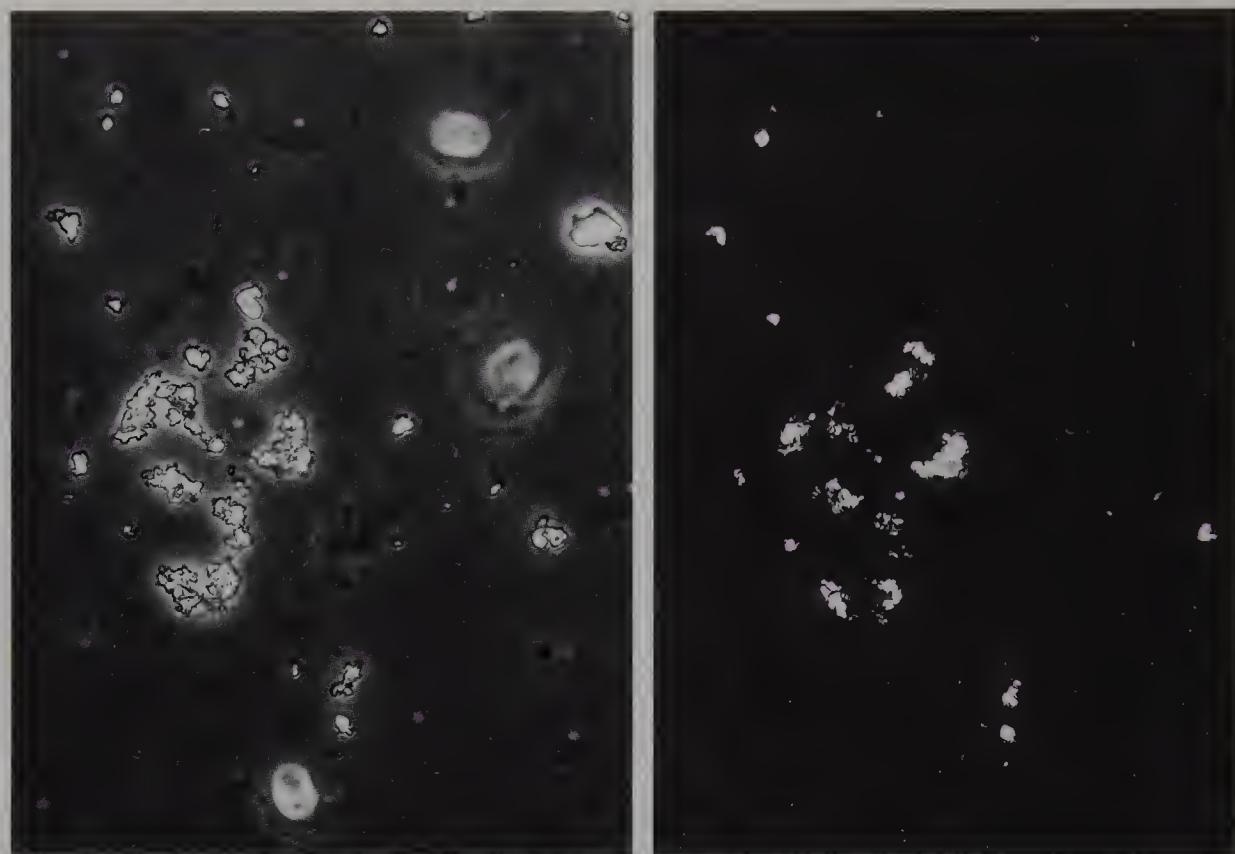


Figure 173 Lipofuscin from the same specimen as in the previous figure, with polars uncrossed (left) and with polars crossed (right) to show birefringence (polarized light, $\times 700$).

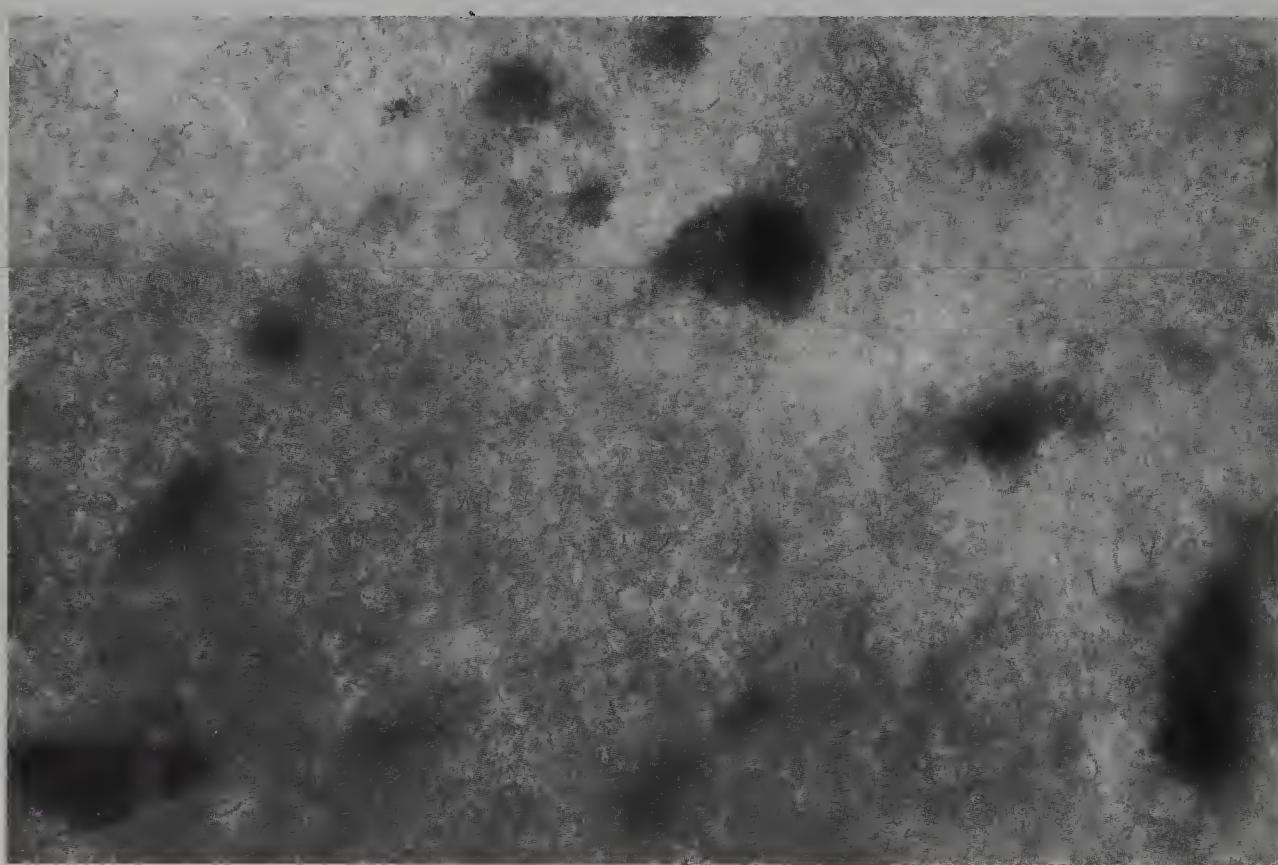


Figure 174 Thin slab of human superior colliculus from a 75-year-old male, lightly coloured with methylene blue to show the incidence of neurons (phase contrast, $\times 700$).

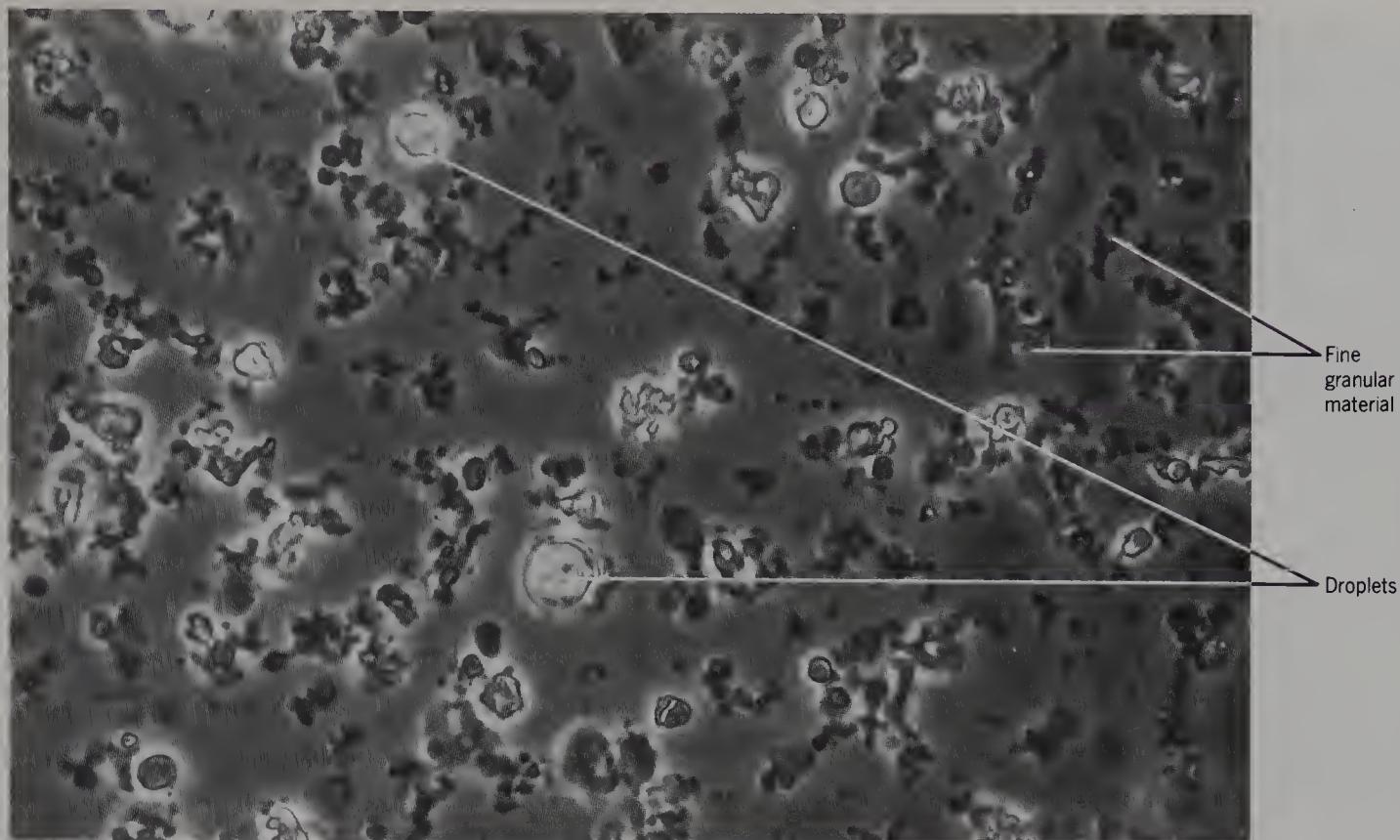


Figure 175 Teased human superior colliculus from a 75-year-old male, to show large refractile droplets and fine granules (phase contrast, $\times 700$).

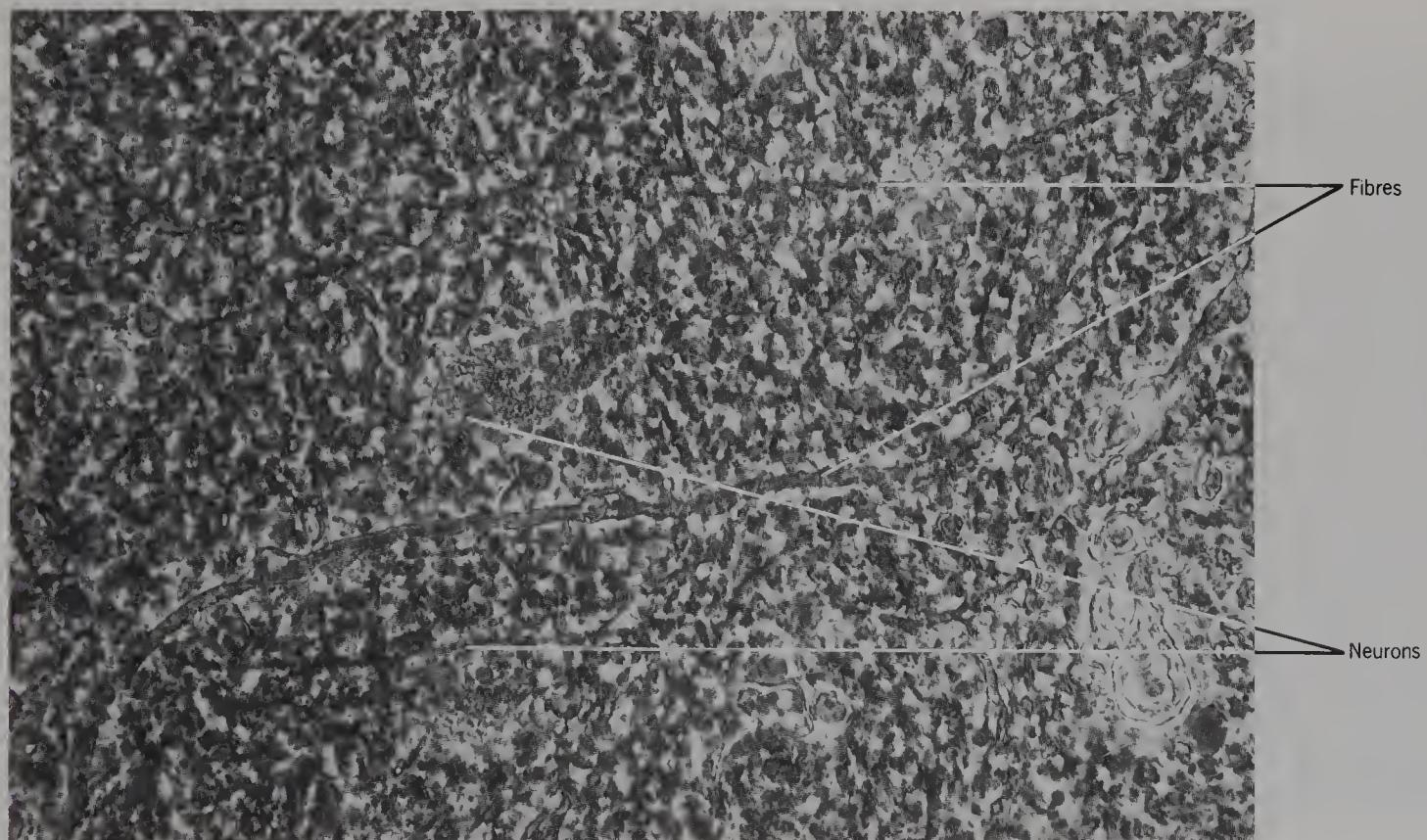


Figure 176 Thin slab of human inferior colliculus from a 75-year-old male (phase contrast, $\times 700$).

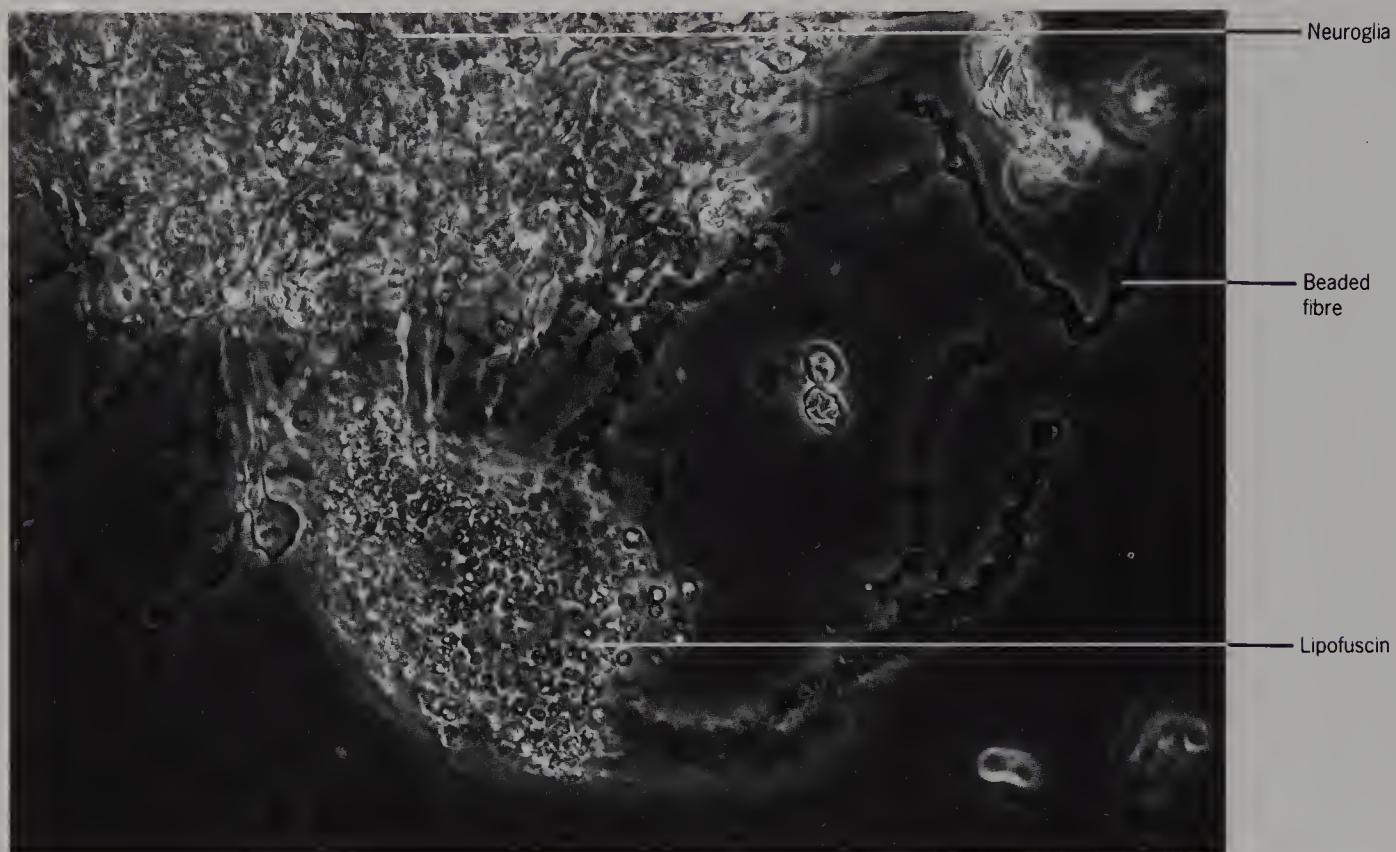


Figure 177 Teased human inferior colliculus from a 75-year-old male, to show a neuron covered with lipofuscin and associated neuroglia (phase contrast, $\times 700$).

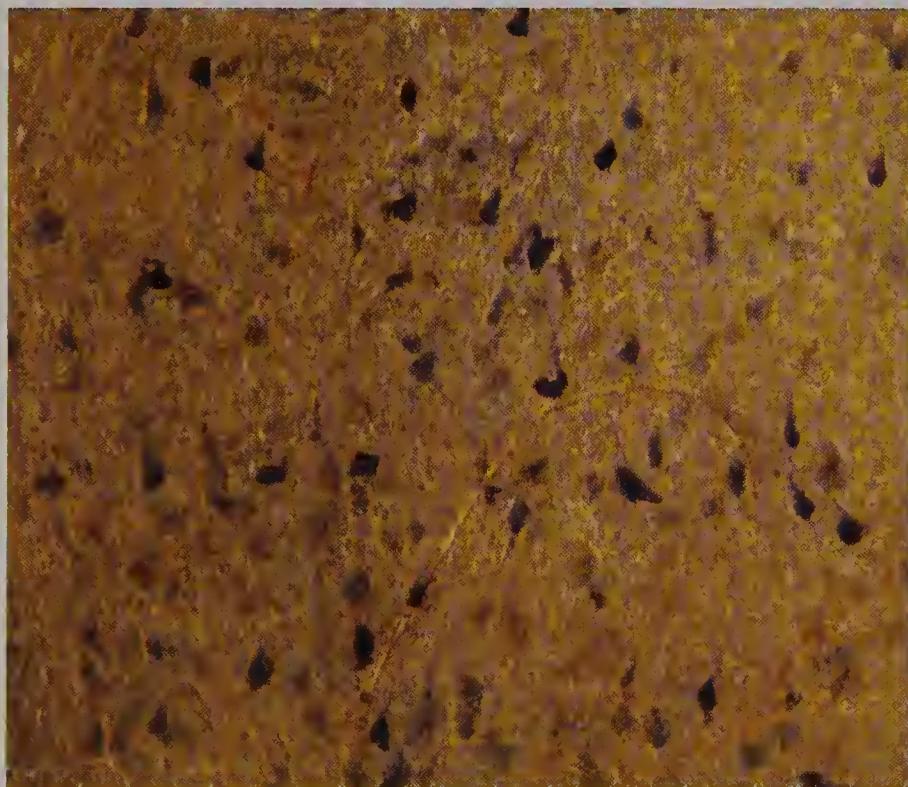


Figure 178 Thin slab of the human hippocampus from a 60-year-old male, lightly coloured with methylene blue to show the incidence of neurons (bright field, $\times 100$).

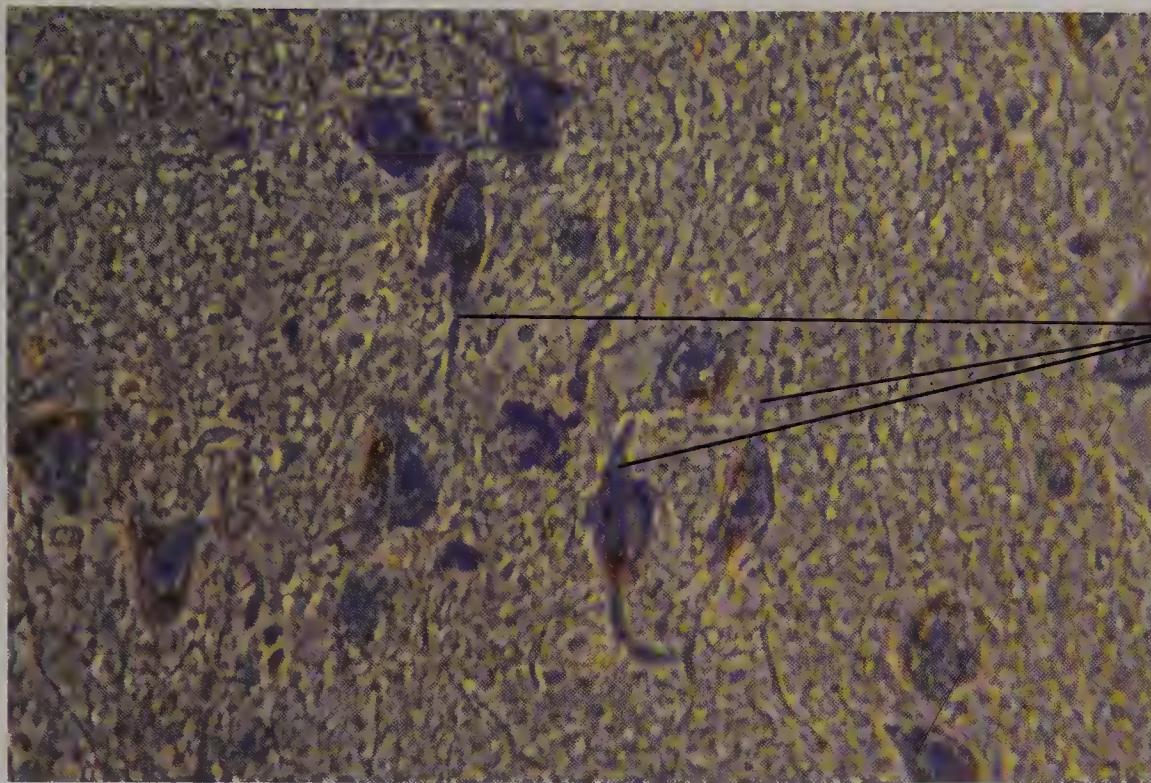


Figure 179 Thin slab of the human hippocampus from a 60-year-old male, lightly coloured with methylene blue to show the incidence and appearance of pyramidal neuron somas (bright field, $\times 255$).

There is lipofuscin in the cytoplasm of some neurons.

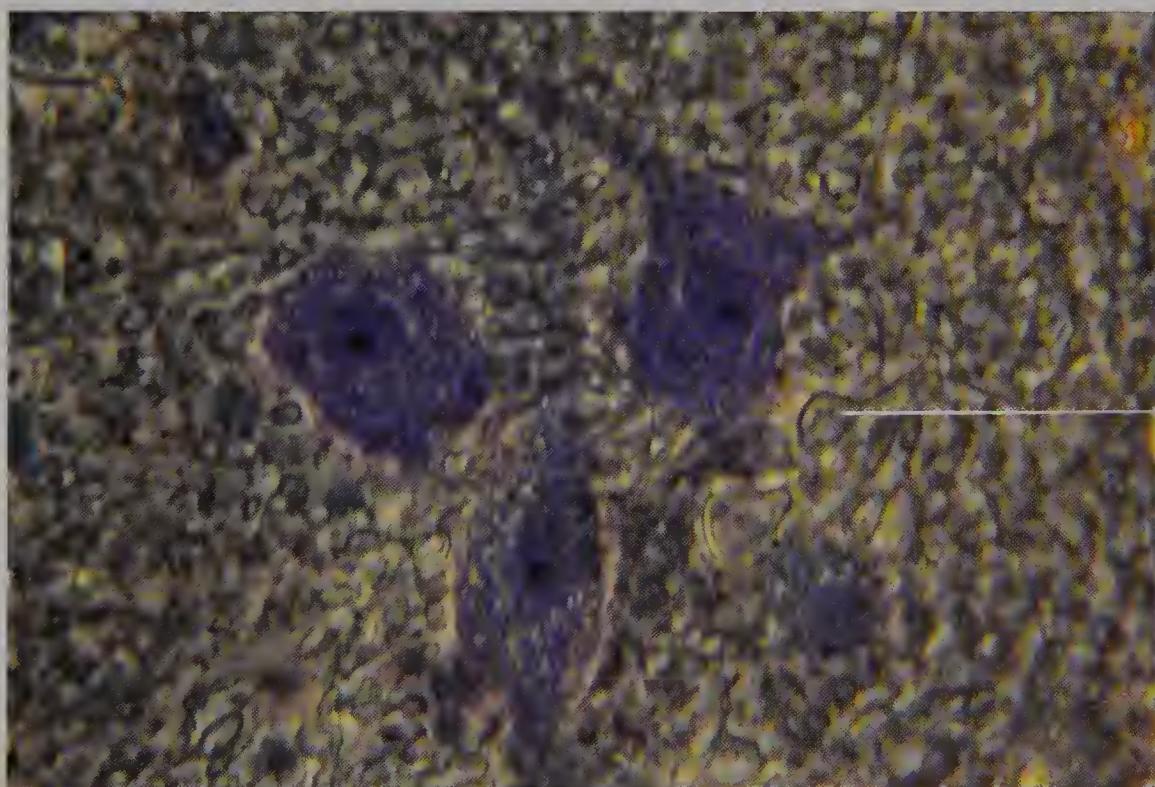


Figure 180 Higher power view of the same specimen as in the previous figure, to show pyramidal neurons *in situ* and fine beaded fibres (bright field, $\times 610$).

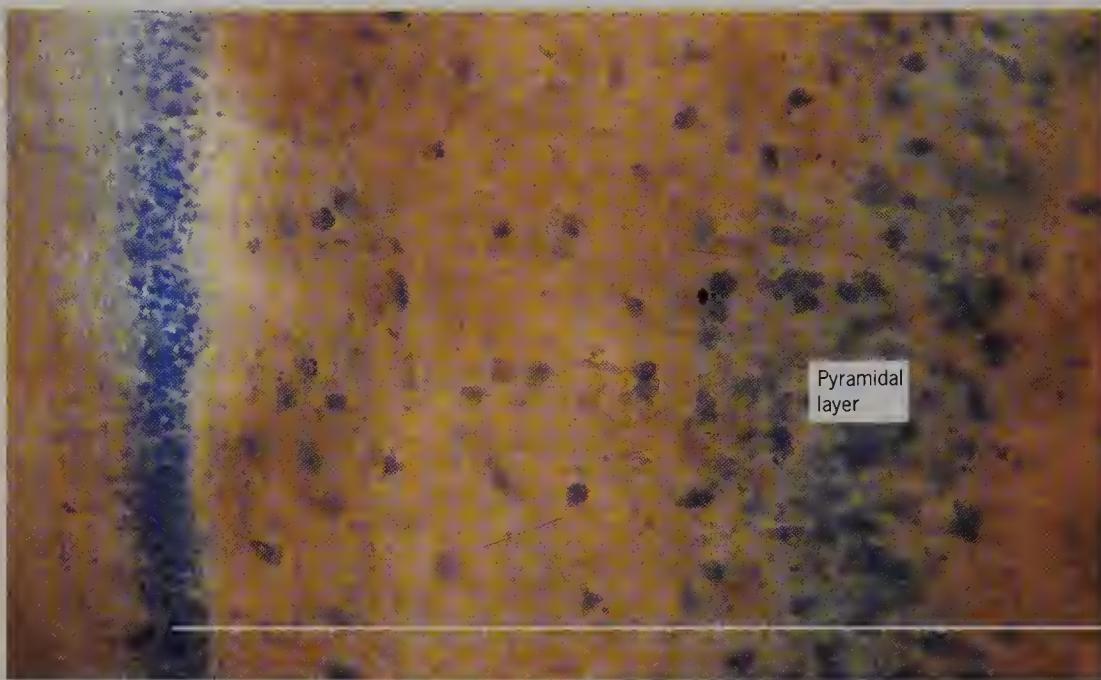


Figure 181 Thin slab of rabbit hippocampus, lightly coloured with methylene blue, to show pyramidal layer (right) and granule cell layer (left) (bright field, $\times 100$).

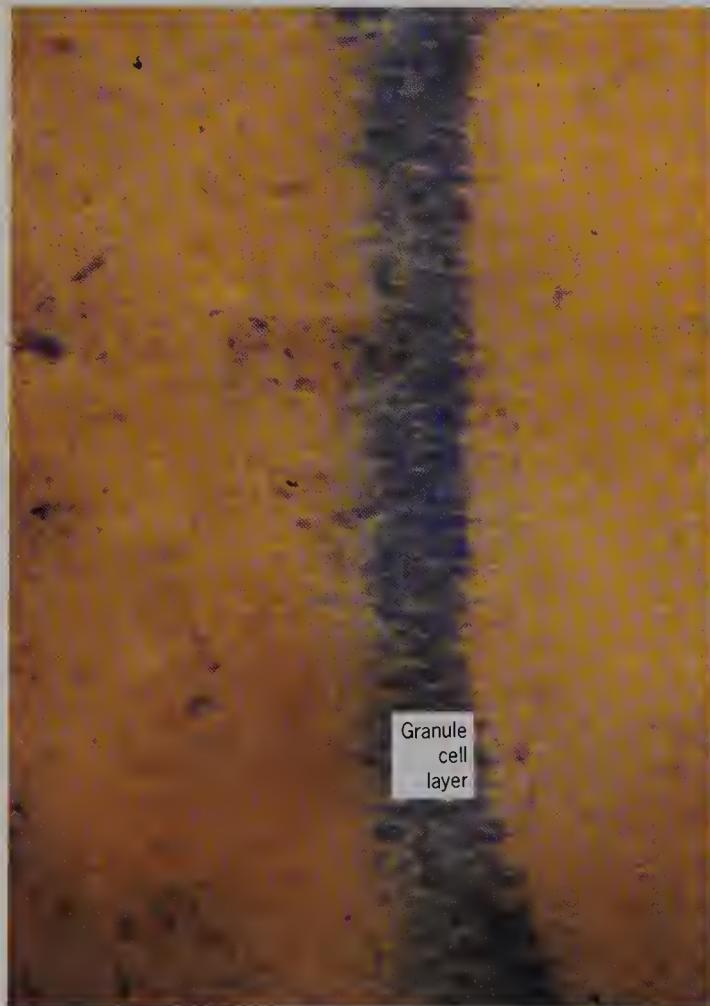


Figure 182 Higher power view of the same specimen as in the previous figure, but enlarged granule cell layer with fine processes proceeding from the cells (bright field, $\times 255$).

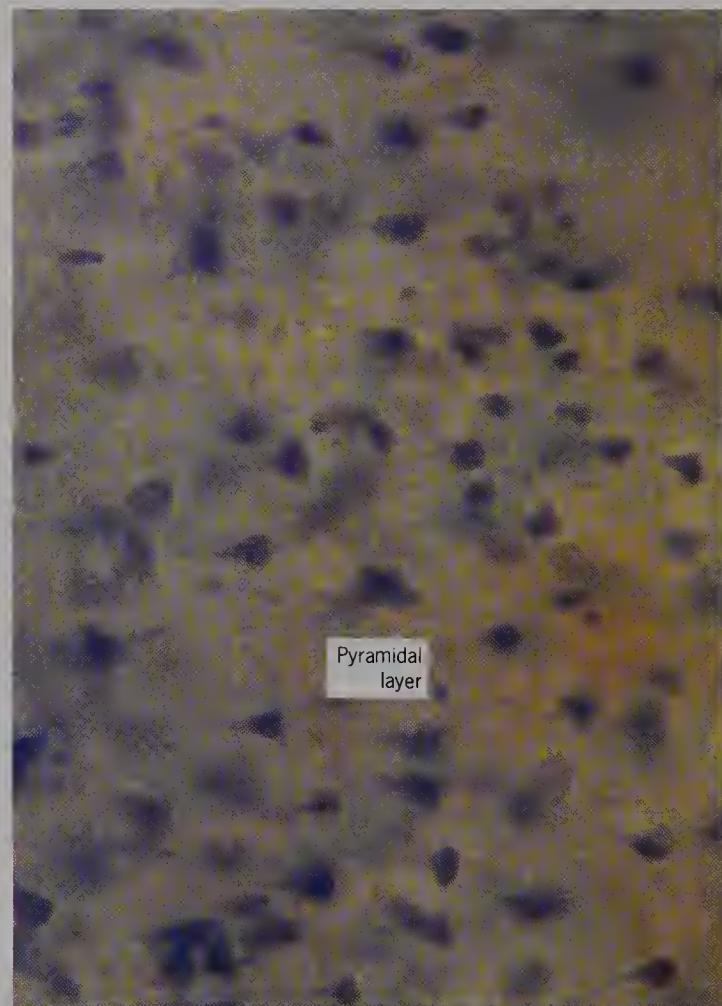


Figure 183 Higher power view of the same specimen as in the previous figure, with the pyramidal cell layer enlarged (bright field, $\times 255$).

The somas of granule cells are smaller than those of the pyramidal neurons.

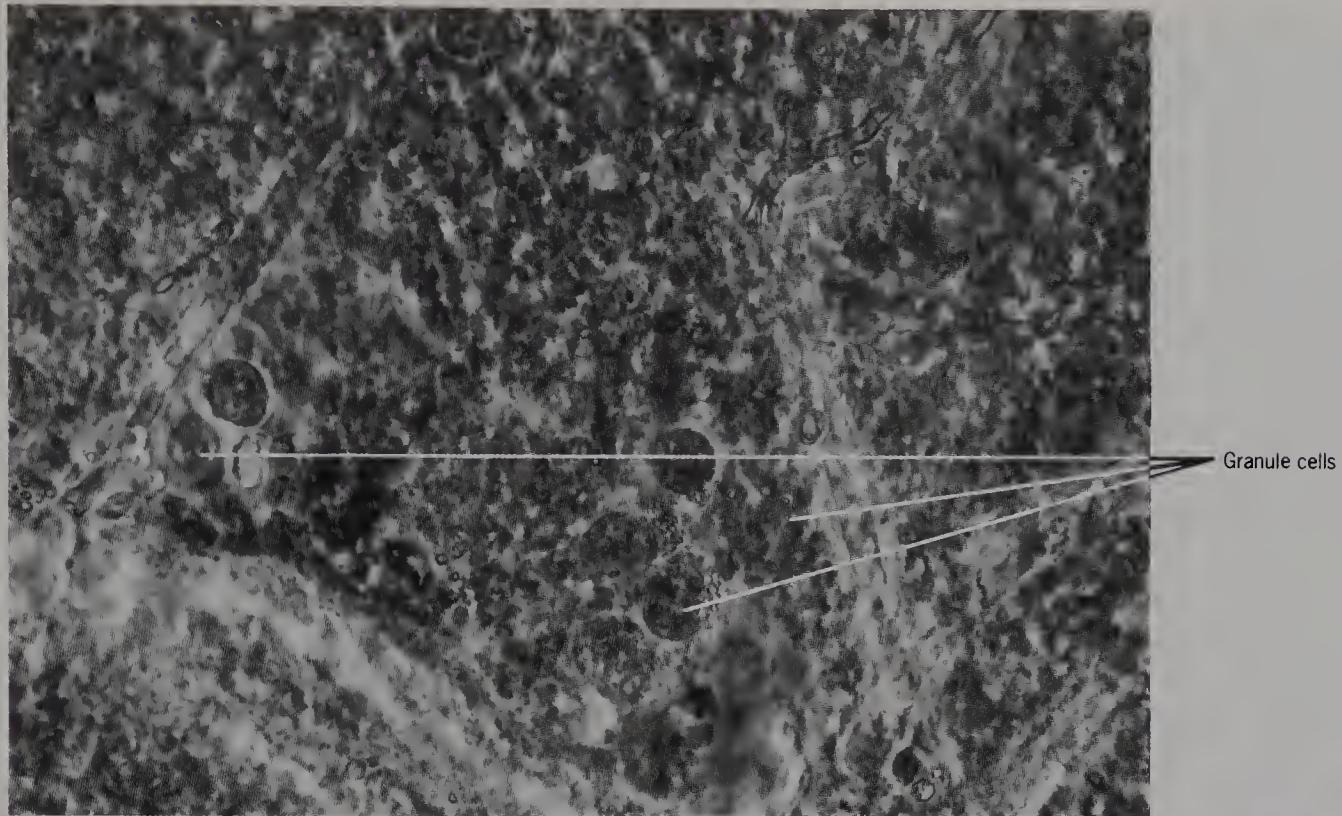


Figure 184 Thin slab of the human hippocampus from an 80-year-old female, to show granule cell somas (phase contrast, $\times 700$).

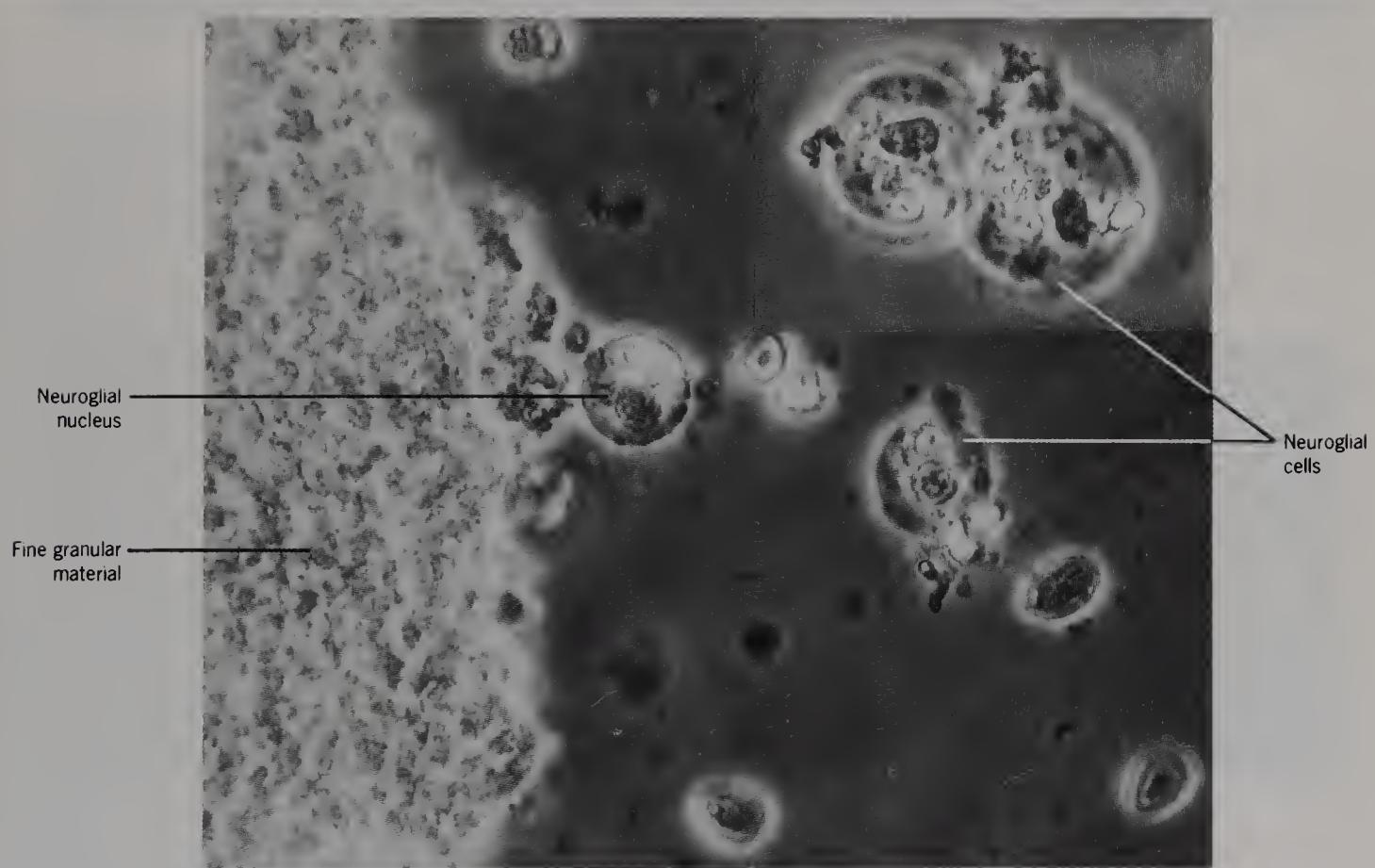


Figure 185 Teased human hippocampus from the previous specimen to show granule cells and neuroglial nuclei (phase contrast, $\times 700$). Inset : two isolated granule cells.

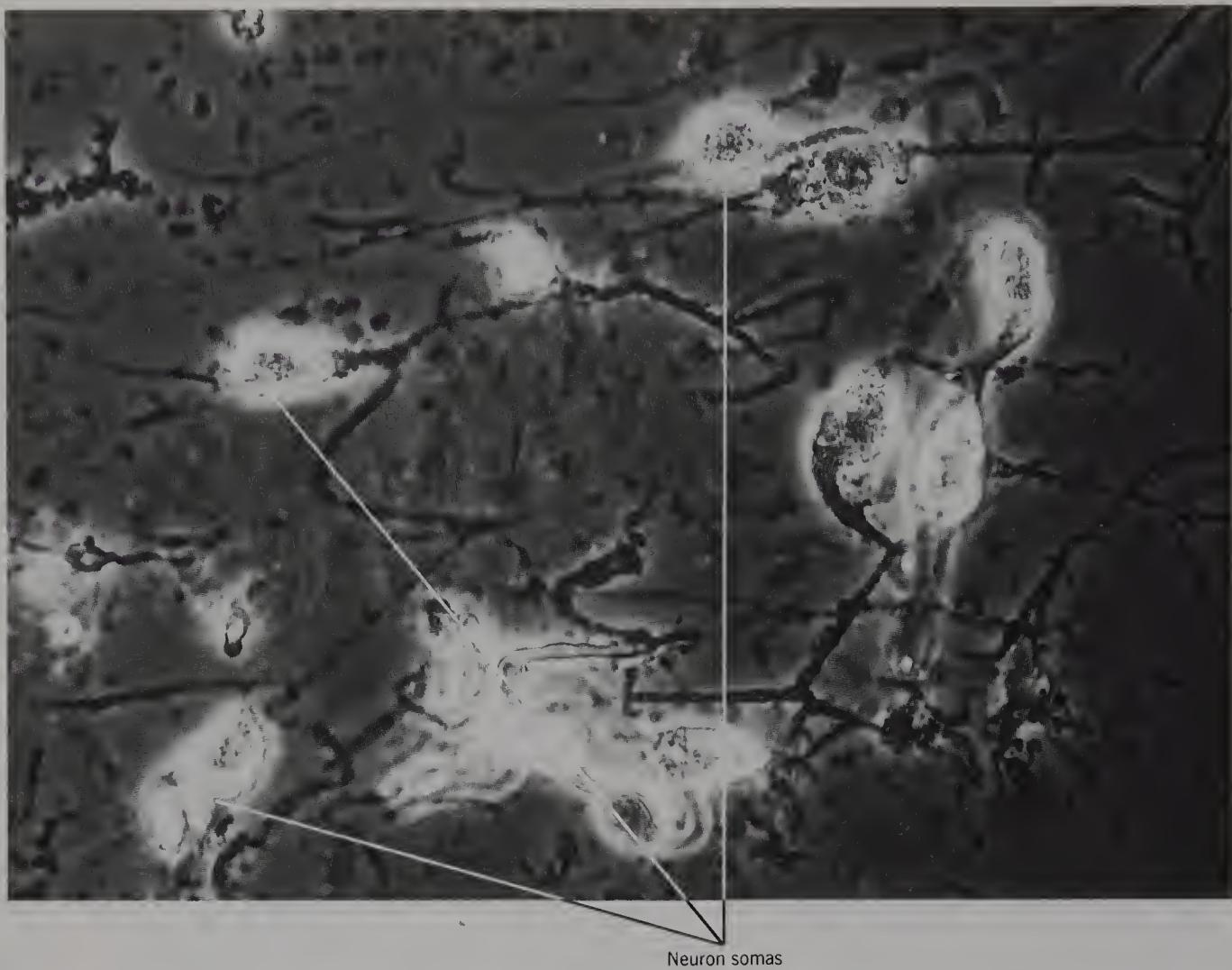


Figure 186 Teased human hippocampus from a 54-year-old male, to show pyramidal neurons and their processes (phase contrast, $\times 800$).

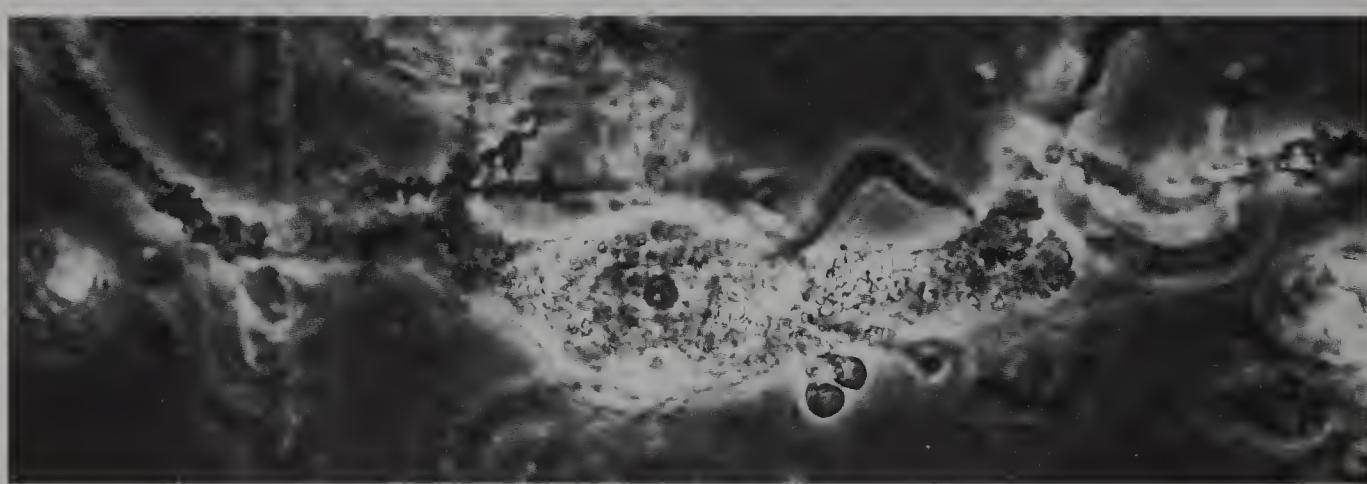


Figure 187 Teased human hippocampal pyramidal neuron from the previous specimen (phase contrast, $\times 800$).

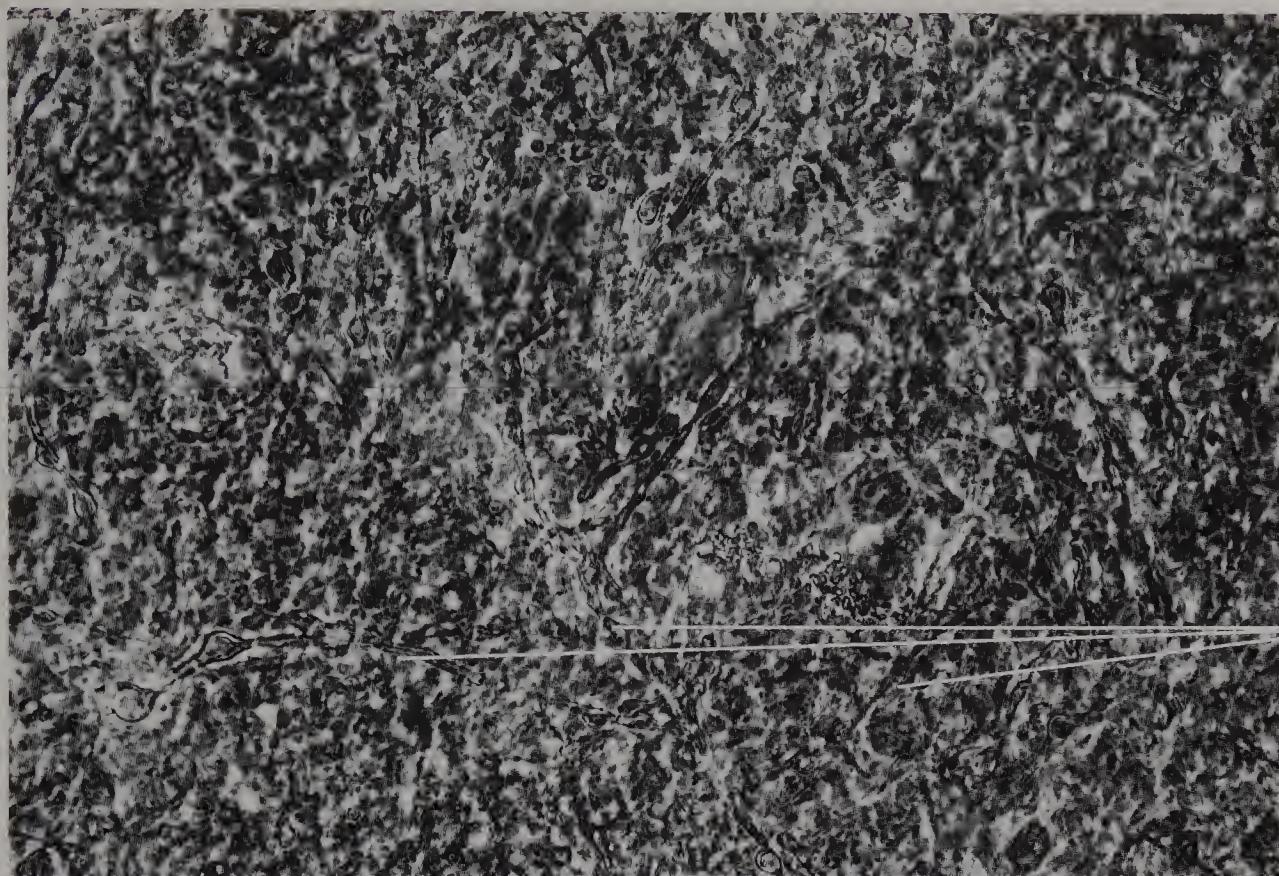


Figure 188 Thin slab of the human amygdala from a 73-year-old male, to show neuron somas and beaded fibres (phase contrast, $\times 700$).

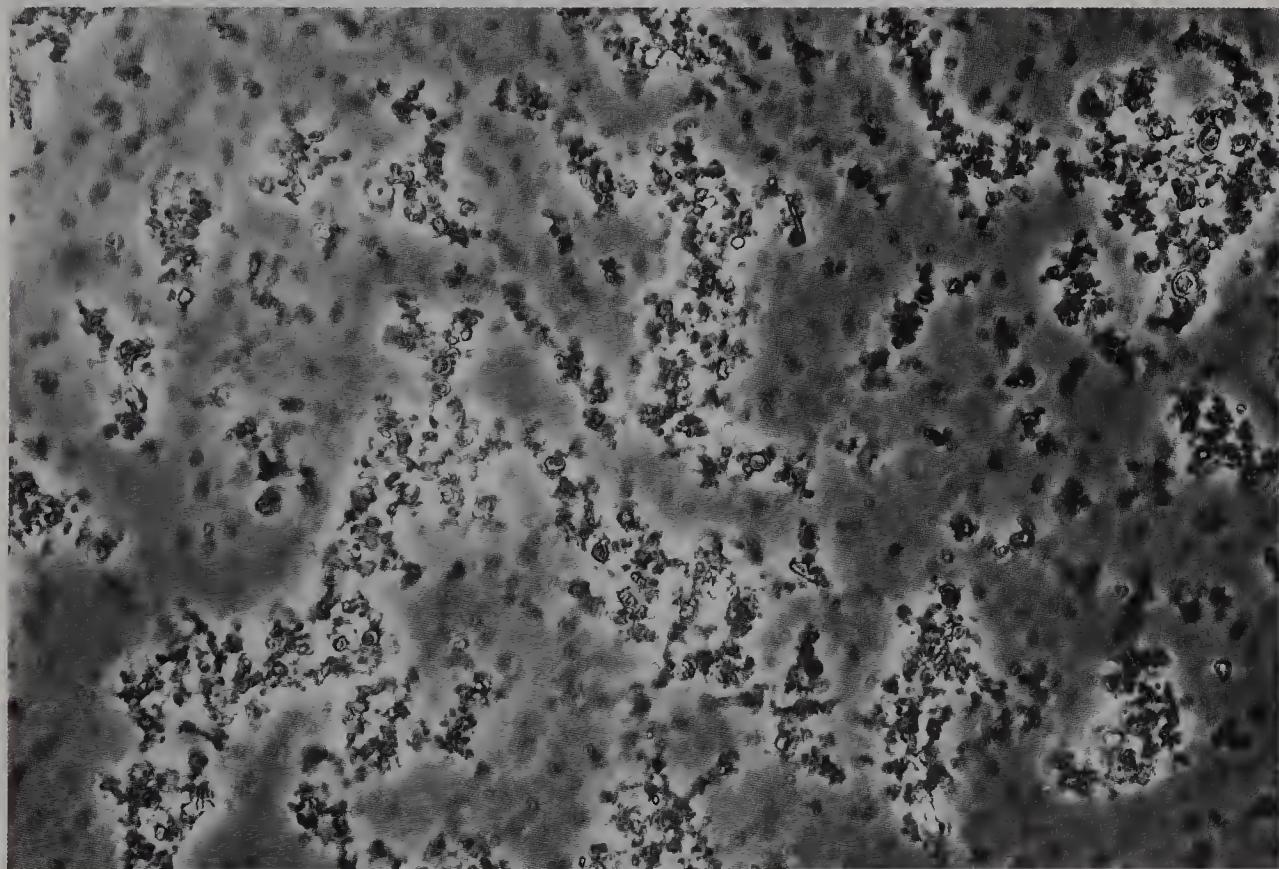
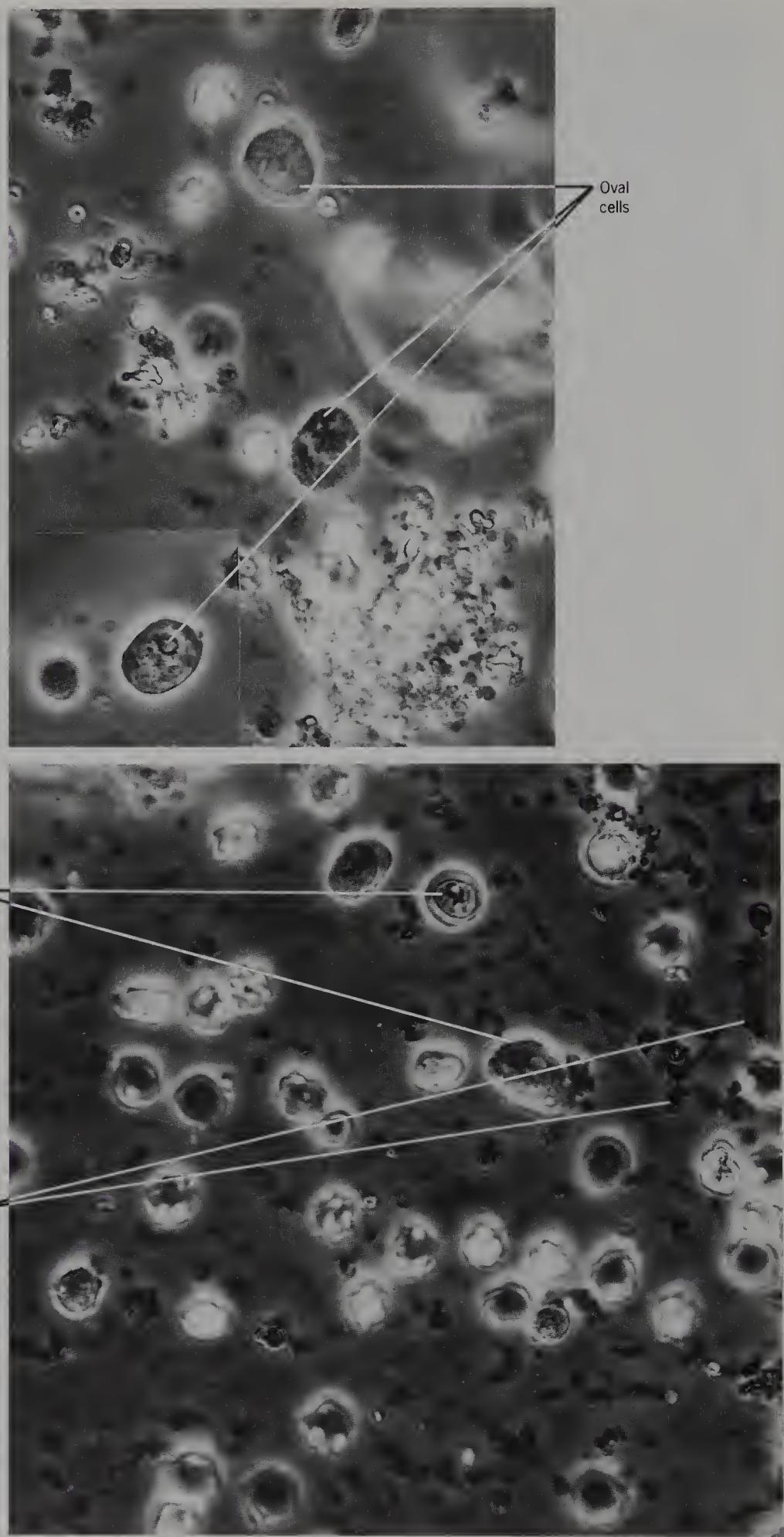


Figure 189 Teased human amygdala from the previous specimen, to show fine granular material (phase contrast, $\times 700$).

Figure 190 Teased human amygdala from the previous specimen, to show round and oval cells and fine granular material (phase contrast, $\times 800$).



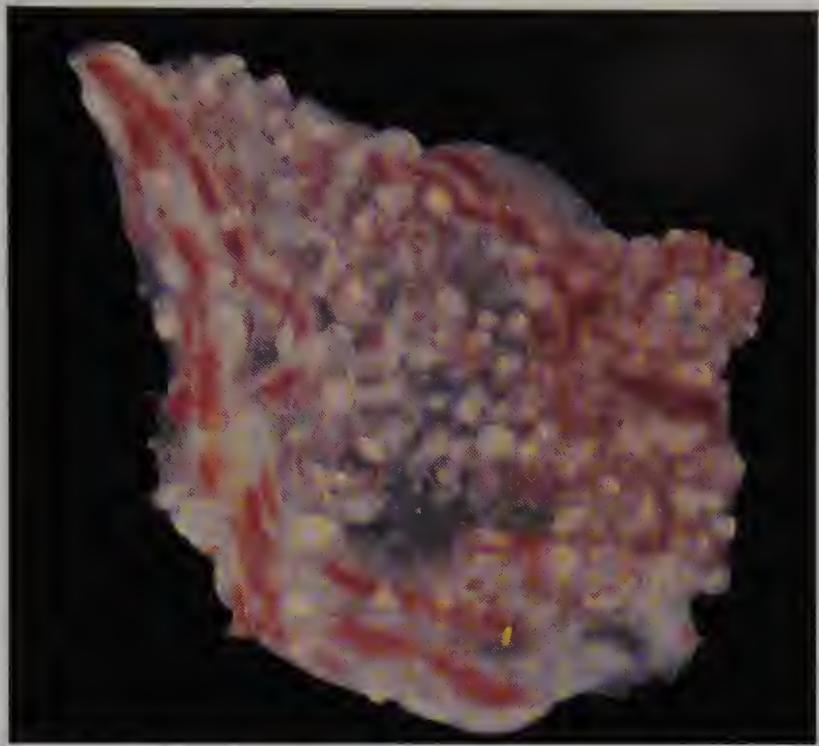


Figure 191 Human choroid plexus from the posterior horn of the lateral ventricle, right side, from a 60-year-old male (bright field, $\times 15$).

The large blood vessels can be seen.

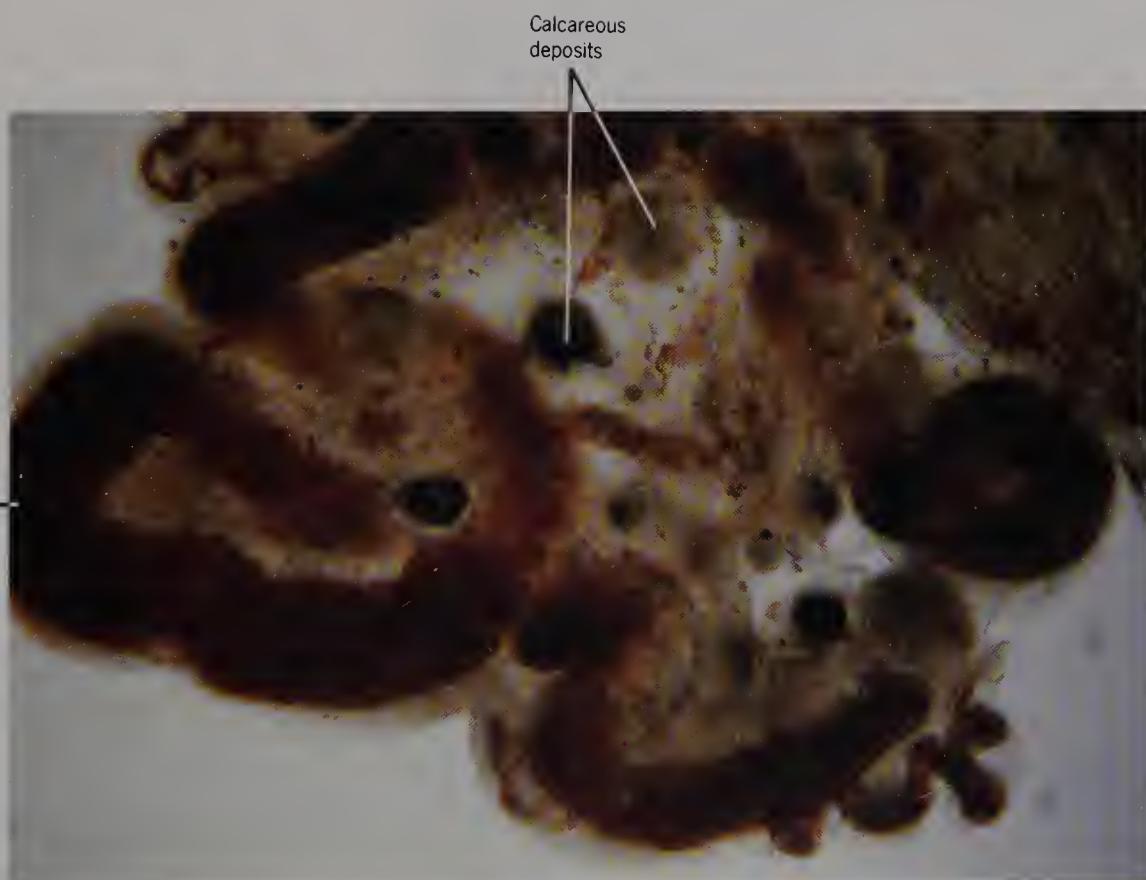


Figure 192 Human choroid plexus from the previous specimen, to show blood vessels and villi (bright field, $\times 100$).

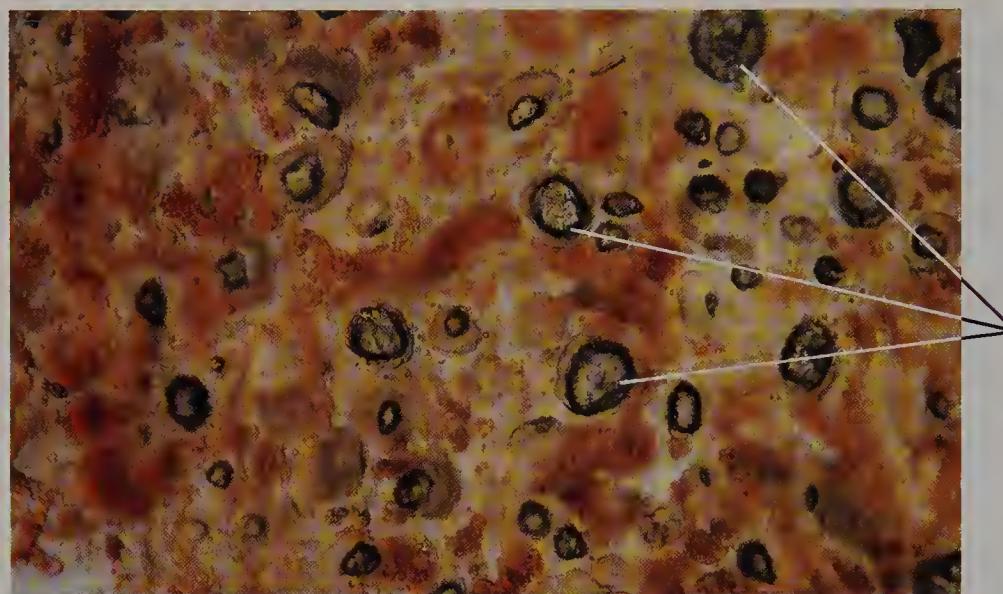


Figure 193 Human choroid plexus from the previous specimen, to show capillaries and what are believed to be calcareous deposits (bright field, $\times 85$).

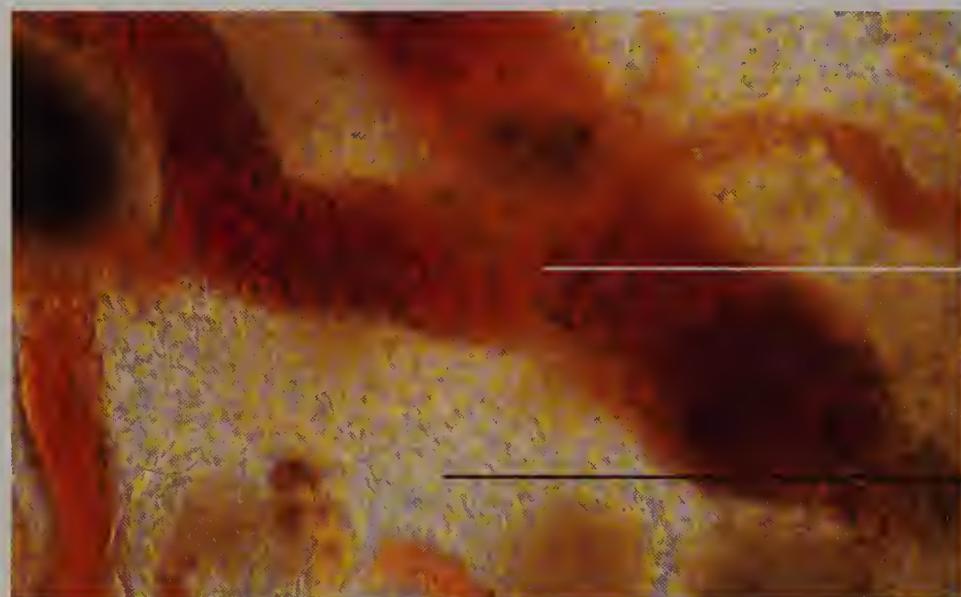


Figure 194 Human choroid plexus from the previous specimen, to show blood vessels and calcareous deposits (phase contrast, $\times 215$).

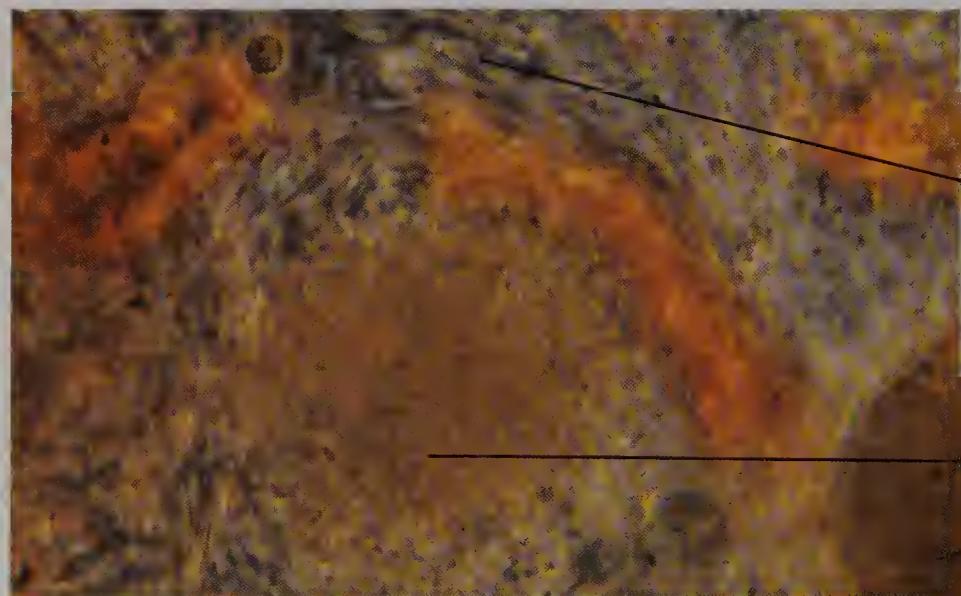


Figure 195 Human choroid plexus from the previous specimen, to show a 'whorl' and connective tissue fibres (phase contrast, $\times 520$).

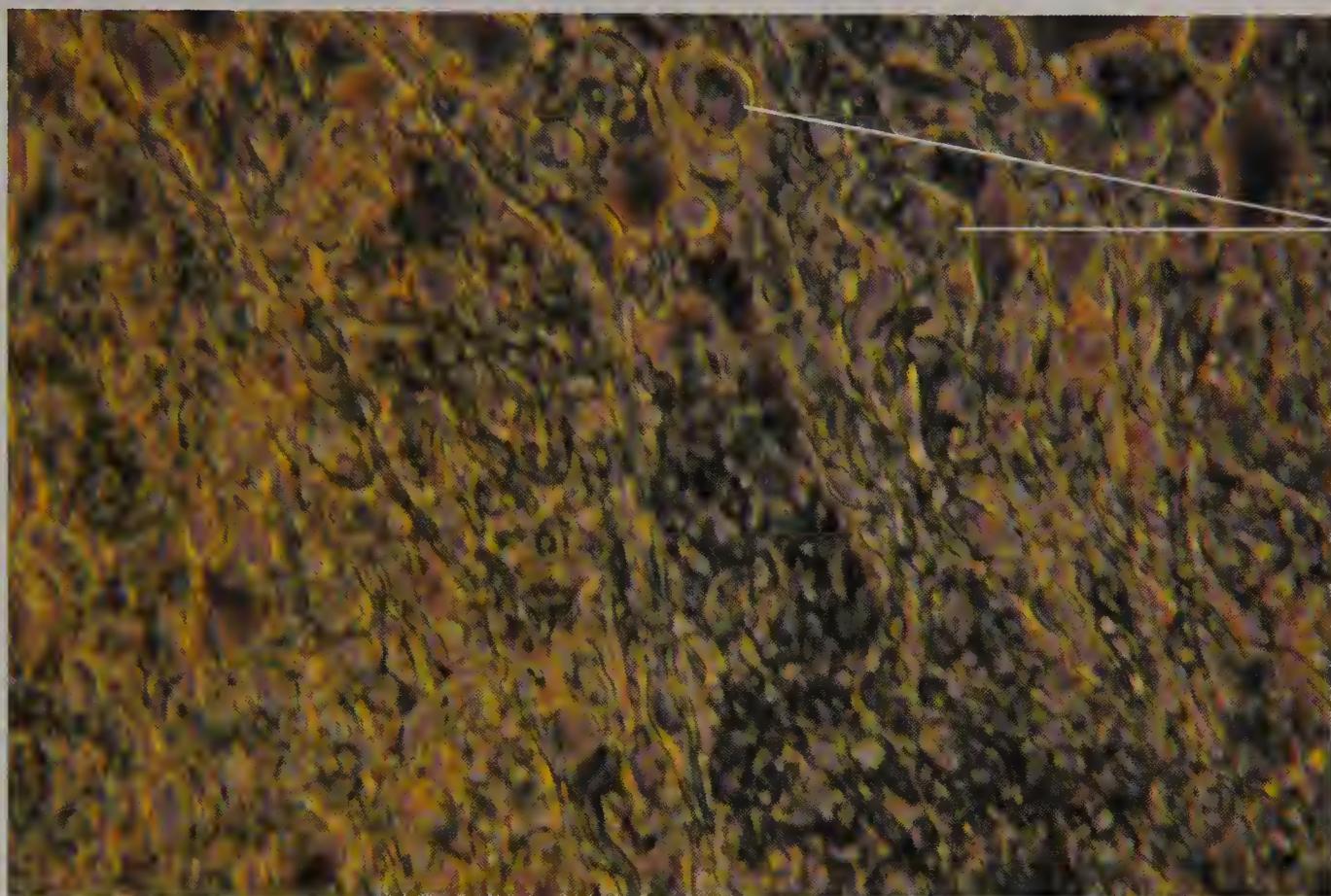


Figure 196 Rabbit paraventricular white matter to show droplets (phase contrast, $\times 720$).

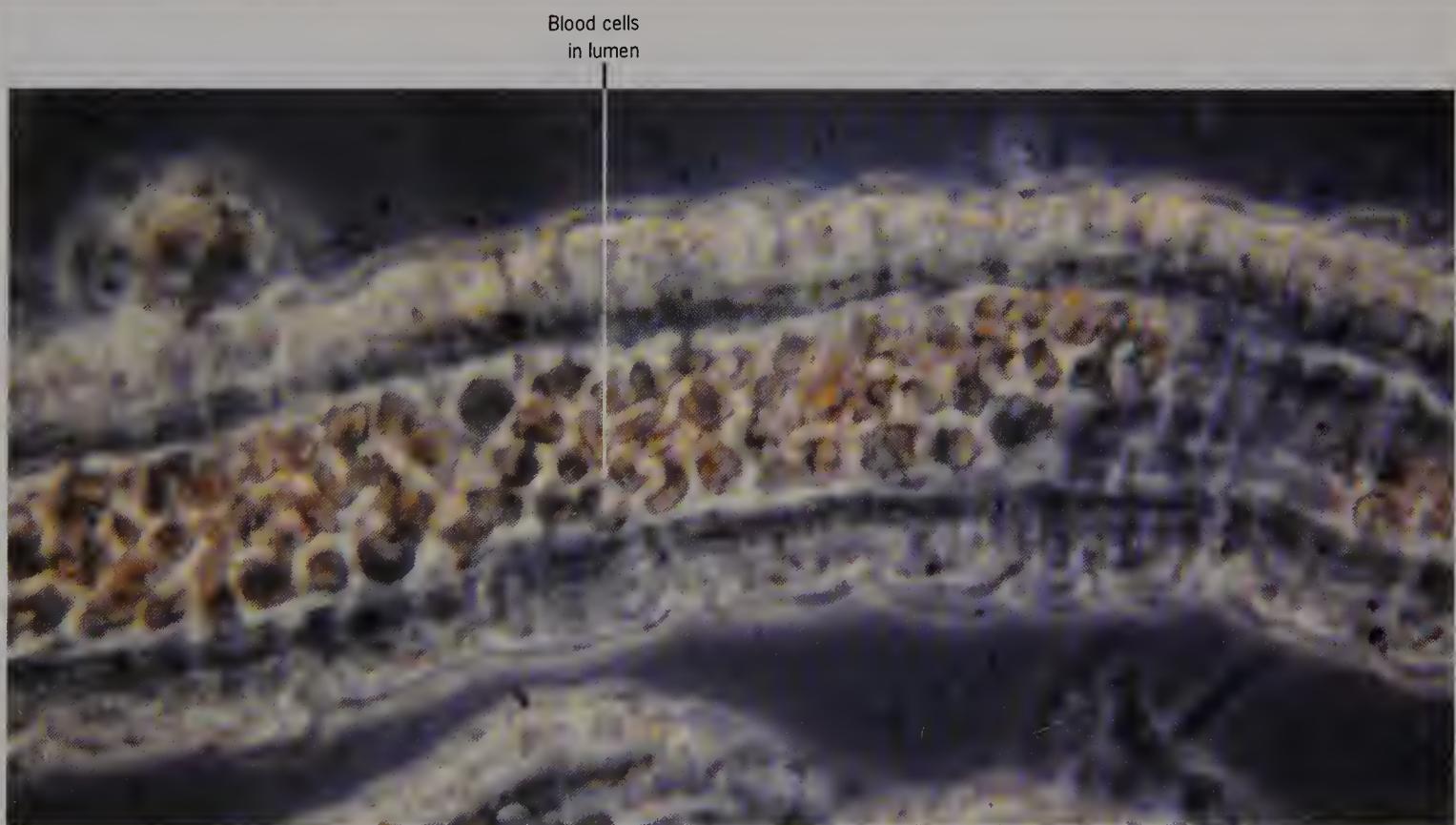


Figure 197 Teased artery from rabbit choroid plexus from the lateral ventricle (phase contrast, $\times 800$).

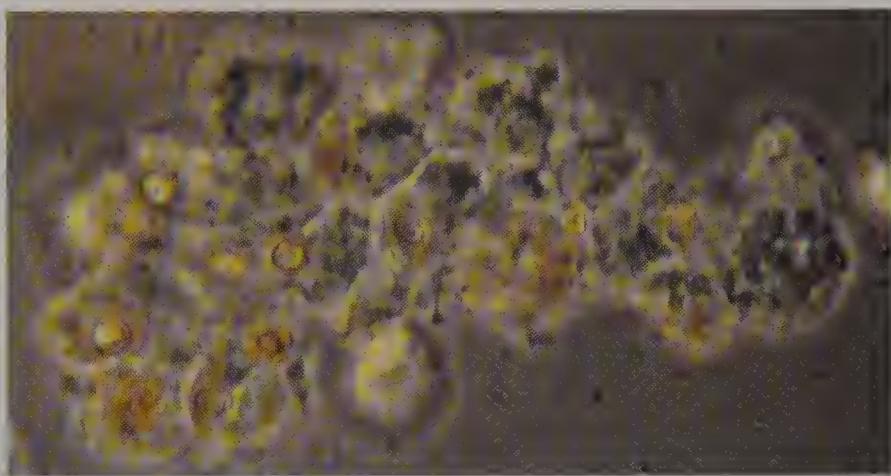


Figure 198 Isolated human epithelial cells from the choroid plexus of a 60-year-old male (phase contrast, $\times 600$).

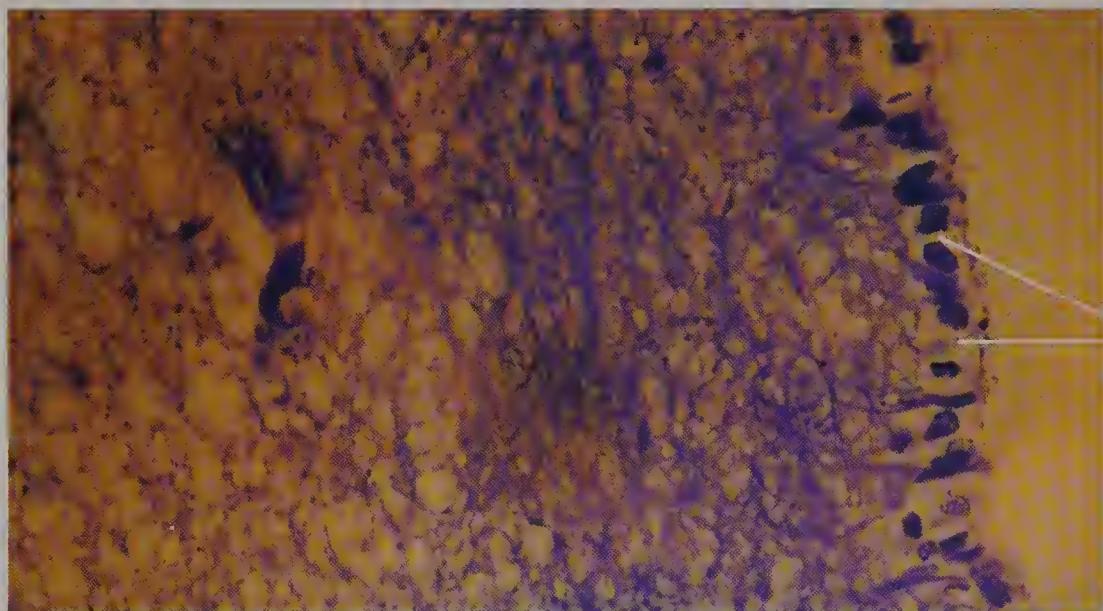


Figure 199 Human ependymal cells and adjacent white matter stained with Holzer's stain (bright field, $\times 600$).

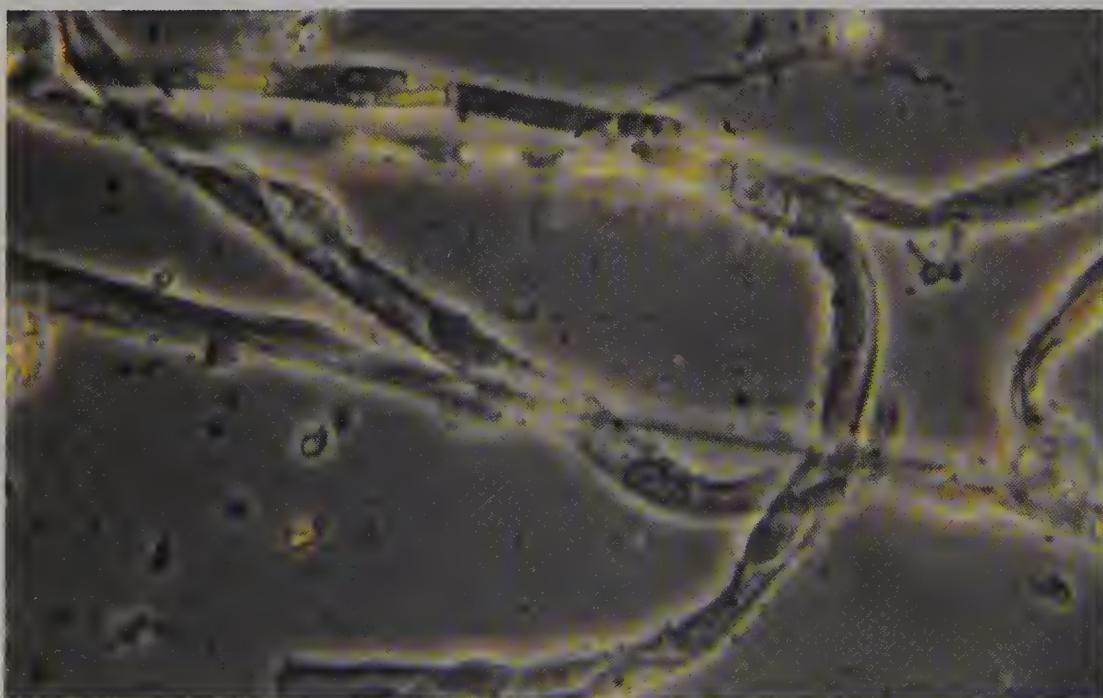


Figure 200 Rabbit capillary from the white matter adjacent to the third ventricle (phase contrast, $\times 600$).

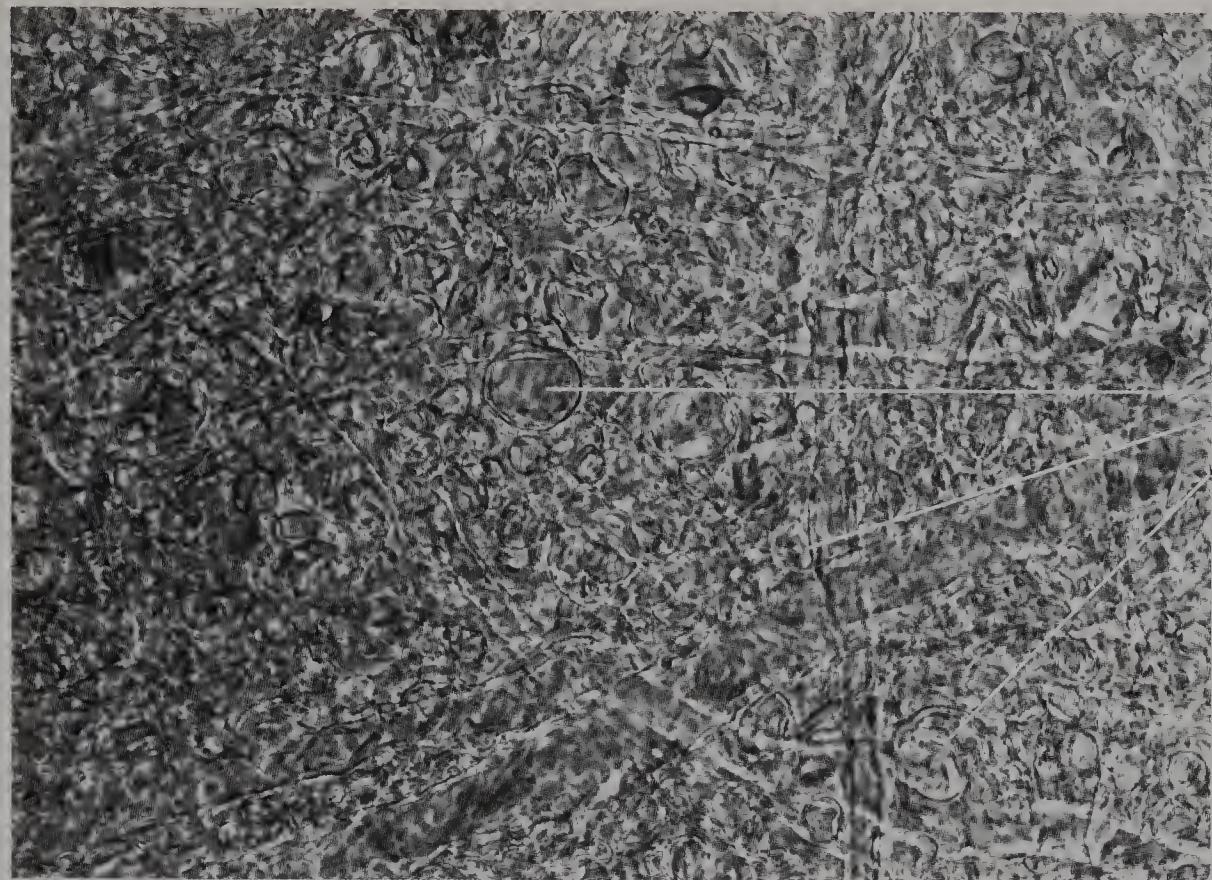


Figure 201 Thin slab of human pyramid from a 95-year-old female, to show fibres and large and small droplets (phase contrast, $\times 700$).

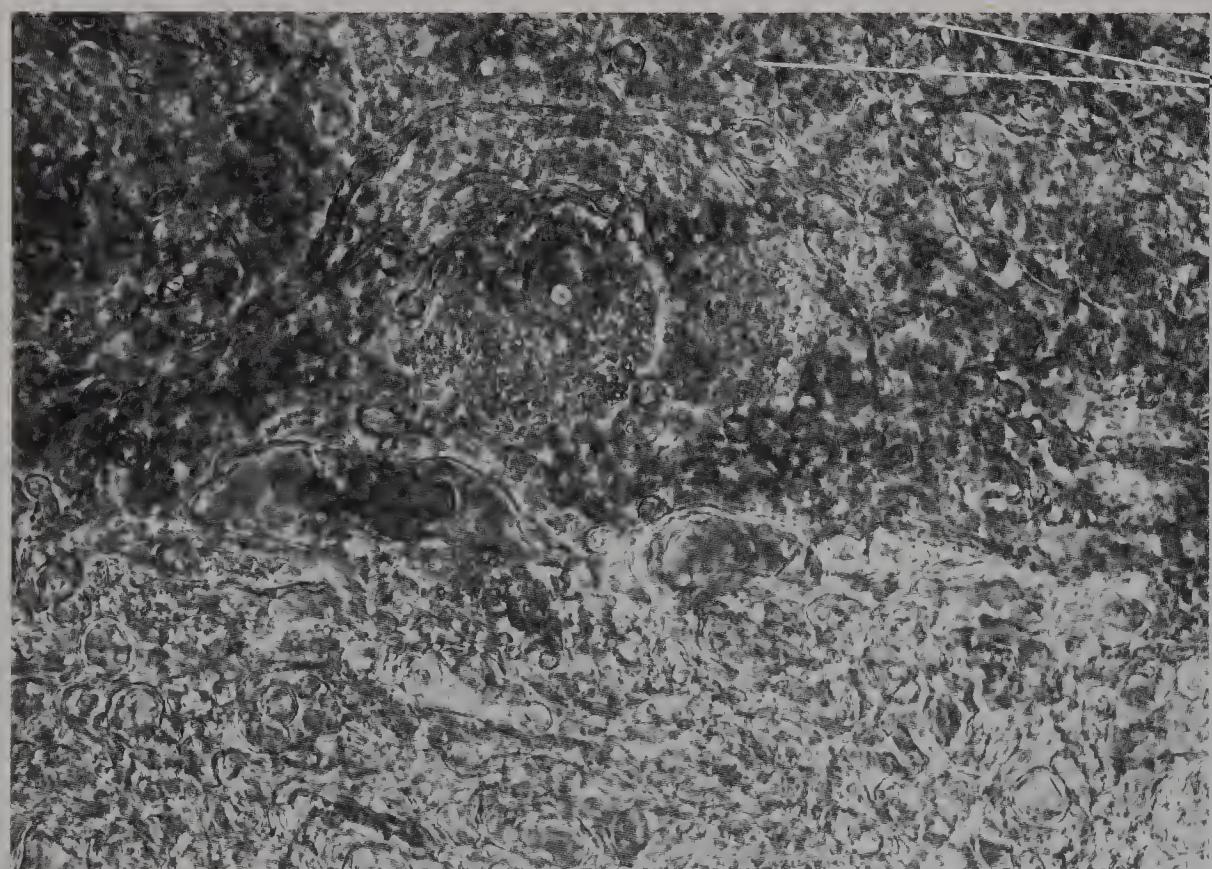


Figure 202 Thin slab of human pyramid from the previous specimen, to show the pyramid/arcuate nucleus boundary (phase contrast, $\times 700$).

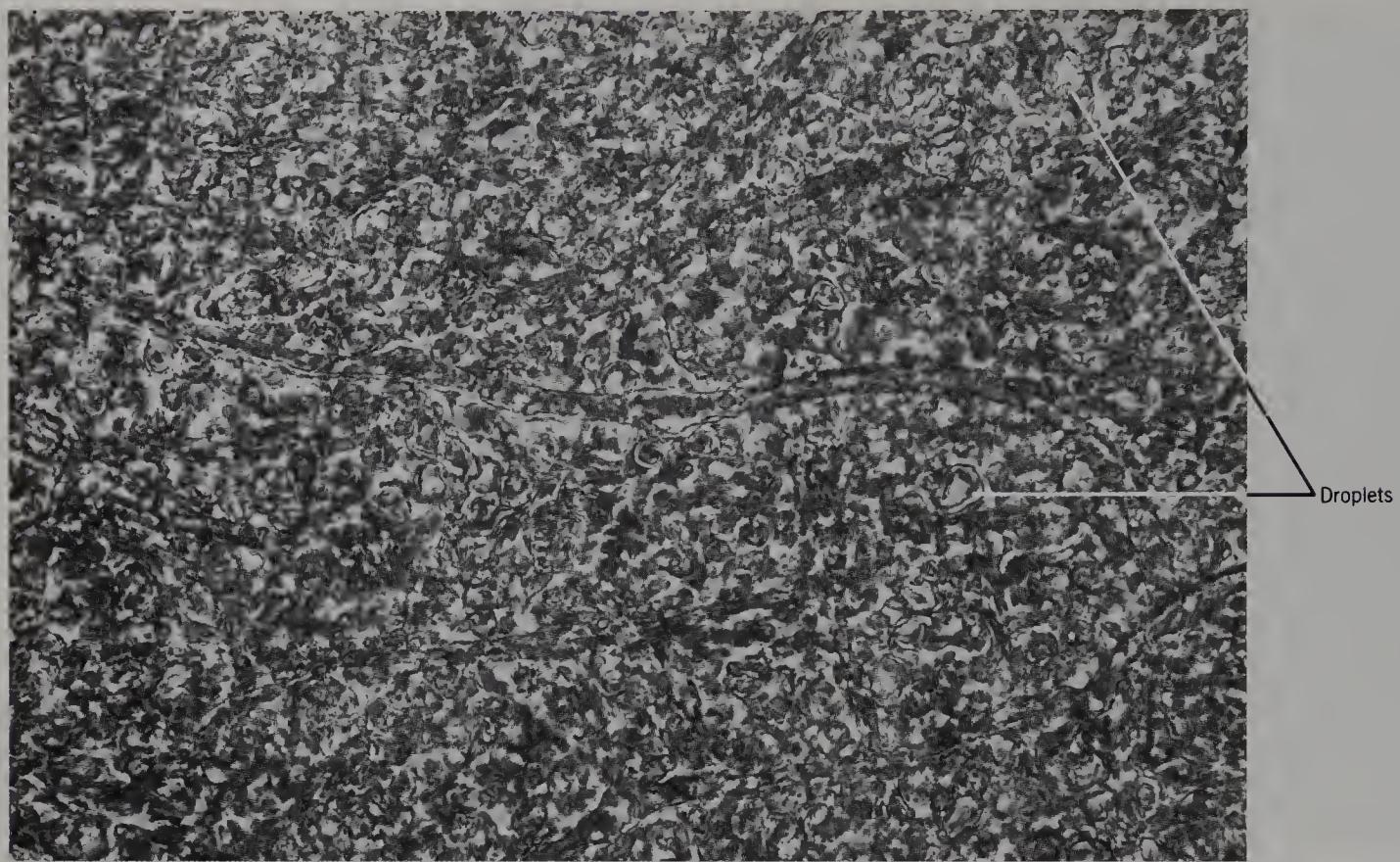


Figure 203 Thin slab of human pons from a 95-year-old female, to show beaded fibres and droplets (phase contrast, $\times 700$).



Figure 204 Partially teased human pons from the previous specimen, to show beaded fibres (phase contrast, $\times 700$).

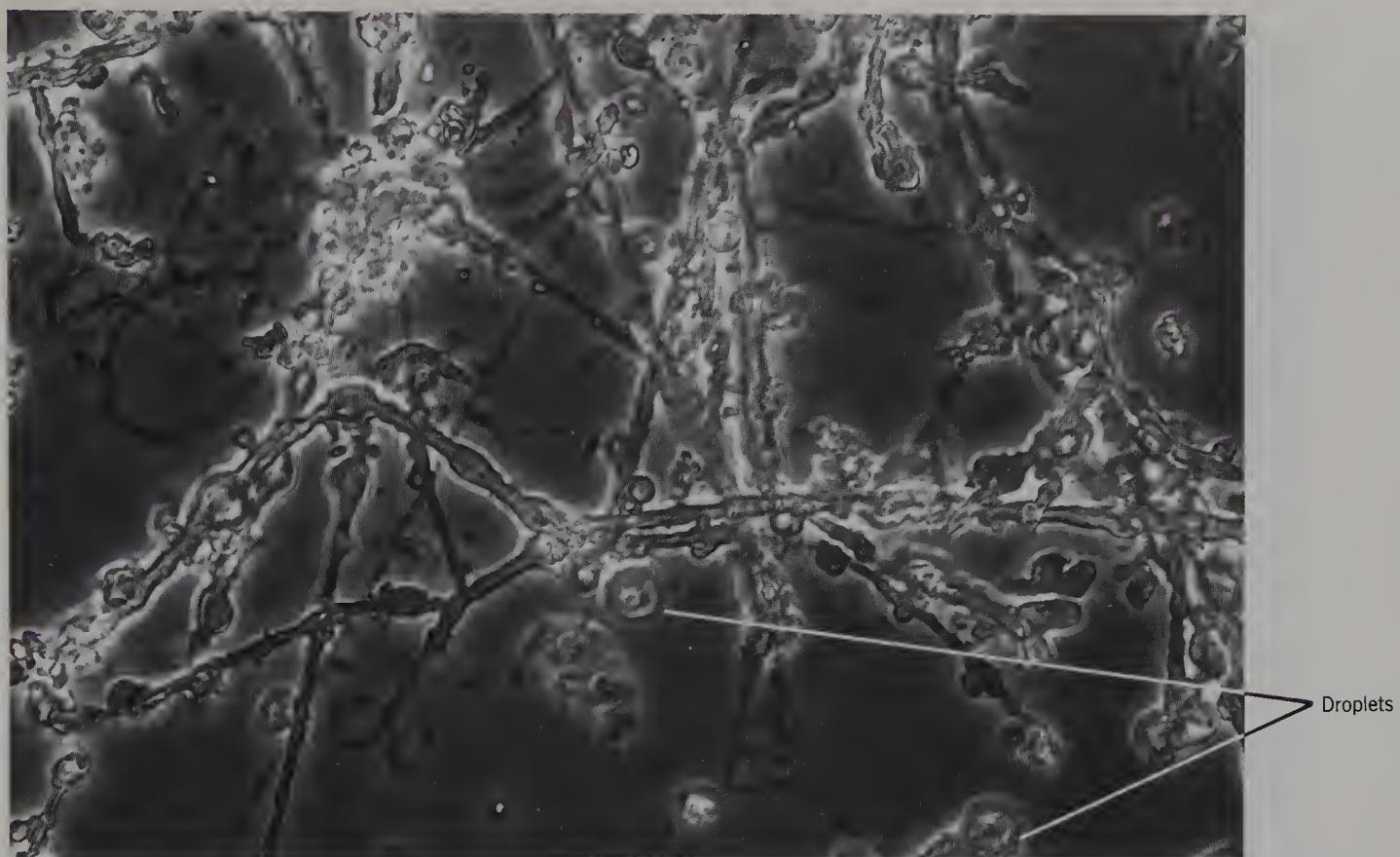


Figure 205 Teased human pons from the previous specimen, to show beaded fibres and droplets (phase contrast, $\times 700$).

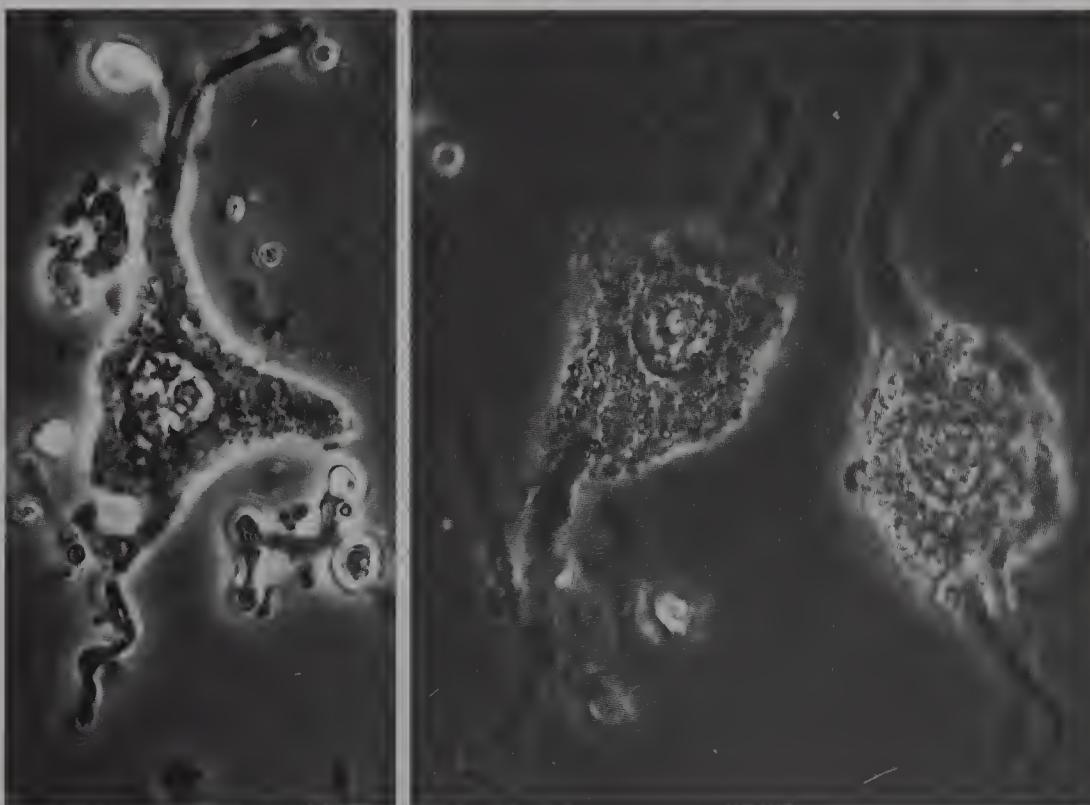


Figure 206 Isolated neurons from the teased human pontine nucleus from a 54-year-old male (phase contrast, $\times 700$).

Note how small these neurons are.

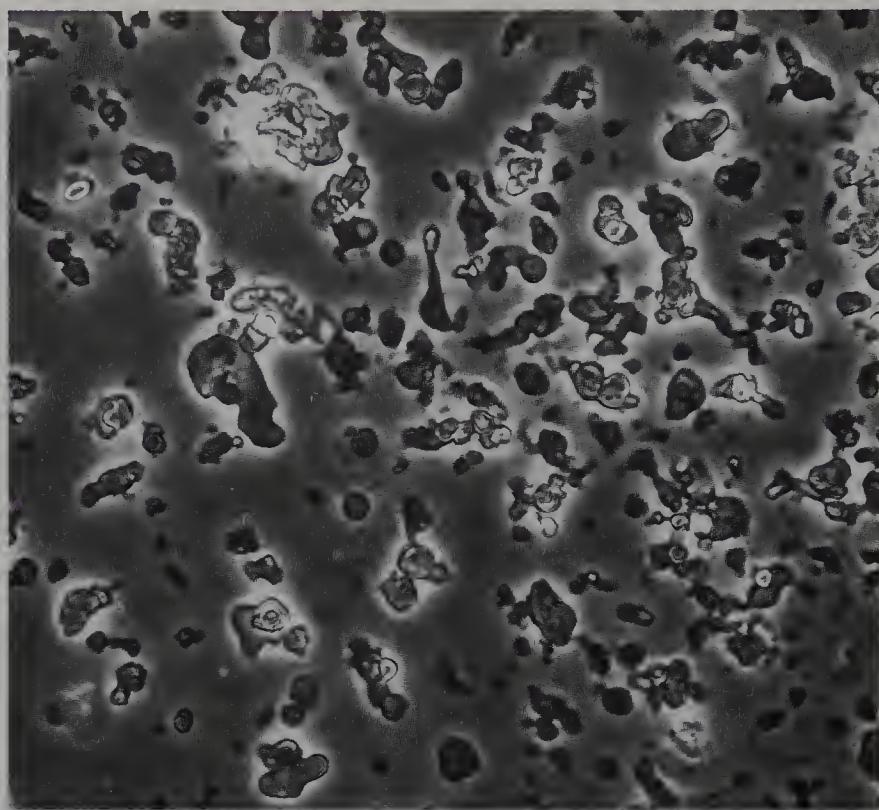


Figure 207 Teased guinea-pig pons to show refractile droplets (phase contrast, $\times 700$).

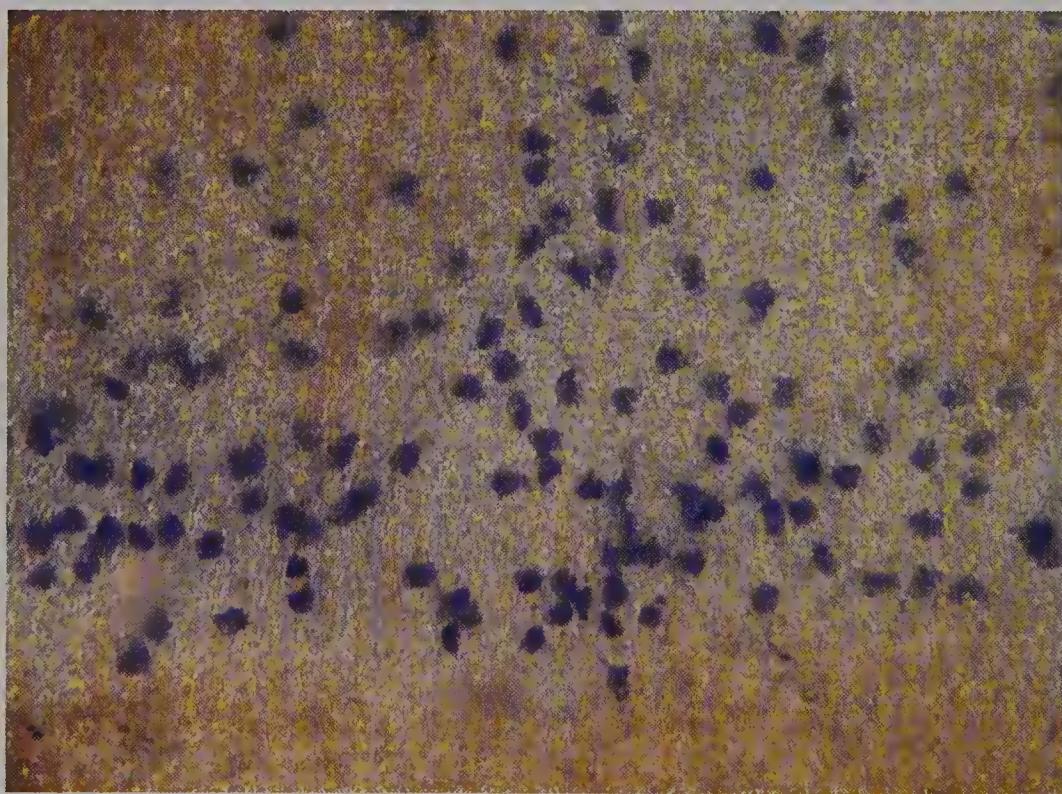


Figure 208 Thin slab of human olfactory nucleus from a 60-year-old male, lightly coloured with methylene blue to show the incidence of neuron somas (bright field, $\times 100$).

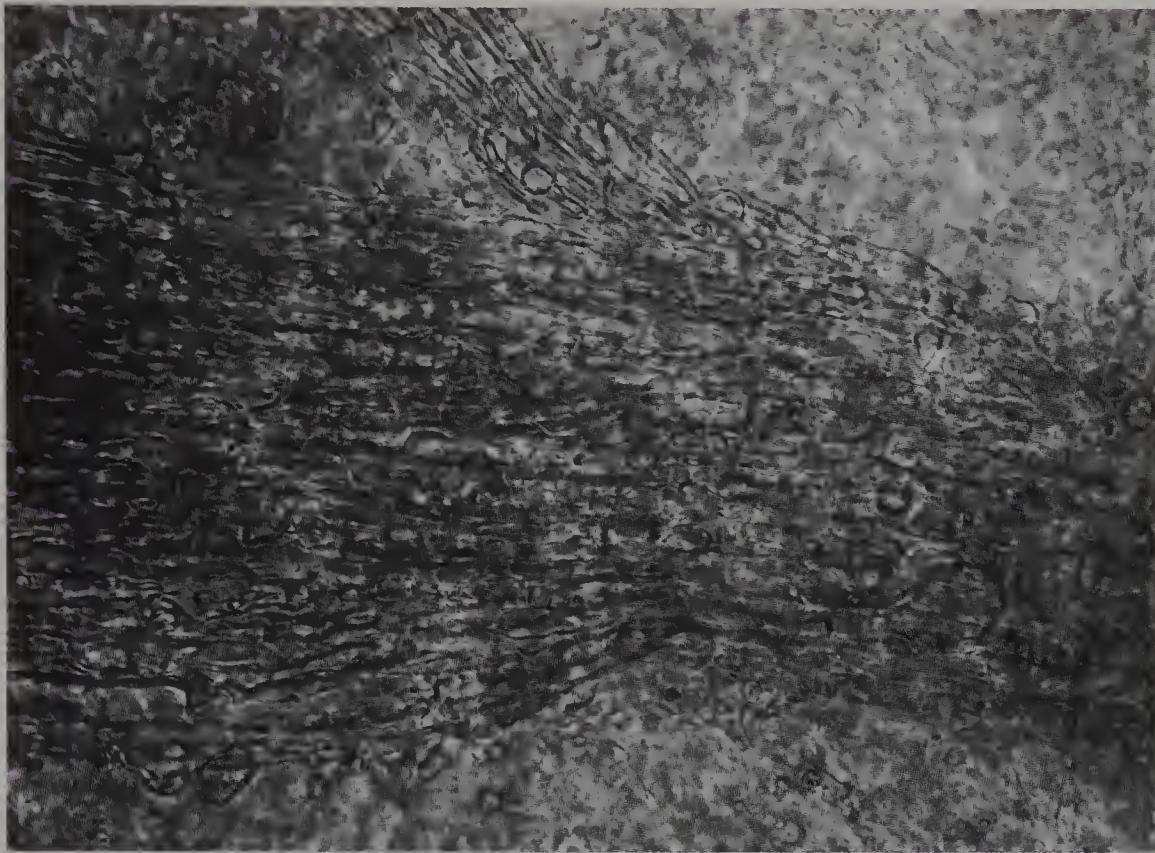


Figure 209 Thin slab of human olfactory nucleus from a 77-year-old male, to show a fibre tract *in situ* (phase contrast, $\times 700$).



Figure 210 The same thin slab of human olfactory nucleus as in the previous specimen, to show birefringence of some fibres (polarized light, $\times 700$).

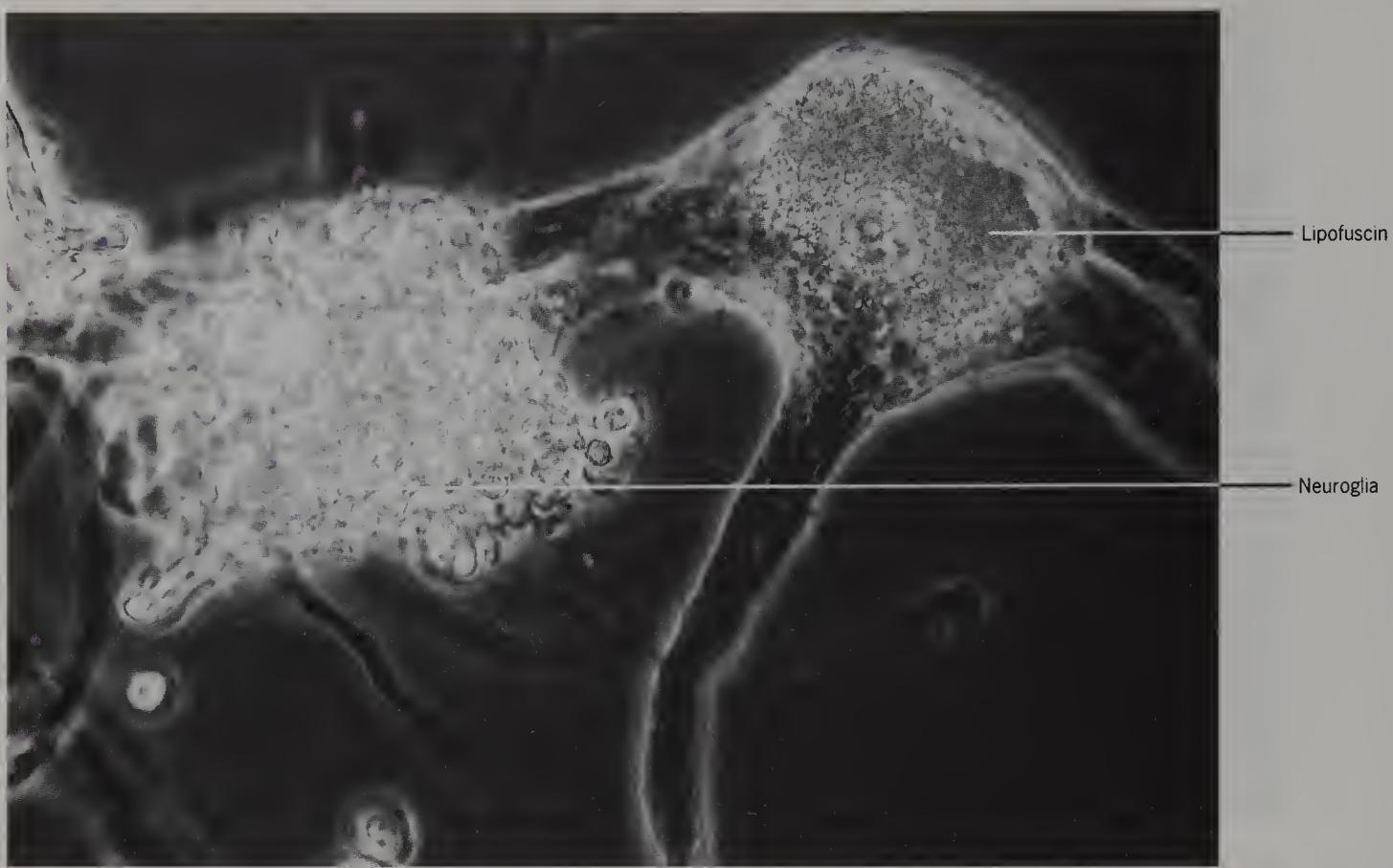


Figure 211 Isolated neuron from teased human olfactory nucleus from a 77-year-old male, with adherent neuroglia (phase contrast, $\times 700$).

The neuron soma is more than half full of lipofuscin.



Figure 212 Isolated capillaries from teased human olfactory nucleus from a 77-year-old male (phase contrast, $\times 700$).

Note the thinness of the walls.

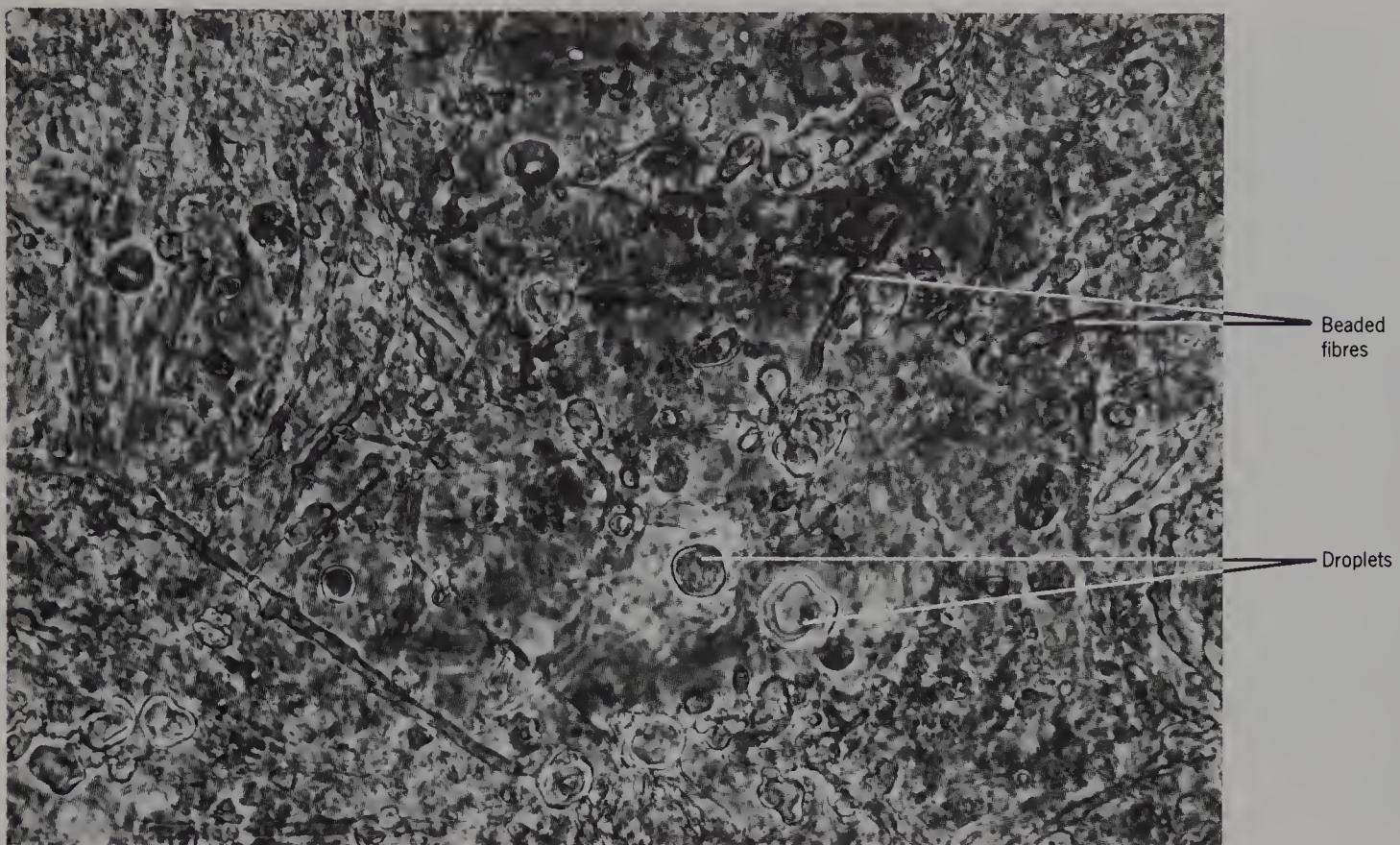


Figure 213 Thin slab of human medial lemniscus from a 95-year-old female, to show beaded fibres and droplets (phase contrast, $\times 700$).

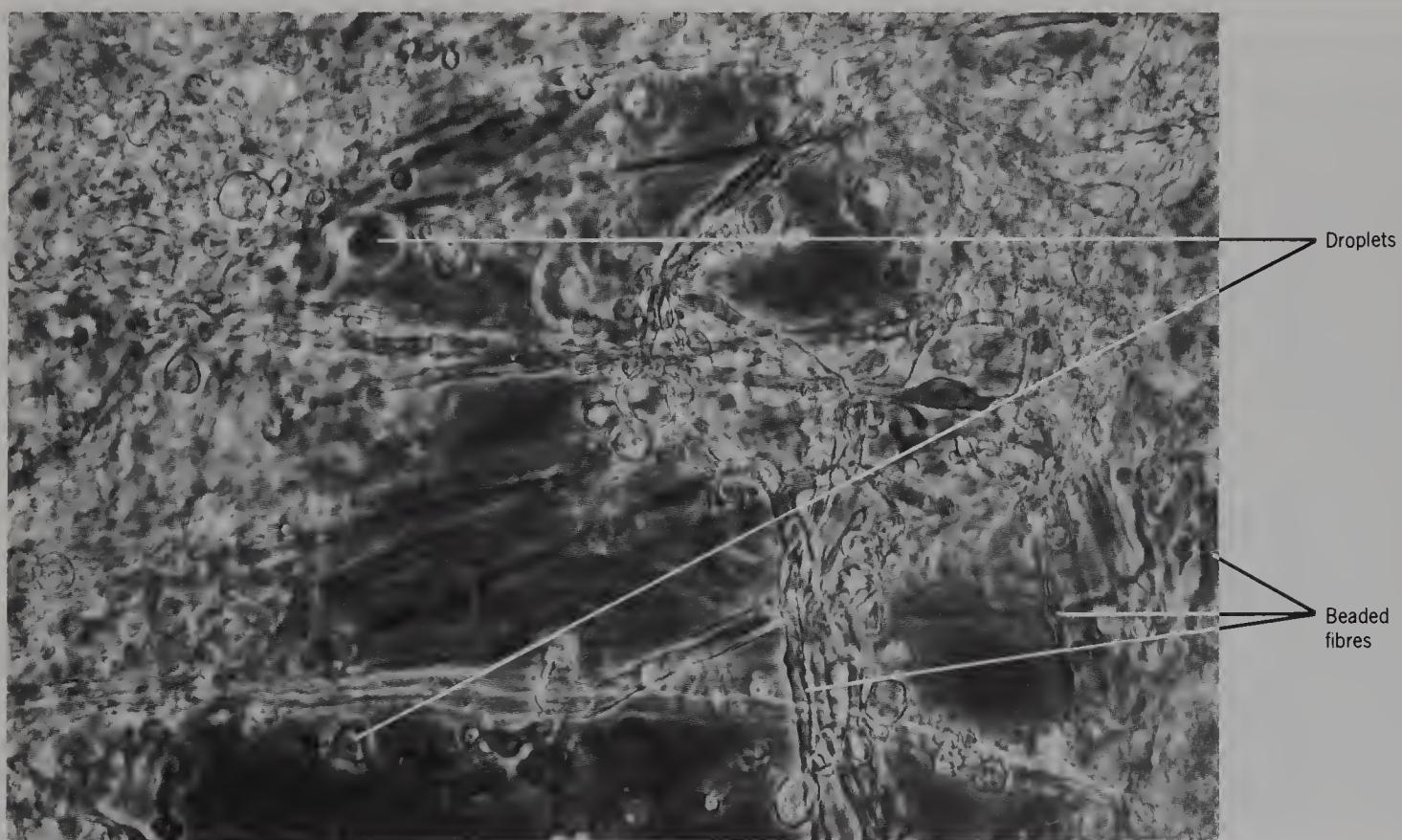


Figure 214 Partially teased human medial lemniscus from the previous specimen, to show beaded fibres and droplets (phase contrast, $\times 700$).

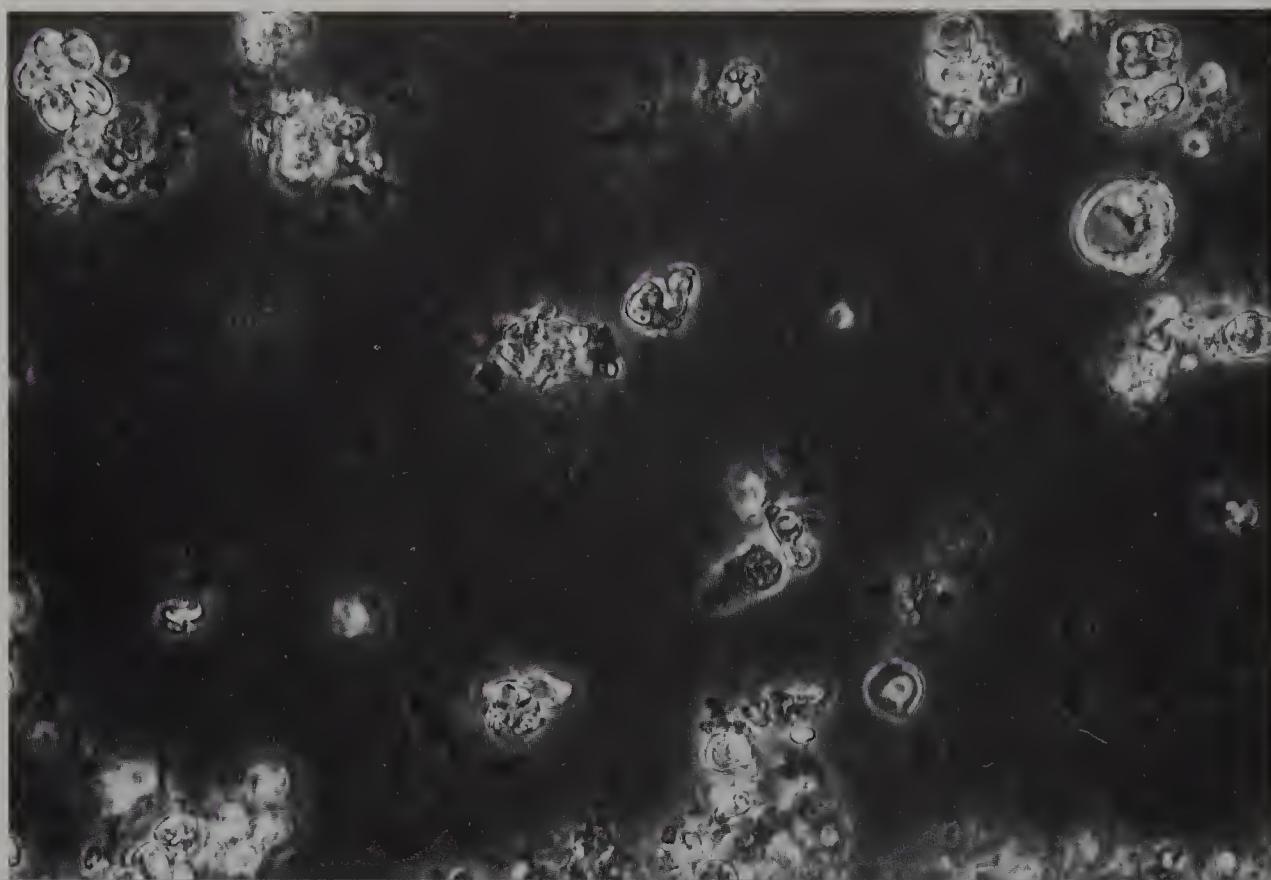


Figure 215 Teased human medial lemniscus from the previous specimen, to show isolated droplets (phase contrast, $\times 700$). These droplets appear refractile and transparent compared with granules, which are dark.

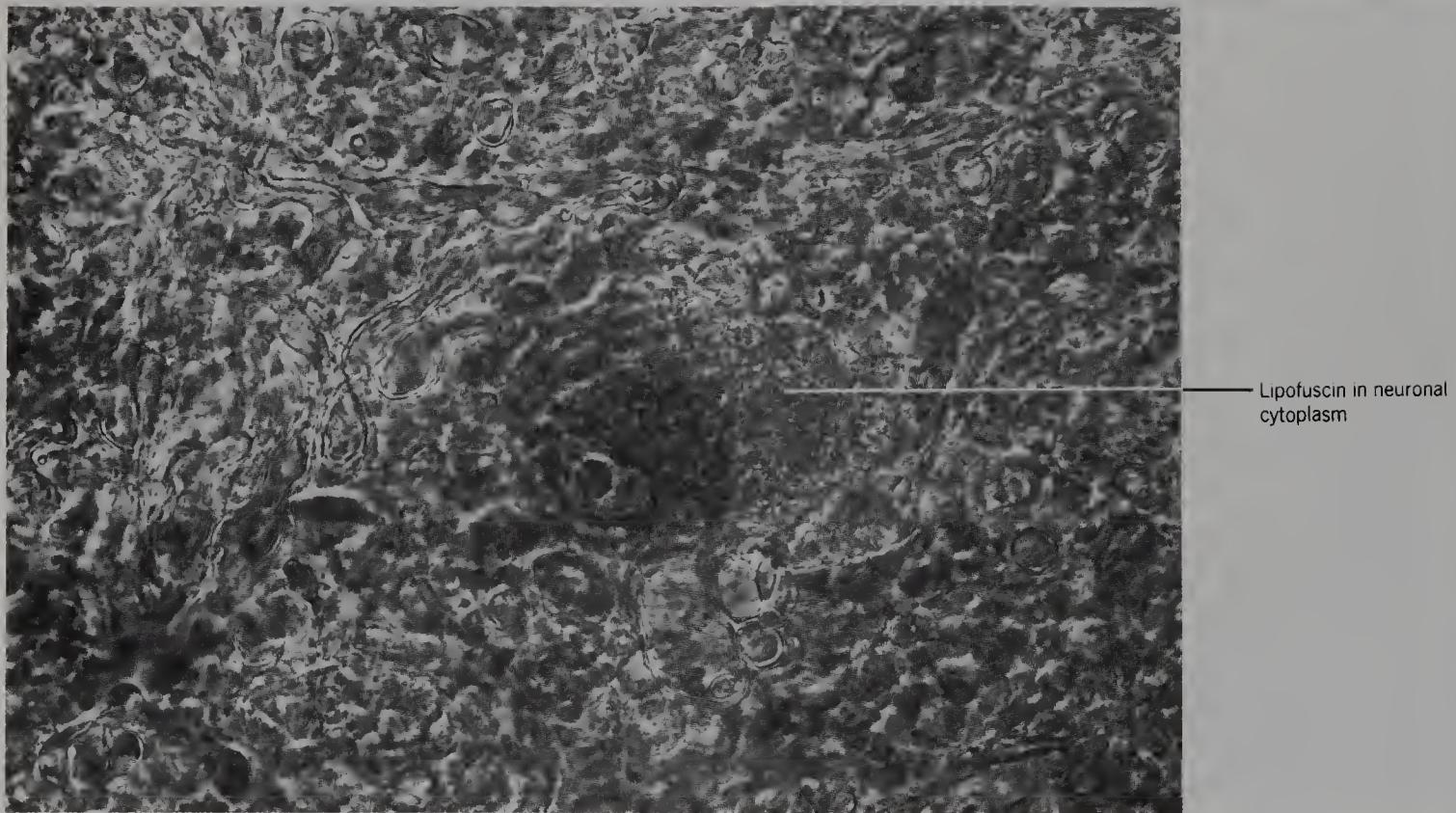


Figure 216 Thin slab of human inferior vestibular nucleus from a 68-year-old male, to show a neuron with lipofuscin *in situ* and beaded fibres (phase contrast, $\times 700$).

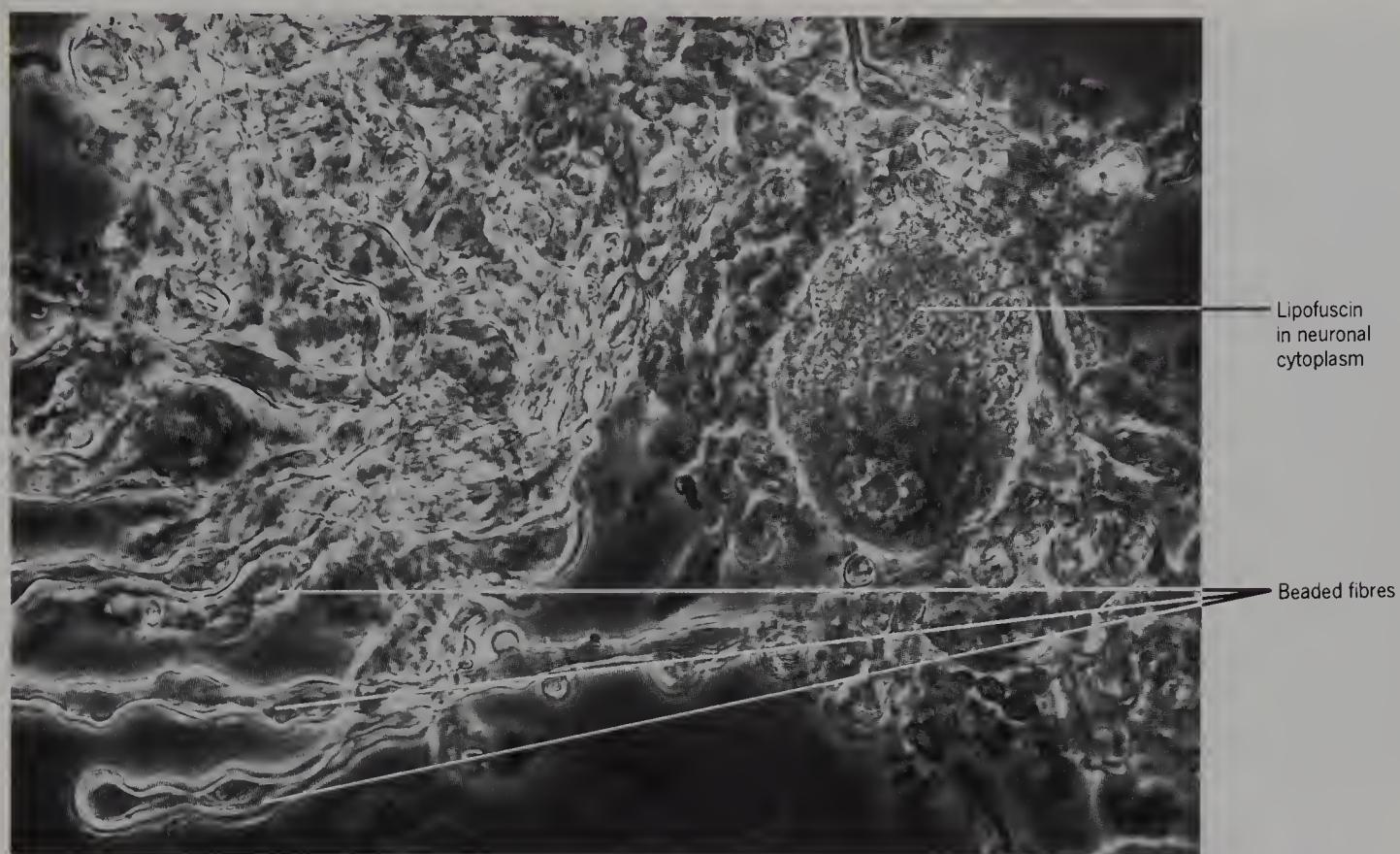


Figure 217 Partially teased human inferior vestibular nucleus from the previous specimen to show neuron and beaded fibres (phase contrast, $\times 700$).



Figure 218 Isolated neuron from teased human inferior vestibular nucleus from a 53-year-old male, with adherent neuroglia (phase contrast, $\times 280$).

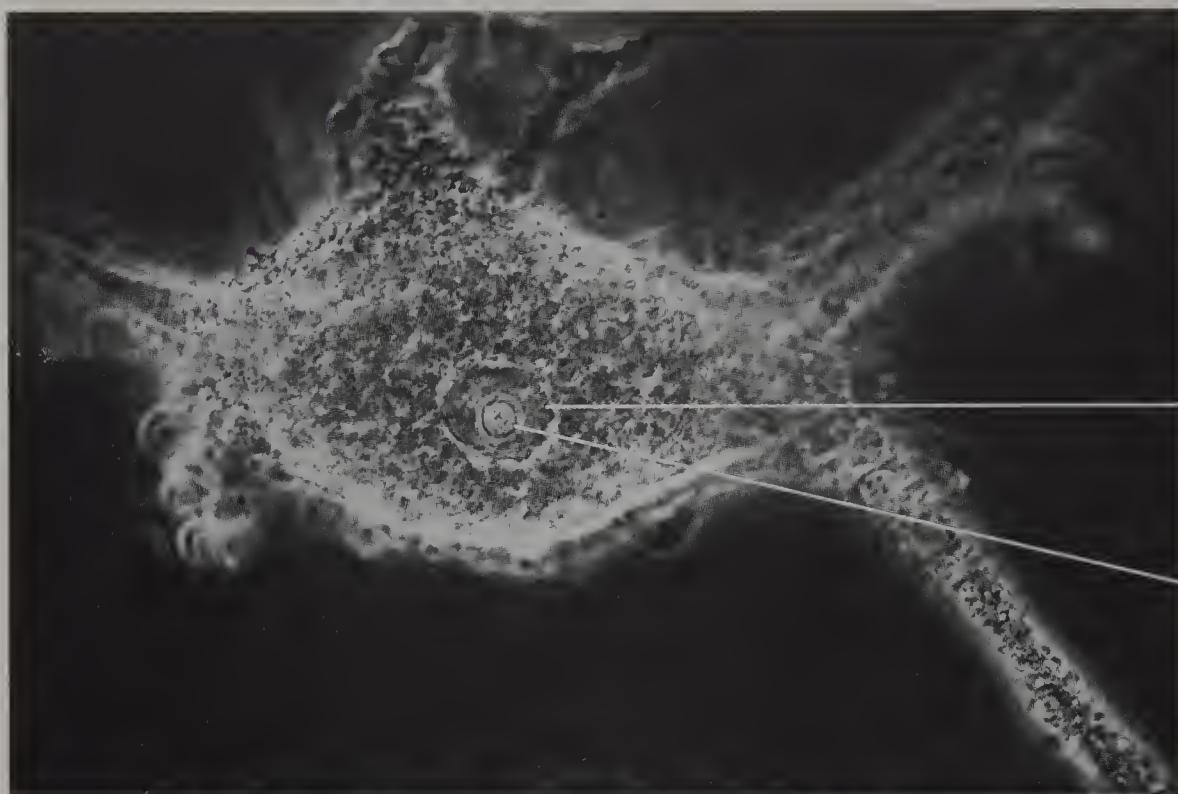


Figure 219 Isolated rabbit neuron from teased lateral vestibular nucleus to show nuclear and nucleolar membranes (phase contrast, $\times 700$).

The nucleolar membrane is seen when the somas are dissected out in saline, but not in sucrose (Hussain *et al.*, 1974).

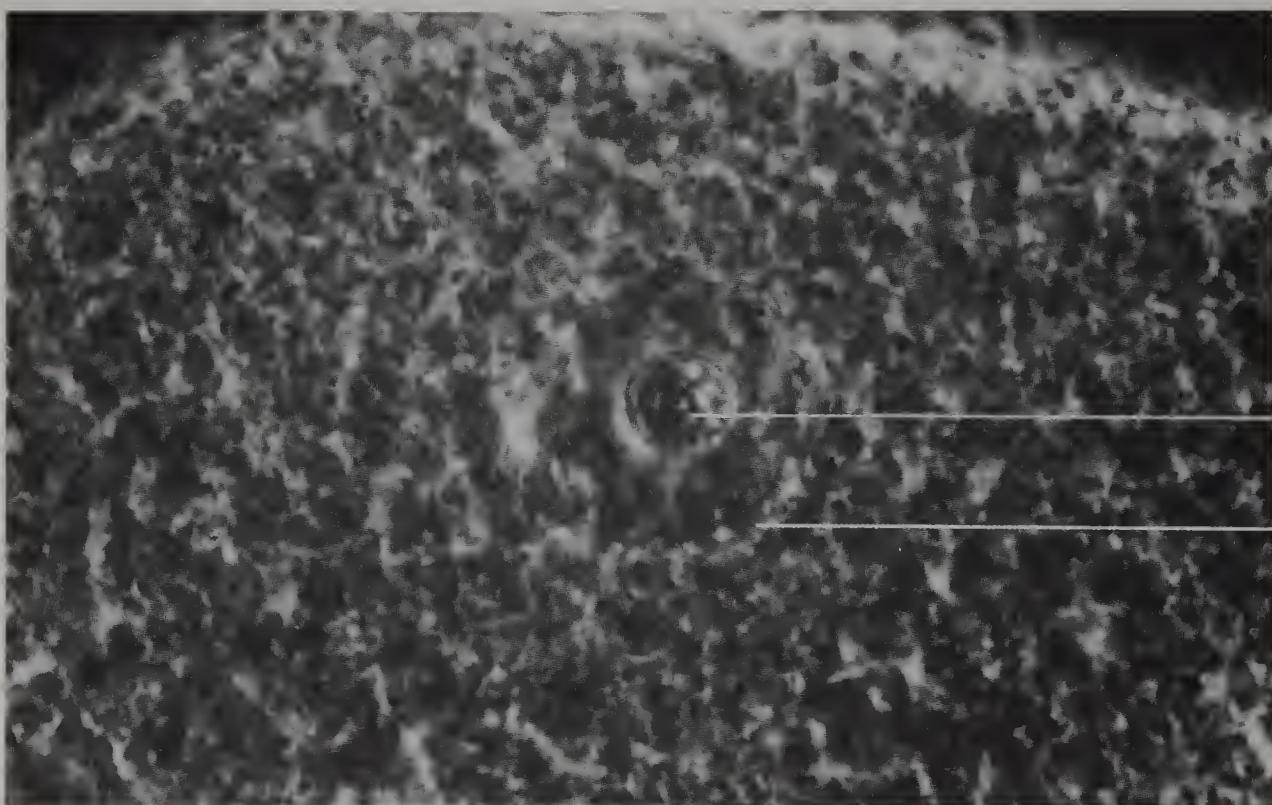


Figure 220 Isolated rabbit neuron soma from teased lateral vestibular nucleus, to show details of nucleolus (phase contrast, $\times 2000$).

The nucleolonema moves during life (Sartory *et al.*, 1971).

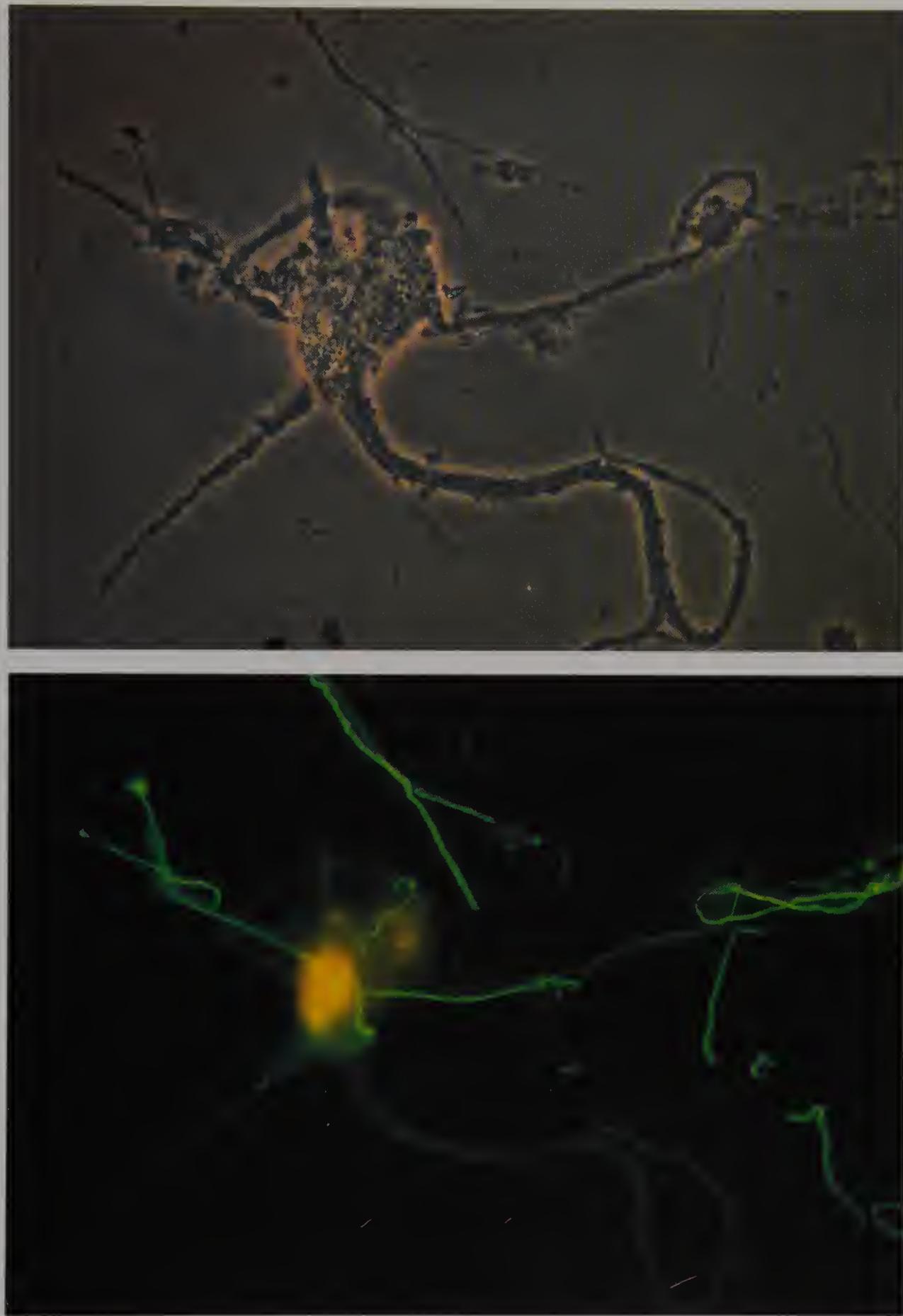


Figure 221 Isolated human neuron from the lateral vestibular nucleus of an 82-year-old male, stained with anti-neurofilament 200 kD protein, by phase contrast (above) and after excitation with blue light of 450–490 nm (below) ($\times 500$).

Fibres probably unmyelinated can be seen fluorescing, but the fine granular material does not.

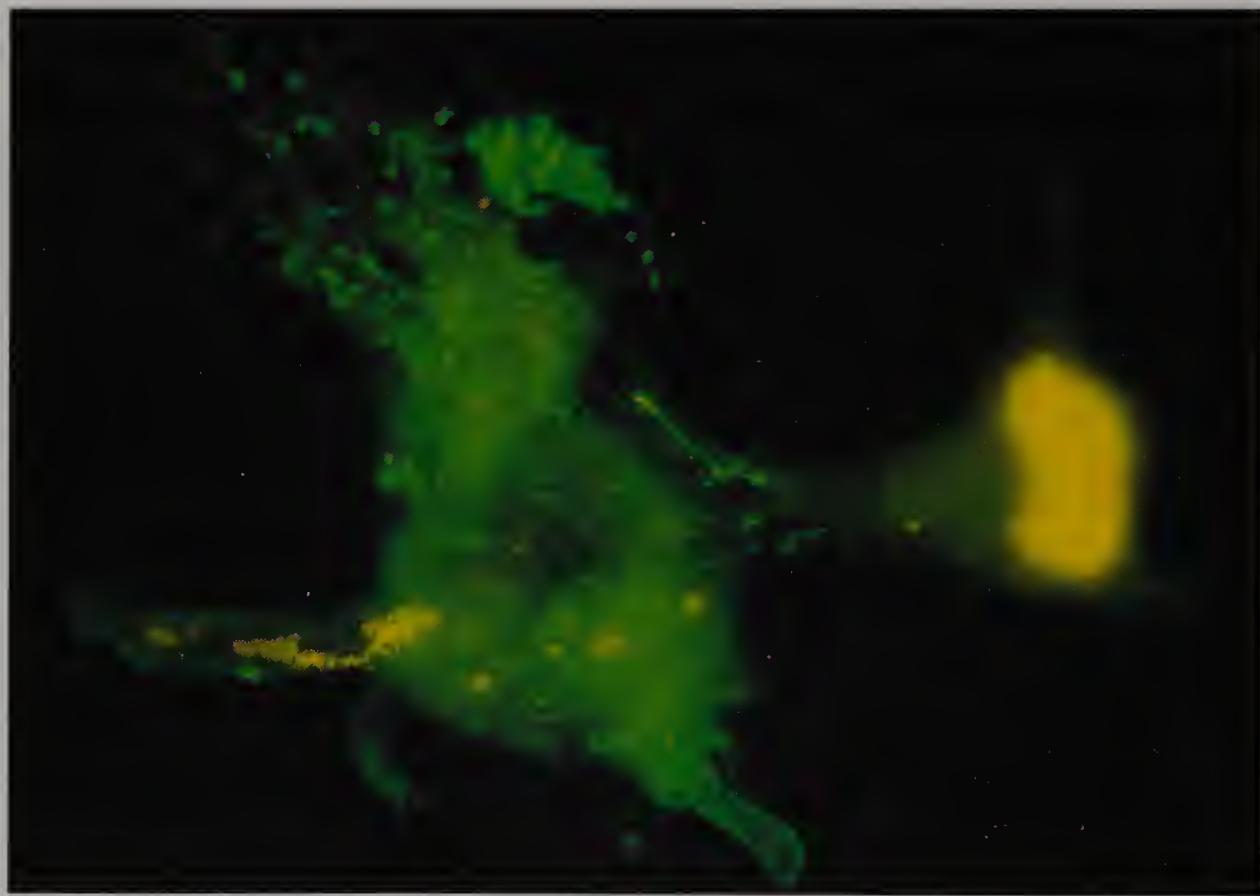
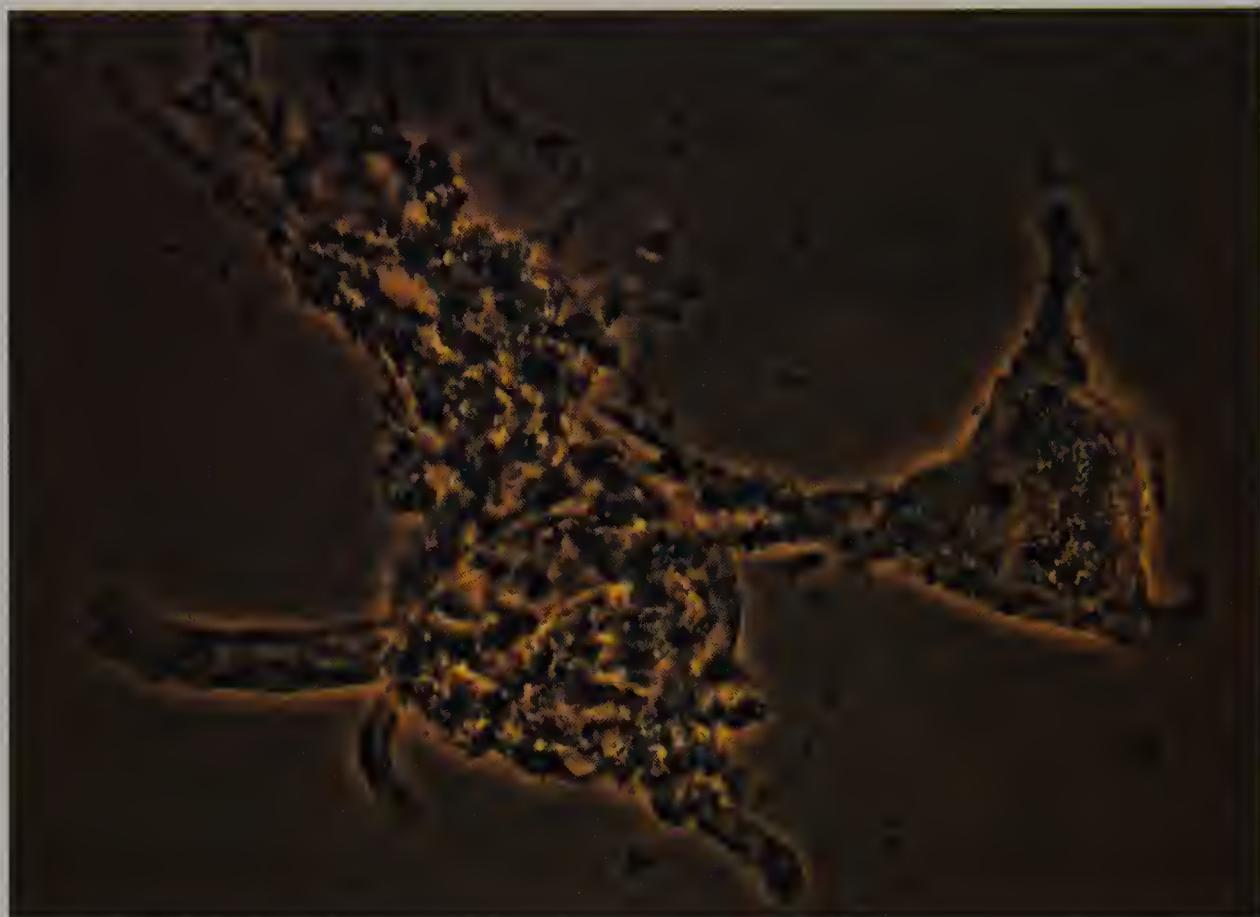


Figure 222 Isolated human neuron from the lateral vestibular nucleus of a 64-year-old male, stained with anti-glial fibrillary acidic protein, by phase contrast (above) and after excitation with blue light of 450–490 nm (below) ($\times 500$).

Some fine granules can be seen fluorescing, compare with the previous figure.

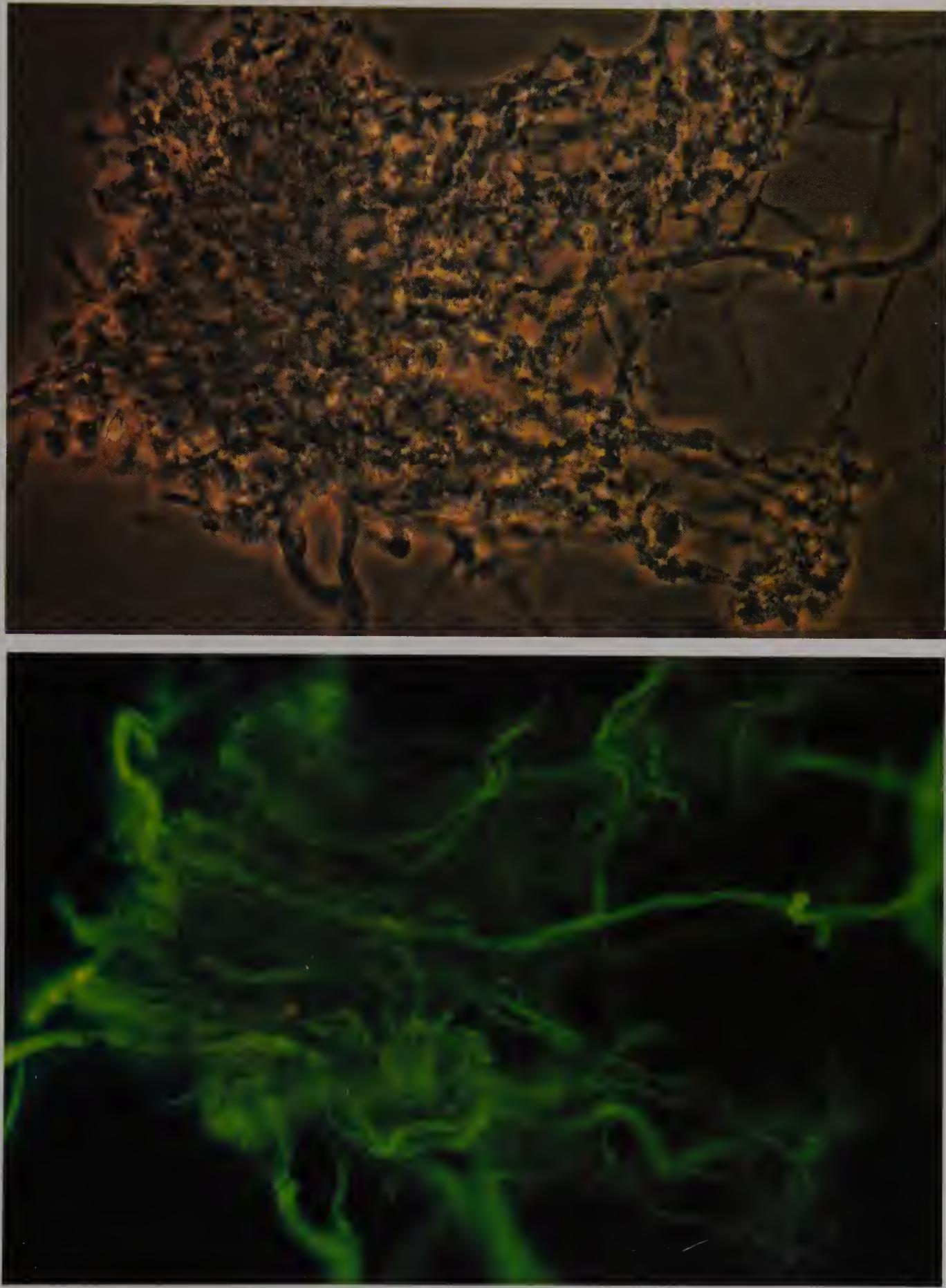


Figure 223 Isolated human neuroglia from the lateral vestibular nucleus of an 82-year-old male, stained with anti-neurofilament 200 kD protein, by phase contrast (above) and after excitation with blue light of 450–490 nm (below) ($\times 500$).

The lipofuscin fluoresces brightly, as do probably unmyelinated fibres, but the main dendrites only weakly.



Figure 224 Thin slab of human medullary white matter from a 95-year-old female, to show beaded fibres *in situ* (phase contrast, $\times 700$).

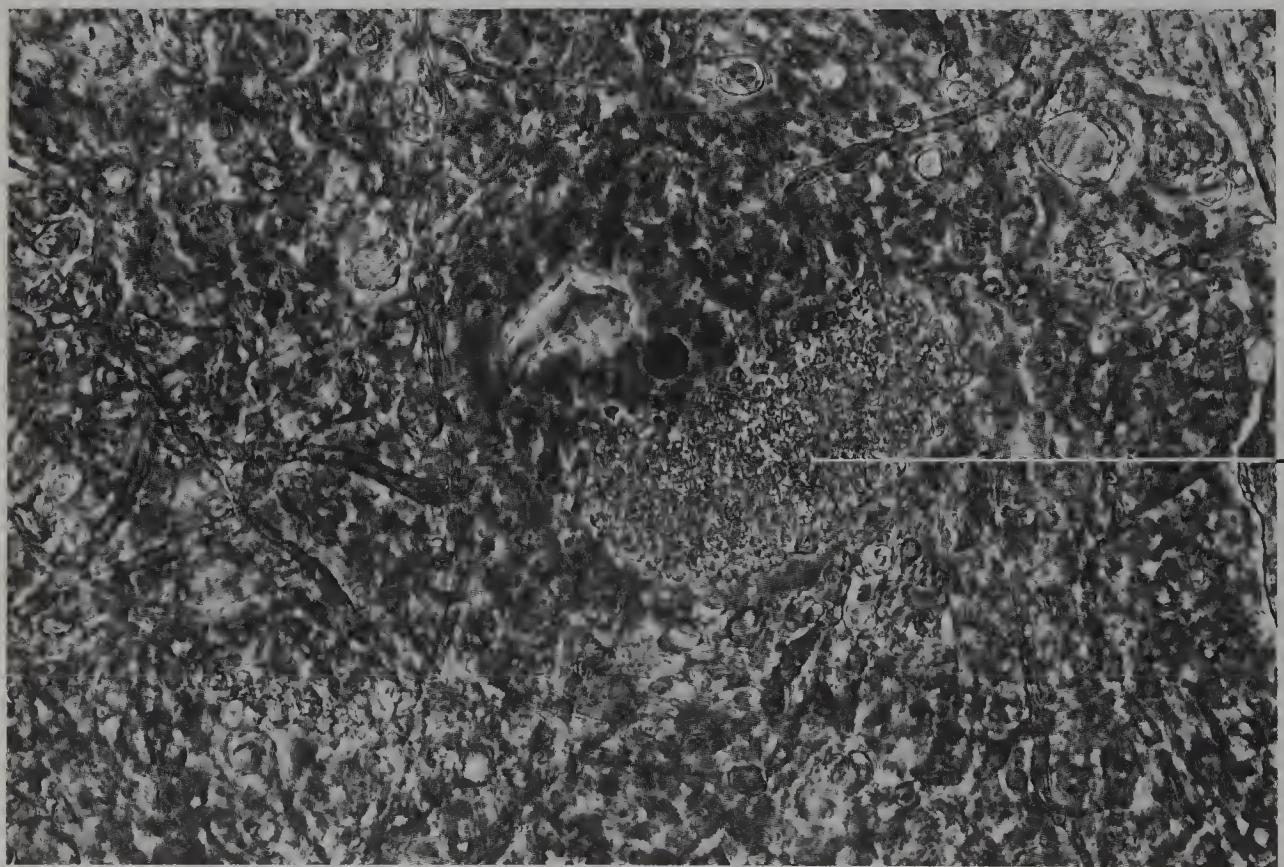


Figure 225 Thin slab of human dorsal nucleus of the vagus from a 95-year-old female, to show a neuron *in situ* with large lipofuscin deposit (phase contrast, $\times 700$).

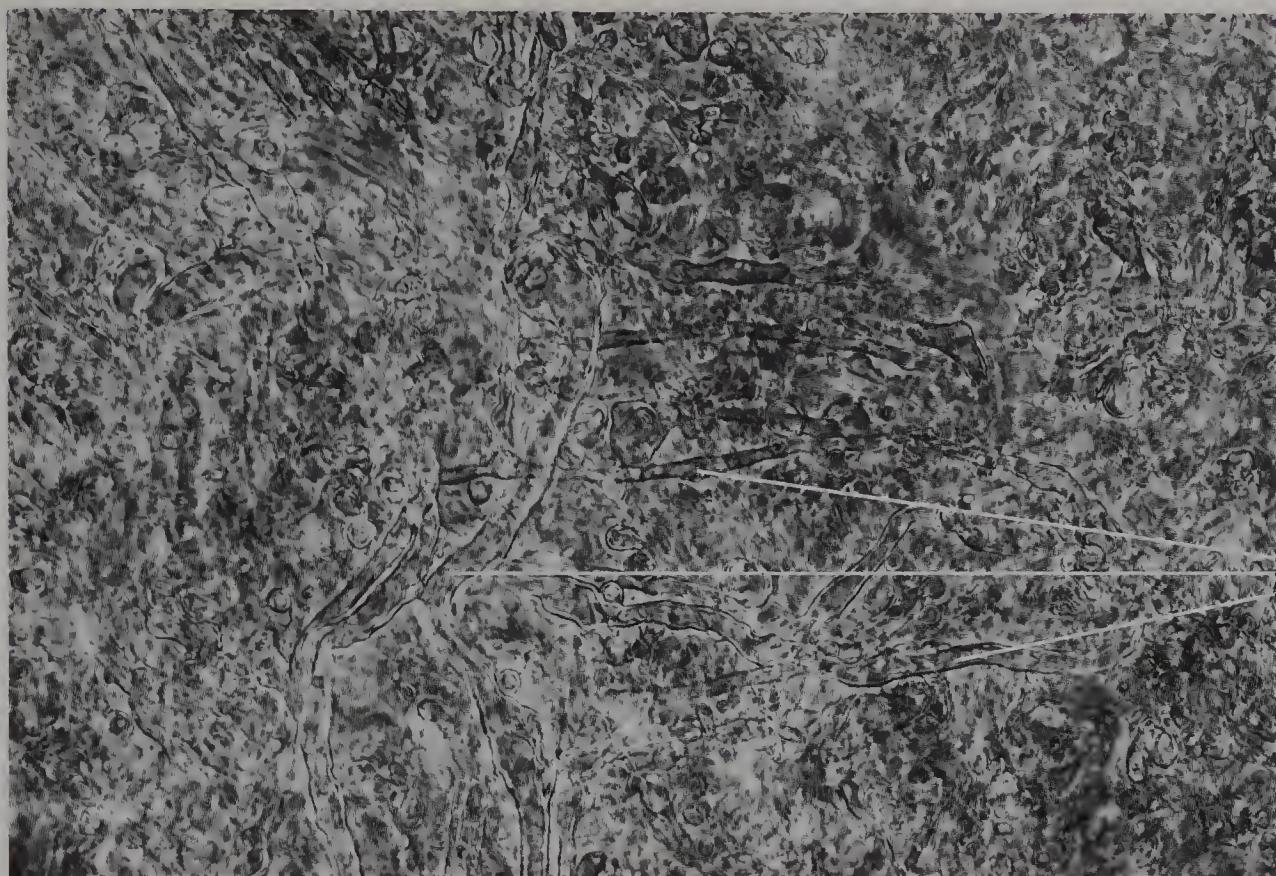


Figure 226 Thin slab of human dorsal nucleus of the vagus from a 95-year-old female, to show beaded fibres *in situ* (phase contrast, $\times 700$).



Figure 227 Partially teased human dorsal nucleus of the vagus from the previous specimen, to show beaded fibres (phase contrast, $\times 700$).

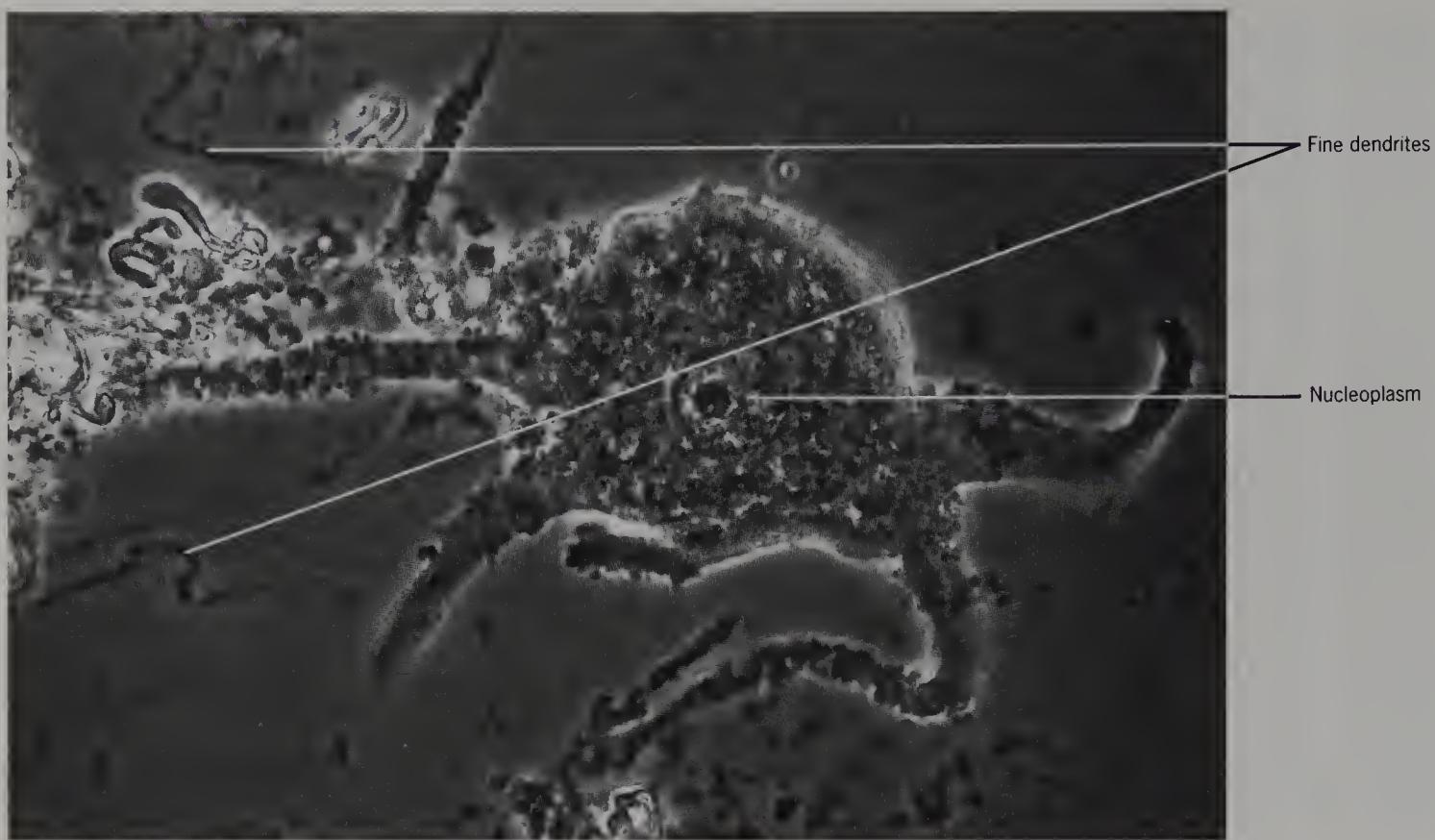


Figure 228 Isolated neuron from the dorsal nucleus of the vagus from a 53-year-old male (phase contrast, $\times 700$).

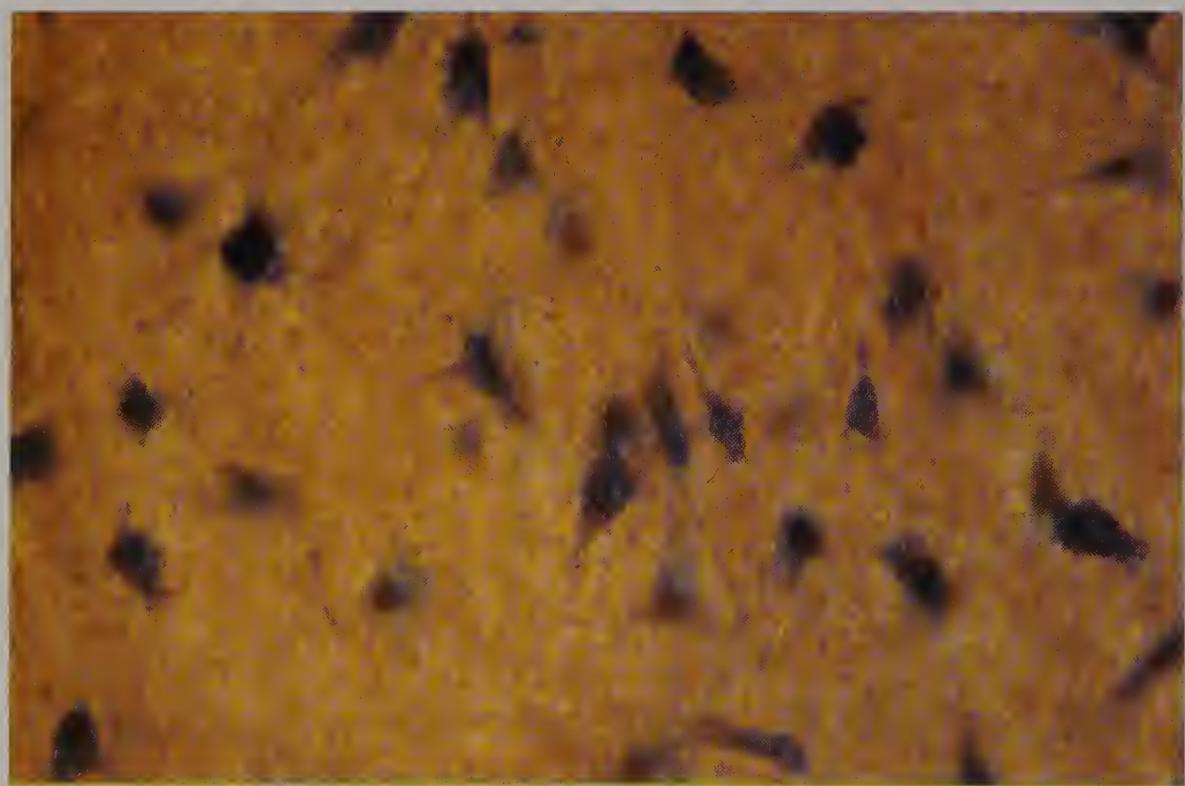


Figure 229 Thin slab of human hypoglossal nucleus from a 60-year-old male, lightly coloured with methylene blue to show the incidence and appearance of neuron somas (bright field, $\times 100$).



Figure 230 Thin slab of human hypoglossal nucleus, from the previous specimen, lightly coloured with methylene blue to show the appearance of the neuron soma *in situ* (phase contrast, $\times 610$).

Note the lipofuscin deposit to one side of the nucleus.

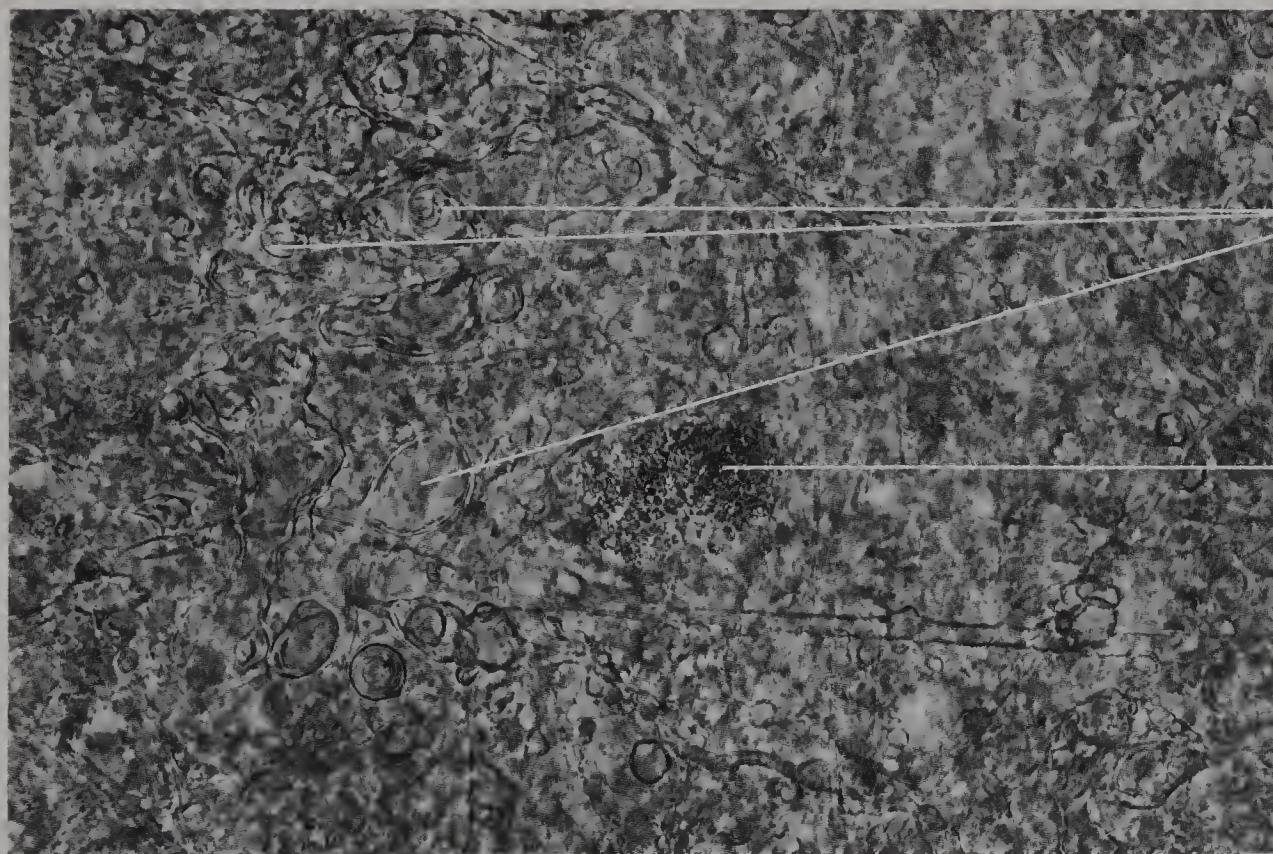


Figure 231 Thin slab of human hypoglossal nucleus, from a 95-year-old female, to show lipofuscin, beaded fibres and droplets (phase contrast, $\times 700$).

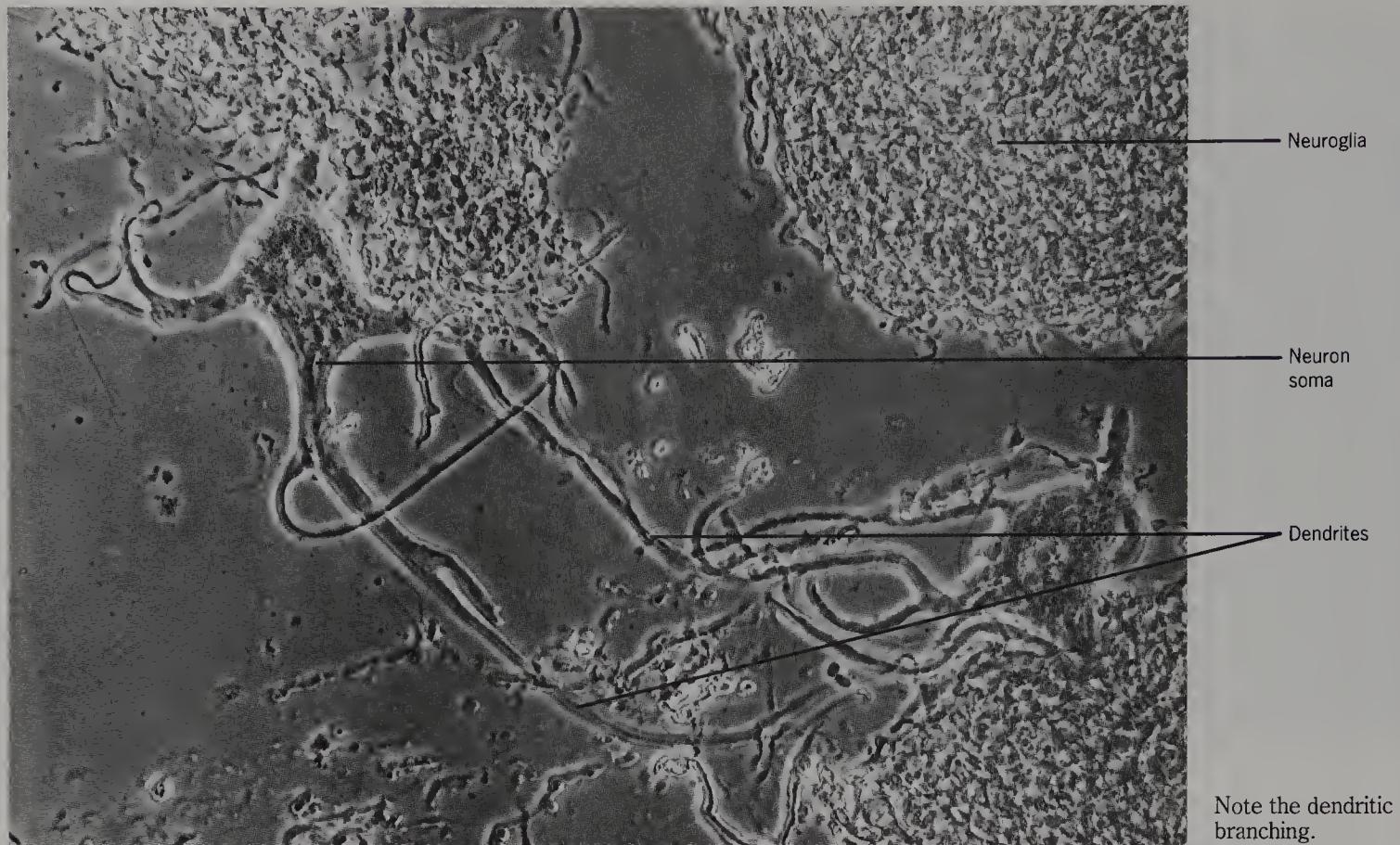


Figure 232 Teased human hypoglossal nucleus from a 62-year-old female, to show neurons and neuroglia (phase contrast, $\times 300$).

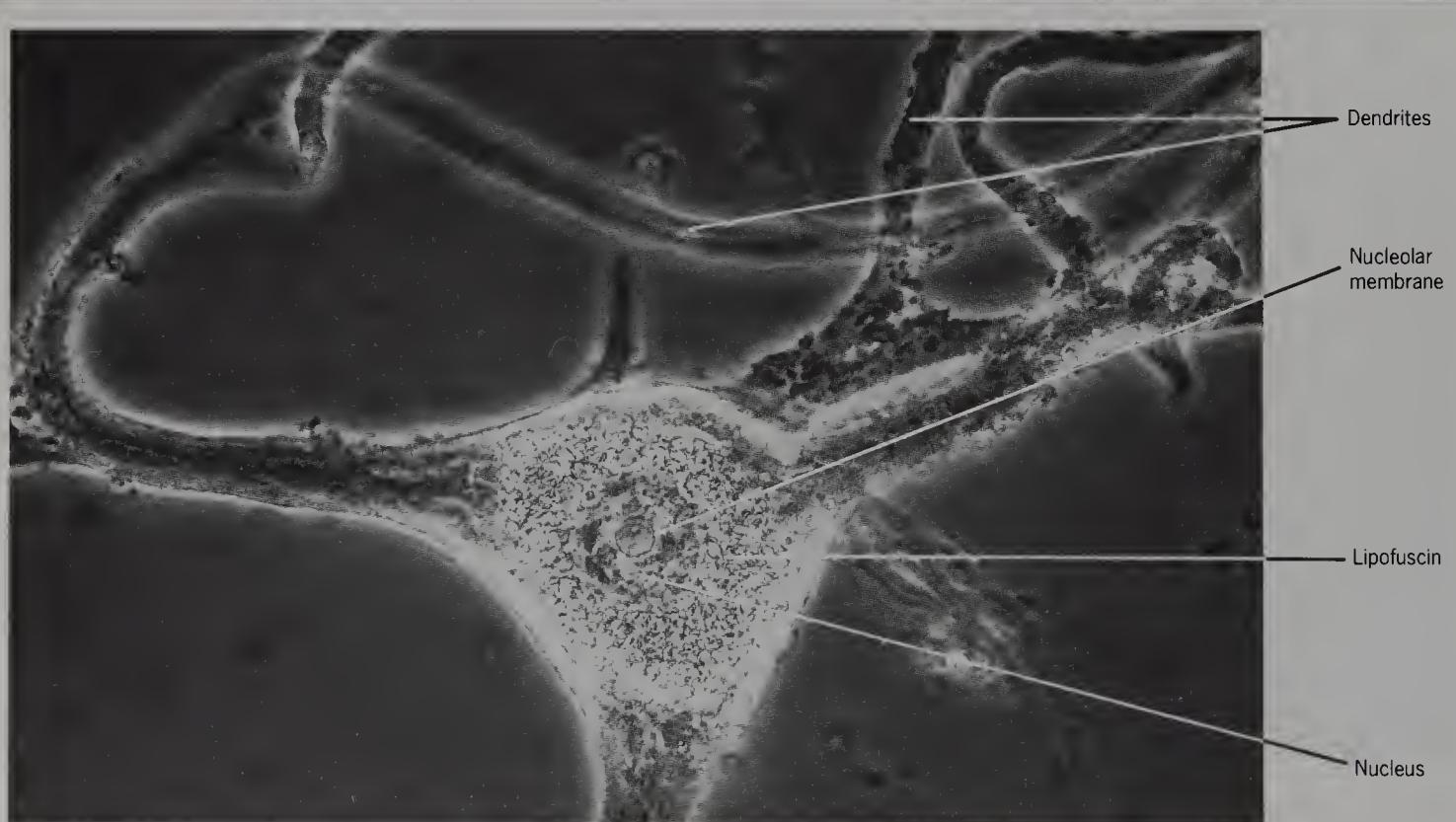


Figure 233 Isolated human neuron from the hypoglossal nucleus of the previous specimen (phase contrast, $\times 700$).

Near the soma, it is usually difficult to distinguish with certainty between small primary dendrites and axons.

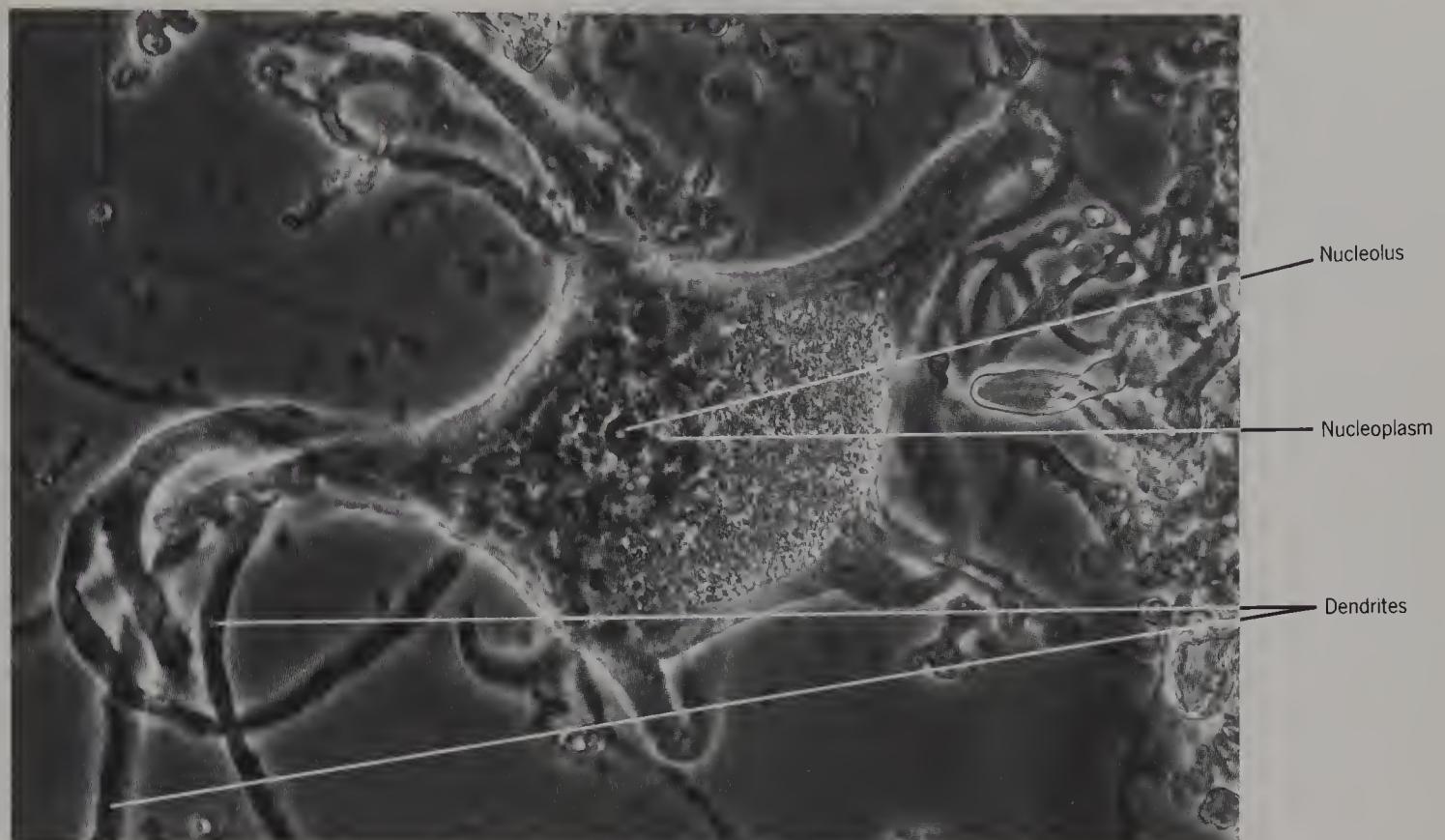


Figure 234 Isolated human neuron from the hypoglossal nucleus of the previous specimen (phase contrast, $\times 700$). Note the dense material in the cytoplasm and dendrites.

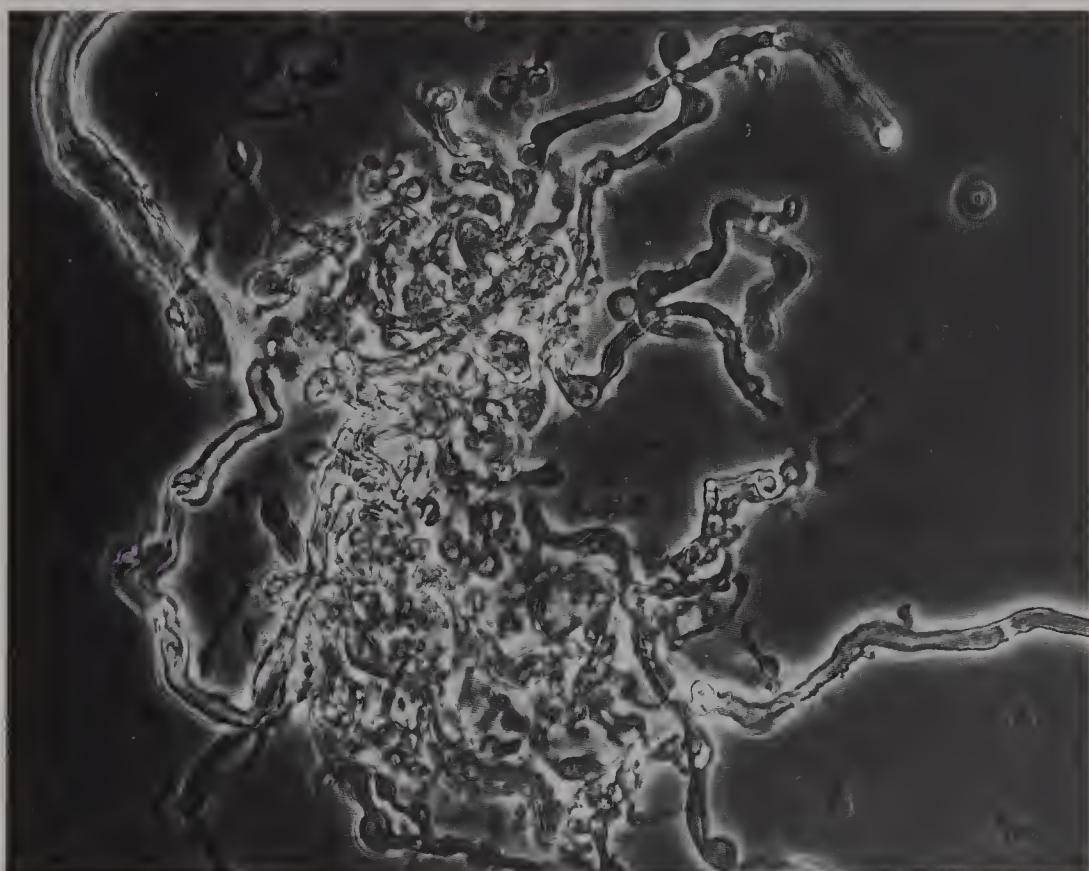


Figure 235 Teased human white matter adjacent to the hypoglossal nucleus of a 62-year-old female, to show beaded fibres (phase contrast, $\times 700$).

SECTION

5

CEREBELLUM

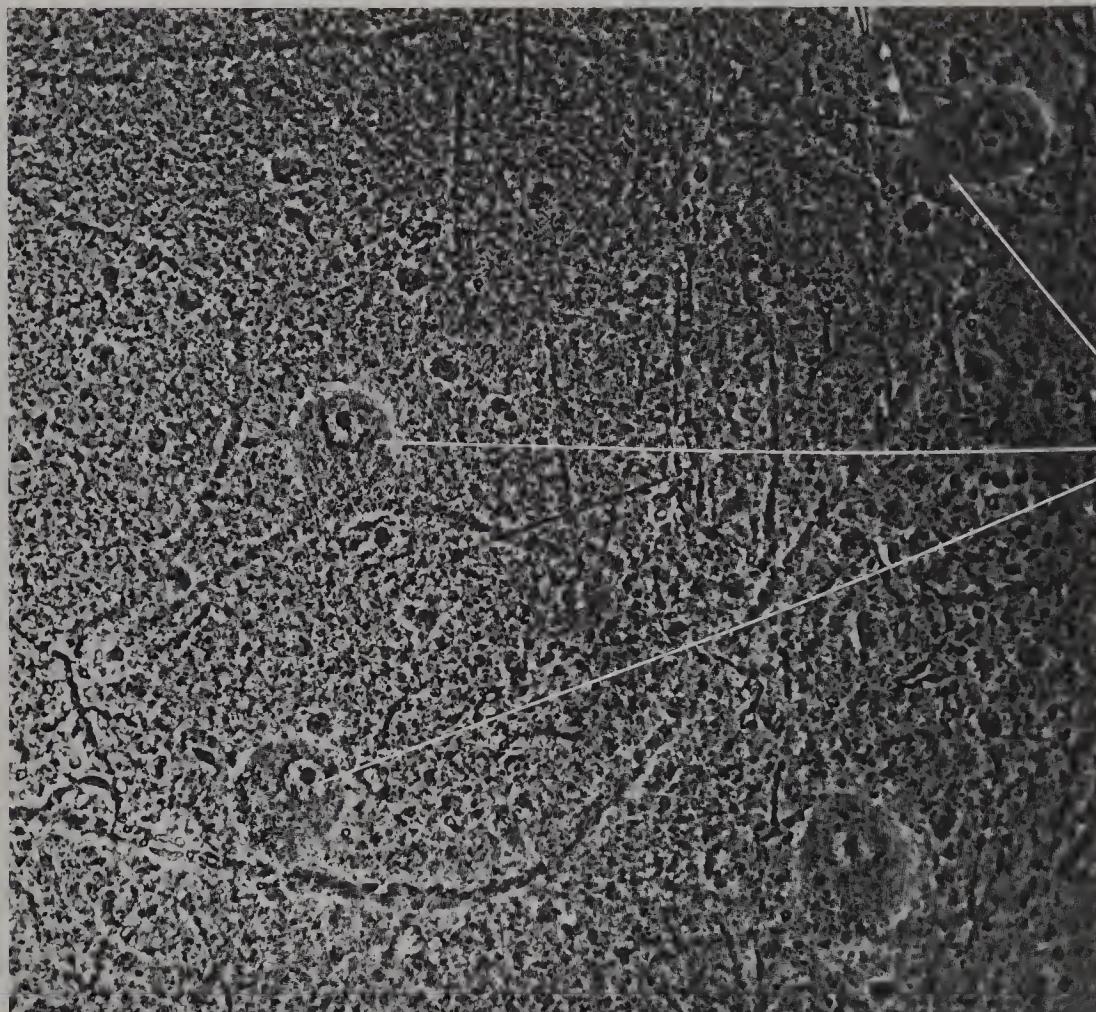


Figure 236 Thin slab of human cerebellar cortex from a 71-year-old male, to show Purkinje cells with dendrites *in situ* (phase contrast, $\times 335$).

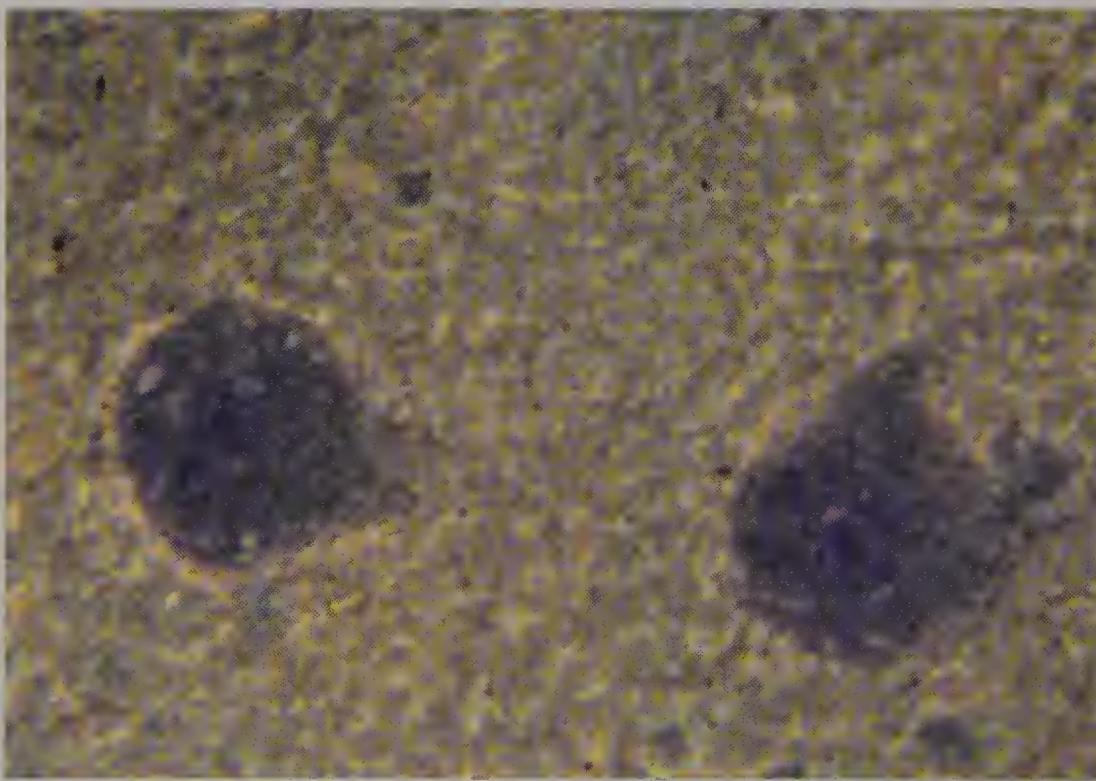


Figure 237 Thin slab of human cerebellar cortex from an 84-year-old male, lightly coloured with methylene blue to show Purkinje cell somas *in situ* (bright field, $\times 610$).

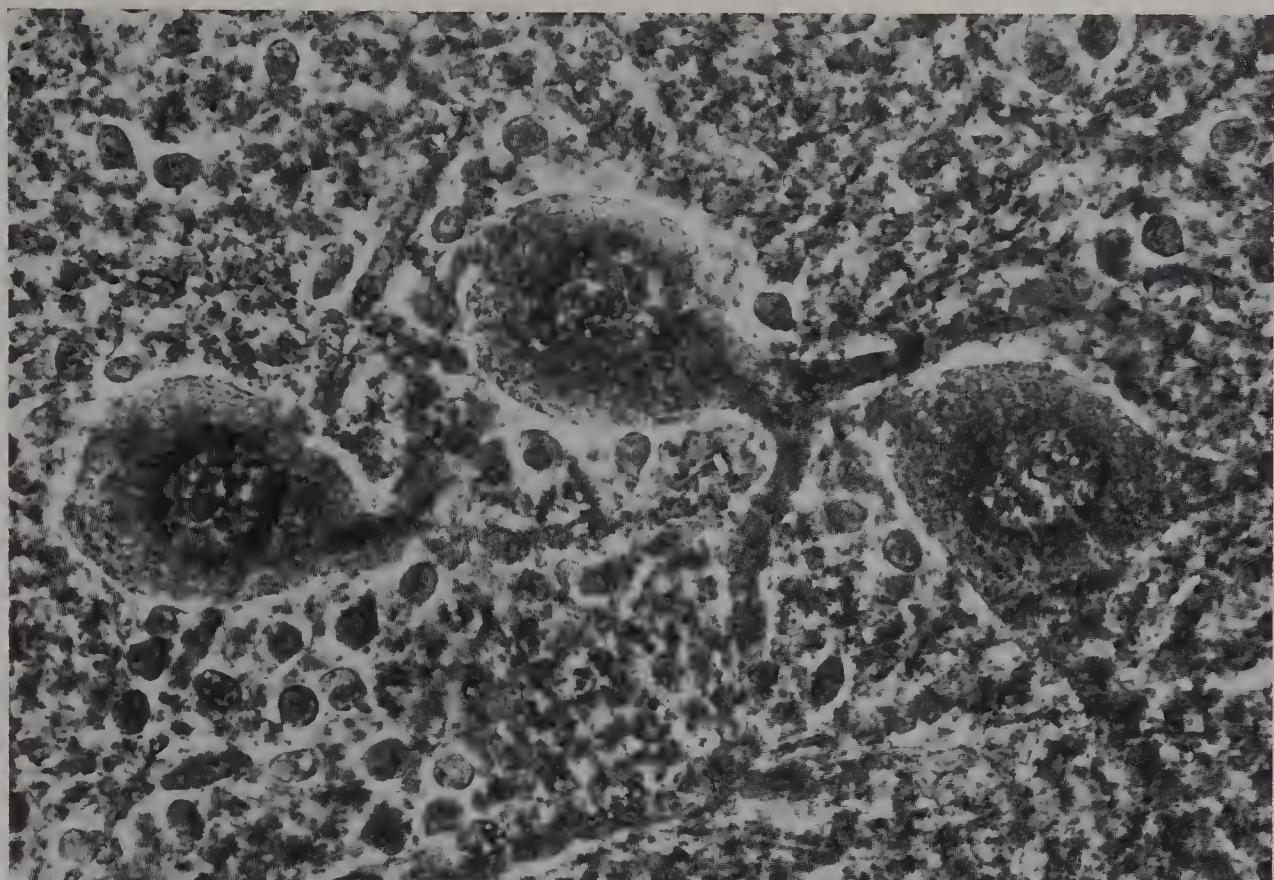


Figure 238 Thin slab of lamb cerebellar cortex to show Purkinje and granule cells *in situ* (phase contrast, $\times 700$). These cells were originally described by Purkinje in 1838.

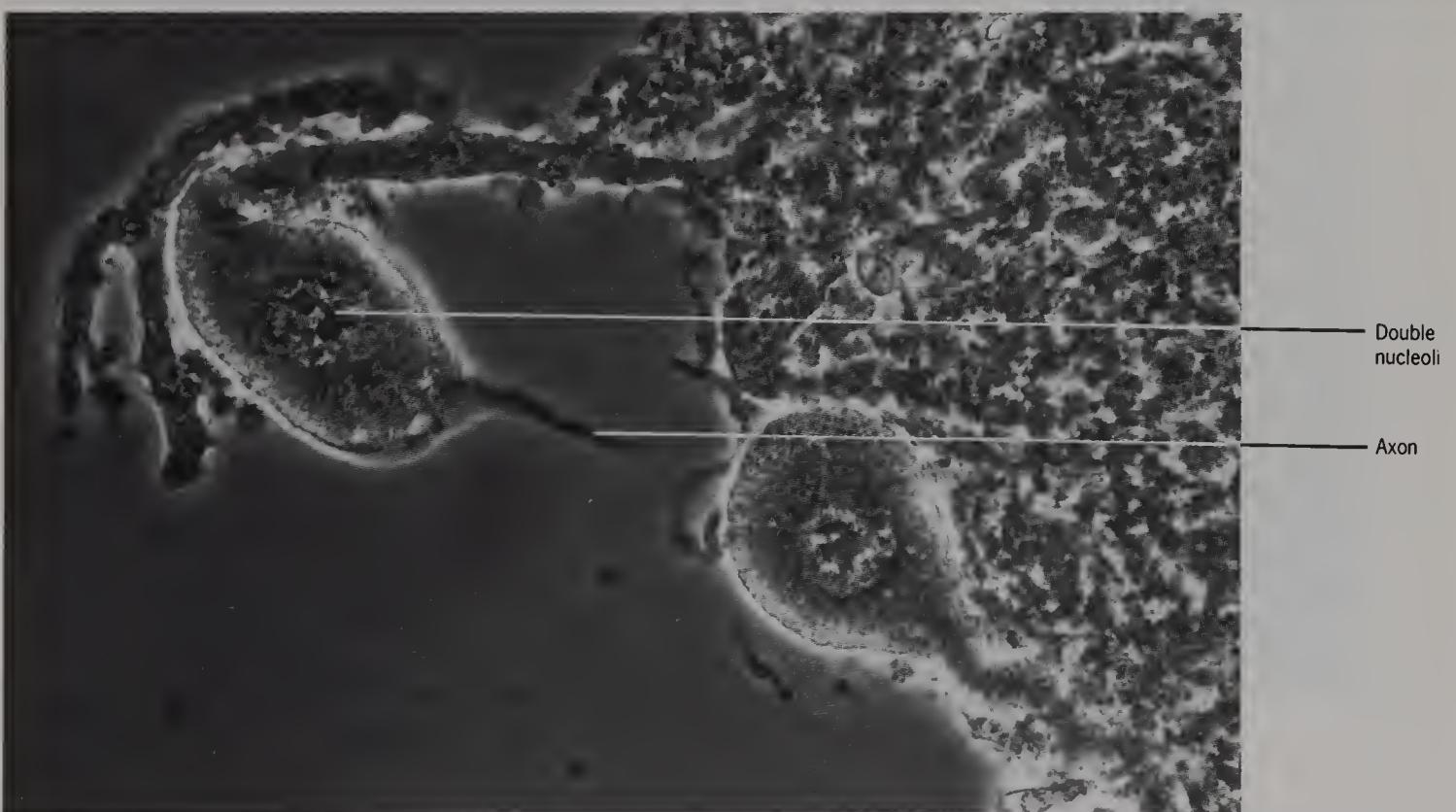


Figure 239 Partially teased lamb cerebellar cortex to show two Purkinje cells, one with two nucleoli and associated neuroglia (phase contrast, $\times 700$).

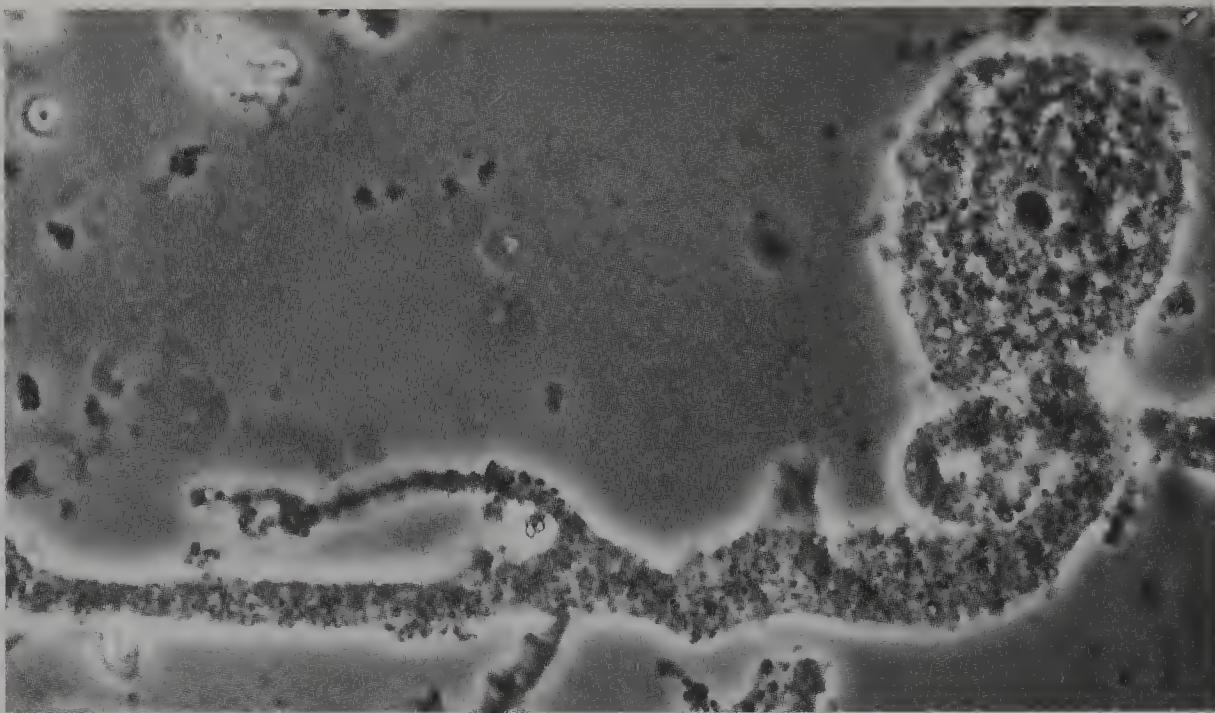
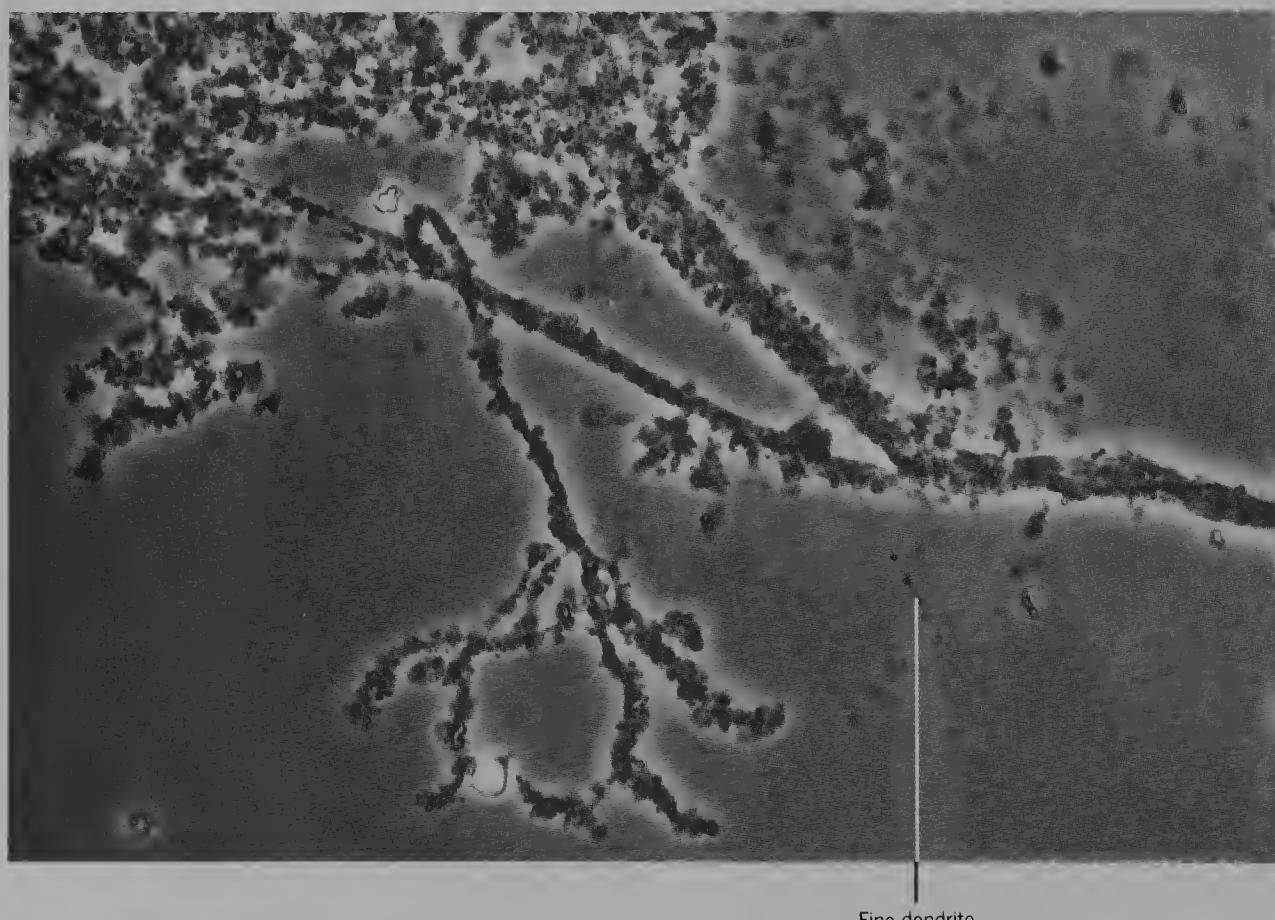


Figure 240 Isolated human Purkinje cell from a 53-year-old male (phase contrast, $\times 700$).



Fine dendrite

Figure 241 Teased dendrites from the human Purkinje cell of the previous specimen (phase contrast, $\times 700$).

Fine granules adhere to the dendrites.

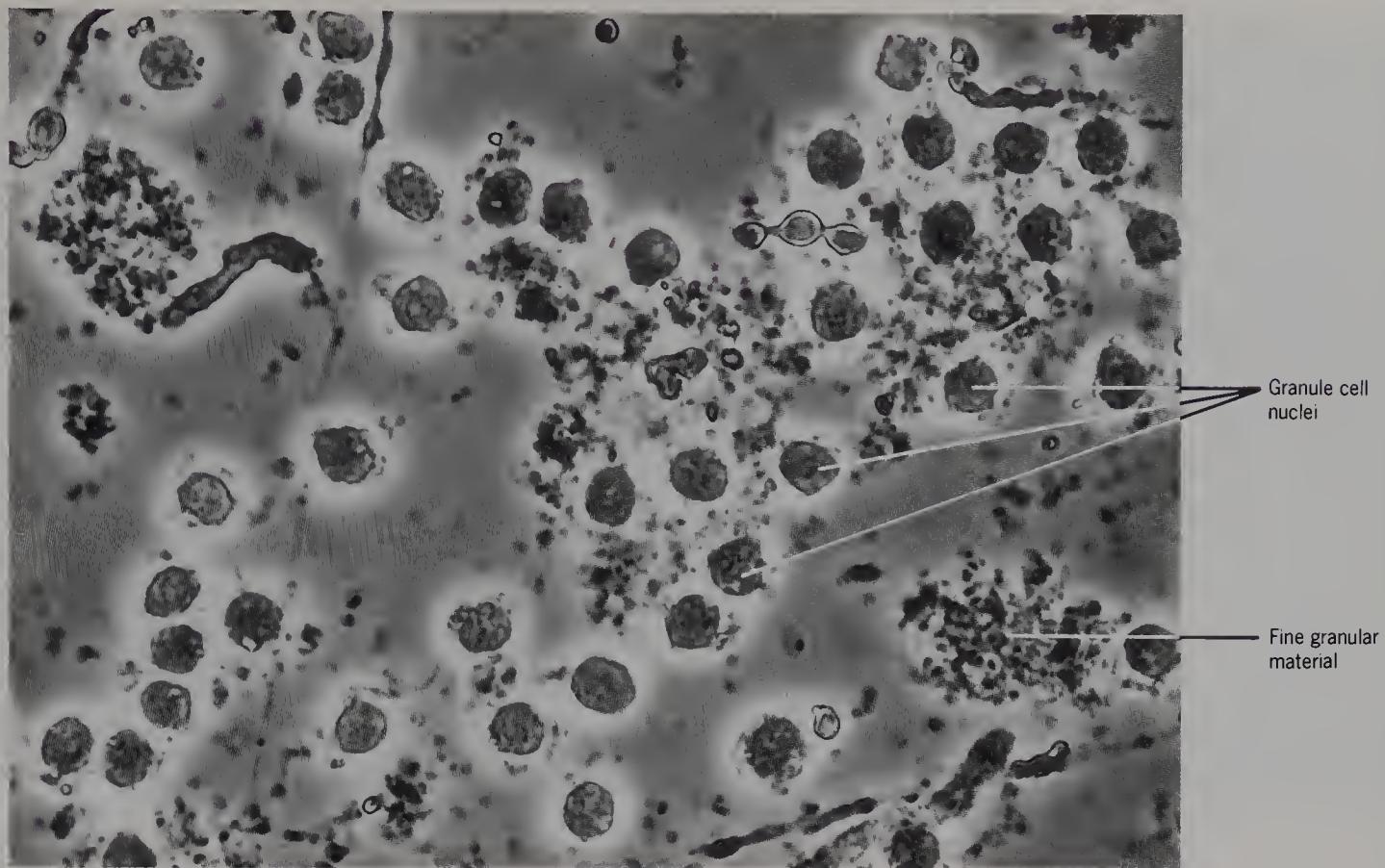


Figure 242 Isolated human cerebellar granule cells and fine granular material from a 55-year-old male (phase contrast, $\times 700$). It is difficult to see cytoplasm around these cells.

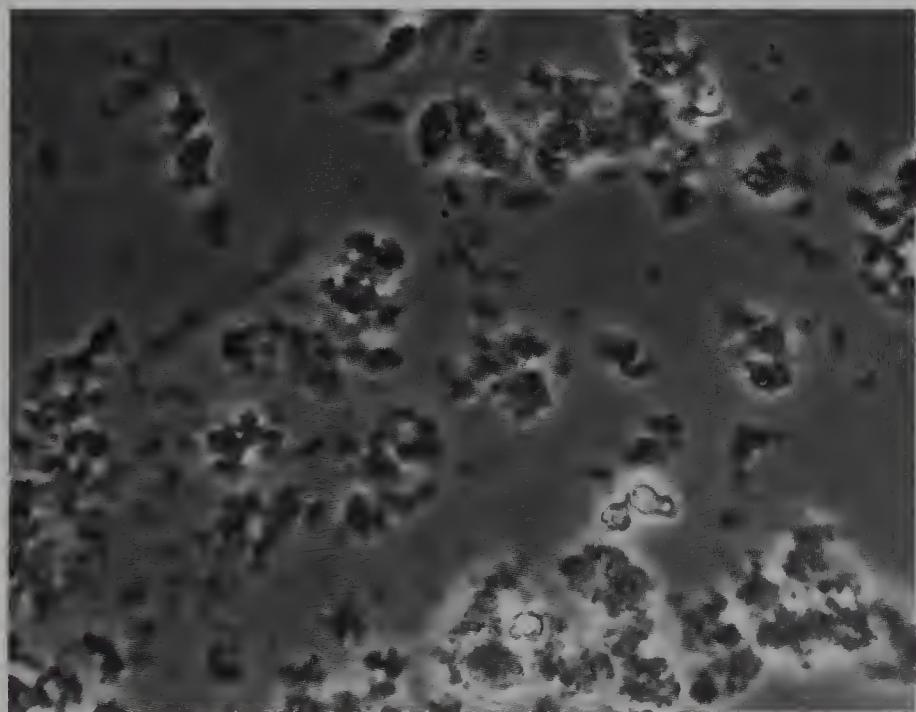


Figure 243 Isolated fine granular material of human cerebellar grey matter from an 80-year-old female (phase contrast, $\times 700$).

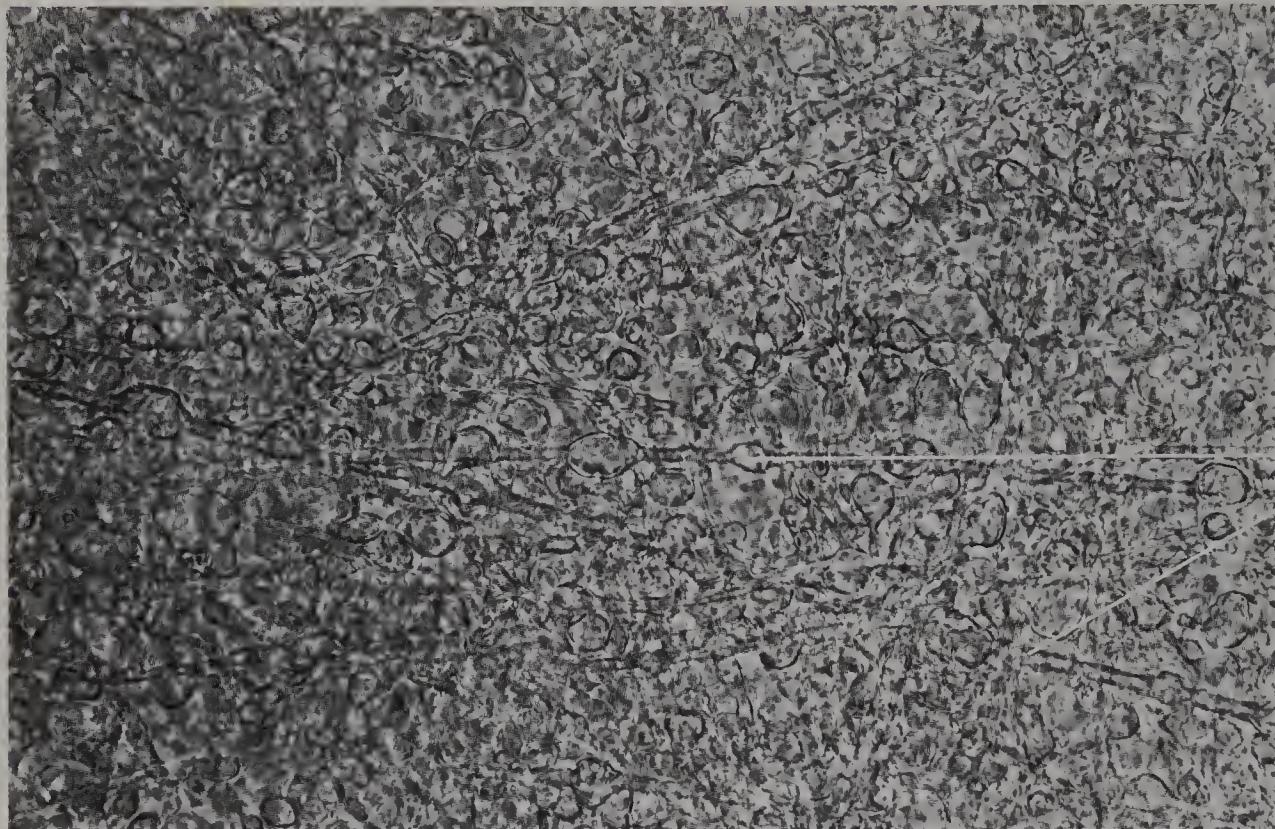


Figure 244 Thin slab of human cerebellar white matter from the centre of a folium from a 71-year-old male, to show fine beaded fibres (phase contrast, $\times 700$).

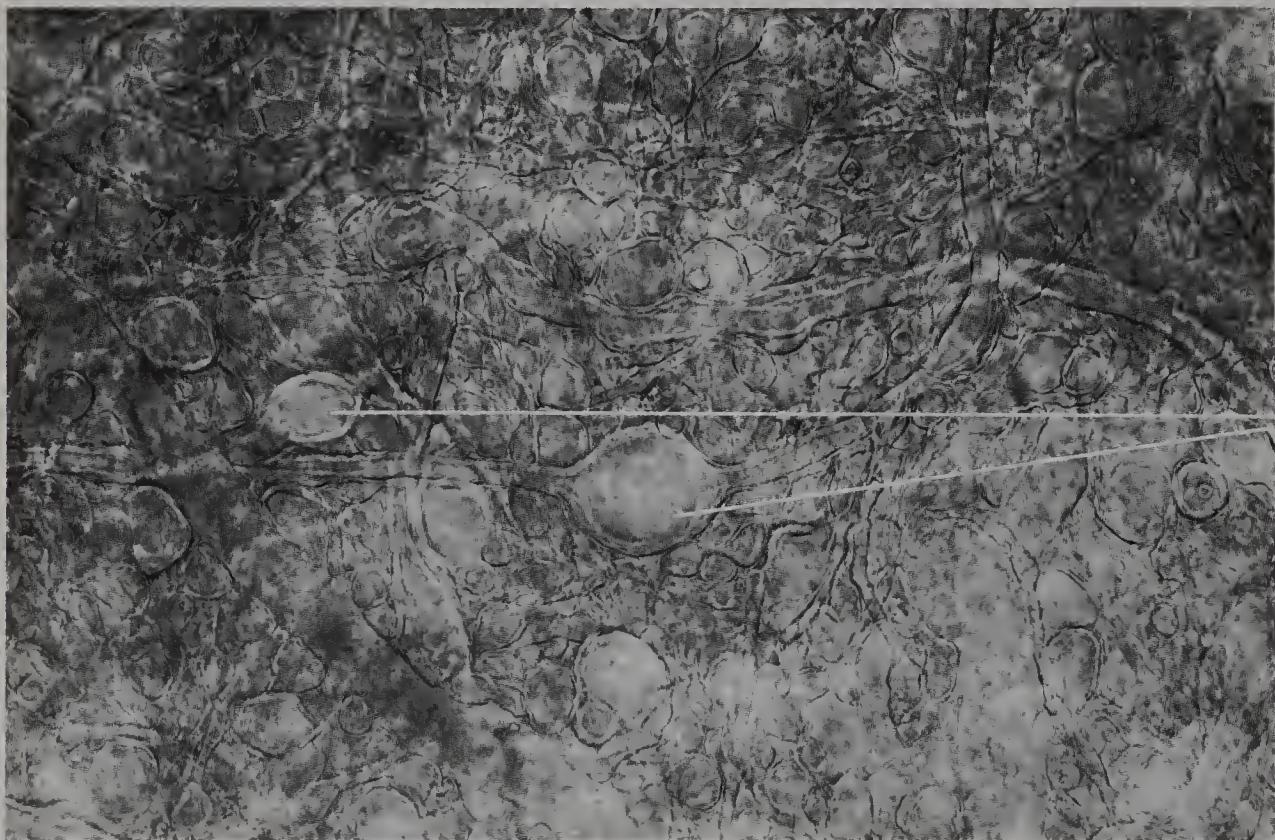


Figure 245 Thin slab of human cerebellar white matter adjacent to the dentate nucleus, from the previous specimen, to show large beaded fibres and droplets (phase contrast, $\times 700$).

There is a large variation in fibre diameters between the fibres seen in this and the previous figure.

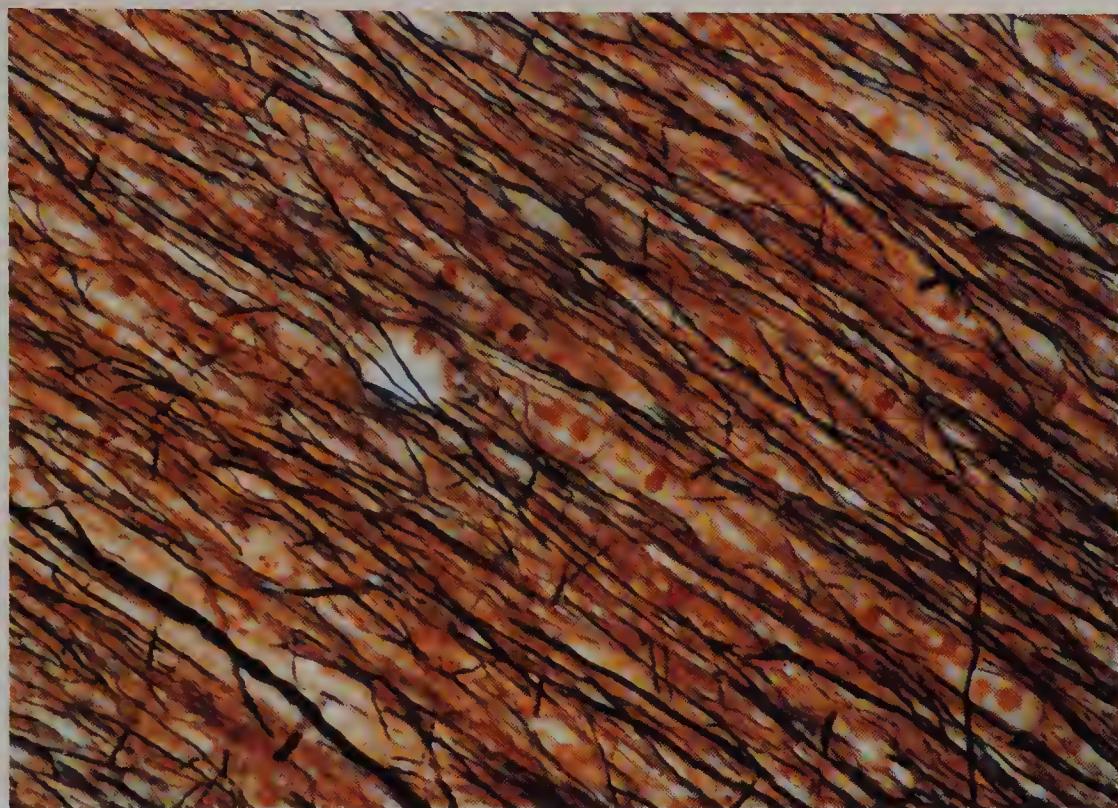


Figure 246 Section of human cerebellar white matter, stained with Palmsgren's stain, to show a tract of fine fibres (bright field, $\times 610$).

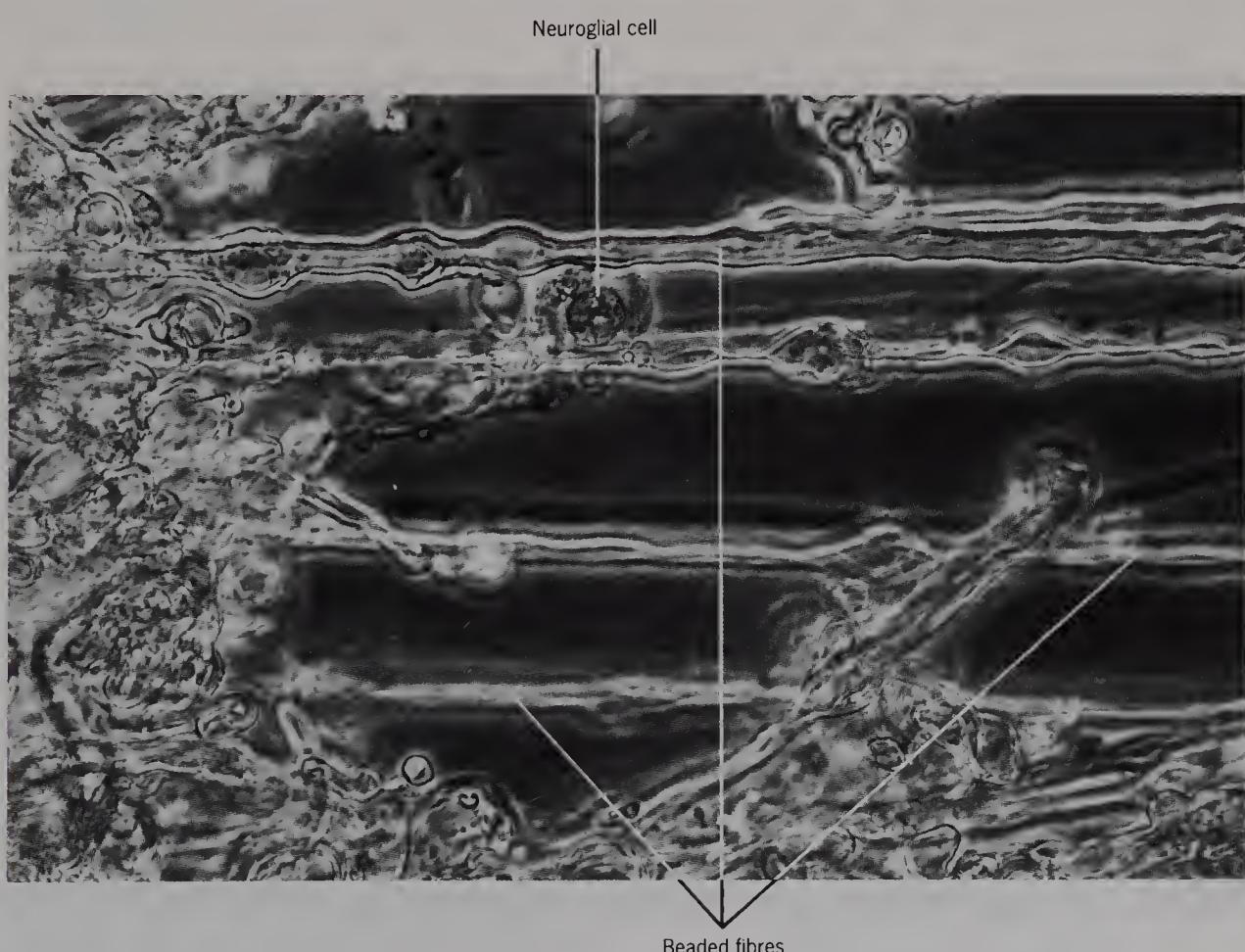


Figure 247 Partially teased human cerebellar white matter adjacent to the dentate nucleus, from a 71-year-old male, to show beaded fibres and neuroglial cells (phase contrast, $\times 700$).

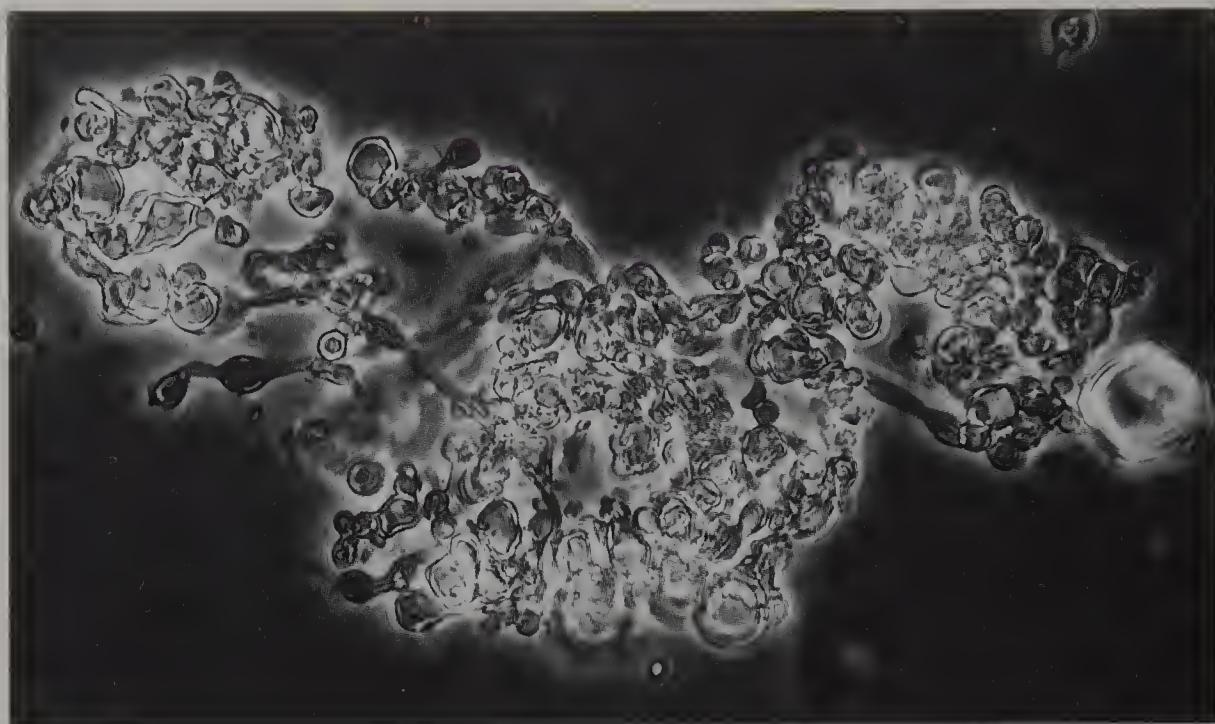


Figure 248 Teased human cerebellar white matter from an 80-year-old female, to show beaded fibres and droplets (phase contrast, $\times 800$).

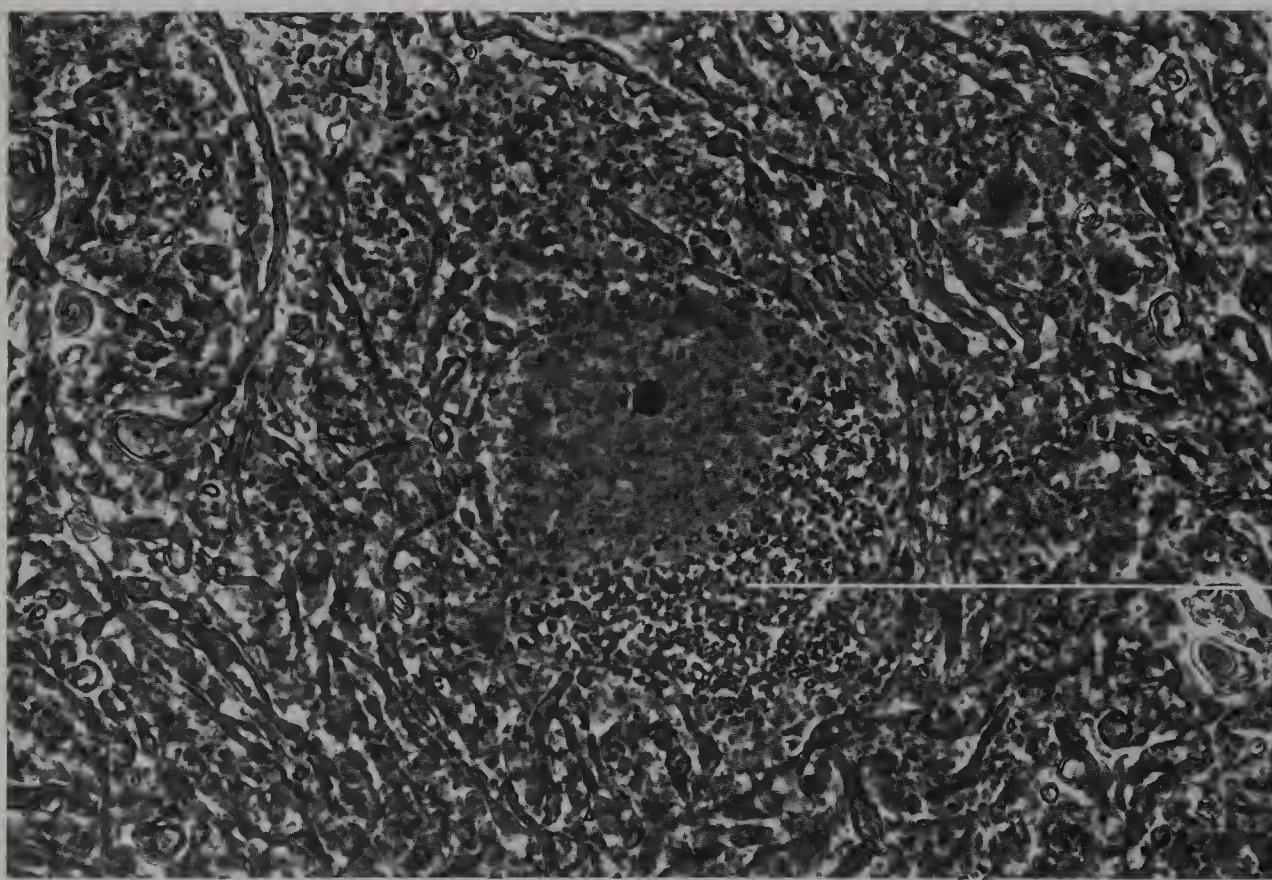


Figure 249 Thin slab of human dentate nucleus from a 71-year-old male, to show a neuron with lipofuscin *in situ* and beaded fibres (phase contrast, $\times 700$).

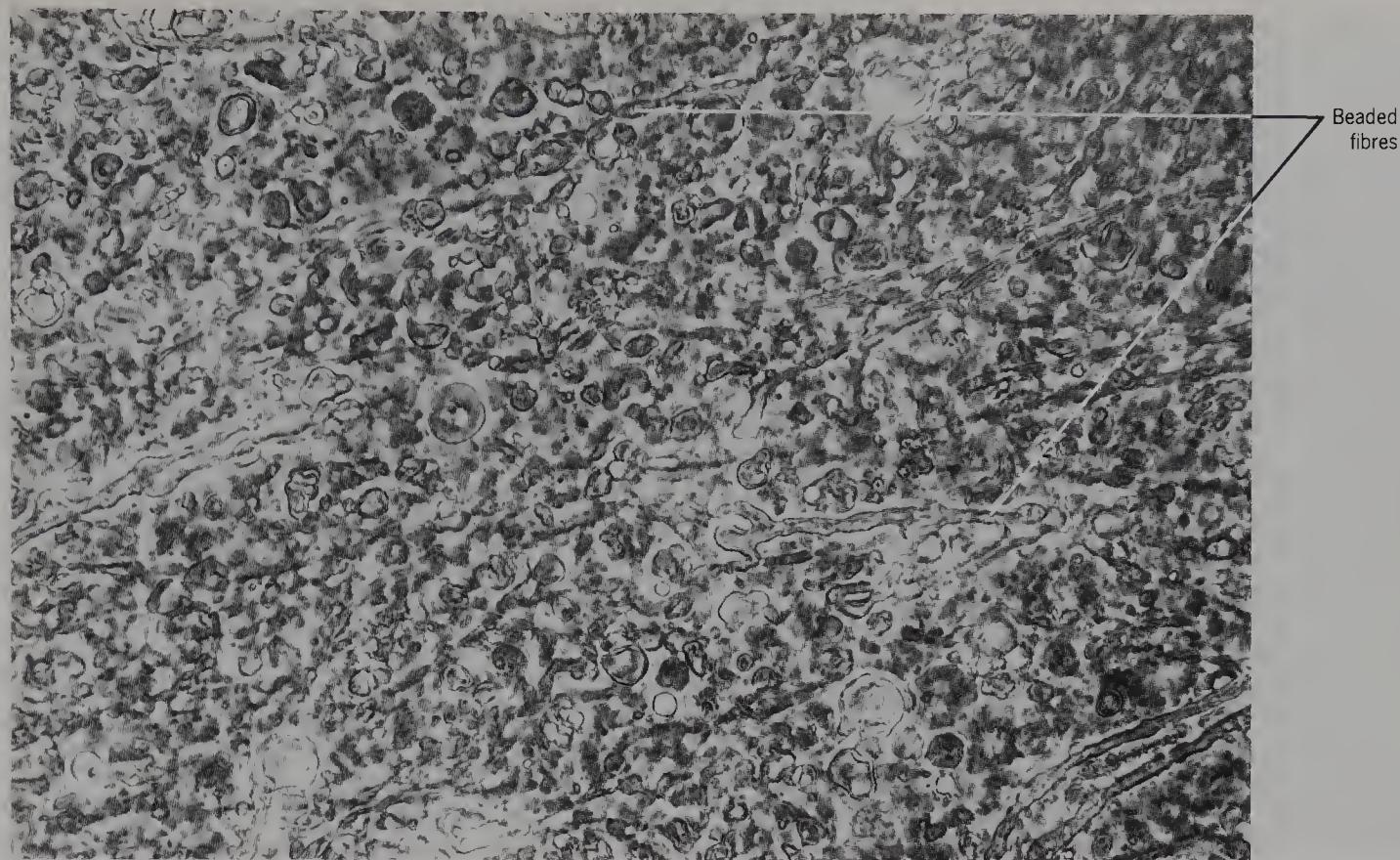


Figure 250 Thin slab of human dentate nucleus from the previous specimen, to show beaded fibres and droplets (phase contrast, $\times 700$).

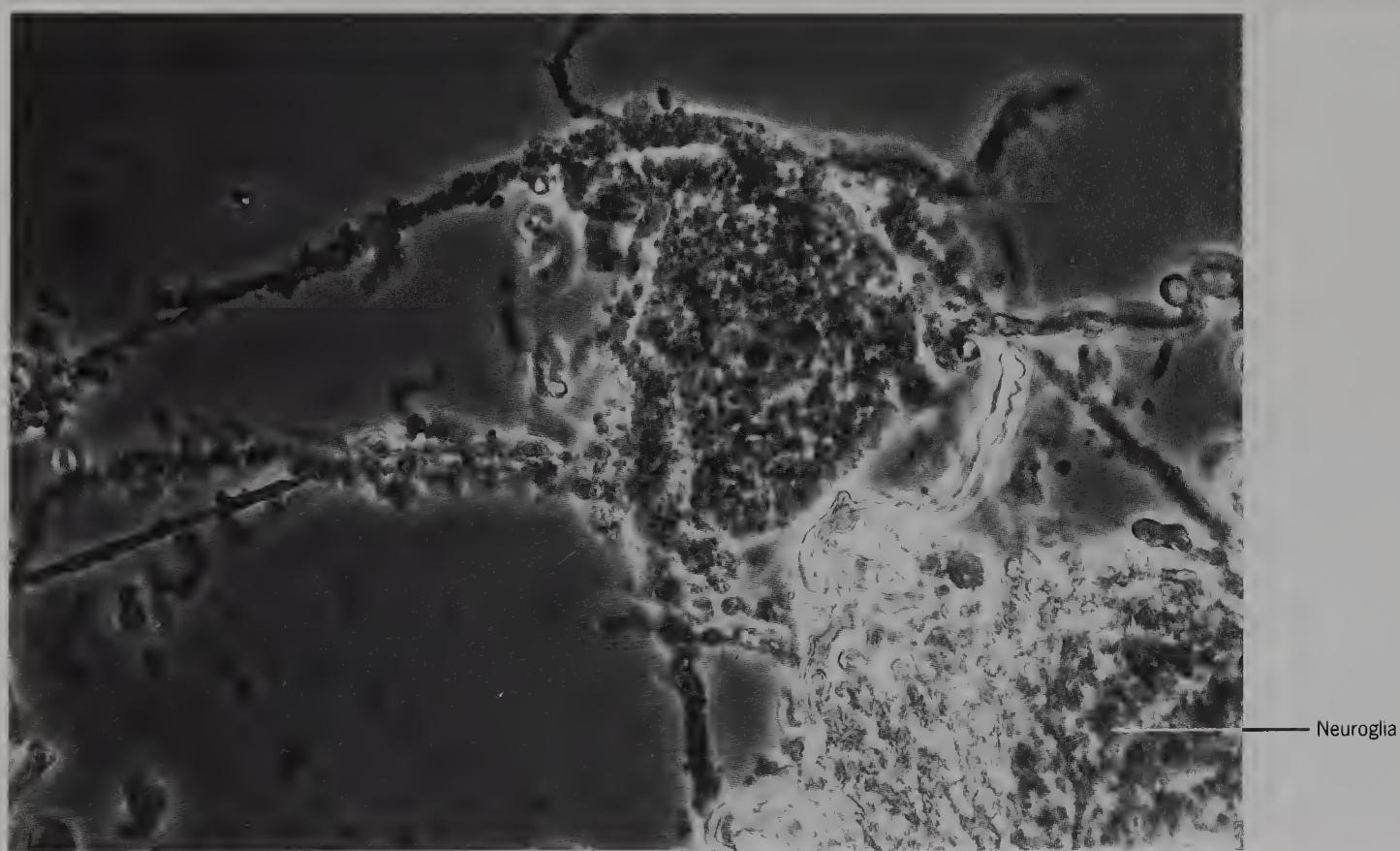


Figure 251 Isolated guinea-pig neuron with associated neuroglia from the dentate nucleus (phase contrast, $\times 700$).

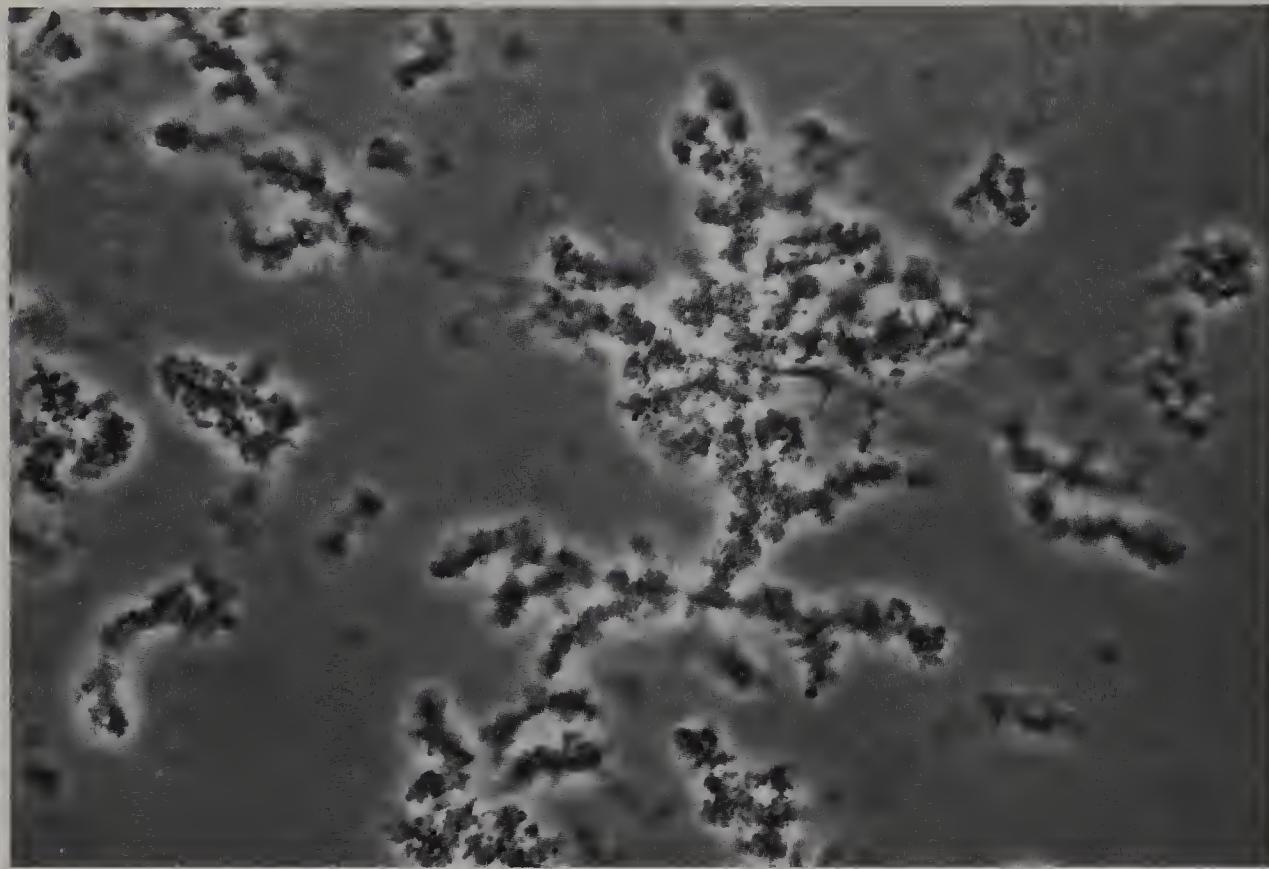


Figure 252 Teased neuroglia from the rabbit dentate nucleus, to show fine granular material (phase contrast, $\times 700$).

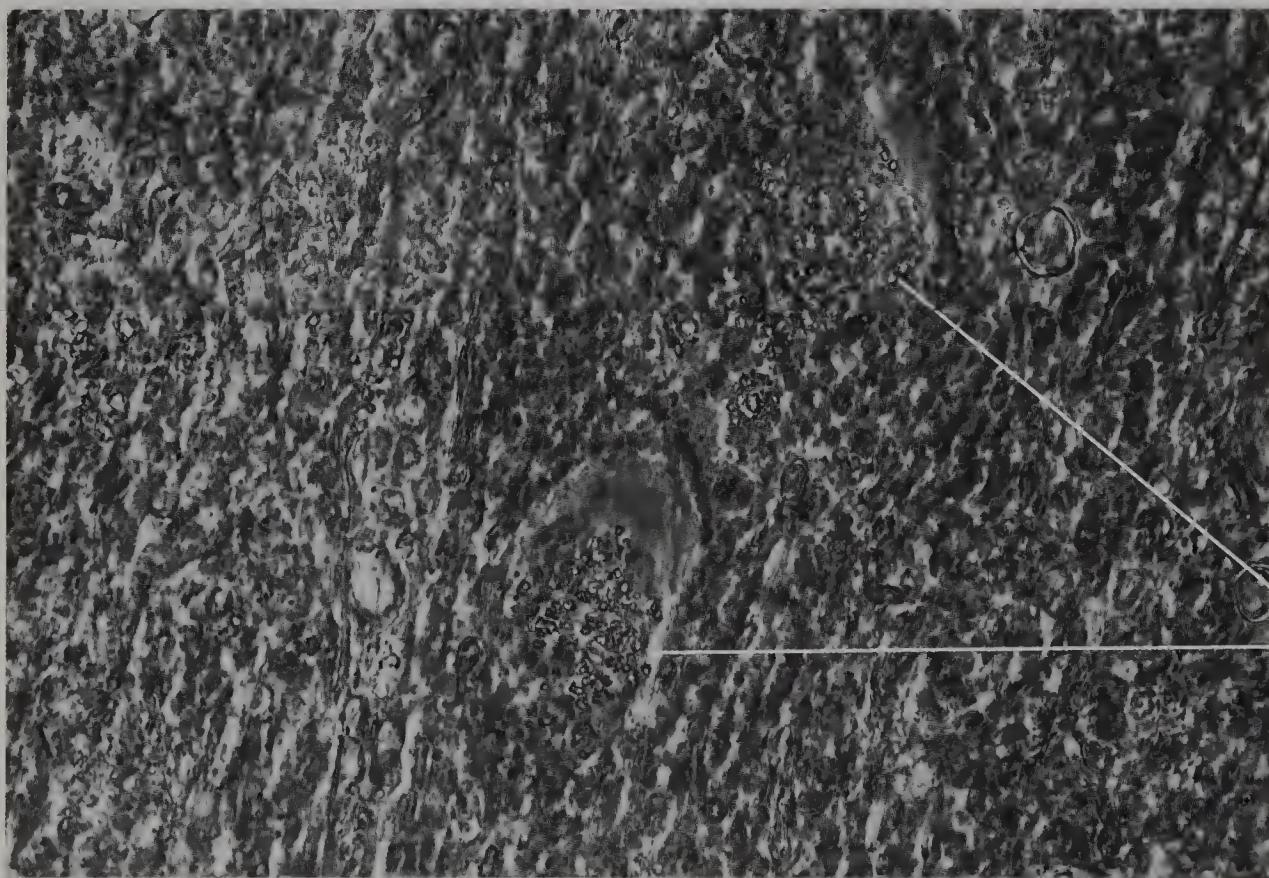


Figure 253 Thin slab of human fastigial nucleus from a 71-year-old male, to show neurons *in situ* with associated lipofuscin (phase contrast, $\times 700$).



Figure 254 Thin slab of human white matter adjacent to the fastigial nucleus, from the previous specimen, to show beaded fibres and droplets (phase contrast, $\times 700$).

SECTION**6****SPINAL CORD AND
GANGLIA**

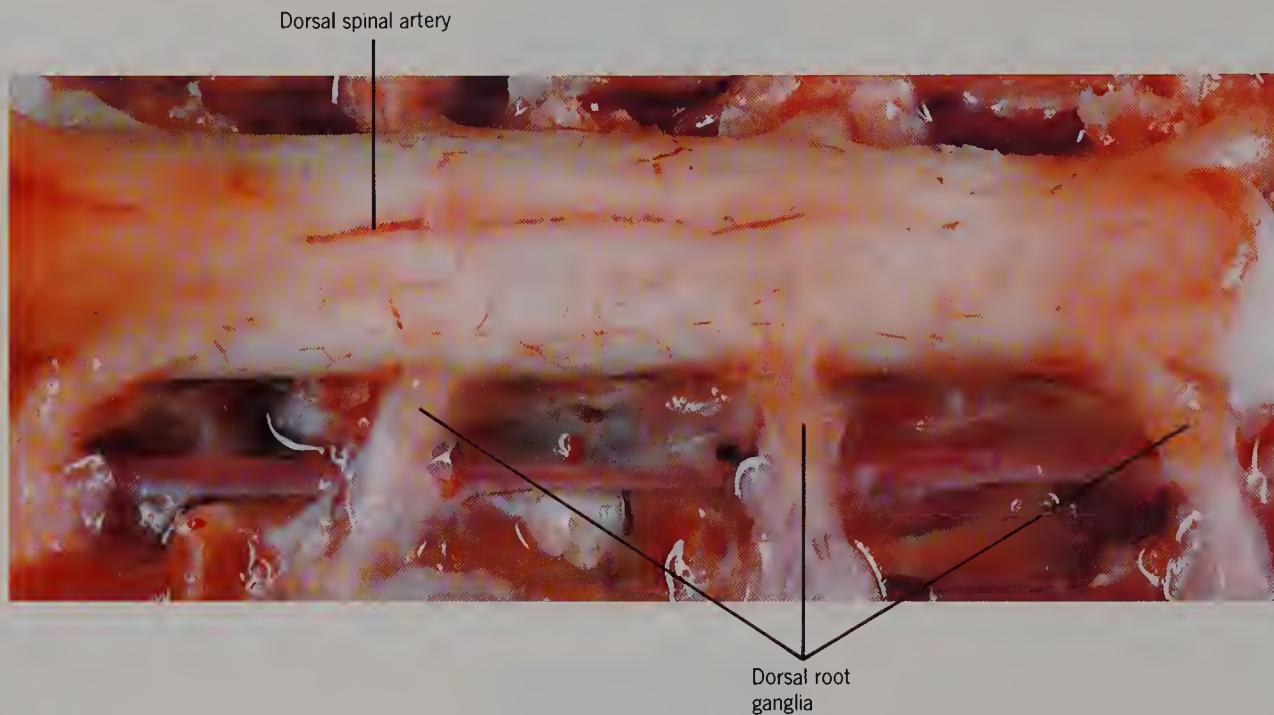


Figure 255 Dissection of rat spinal cord to show the position of dorsal root ganglia ($\times 6$).

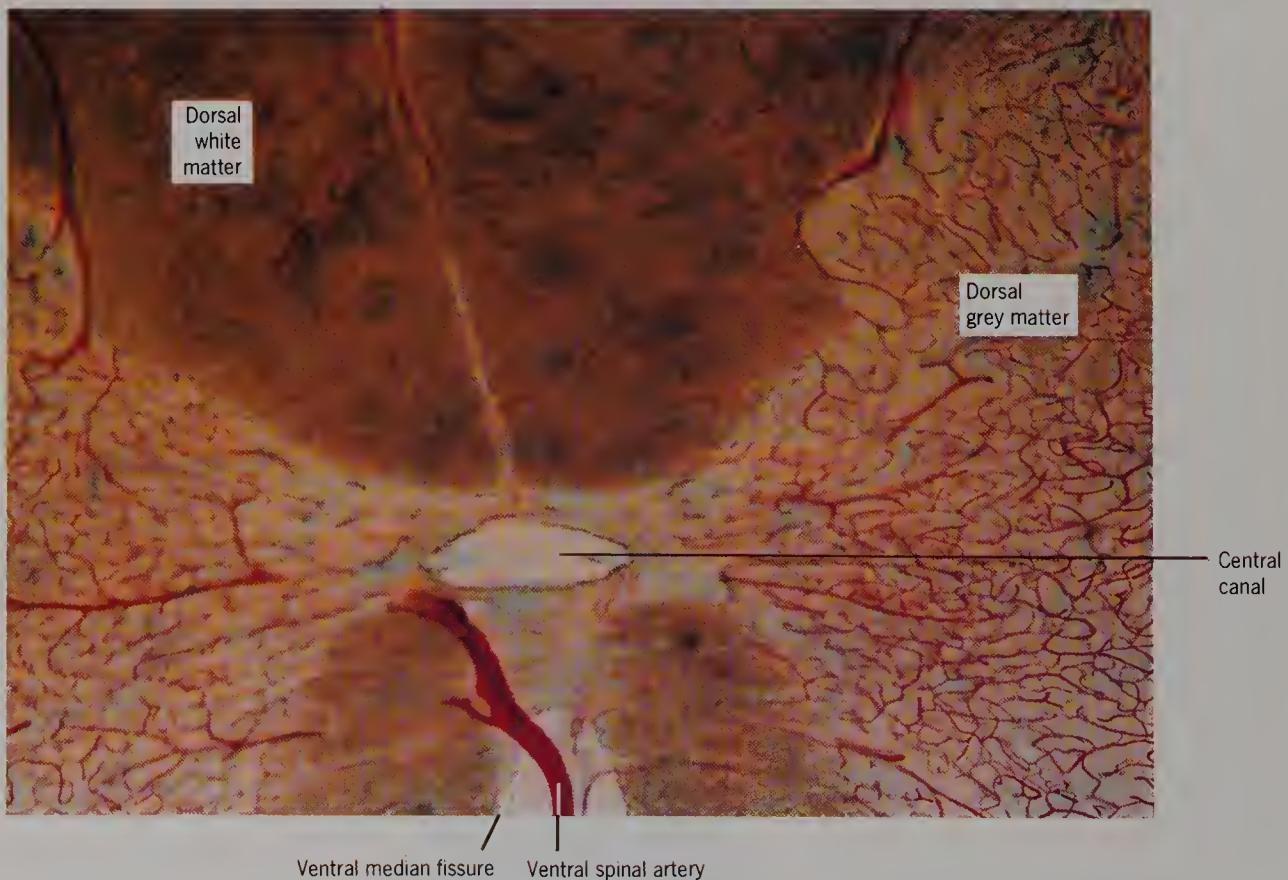


Figure 256 Section of injected cat spinal cord to show that there are more blood vessels in the grey than the white matter ($\times 60$).



Figure 257 Section of cat spinal cord stained with a silver stain to show the distribution of black-staining ventral horn cells in the grey matter (bright field, $\times 40$).

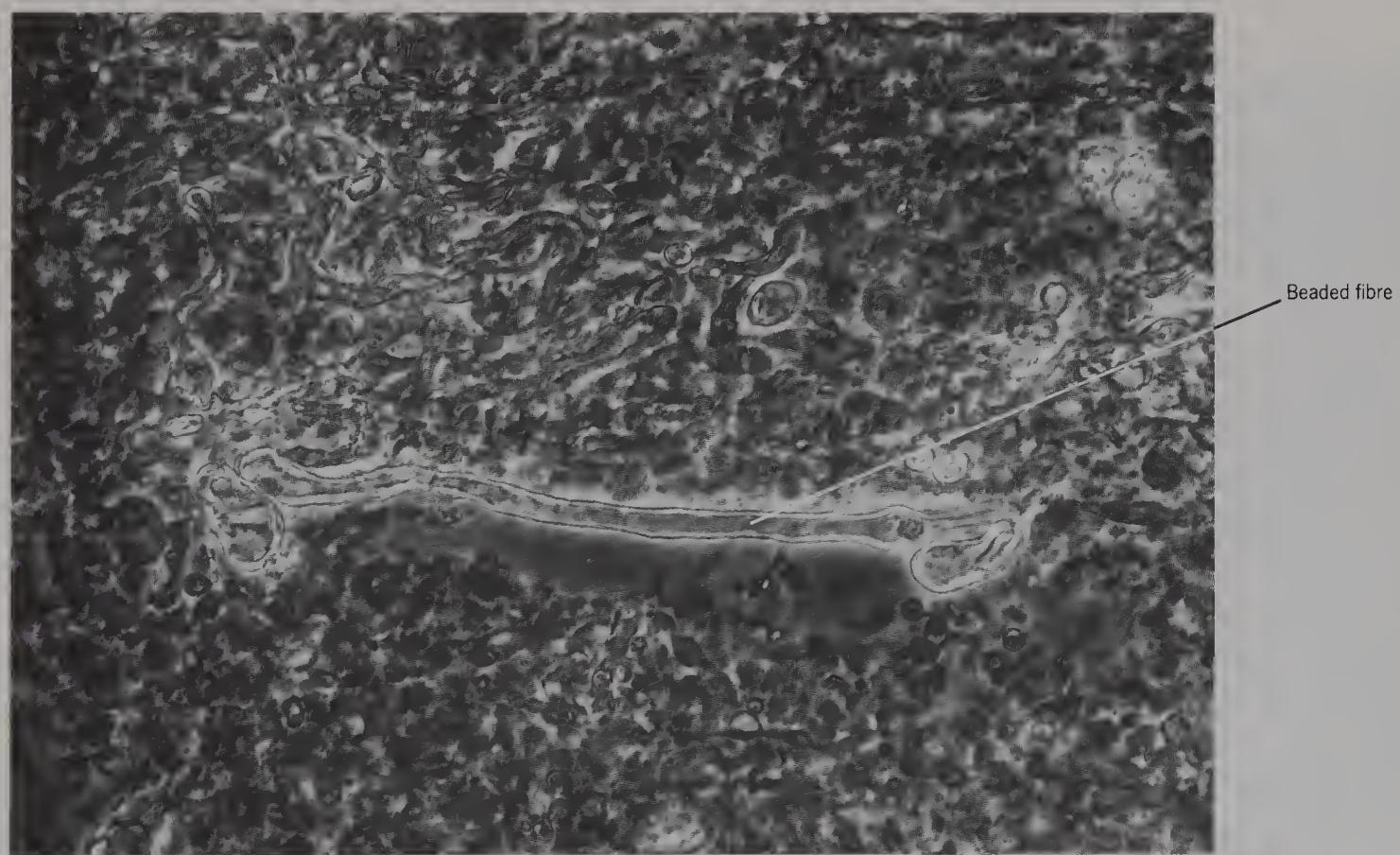


Figure 258 Partially teased rabbit substantia gelatinosa from the cervical spinal cord, to show fibres, believed to be myelinated (phase contrast, $\times 700$).

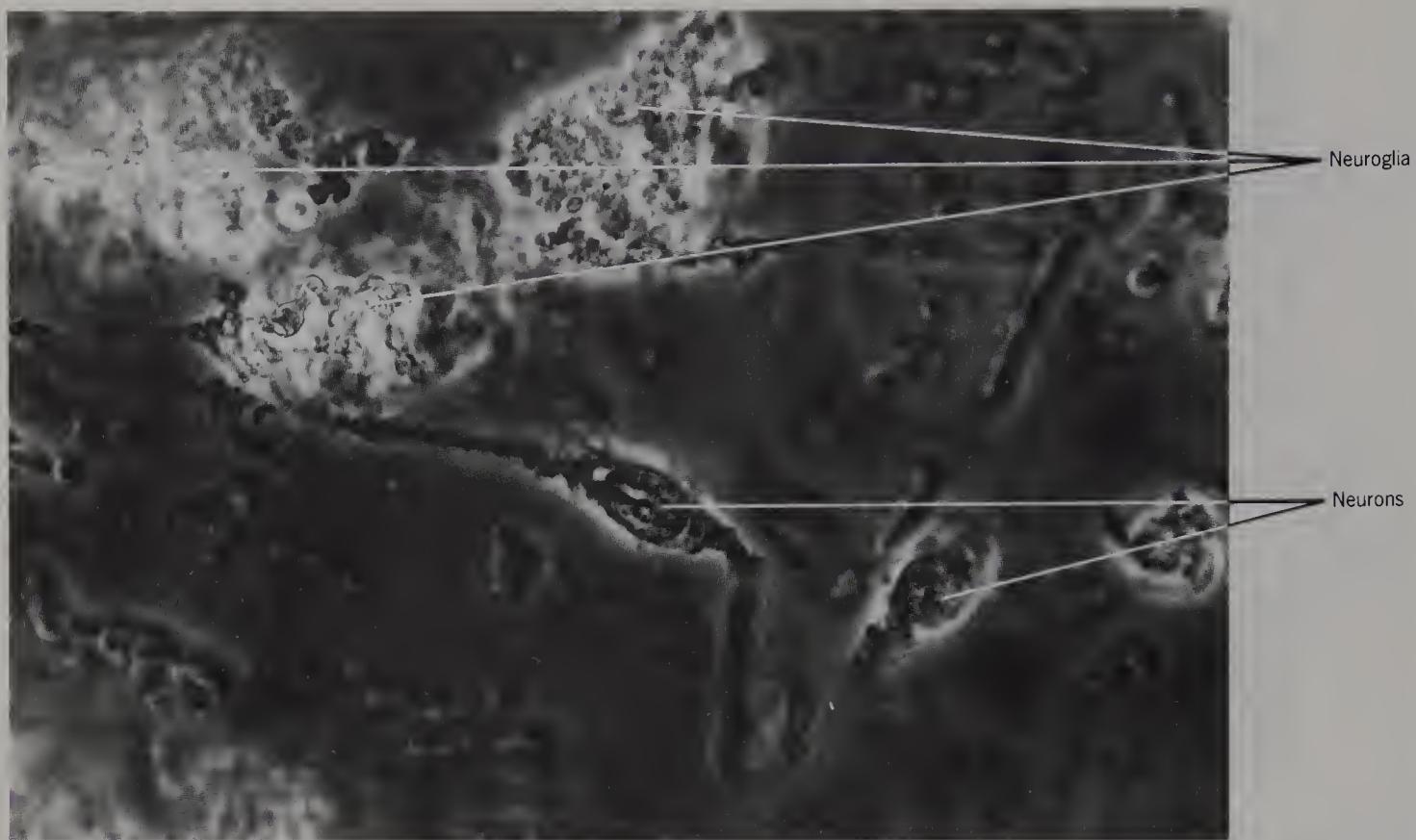


Figure 259 Teased rabbit substantia gelatinosa from the cervical spinal cord, to show bipolar neurons and associated neuroglia (phase contrast, $\times 700$).

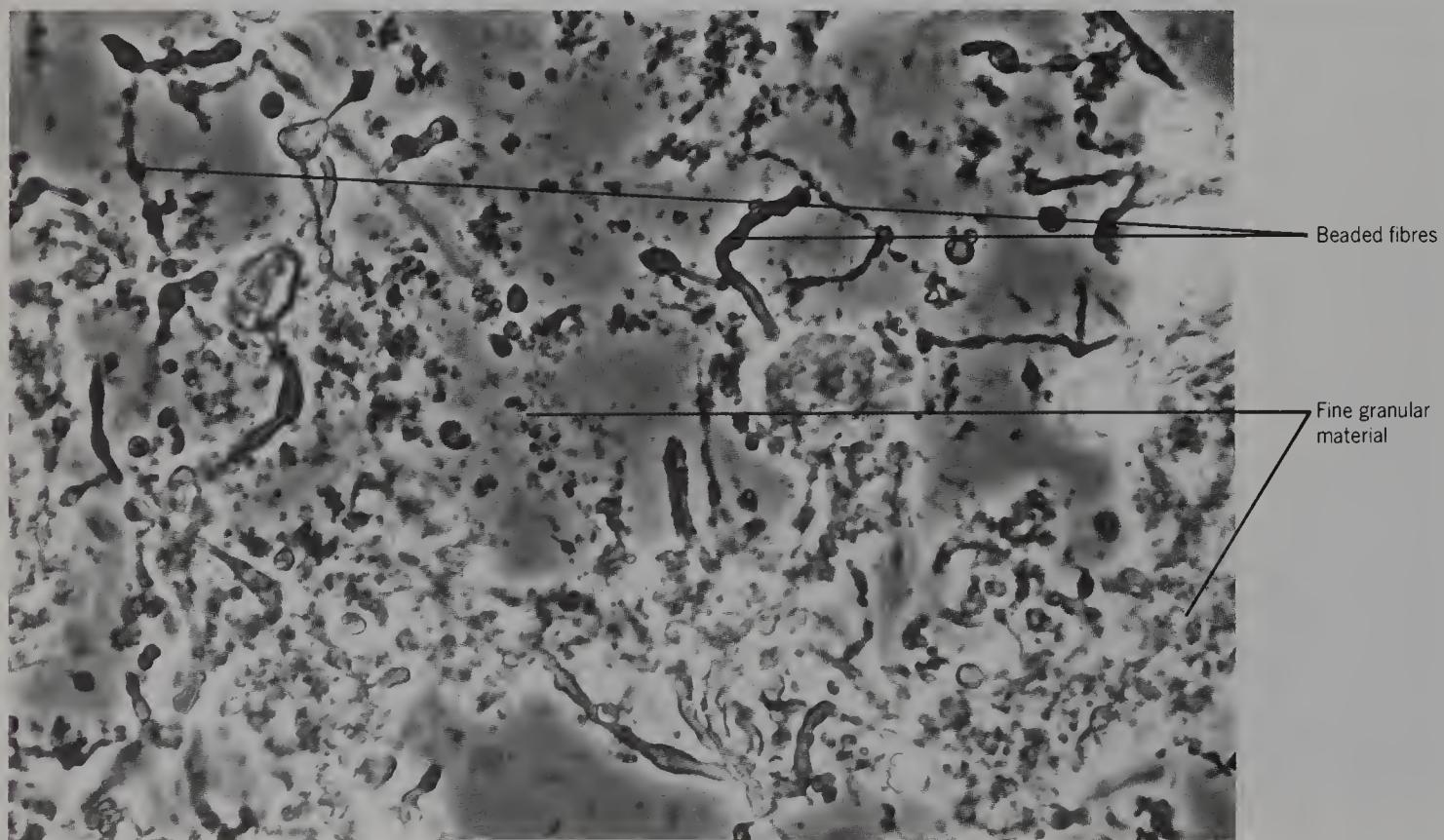
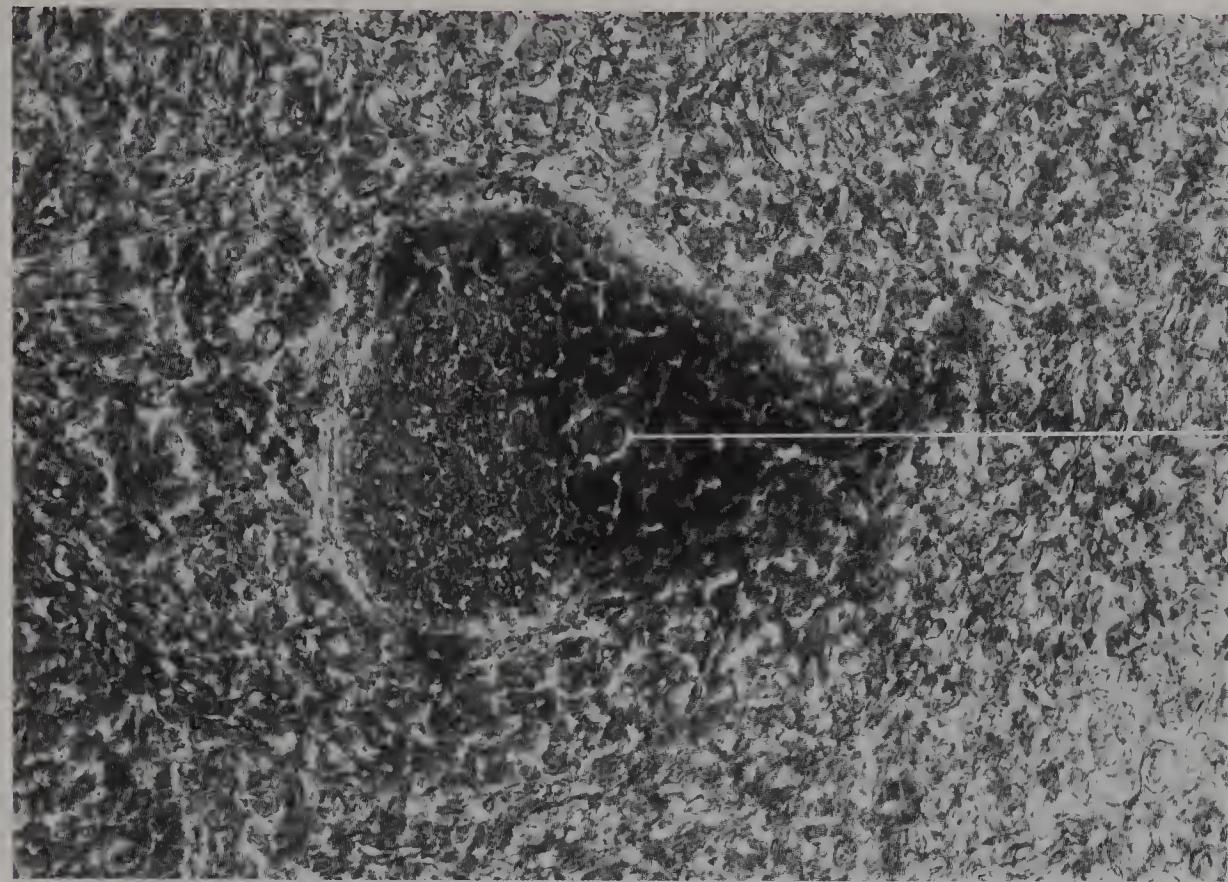


Figure 260 Teased guinea-pig substantia gelatinosa from the cervical spinal cord, to show a small neuron, beaded fibres and fine granular material (phase contrast, $\times 700$).



Nucleolar
membrane

A nucleolar membrane can
be seen.

Figure 261 Thin slab of human anterior horn from the cervical spinal cord from an 89-year-old female, to show anterior horn cell *in situ* (phase contrast, $\times 700$).

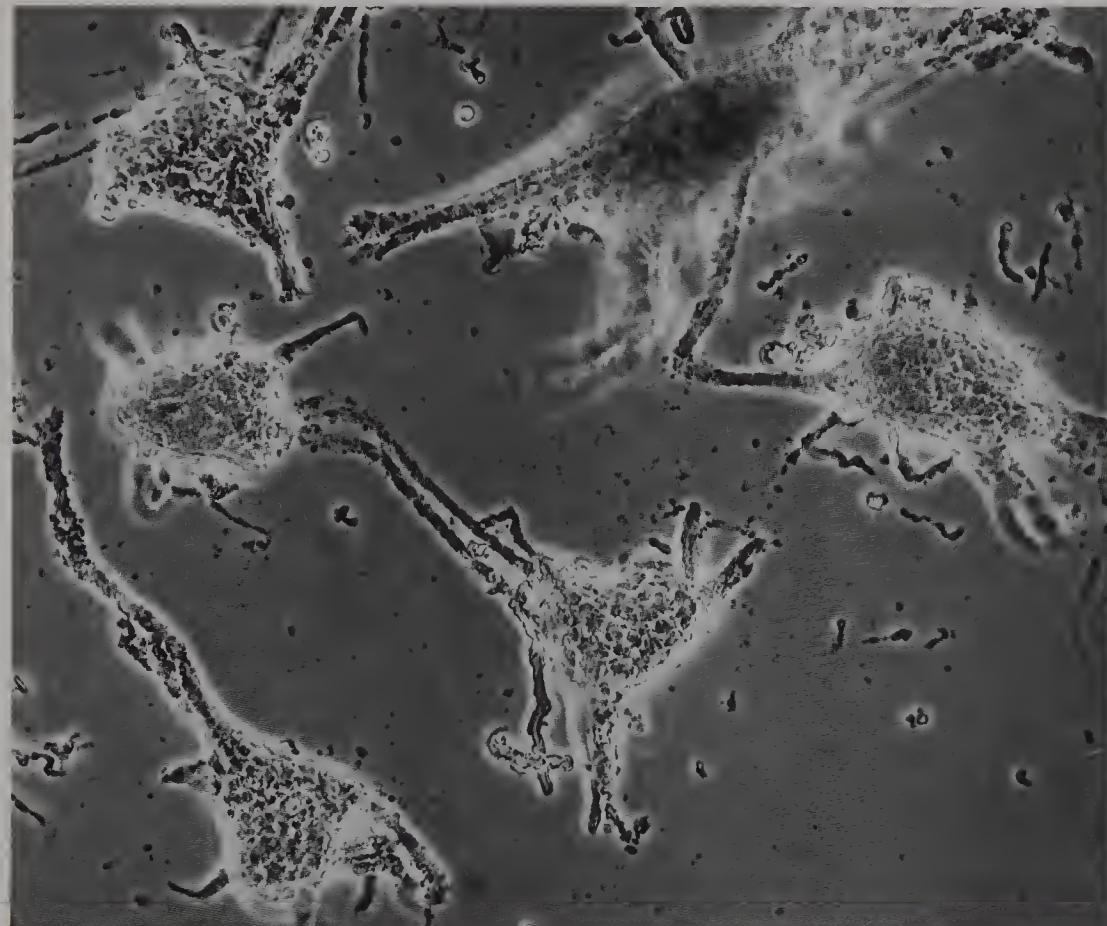


Figure 262 Isolated rabbit ventral horn cells from the cervical spinal cord (phase contrast, $\times 335$).

The term 'neuron' was coined by Waldeyer-Hartz in 1891.

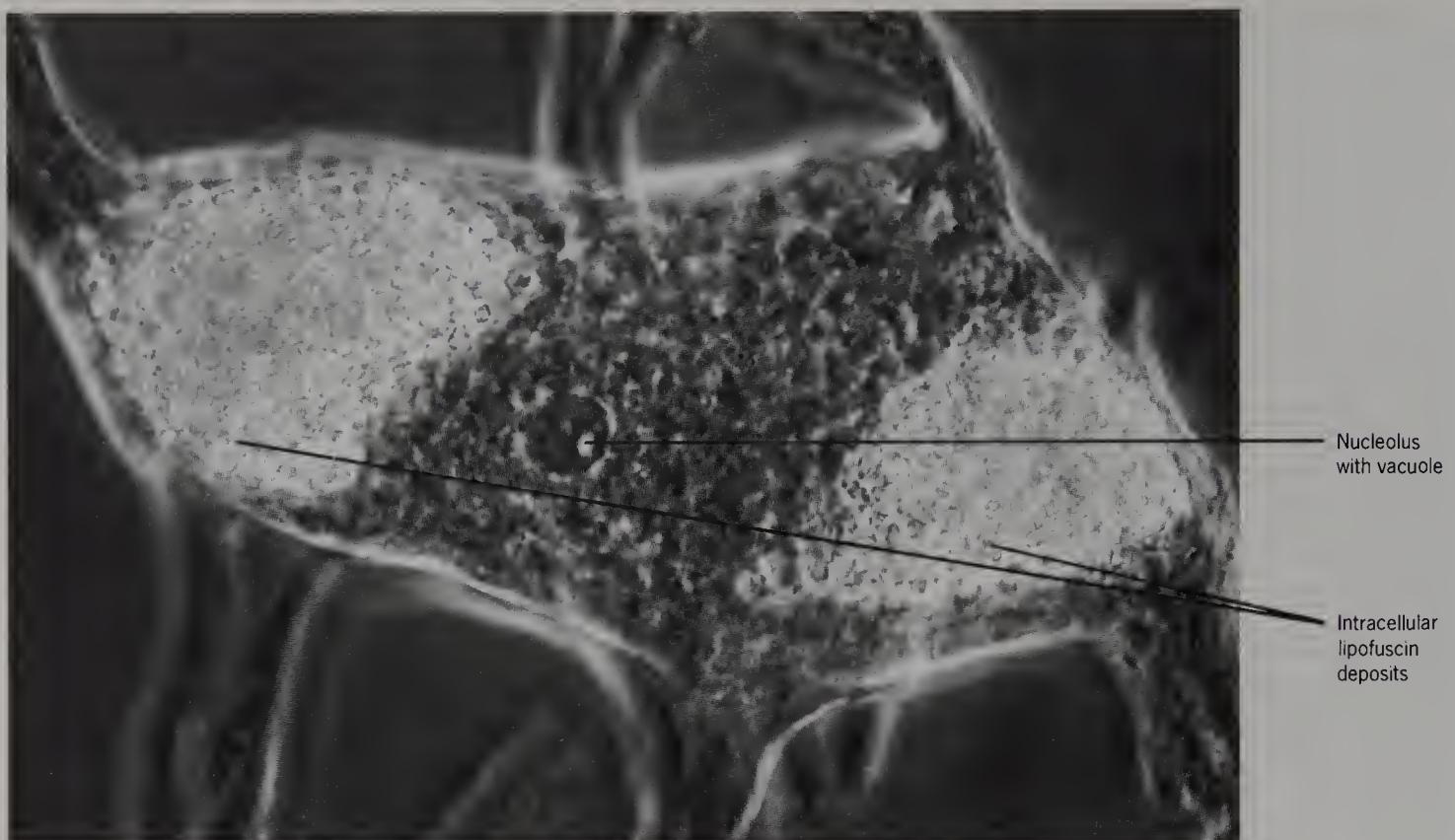


Figure 263 Isolated human anterior horn cell from the cervical spinal cord of a 75-year-old male, to show the large intracellular lipofuscin deposits, the nucleus and the nucleolus (phase contrast, $\times 1100$).

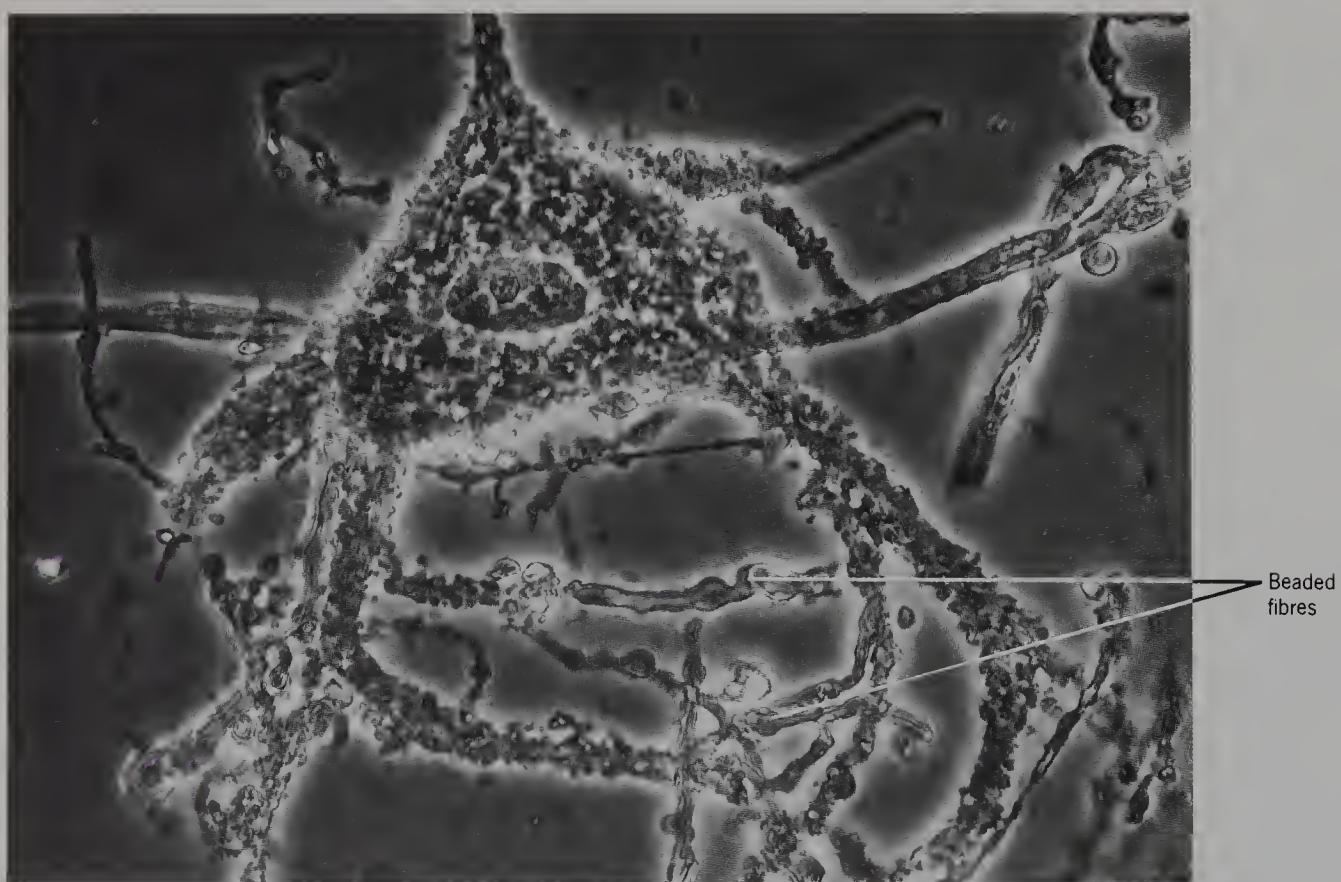


Figure 264 Isolated rabbit anterior horn cell from the cervical spinal cord, to show the nucleolar membrane, small and medium size beaded fibres, and a capillary (phase contrast, $\times 700$).

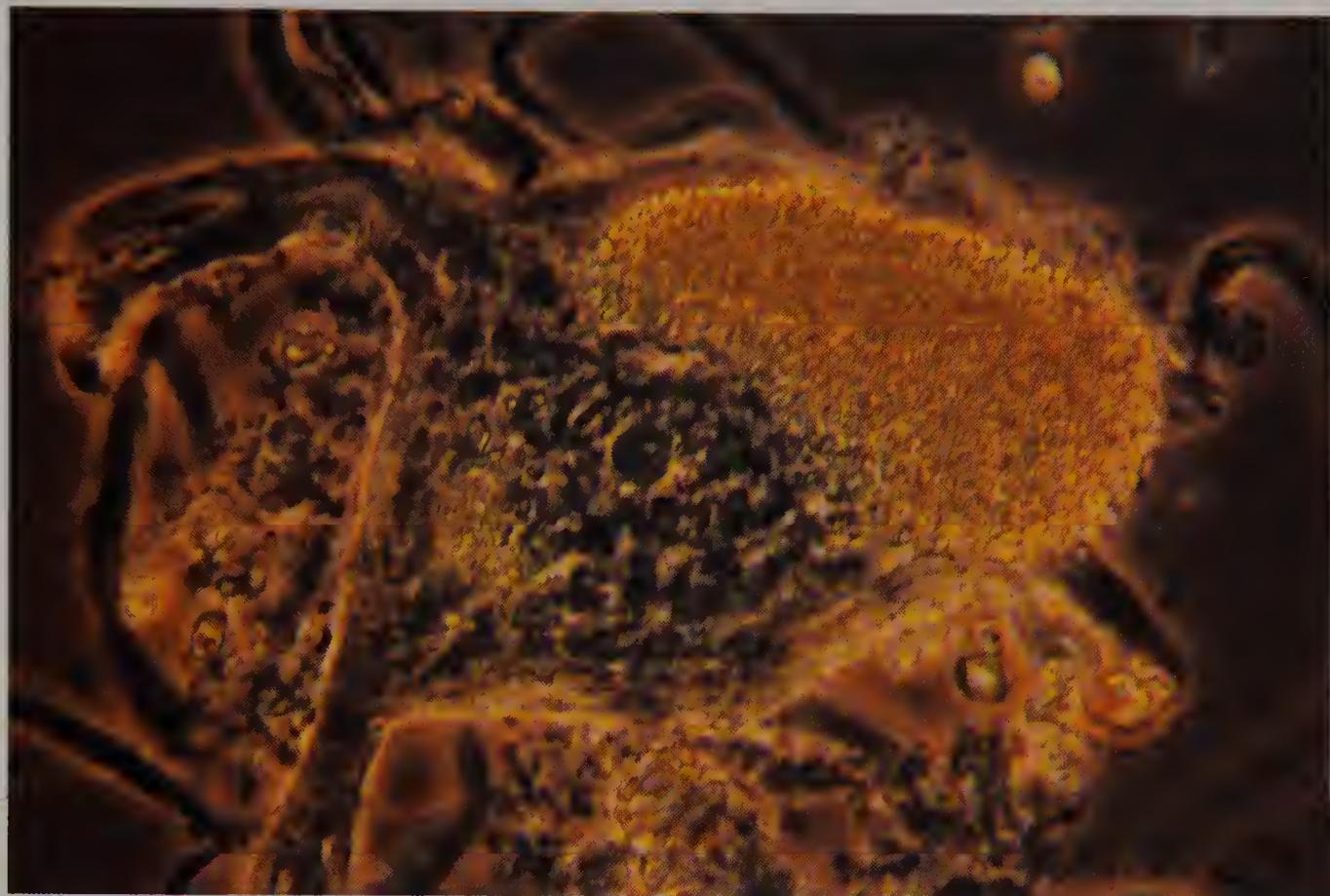


Figure 265 Isolated human anterior horn cell from a 74-year-old male (phase contrast, $\times 720$).

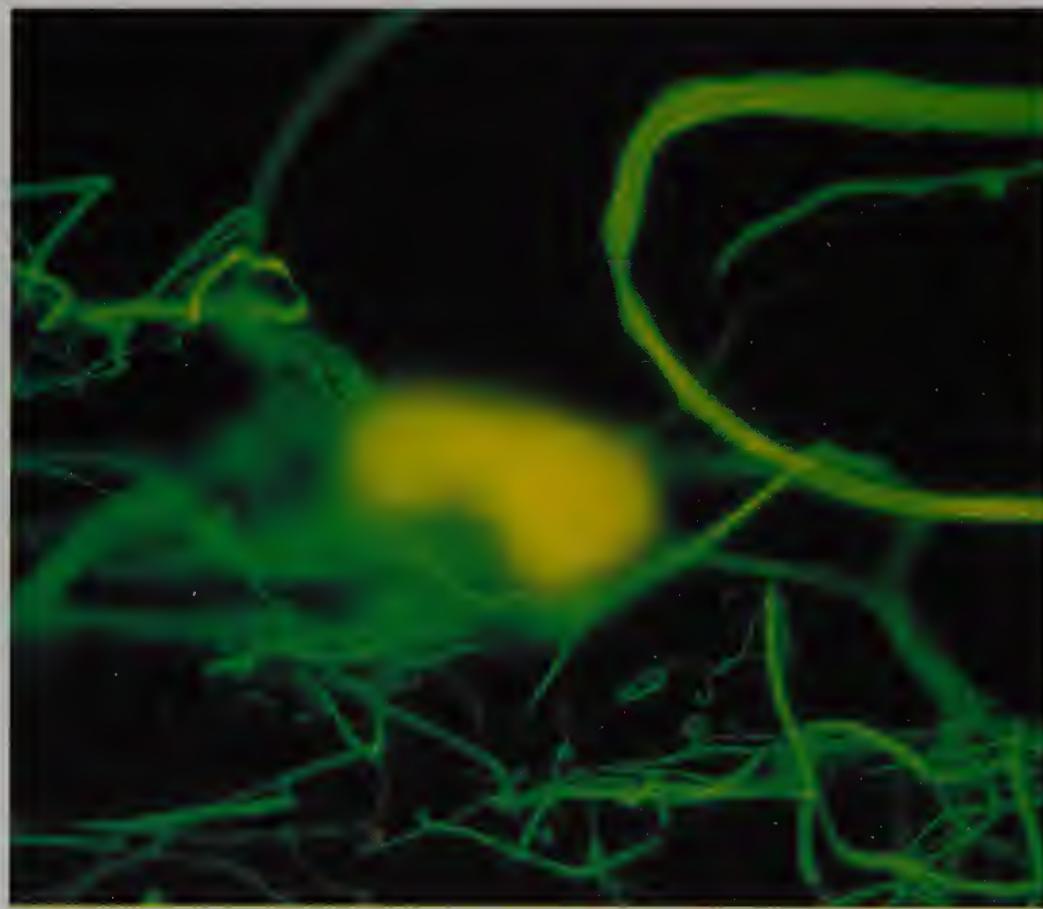
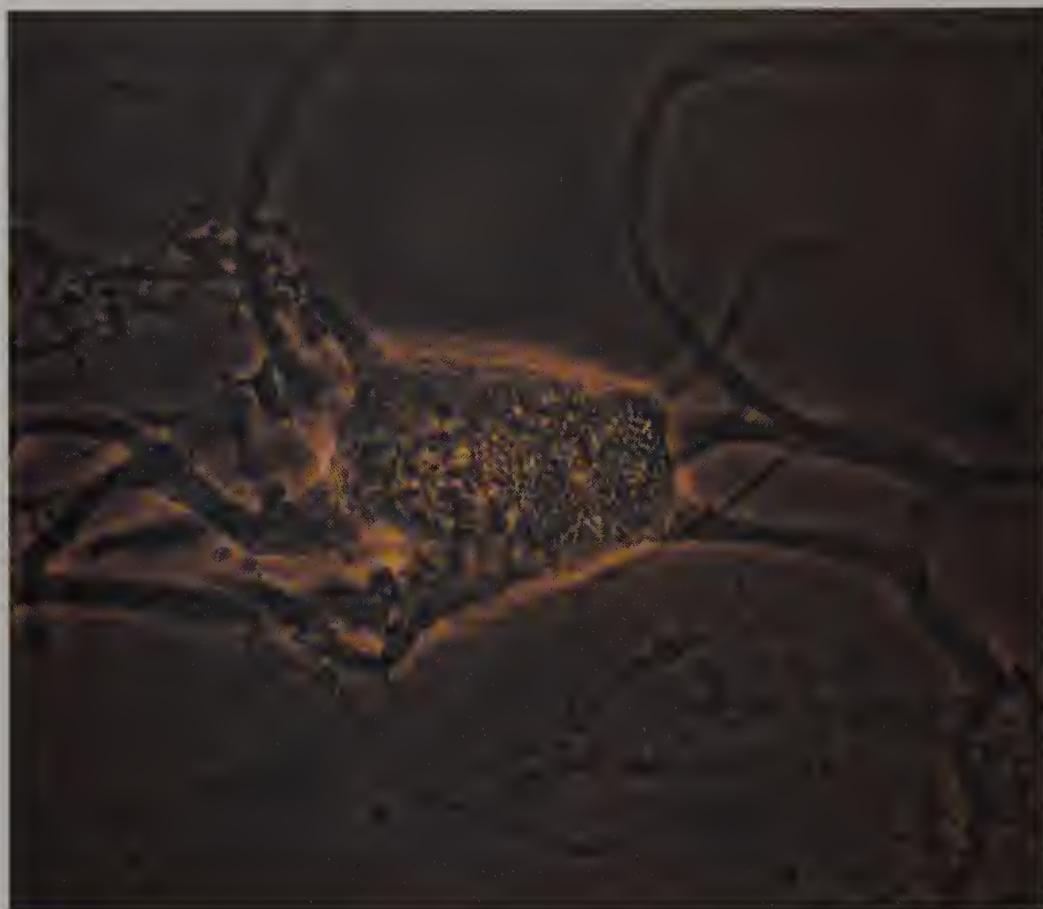


Figure 266 Isolated human anterior horn cell of an 82-year-old male, stained with anti-neurofilament 200 kD protein, by phase contrast (above) and after excitation with blue light of 450–490 nm (below) ($\times 500$).

As in Figure 221, the lipofuscin fluoresces brightly as do probably unmyelinated fibres, but the main dendrites only weakly.

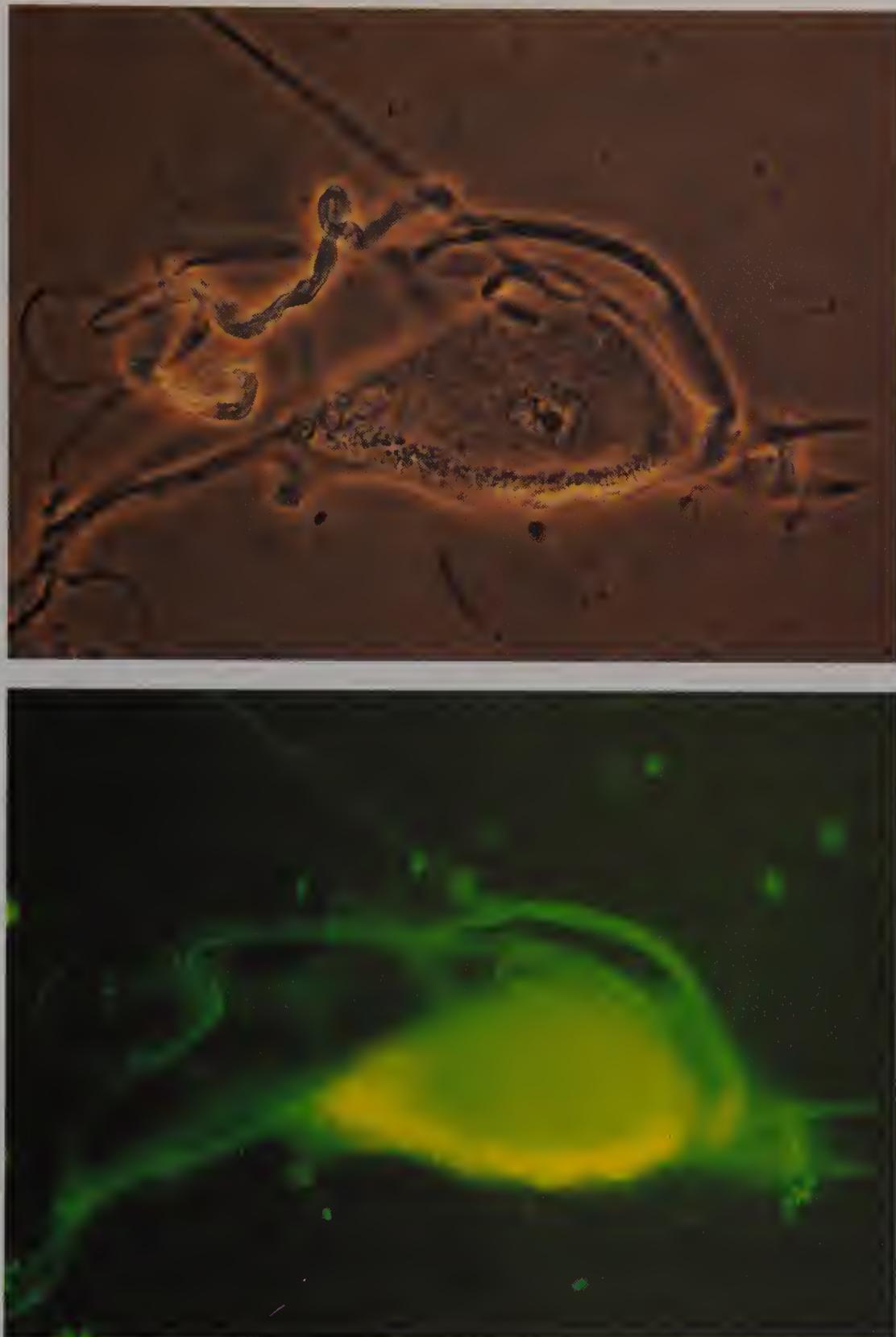


Figure 267 Isolated human anterior horn cell of a 64-year-old male, stained with anti-glial fibrillary acidic protein, by phase contrast (above) and after excitation with blue light of 450–490 nm (below) ($\times 500$).

Compare with the previous figure.

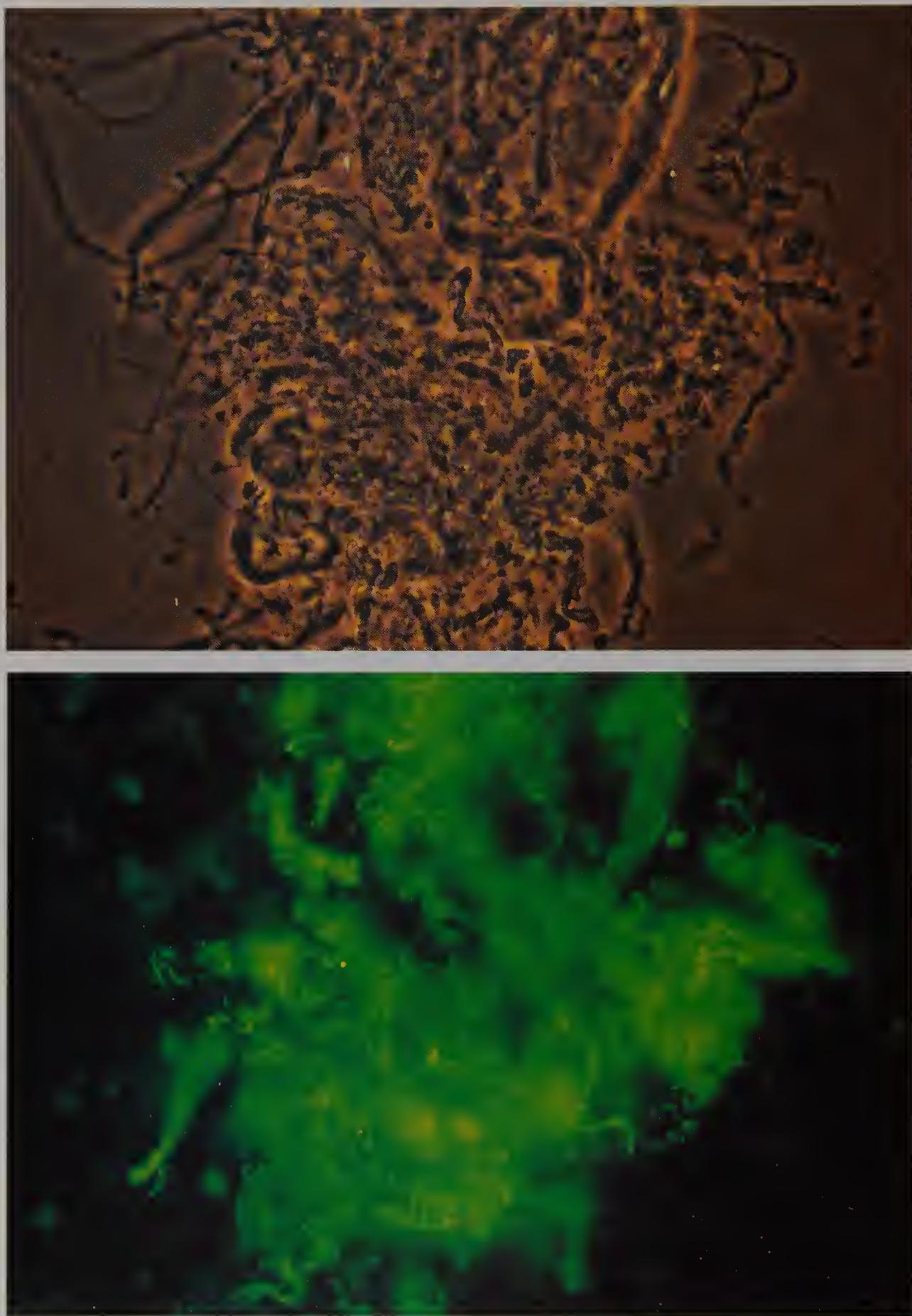


Figure 268 Isolated human neuroglia from the anterior horn of a 64-year-old male, stained with anti-glial fibrillary acidic protein, by phase contrast (above) and after excitation with blue light of 450–490 nm (below) ($\times 500$).

Short fine fibres are fluorescing brightly. Compare with the fibres in Figure 226.



Figure 269 Thin slab of human gracile tract from the cervical spinal cord of an 89-year-old female, to show beaded fibres *in situ* (phase contrast, $\times 700$).



Figure 270 Thin slab of human cuneate tract from the cervical spinal cord of an 89-year-old female, to show beaded fibres *in situ* and droplets (phase contrast, $\times 700$).

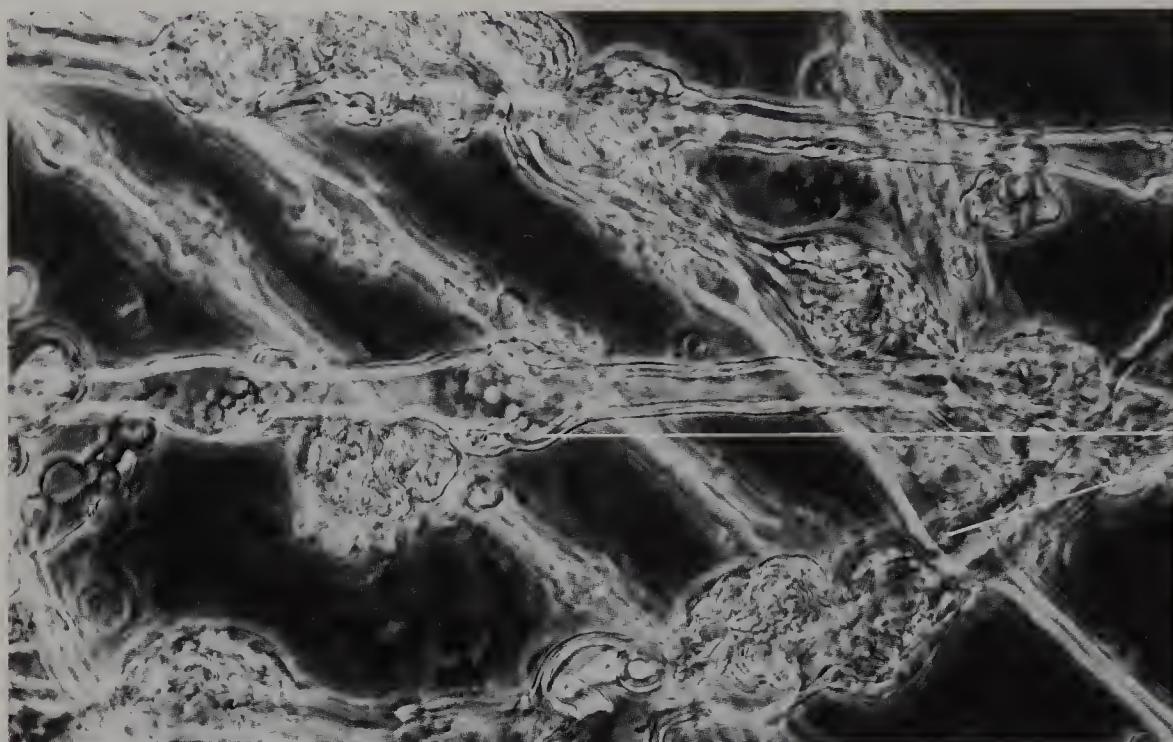


Figure 271 Teased human cuneate tract from the previous specimen, to show beaded fibres (phase contrast, $\times 700$).



Figure 272 Thin slab of fresh rat dorsal region of cervical spinal cord, to show beaded fibres and droplets (phase contrast, $\times 700$).

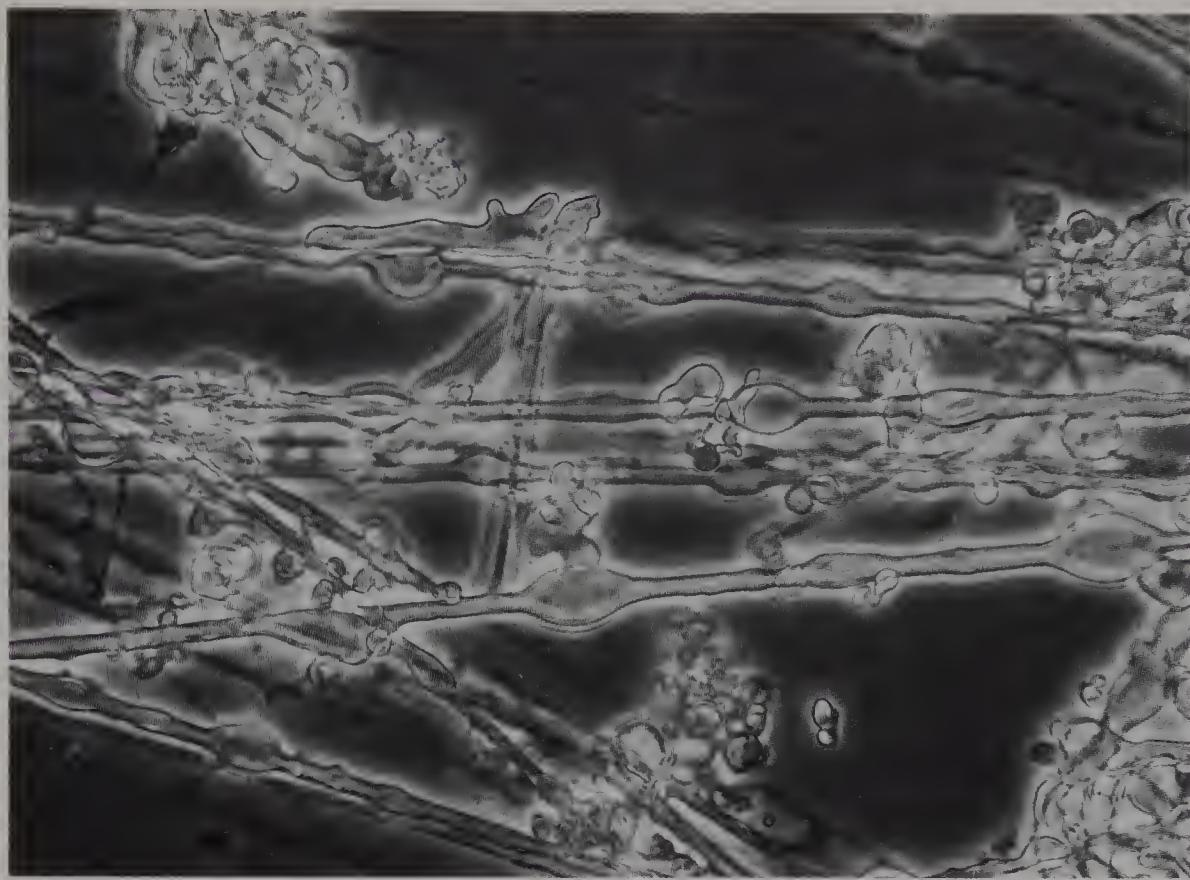


Figure 273 Teased fresh rat beaded fibres from the dorsal cervical spinal cord (phase contrast, $\times 700$).

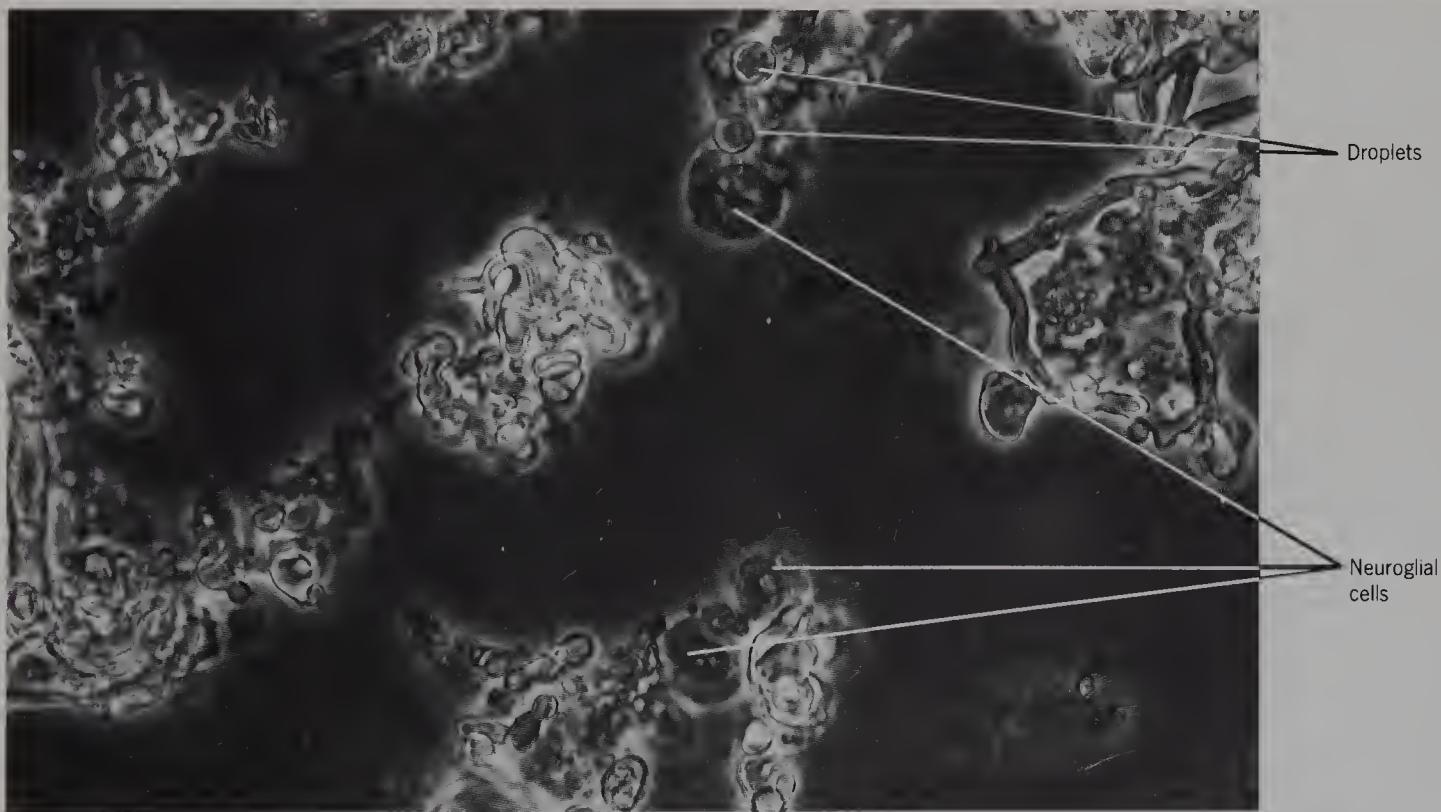


Figure 274 Teased fresh guinea-pig dorsal white matter from the sacral spinal cord, to show droplets and neuroglial cells (phase contrast, $\times 700$).

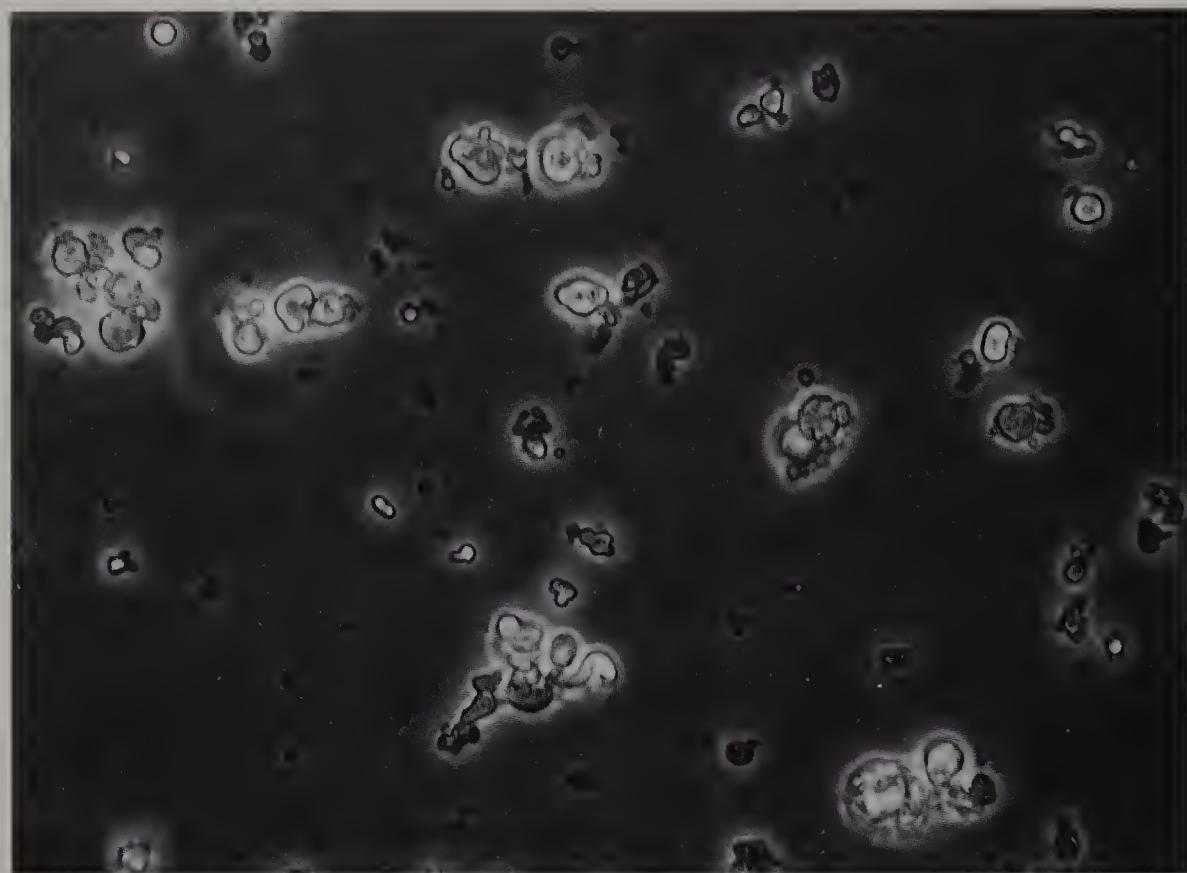


Figure 275 Teased freshly killed rabbit dorsal white matter from the cervical spinal cord, to show isolated droplets (phase contrast, $\times 700$).



Figure 276 Thin slab of fresh guinea-pig lateral white matter from the cervical spinal cord to show fibres and droplets *in situ* (phase contrast, $\times 700$).

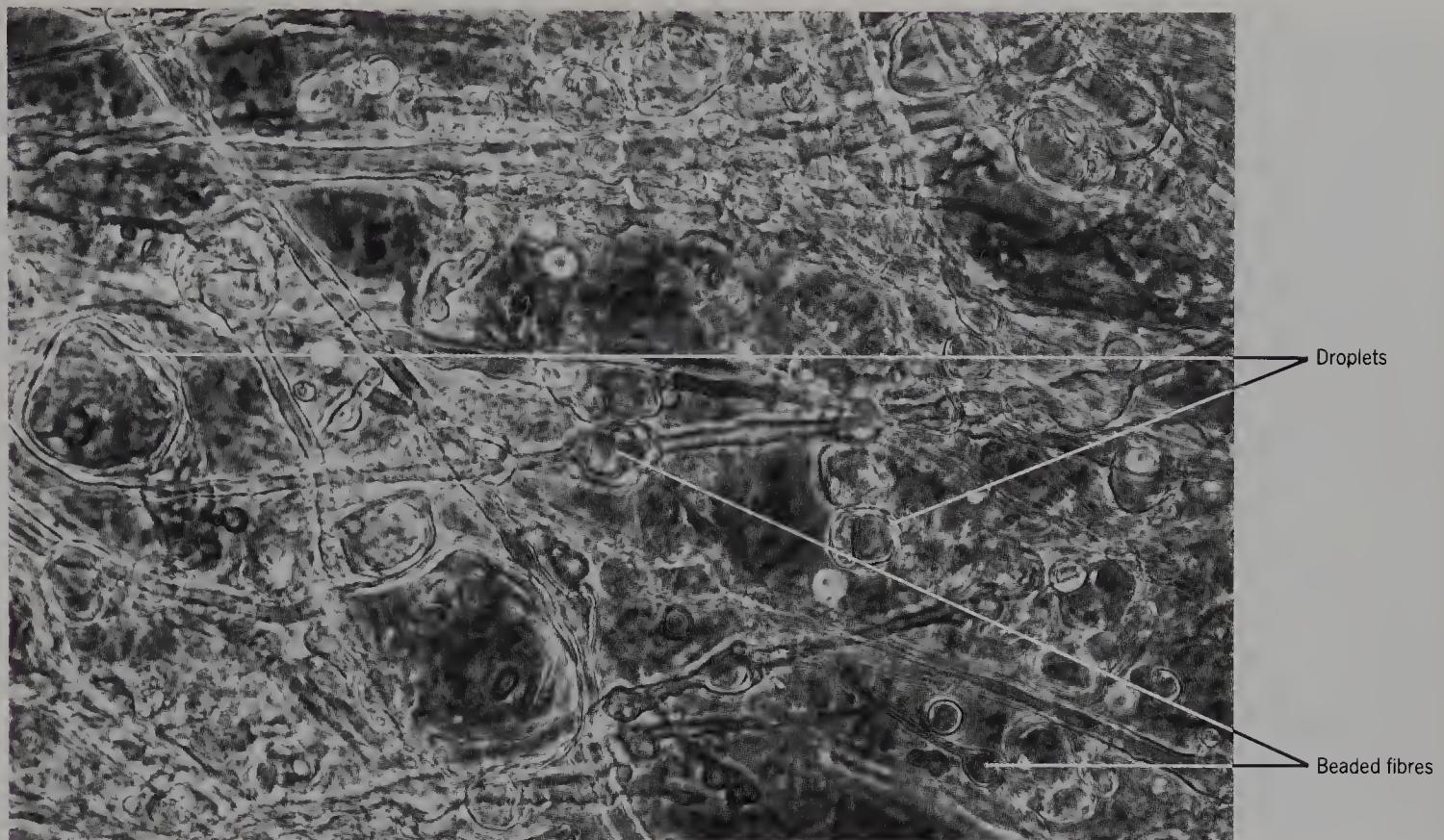


Figure 277 Partially teased human vestibulospinal tract from the cervical spinal cord of an 89-year-old female, to show beaded fibres and droplets (phase contrast, $\times 700$).

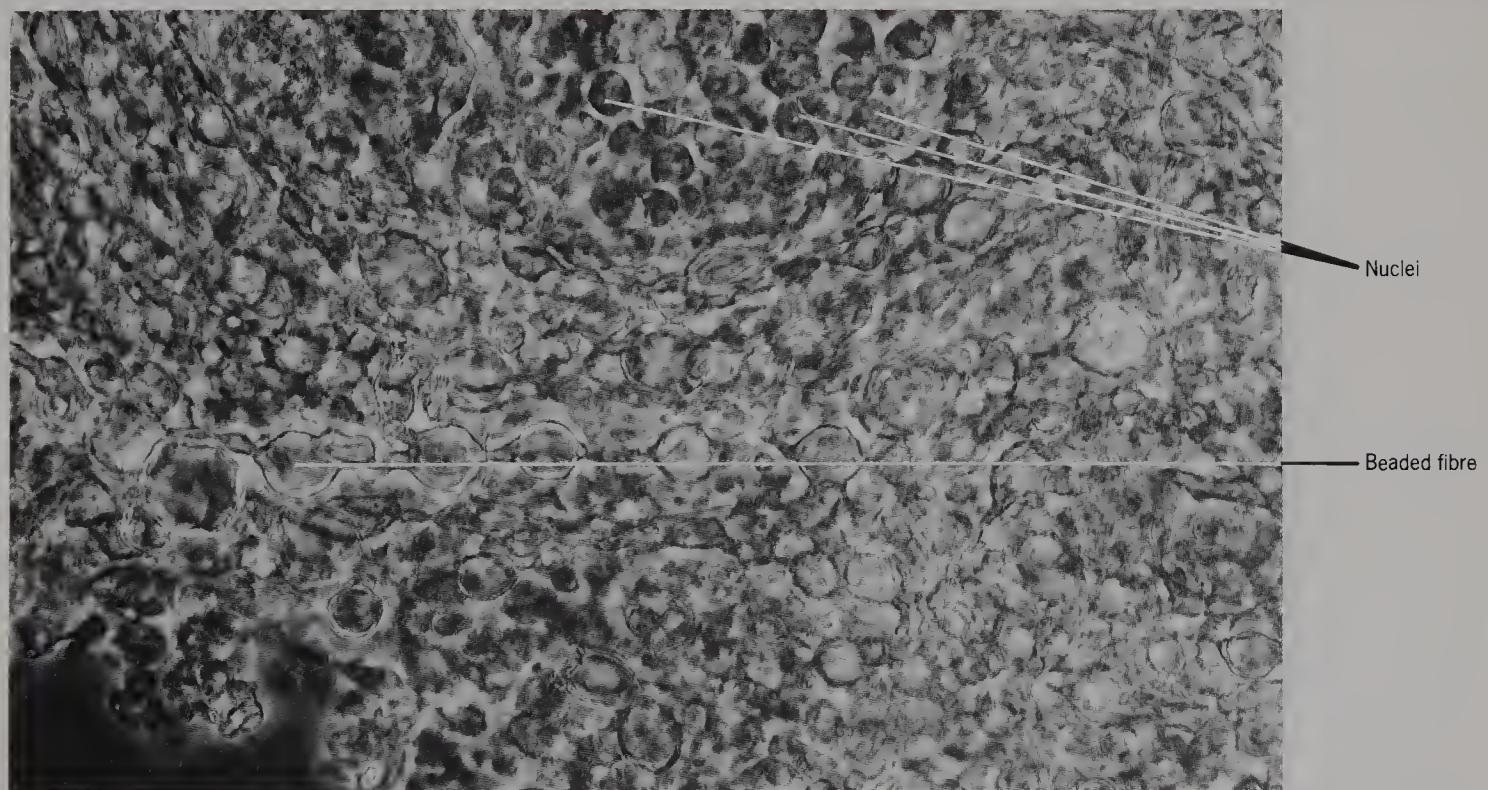


Figure 278 Thin slab of guinea-pig filum terminale to show beaded fibres, droplets and neuroglial nuclei (phase contrast, $\times 700$).

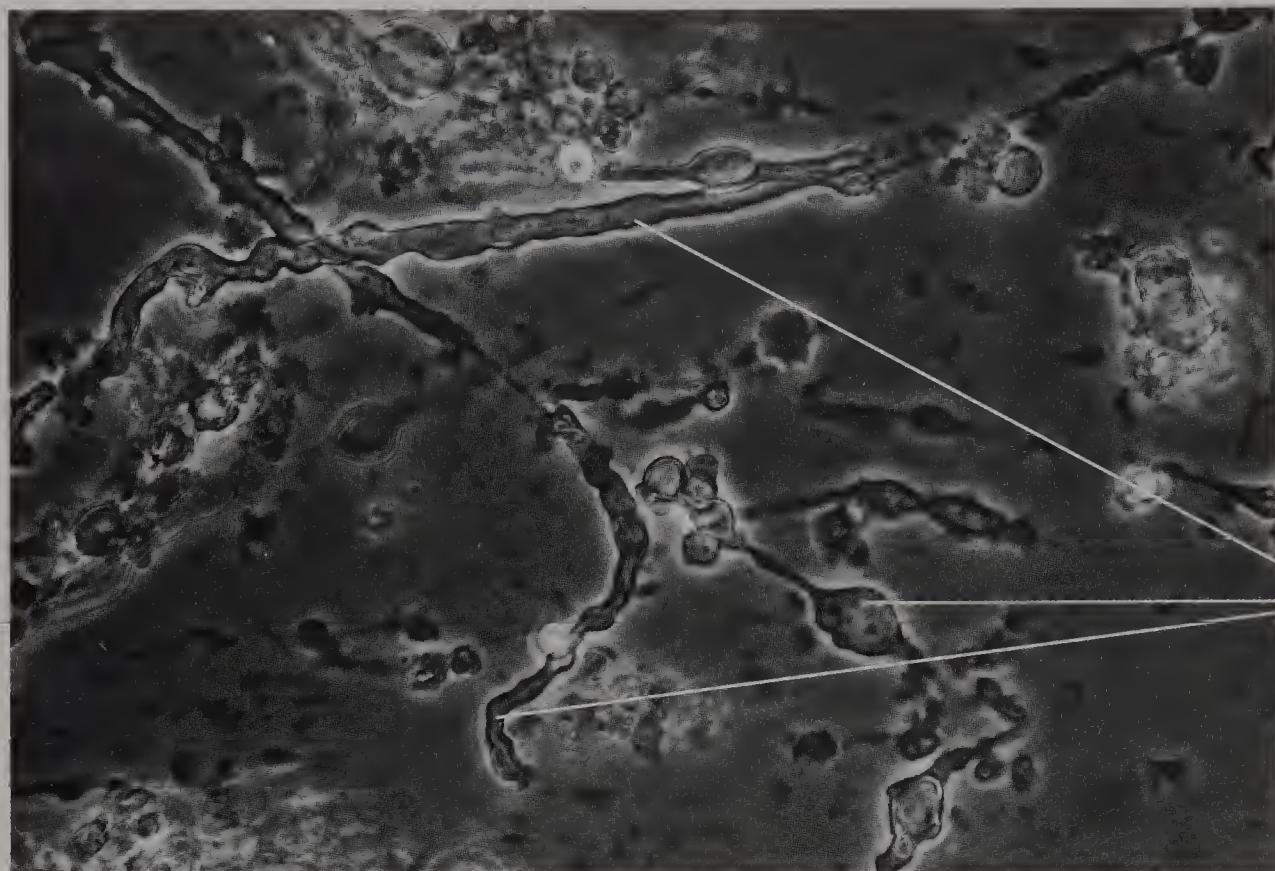


Figure 279 Teased fresh guinea-pig filum terminale to show beaded fibres (phase contrast, $\times 700$).

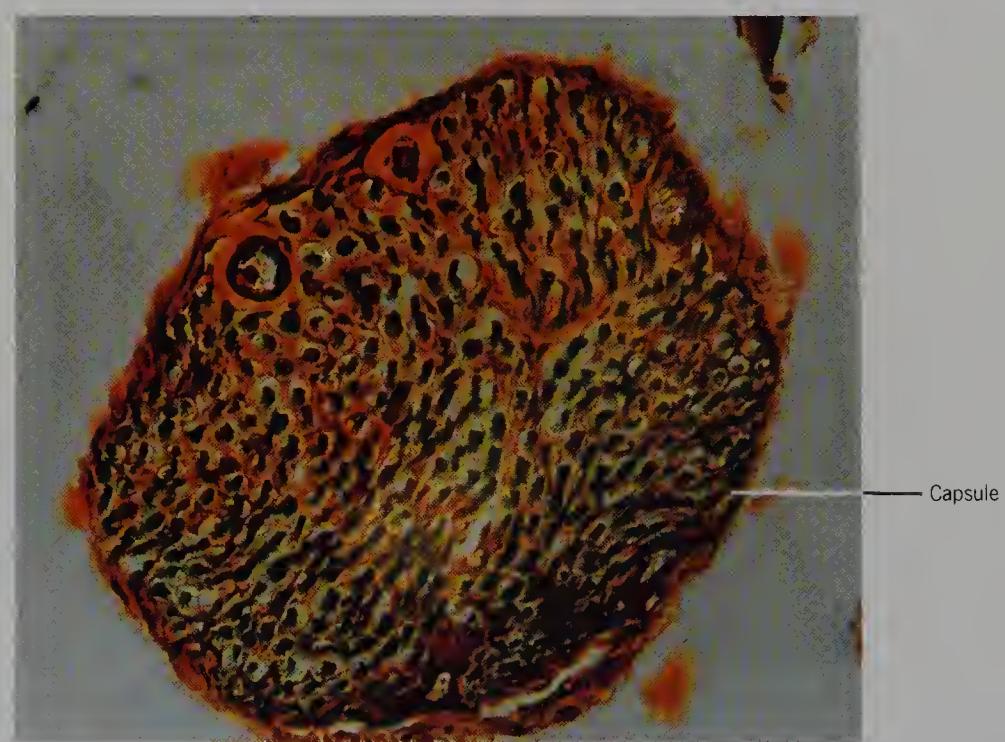


Figure 280 Transverse section of a human ventral root stained with Palmsgren's stain to show nerve fibres (bright field, $\times 610$).



Figure 281 Section of a human dorsal root ganglion stained with haematoxylin and eosin (bright field, $\times 610$).



Figure 282 Isolated rat cervical spinal ganglion (vertical illumination, $\times 20$).

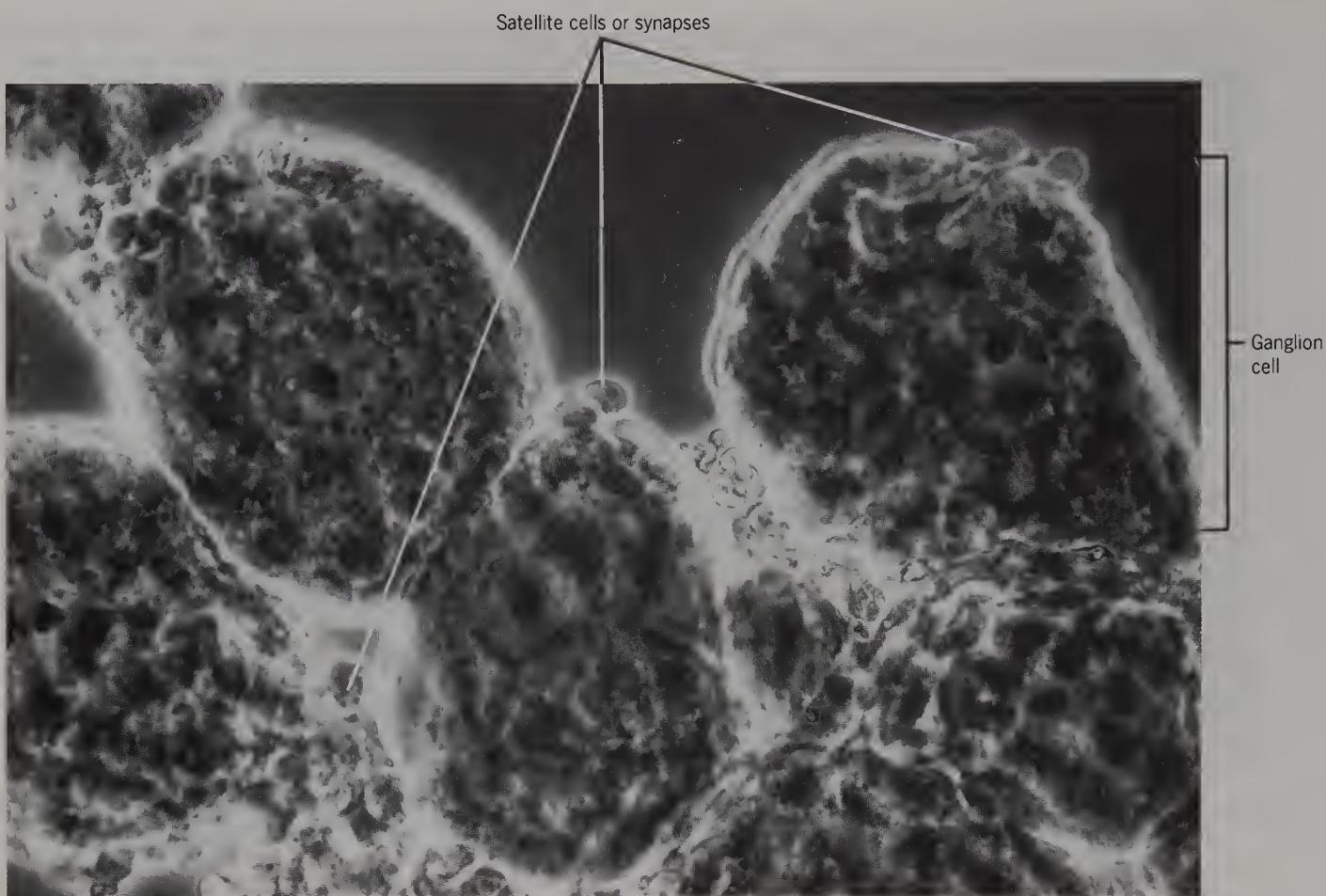


Figure 283 Partially teased rabbit cervical spinal ganglion, to show ganglion cells (phase contrast, $\times 700$).



Figure 284 Isolated rat ganglion cell from cervical spinal ganglion (phase contrast, $\times 800$).

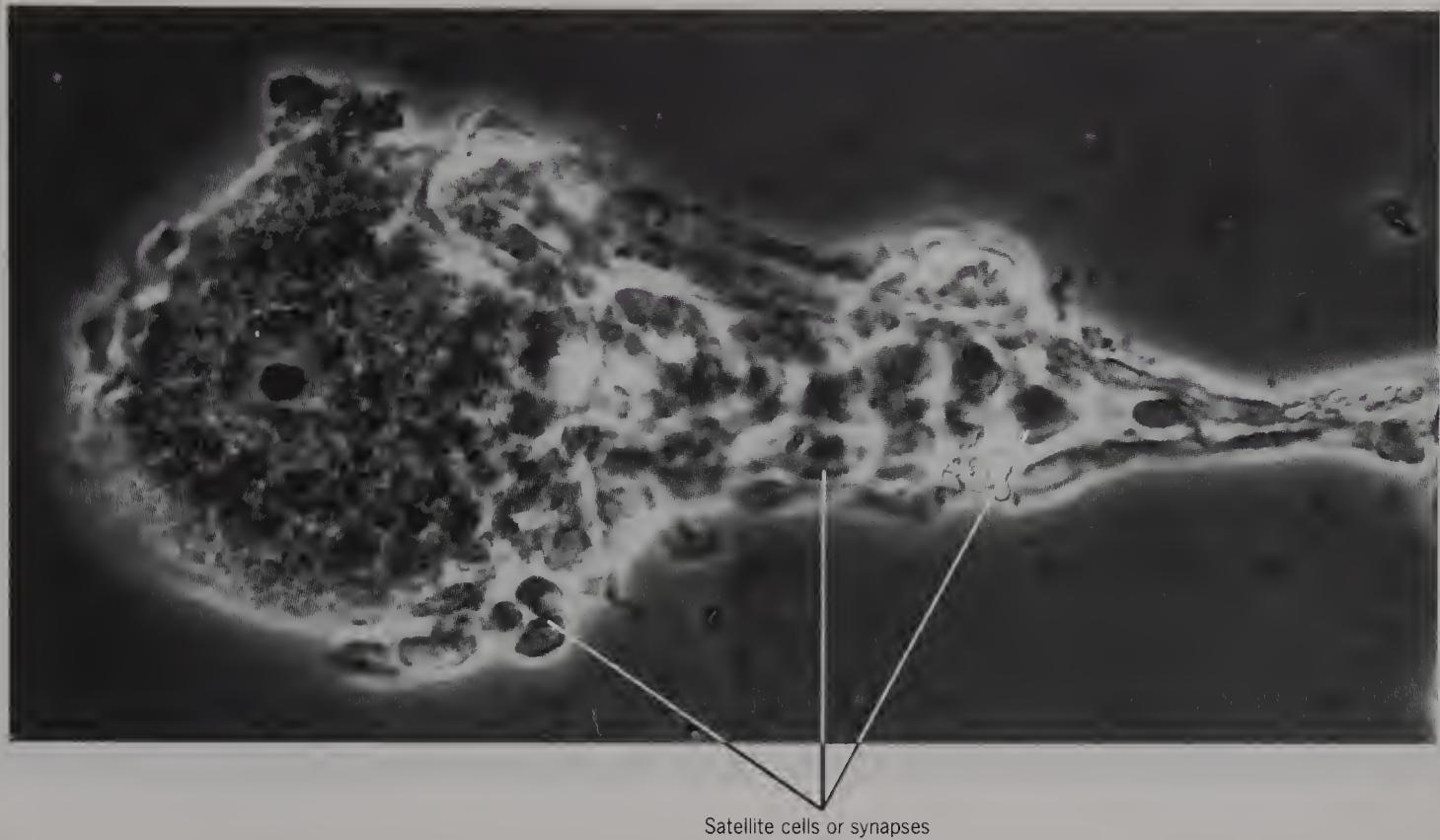


Figure 285 Isolated rabbit ganglion cell from cervical spinal ganglion to show associated 'satellite' cells or synapses (phase contrast, $\times 800$).



Figure 286 Dissected rabbit superior cervical ganglion (vertical illumination, $\times 20$).

This ganglion is sympathetic.



Figure 287 Rat superior cervical ganglion to show nerve fibres *in situ* (bright field, $\times 800$).

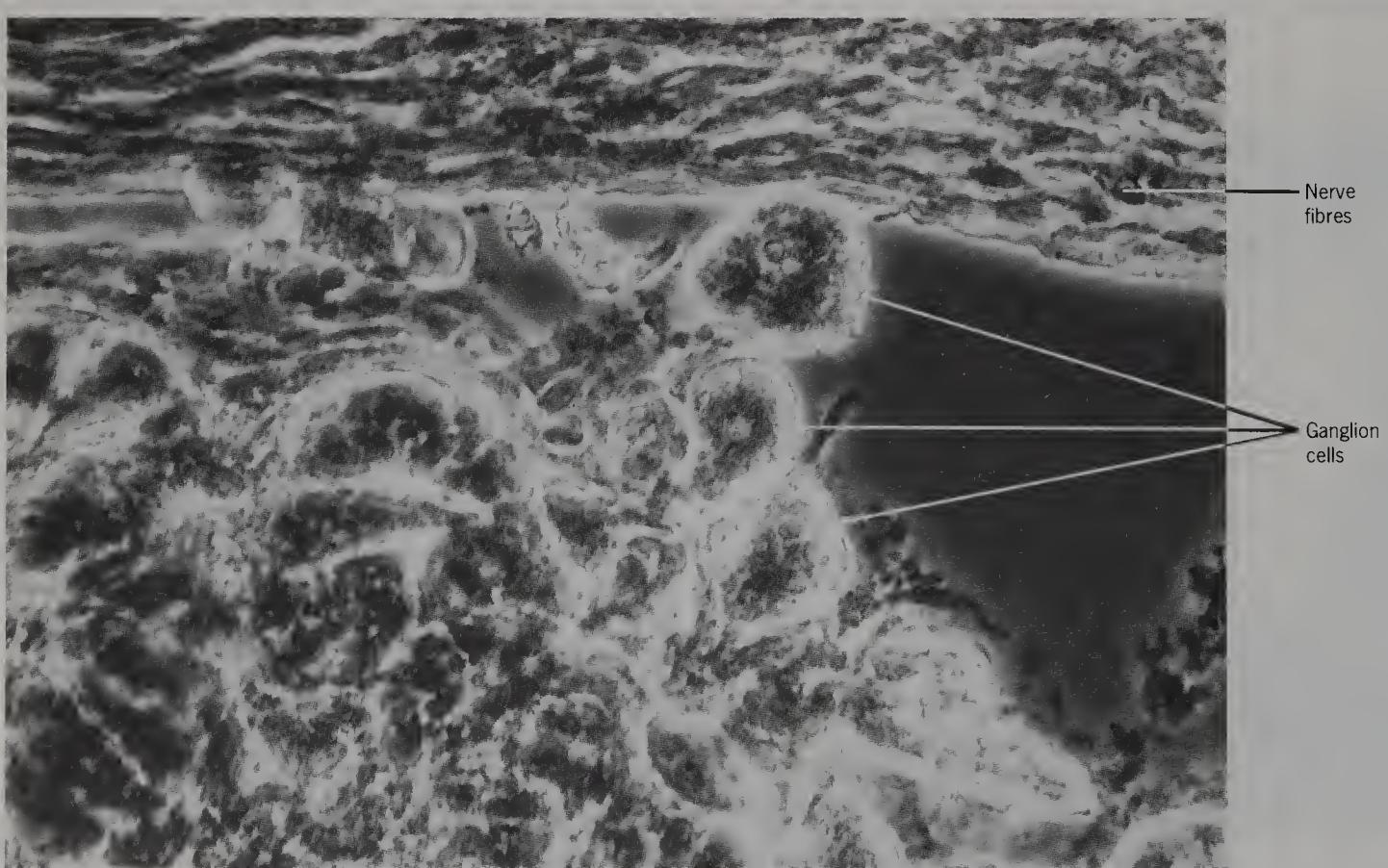


Figure 288 Partially teased superior cervical ganglion from 4-week-old rat, to show ganglion cells and nerve fibres (phase contrast, $\times 700$).



Figure 289 Dissected rabbit vagal ganglion (vertical illumination, $\times 20$).

This ganglion is parasympathetic.

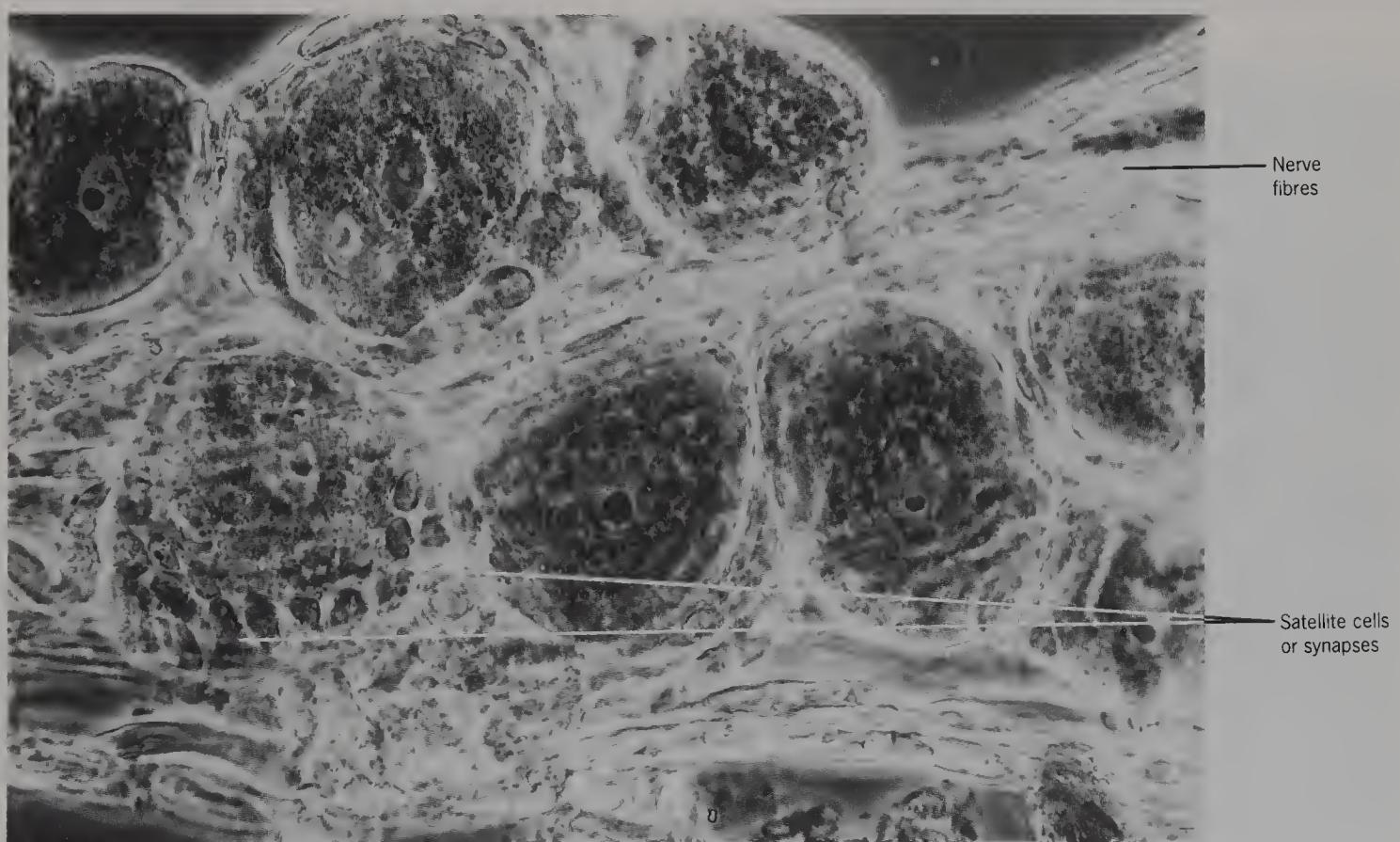


Figure 290 Partially teased rabbit vagal ganglion, to show ganglion cells, 'satellite' cells or synapses, and nerve fibres (phase contrast, $\times 700$).

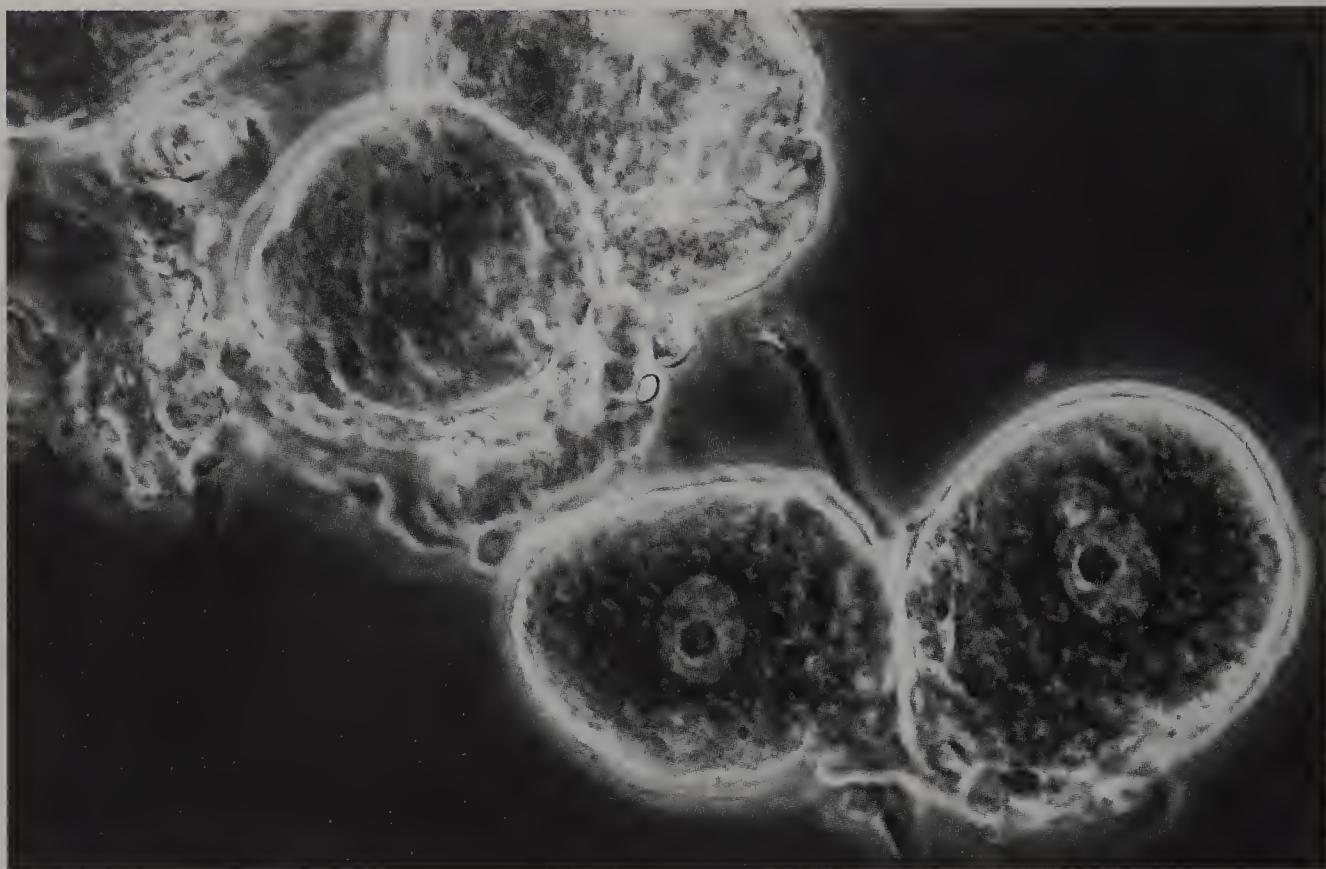


Figure 291 Teased rabbit ganglion cells from the previous specimen (phase contrast, $\times 800$).

Note the low refractive index of the nucleoplasm.

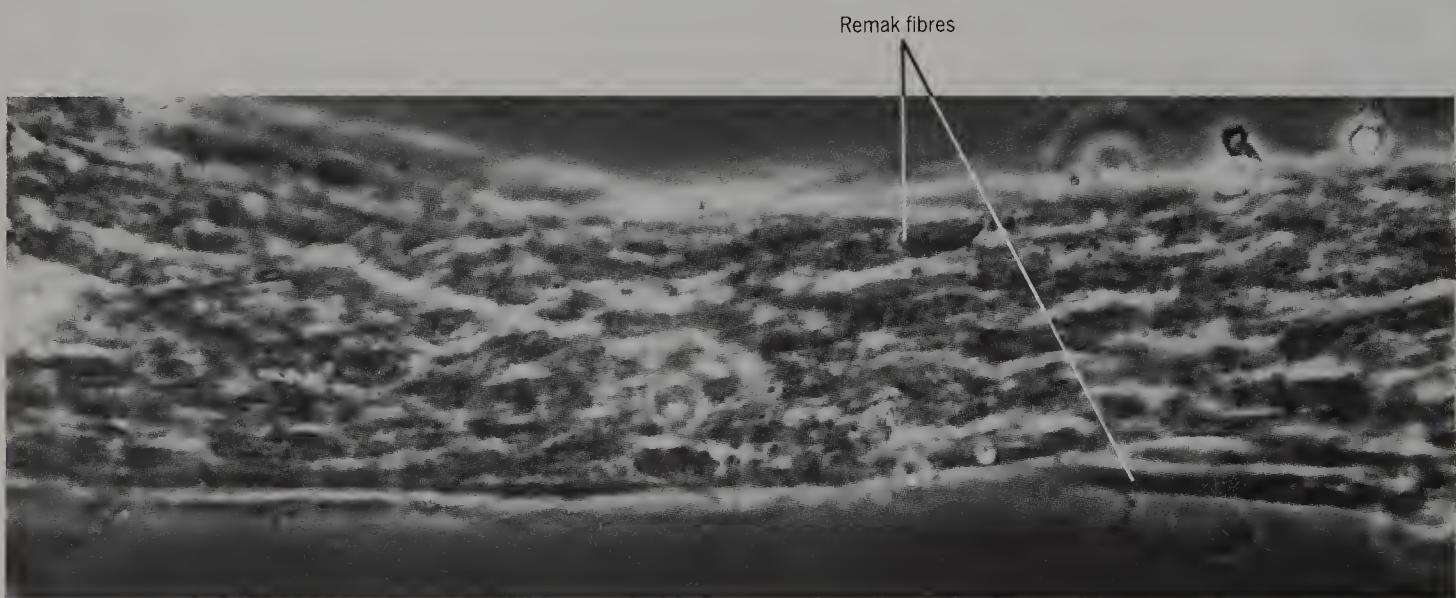


Figure 292 Partially teased mouse sympathetic nerve to the ileum, to show Remak fibres *in situ* (phase contrast, $\times 800$).

These fibres were described by Remak in 1836.

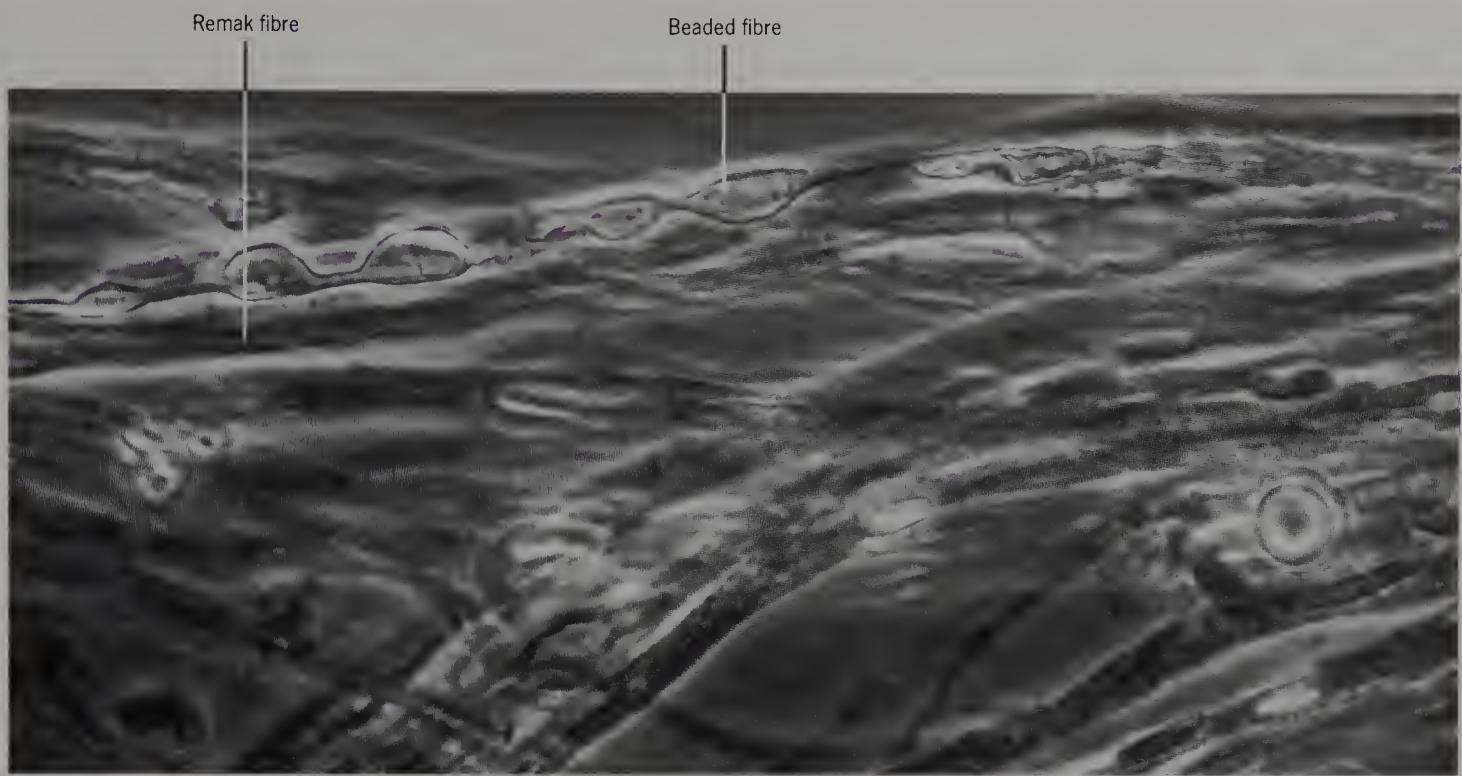


Figure 293 Teased rabbit cervical sympathetic nerve, to show a beaded fibre and Remak fibres (phase contrast, $\times 800$).

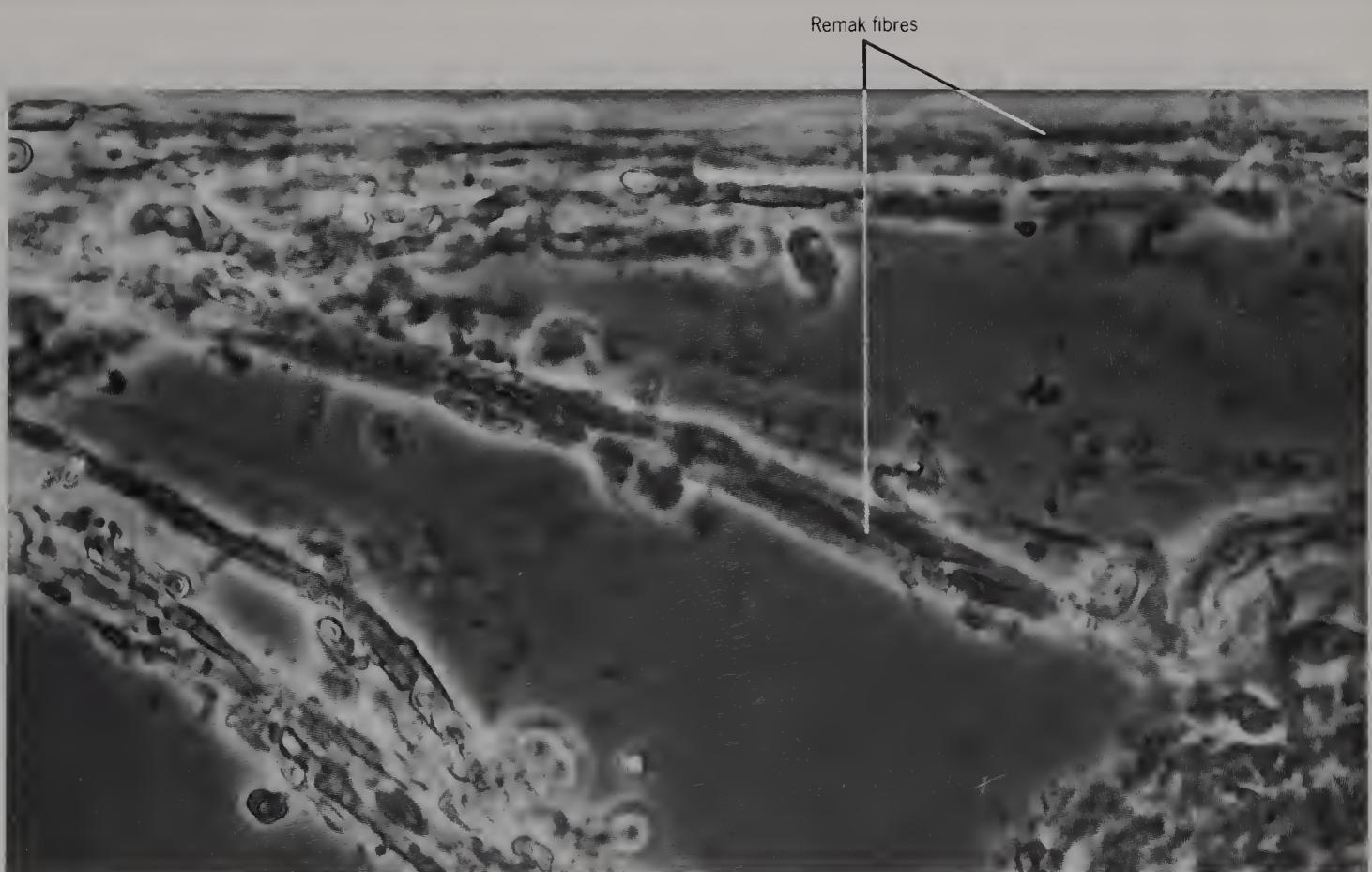


Figure 294 Teased guinea-pig cervical sympathetic nerve, to show Remak fibres (phase contrast, $\times 800$).

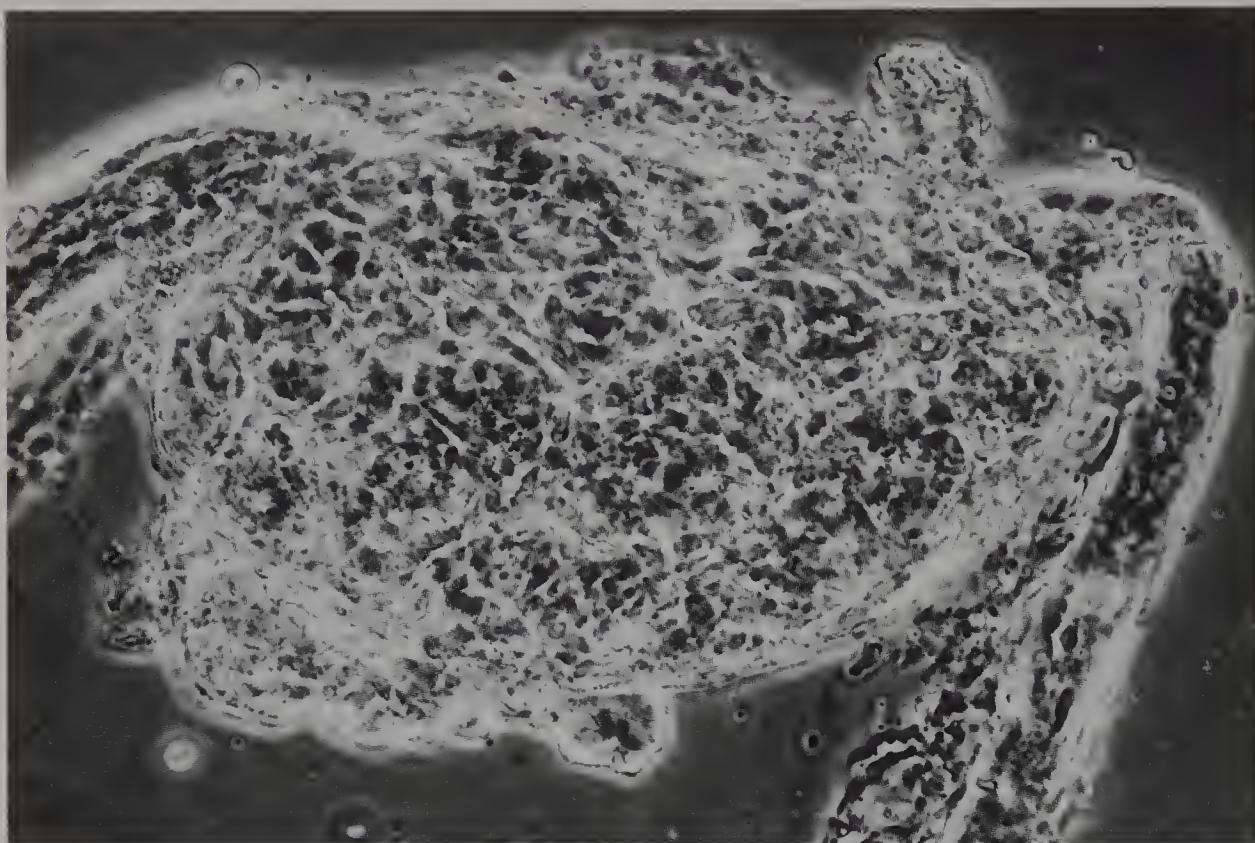


Figure 295 Isolated mouse sublingual ganglion, to show ganglion cells *in situ* (bright field, $\times 500$).

This ganglion is parasympathetic.

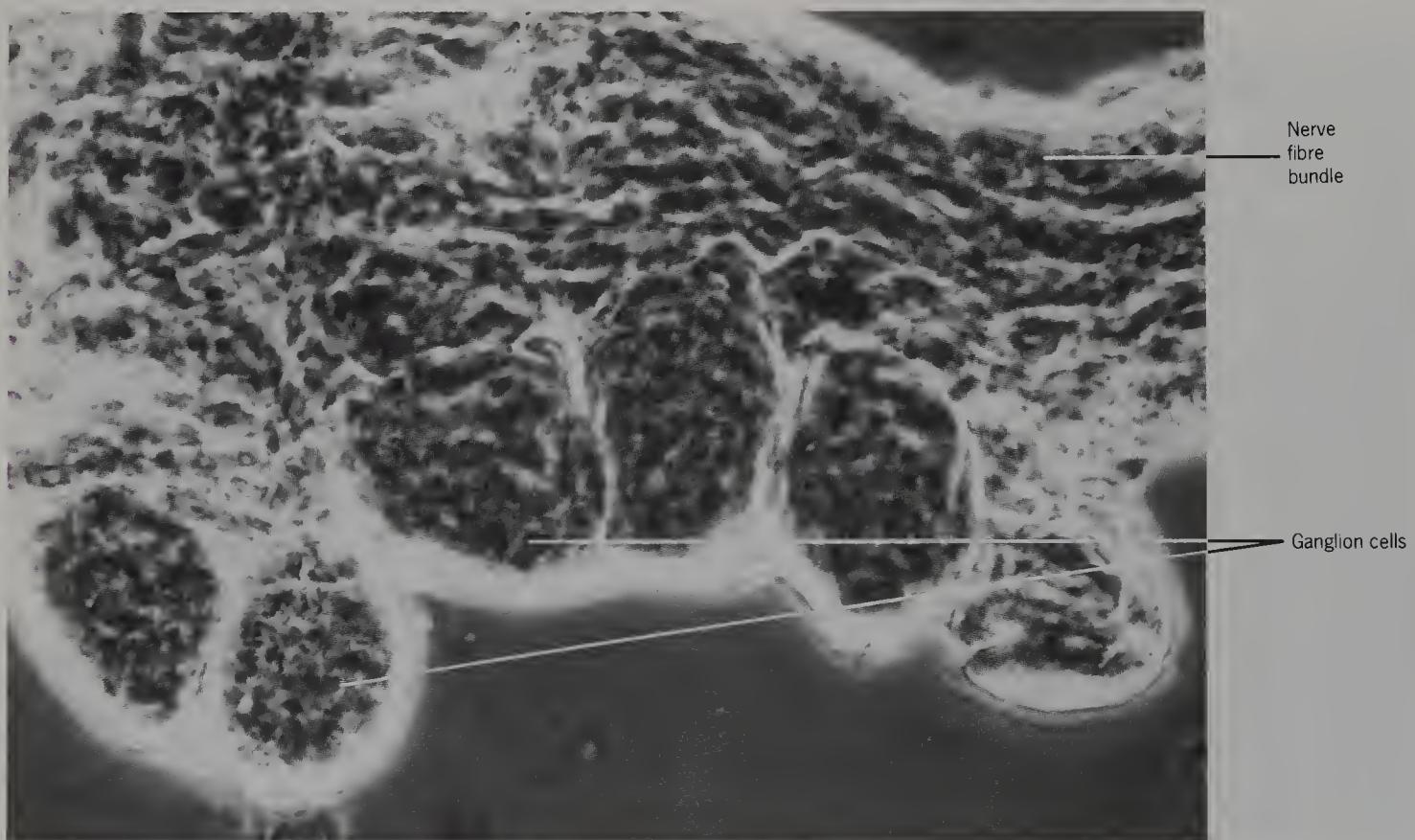


Figure 296 Partially teased mouse sublingual ganglion, to show ganglion cells and associated nerve fibres (phase contrast, $\times 1100$).



Figure 297 Myenteric plexus in guinea-pig colon *in situ* (bright field, $\times 270$).

This plexus is parasympathetic.

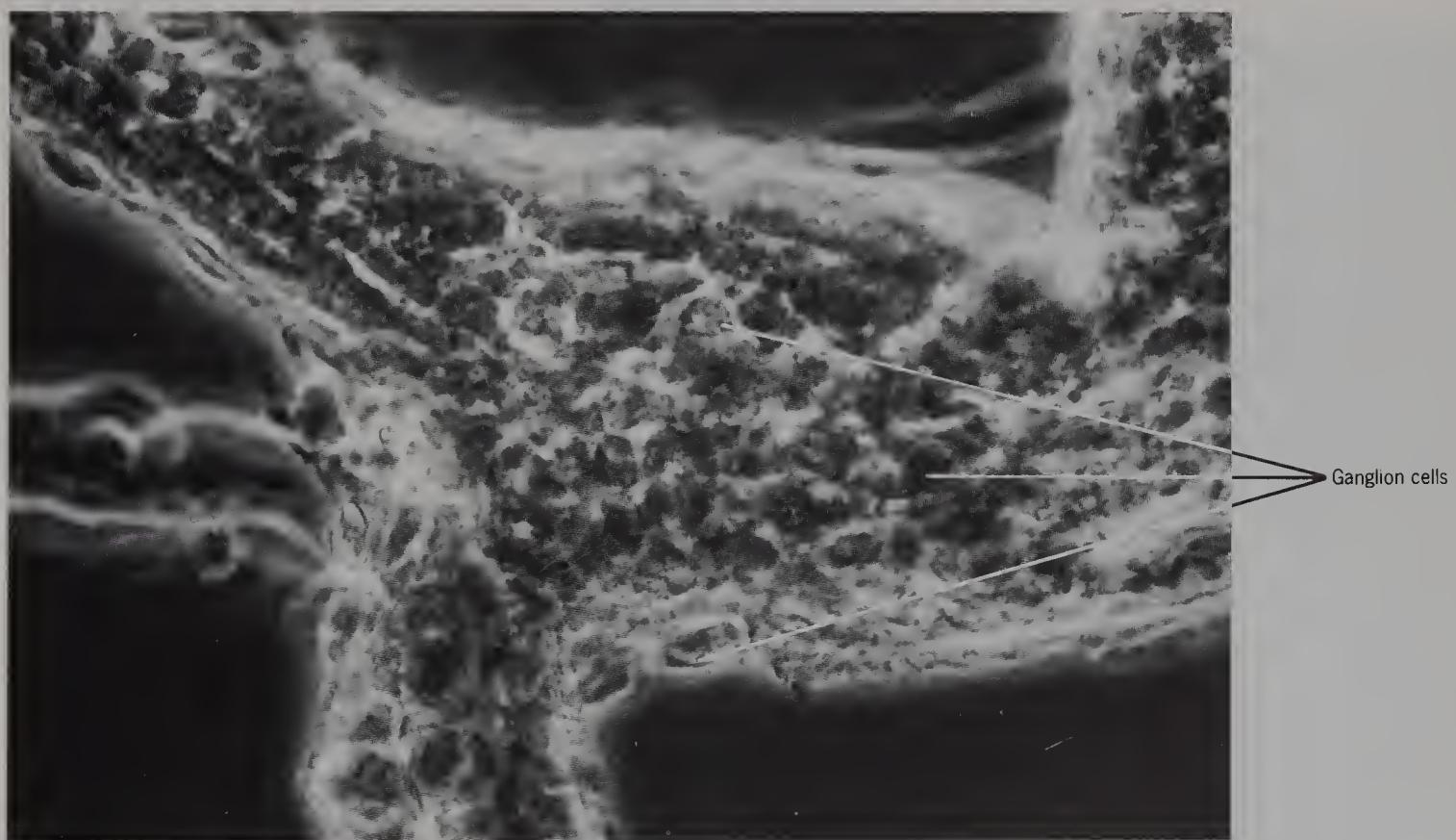


Figure 298 Dissected guinea-pig myenteric plexus of colon, to show ganglion cells *in situ* (bright field, $\times 700$).

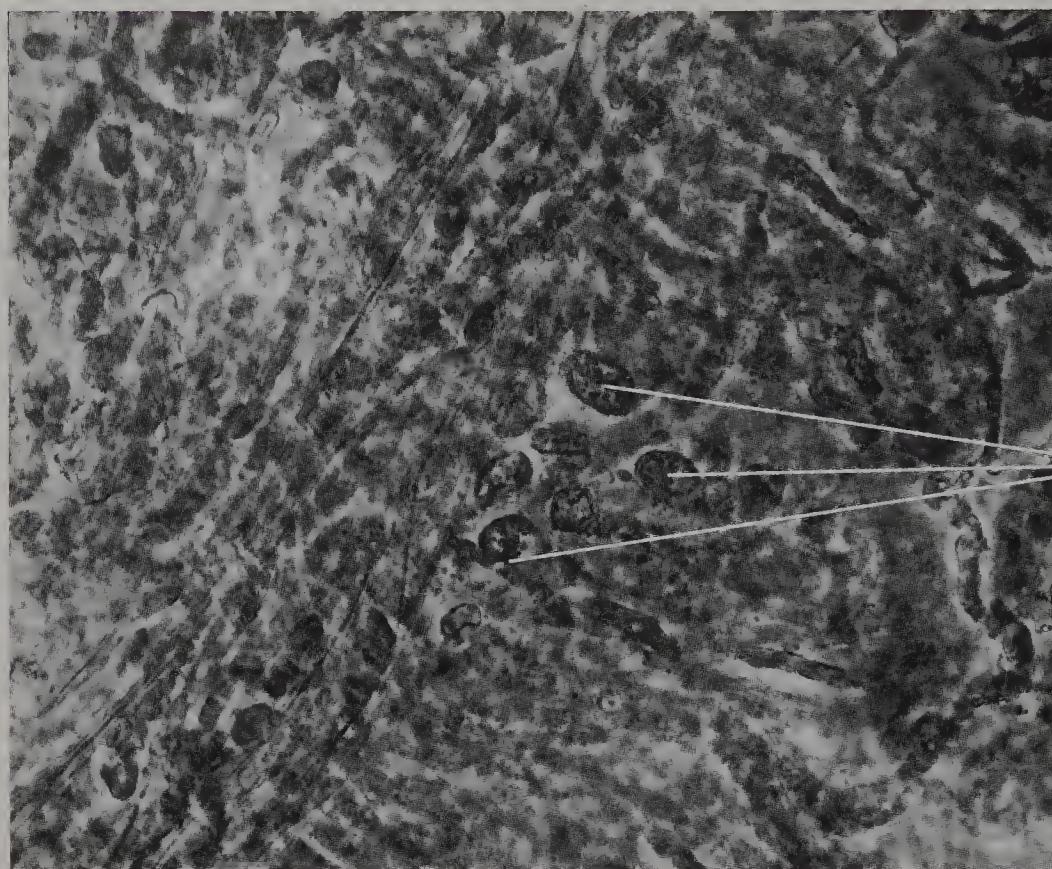


Figure 299 Guinea-pig myenteric plexus of colon *in situ*, to show ganglion cells (bright field, $\times 700$).



Figure 300 Isolated guinea-pig ganglion cells from the myenteric plexus of colon to show multiple nucleoli (phase contrast, $\times 1300$).

Nucleus with
multiple
nucleoli

SECTION
7

CRANIAL NERVES AND RETINA

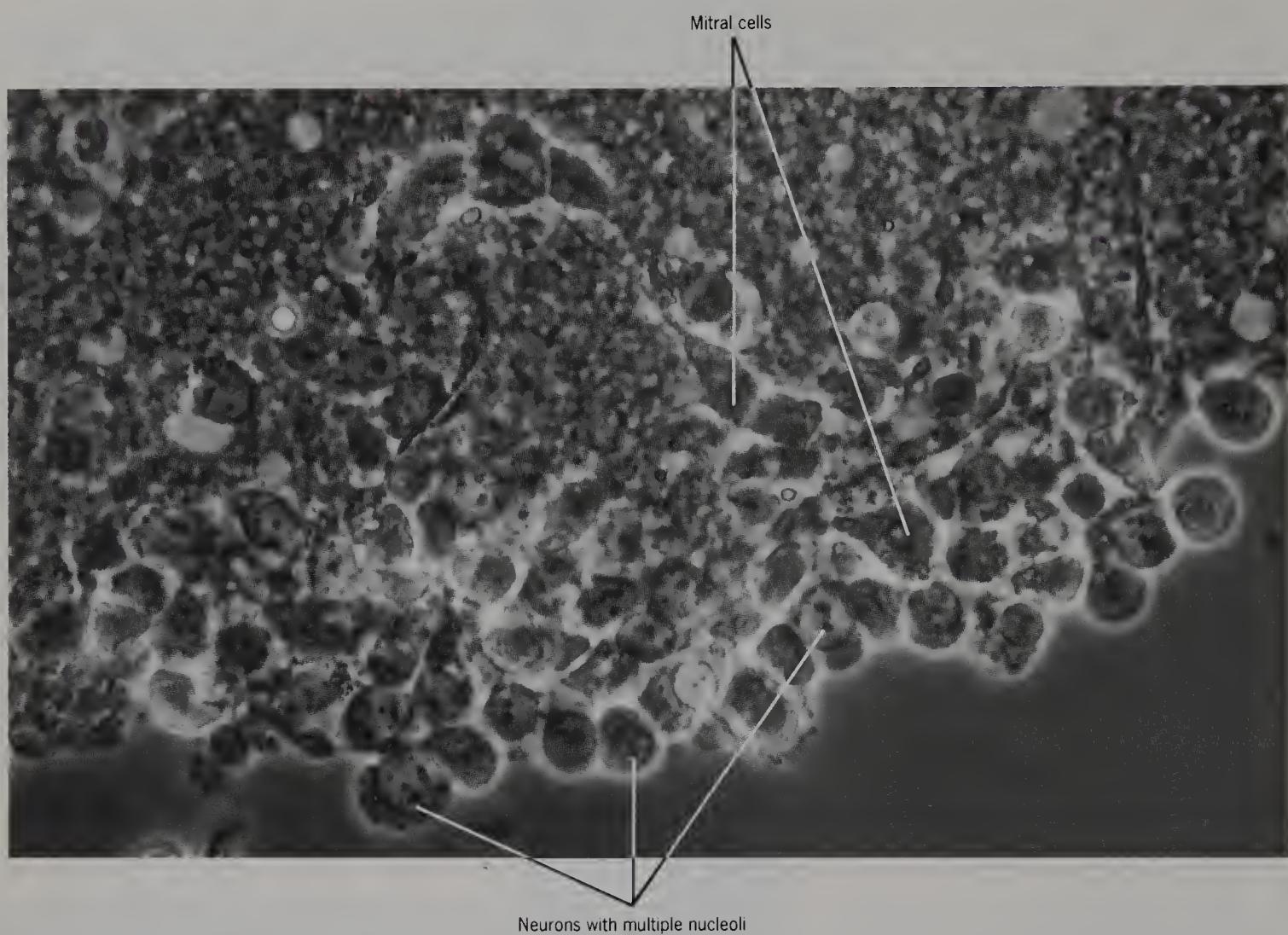


Figure 301 Partially teased rabbit olfactory bulb to show different cell types (phase contrast, $\times 800$).

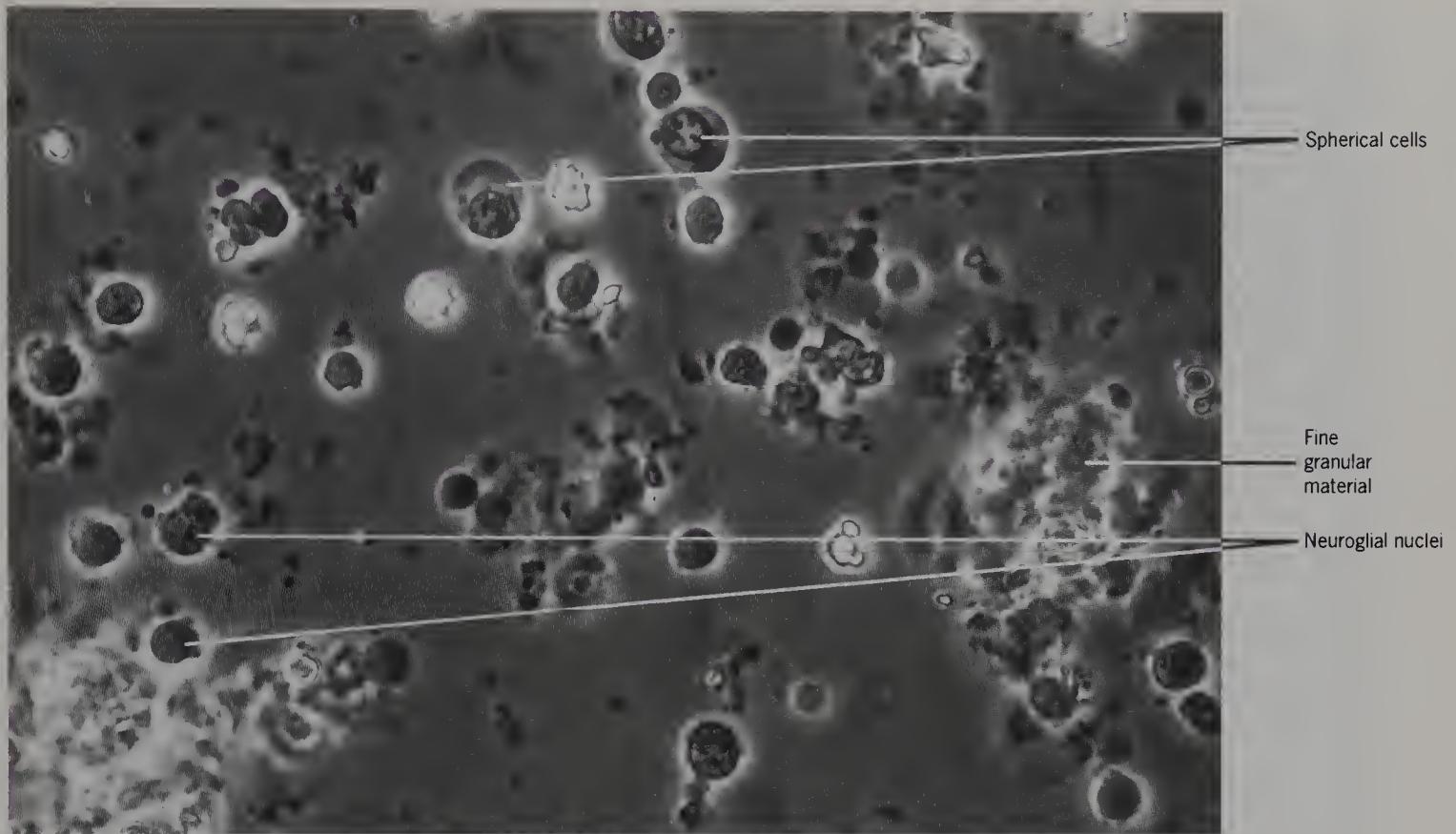


Figure 302 Teased human olfactory bulb from a 75-year-old male, to show spherical cells (phase contrast, $\times 700$).

These are probably neuroglia.



Figure 303 Thin slab of human olfactory tract from a 55-year-old male, to show beaded fibres *in situ* (phase contrast, $\times 700$).

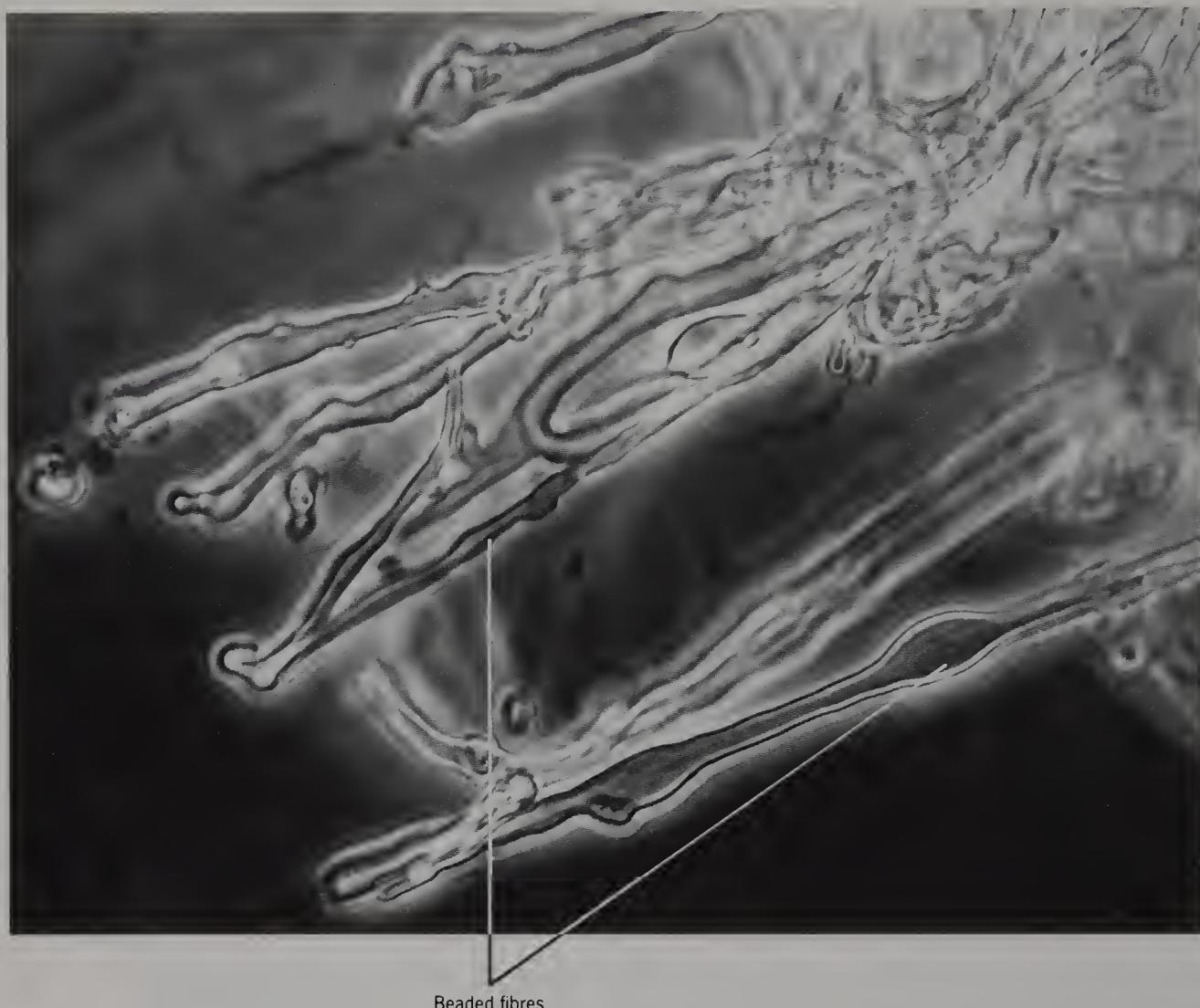


Figure 304 Partially teased human olfactory tract from a 75-year-old male, to show fibres (phase contrast, $\times 1200$).

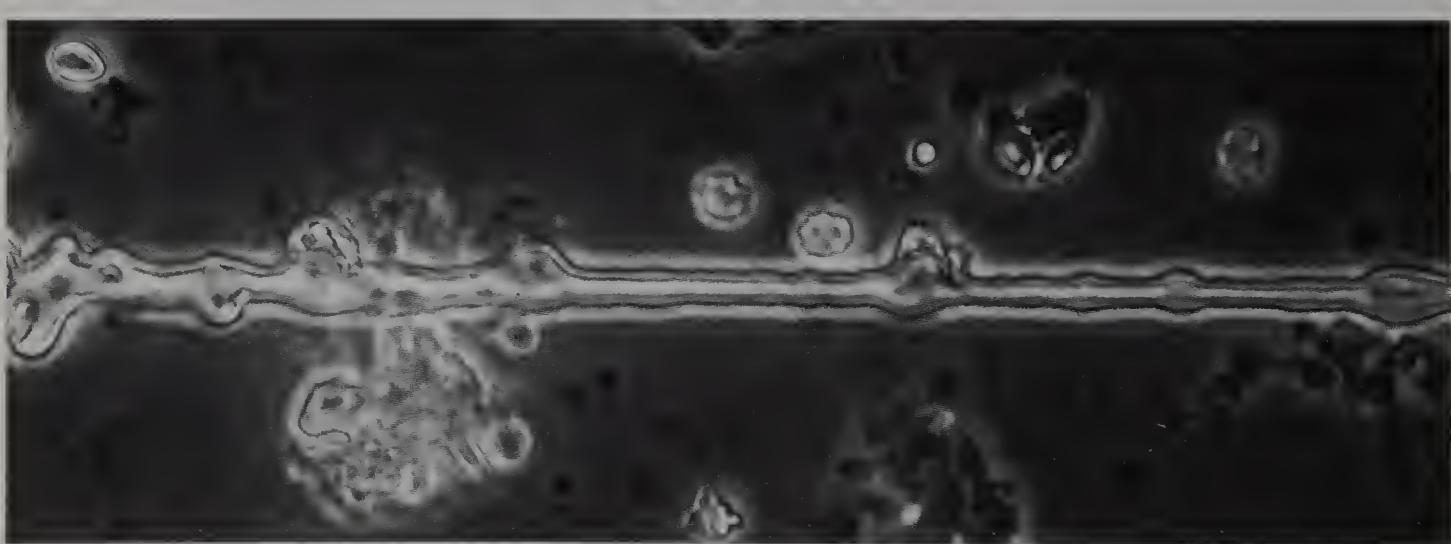


Figure 305 Isolated beaded fibre from the previous specimen (phase contrast, $\times 800$)

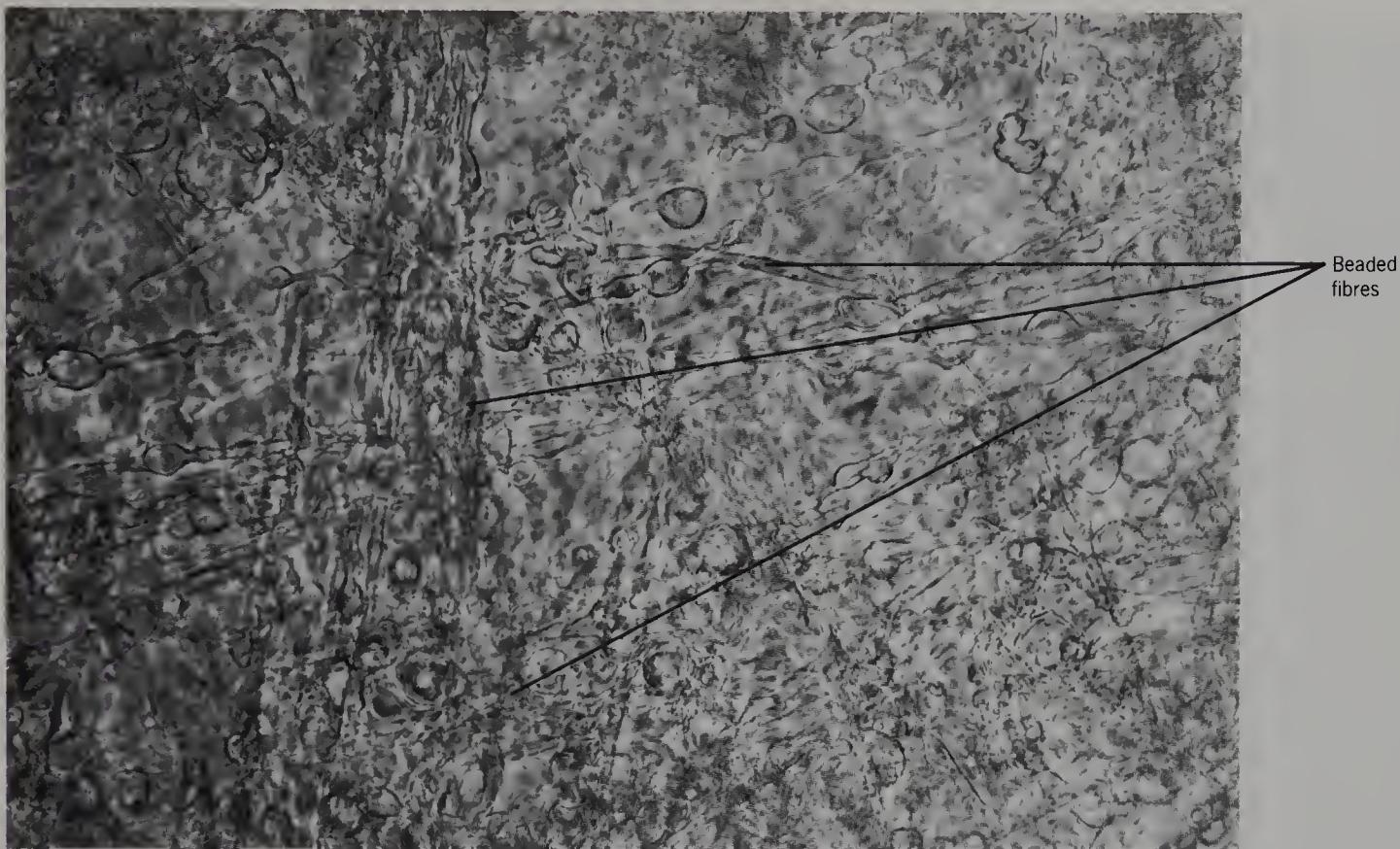


Figure 306 Thin slab of human optic nerve from an 85-year-old female, to show beaded fibres *in situ* (phase contrast, $\times 700$).

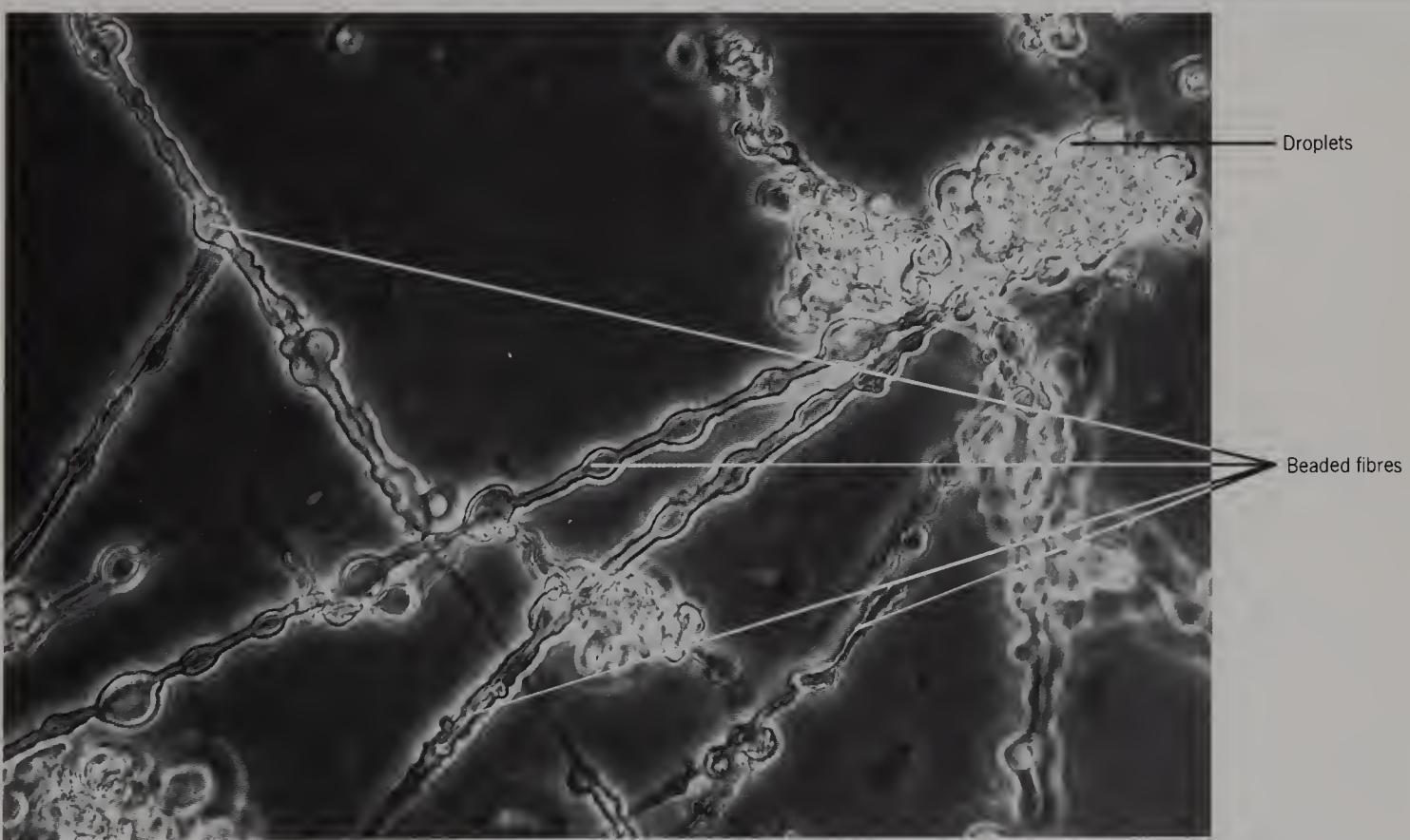


Figure 307 Teased human optic nerve from an 87-year-old female, to show beaded fibres (phase contrast, $\times 700$).

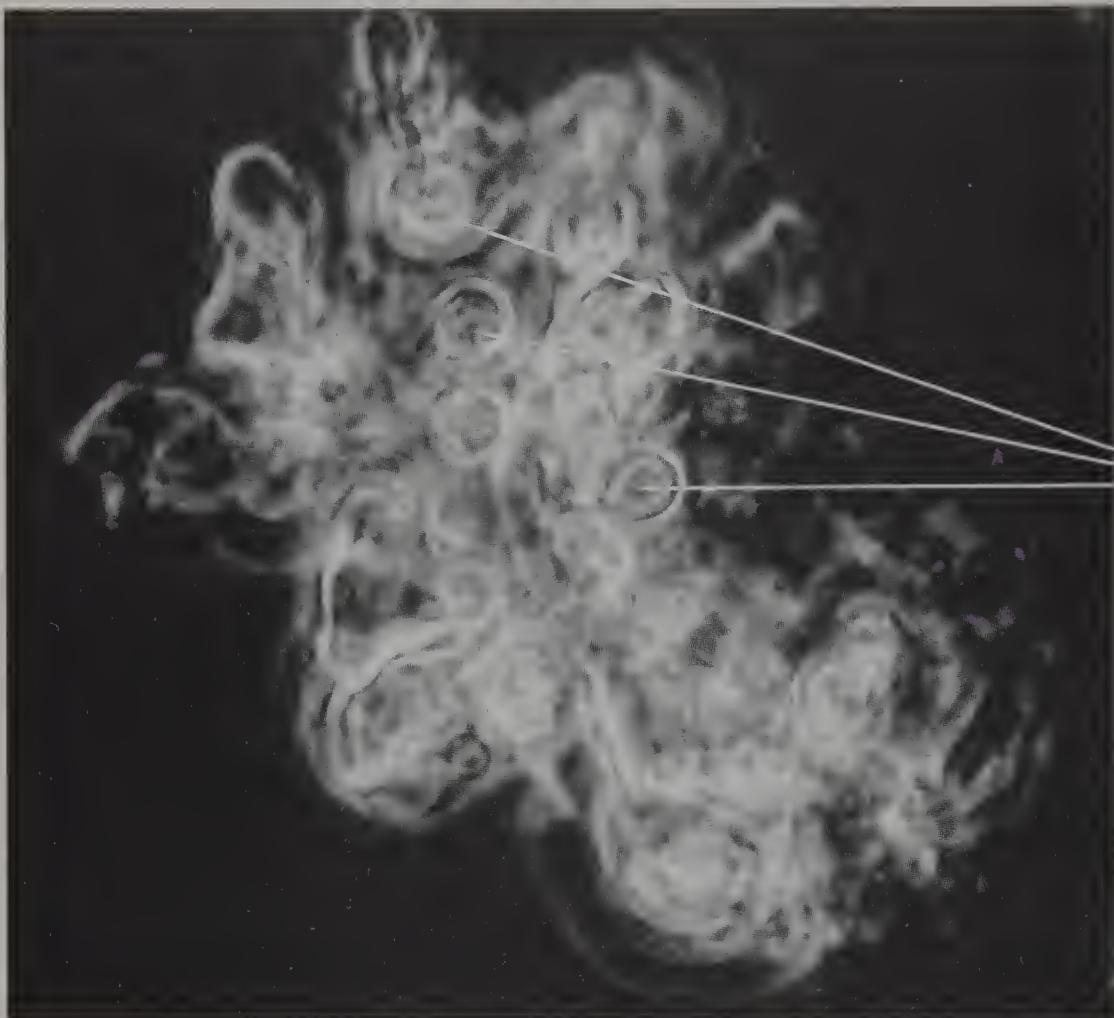


Figure 308 Teased human neuroglial clump from the optic nerve of a 43-year-old male (phase contrast, $\times 2000$).

This consists of refractile droplets.



Figure 309 Isolated droplet (above) and neuroglial cell (below) from the previous specimen (phase contrast, $\times 2000$).

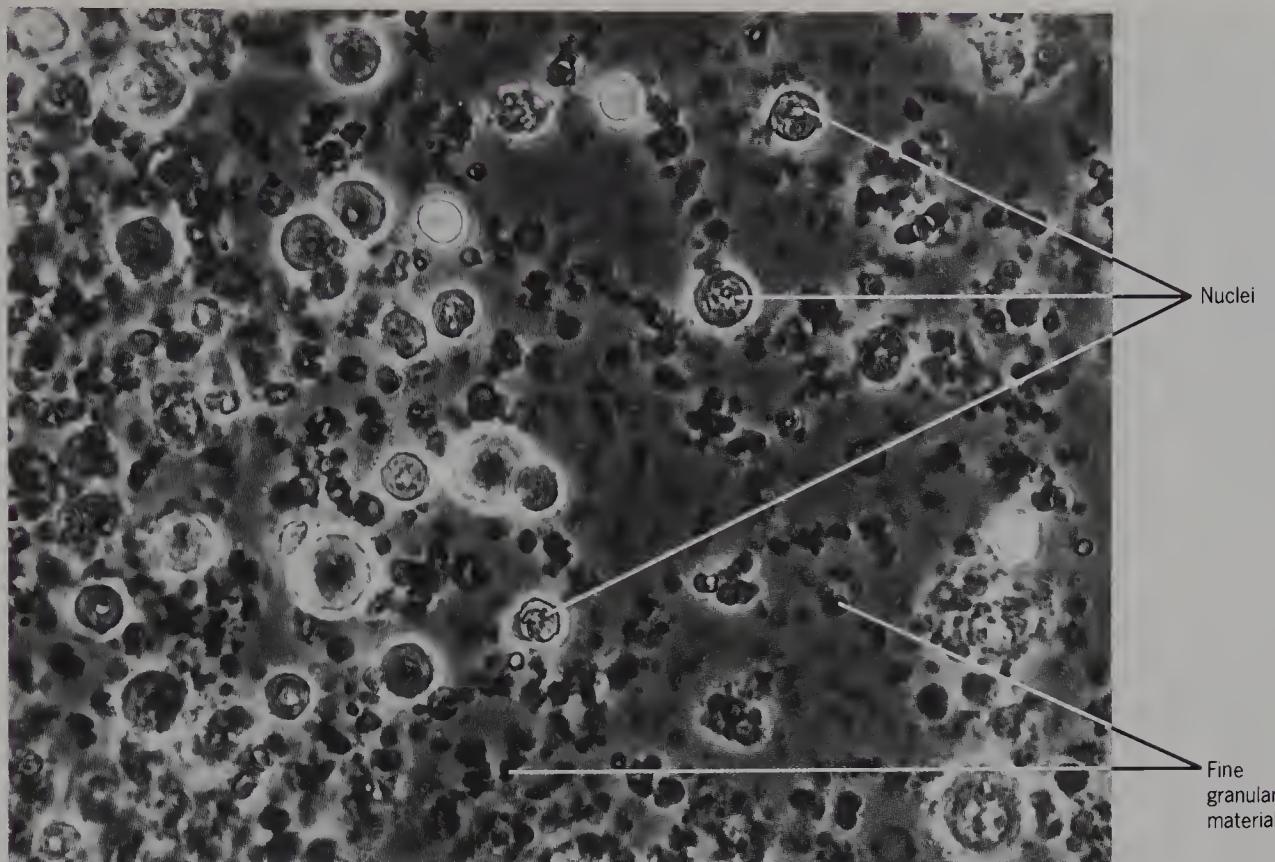


Figure 310 Neuroglial nuclei and fine granular material teased from the optic nerve of a 1-week-old rat (phase contrast, $\times 700$).

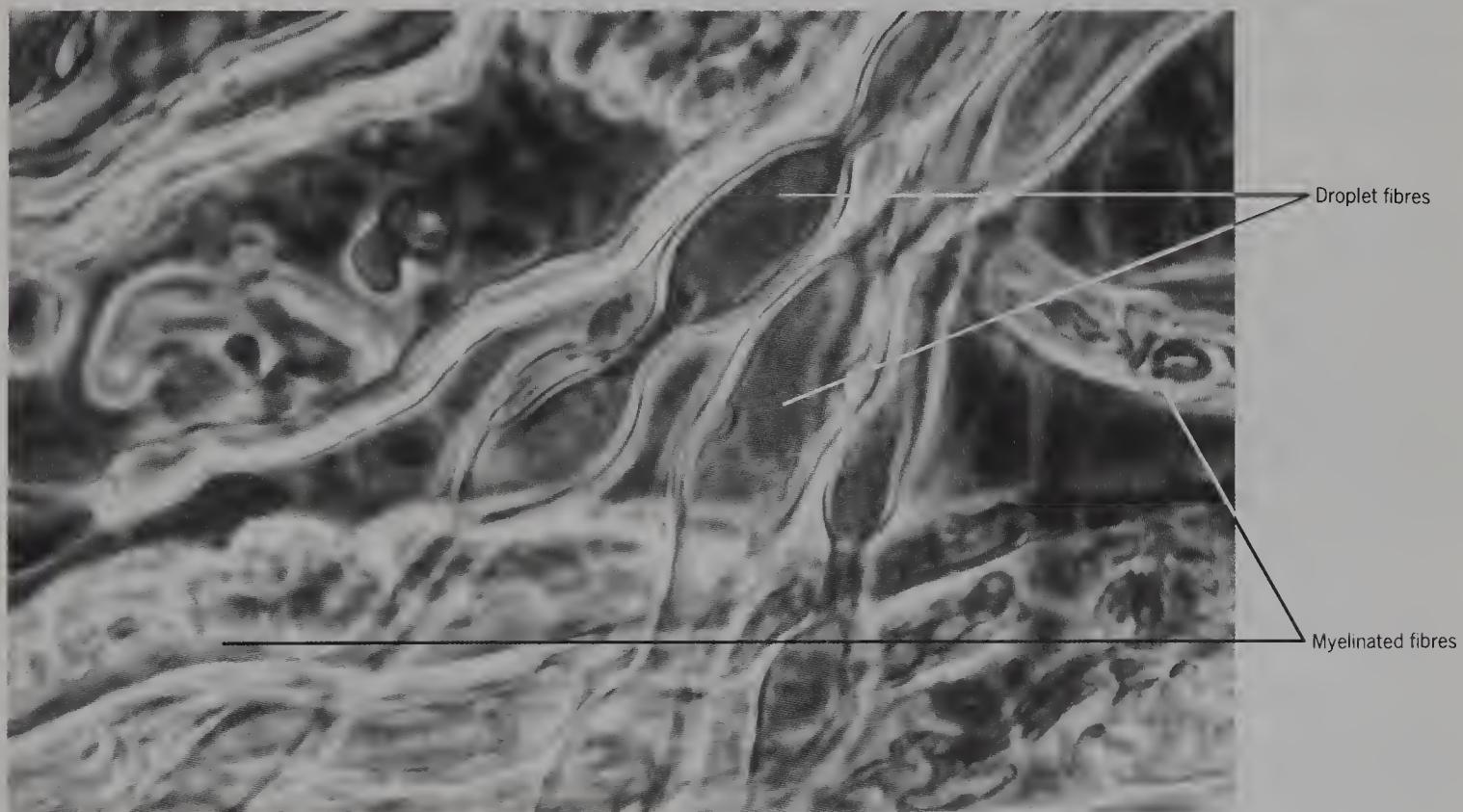


Figure 311 Teased rat oculomotor nerve, to show beaded and myelinated nerve fibres (phase contrast, $\times 1750$).

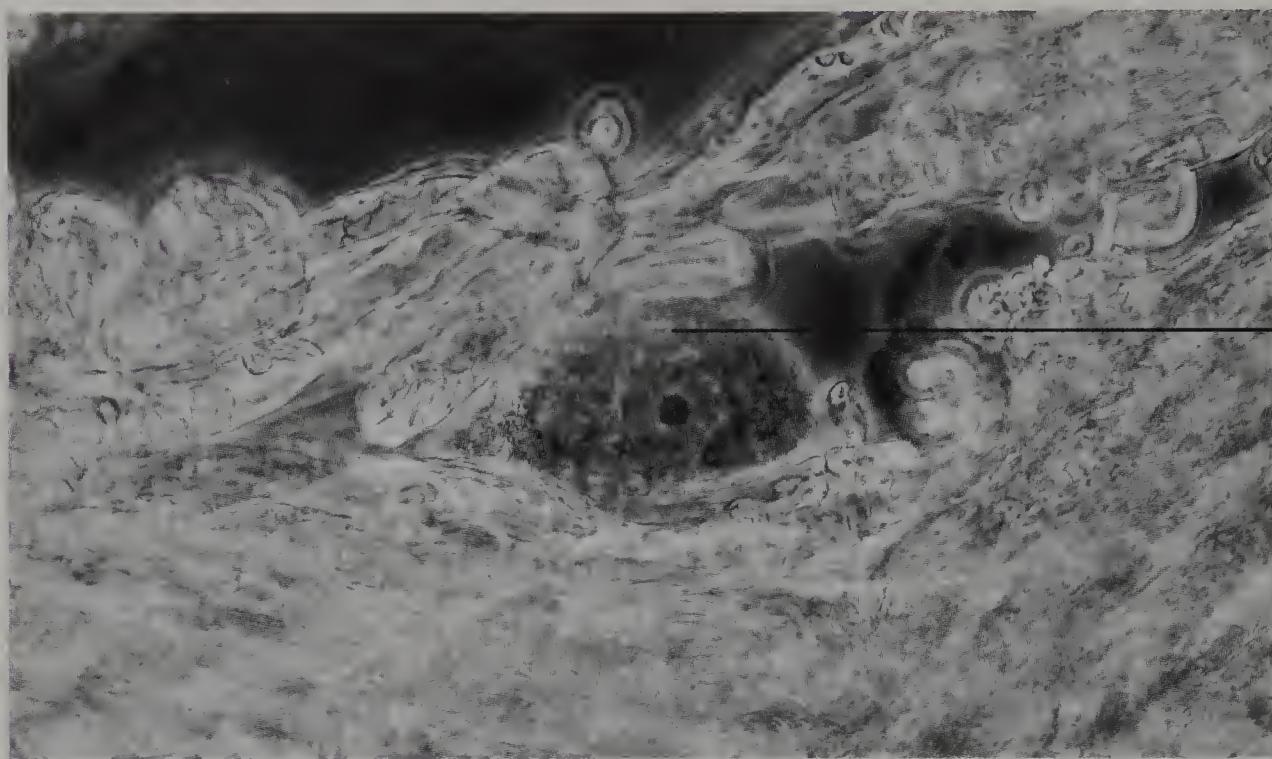


Figure 312 Partially teased rat trigeminal nerve to show a ganglion cell and myelinated fibres (phase contrast, $\times 700$).

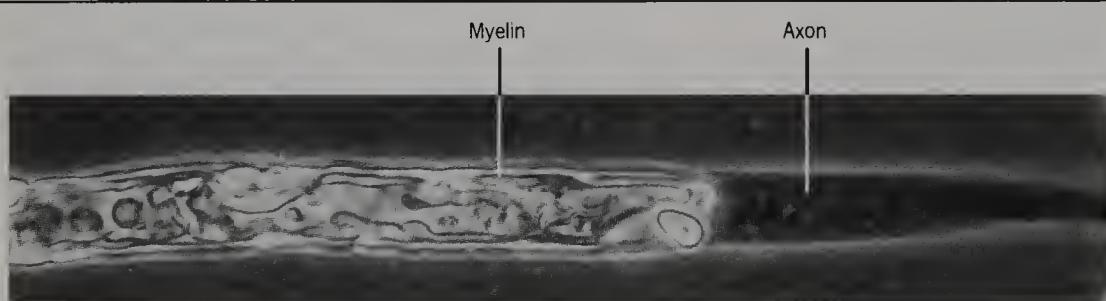


Figure 313 Isolated rabbit myelinated nerve fibre of the abducens nerve, showing the axon from which the sheath has been partly pulled off by teasing (phase contrast, $\times 700$).

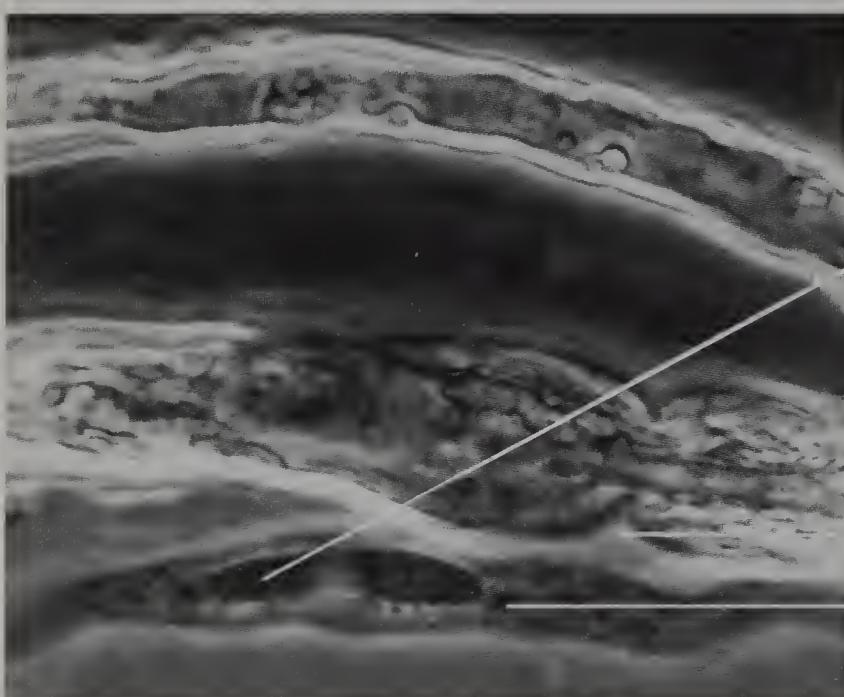


Figure 314 Isolated rat myelinated and unmyelinated (Remak) fibres from the facial nerve (phase contrast, $\times 1750$).

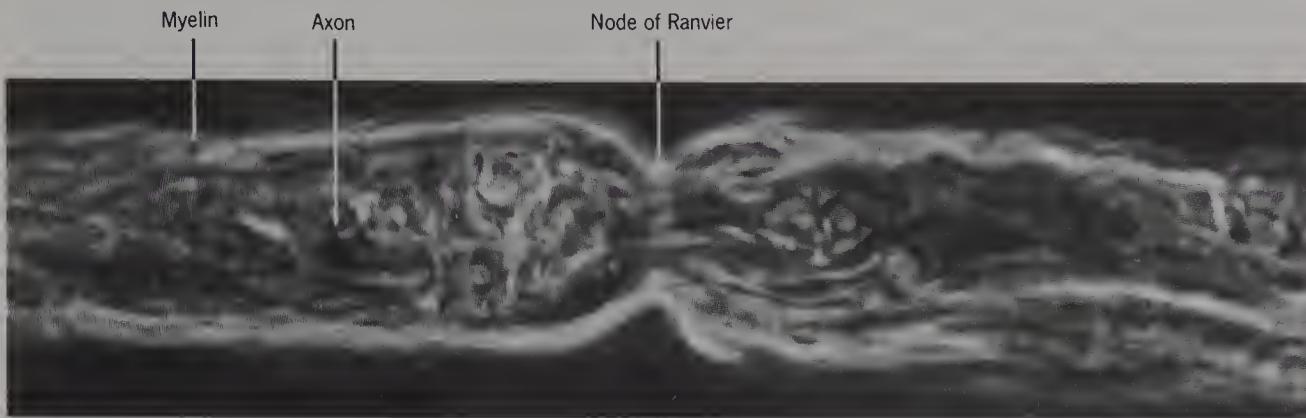


Figure 315 Isolated rat myelinated fibre from the glossopharyngeal nerve, to show a node of Ranvier (phase contrast, $\times 1750$). Ranvier described them in 1871.

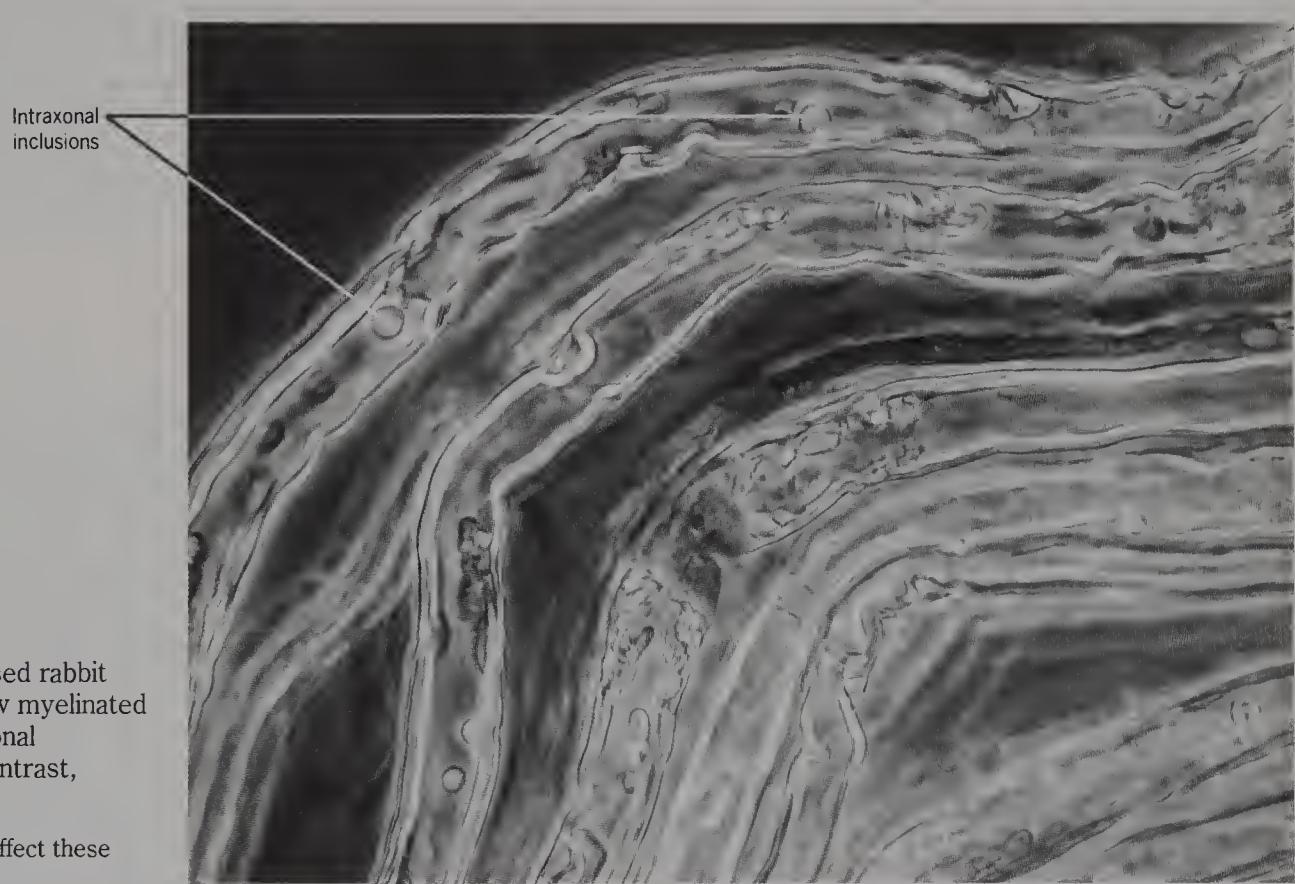


Figure 316 Teased rabbit vagus nerve to show myelinated fibres with intra-axonal inclusions (phase contrast, $\times 700$).

It is not known what effect these inclusions have.



Figure 317 Isolated beaded fibre in rabbit vagus nerve (phase contrast, $\times 1750$).

Schmidt-Lanterman incisure



Figure 318 Normal fundus of a left eye, 30 degrees view. The optic nerve head shows a physiological cup with a cup to disc ratio of 0.2.

The veins are darker than the arteries, and the colour is given by the pigment layer and the fine blood vessels. People with darker complexions have darker fundi.

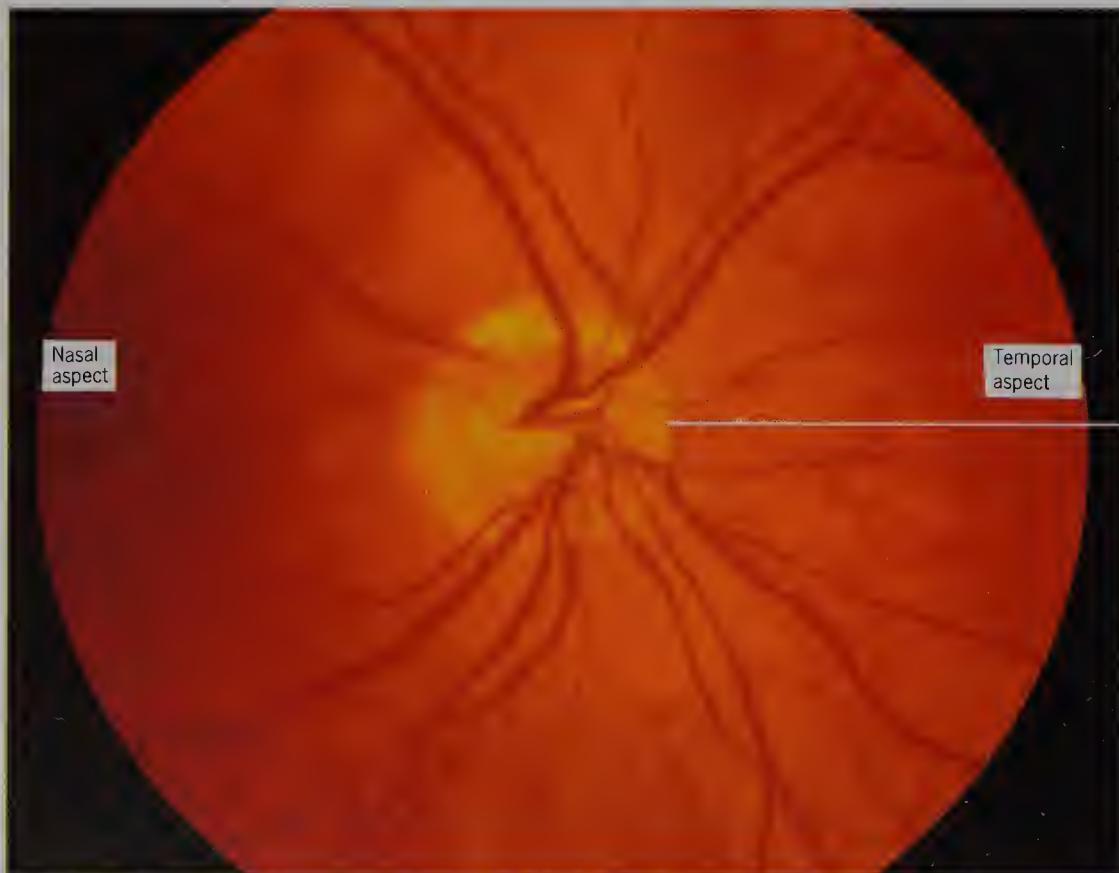


Figure 319 As above, fundus of the right eye of another subject, to show variation of normal appearances.

The ophthalmoscopic views in this and the previous figure were kindly provided by Mr E. S. Rosen, of Manchester.



Figure 320 Unteased rabbit retina to show blood vessels and bundles of nerve fibres (bright field, $\times 85$).

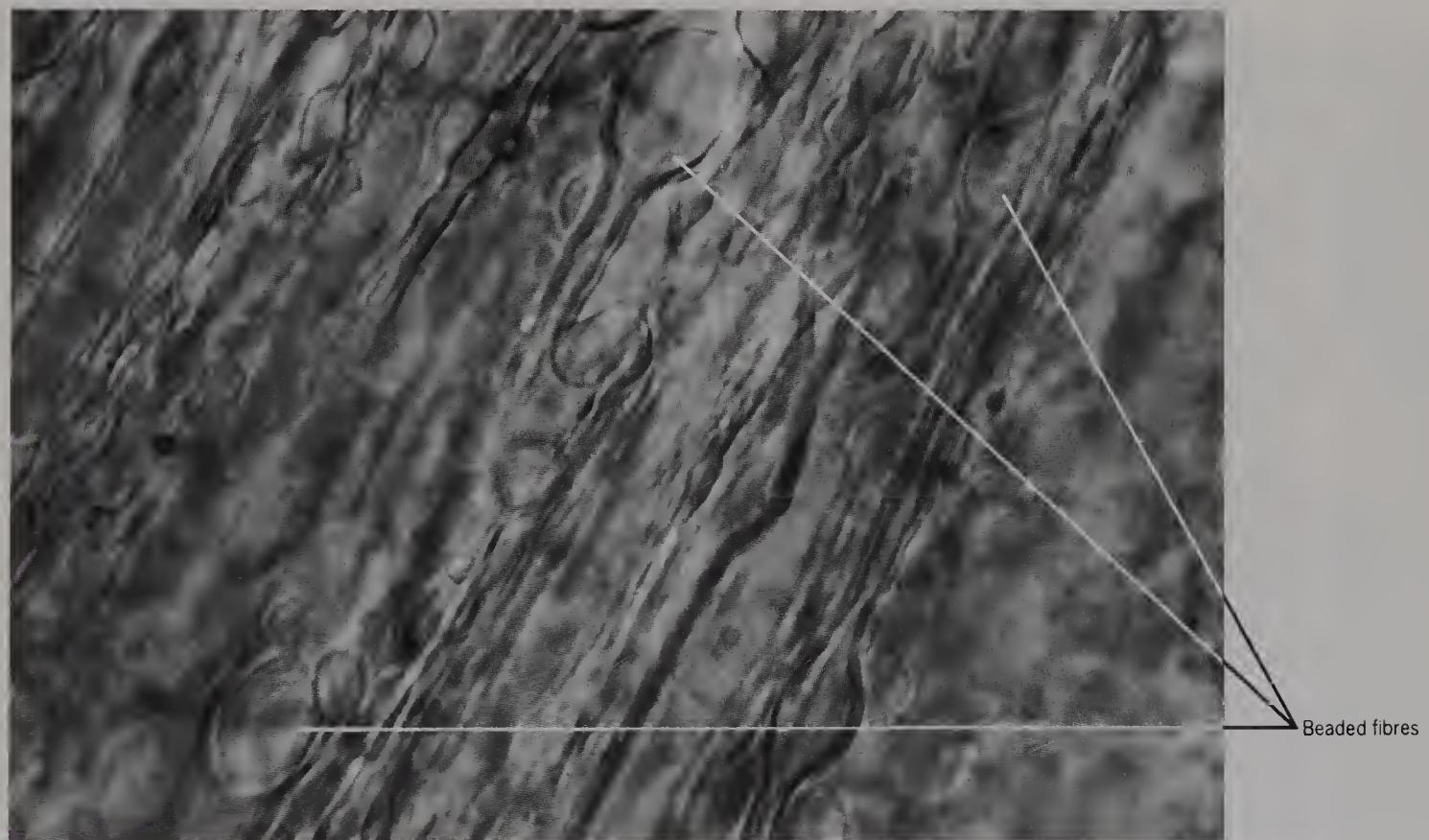


Figure 321 Partially teased rabbit retina to show beaded fibres (phase contrast, $\times 1750$).

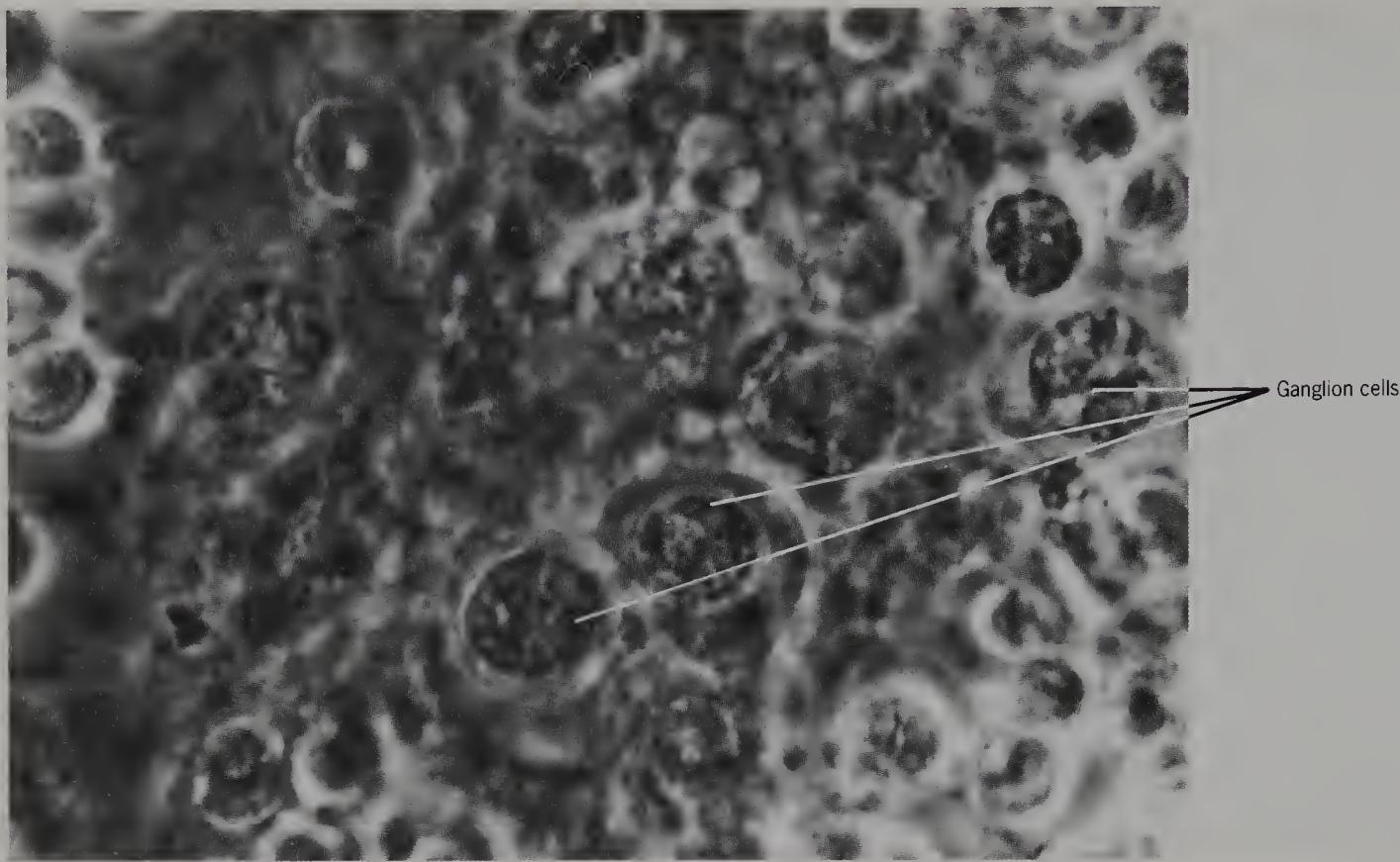


Figure 322 Partially teased rabbit retina to show ganglion cells (phase contrast, $\times 1750$).

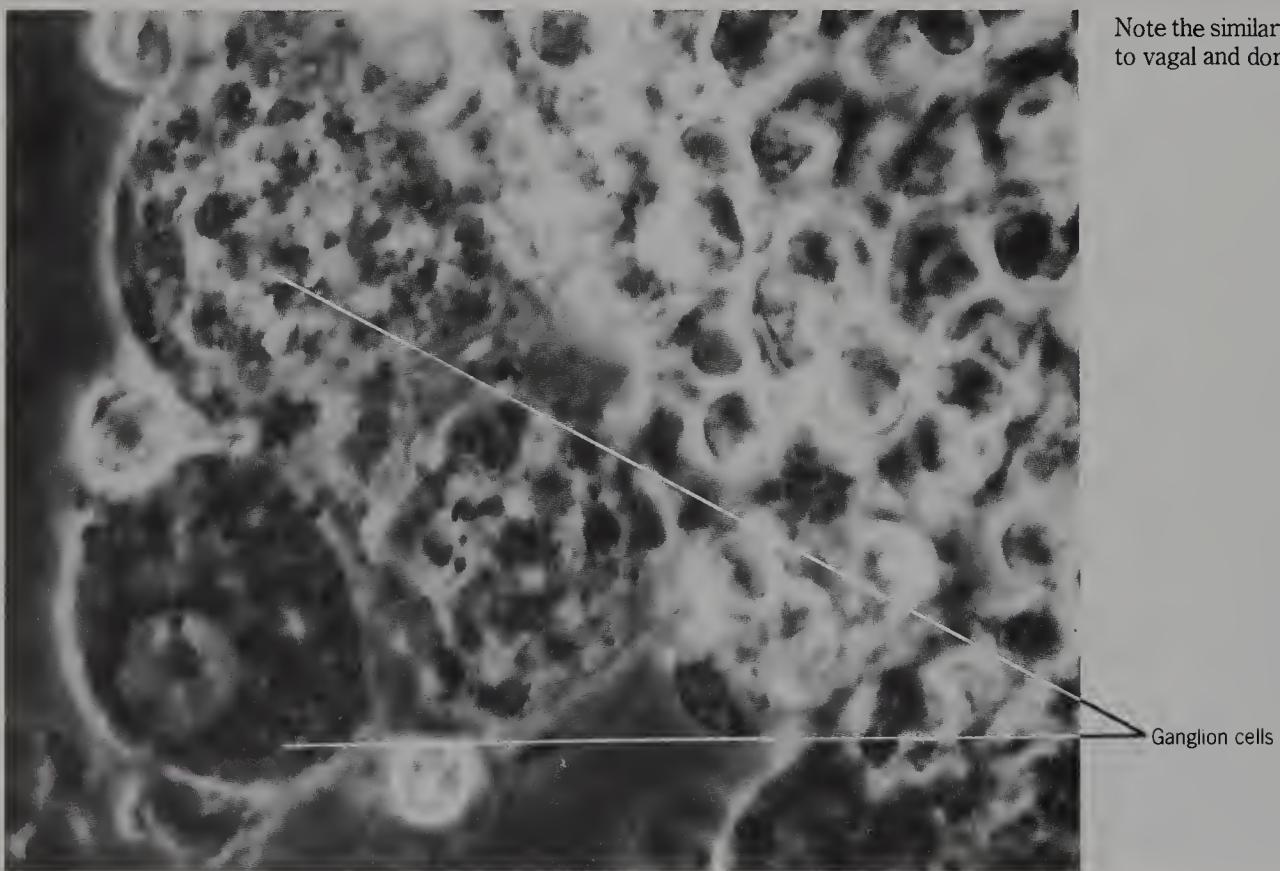


Figure 323 Partially teased rabbit retina to show ganglion cells (phase contrast, $\times 1750$).

Note the similarity of these ganglion cells to vagal and dorsal root ganglion cells.

Figure 324 Partially teased rabbit retina to show small ganglion cells and fine fibres (phase contrast, $\times 700$).

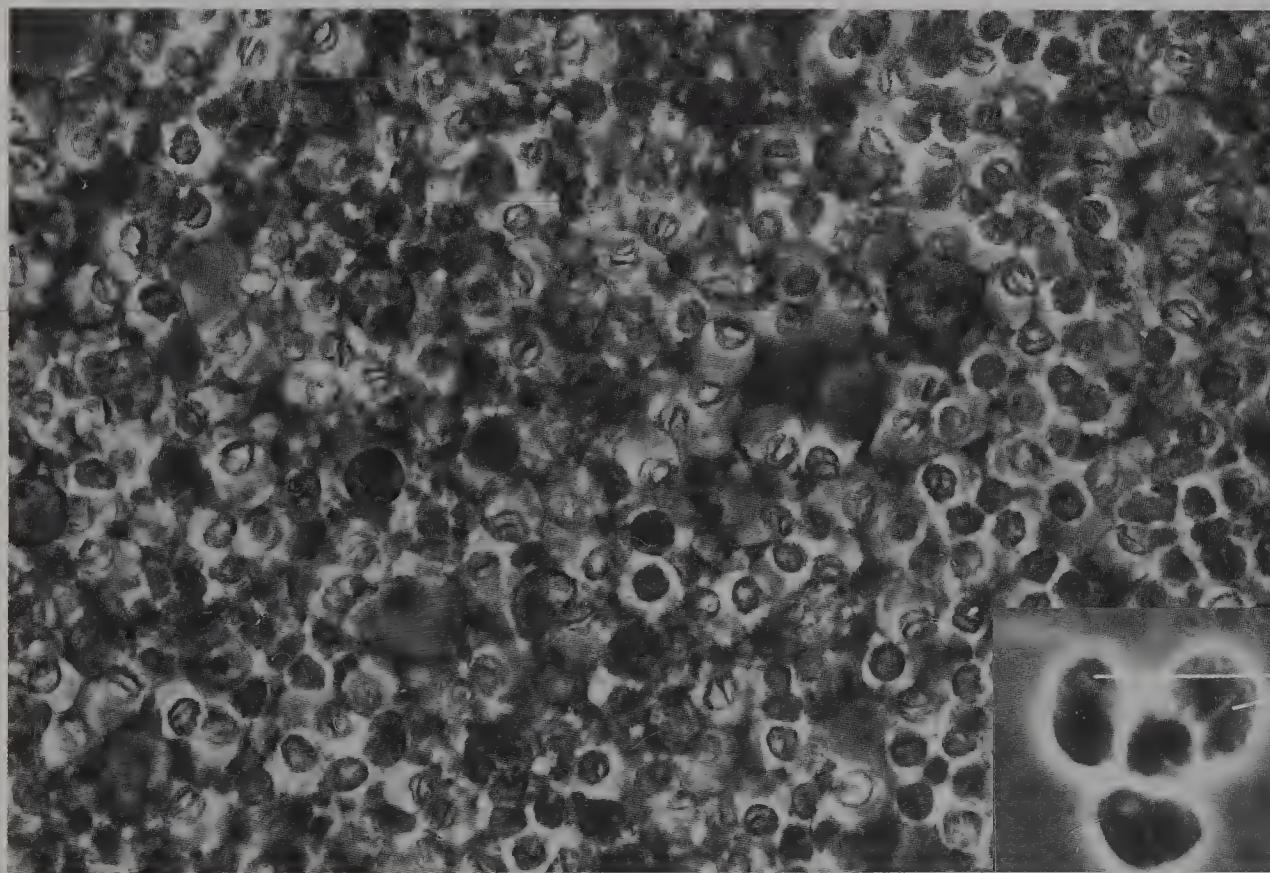
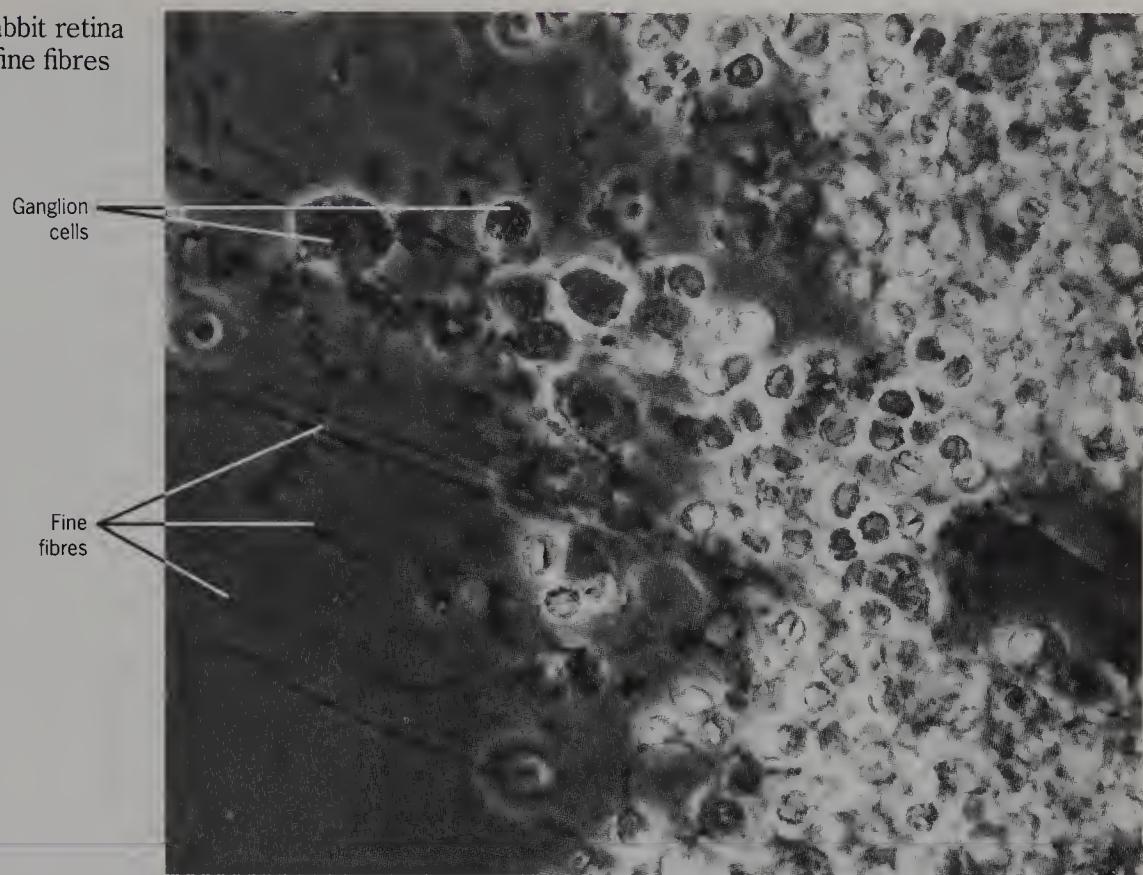


Figure 325 Partially teased rabbit retina, to show cell bodies of rods and cones (phase contrast, $\times 700$). Inset: rod nuclei (phase contrast, $\times 1750$).

Banding can be seen in rod nuclei.

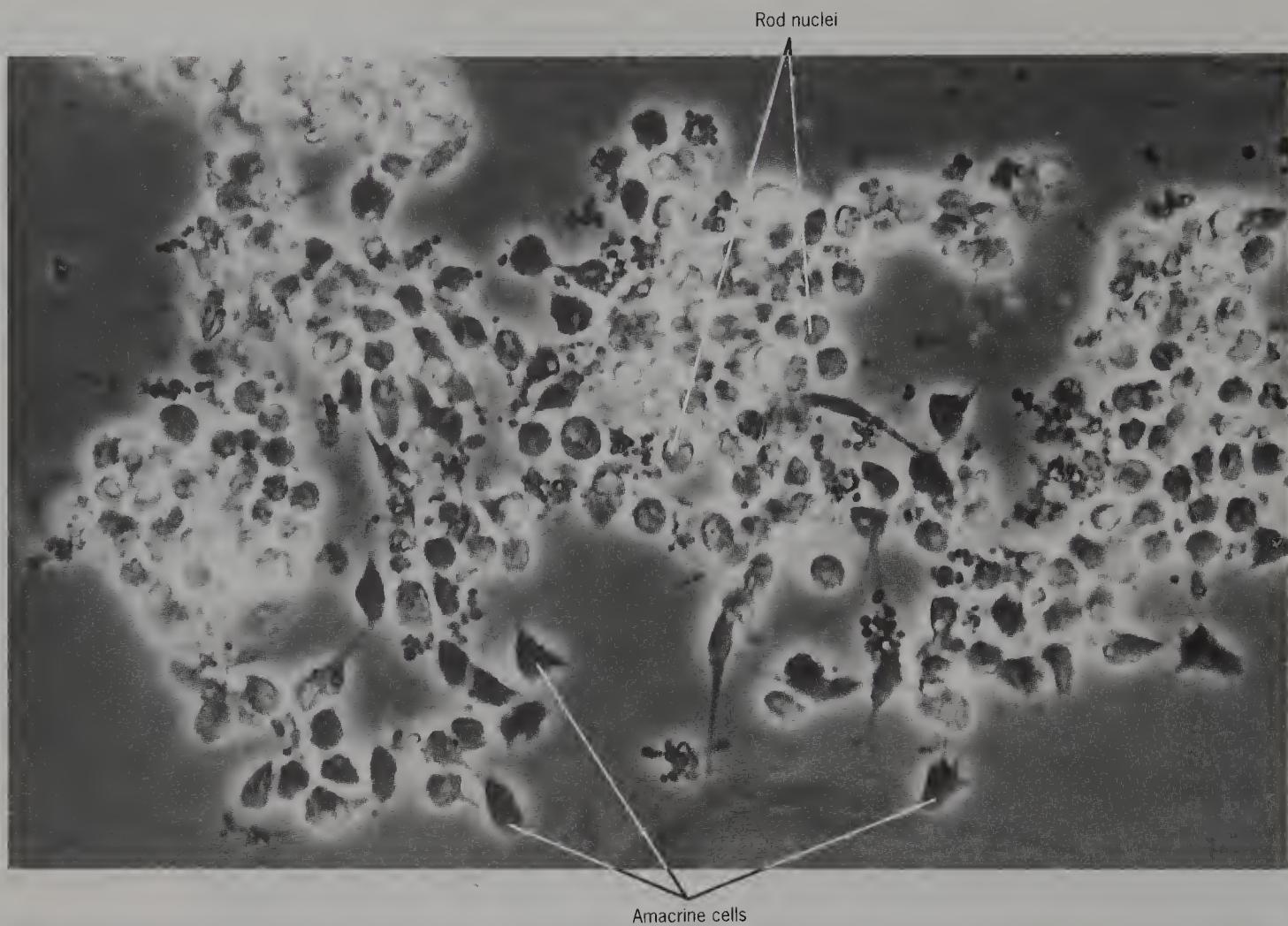


Figure 326 Teased rabbit retina to show amacrine cells and rod nuclei (phase contrast, $\times 800$).

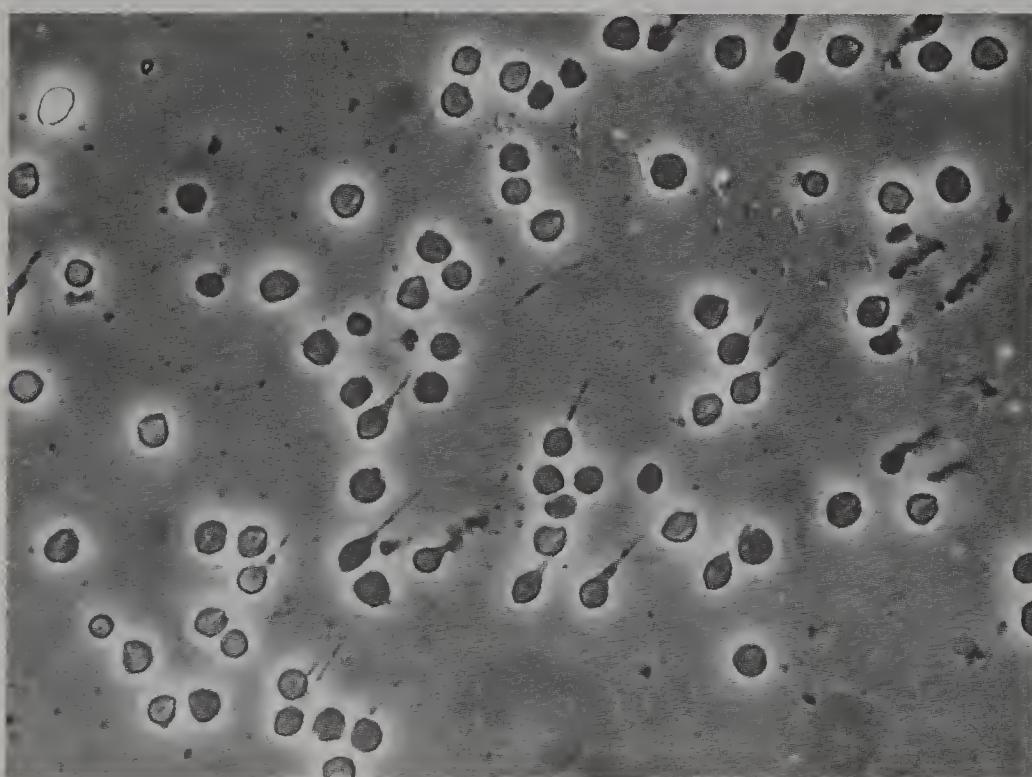


Figure 327 Isolated nuclei, probably of cones, from the central area of rat retina (phase contrast, $\times 800$).



Figure 328 Isolated nuclei, probably of rods, from the central area of rat retina (phase contrast, $\times 800$).

In isolated preparations, it is difficult to differentiate between the nuclei of rods and cones. Their appearances vary between species (Ramon y Cajal, 1892).

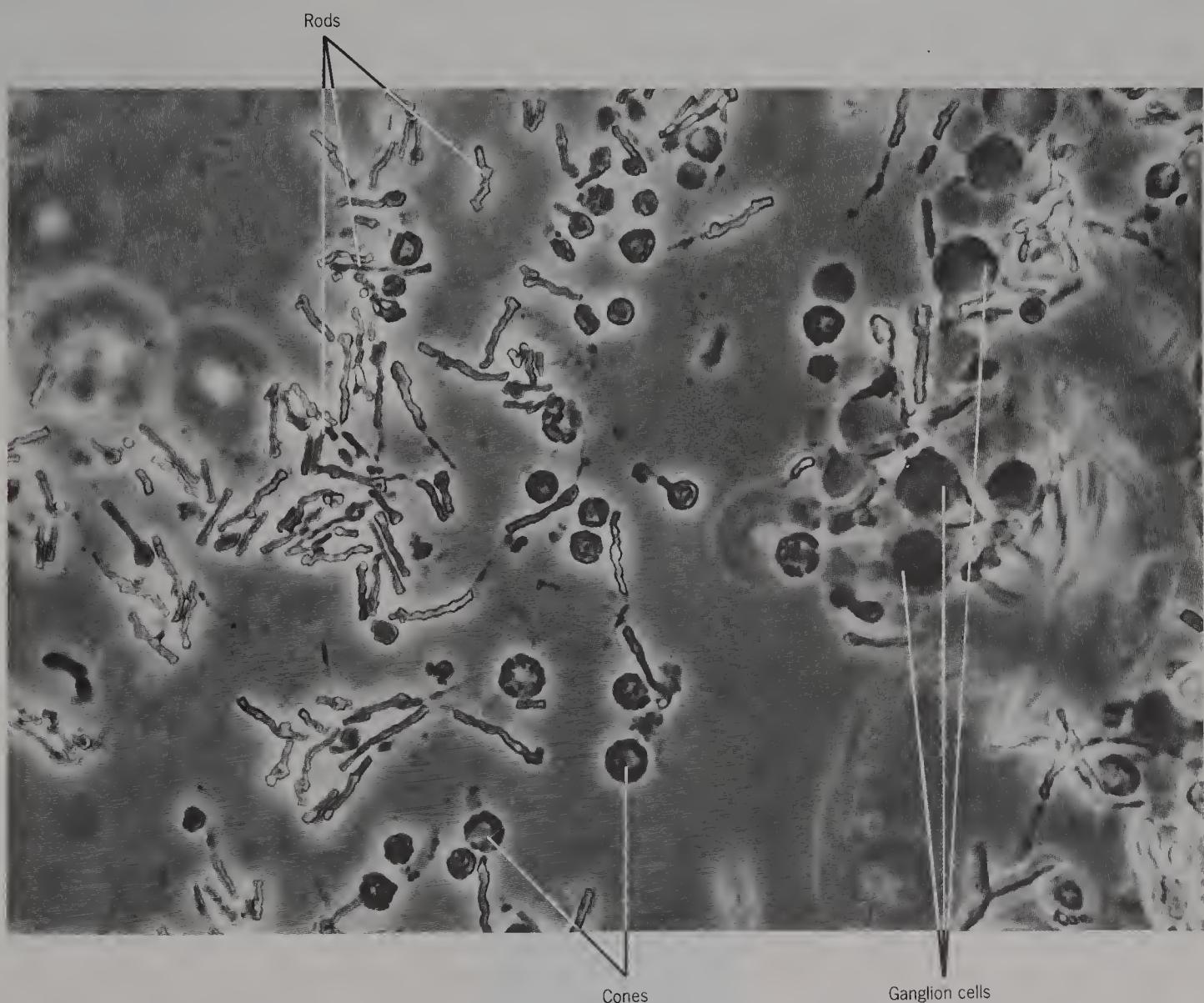


Figure 329 Teased outer segments of rods and ganglion cells from rat retina (phase contrast, $\times 800$).

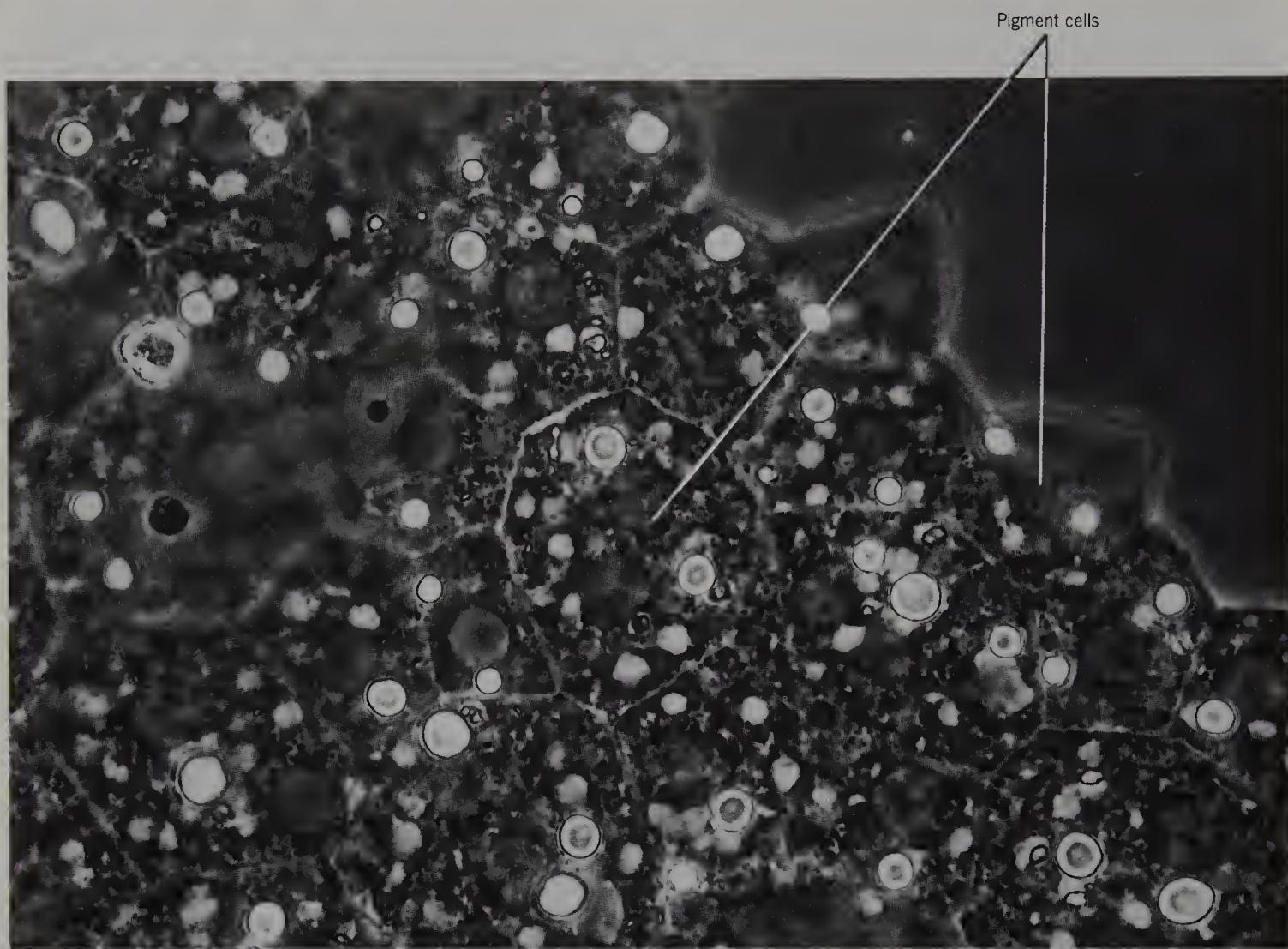


Figure 330 Partially teased rabbit retina to show pigment cell layer (phase contrast, $\times 800$).

SECTION
8

PERIPHERAL NERVES

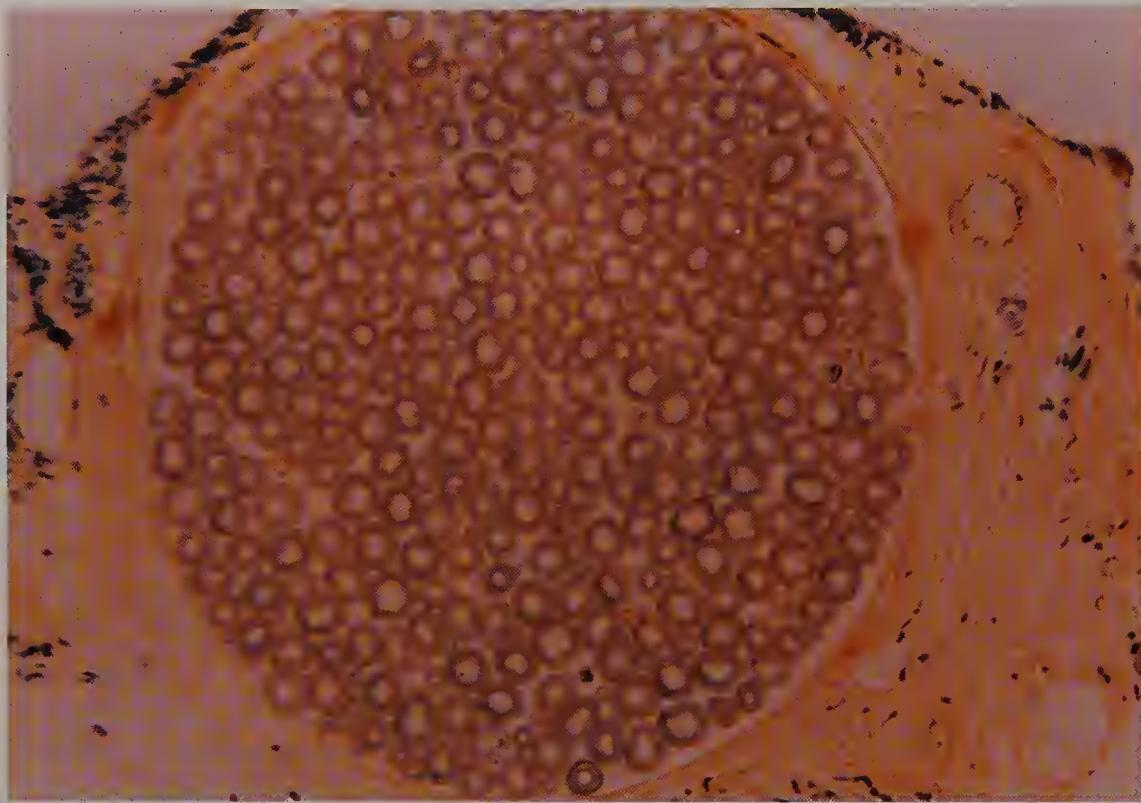


Figure 331 Transverse section of a branch of rabbit sciatic nerve, stained by the Weigert–Pal method, to show the incidence of myelinated fibres (bright field, $\times 610$).

A section of unfixed nerve was first seen by van Leeuwenhoek in 1719.

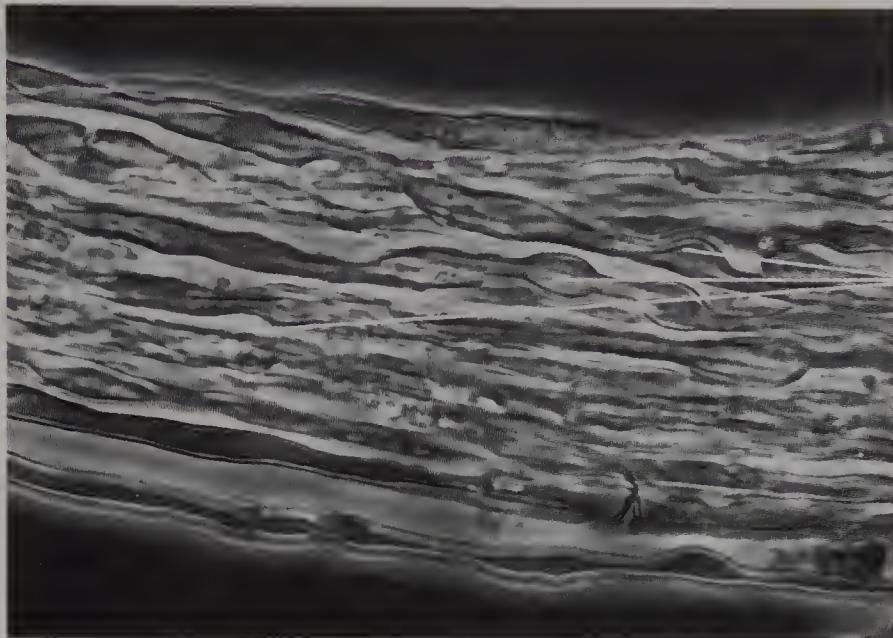


Figure 332 Partially teased 9-day-old mouse phrenic nerve, to show beaded fibres (phase contrast, $\times 1800$).

Myelination was not complete.

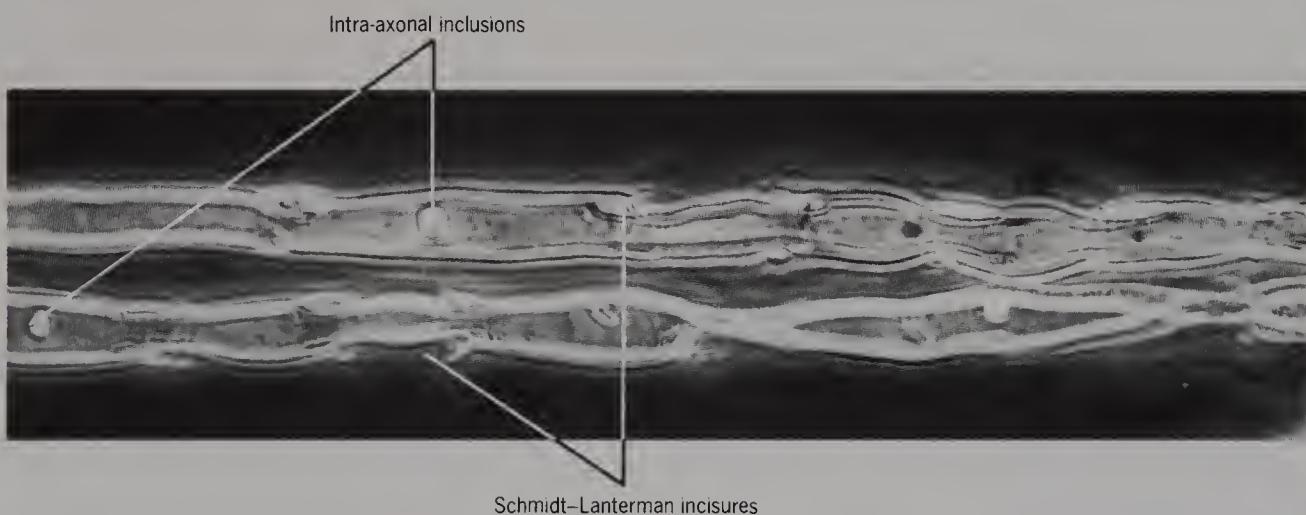


Figure 333 Isolated guinea-pig myelinated nerve fibres from phrenic nerve (phase contrast, $\times 800$).

There are intra-axonal inclusions.

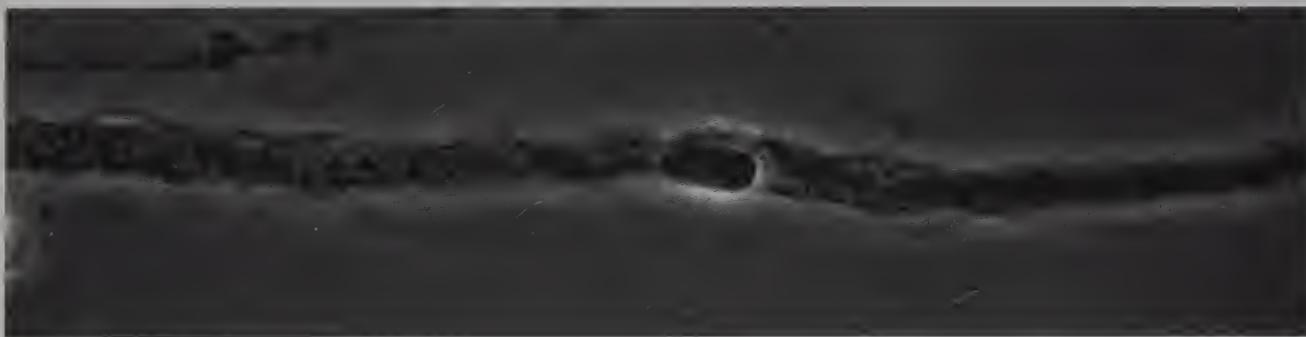


Figure 334 Isolated guinea-pig Remak fibre from phrenic nerve (phase contrast, $\times 800$).

These fibres are rather rare in mixed peripheral nerves.

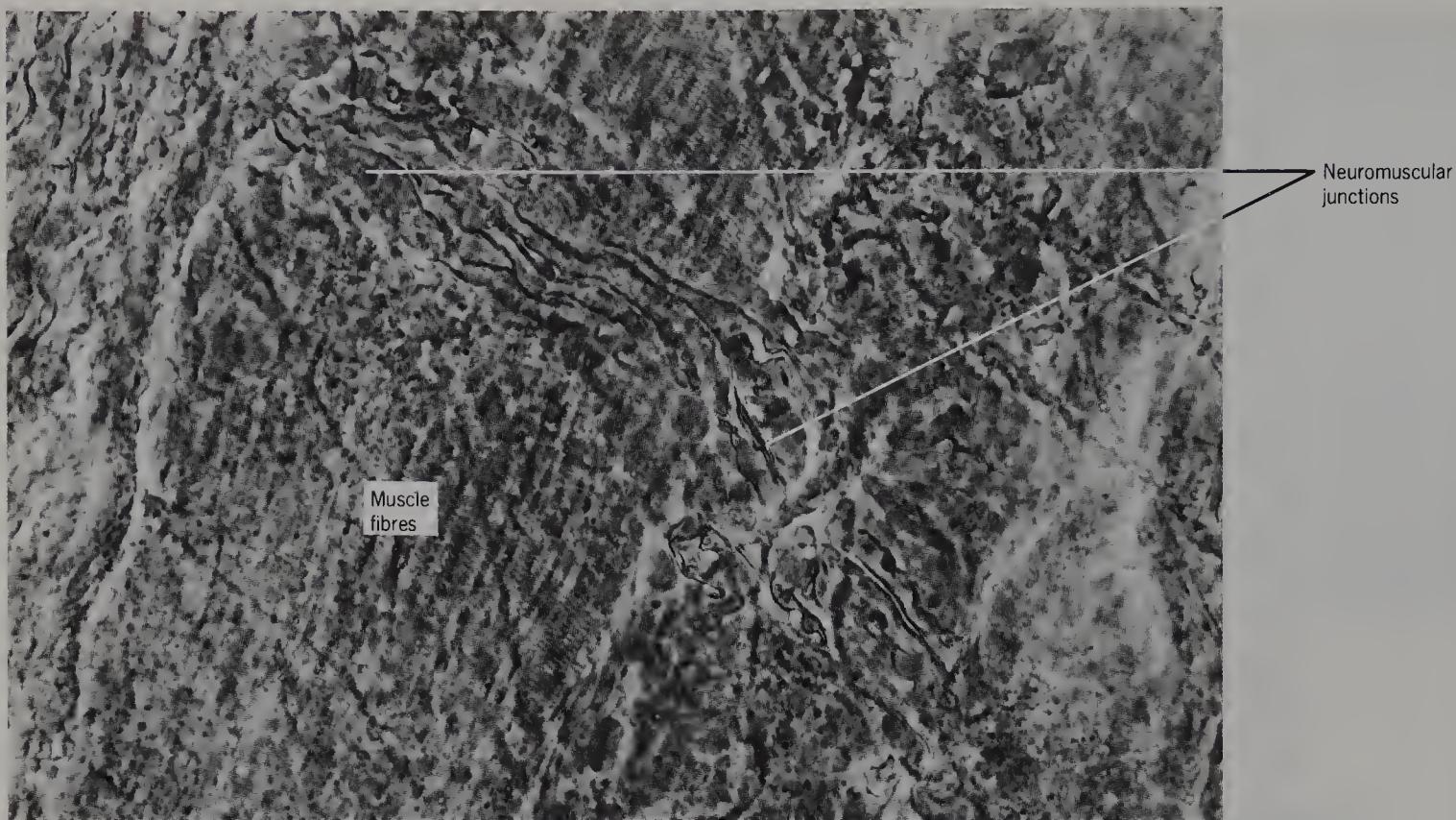


Figure 335 Thin slab of guinea-pig diaphragm including terminations of phrenic nerve, to show neuromuscular junctions (phase contrast, $\times 700$).

Neuromuscular junctions were first seen by Kuhne in 1862.

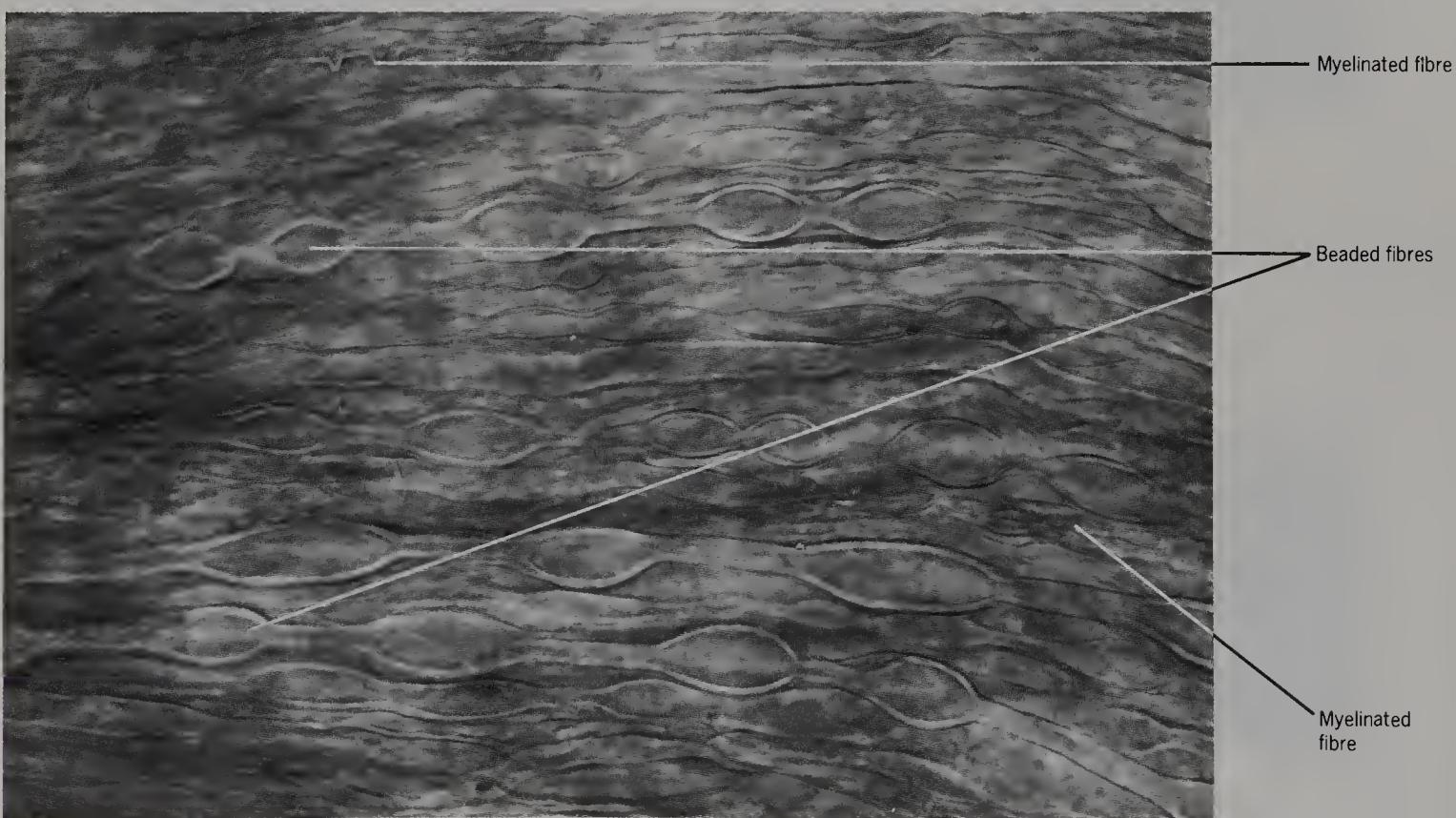


Figure 336 Unteased guinea-pig median nerve, to show beaded and myelinated fibres *in situ* (bright field, $\times 700$).

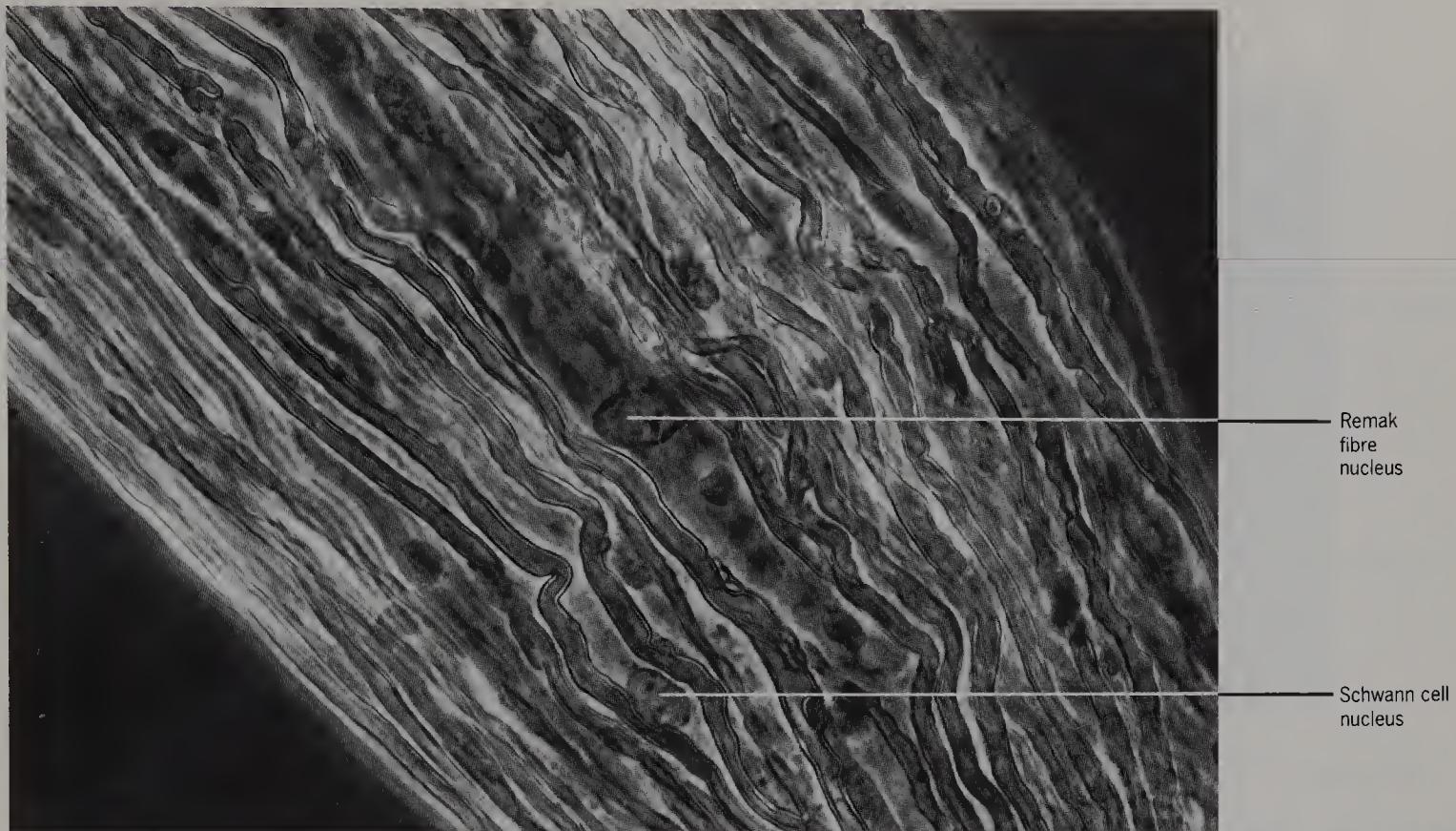


Figure 337 Partially teased 9-day-old mouse median nerve, to show developing myelinated nerve fibres and Schwann cells *in situ* (phase contrast, $\times 700$).

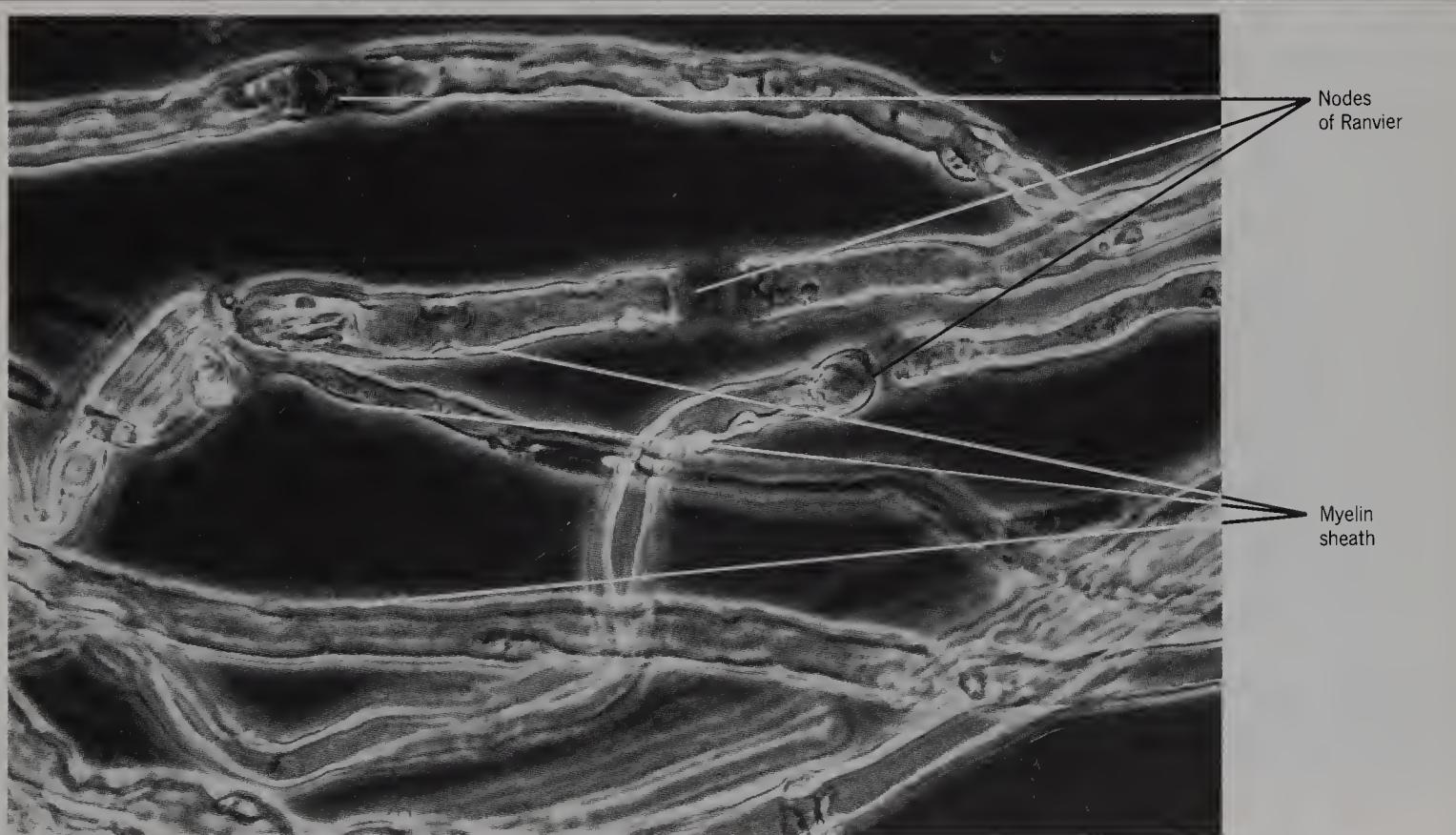


Figure 338 Isolated guinea-pig myelinated nerve fibres from median nerve (phase contrast, $\times 700$).

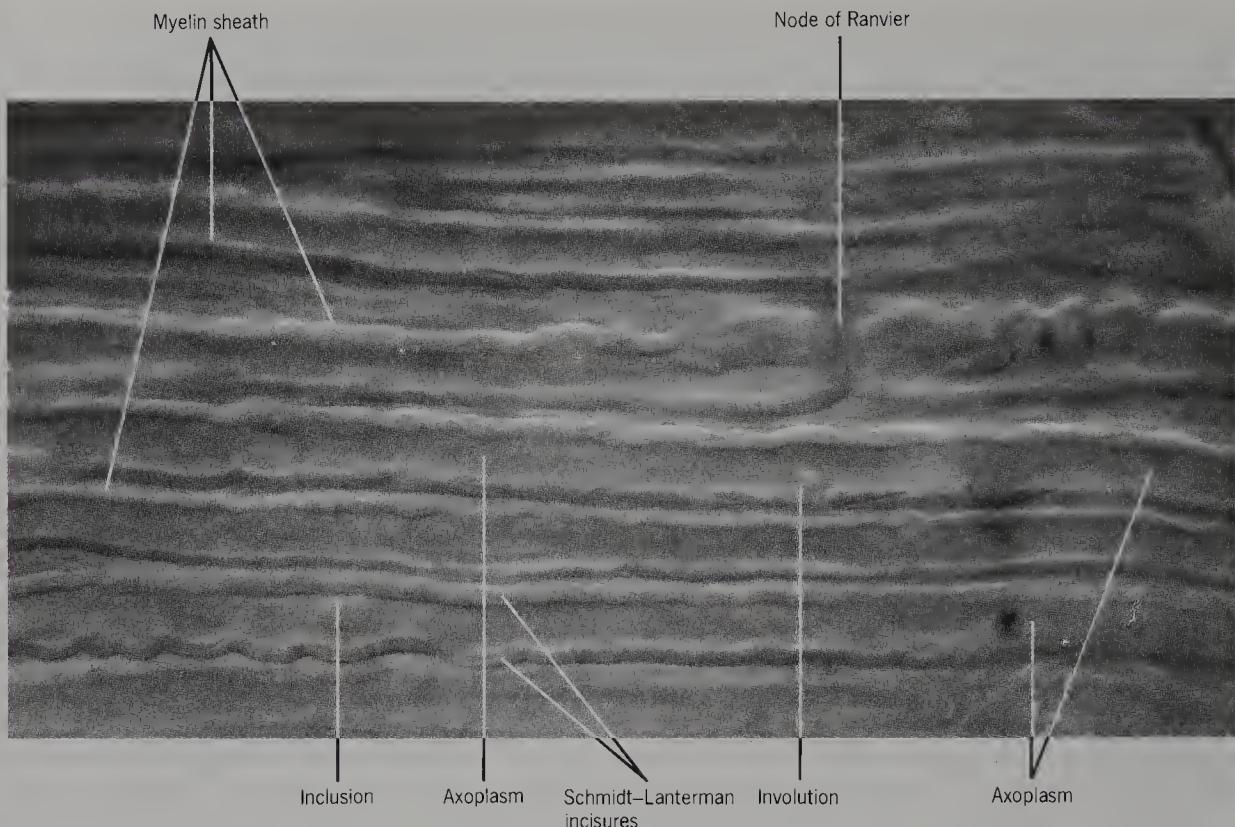


Figure 339 Sciatic nerve of a living mouse *in situ* (incident light, dark ground, $\times 1000$). (By kind permission of Dr S. Hall.)

Note the presence of narrow Schmidt–Lanterman incisures and intra-axonal inclusions (Williams and Hall, 1970).

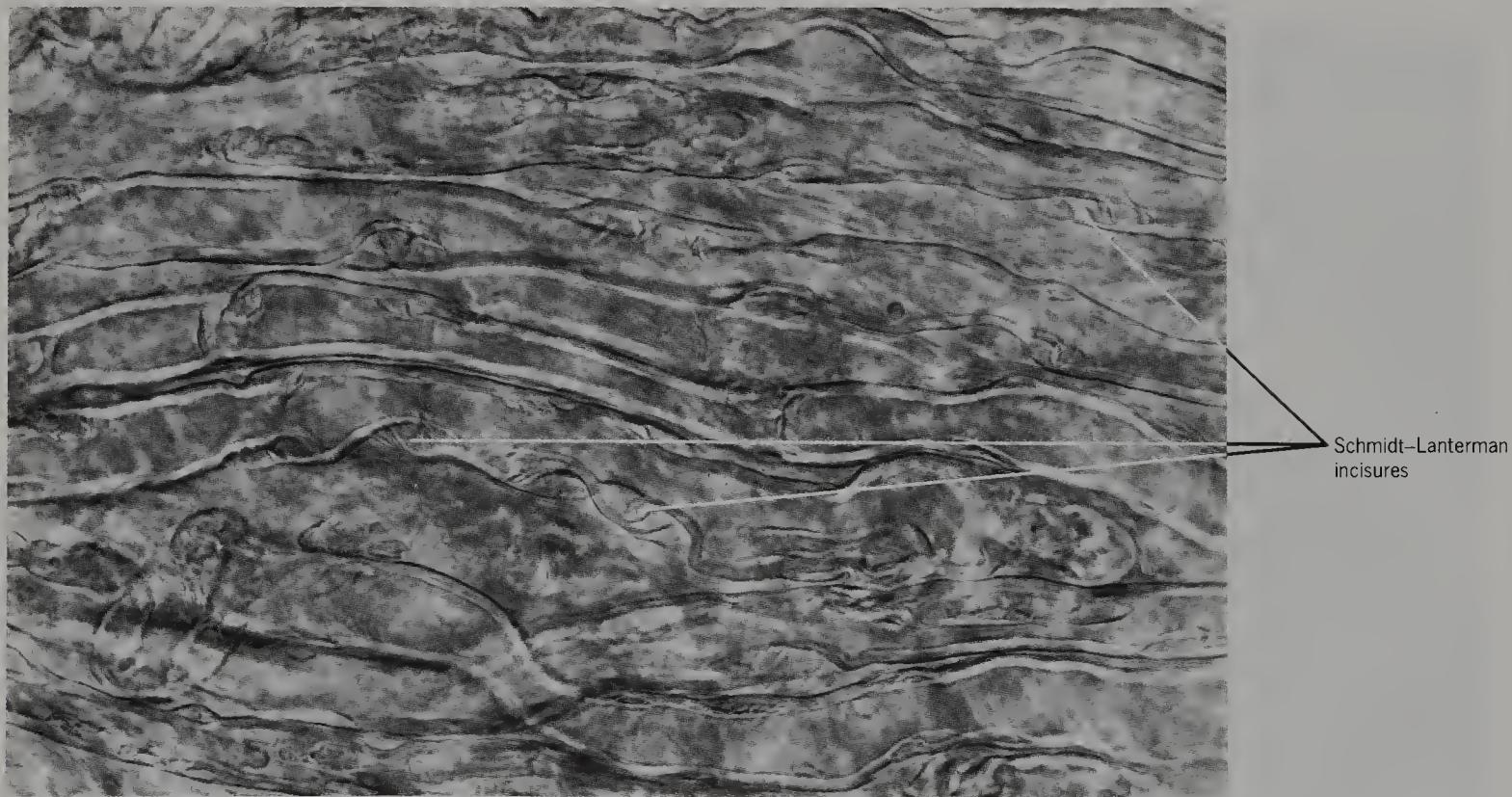


Figure 340 Unteased guinea-pig sciatic nerve, to show myelinated fibres (phase contrast, $\times 700$).

It will be seen by comparison with the previous figure that the Schmidt–Lanterman incisures were wider in the excised nerve than in the intact nerve. The incisures were originally seen in 1877 by Schmidt and Lanterman.

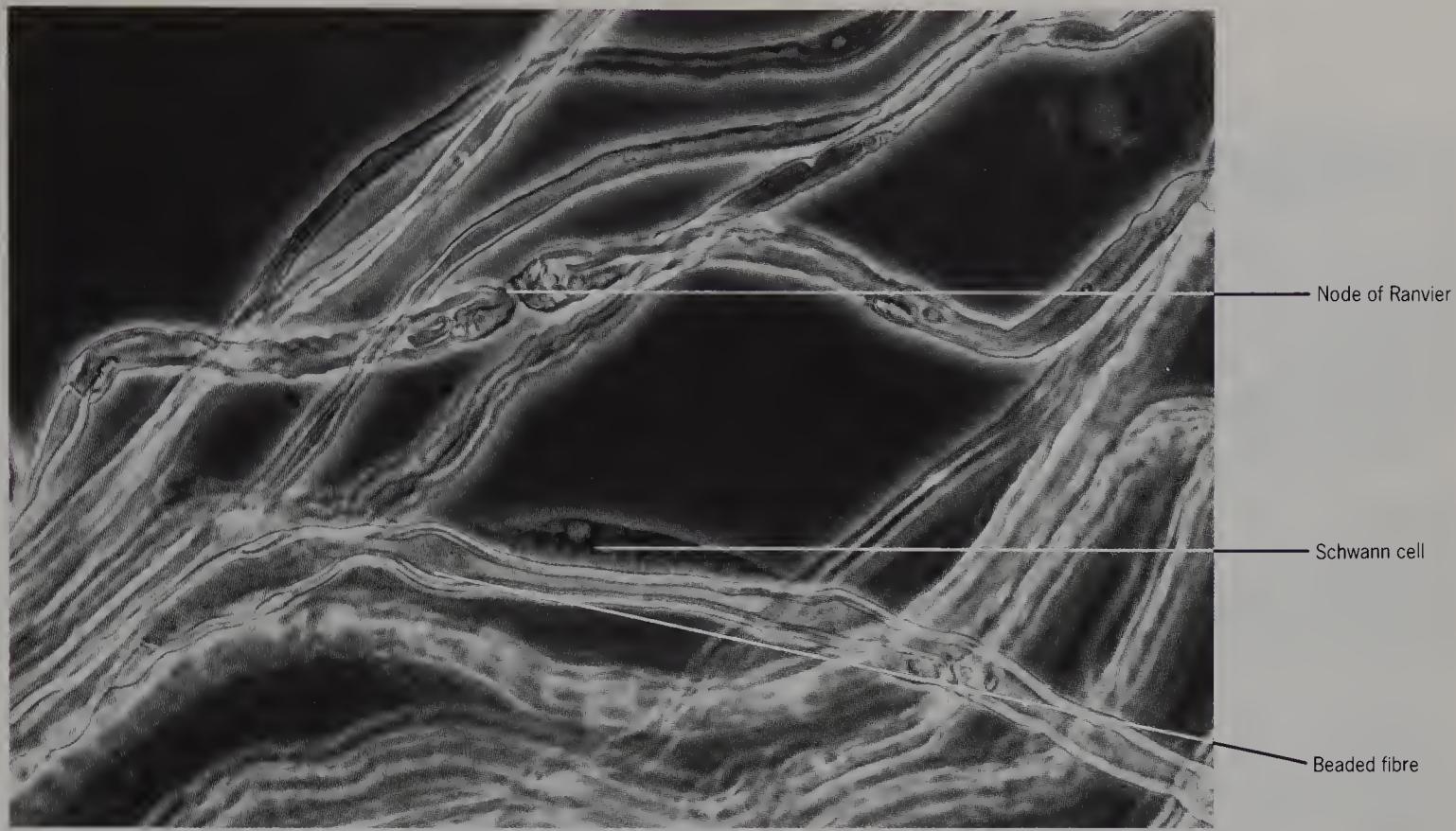


Figure 341 Teased 4-week-old rat sciatic nerve, to show myelinated nerve fibres and a Schwann cell (phase contrast, $\times 700$).

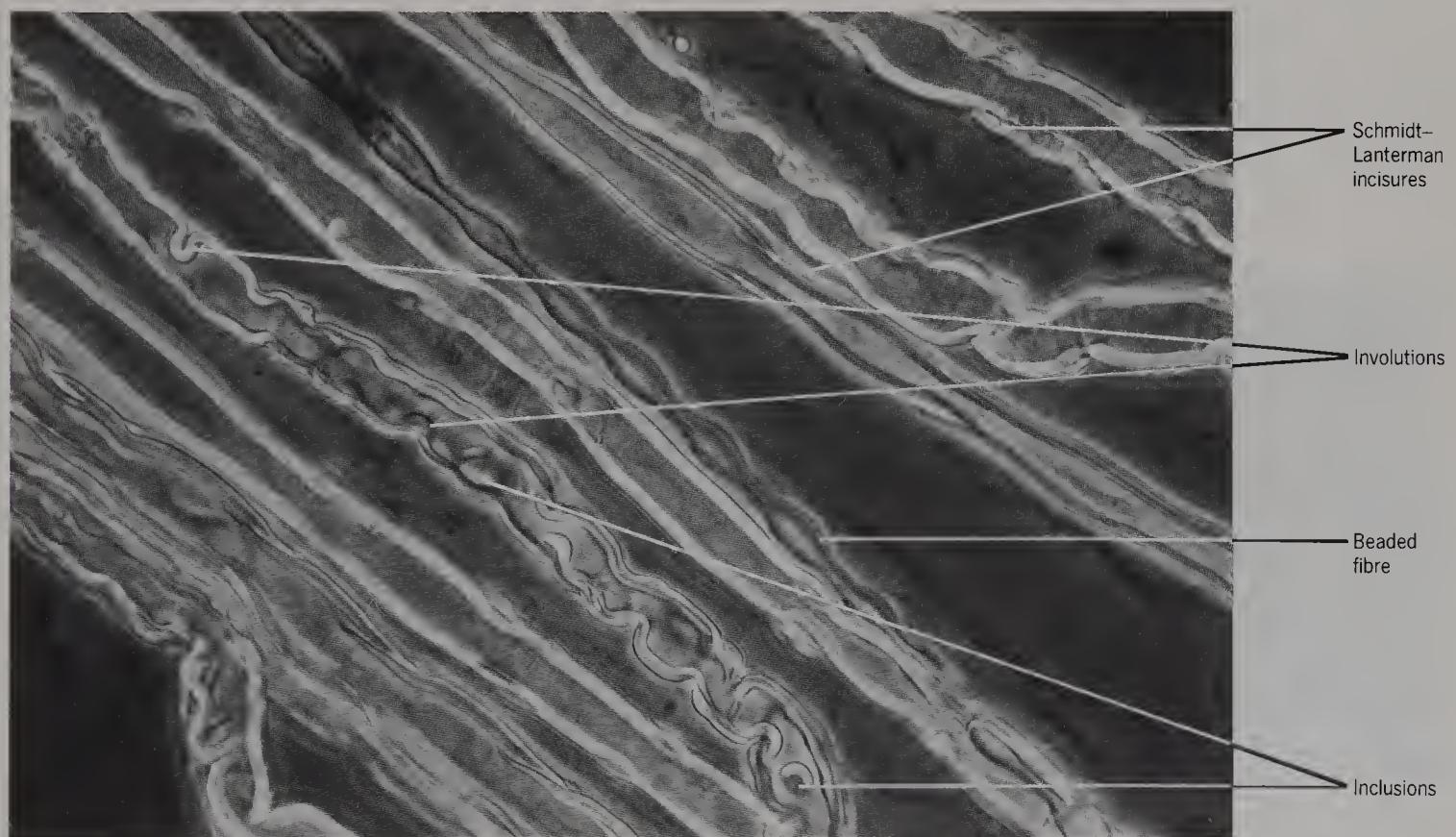


Figure 342 Teased rabbit sciatic nerve, to show beaded and myelinated nerve fibres and a Schwann cell (phase contrast, $\times 700$).

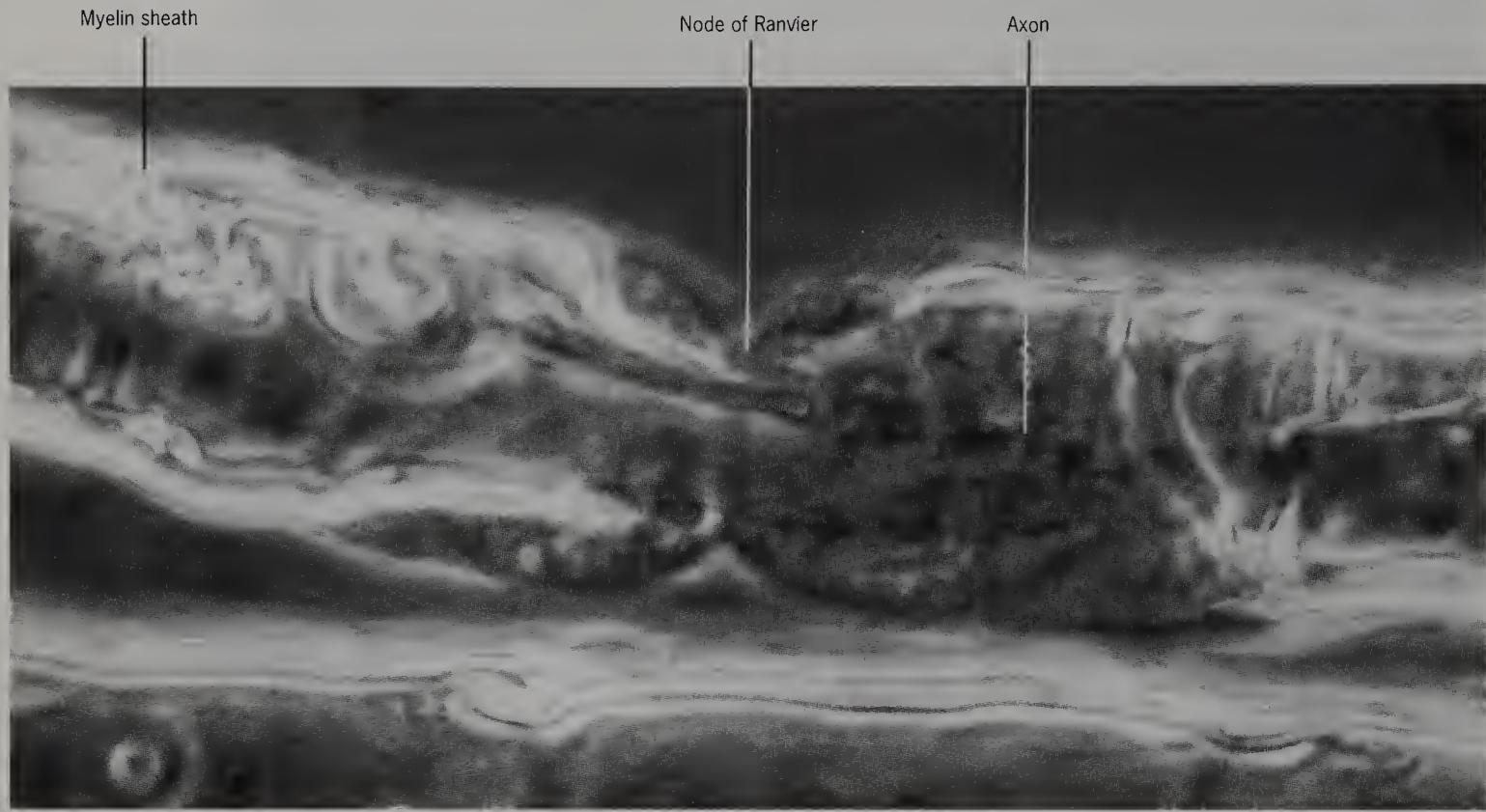


Figure 343 Isolated rabbit myelinated fibres from sciatic nerve, to show node of Ranvier (phase contrast, $\times 2000$). Note the central position of the axon.



Figure 344 Isolated rat myelinated fibre from the sciatic nerve, to show Schmidt-Lantermann incisure on one side and intra-axonal particles (phase contrast, $\times 1300$).

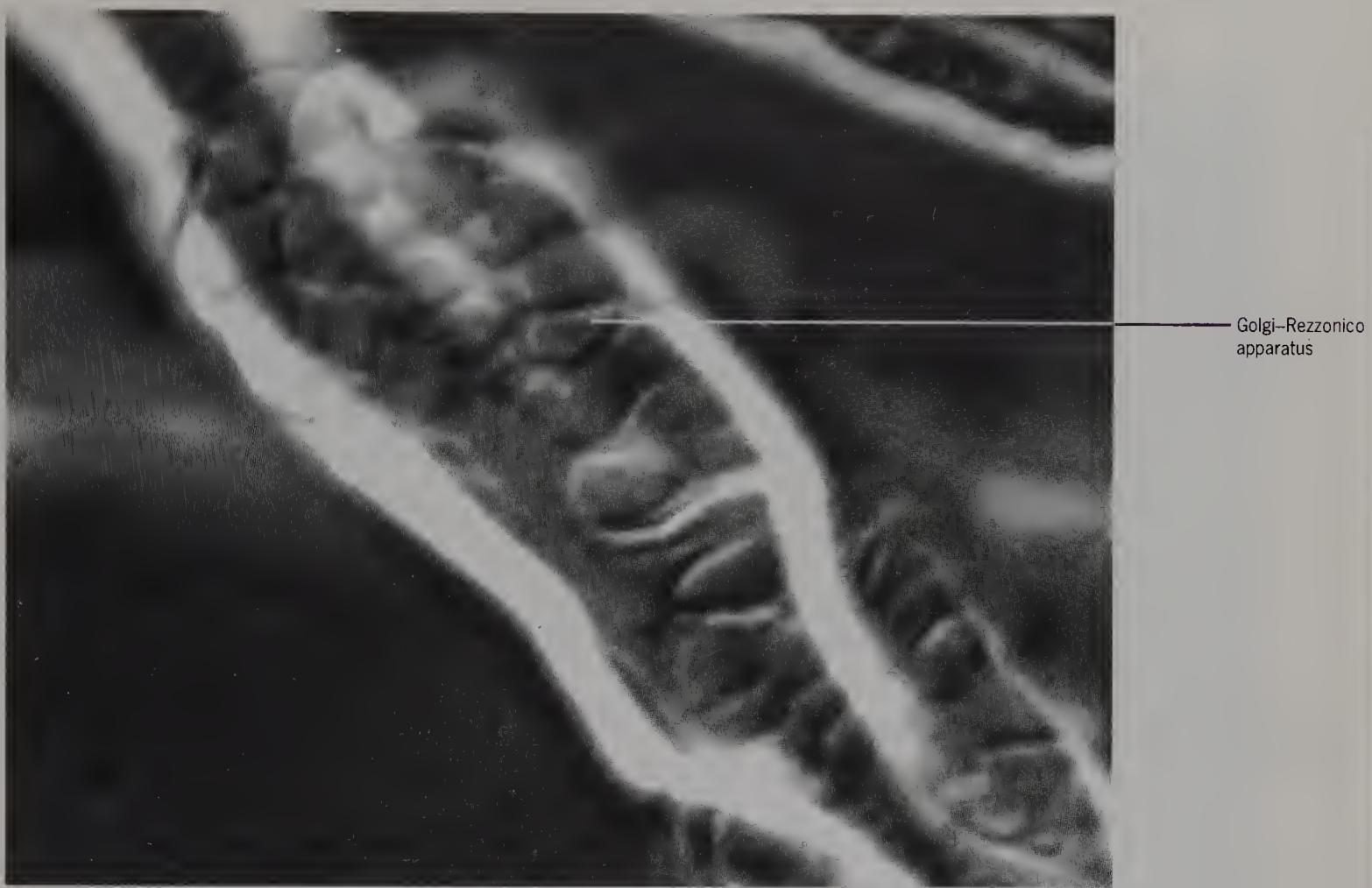


Figure 345 Isolated rabbit sciatic fibre, to show apparatus of Golgi–Rezzonico (Zeiss scanning differential interference contrast, $\times 4300$). (By kind permission of Miss P. Gunter, of Zeiss Oberkochen.)

This was first reported in 1881 by Golgi.

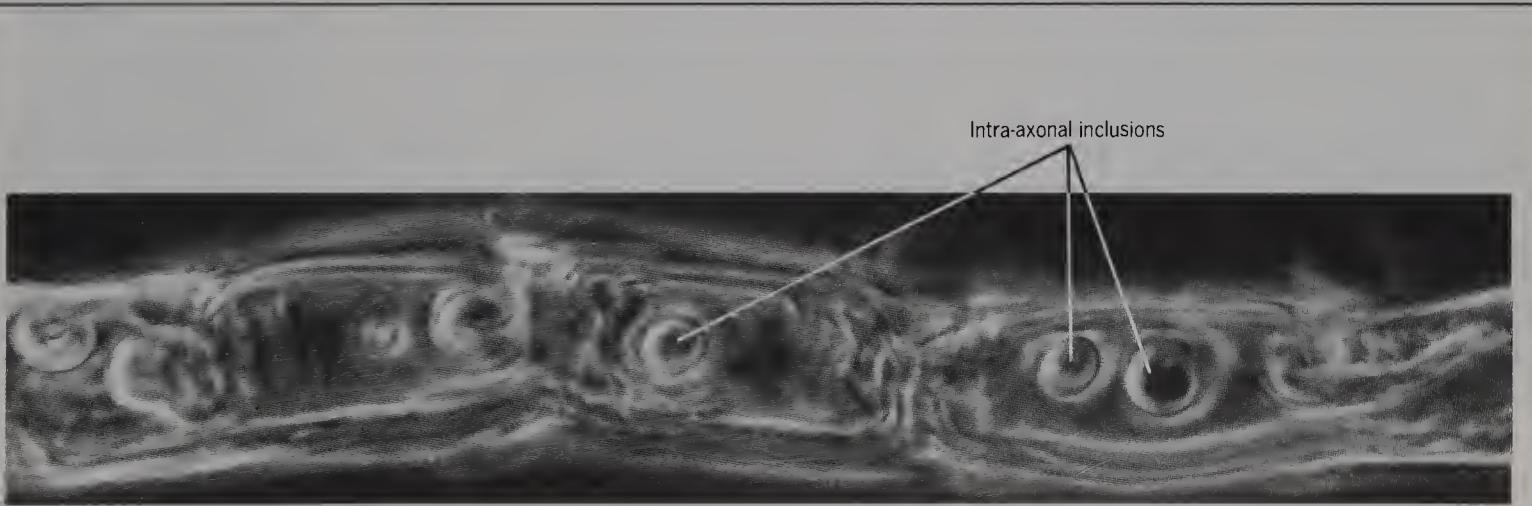


Figure 346 Isolated rabbit myelinated fibre from the sciatic nerve, to show intra-axonal inclusions (phase contrast, $\times 800$).

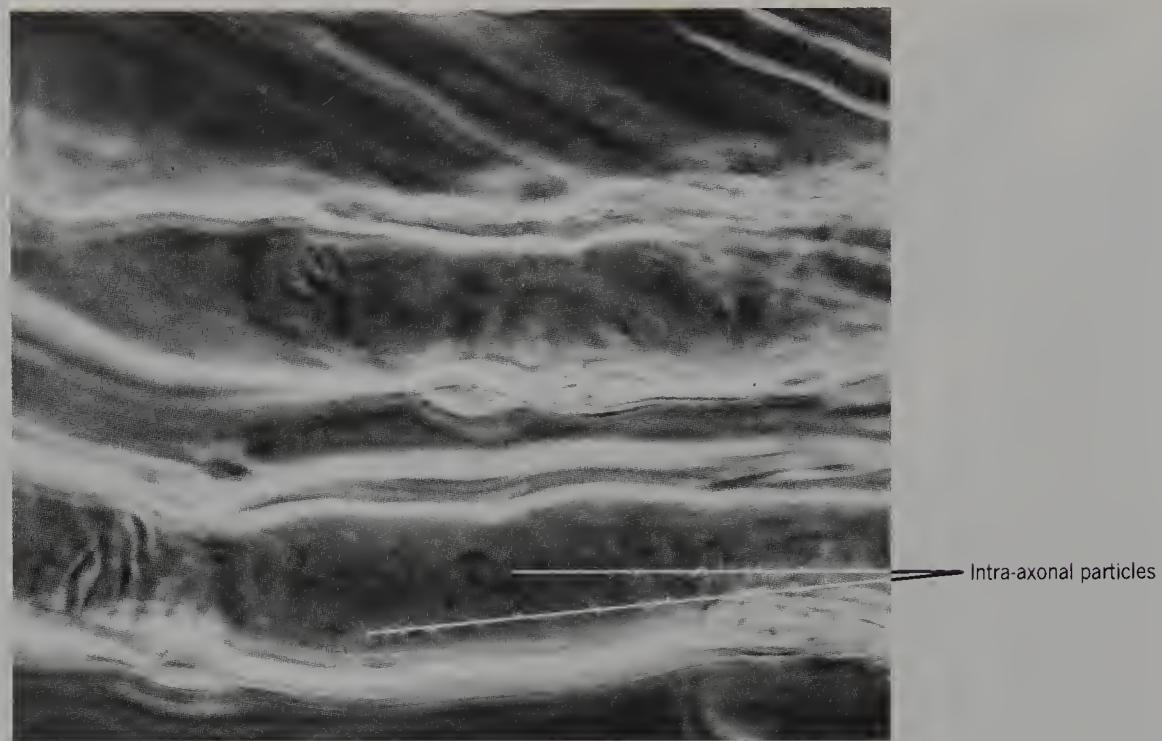


Figure 347 Isolated rabbit myelinated fibres from the sciatic nerve to show intra-axonal particles (phase contrast, $\times 1300$).
Particles can be seen moving in fresh axons.

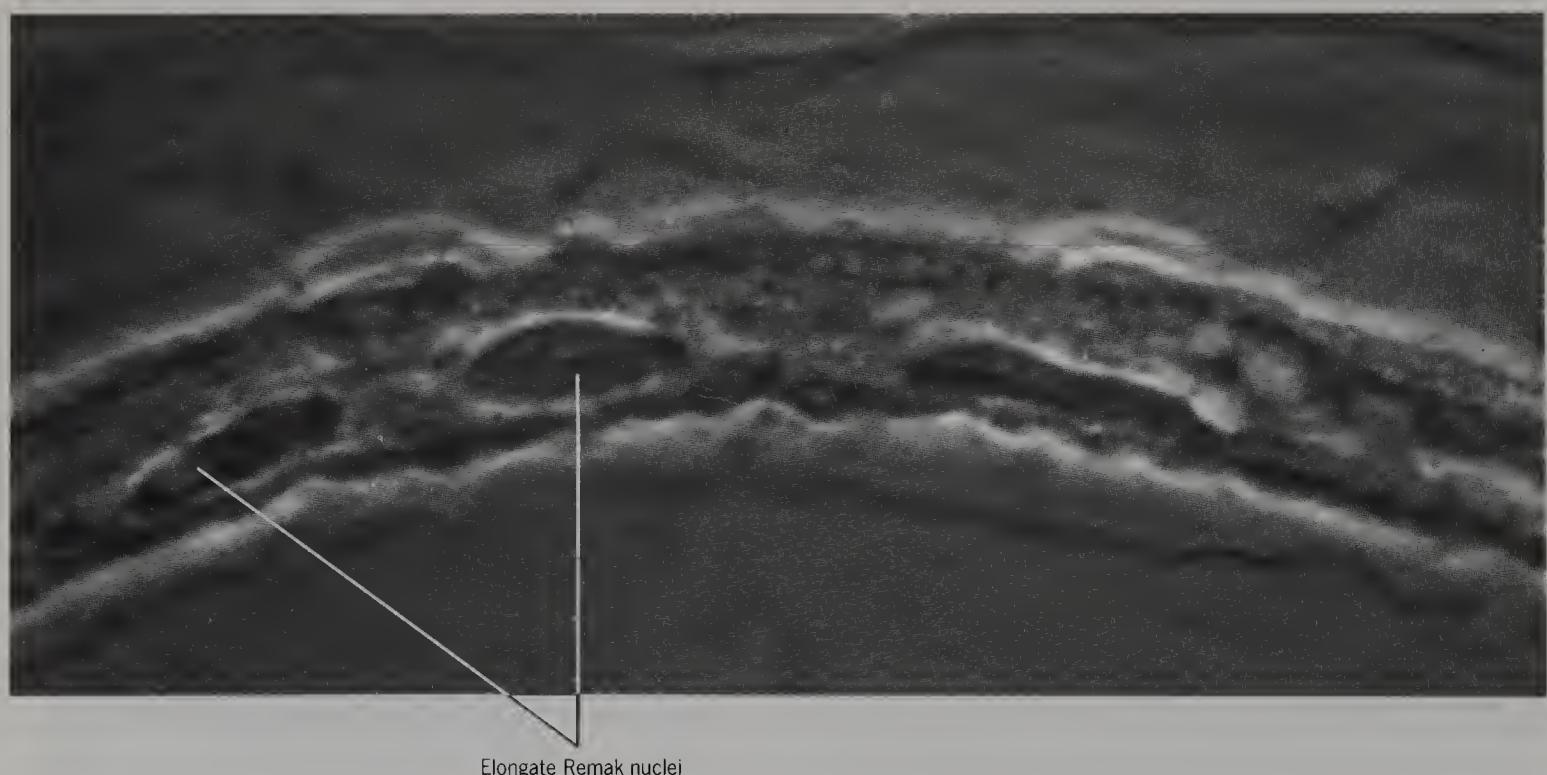


Figure 348 Isolated Remak fibre from rabbit sciatic nerve (phase contrast, $\times 2000$).

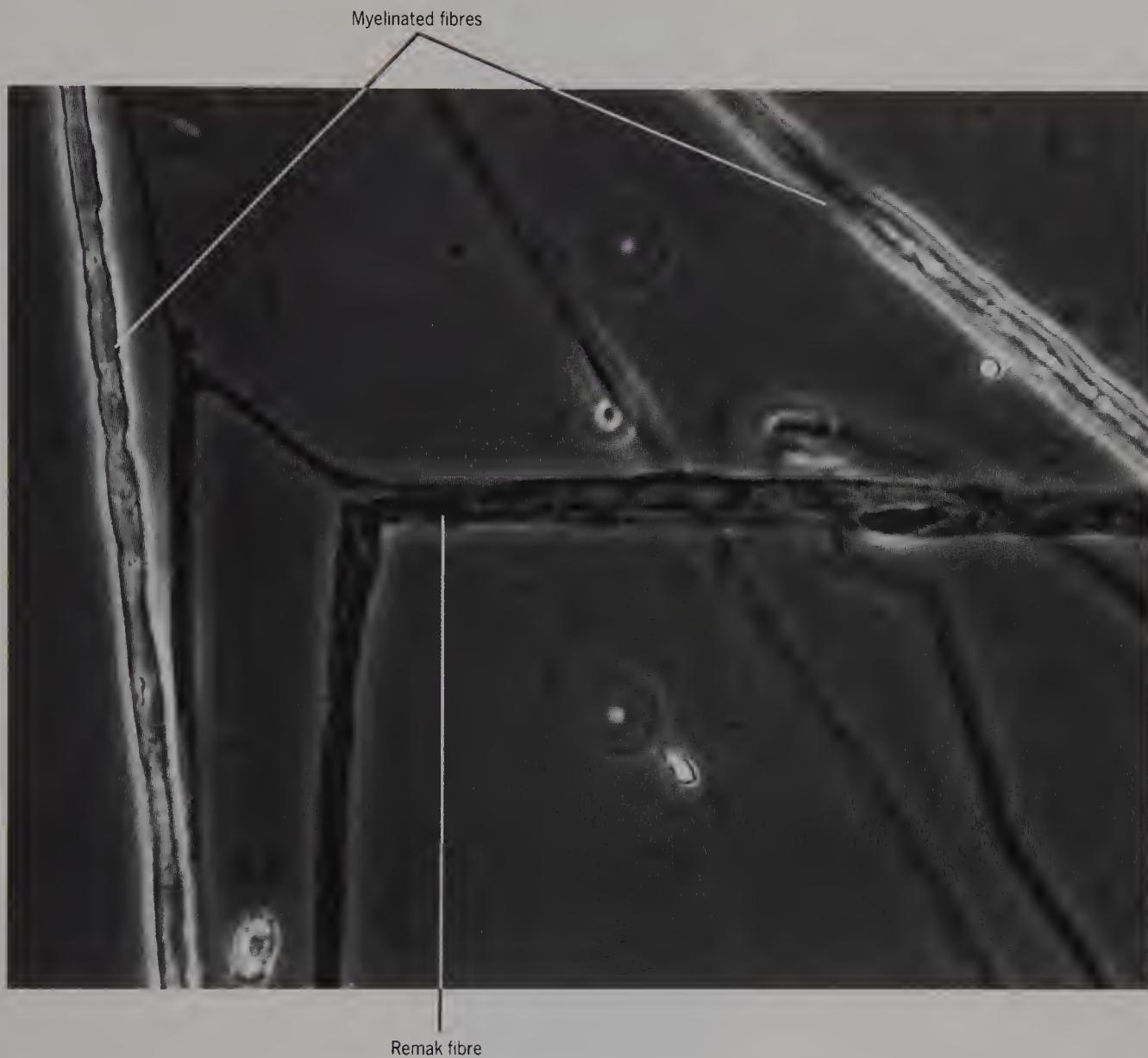


Figure 349 Teased rabbit sural nerve to show myelinated and Remak fibres (phase contrast, $\times 800$).

Note the branching of the Remak fibre.

SECTION**9****PITUITARY, PINEAL AND
ADRENAL GLANDS**

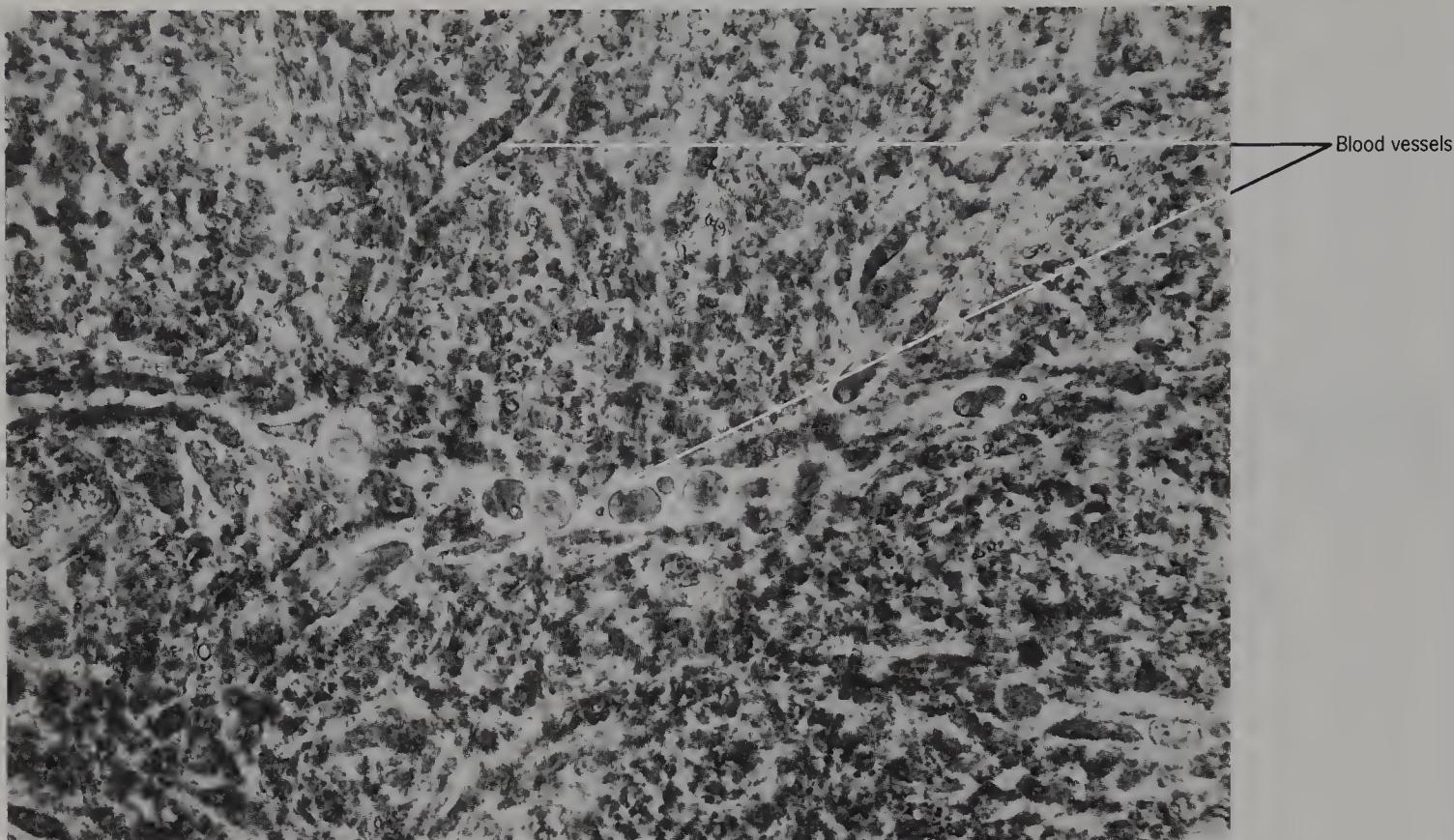


Figure 350 Unteased human posterior pituitary gland from a 73-year-old male, to show blood vessels *in situ* (phase contrast, $\times 700$).

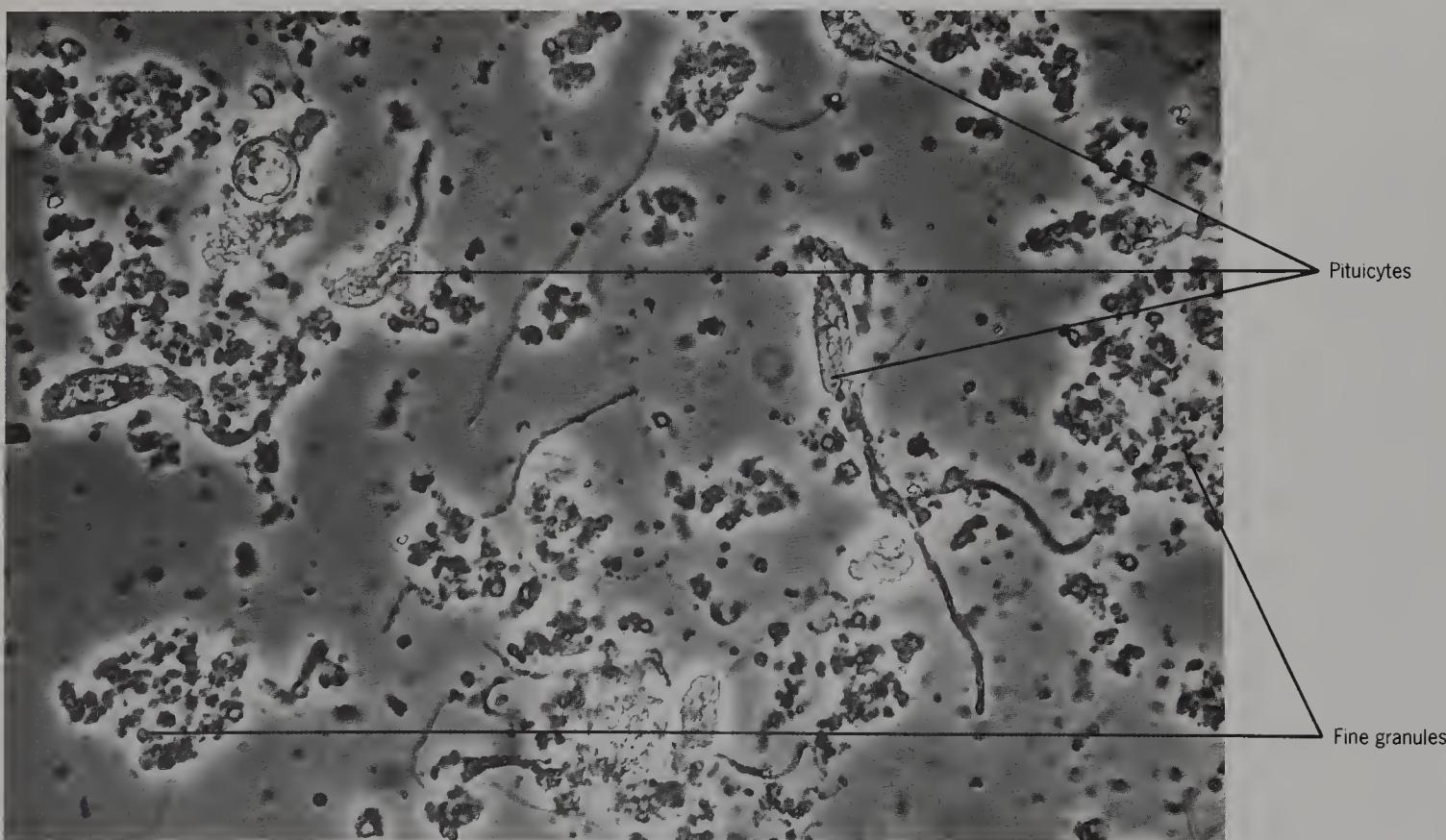


Figure 351 Isolated human pituicytes from the posterior lobe of a 73-year-old male; fine granules can also be seen (phase contrast, $\times 700$).

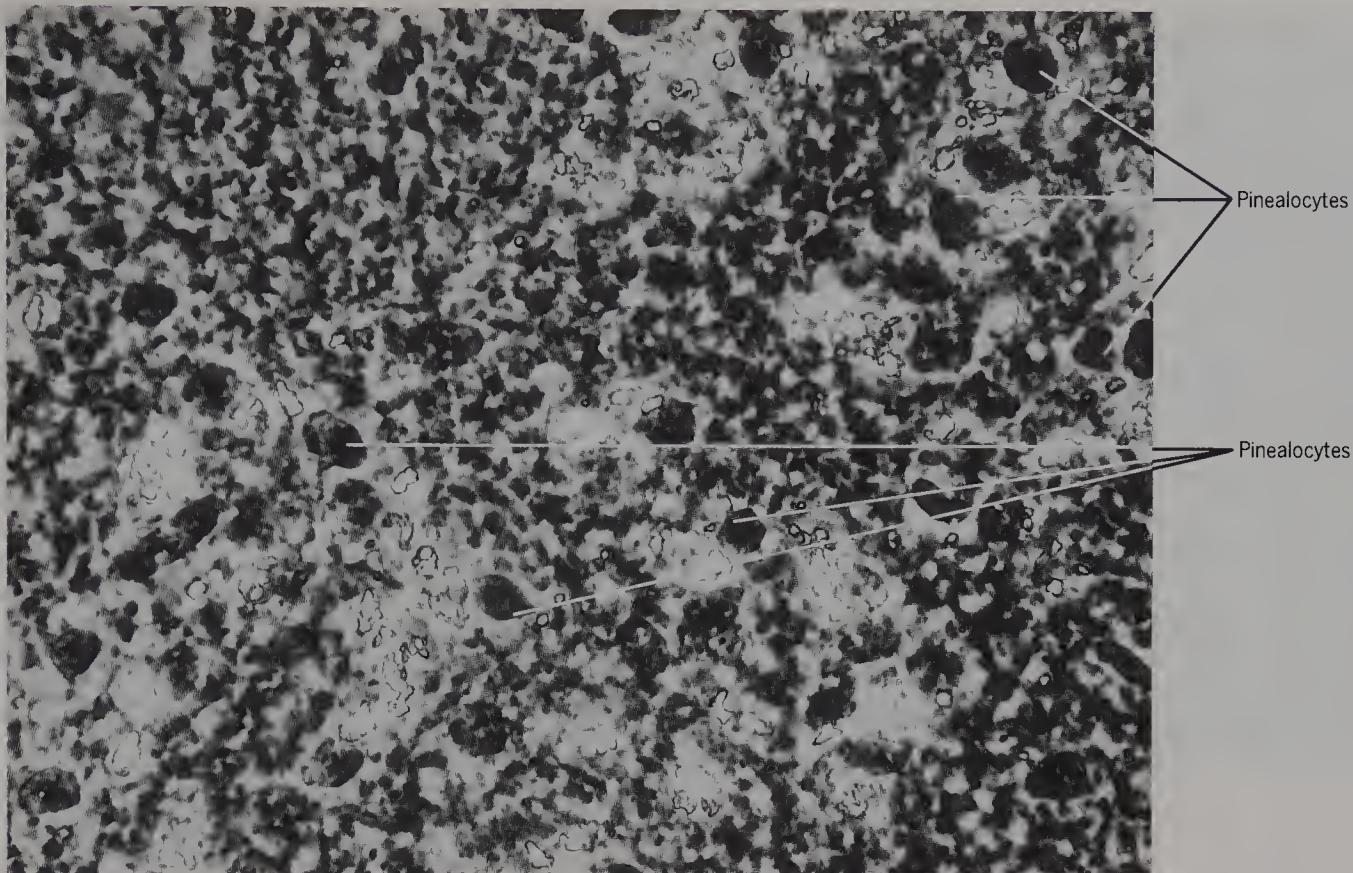


Figure 352 Thin slab of human pineal gland from a 66-year-old male, showing pinealocytes *in situ* (phase contrast, $\times 700$).

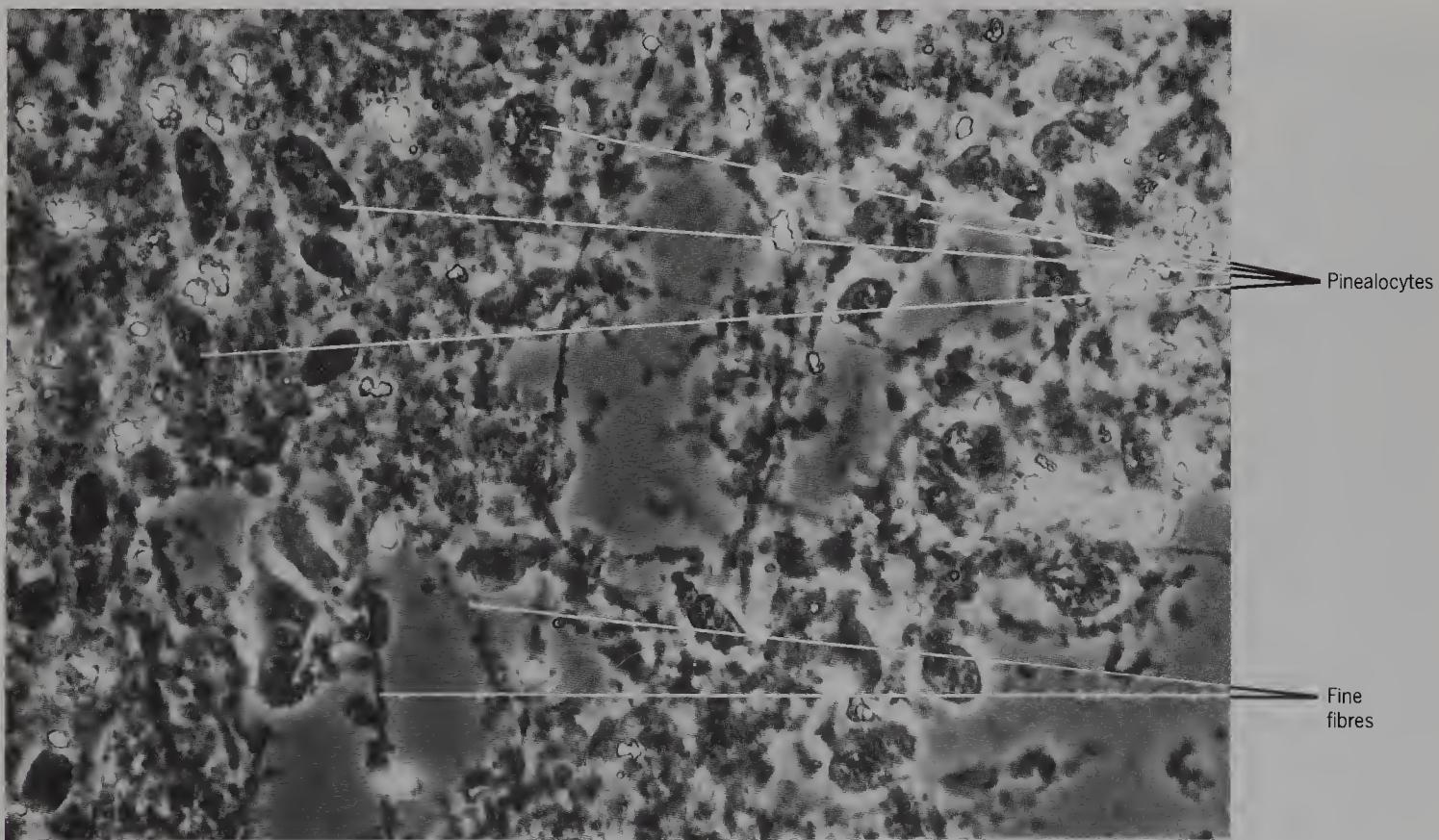


Figure 353 Partially teased human pineal gland from a 66-year-old male, to show pinealocytes, fine nerve fibres and fine granular material (phase contrast, $\times 700$).

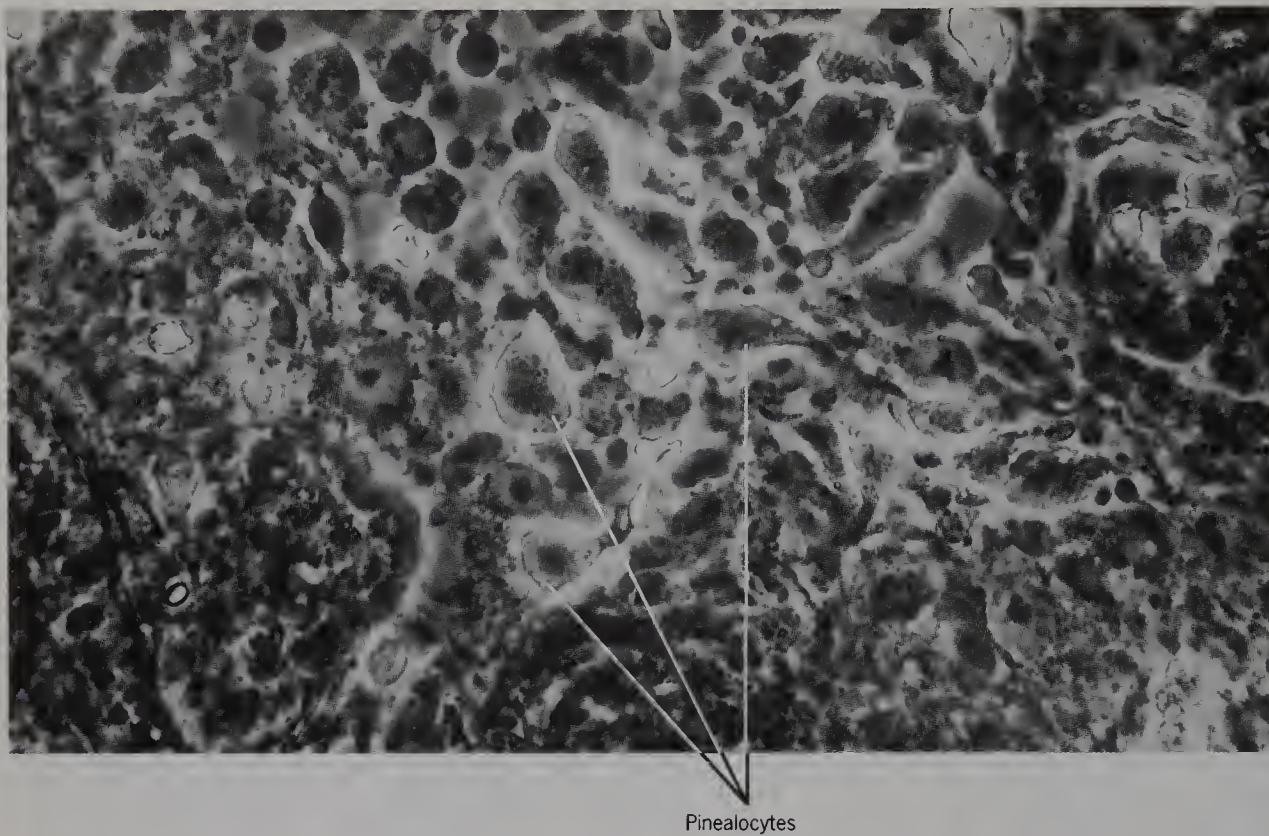


Figure 354 Partially teased guinea-pig pineal gland, to show pinealocytes (phase contrast, $\times 700$).

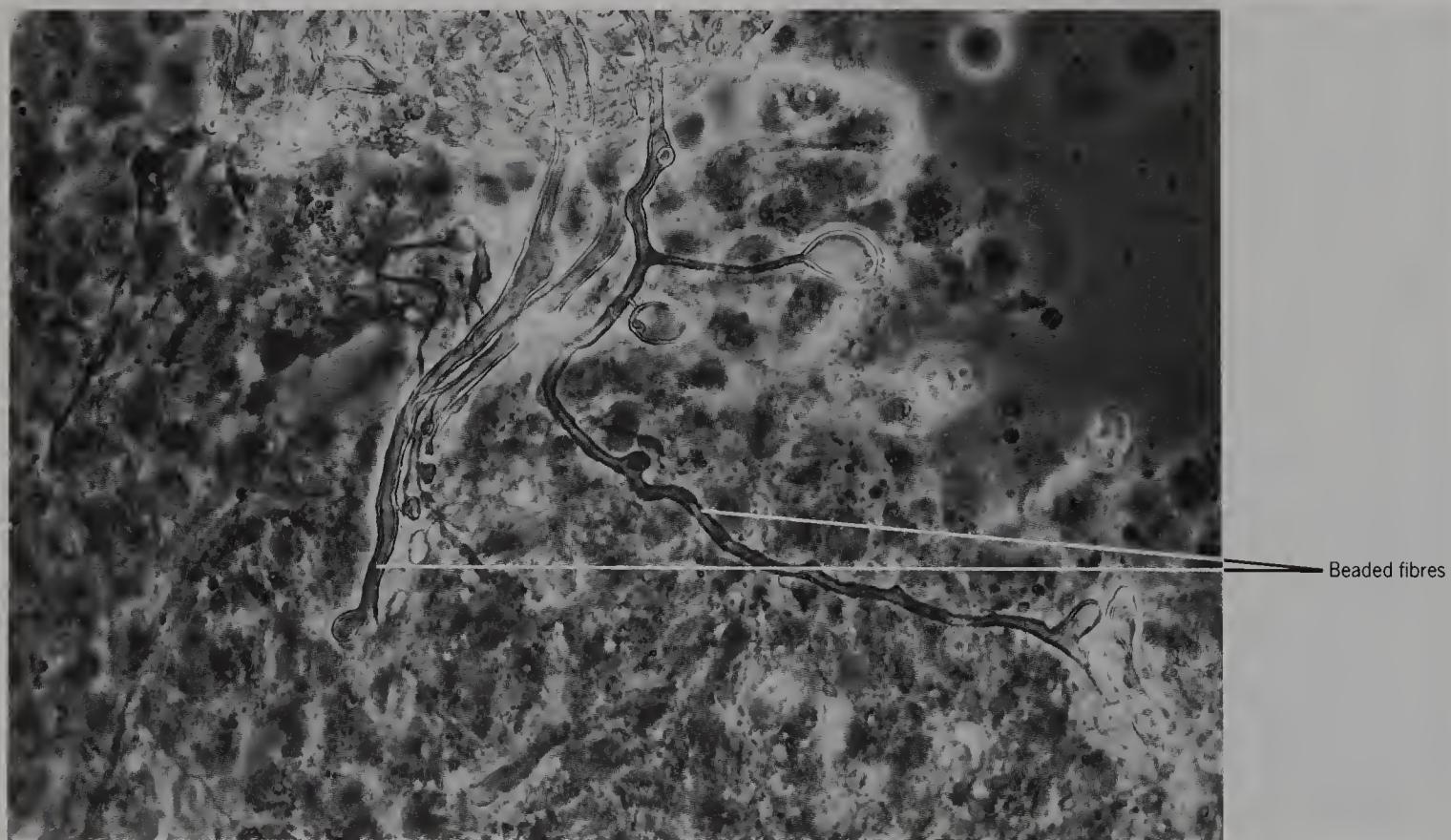


Figure 355 Partially teased guinea-pig pineal stalk, lower end, to show beaded fibres and endings (phase contrast, $\times 700$).

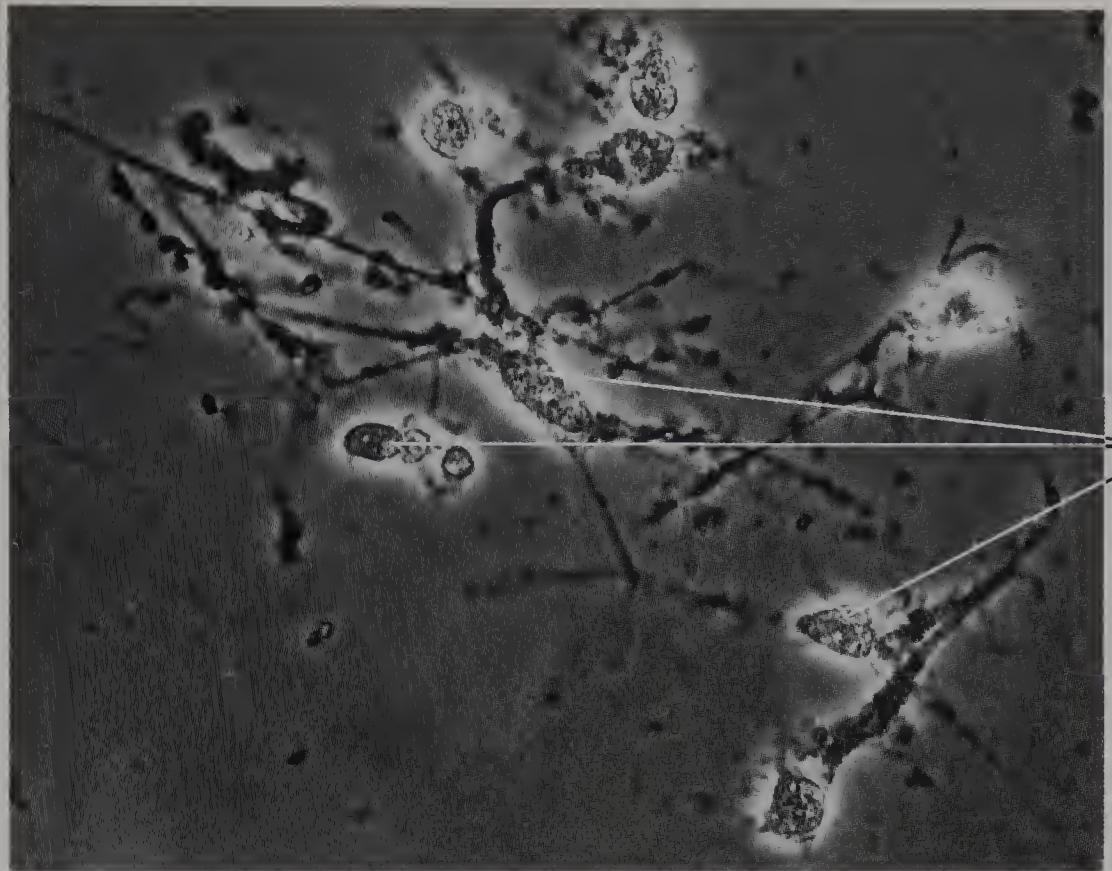


Figure 356 Isolated human pinealocytes from a 66-year-old male (phase contrast, $\times 700$).

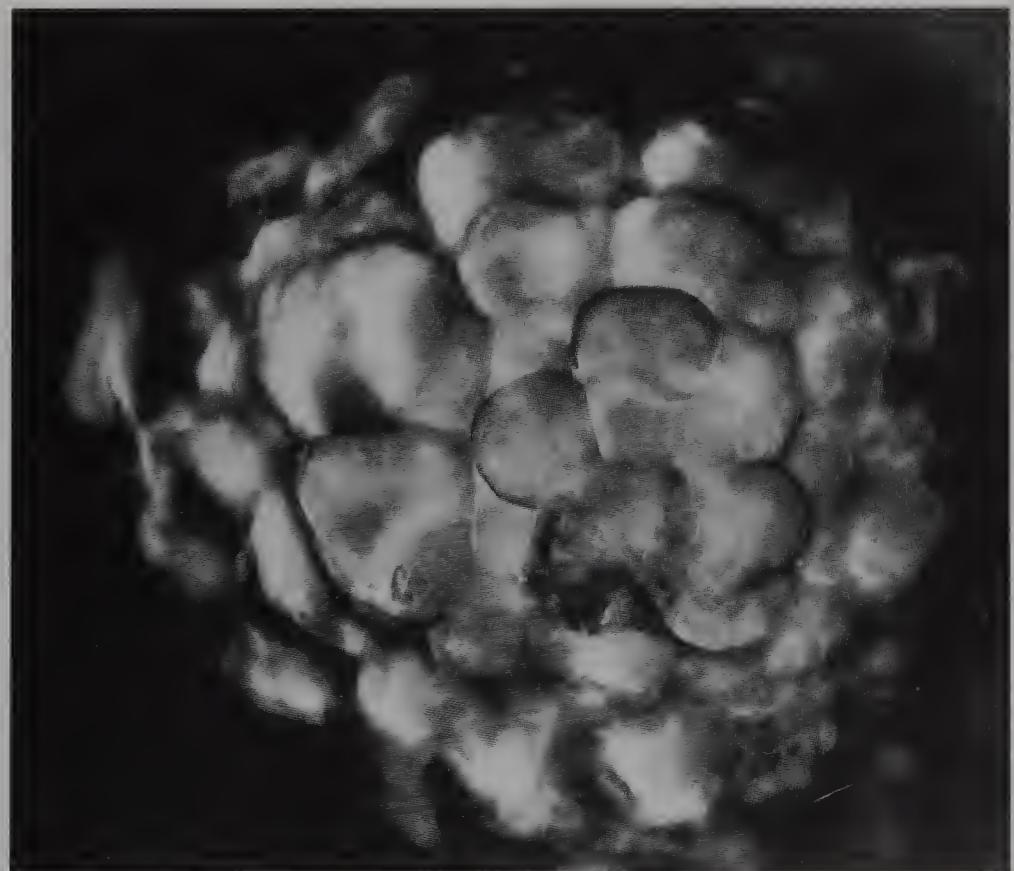


Figure 357 Brain sand from the previous specimen (phase contrast, $\times 335$).

This is composed of the calcium salts, hydroxyapatite, laid down in lamellae. It provides a landmark for the position of the pineal gland in radiographs.

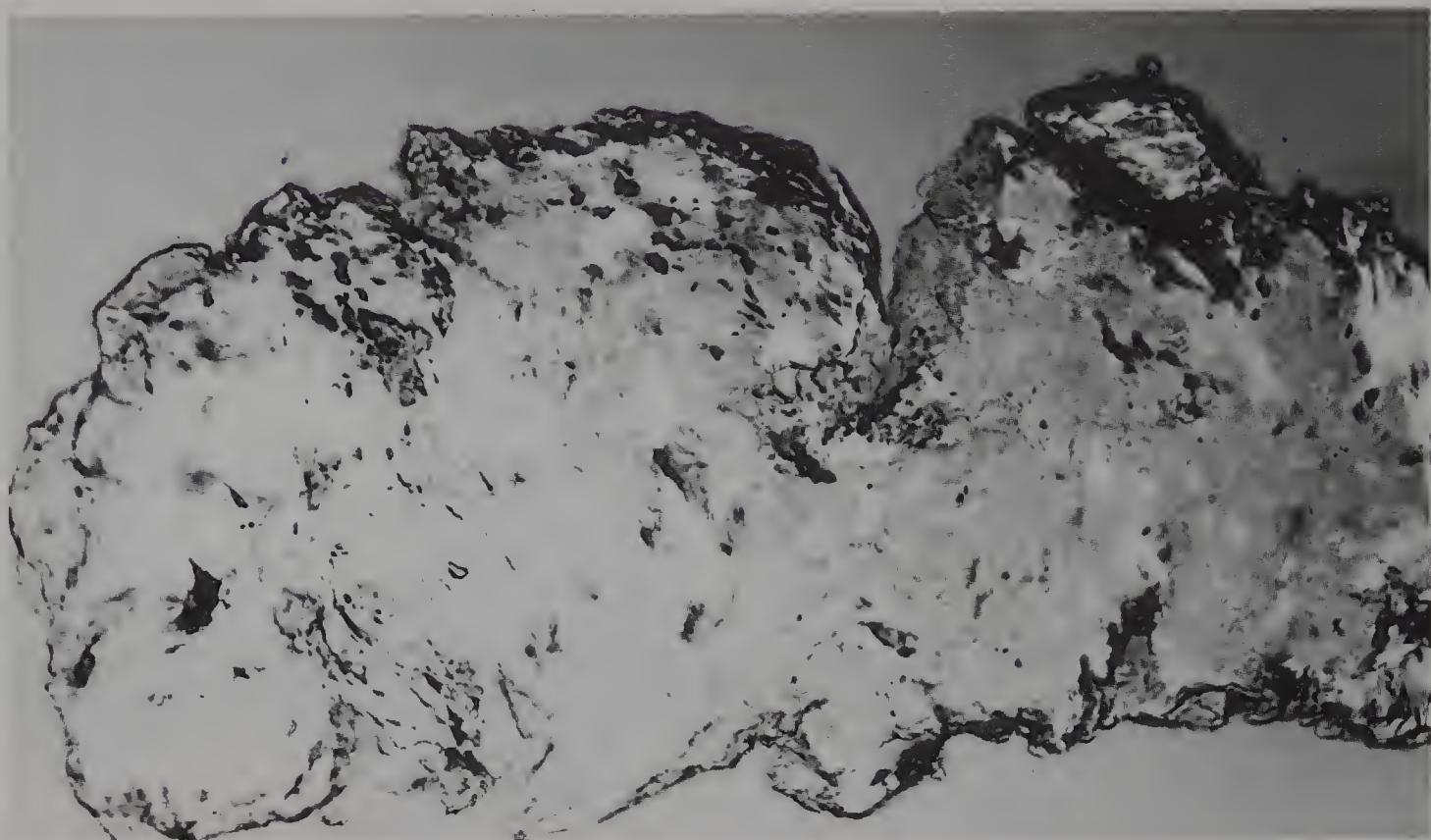


Figure 358 Another piece of human brain sand (bright field, $\times 800$).

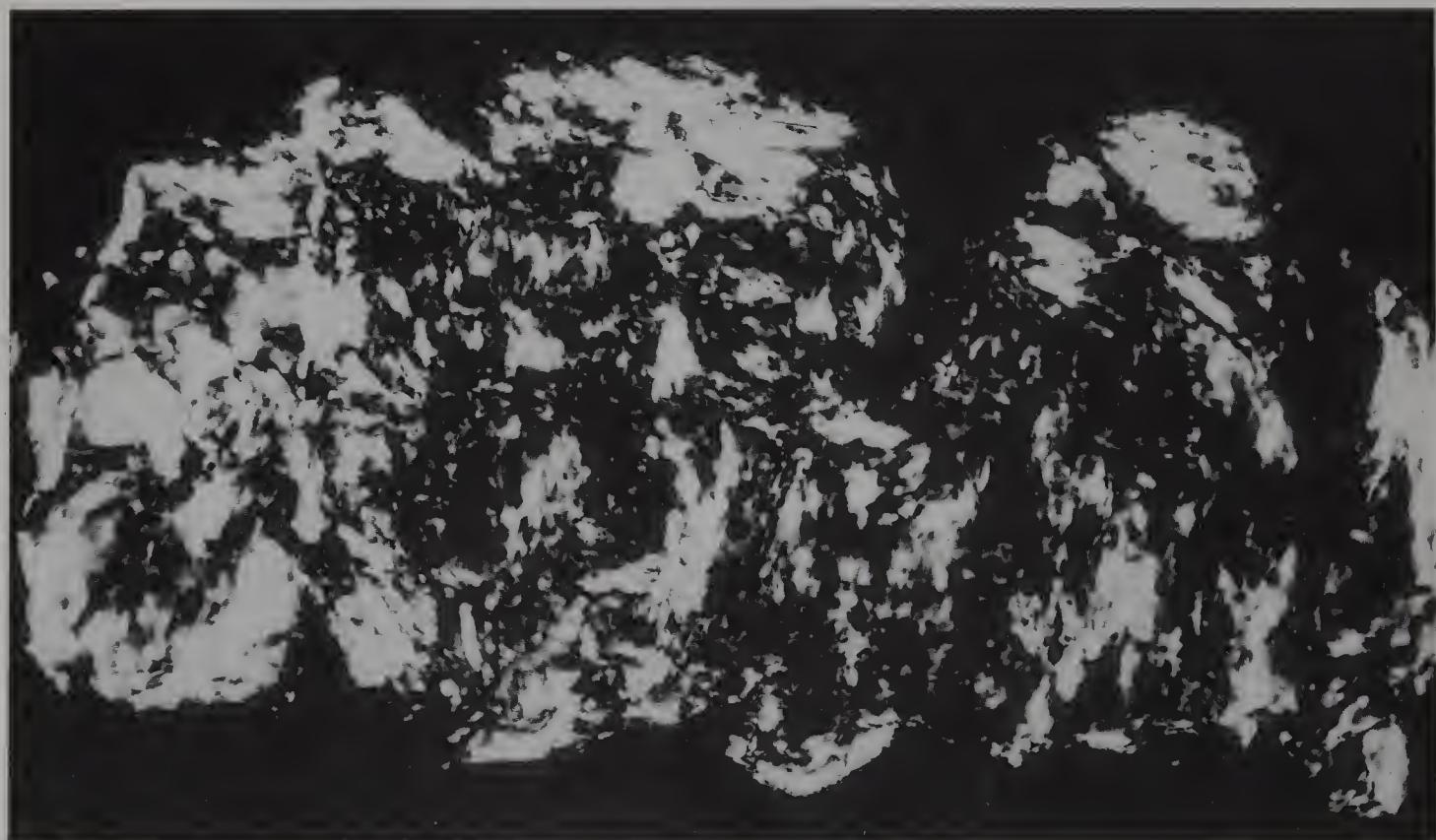


Figure 359 The same piece of brain sand as in the previous figure, but viewed through cross polars to show its birefringence ($\times 800$).

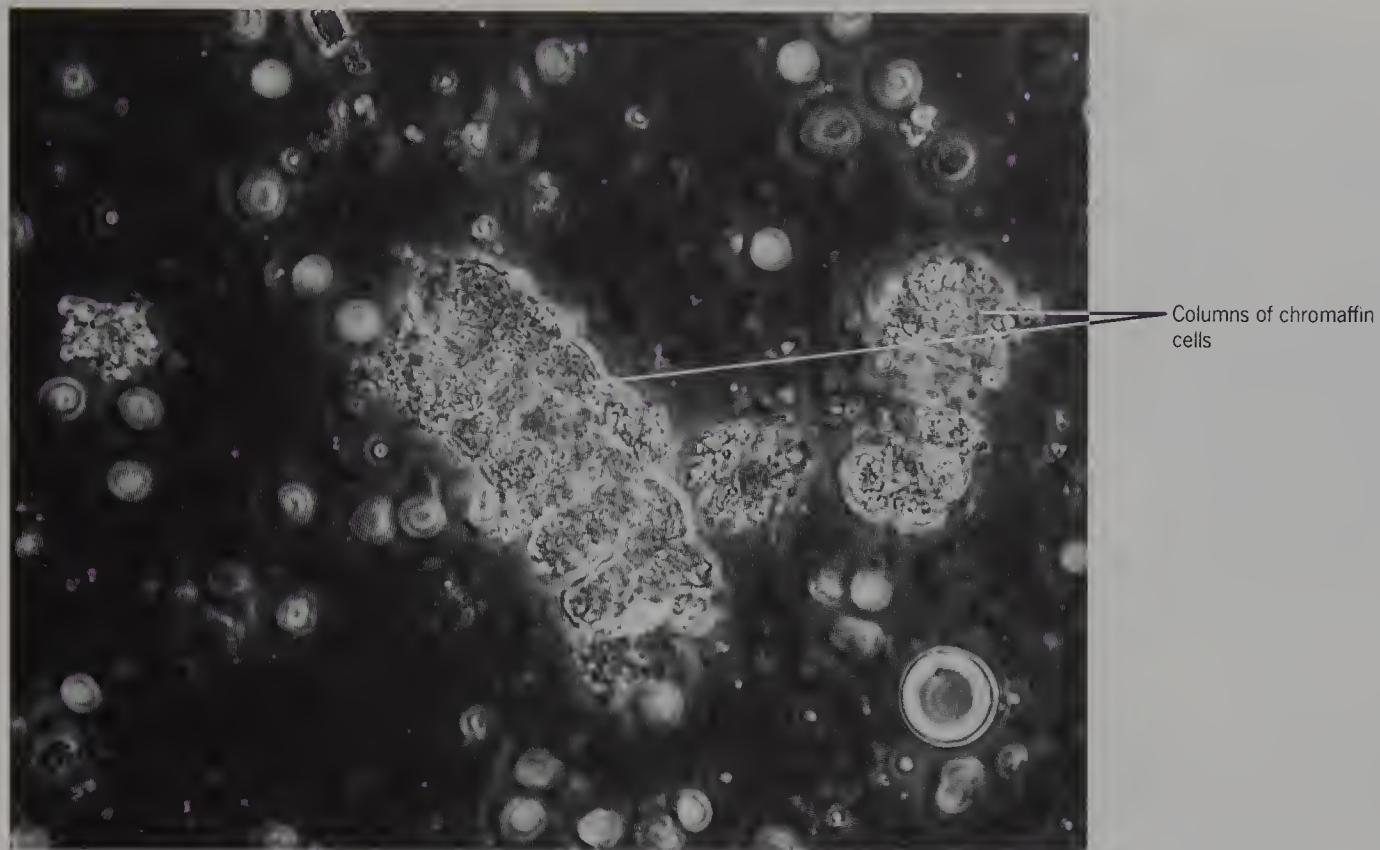


Figure 360 Partially teased rabbit adrenal medulla to show chromaffin cells in columns (phase contrast, $\times 700$).

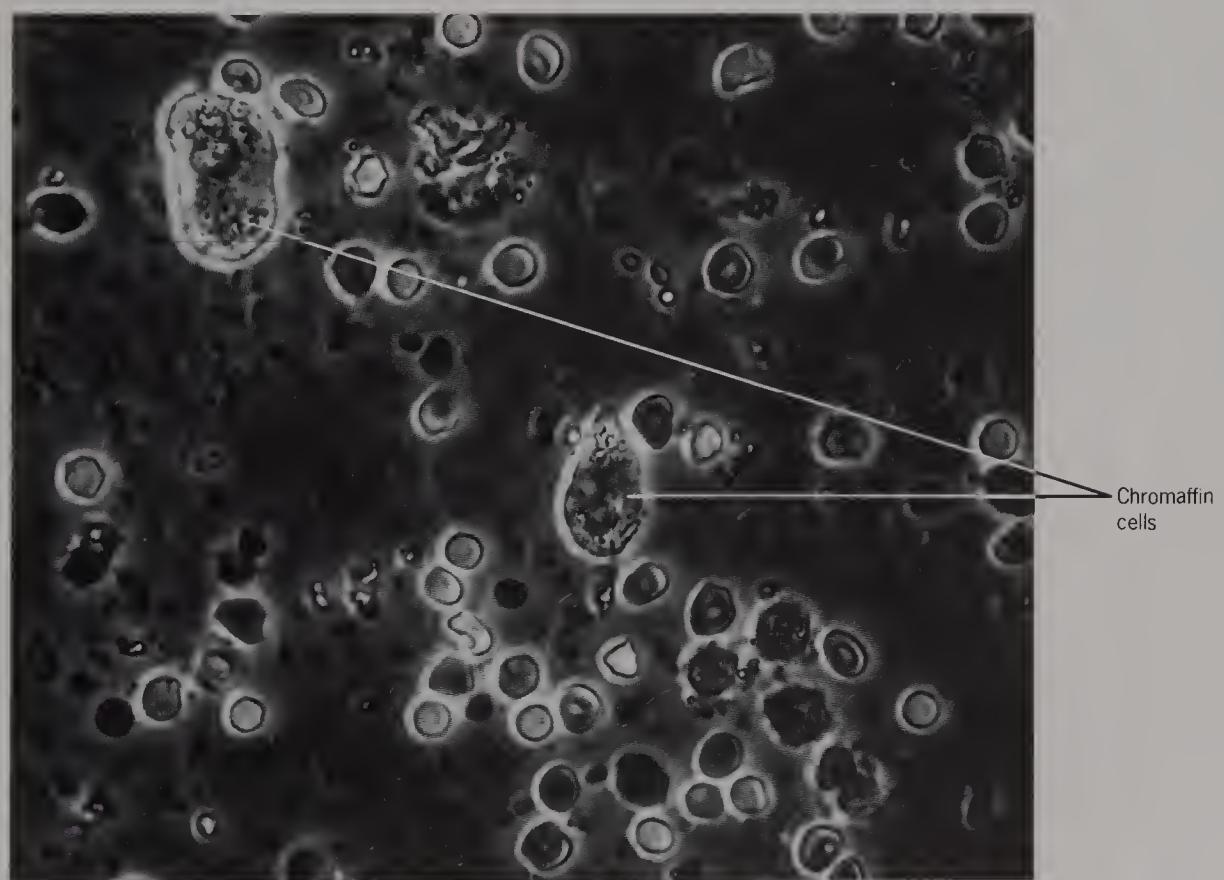


Figure 361 Teased rabbit adrenal medulla to show chromaffin cells (phase contrast, $\times 700$).

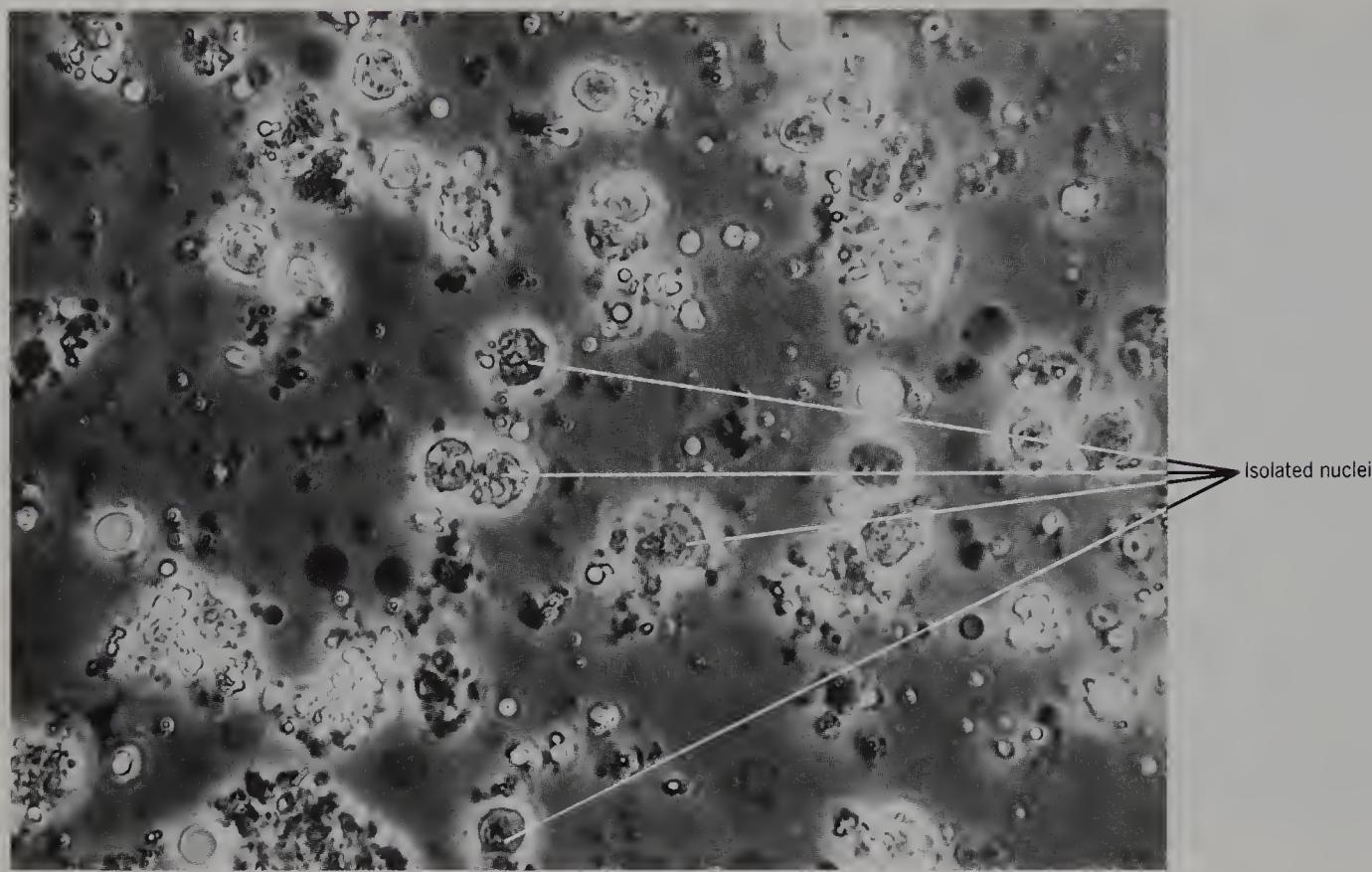


Figure 362 Isolated nuclei and fine granular material from rabbit adrenal medulla (phase contrast, $\times 700$).

SUMMARY OF THE STRUCTURE OF THE NERVOUS SYSTEM

The grey matter in fresh tissue appears brownish due to the presence of blood vessels, blood and neuron somas. Its main elements are neuron somas, dendrites, axons, neuroglial nuclei, beaded fibres, fine granular material and fine fibres. It also contains blood vessels of the different sizes, as do nearly all other tissues. A large proportion of the volume of grey matter is occupied by a fine granular material, which is frequently illustrated in this atlas. It may not have been seen before by light or electron microscopy, because it may have been washed out or extracted by the chemicals used in the staining and mounting procedures. The whole nervous system contains a network of fine dendrites or unmyelinated fibres, which are too thin and transparent to be seen, unless the surrounding tissue is stretched away from it.

The white matter consists of fibre tracts, large fibres, beaded fibres and droplets. The droplets and the beads in fibres vary in size and are translucent. They are found in freshly killed animal white matter, as well as in human post-mortem material, so that it is unlikely that they are fungi, bacteria, spores, or their products. Both the droplets and beads are shrunk or disappear

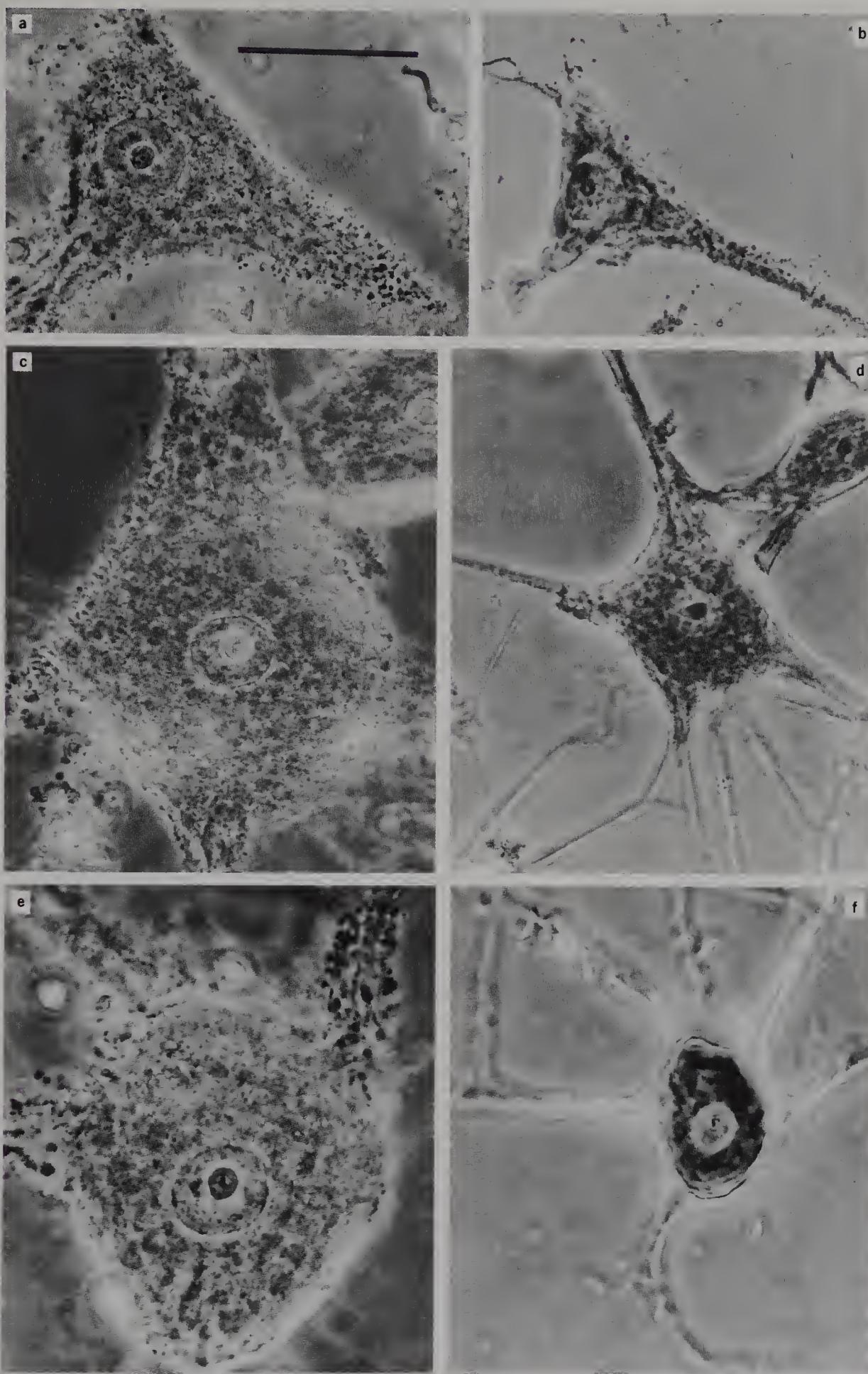
as a consequence of staining and embedding procedures (Chughtai *et al.*, 1988). In life, they are obviously insoluble in the aqueous cellular fluids and tend to be spherical, so they may contain a high proportion of lipid.

The basal ganglia and the cranial nerve nuclei are intermediate between grey and white matter at the cellular level. They contain neuron somas, beaded fibres, fine fibres and fine granular material. Unidentified spherical cells with little cytoplasm and no dendrites can be seen occasionally.

The peripheral nervous system is dominated by myelinated nerve fibres with nodes of Ranvier. The Schmidt-Lanterman incisures are present in the living nerves, but are probably widened by manipulations of the tissue. Many axons are slightly invaginated and involutions can be seen within them. The peripheral nerves contain occasional Schwann cells with elongate nuclei on their periphery. Very fine fibres may be teased out, and it is impossible to know for certain whether they are nerve fibres or collagen fibres. Remak fibres appear black, and are very rare in cranial or peripheral nerves. No other unmyelinated fibres were seen.

APPENDIX

The effects of staining procedures on the appearances of rabbit medullary neuron somas. The micrographs **a**, **c** and **e** are of fresh neurons in normal saline. Micrographs **b**, **d** and **f** show the same neurons after staining with haematoxylin and eosin (**b**), Palmgren's procedure (**d**) and buffered osmic acid (**f**) (phase contrast, $\times 700$). The bar is 50 μm . The shrinkages of the somas were to 22, 21 and 14 per cent, respectively, of the original areas (Chughtai *et al.*, 1987). (These photographs are reproduced by kind permission of the editor of *Microscopy* and the Quekett Microscopical Club.)



Unfixed

After staining and mounting

SELECTED REFERENCES

- Baker, J. R. (1958). *The Principles of Biological Microtechnique*, p. 19. Methuen, London.
- Betz, V. A. (1874). Anatomische Nachweis zweier Gehirnzentra. *Zbl. med Wiss.* **12**, 578–580; 595–599.
- Chambers, R. and Chambers, E. D. (1961). *Explorations into the Living Cell*. Commonwealth Fund, Harvard University Press, Cambridge, Massachusetts.
- Chughtai, I., Hillman, H. and Jarman, D. (1987). The effect of haematoxylin and eosin, Palmgren's and osmic acid procedures on the dimensions and appearance of isolated rabbit medullary neurons. *Microscopy* **35**, 625–659.
- Chughtai, I., Hillman, H. and Jarman, D. (1988). The effect of staining with haematoxylin and eosin, Golgi's stain and osmic acid on the appearance of single sciatic nerve and corpus callosal fibres of rat and guinea-pig. *Microscopy* **36**, 76–83.
- Clarke, E. and O'Malley, C. D. (1968). *The Human Brain and Spinal Cord*. University of California, Berkeley.
- Debus, E., Weber, K. and Osborn, M. (1983). Monoclonal antibodies specific for glial fibrillary acid (GFA) protein and for each of the neurofilament triplet polypeptides. *Differentiation* **25**, 193–203.
- Dossel, W. E. (1966). Preparation of tungsten microneedles with a propane torch. *Stain Technol.* **41**, 61–63.
- Ehrenberg, C. G. (1833). Nottwendigkeit einer feineren mechanischen Zerlegung des Gehirns und der Nerven vor der chemischen, dargestellt aus Beobachtungen von C. G. Ehrenberg. *Poggendorffs Ann. Phys.* **28**, 449–473.
- Fernandez-Moran, H. (1952). The submicroscopic organization of vertebrate nerve fibres. *Exptl. Cell Res.* **3**, 283–359.
- Golgi, C. (1881). Sulla struttura delle fibre nervosa midollate periferiche e centrali. *Arch. Scienze Med.* **4**, 221–245.
- Gray, J. (1931). *A Textbook of Experimental Cytology*. Cambridge University Press, Cambridge.
- Heilbrunn, L. V. (1956). *Dynamics of Living Protoplasm*. Academic Press, New York.
- Hillman, H. (1986a). Hyden's technique of isolating mammalian cerebral neurons by hand dissection. *Microscopy* **35**, 382–389.
- Hillman, H. (1986b). *The Cellular Structure of the Living Mammalian Nervous System*. MTP Press, Lancaster.
- Hussain, T. S., Hillman, H. and Sartory, P. (1974). A nucleolar membrane in neurons. *Microscopy* **32**, 348–352.
- Hyden, H. (1959). Quantitative assay of compounds in isolated fresh nerve cells and glial cells from control and stimulated animals. *Nature* **184**, 433–435.
- Kuhne, W. (1862). *Über die Peripherischen Endorgane der motorischen Nerven*, pp. 17–18. Englemann, Leipzig.
- Lanterman, A. J. (1877). Über den feineren Bau der markhaltigen Nervenfasern. *Arch. Mikroskop. Anat. Entwickl. Mech.* **13**, 1–8.
- Leeuwenhoek van, A. (1674). More observations from Mr. Leeuwenhoek. *Phil. Trans. Roy. Soc. B* **9**, 178–182.
- Leeuwenhoek van, A. (1719). *Epistolae Physiologicae Super Compluribus Naturae Arcanis*, p. 312. Beman, Delft.
- Meynert, T. (1872). The brain of mammals. In: (ed. Stricker, S., trans. Power, H.) *Manual of Human and Comparative Histology*, Vol. 2, p. 391. New Sydenham Society, London.
- Obersteiner, H. (1903). Über das hellgelbe Pigment in den Nervenzellen und das vorkommen weitere fettanlicher Körper im Centralnervensystem. *Arb. A. Neurol. Inst., Wein* **10**, 245–274.
- Purkinje, J. E. (1838). Neueste Untersuchungen aus der Nerven und Hirn-Anatomie. *Bericht über die Versammlung Deutscher Naturforscher und Ärzte in Prag in September 1837*, pp. 177–180. Hasse, Prague.
- Ramon y Cajal, S. (1892). Trans. Thorpe, S. A. and Glickstein, M. (1972). *The Structure of The Retina*. Charles Thomas, Springfield, Illinois.
- Ranvier, L. A. (1871). Contributions à l'histologie et à la physiologie des nerfs périphériques. *Compt. Hebd. Acad. Sci., Paris* **73**, 1168–1171.
- Remak, R. (1836). Verlaufige Mittheilung mikroskopischer Beobachtungen über den innern Bau der Cerebrospinalnerven und über die Entwicklung ihrer Formelemente. *Arch. Anat. Physiol.* **145**–161.
- Remak, R. (1838). *Observationes Anatomicae et Microscopicae de Systematis Nervosi Structura* (thesis). Reimerionis, Berlin.
- Sartory, P., Fasham, J. and Hillman, H. (1971). Microscopic observations of the nucleoli in unfixed rabbit Deiters' neurons. *Microscopy* **32**, 93–100.
- Schmidt, H. D. (1877). On the construction of the dark or

- double bordered nerve fibres. *Month. Microsc. J.* **11**, 200–221.
- Schwann, T. (1839). *Mikroskopisches Untersuchungen über die Uebereinstimmung in der Struktur und dem Wachstum der Thiere und Pflanzen*, pp. 174–175. Reimer, Berlin.
- Stilling, B. and Wallach, J. (1842). *Untersuchungen über den Bau des Nervensystems*. Wigand, Leipzig.
- Tellesniczky, K. (1898). Ueber die Fixierungs — (Haertung's) — Flussigkeiten. *Arch. Mikrosk. Anat.* **52**, 202–280.
- De Vieussens, R. (1684). *Neuronographia Universalis*, pp. 55–56. Certe, Lyons.
- Virchow, R. (1846). Über das granulirte Ansehen der Wanderungen der Gehirnventrikel. *Allg. Z. Psychiat.*, Berlin **3**, 242–250.
- Virchow, R. (1856). *Gesammelte Abhandlungen Zur Wissenschaftlichen Medizin*, p. 890. Meidinger, Frankfurt.
- Waldeyer-Hartz, H. W. G. (1891). Über einige neuere Forschung im Gebiete der Anatomie des Centralnervensystems. *Deutsch. med Wschr.* **17**, 1213–1218.
- Williams, P. L. and Hall, S. M. (1970). *In vivo* observations on mature, myelinated nerve fibres of the mouse. *J. Anat.* **107**, 31–38.
- Zernike, F. (1934). Begungstheorie des Schneidenverfahrens und Seiner verbesserte Form der Phasenkontrastmethode. *Physica* **1**, 689–704.

NIH Library, Building 10
National Institutes of Health
Bethesda, Md. 20892



<http://nihlibrary.nih.gov>

10 Center Drive
Bethesda, MD 20892-1150
301-496-1080

3 1496 00453 7844

The *Atlas of the Cellular Structure of the Human Nervous System* covers all the main areas of the brain, the cranial nerves, ganglia and peripheral nerves, viewed mainly by phase-contrast microscopy.

The atlas is unique in using photographs of *unfixed* tissue, seeking to show structures in as near natural a state as possible.

Particular features include:

- photographs of the neuroglia, white matter, droplet fibres and fine structure of the nucleolus
- observations by scanning differential interference microscopy, Hoffman modulation contrast, and polarizing microscopy
- photographs of cells identified by fluorescent monoclonal antibody studies.

ACADEMIC PRESS

Harcourt Brace Jovanovich, Publishers

LONDON • SAN DIEGO
NEW YORK • BOSTON
SYDNEY • TOKYO

ISBN 0-12-348770-6



9 780123 487704